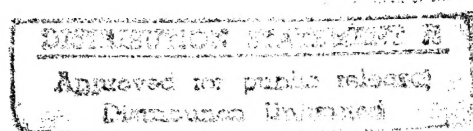


High Temperature Polymer Matrix Composites

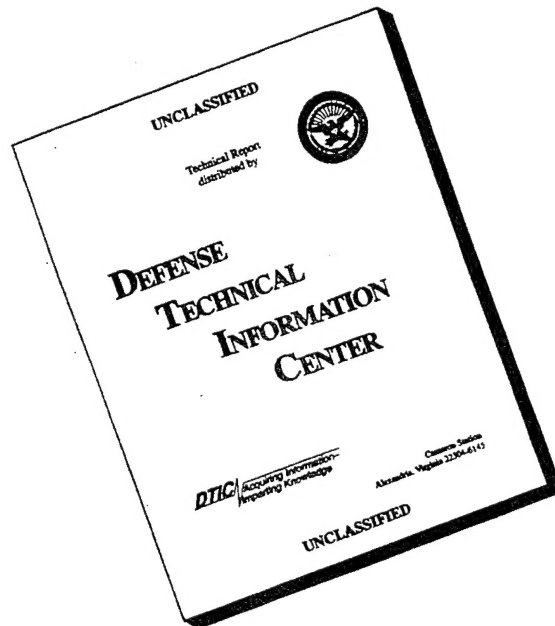


*Proceedings of a conference held at
NASA Lewis Research Center
Cleveland, Ohio
March 16-18, 1983*

19960306 017

NASA

DISCLAIMER NOTICE



THIS DOCUMENT IS BEST
QUALITY AVAILABLE. THE
COPY FURNISHED TO DTIC
CONTAINED A SIGNIFICANT
NUMBER OF PAGES WHICH DO
NOT REPRODUCE LEGIBLY.

Date: 9/1/95 Time: 5:59:09PM

Page: 1 Document Name: untitled

DTIC DOES NOT HAVE THIS ITEM

-- 1 - AD NUMBER: D439681
-- 5 - CORPORATE AUTHOR: NATIONAL AERONAUTICS AND SPACE ADMINISTRATION
-- CLEVELAND OH LEWIS RESEARCH CENTER
-- 6 - UNCLASSIFIED TITLE: HIGH TEMPERATURE POLYMER MATRIX COMPOSITES.
--11 - REPORT DATE: SEP , 1985
--12 - PAGINATION: 421P
--14 - REPORT NUMBER: NASA-CP-2385
--20 - REPORT CLASSIFICATION: UNCLASSIFIED
--21 - SUPPLEMENTARY NOTE: PROCEEDINGS: HIGH TEMPERATURE POLYMER
-- MATRIX COMPOSITES CONFERENCE HELD AT NASA LEWIS RESEARCH CENTER ON
-- 16-18 MARCH 1983. (SEE PL-48468-PL-48498).
--22 - LIMITATIONS (ALPHA): APPROVED FOR PUBLIC RELEASE; DISTRIBUTION
-- UNLIMITED. AVAILABILITY: NATIONAL TECHNICAL INFORMATION SERVICE,
-- SPRINGFIELD, VA. 22161. NASA CP-2385.
--33 - LIMITATION CODES: 1 24

High Temperature Polymer Matrix Composites

DTIC QUALITY INSPECTED 4

*Proceedings of a conference held at
NASA Lewis Research Center
Cleveland, Ohio
March 16-18, 1983*

NASA
National Aeronautics
and Space Administration
Scientific and Technical
Information Branch
1985

PREFACE

This is the proceedings of the High Temperature Polymer Matrix Composites Conference held at the NASA Lewis Research Center on March 16-18, 1983.

The purpose of the conference was to provide scientists and engineers working in the field of high temperature polymer matrix composites an opportunity to review, exchange, and assess the latest developments in this rapidly expanding area of materials technology.

Technical papers were presented in the following areas:

1. Matrix Development
2. Adhesive Development
3. Characterization
4. Environmental Effects
5. Applications

Tito T. Serafini
Conference Chairman

Confas-a-whale
PL-048467

CONTENTS

	Page
Preface	111
 SESSION I - MATRIX DEVELOPMENT	
Chairman: Robert J. Jones, TRW, Inc.	
 Acetylene Terminated Matrix Resins	
I.J. Goldfarb, C.Y-C. Lee, F.E. Arnold, and T.E. Helminiatk Air Force Wright Aeronautical Laboratories	PL-48468 . 1
 An Improved Processible Acetylene-Terminated Polyimide for Composites	
Abraham L. Landis and Arthur B. Naselow Hughes Aircraft Company	PL-48469 . 11
 PMR Polyimides from Solutions Containing Mixed Endcaps	
Peter Delvigs, NASA Lewis Research Center	PL-48470 . 23
 Matrix Resin Development at NASA Langley Research Center	
Terry L. St. Clair, NASA Langley Research Center	PL-48471 . 35
 Bismaleimides and Related Maleimido Polymers as Matrix Resins for High Temperature Environments	
John A. Parker, Demitrius A. Kourtides, and George M. Fohlen, NASA Ames Research Center	PL-48472 . 55
 The Synthesis, Characterization and Thermal Chemistry of Modified Norbornenyl PMR Endcaps	
Chaim N. Sukenik, William M. Ritchey, Vinay Malhotra, and Uday Varde, Case Western Reserve University	PL-48473 . 79
 All-Aromatic Biphenylene End-Capped Polyquinoline and Polyimide Matrix Resins	
John P. Droske and John K. Stille, Colorado State University, and William B. Alston, NASA Lewis Research Center	PL-48474 . 91
 SESSION II - ADHESIVE DEVELOPMENT	
Chairman: S.E. Wentworth, U.S. Army Materials and Mechanics Research Center	
 Evaluation of a High Temperature Adhesive for Fabricating Graphite/PMR-15 Polyimide Structures	
S.G. Hill and J.B. Cushman, Boeing Aerospace Company . . .	PL-48475 . 97
 New Processable Modified Polyimide Resins for Adhesive and Matrix Applications	
David Landman, The Dexter Corporation	PL-48476 . 109

Recent Developments in Polyimide and Bismaleimide Adhesives
Robert E. Politi, American Cyanamid Company PL-48477. 125

SESSION III - CHARACTERIZATION
Chairman: M.G. Maximovich, Lockheed Missiles
and Space Company

Chemical Control of Rate and Onset Temperature of Nadimide
Polymerization
Richard W. Lauver, NASA Lewis Research Center PL-48478 137

Characterization Methodology for PMR-15
A.B. Hunter, Boeing Aerospace Company PL-48479 151

Characterization of Polyimide Matrix Resins and Prepregs
M.G. Maximovich and R.M. Galeos, Lockheed Missiles
and Space Company PL-48480 157

Quality Assurance Procedures for V378A Matrix Resin
Charles L. Hamermesh and Paul J. Dynes,
Rockwell International Science Center PL-48481 171

SESSION IV - ENVIRONMENTAL EFFECTS
Chairman: C.H. Sheppard, Boeing Aerospace Company

Replacement of MDA with more Oxidatively Stable Diamines
in PMR-Polyimides
William B. Alston, U.S. Army AVRADCOM Research and
Technology Laboratories, NASA Lewis Research Center . . . PL-48482 187

Properties of Autoclaved Gr/PI Composites Made from Improved
Tack PMR-15 Prepreg
Raymond D. Vannucci, NASA Lewis Research Center . . . PL-48483 207

Thermo-Oxidative Stability of Graphite Fiber/PMR-15
Polyimide Composites at 350°C
Daniel A. Scola, United Technologies Research Center . . . PL-48484 217

Rheological, Processing, and 371 °C Mechanical Properties
of Celion 6000/N-Phenylnadimide Modified PMR Composites
Ruth H. Pater, NASA Lewis Research Center . . . PL-48485 243

High Temperature, Short Term Tensile Strength of
C6000/PMR-15 Composites
P.R. DiGiovanni and D. Paterson, Raytheon Company . . . PL-48486 257

Polyimide Matrix Resins for up to 700°F Service
R.J. Jones, G.E. Chang, S.H. Powell, and H.E. Green,
TRW Energy Development Group PL-48487 271

Surface Protection of Graphite Fabric/PMR-15 Composites
 Subjected to Thermal Oxidation
 M.P. Hanson and T.T. Serafini, NASA Lewis Research Center . *PL-48488* 287 (21)

Microscopic Evaluation of a Polyimide (PMR15) - Graphite Composite
 Jeffry J. Fedderly and Joseph M. Augl,
 Naval Surface Weapons Center *PL-48489*. 299 (22)

Effects of Real-Time Thermal Aging on Graphite/Polyimide Composites
 J.F. Haskins and J.R. Kerr, General Dynamics Convair Division *PL-48490* 315 (23)

Environmental Stability Graphite/PMR-15 Composites *PL-48491*
 Clyde H. Sheppard and Doug McLaren, Boeing Aerospace Company 329 (24)

SESSION V - DESIGN/ANALYSIS
 Chairman: *D. Mulville, Naval Air Systems Command*

Development of Design Data for Propulsion PMR-15 Composites
 J. Postlewaite and D. McLaren, Boeing Commercial
 Airplane Company *PL-48492* 335 (25)

SESSION VI - APPLICATIONS I
 Chairman: *T. Cordell, Air Force Wright
 Aeronautical Laboratories*

Polyimide Composites - Application Histories *PL-48493* 339 (26)
 Leonard M. Poveromo, Grumman Aerospace Corporation

V-378A, A Modified Bismaleimide for Advanced Composites *PL-48494* 359 (27)
 S.W. Street, HITCO Materials Division

Transfer Molding of PMR-15 Polyimide Resin
 J.P. Reardon, D.W. Moyer, and B.E. Nowak,
 Tribon Bearing Company *PL-48495* 379 (28)

SESSION VII - APPLICATIONS II
 Chairman: *T. Cordell, Air Force Wright
 Aeronautical Laboratories*

Application of GR/PMR-15 to Commercial Aircraft
 Propulsion Installation Structures
 J. Postlewaite, K. Porter, and D. McLaren,
 Boeing Commercial Airplane Company *PL-48496*. 393 (29)

Fabrication Process of a High Temperature Polymer Matrix
 Engine Duct
 R.D. Pratt and A.J. Wilson, General Electric Company . . . *PL-48497*. 401 (30)

Current and Future Engine Applications of Gr/PI Composites
 P.J. Cavano and T.E. Schmid, Pratt & Whitney Aircraft . . *PL-48498* 409 (31)

ACETYLENE TERMINATED MATRIX RESINS

I. J. Goldfarb, C. Y-C. Lee, F. E. Arnold, and T. E. Helminiak
Materials Laboratory
Air Force Wright Aeronautical Laboratories

601

The synthesis of resins with terminal acetylene groups have provided a promising technology to yield high performance structural materials. Because these resins cure through an addition reaction, no volatile by-products are produced during the processing. The cured products have high thermal stability and good properties retention after exposure to humidity. Resins with a wide variety of different chemical structures between the terminal acetylene groups have been synthesized in the Materials Laboratory, and their mechanical properties have been studied. The ability of the acetylene cured polymers to give good mechanical properties has been demonstrated by the resins with quinoxaline structures. Processibility of these resins can be manipulated by varying the chain length between the acetylene groups or by blending in different amounts of reactive diluents. Processing conditions similar to the state-of-the-art epoxy can be attained by using backbone structures like ether-sulfone or bis-phenol-A. The wide range of mechanical properties and processing conditions attainable by this class of resins should allow them to be used in a wide variety of applications.

INTRODUCTION

A variety of aromatic and aromatic heterocyclic oligomers with terminal acetylene units have been reported (Ref 1-3) in recent years for use as addition curable moisture resistant thermoset resins. Long term use temperatures for these materials are in the range of 250-550°F with short term usage at 600-650°F depending on the specific molecular structure between acetylene cure sites. A substantial effort in our laboratory has been directed toward the synthesis and characterization of acetylene terminated oligomers. These materials can be classified into rigid (high T_g) and flexible (low T_g) systems. For higher use temperatures, the rigid aromatic heterocyclic oligomeric backbones are employed which exhibit higher T_g 's after cure. Materials which process analogous to the state-of-the-art epoxides require the more flexible (e.g. phenylene R systems) where R refers to the functional group which imparts the flexibility to the oligomeric backbone. This paper is an attempt to scope the chemistry and the range of processing and mechanical properties presently attainable by this class of resins. It is not a complete survey of previous work in this technology area but selective resins are chosen to demonstrate their versatility and properties. The data reported are in general not optimized because of the limited quantities of these resins.

CURE CHEMISTRY

Studies of various acetylene terminated monomers have demonstrated that the polymerization is a free radical propagation of the acetylene moiety to a linear conjugated polyene (Ref 4). The kinetic chain length of this reaction is unusually short (6-8 acetylene units) and termination is first order. This early stage of reaction of a difunctional acetylene is depicted in Figure 1. A proposed model to account for these observations is as follows: A thermally induced free radical probably involving two molecules of monomer initiates the propagation of one acetylene per monomer unit into a conjugated polyene. This results in a cluster-shaped species whose growth is inhibited by the steric hindrance of the pendant groups attached to the acetylene. Although the free radical at the hub of the cluster is still reactive, its growth becomes increasingly more difficult as the reaction proceeds reaching a finite limit. Based on this model one would predict a steady growth of free radicals to a high concentration. Electron paramagnetic resonance of polymerizing acetylene terminated sulfone verifies such a growth of free radicals to unusually high concentrations (Ref 5). Involvement of the pendant acetylenes of a cluster in subsequent polyene formation reactions yields a crosslinked network whose crosslink sites are the polyenes. This model would lead to the prediction that a high degree of cure completion would be required in order to obtain good tensile properties. In addition it would be expected that the monomer size should influence the average polyene length and hence the number of arms per cluster. This in turn would have a direct effect on the network topology which should manifest itself in mechanical behavior. Studies to explore the size effect are currently underway. Studies to date support the proposed model with no evidence of any further reaction of the polyene species, but trimerization to an aromatic species, although sterically improbable, is possible and has been observed in small quantities. It has been demonstrated that polymerization of acetylene terminated monomers can be initiated at lower temperatures using transition metal-organic compounds (Ref 6). Although the effect on network structure has not been determined, preliminary mechanical characterization of initiated polymers indicates an effect may be present. As might be expected for a free radical polymerization, cure studies in air and nitrogen have clearly shown that the rate of cure is markedly reduced in air (Ref 7). The mechanical properties are apparently favorably influenced by an air cure (Ref 8).

MECHANICAL PROPERTIES

To demonstrate that AT cured systems can attain good mechanical properties, the results for a quinoxaline resin (ATQ) are shown as an example. This quinoxaline resin, whose structure is as shown in Figure 2, is prepared by endcapping quinoxaline oligomers with 3-(3,4-diaminophenoxy)phenylacetylene (Ref 1). The neat resin mechanical properties of this system are listed in Table I (Ref 9). The test specimens were post-cured at 700°F under nitrogen for 1 hour. The fully cured T_g of this resin is 321°C. The data listed in Table I indicate good tensile strength at room temperature. The resins have also been tested at 450°F. The mechanical properties at both temperatures are not affected by aging at 200°F, 94% humidity environment. This resin has also been evaluated as a matrix in an unidirectional graphite composite. Prepreg tapes were prepared by drum winding at room temperature using Hercules HT-S fiber and solutions of the ATQ resin in

methylene chloride (Ref 10). The laminates were fabricated in a press at 550°F for 2 hours under 200 psi pressure and post-cured in an oven at 600°F for 16 hours. The composite data are listed in Table II (Ref 1). Again the properties are good and seemingly unaffected after 30 days of aging at 160°F/95% relative humidity environments. The ability of the cured AT systems to maintain high temperature properties, even with relatively flexible backbones, can be demonstrated by the mechanical properties of the bis-phenol-A (ATB) resin. The synthesis and characterization of this resin are being reported elsewhere (Ref 11). The structure is shown in Figure 3. The neat resin tensile data are listed in Table III. This resin has good retention of properties at 350°F. Again, aging in severe wet environment (immersed in 160°F water till saturation) does not seriously affect its mechanical properties. Preliminary short beam shear data of the ATB/graphite composite (Ref 12) show values of 12 ksi at room temperature and 7.5 ksi at 350°F.

PROCESSABILITY

The AT resins can be used in a wide range of processing temperature and conditions. Resins with high molecular weight and rigid backbones usually have very short time in the melt state, and require rather extreme processing conditions like compression molding at high temperature. At the other extremes, resins with flexible backbones can exhibit the "tack and drape" characteristics of the state-of-the-art epoxy resins. At moderately high temperature, this type of resin remains in the liquid state for an extended period of time. Because they are single component systems, these resins do not have the problems associated with mixing-in high temperature melting components. An example of an AT system that shows the high temperature processing characteristic is another quinoxaline resin that is end-capped with 4-(3-ethynylphenoxy)benzil (Ref 1). The structure of this resin (BATQ) is shown in Figure 4. This resin has a high uncured T_g of 185°C. The isothermal viscosity curves as a function of cure time are shown in Figure 5. In order to mold this resin into tensile dog-bone specimens for testing, the resins were processed at 180°C under 18 ksi pressure for 1 hour, then cured for 1 hour at 220°C in the mold under the same pressure. The tensile data of these specimens after post curing at 250°C for 4½ hours are quite good; with a tensile strength of 13.4 ksi and 13.1 ksi before and after moisture aging respectively. The viscosity profile of the ATB however, is quite different. At 25°C, the viscosity of this resin is 10^3 poise (as measured by dynamic measurement at 10 rad/sec) (see Fig. 6). At 80°C, the viscosity level is less than 1 poise and can be poured through narrow channels of processing molds. Because of the low uncured viscosity, this resin can be tailored to suit different viscosity requirements for specific processing needs by B-staging the resin to appropriate degrees.

Molecular Weight Effect

By changing the molecular weight between the acetylene groups the thermo-rheological profiles of a system can be drastically modified. Figure 5 shows the isothermal viscosity curves of a series of quinoxaline resins. The lowest molecular weight structure, shown in Figure 4, is referred to as SBQ (Ref 1). It is obvious that with decreasing oligomer chain lengths, the processing window (time in melt state) is increased to allow easier processing. The fracture toughness (K_{Ic}) measurement of this series also indicate that the toughness decreases with decreasing chain length (Fig. 7).

Reactive Diluents

Another approach that can improve the processability of a resin is to blend it with reactive diluents (Ref 13). The BATQ described in the previous section is very difficult to process because of its high uncured T_g. When a reactive diluent is blended in with a resin, the glass transition temperature of the mixture is lowered than the unblended resin. The mixture can then be processed at a temperature unreachable by the unblended resin. Also because of the lower processing temperature, the kinetic rate of the cure is slower as well, thus affording further improvement of the processing window. Because of the reactivity of the diluents, they will be incorporated into the final network during cure. Both difunctional and monofunctional acetylene terminated phenylene oxide have been used as reactive diluents with BATQ resin. The isothermal cure viscosity curves of the blends are shown in Figure 8. Substantial improvement in processing can be realized by the small amount of diluents added. At low concentration, the diluents do not appear to adversely affect the mechanical properties of the resin. However, at higher concentration, the properties of the resin can be seriously compromised.

CONCLUSIONS

The acetylene terminated resins are a promising thermoset technology because of its addition cure reaction, good thermal properties and excellent properties retention after exposure to humid environments. By incorporating appropriate chemical structures between the terminal acetylene groups, one can obtain matrices with good mechanical properties after cure. The wide range of viscosity profiles before cure attainable by these resins makes them a versatile technology for designing thermoset systems for specific application requirements.

REFERENCES

1. F. L. Hedberg, R. F. Kovar and F. E. Arnold: Acetylene Containing Aromatic Heterocyclic Polymers, in Contemporary Topics in Polym. Sci. (ed. Eli M. Pearce) Vol 2, Plenum Publishing Corp., NY, 235 (1977).
2. P. M. Hergenrother: Acetylene-Containing Precursor Polymers, J. Macromol. Sci. Rev. Macromol. Chem., C19 (1) 1 (1980).
3. N. Bilow: Acetylene-Substituted Polyimides as Potential High Temperature Coatings, in Resins for Aerospace, ACS Symposium #132, 139 (1982).
4. J. M. Pickard, E. G. Jones and I. J. Goldfarb: The Kinetics and Mechanism of the Bulk Thermal Polymerization of Bis 4-(3-Ethynyl-Phenoxy) Phenyl Sulfone, Am. Chem. Soc. Div. of Polym. Prepr. 20 (2), 375 (1979).
5. T. C. Sandreczki and C. Y-C. Lee: Characterization of Acetylene Terminated Resin Cure States Using EPR Spectroscopy, Am. Chem. Soc. Div. of Polym. Prepr. 23 (2), 185 (1982).

6. L. G. Picklesimer, M. A. Lucarelli, W. B. Jones, T. E. Helminiak and C. C. Kang: Acetylene Terminated Sulfone Monomer Polymerization by INitiator, Am. Chem. Soc. Div. of Polym. Chem. Prepr., 22 (2), 97 (1981).

7. C. C. Kuo, C. Y-C. Lee and I. J. Goldfarb: Effects of Air and Nitrogen Environment on Cure of Acetylene Terminated Resins, Am. Chem. Soc. Div. Org. Coat. Plast. Chem. Prepr. 47 595 (1982).

8. C. C. Kuo and C. Y-C. Lee: Environmental Cure Effects on Mechanical Properties of Acetylene Terminated Sulfone, Am. Chem. Soc. Org. Coat. and Appl'd. Polym. Sci. Proc. 47, 144 (1982).

9. T. E. Helminiak, W. B. Jones, Jr.: Influence of Molecular Weight on Fracture Behavior of Quinoxaline Thermosets Am. Chem. Soc. Org. Coat. Plast. Chem. Prepr., 48 (1983).

10. C. E. Browning, A. Wereta, J. T. Hartness and R. F. Kovar: Initial Development of An ATQ Matrix Resin, Nat'l SAMPE Tech. Conf. Series, 21, 83 (1976).

11. C. Y-C. Lee, L. R. Denny and I. J. Goldfarb: Characterization of a BisPhenol-A Based Resin with Terminal Acetylene Groups, Am. Chem. Soc. Polym. Prepr., 24, (1983).

12. F. L. Abrams and C. E. Browning: Influence of Molecular Structure on Mechanical Properties of Acetylene Terminated Resins, Am. Chem. Soc. Org. Plast. Chem. Prepr., 48 (1983).

13. B. A. Reinhardt, W. B. Jones, T. E. Helminiak and F. E. Arnold: Reactive Diluents for an Acetylene Terminated Quinoxaline System, Am. Chem. Soc. Polym. Prepr. 22 (2), 100 (1981).

TABLE I
Mechanical Properties of Neat Resin ATQ

Test Temperature	Tensile Strength MPa (ksi)	
	Dry	Wet
RT	98(14)	98(14)
450°F	27(3.8)	32(4.5)

TABLE II
ATO/HT-S Composite Properties

Property	RT	500°F	300°F Aged*	450°F Aged*
Flexural Strength - ksi	221	194	221	198
Flexural Modulus - Msi	19.5	18.1	19.5	19.1
Short Beam Shear - ksi	15	-	-	-

*30 days at 71°C 95% RH.

TABLE III
ATB Neat Resin Mechanical Properties

	RT		200°F		350°F	
	Dry	Aged*	Dry	Aged*	Dry	Aged*
Elongation at Break - %	3.5	3.1	4.4	3.4	6	7
Tensile Strength - ksi	9.8	8.5	8.3	7.2	5.8	5.5

*Immersed in 160°F water till saturation.

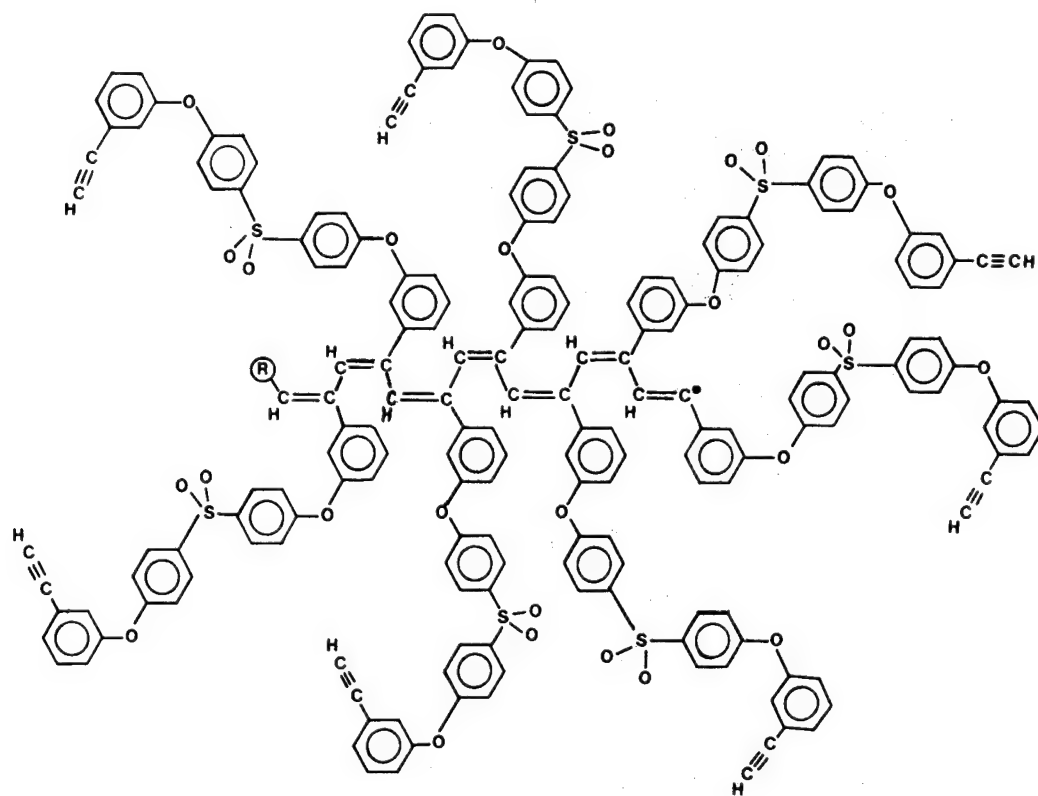


FIGURE 1. Early Stage of Cure.

ATQ

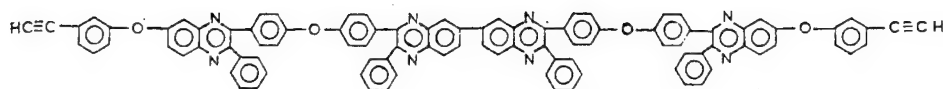


FIGURE 2. Molecular Structure of ATQ.

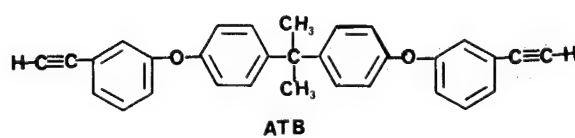


FIGURE 3. Molecular Structure of ATB.

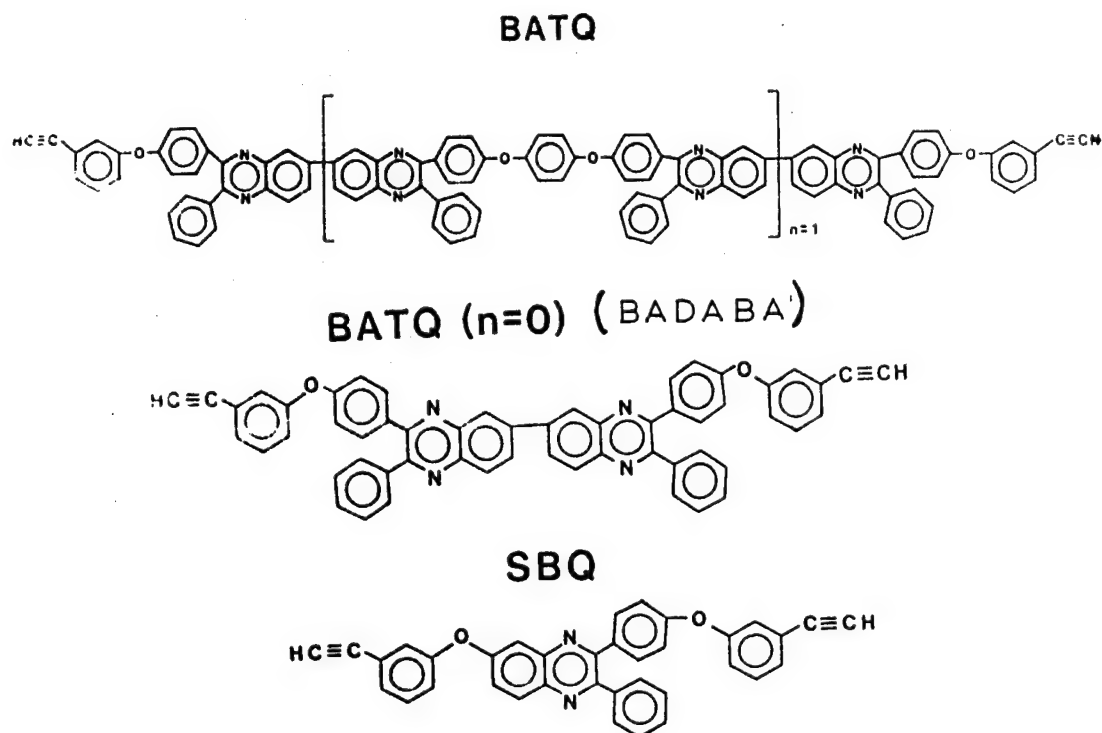


FIGURE 4. Molecular Structure of BATQ, BADABA, and SBQ.

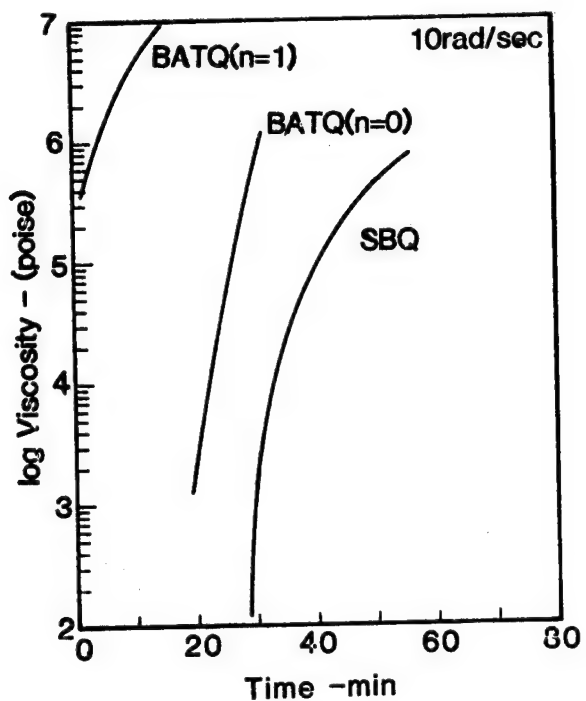


FIGURE 5. Isothermal Cure Viscosity of the Quinoxaline Resins.

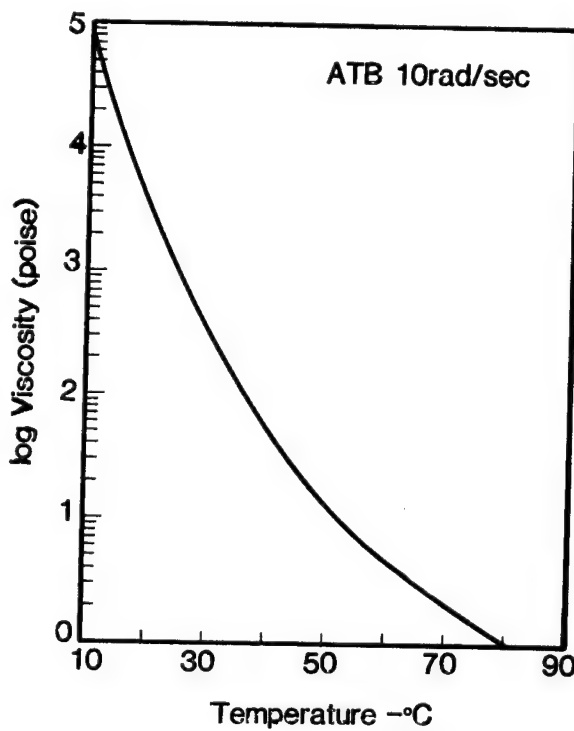


FIGURE 6. Viscosity of ATB.

FRACTURE TOUGHNESS VS NORMALIZED CHAINLENGTH
FOR ACETYLENE TERMINATED QUINOXALINES

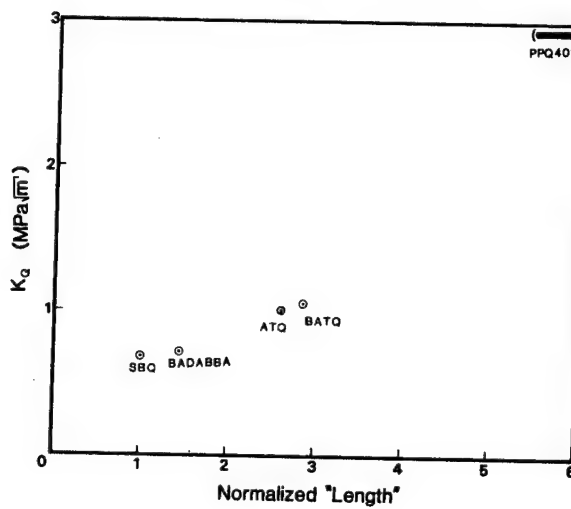


FIGURE 7. Fracture Toughness of the Quinoxaline Resins.

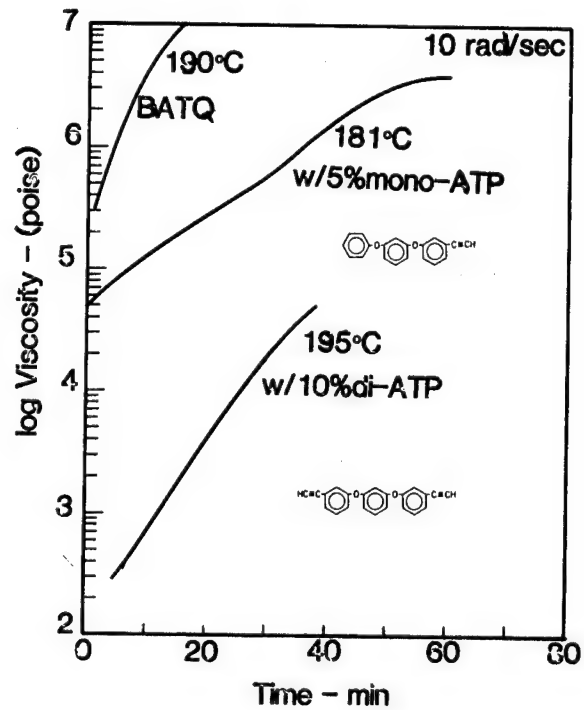


FIGURE 8. Isothermal Cure Viscosity of BATQ with Reactive Diluents.

-02

AN IMPROVED PROCESSIBLE ACETYLENE-TERMINATED POLYIMIDE FOR COMPOSITES

Abraham L. Landis and Arthur B. Naselow
Hughes Aircraft Company
Technology Support Division

HR600P is the newest member of a family of thermosetting acetylene-substituted polyimide oligomers. This oligomer is the isoimide version of the oligomer known as HR600P and Thermid 600.* Although both types of material yield the same heat resistant end products after cure, HR600P has much superior processing characteristics. This is attributed to its lower melting temperature ($160 \pm 10^\circ\text{C}$, $320 \pm 20^\circ\text{F}$) in contrast to 202°C (396°F) for Thermid MC-600, its longer gel time at its processing temperature (16-30 minutes vs 3 minutes), and its excellent solubility in low boiling solvents such as tetrahydrofuran, glymes, or 4:1 methyl ethyl ketone/toluene mixtures. These advantages provide more acceptable coating and impregnation procedures, allow for more complete removal at lower temperatures, provide a longer pot life or working time, and allow composite structure fabrication in conventional autoclaves used for epoxy composite curing. The excellent processing characteristics of HR600P allow its use in large area laminated structures, structural composites, and molding compositions. The HR600P and HR60XP, where X is the degree of polymerization of the oligomer, materials will be produced in the future by National Starch and Chemical Company, Bridgewater, New Jersey.

DISCUSSION

In 1961, research was initiated, under U.S. Air Force Material Laboratory sponsorship (reference 1), aimed at the development of high temperature resins for composites which cure by addition reactions. A unique system of resins was developed based on the homopolymerization of an acetylene end group by heat alone. These oligomers were difunctional acetylene-terminated polyimides, sufficiently low in molecular weight and having the necessary structural features to impart solubility and fusibility during their processing.

Polyimides in general tend to be insoluble, intractable materials. Even as low molecular weight prepolymers special consideration had to be given to the polymer backbone to impart fusibility and solubility to the acetylene-terminated polyimide prepolymer. Numerous combinations of aryl diamines, difunctional aromatic acid anhydrides and 3-aminophenylacetylene finally gave a composition of an oligomer depicted by Figure 1 which had reasonably good processibility.

*Gulf Oil Chemical Company Trade Mark

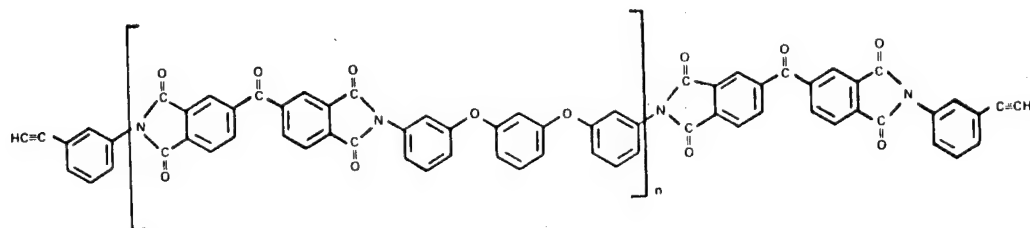


Figure 1. Specific designations: Thermid 600 when $n = 1$,
HR-60X when $n = X$.

This oligomer was prepared by the reaction of benzophenonetetracarboxylic dianhydride (BTDA), 1,3-bis(3-aminophenoxy)benzene (APB) and 3-aminophenylacetylene (APA) in molar ratios of 2:1:2. By varying the molar ratio of the reactants, the value of n , also called the degree of polymerization DP, could be varied. The oligomer with a DP of one was found to be very promising both as a molding and as a matrix resin and was initially licensed to Gulf Oil Chemical Company and marketed under the trade name Thermid 600. It has found utility as matrix resin for glass and graphite reinforced composites, chopped graphite reinforced molding compounds, adhesives for polytitanium, self-lubricating composites, bearing retainers, adhesives for other polyimides such as Kapton, and matrix resin for printed wiring boards. Thermid 600 has the proven ability to meet both long term (under 550°F) and short term exposure (over 550°F) with minimal degradation of mechanical properties. In the past, these resins have had limited acceptability because their high melting point and rapid cure allow a very limited time at viscosities acceptable for processing.

Also, the resins have a relatively limited solubility in common solvents. The processing window becomes even smaller with higher DP oligomers. In the past, a number of approaches have been tried to improve the processibility of these oligomers. For example, the incorporation of acetylene-terminated reactive diluents met with limited success because of the lack of mutual solubility of the oligomer and diluent.

A new approach was tried several years ago to improve the processibility of these oligomers. It was found that, under specific conditions, an isomeric form of these oligomers can be made which has a lower melting temperature and is soluble in a wide variety of common solvents when compared to the imides. This isomeric form is the iminolactone or isoimide form and is depicted by the structure shown in Figure 2.

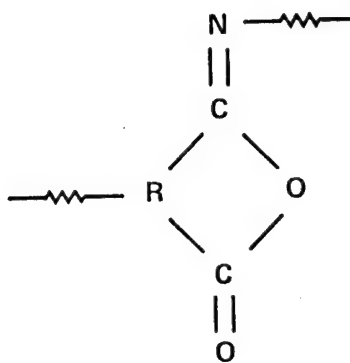


Figure 2. - Isoimide form of oligomer.

This structure is metastable and readily converts irreversibly to the imide form, either by heat or by catalysis. There are numerous references in the literature to this phenomenon (reference 2 and 3). The formation of the isoimide structure is through the cyclodehydration of the amic acid precursor by selected dehydrating agents. Thus, depending upon the cyclodehydration method used, the imide or isoimide structure is formed. This is depicted in Figure 3.

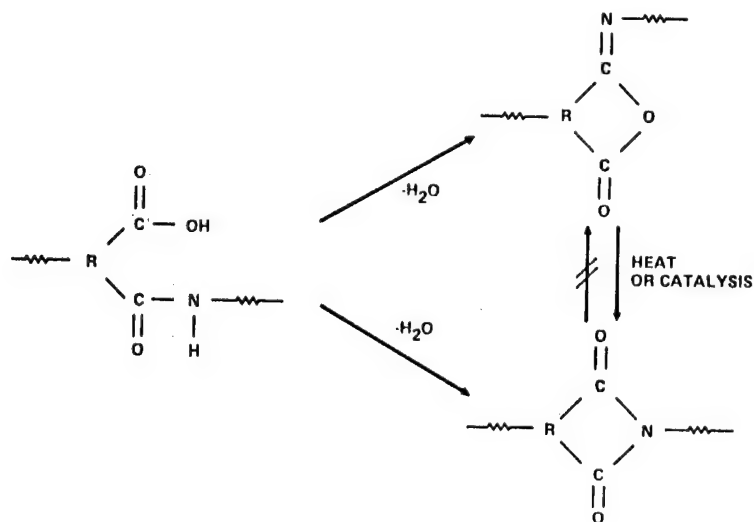


Figure 3. - Imide-Isoimide formation and conversion.

Because of the number of isomers possible for the isoimide compared to the imide and due to its asymmetry, the isoimide version of the Thermid 600 is known as HR600P oligomer. It is prepared by chemical rather than thermal cyclodehydration of the amic acid precursor. Generally, the HR600P has an isoimide content greater than 80 percent. The theoretical structure is depicted in Figure 4.

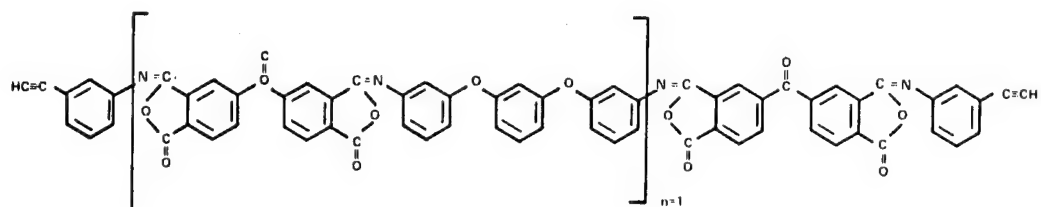


Figure 4. - HR600P Acetylene-terminated polyisoimide oligomer.

The spectrum for the imide form is depicted in Figure 5 and that of the isoimide version in Figure 6. The I.R. spectrum of the imide form shows the expected C=O (sym 1707-1730 cm^{-1} , asym 1776-1794 cm^{-1}). The I.R. spectrum of the isoimide shows C=O at 1789-1841 cm^{-1} , C=N at 1680-1730 cm^{-1} , and a characteristic broad band base at 900-950 cm^{-1} which can be attributed to the lactone ring with an exo-double bond.

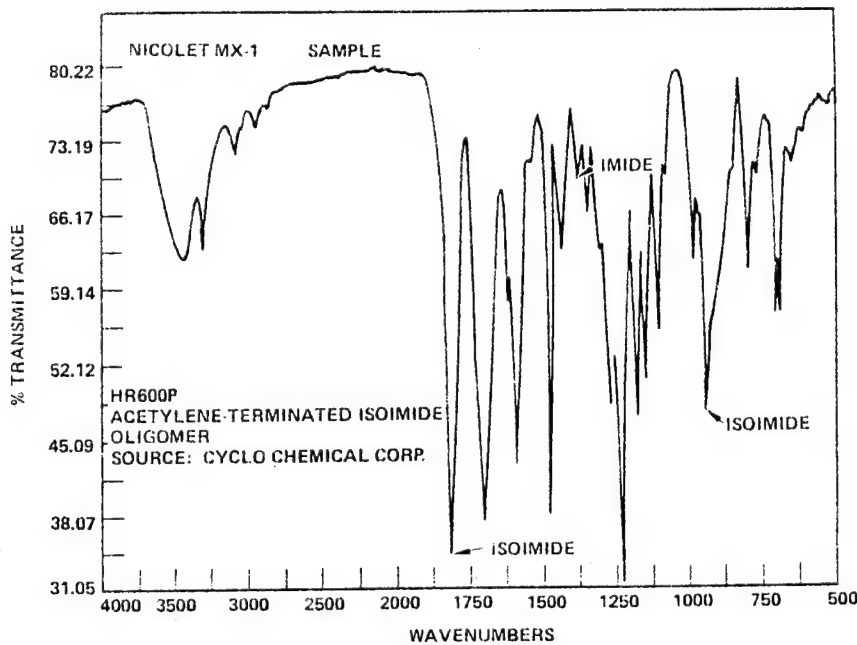


Figure 5. - HR600P Acetylene-terminated isoimide oligomer.

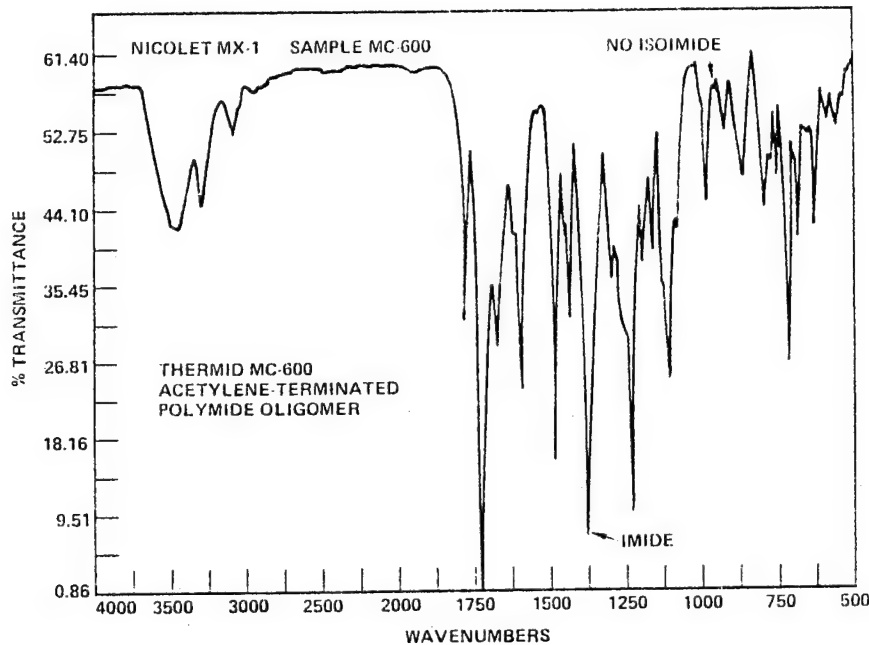


Figure 6. - Thermid MC-acetylene-terminated polyimide oligomer.

A study reported in the literature with N-substituted phthaloisoimide, Figure 7,

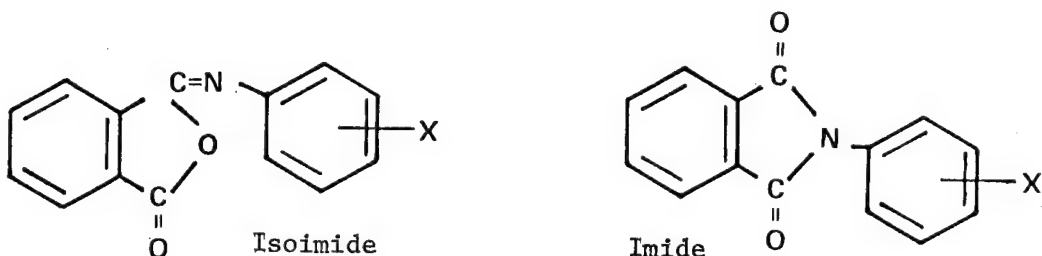


Figure 7. - Configurations of isoimide and imide forms of N-substituted phthaloisoimide.

shows a significant difference in melting point of the isoimide form over that of the imide. Table I depicts this difference. The dramatic decrease in melting point is very significant. Also, the solubility of the isoimide form in a number of common solvents in which the imide version is sparingly soluble is greatly increased.

TABLE I - Melting Points Of Comparable Imides and Isoimides (reference 3)

N-Substituted Phthaloisoimide	M.P. °C	
	Imide	Isoimide
C ₆ H ₅ -	207-8	110-2
o-CH ₃ C ₆ H ₄ -	180-1	135-6
p-CH ₃ OC ₆ H ₄ -	203-4	112-4
o-CH ₃ OC ₆ H ₄ -	158-9	116-7

The structure of the acetylene-terminated isomeric oligomers differs from that of the corresponding imide oligomers only in the arrangement of atoms in the functional heterocycle formed. Thus, the preparation of both oligomers requires the same stoichiometry of the reacting monomers but different reaction conditions. The acetylene-terminated polyisoimide analogous to Thermid MC-600, and having a degree of polymerization of 1 (DP=1), is referred to an HR600P in this discussion. The DP and DP_x materials are referred to as HR602P and HR60XP, respectively. The HR600P oligomer melts at about 150-160°C, whereas Thermid MC-600 melts at 195-205°C. Also, HR600P has excellent solubility in such solvents as tetrahydrofuran, glyme, N,N-dimethylacetamide, N-methylpyrrolidone and other amide or ketone solvents.

Upon heating and curing the HR600P converts to a thermally and oxidatively stable polymer having good physical properties. Figure 8 compares the infra-red spectra of molded and cured specimens of HR600P and MC-600. The similarity of the spectra is striking. The enhanced processibility permits the use of a wider range of DP's than has been possible with acetylene-terminated polyimides. Oligomers with high DP's are still very processible and have been particularly useful for coatings where flexibility and toughness are important. The fabrication of good quality composites using conventional autoclaving techniques (starting with a cold mold and curing at moderate temperatures) has been demonstrated. Sharp angular shapes were molded from graphite fiber composites. Such shapes are very difficult to produce with other high performance polyimides.

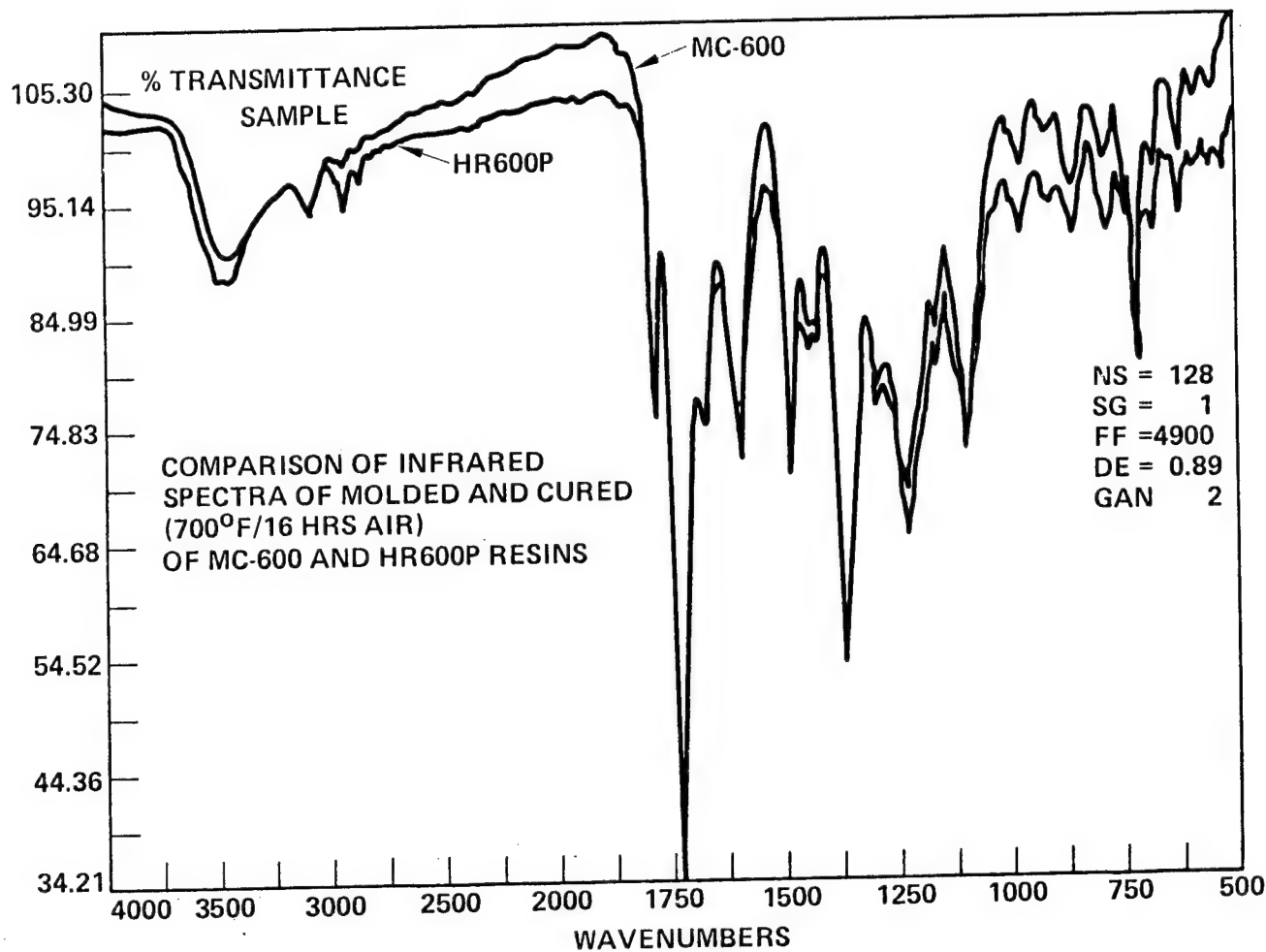


Figure 8. - Comparison of infrared spectra of molded and cured (700 °F/16 hrs air) of MC-600 and HR600P resins.

Properties and Processibility of HR60XP Oligomers

The uncured resin is a dry, free flowing, yellow powder. Its properties are shown in Table II.

TABLE II - Properties of HR600P

Melting Range	$320 \pm 20^{\circ}\text{F}$ ($160 \pm 10^{\circ}\text{C}$)
Gel Time (see Figure 9)	Traditional Method 6-7 minutes @ 190°C 6 minutes @ 218°C Rheometrics 30 minutes @ 190°C 8 minutes @ 210°C
Solubility	tetrahydrofuran dimethylformamide 4:1 methyl ethyl ketone/toluene N-methylpyrrolidinone Cellosolve
Molecular Weight	$M_w \sim 2600$ $M_n \sim 1100$
Viscosity (Rheometric)	<u>Minimum</u> 2.3×10^4 poise @ 190°C 3.6×10^3 poise @ 210°C <u>Time to reach 10^5 poise</u> 8 minutes @ 190°C 8 minutes @ 210°C

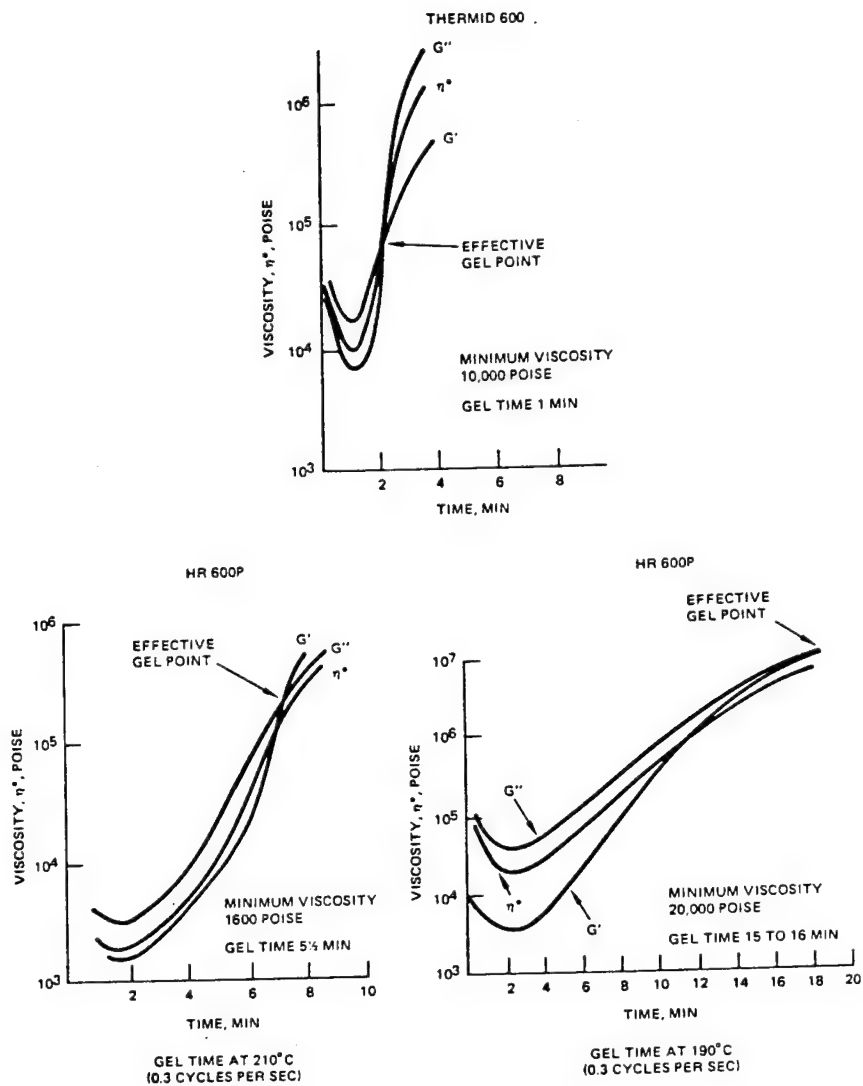


Figure 9. - Gel times of Thermid 600 and HR600P.

Figure 10 depicts a comparison of the differential scanning calorimetric curves (DSC) for HR600P and Thermid MC-600. The increase in the width of the HR600P curve over the MC-600 indicates a wider processing window. The neat resin can be molded below 400°F (210°C) by compression molding. By postcuring through a controlled temperature cycle up to 600°F (316°C) and then at 700°F (371°C) for approximately eight hours in air, a T_g of approximately 662°F (350°C) can be achieved, which is approximately that obtained for Thermid MC-600.

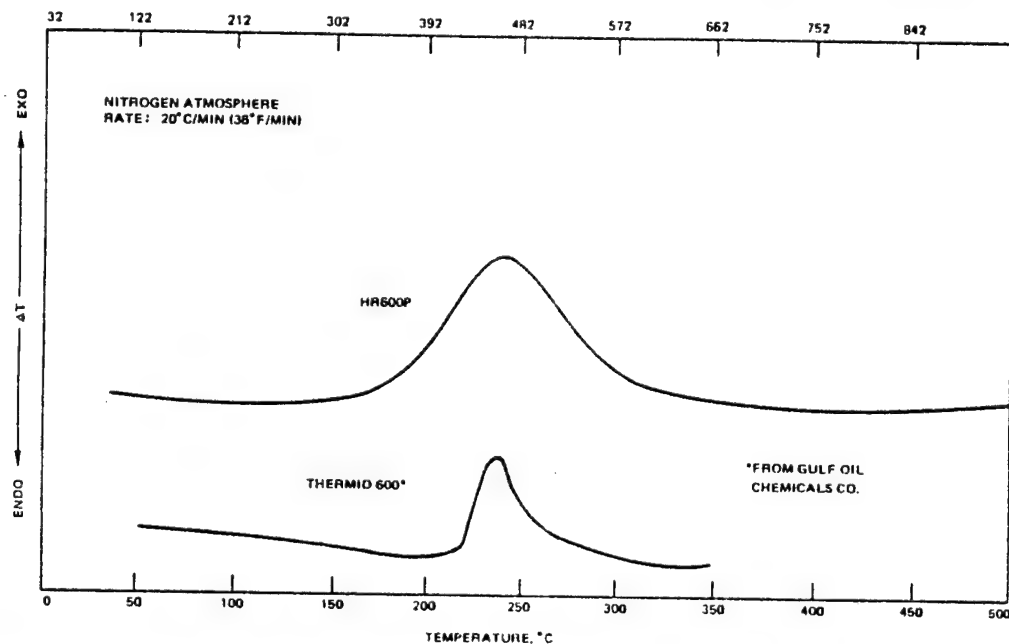


Figure 10. - Differential scanning calorimetry curves for Thermid MC-600 and HR600P resins.

Some select thermal mechanical properties for the molded HR600P oligomer are shown in Table III.

TABLE III - Select Thermal Mechanical Properties of Molded HR600P Oligomer

Neat Resin Properties	Values
Tensile Strength (Specimen size, 2 in. gauge length) (Rate at loading, .05 in./min.)	8500 psi at 21°C (70°F) 4000 psi at 316°C (600°F)
Tensile Modulus	730,000 psi at 21°C (70°F) 180,000 psi at 316°C (600°F)
Elongation at Break	1.2% at 21°C (70°F) 4.2% at 316°C (600°F)
Glass Transition Temperature, T _g by TMA	300°C after 8 hrs. @ 370°C air postcure 350°C after 15 hrs. @ 370°C air postcure 330°C after 4 hrs. @ 400°C air postcure 354°C after 8 hrs. @ 400°C air postcure
Density	1.34 g/cc

Composites

The high processibility of the HR600P oligomer makes this oligomer particularly amenable to the state-of-the-art autoclaving molding techniques. The processibility is compared to two other high temperature, high performance resins, namely LARC-160 and NRC-150 in Figure 11. It should be noted that with the HR600P oligomer, the part can be easily formed at 375°F starting with a cold mold. After several hours, the part can be removed from the autoclave and postcured in an oven. This cannot be easily accomplished with the other two resins.

Typically, a glass clogh prepreg is prepared by coating the cloth with a lacquer containing 25 percent by weight of HR600P resin in tetrahydrofuran containing one percent of N-methylpyrrolidinone. In the case of graphite, the tow is coated with the same lacquer using a dip tank and a collimation drum. The prepreg is placed between Mylar film to preserve tack and drape. Tetrahydrofuran is used to reactivate the tack and drape. The bulk may be reduced every fourth ply by vacuum bagging for thirty minutes. After the final ply, the layup is oven dried at 140°F for 16 hours under vacuum. The debulked preform is then molded using the cycle shown in Figure 11. A typical postcure involves 150°F to 450°F in 2 hours, hold at 450°F

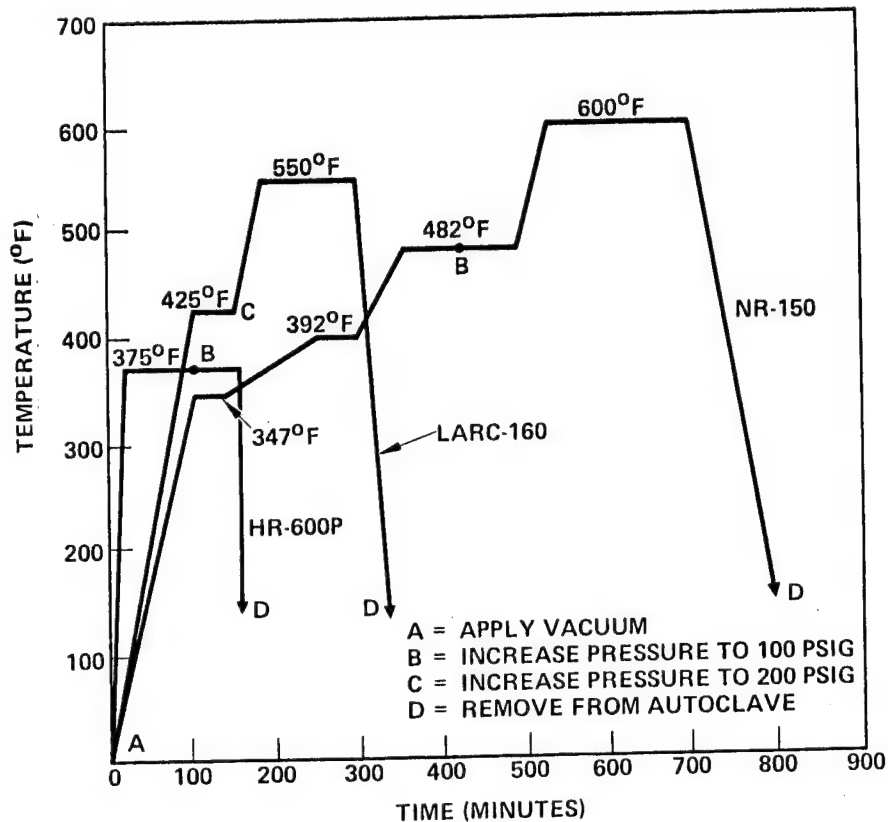


Figure 11. - Comparison of autoclave cycles of HR600P with high performance resins LARC-160 and NR-150.

for 1 hour, 450°F to 600°F in 2 hours, hold at 600°F in 3 hours, 600°F to 700°F in 1.5 hours, and hold at 700°F for 6 hours. In the case of compression molding, it is necessary to introduce about 5 percent by weight of Cab-O-Sil to the resin to prevent excessive squeeze-out of the resin or to advance the resin to a suitable viscosity for molding.

Recent test results of HR600P HTS unidirectional graphite laminates show that the strength retention properties are good. It is difficult to compare this data with that of Thermid 600 since those laminates were made by compression molding techniques whereas HR600P laminates were made by vacuum bag autoclaving techniques. Figures 12 and 13 depict the change in flexural strength and shear strength as a function of heat aging in air at 550°F up to 1000 hours. Most noteworthy is the small change in these values when measured at room temperature. It should be noted that these measurements were made on samples prepared by an unoptimized process.

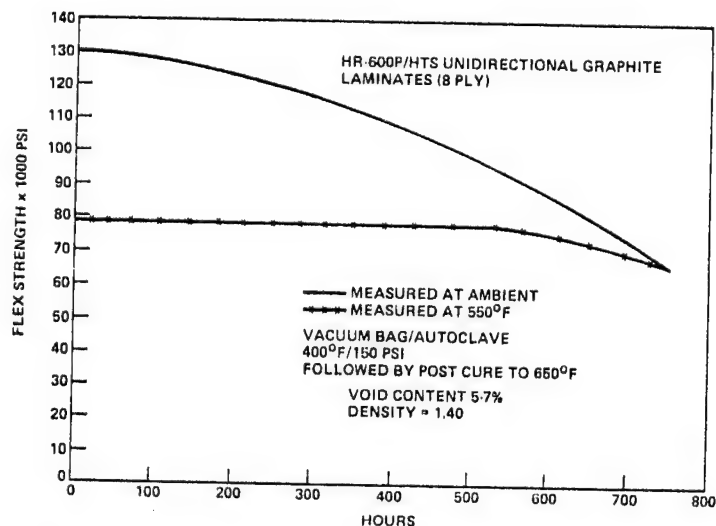


Figure 12. - Change in flexural strength as function of air aging at 550 °F.

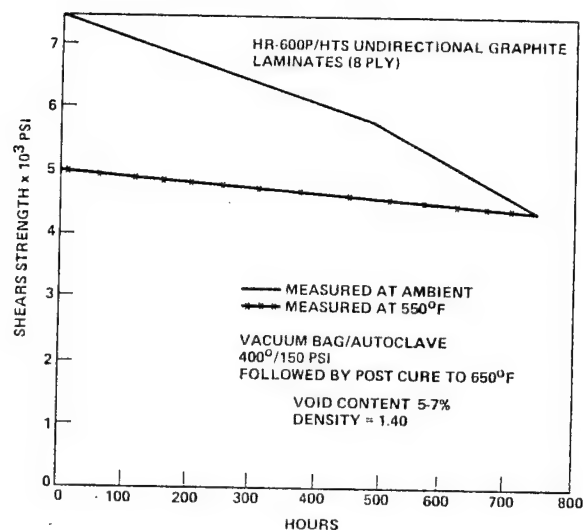


Figure 13. - Change in shear strength as function of air aging at 550 °F.

Coatings and Films

Good quality films and coatings could be made from the HR60XP oligomers having DP's of five or greater. High solid content resins can be formulated in a solvent mixture containing tetrahydrofuran and N-methylpyrrolidone. After drying, these coatings can be cured at the usual cure temperature where homopolymerization of the acetylene group takes place (500-600°F). Steel test specimens coated with HR605P oligomer and cured at 600°F had excellent corrosion and moisture resistance. Good quality films could be cast from lacquers formulated from HR605P and HR610 oligomers.

REFERENCES

1. Air Force Contracts F33615-69-C-1458; F33615-73-C-5062; F33615-73-C-5063; F33615-71-C-1228; F33615-69-C
2. M. L. Ernst And G. L. Schmir, J. Am. Chem. Soc., 88, 5001 (1966)
3. William I. Awad, Adel S. Wasfi and Mohammad J. S. Ewad, J. Iraqi Chem. Soc., 2, 5-15 (1977)

PMR POLYIMIDES FROM SOLUTIONS CONTAINING MIXED ENDCAPS

Peter Delvigs
National Aeronautics and Space Administration
Lewis Research Center

Previous studies have shown that partial substitution of p-aminostyrene (PAS) for the monomethylester of endo-5-norbornene-2, 3-dicarboxylic acid (NE) lowered the cure temperature of PMR polyimides from 316 to 260° C, but the modified PMR polyimides required higher compression-molding pressures than state-of-the-art PMR-15. In this study PMR polyimides were prepared employing three endcaps: NE, PAS, and endo-N-phenyl-5-norbornene-2,3-dicarboximide (PN). The effect of PN addition on the processing characteristics and glass transition temperatures of graphite fiber-reinforced PMR composites was studied. The room temperature and short-time 316° C mechanical properties of the composites were determined. The weight loss and mechanical property retention characteristics of the composites after exposure in air at 316° C were also determined.

INTRODUCTION

Studies at NASA Lewis Research Center led to the development of a class of readily processable polyimides known as PMR polyimides (refs. 1 and 2). The commercially available version known as PMR-15 uses an alcohol solution of three monomer reactants: 4,4'-methylenedianiline (MDA), the dimethylester of 3,3',4,4'-benzophenonetetracarboxylic acid (BTDE), and the monomethylester of 5-norbornene-2,3-dicarboxylic acid (NE) as an endcapping reagent. Because of its excellent processability and thermo-oxidative stability, PMR-15 has made it possible to design and fabricate composite structures for use at temperatures up to 316° C. Final curing of PMR-15 requires temperatures in the range of 288 to 316° C, preferably the higher temperature. These requirements exceed the capability of many existing autoclave facilities which were originally acquired for curing epoxy resins. A lower-curing-temperature PMR polyimide would be more compatible with existing facilities and increase the applications of PMR polyimides.

A previous study showed that the use of an alternate endcap, m-aminostyrene, lowered the final cure temperature of PMR polyimides from 316 to 260° C (ref. 3). However, the glass transition temperatures (T_g) of these polyimides were in the range of 270 to 280° C, limiting their use to temperatures not exceeding 260° C.

More recently, PMR polyimides were prepared from monomer solutions containing equimolar amounts of NE and p-aminostyrene (PAS) endcapping reagents (ref. 4). It was shown that these polyimides (designated PMR-NV polyimides) could be cured at 260° C, and exhibited T_g values in excess of 325° C. Compression-molded graphite-fiber/PMR-NV composites exhibited short-term mechanical properties as well as mechanical property retention characteristics at 316° C equivalent to those of PMR-15 composites. The PMR-NV composites, however, exhibited considerably reduced resin flow during compression molding. In order to achieve void-free composites, it was necessary to double the molding pressure compared to state-of-the-art PMR-15 composites.

The purpose of this study was to investigate the effects of incorporating an additional endcap, endo-N-phenyl-5-norbornene-2, 3-dicarboximide (PN), on the processing characteristics and properties of PMR-NV polyimides. Compression-molded

Celion 6000 graphite fiber-reinforced composites were fabricated from monomer solutions containing MDA, BTDE, equimolar amounts of NE and PAS, and various amounts of PN. The resin flow characteristics of the PMR-NV polyimides were determined. The effect of various posture conditions on the T_g values of the composites was studied. The room temperature and short-time 316° C mechanical properties of the composites were determined. Composite weight loss and mechanical property retention characteristics as a function of exposure time in air at 316° C were also determined.

EXPERIMENTAL PROCEDURES

Monomers and PMR Solutions

The monomers used in this study are shown in table I. The dimethylester of 3,3',4,4'-benzophenonetetracarboxylic acid (BTDE) was prepared by refluxing a suspension of the corresponding dianhydride in a calculated amount of anhydrous methanol until the solid dissolved, and then for an additional 2 hr to give a 50 wt % solution of BTDE. The endo-N-phenyl-5-norbornene-2,3-dicarboximide (PN) was prepared as follows: a solution of endo-5-norbornene-2,3-dicarboxylic anhydride (41.0 g, 0.25 mole) and aniline (24.2 g, 0.26 mole) in N, N-dimethylacetamide (50 ml) was stirred at room temperature for 10 min, then heated to reflux for 1 hr. The solution was cooled to below 100° C, and water was added to cloudiness. After cooling in ice, the precipitate was filtered, washed with a mixture of water and N, N-dimethylacetamide (2:1), and dried in a vacuum at 60° C. The crude product was recrystallized from methanol to yield 52.9 g (88 %) of PN, m.p. 142.5 to 143° C. The other monomers shown in table I were obtained from commercial sources and used as received.

Prepreg solutions were prepared at room temperature by dissolving the monomers in a calculated amount of anhydrous methanol to give solutions containing 40 wt % solids. The stoichiometric ratios of the reactants used in this study are shown in table II. Differential scanning calorimetry (DSC) measurements were performed by evaporating small aliquots of the prepreg solutions to dryness, then staging for 1 hr at 150° C. The runs were performed in a commercial pressure DSC cell under 50 psi of nitrogen at a heating rate of 10° C/min.

Composite Fabrication

Prepreg tapes were made by drum winding and impregnating Celion 6000 graphite fiber with PMR solutions calculated to give composites having approximately 58 vol % fiber. The prepreg tapes were dried on the rotating drum for 1 hr, then dried further at room temperature overnight. The tapes were removed from the drum, cut into 10.16 by 10.16 cm plies and stacked unidirectionally into a preforming mold, 11 plies thick. The stack was imidized for 1 hr at 150° C under a pressure of approximately 690 Pa. After staging the stack was placed into a matched metal die and a thermocouple attached to the die. The die was inserted into a press preheated to 260° C, and a pressure of 3.45 MPa was applied when the die temperature had reached 232° C. After reaching 260° C, pressure and temperature were maintained for 2 hr. The composites were then cooled to 204° C prior to removal from the mold. The control composites (prepared from solutions without added PN) were fabricated using the same procedure, except that a molding pressure of 6.89 MPa was employed.

Composite Testing

Postcure and isothermal exposure of the composites was performed in forced air convection ovens having an air change rate of 100 cm³/min. All composites were postcured by heating to 316° C during 2 hr, holding at 316° C for 24 hr, followed by heating at 343° C for 16 hr. Prior to specimen preparation the composites were inspected for acceptance by an ultrasonic C-scan technique. The fiber content was determined by H₂SO₄/H₂O₂ digestion. Glass transition temperatures (T_g) were determined with a thermal mechanical analysis (TMA) apparatus using a penetration probe at a heating rate of 10° C/min. The probe was loaded with a 5-g weight.

Resin flow during cure was calculated according to the following equation:

$$F = \frac{W_2}{W_1 + W_2} \times 100 \quad (1)$$

where

F resin flow, wt %

W₁ weight of resin in molded composite as determined by acid digestion method

W₂ weight of staged prepreg - weight of molded composite after removal of resin flash

Isothermal exposure at 316° C was carried out using 0.508 by 10.16 cm specimens. The thickness of the specimens varied from 0.188 to 0.201 cm.

Flexural strength tests were performed in accordance with ASTM D-790 using a three-point loading fixture and a span of 5.08 cm. The span/depth ratio ranged from 25.3 to 27.0. The rate of center loading was 1.27 cm/min. Interlaminar shear strength tests were performed essentially in accordance with ASTM D-2344 at a constant span/depth ratio of 5. Elevated temperature tests were conducted in an environmental heating chamber following a 15-min soak at the test temperature. The reported mechanical property values are averages of four or more tests at each condition.

RESULTS AND DISCUSSION

It has been demonstrated (ref. 5) that addition of PN to PMR-15 increases the resin flow during compression molding. It was felt that incorporation of this additive in the PMR-NV polyimide system would increase the resin flow to a level that would permit compression molding of the composites at pressures not exceeding 3.45 MPa. It remained to be demonstrated that addition of PN in amounts up to 10 mole percent would not significantly increase the final cure temperature of the PMR-NV composites above 260° C. The monomer stoichiometry of the PMR-NV formulations used in this study is shown in table II. Differential scanning calorimetry (DSC) analysis of the various formulations indicated that it is feasible to cure the resins at 260° C. A typical DSC scan is shown in figure 1 for the PMR-NV15-PN10 formulation that had been staged for 1 hr at 150° C. The DSC scan exhibits a melt endotherm peaking at about 225° C, and a single reaction exotherm centered at about 285° C. This exotherm temperature is comparable to that of PMR-NV15 without added

PN, and is substantially lower than the cure exotherm temperature of 340° C for PMR-15 (ref. 6).

The chemistry of the PMR-NV resins prepared from solutions containing the three endcaps is shown in figure 2. Most of the methanol solvent is first evaporated at room temperature. The prepreg is then staged for 1 hr at 150° C. During this step the PAS, NE, MDA, and BTDE monomers react to form the endcapped imide oligomer structure shown in figure 2. Water and methanol are evolved during this cyclodehydration step. The PN monomer is unreactive during this step. It should be pointed out that the structure shown for the endcapped imide oligomer is an idealized one, reflecting the overall stoichiometry of each monomer formulation. It is to be expected that the actual composition consists of a mixture of oligomers having varying chain lengths.

The final cure is carried out under a pressure of 3.45 MPa at 260° C without the evolution of volatile reaction by-products to yield a crosslinked polyimide. The cure probably occurs through a very complex set of reactions. A detailed study of the cure mechanism was beyond the scope of this investigation. A few comments, however, can be made regarding the most likely cure reactions. Some possible crosslinking reactions are outlined in figure 3. If only styryl endcaps were present, a straightforward addition reaction of the vinyl groups could be expected to yield the substituted polystyrene structure shown in Scheme A. The thermal polymerization of norbornenyl endcaps follows a more complex mechanism. It is well established that the first step is a retrograde Diels-Alder reaction to yield a substituted maleimide and cyclopentadiene. It has been proposed that these species coreact to yield the structure shown in Scheme B (ref. 7).

When both styryl and norbornenyl endcaps are present, the crosslinking mechanism is very likely more complicated. It is expected that some homopolymerization of the styryl endcaps occurs. It is more likely that the styryl endcaps coreact with the Diels-Alder reversion products, as shown in Scheme C. Another possibility is the coreaction of styryl and intact norbornenyl endcaps (Scheme D).

A study of resin flow was performed on unidirectional composites prepared from unsized Celion 6000 graphite fiber and the various monomer solutions listed in table II. The prepreg was imidized at 150° C because it had been shown in the previous study (ref. 4) that imidization at temperatures above 150° C caused a significant level of resin advancement due to the presence of styryl endcaps. The imidized prepreg was placed in a mold at room temperature and inserted into a press preheated to 260° C. Pressure was applied when the temperature of the prepreg stack reached 232° C, and final cure was conducted for 2 hr at 260° C. A cure pressure of 3.45 MPa was employed in this series of experiments, compared to 8.27 MPa used for PMR-NV formulations containing no added PN (ref. 4). The results are summarized in figure 4. It can be seen that both the PMR-NV15 and PMR-NV12.5 formulations exhibited a resin flow level of less than 0.5 percent, compared to 3.85 percent for PMR-15. The incorporation of five mole percent of PN caused a significant increase of flow, to 2.6 percent for PMR-NV15-PN5 and 3.4 percent for PMR-NV12.5-PN5. Addition of ten mole percent of PN further increased the flow to levels comparable to that for PMR-15. Ultrasonic C-scan examination indicated that all panels prepared from formulations containing PN exhibited no voids.

It is well known that PMR-15 polyimides must be subjected to a free-standing postcure in air at 316° C for at least 16 hr to achieve a sufficiently high glass transition temperature (T_g) for 316° C applications. In the previous study (ref. 4) it was found that a postcure cycle of 24 hr in air at 316° C was necessary

to achieve T_g values above 320° C for PMR-NV. However, when the latter postcure cycle was used for PMR-NV composites containing PN, the T_g values did not exceed 316° C (table III). Interlaminar shear strength tests performed at 316° C exhibited thermoplastic failure. The low T_g values are not surprising, since incorporation of monofunctional PN segments is expected to decrease the crosslink density of the polymer structure and hence decrease the T_g . Consequently, a study of postcure conditions to increase the T_g of the PN-containing PMR-NV composites was performed. The results are shown in table III. It can be seen that extending the postcure time at 316° C from 24 to 48 hr did not produce a significant increase in T_g values. An attempt was made to postcure the composites at 343° C. However, blistering of the specimens occurred in several instances, even when the temperature was gradually increased to 343° C during 4 hr. It is possible that after the cure at 260° C some residual unreacted norbornenyl endcaps remain, and release volatiles during the postcure causing blister formation. When the composites were postcured for 24 hr at 316° C, followed by 343° C for 16 hr, no blistering occurred. It can be seen in table III that the T_g values of all composites were increased to levels suitable for 316° C applications.

Using the cure and postcure schedules established in the previously described resin flow and postcure studies, a new series of 10.16 by 10.16 cm unidirectional composites were fabricated from unsized Celion 6000 graphite fibers and each of the resins listed in table II. Ultrasonic C-scan examination of the composites after postcure indicated that they were free of defects. The room temperature and initial 316° C mechanical properties of the composites are summarized in table IV. It can be seen that both the 25° C properties and short-term 316° C properties of the PMR-NV composites containing PN are essentially equivalent to those of the control, PMR-NV15, composite. Furthermore, the PMR-NV composite properties are equivalent to those of state-of-the-art PMR-15 composites (ref. 4).

The weight loss characteristics of the composites after exposure in air at 316° C are shown in figure 5. There appears to be a slight trend toward higher weight loss with increasing PN content, as well as decreasing formulated molecular weight values. This can be attributed to increase of alicyclic content in both cases. However, the differences are not considered to be significant.

The interlaminar shear strength (ILSS) retention characteristics of the composites after exposure and testing in air at 316° C are compared in figure 6. The composites prepared from formulations containing PN exhibit slightly lower ILSS values after long term exposure at 316° C, compared to those of the control sample. This is probably due to the lower matrix modulus values resulting from incorporation of the monofunctional PN segments into the polymer chain. It has been shown (ref. 8) that composite ILSS is influenced by the modulus of the polymer matrix. Therefore, the lower ILSS values are probably due to the lower matrix modulus resulting from incorporation of the monofunctional PN segments into the polymer chain.

The flexural strength retention characteristics of the composites are shown in figure 7. All composites exhibit an increase in flexural strength up to approximately 900 hr of exposure at 316° C. This increase can be attributed to an increase of favorable crosslinking reactions of the resin matrix. The PN-containing composites exhibit slightly lower flexural strength values during this period, but on further exposure their flexural strength values are essentially equivalent to those of the control composite.

The flexural modulus values of the PN-containing composites (shown in figure 8) coincide quite closely with those of the control. This is to be expected, since composite modulus is a fiber-dominated property.

CONCLUSIONS

Based on the results of this investigation, several conclusions can be drawn. PMR polyimide composites prepared from monomer solutions containing equimolar amounts of the monomethylester of endo-5-norbornene-2, 3-dicarboxylic acid (NE) and p-aminostyrene (PAS) and 5 to 10 mole percent of endo-N-phenyl-5-norbornene-2, 3-dicarboximide (PN): (1) can be compression-molded at 260° C compared to 316° C for state-of-the-art PMR-15 composites; (2) exhibit resin flow comparable to that of PMR-15 composites; (3) require a postcure temperature of 343° C compared to 316° C for PMR-15 composites; (4) exhibit room temperature and short-term 316° C mechanical properties essentially equivalent to those of control composites; (5) exhibit slightly lower interlaminar shear strength values during 1500 hr of exposure and slightly lower flexural strength values during 900 hr of exposure in air at 316° C, compared to those of control composites.

REFERENCES

1. Serafini, T.T.; Delvigs, P.; and Lightsey, G.R.: *J. Appl. Polym. Sci.*, Vol. 16, p. 905, 1972.
2. Serafini, T.T.; Delvigs, P.; and Lightsey, G.R.: U.S. Patent 3,745,149, July 1973.
3. Serafini, T.T.; Delvigs, P.; and Vannucci, R.D.: *NASA TM-81705*, 1981.
4. Delvigs, P.: *NASA TM-82958*, 1982.
5. Pater, R.H.: *NASA TM-82733*, 1981.
6. Lauver, R.W.: *J. Polym. Sci., Polym. Chem.*, Vol. 17, p. 2529, 1979.
7. Burns, E.A.; Jones, R.J.; Vaughan, R.W.; and Kendrick, W.P.: *NASA CR-72633*, 1970.
8. Chamis, C.C.; Hanson, M.P.; and Serafini, T.T.: *Modern Plastics*, p. 90, May 1973.

TABLE I. - MONOMERS USED FOR POLYIMIDE SYNTHESIS

STRUCTURE	NAME	ABBREVIATION
	MONOMETHYL ESTER OF ENDO-5-NORBORNENE-2, 3-DICARBOXYLIC ACID	NE
	P - AMINOSTYRENE	PAS
	ENDO-N-PHENYL-5-NORBORNENE-2, 3-DICARBOXYIMIDE	PN
	DIMETHYL ESTER OF 3, 3', 4, 4' - BENZO-PHENONETETRACARBOXYLIC ACID	BTDE
	4, 4' - METHYLENEDIANILINE	MDA

CS-83-0960

TABLE II. - COMPOSITION OF PMR-NV POLYIMIDES

RESIN	PN MOLE percent	MOLES OF REACTANTS				
		PAS	NE	MDA	BTDE	PN
PMR-NV 15 (CONTROL)	0	1	1	2.5	2.5	0
PMR-NV 15-PN 5	5	1	1	2.5	2.5	0.368
PMR-NV 15-PN 10	10	1	1	2.5	2.5	.778
PMR-NV 12.5-PN 5	5	1	1	2	2	.316
PMR-NV 12.5-PN 10	10	1	1	2	2	.667

CS-83-0957

TABLE III. - GLASS TRANSITION TEMPERATURES OF CELION 6000
GRAPHITE FIBER/PMR-NV POLYIMIDE COMPOSITES

RESIN	T _g , °C AFTER POSTCURE		
	24 hr @ 316° C	48 hr @ 316° C	24 hr @ 316° C + 16 hr @ 343° C
PMR-NV 15	328	332	358
PMR-NV 15-PN 5	314	320	353
PMR-NV 15-PN 10	303	308	342
PMR-NV 12.5	330	335	358
PMR-NV 12.5-PN 5	316	321	344
PMR-NV 12.5-PN 10	304	310	341

CS-83-0961

TABLE IV. - MECHANICAL PROPERTIES OF CELION 6000 GRAPHITE
FIBER/PMR-NV POLYIMIDE COMPOSITES^a

RESIN	INTERLAMINAR SHEAR STRENGTH, MPa		FLEXURAL ^b STRENGTH, MPa		FLEXURAL ^b MODULUS, GPa	
	25° C	316° C	25° C	316° C	25° C	316° C
PMR - NV 15	113	50.3	1740	960	127	116
PMR-NV 15-PN 5	109	49.6	1750	950	121	112
PMR-NV 15-PN 10	112	49.6	1710	910	120	112
PMR-NV 12.5-PN 5	112	49.6	1850	940	123	115
PMR-NV 12.5-PN 10	110	48.9	1860	900	125	113

^a POSTCURED 24 hr IN AIR AT 316° C PLUS 16 hr IN AIR AT 343° C

^b NORMALIZED TO 60 v/o FIBER

CS-83-0962

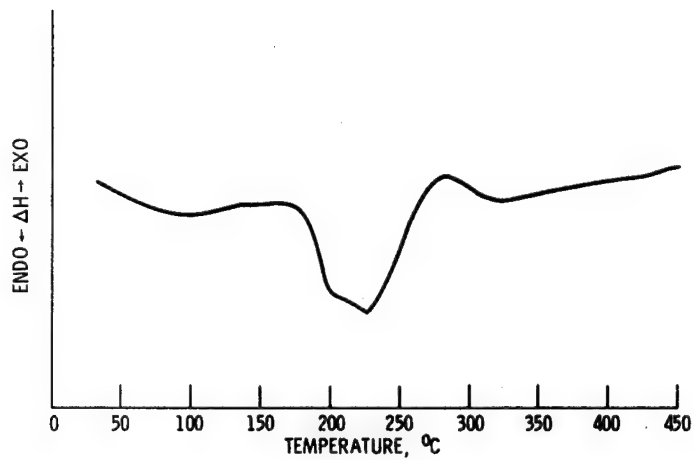


Figure 1. - DSC scan of PMR-NV15-PN10 prepeg
staged for 1 hr at 150° C.

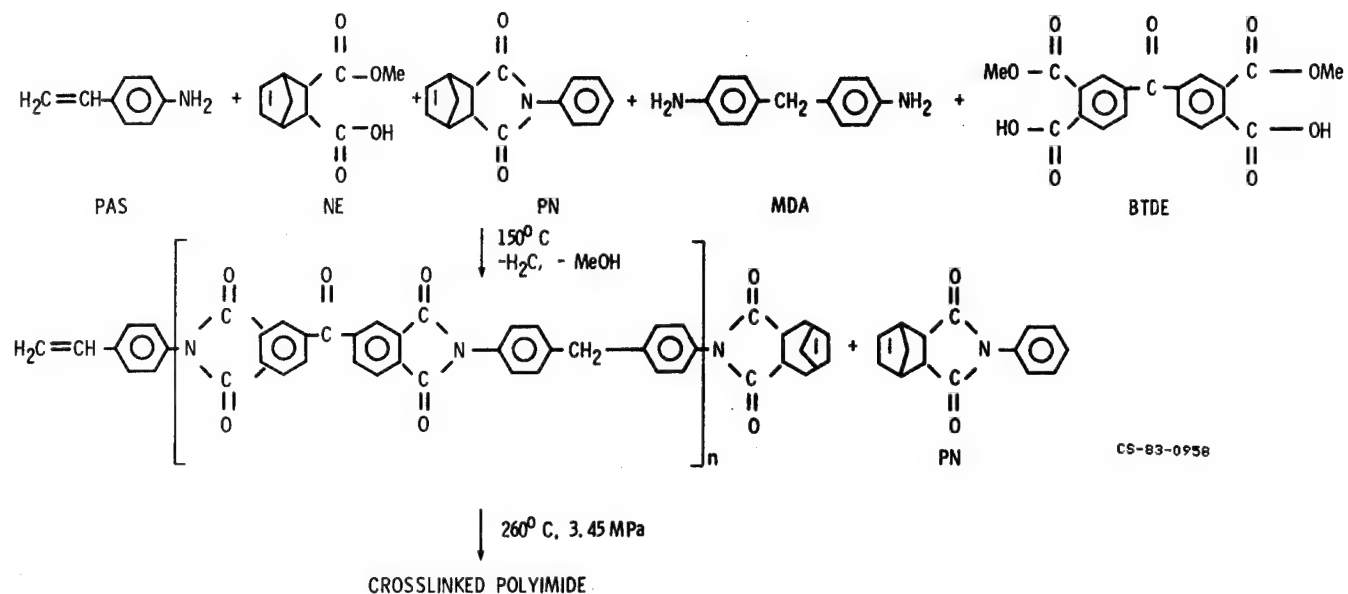


Figure 2. - PMR-NV polyimide chemistry.

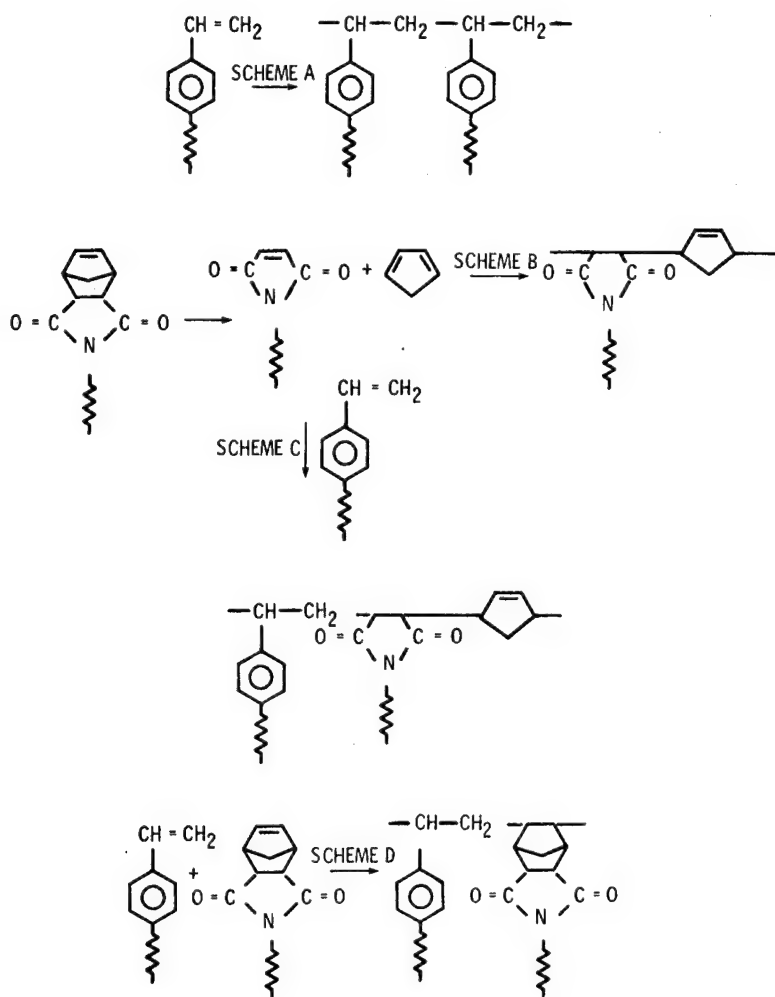


Figure 3. - Possible crosslinking reactions of PMR-NV polyimides.

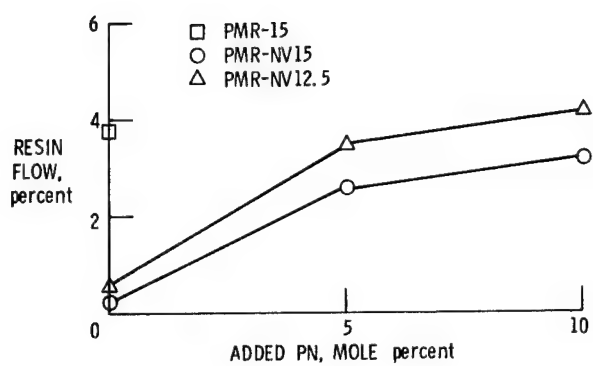


Figure 4. - Resin flow of PMR-NV polyimides.

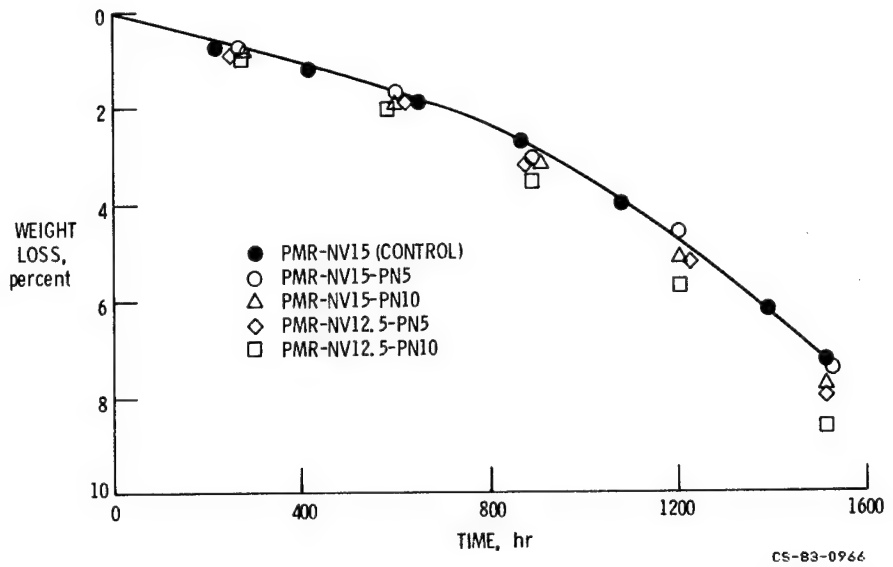


Figure 5. - Weight loss of Celion 6000 graphite fiber/PMR-NV polyimide composites in air at 316° C.

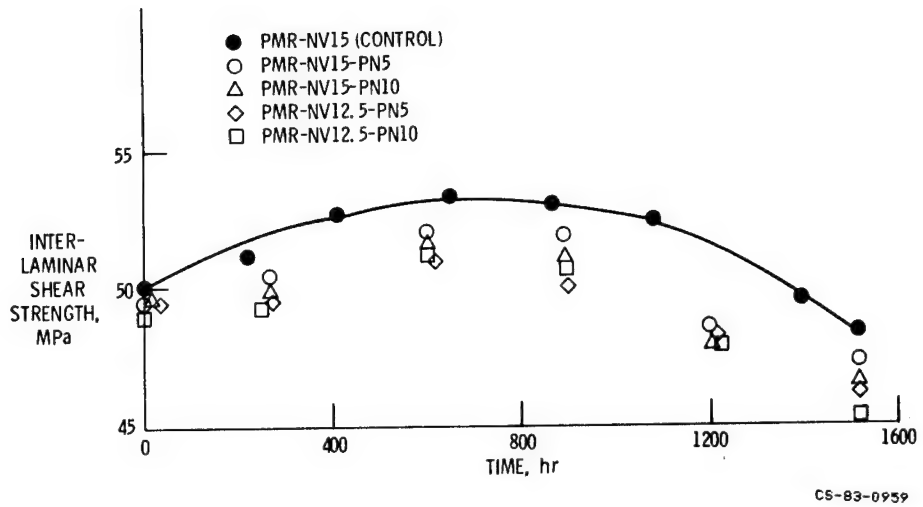


Figure 6. - Interlaminar shear strength of Celion 6000 graphite fiber/PMR-NV polyimide composites exposed and tested in air at 316° C.

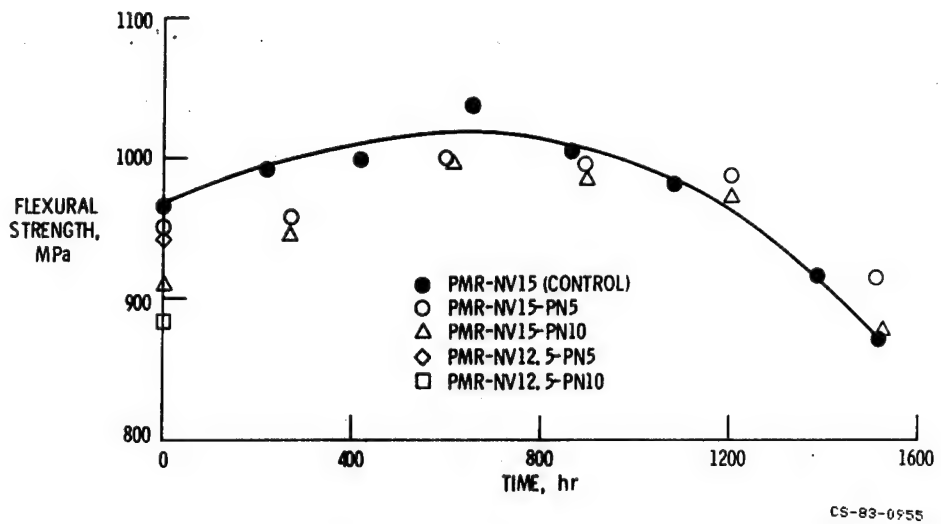


Figure 7. - Flexural strength of Celion 6000 graphite fiber/PMR-NV polyimide composites exposed and tested in air at 316° C.

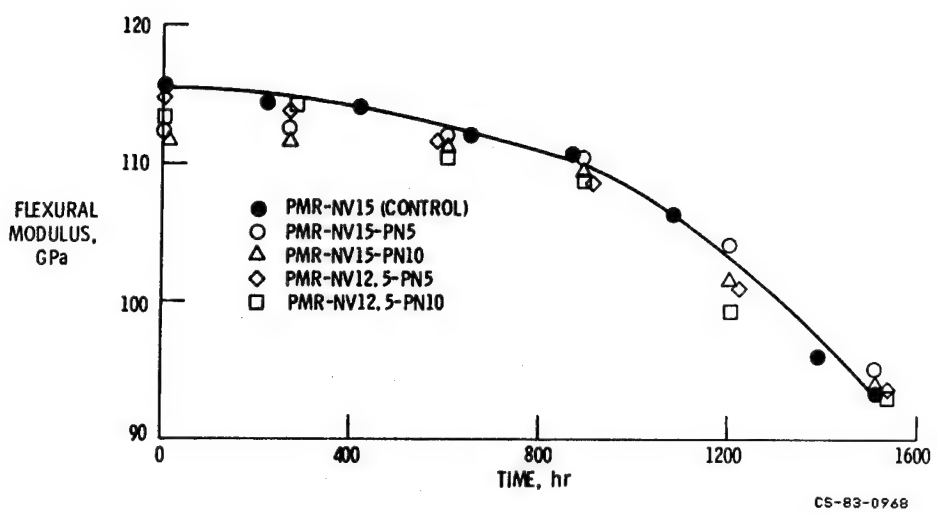


Figure 8. - Flexural modulus of Celion 6000 graphite fiber/PMR-NV polyimide composites exposed and tested in air at 316° C.

MATRIX RESIN DEVELOPMENT AT NASA Langley Research Center

Terry L. St. Clair
National Aeronautics and Space Administration
Langley Research Center

The polymer program at NASA Langley Research Center has as a focus the synthesis and characterization of polymers for aerospace applications. Requirements for these materials vary according to the specific programs.

The synthesis effort involves preparation of polymers for both intermediate- and high-temperature applications. The systems under investigation are thermoplastics, thermosets, and hybrids of these two.

The characterization effort includes a wide variety of programs, such as methodology development, general testing, and specialized studies. This work deals with the elucidation of polymer behavior in composite, adhesive, and film applications for the various aerospace applications.

FOCUS

- o Polymer Synthesis
 - Thermoplastics
 - Pseudothermoplastics
 - Thermosets
- o Characterization
 - Methodology Development
 - General Testing
 - Specialized Studies

POTENTIAL APPLICATIONS

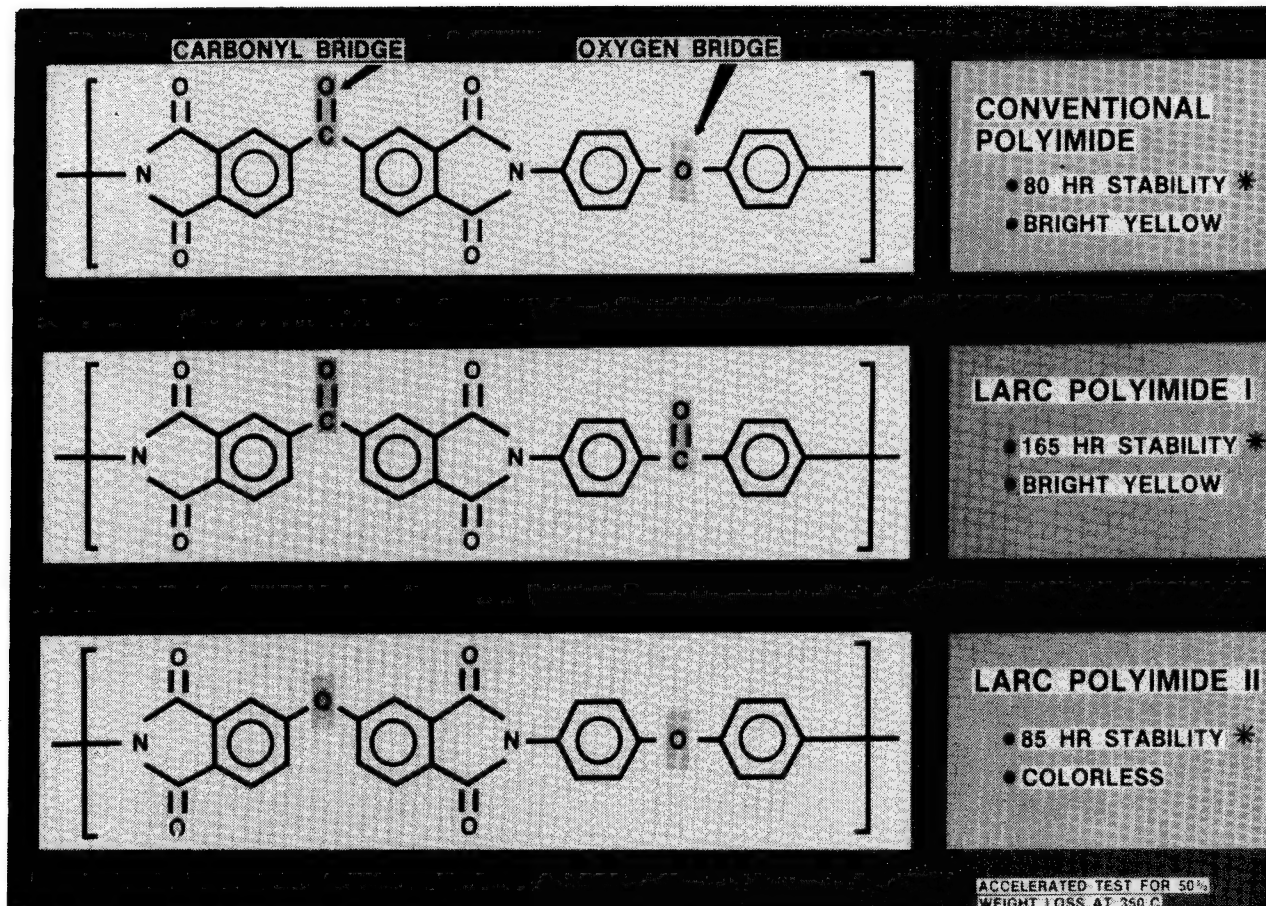
- o Matrix Resins
- o Adhesives
- o High Performance Films

TAILORING POLYMER STRUCTURES TO CONTROL PROPERTIES

The oxidative stability and color (transparency) of linear aromatic polymers can be tailored by altering chemical groups that bridge the aromatic rings. In

the figure below, the $-\overset{\text{O}}{\text{C}}-$ (carbonyl) bridging group is in the dianhydride-derived portion of the polymer and the $-\overset{\text{O}}{\text{C}}\text{---O}-$ (oxygen) bridging group is in the diamine-derived portion of the commercial polyimide. When this polyimide was tested at 350°C the polymer film lost half of its initial weight in 80 hours. Other experimental polyimides were prepared and tested in the same manner, but the bridging groups were altered as shown in the figure. With the carbonyl bridge in both components (LARC Polyimide I), oxidative stability was improved by a factor of 2 without affecting the color transparency. Altering the structure by placing the oxygen bridge in both components (LARC Polyimide II) provided a polymer film with good transparency (colorless) and oxidative stability comparable to the commercial polyimide.

These results indicate the progress we are making in understanding how to control properties by tailoring the chemical structure of the polymer. For polymer coatings we can achieve good transparency without sacrificing oxidative stability, or the structure can be altered to achieve excellent gains in thermooxidative stability (ref. 1).



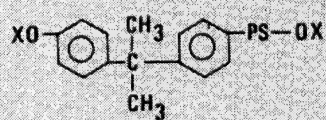
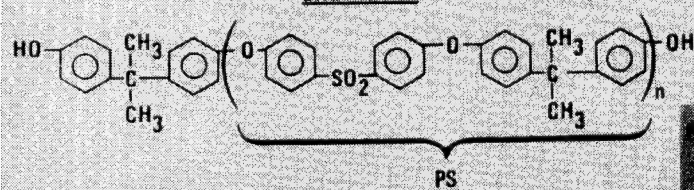
TOUGH SOLVENT RESISTANT POLYSULFONES

Polysulfones are engineering thermoplastics which are widely used in a variety of applications. They exhibit an excellent combination of processability, mechanical properties including impact strength, and cost. Their use, however, is generally restricted to environments where there is no exposure to polar organic solvents. Polysulfones are prone to solvent attack, especially in a stressed condition, undergoing solvent-induced crazing and cracking. As a result their use as structural adhesives and composite matrices on aerospace vehicles has been restricted.

Several synthetic routes are under investigation to transform polysulfones into solvent resistant materials while retaining their attractive properties. As shown in the figure, cured polymers from polysulfones endcapped with crosslinkable groups exhibit better solvent resistance and higher use temperatures than commercial polysulfone. As the solvent resistance of the polymer is improved, there is a corresponding loss of toughness. Acceptable trade-offs can be made by adjusting the molecular weight to maximize the attractive features without severely compromising other properties (e.g., toughness and thermoformability). This approach, along with other routes, offers the promise of providing polysulfones with improved solvent resistance, thereby making them more acceptable for use as structural adhesives and composite matrices on airplanes (ref. 2).

**OBJECTIVE: DEVELOP SOLVENT RESISTANT, TOUGH, THERMOFORMABLE POLYSULFONES
FOR MODERATE TEMPERATURE USE**

CHEMISTRY



CROSSLINKED POLYSULFONE
X = CROSSLINKING GROUP

<u>POLYMER PROPERTIES</u>			
<u>TEMPERATURE</u>	<u>Tg°C</u>	<u>PHYSICAL STATE</u>	<u>SOLVENT RESISTANCE</u>
100	200	BRITTLE	INSOLUBLE
150	180	FLEXIBLE	SL. SWELLING
200	190	TOUGH	SWELLS

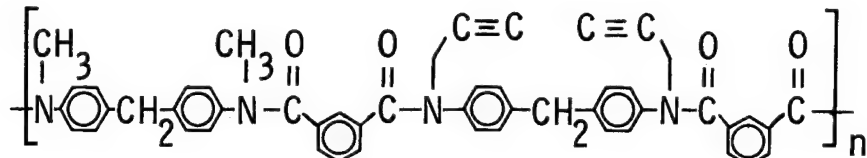
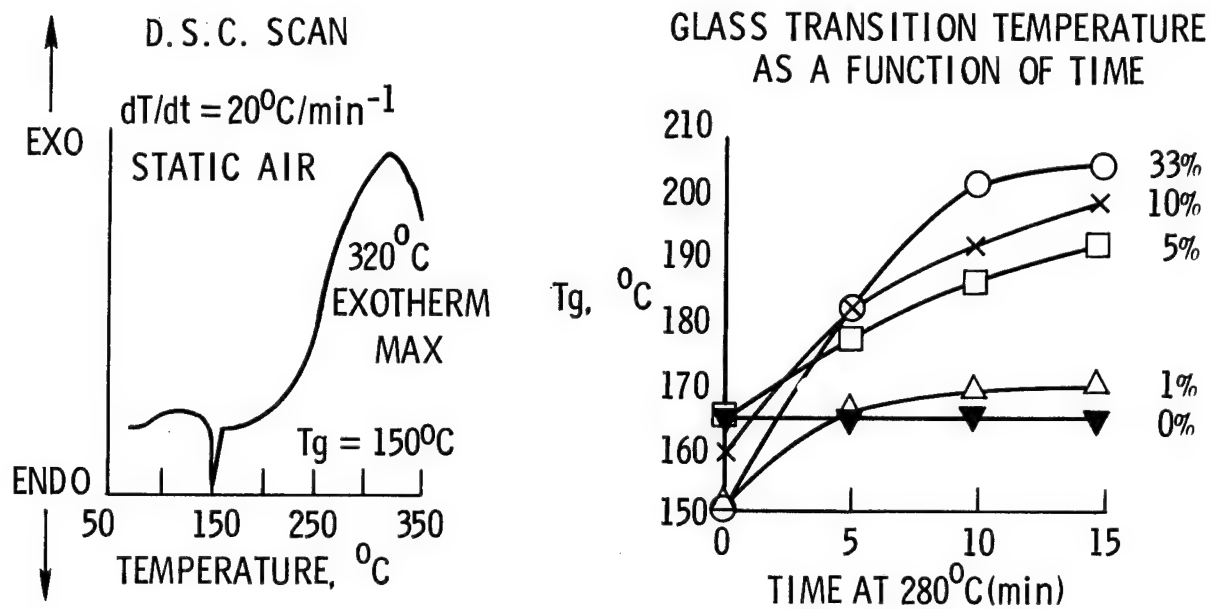
APPLICATIONS

- STRUCTURAL ADHESIVES
- COMPOSITE MATRICES
- COATINGS
- MOLDINGS
- MEMBRANES

N-PROPARGYL-SUBSTITUTED AROMATIC POLYAMIDES

A study was conducted to crosslink methyl-substituted polyamides via pendent propargyl groups for the purpose of improving the applicability of this resin as a matrix for Kevlar fiber composites. Films of the polyamides containing 1-33% propargyl diamine were successfully crosslinked by heating in air at 280°-300°C. The thermal crosslinking of the latent propargyl groups was evidenced by a rise in the glass transition temperature of the films with increasing propargyl concentration, a loss in solubility, and the disappearance of propargyl-related peaks from the infrared film spectra. Thermal crosslinking was accomplished with a slight loss in thermooxidative stability.

From the results of this investigation, propargyl-containing polyamides have been determined to be feasible matrices for polyamide fiber (Kevlar) composites. These materials are processable at advantageously low temperatures and are thermally crosslinkable at temperatures below the relaxation temperature of the fiber. Compatibility of these resins with aromatic polyamide fibers gives them high potential for success as matrix resins for Kevlar composites (ref. 3).

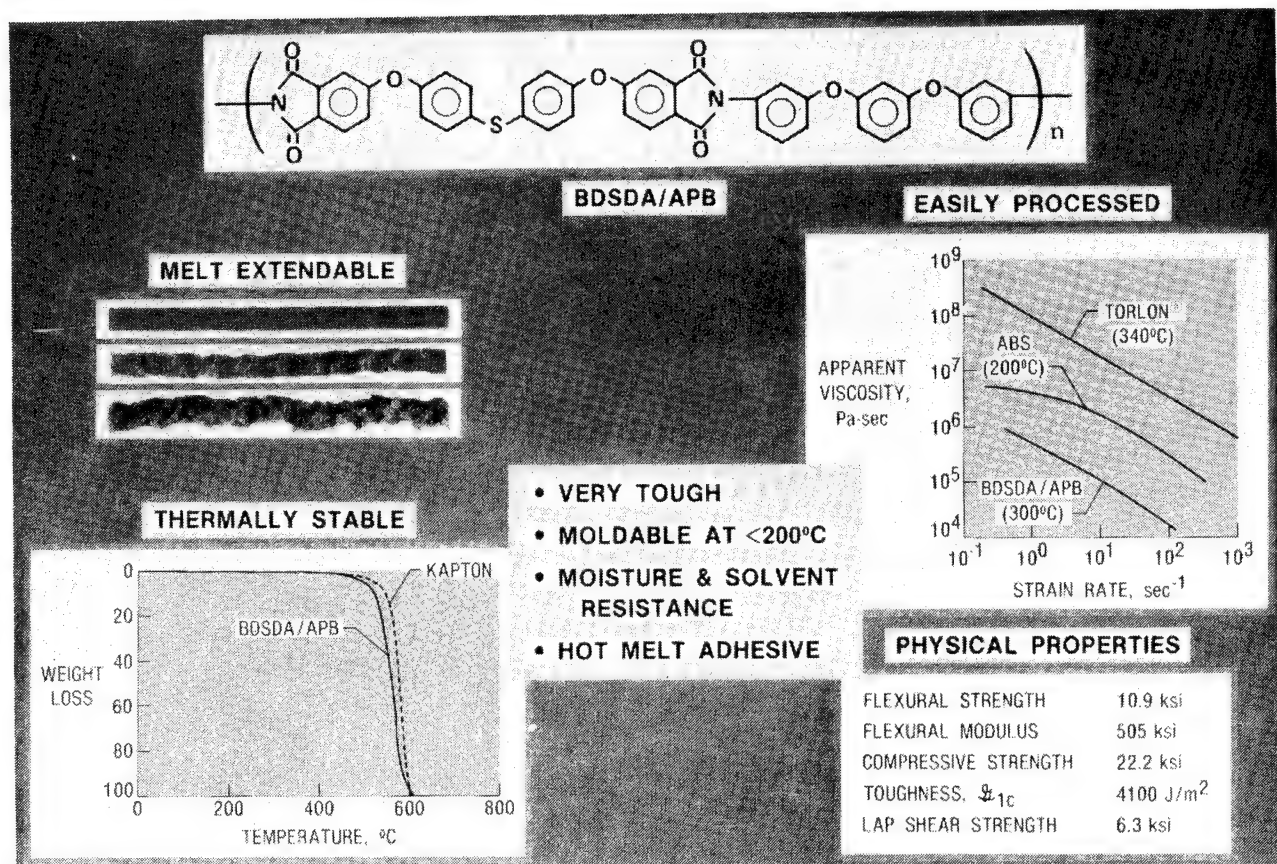


HOT MELT PROCESSABLE POLYIMIDE

Linear aromatic polyimides are a class of polymers which are generally not processable via conventional thermoplastic or hot-melt techniques. This class of polymer is, however, exceptionally thermally stable and has high glass transition temperatures. It is also resistant to attack by common organic solvents.

Linear aromatic polyphenylene oxides and sulfides, on the other hand, are more easily processed than the polyimides, generally exhibit lower glass transition temperatures, and still have relatively good thermal stability, although not equal to the polyimides. These systems also do not possess solvent resistance equal to the polyimides.

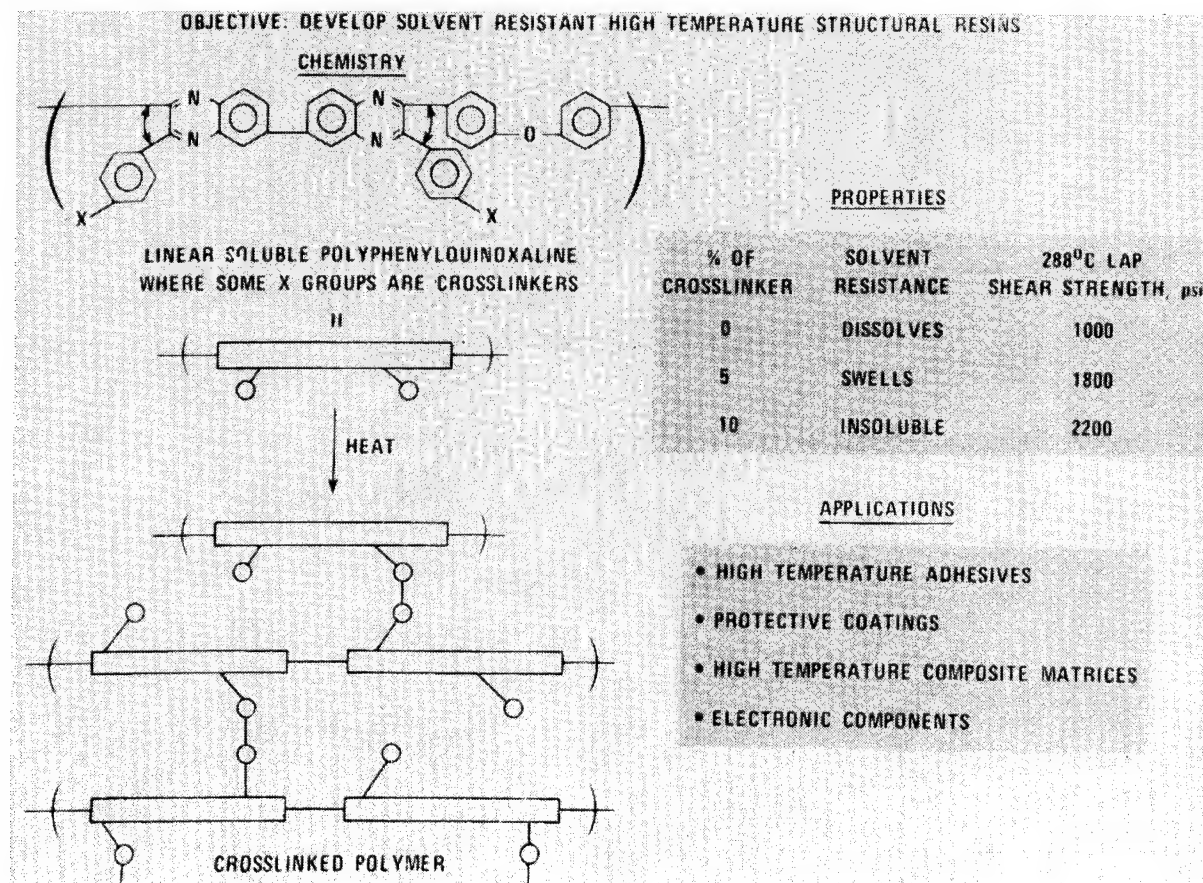
A novel linear aromatic polyphenylene ethersulfideimide has been synthesized which has some of the favorable characteristics of each parent system. The polymer has been molded, used as a resin, and cast into thin films. A limited characterization indicates this system can be processed via conventional thermoplastic techniques and may have a wide variety of applications (ref. 4).



CROSSLINKING OF POLYPHENYLQUINOXALINES

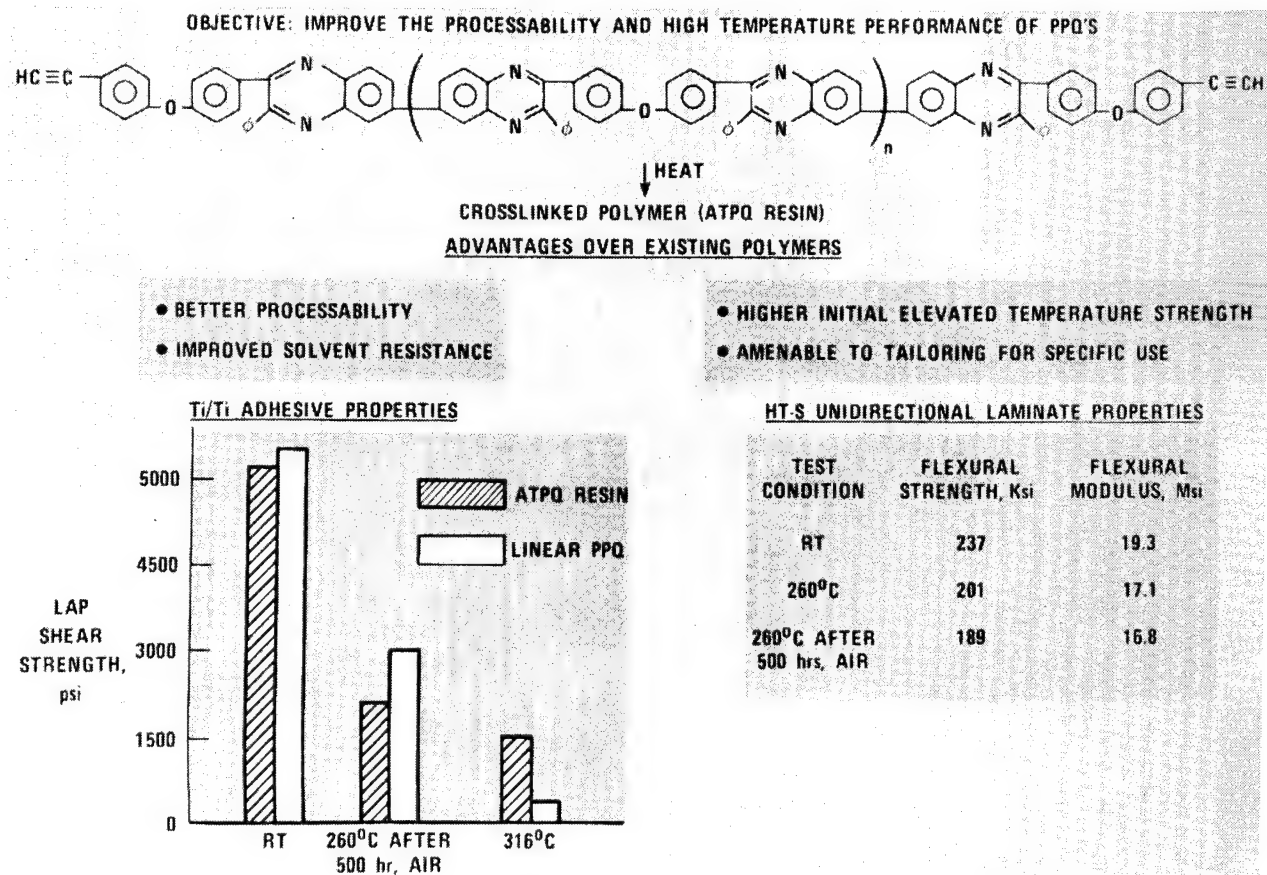
In an attempt to overcome the shortcomings of thermoplastics without severely compromising their attractive features, work was initiated using polyphenyl-quinoxalines (PPQs) as a model system to demonstrate a general concept. Latent pendent groups (e.g. ethynyl and phenylethynyl) were incorporated on the linear molecules. These groups undergo a thermally induced reaction to provide controlled crosslinking. In this way, molecules are tied together (see figure) such that there is a significant improvement in their elevated temperature performance (e.g. creep resistance) and, more importantly, in their fluid and solvent resistance.

As indicated in the table, the T_g of a cured PPQ containing 5% of ethynyl ($C\equiv CH$) or phenylethynyl ($C\equiv C-\phi$) groups was substantially higher than the parent PPQ void of latent crosslinking groups. At the 10% pendent group level, the cured PPQ containing the crosslinking groups became totally insoluble. Preliminary adhesive evaluation has also shown a marked increase in the 288°C lap shear strength. This concept is now being extended to polysulfones, which are lower temperature thermoplastics than PPQs, and it appears to be applicable to other thermoplastics such as polyesters, polyamides, and polyimides. This novel route offers the potential of modifying existing thermoplastics, particularly polysulfones, to improve their performance and make them acceptable for structural uses on future aircraft and spacecraft (ref. 5).



ACETYLENE-TERMINATED PHENYLQUINOXALINES

A series of acetylene-terminated phenylquinoxaline (ATPQ) oligomers of various molecular weights were prepared and subsequently chain-extended by the thermally induced reaction of the ethynyl groups. The processability and thermal properties of these oligomers and their cured resins were compared with those of a relatively high molecular weight linear polyphenylquinoxaline (PPQ) with the same chemical backbone. The ATPQ oligomers exhibited significantly better processability than the linear PPQ but the PPQ displayed substantially better thermooxidative stability. Adhesive (Ti/Ti) and composite (graphite filament reinforcement) work was performed to evaluate the potential of these materials for structural applications. The PPQ exhibited better retention of adhesive and laminate properties than the ATPQ resins at 260°C after aging for 500 hr at 260°C in circulating air (ref. 6).



ADDITION POLYIMIDE ADHESIVES

Addition polyimide oligomers have been synthesized from 3,3',4,4'-benzophenone tetracarboxylic acid dianhydride and 3,3'-methylenedianiline using a variety of latent crosslinking groups as end caps. The nominal 1300-molecular-weight imide prepolymers were isolated and characterized for solubility in amide, chlorinated, and ether solvents; melt-flow and cure properties; glass transition temperature; and thermal stability on heating in an air atmosphere. The general structure of the prepolymer and the end caps is shown below. Adhesive strengths of the polyimides were obtained both at ambient and elevated temperatures before and after aging at 232°C. Properties of the novel addition polyimides were compared to a known nadic end-capped adhesive, LARC-13 (ref. 7).

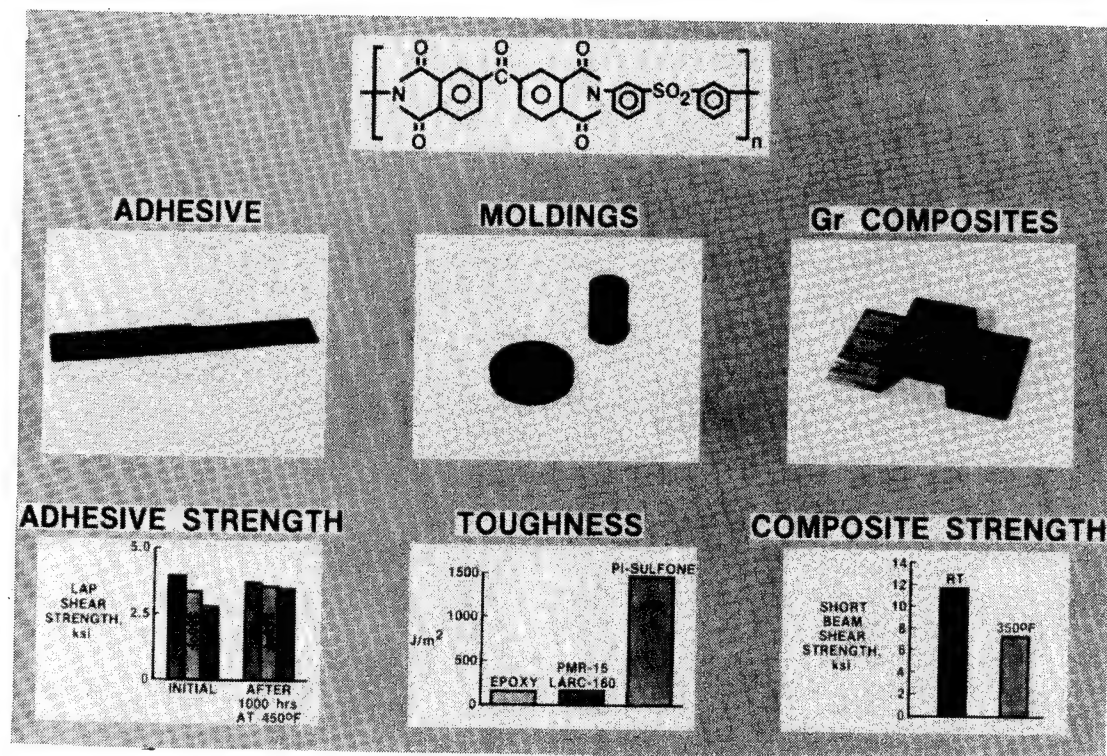
END GROUP R	LAP SHEAR STRENGTHS (LSS) OF ADDITION POLYIMIDES AGED FOR 1000 HOURS AT 232°					
	OLIGOMER END GROUP	INITIAL LSS, psi		LSS AFTER 1000 hr AT 232°C, psi		
		RT	232°C	RT	232°C	
	NADIC (LARC-13)	3200	2600	2600	1960	
	CH ₃ -NADIC	2900	2500	2500	2800	
	Cl ₆ -NADIC	3100	2800	800	1000	
	ACETYLENE					
	N-PROPARGYL					
	CYCLOHEXENE					
	MALEIC					

THERMOPLASTIC POLYIMIDESULFONE

Aromatic polysulfones, a class of high-temperature engineering thermoplastics, have a major deficiency in their tendency to swell and dissolve in many common solvents. This solvation can cause structural components which are fabricated from these polymers to be susceptible to damage by these solvents and thereby lose their structural integrity.

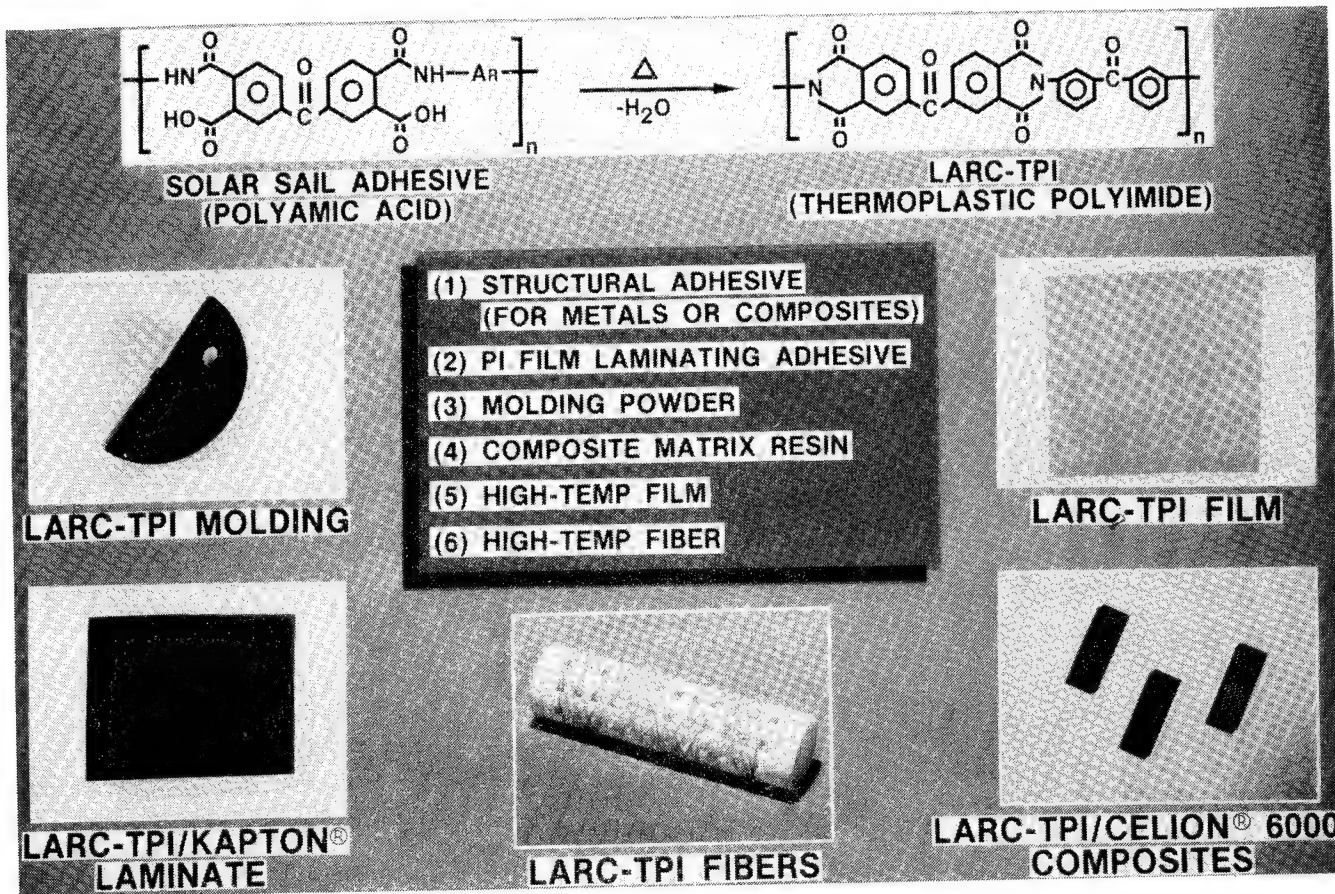
Aromatic polyimides, conversely, are a class of polymers which are known to be resistant to solvents, but they are generally not processable via thermoplastic means. These polyimides are known to be exceptionally thermally stable and like polysulfones and other thermoplastics their use temperature is governed by the softening temperature of each system.

A novel polymer system that possesses the processability of the polysulfones and the solvent resistance of the polyimides has been synthesized and characterized as a film, unfilled molding, filled molding, and adhesive. The structure of this polyimidesulfone (PIS02) is shown below along with some adhesive and molding data (ref. 8).



LARC-TPI

A linear thermoplastic polyimide, LARC-TPI, has been characterized and developed for a variety of high-temperature applications. In its fully imidized form this new material can be used as an adhesive for bonding metals such as titanium, aluminum, copper, brass, and stainless steel. LARC-TPI is being evaluated as a thermoplastic for bonding large pieces of polyimide film to produce flexible, 100% void-free laminates for flexible circuit applications. The further development of LARC-TPI as a potential molding powder, composite matrix resin, high-temperature film, and fiber will also be discussed (ref. 9).



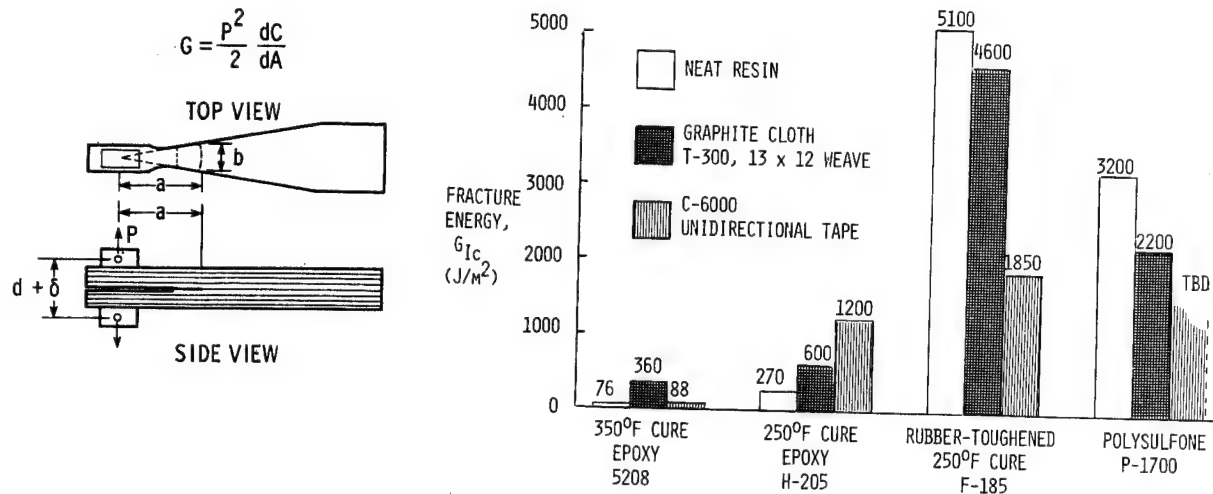
MEASUREMENT OF INTERLAMINAR FRACTURE TOUGHNESS BY COMPOSITE DOUBLE CANTILEVER BEAM TEST

The use of the double-cantilever-beam (DCB) test to measure the fracture toughness (G_{Ic}) of adhesives between metal adherends is well known. The application of the test to composite materials in which the crack is initiated in and propagated between two zero plies at the midplane is just now being pursued after the initial work of Bascom et al. (ref. 10). (See left-hand figure below.) Using a width-tapered DCB specimen, these investigators observed a noticeable improvement in fracture toughness of graphite cloth composites made with rubber-toughened epoxies or thermoplastics (P-1700 polysulfone) compared with state-of-the-art 250°F or 350°F cure epoxy systems. (See right-hand figure below.)

An extension of this work to laminates constructed from unidirectional tape (ref. 11 and right-hand figure) indicates that the G_{Ic} fracture toughness of the matrix varies widely and unpredictably depending upon the type of reinforcement. This work also shows that the G_{Ic} fracture toughness of neat resin cannot be used to predict the G_{Ic} value of composites made from that resin. However, the general trend seems to hold that neat resin G_{Ic} values are relative indicators of and can help rank fracture toughness in the corresponding composites.

NASA is pursuing an in-depth study of the composite DCB test in which the effects of matrix material, strain rate, specimen dimensions, stacking sequence, and environment are being investigated. A detailed analysis of the failure mechanics of various DCB specimens is also being done to help guide the development of an appropriate pure Mode I interlaminar fracture test method. Key investigators at the National Bureau of Standards, Hercules, Inc., and the University of Illinois, Urbana, are participating in this study.

COMPACT TENSION AND WIDTH TAPERED DOUBLE CANTILEVER BEAM TESTS



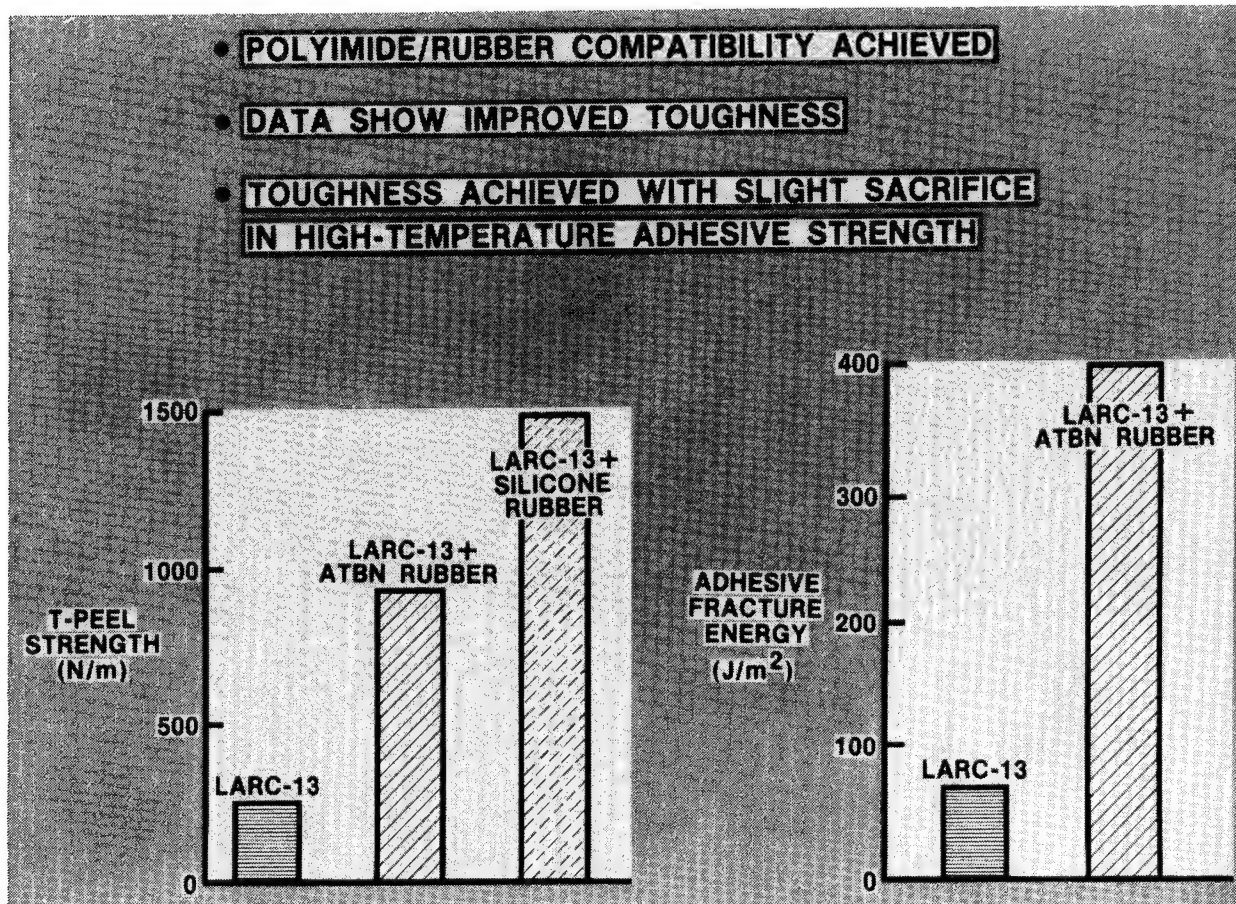
ELASTOMER-TOUGHENED POLYIMIDE ADHESIVES

Addition polyimides are presently being considered as candidate high-temperature adhesives for bonding composite materials and metals such as titanium on future aircraft and spacecraft. These thermoset polyimides undergo cure by an addition reaction involving unsaturated end groups that causes them to be highly crosslinked, insoluble, and extremely brittle.

The elastomer- (rubber) toughening process has been one of the most successful methods for modifying polymer toughness. Incorporation of small amounts of rubber into a polymer matrix has resulted in the significant enhancement of fracture resistance.

This chart illustrates the effects of various added elastomers on the T-peel strength and adhesive fracture energy of a high-temperature addition polyimide, LARC-13 (ref. 12).

- **POLYIMIDE/RUBBER COMPATIBILITY ACHIEVED**
- **DATA SHOW IMPROVED TOUGHNESS**
- **TOUGHNESS ACHIEVED WITH SLIGHT SACRIFICE IN HIGH-TEMPERATURE ADHESIVE STRENGTH**

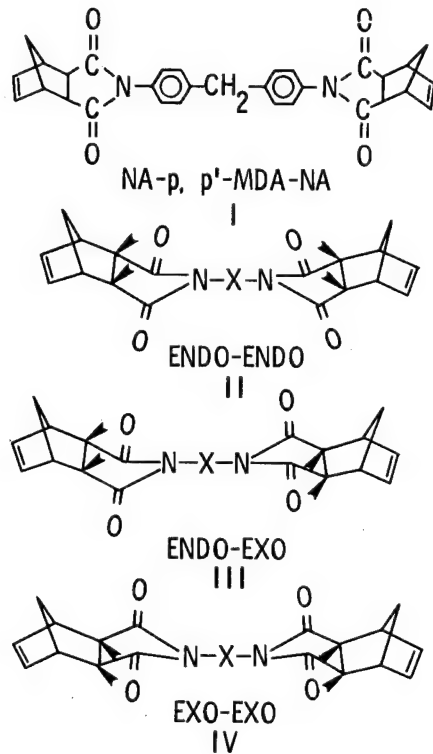
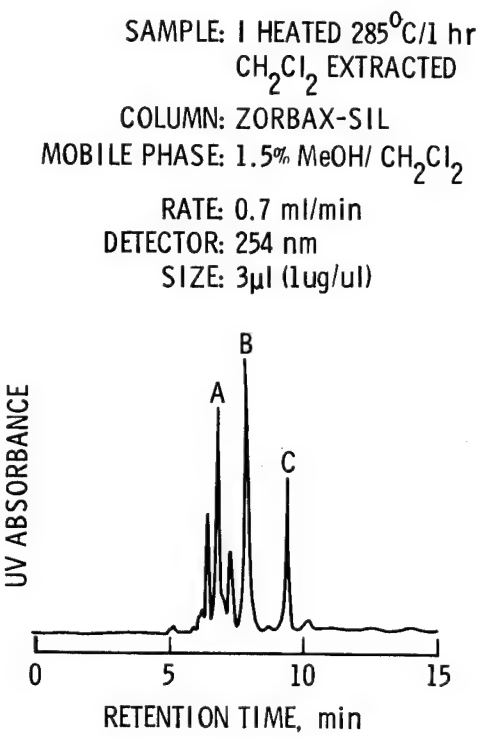


MECHANISM OF CURE IN NORBORNENE END-CAPPED IMIDE MODEL COMPOUNDS

Norbornene end-capped imide oligomers such as LARC-160, PMR-15 and LARC-13 display considerable promise for extensive use in various aerospace adhesive and composite applications (ref. 13). These materials were developed in a successful effort to retain the good thermal performance of linear condensation polyimides while improving overall processability. However, very little is known about the mechanism by which these end-capped oligomers cure. This study (ref. 14) was designed to increase our fundamental understanding of the fate of the norbornene end-capper as the oligomer is heated.

Model compound I was heated to 285°C in air to yield a partially soluble product mixture that was separated by high-pressure liquid chromatography (HPLC) into three main fractions (A, B, and C). Spectroscopic techniques (NMR, FTIR, MS) were used to prove that the thermal reaction products were geometric isomers. Peak C, the only HPLC peak observed before heating, was starting material and proved to be the kinetically favored endo-endo isomer, II. Peaks B and A were shown to be the endo-exo (III) and exo-exo (IV) configurations, respectively. Further work proved that each isomer thermally isomerized to an equilibrium mixture of all three before further curing reactions took place that rendered the mixture insoluble.

Calorimetry and thermogravimetric analysis indicated that these materials behave differently in air than in nitrogen, suggesting different mechanisms of cure depending upon atmosphere. The data obtained is consistent with a reverse Diels-Alder mechanism leading to loss of cyclopentadiene in nitrogen and a more direct chain extension without weight loss in air.

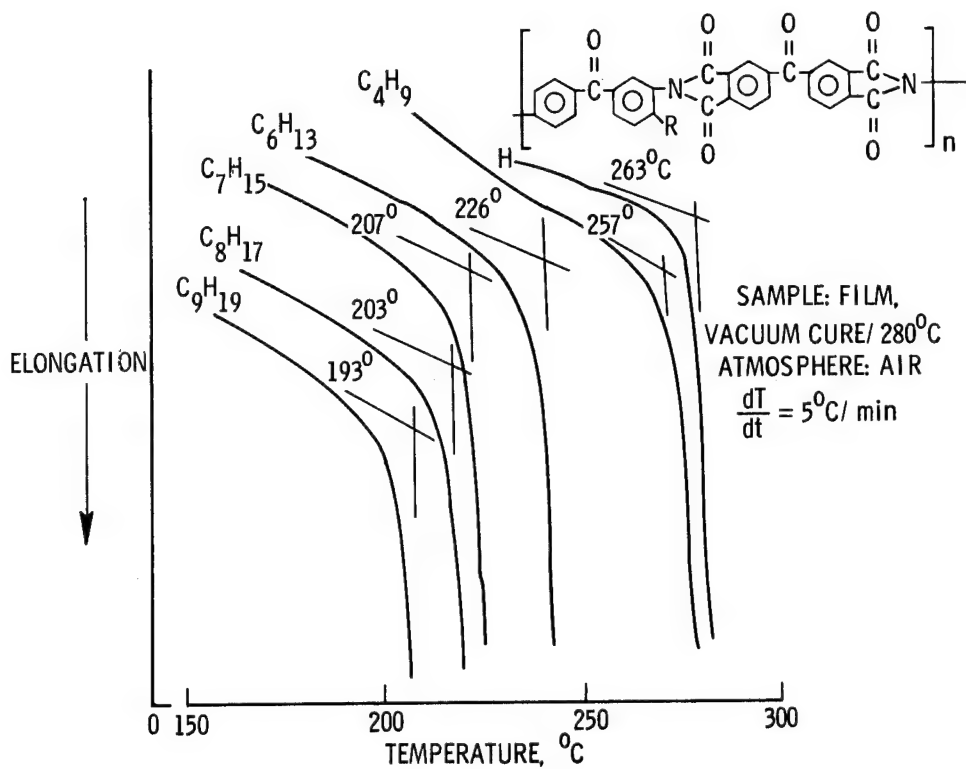


EFFECT OF PENDENT ALKYL GROUPS ON POLYIMIDE PROPERTIES

An investigation was conducted to determine the effect on glass transition temperature (T_g), thermal stability and toughness of a polyimide when alkyl groups are attached pendent to the backbone. A series of polymers was prepared in dimethylacetamide (DMAc) using benzophenone tetracarboxylic dianhydride (BTDA) and five different p-alkyl-m,p'-diaminobenzophenones as monomers. The chemical structures are shown in the figure. The alkyl groups varied in length from C_1 (methyl) to C_9 (nonyl).

Poly(amic) acid solutions in DMAc were vacuum cured to 280°C to afford flexible polyimide films whose T_g decreased with increasing alkyl group length, as determined from thermomechanical analysis. The largest effect, a 70°C decrease in T_g to 193°C, was observed for the polymer containing the nonyl pendent group compared to the T_g of the control polymer (R = H). During thermogravimetric analysis (air, 5°C/min. heating rate), the control exhibited a 10% weight loss at 525°C; the nonyl pendent polymer showed a 10% weight loss at 425°C. The thermooxidative stability of the other films fell between these extremes. Although no increase in the area under the stress-strain curve was observed during film tensile tests, an increase in elongation with a corresponding decrease in tensile strength was noted with increasing alkyl length.

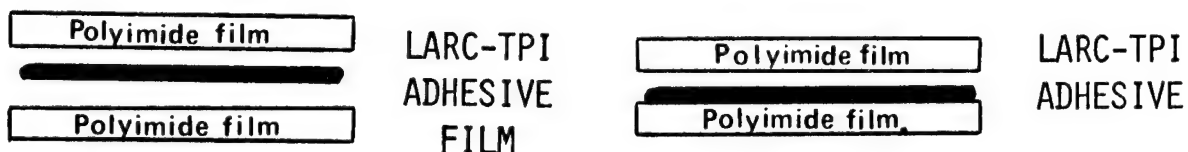
The results of this study indicate that alkyl groups attached pendent to a polyimide backbone can be used to vary the T_g over a wide temperature range. This approach may offer a means of lowering the processing temperature of polyimides without a significant reduction in thermal stability (ref. 15).



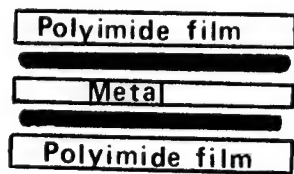
FILM LAMINATING

A need exists in the aerospace industry for reliable flexible electrical circuitry that can withstand extreme temperature variations and retain flexibility. Problems to date have been due partially to the presence of voids in film laminates caused by volatiles generated by the adhesive and/or the inherent rigidity of some adhesives. Because it is both flexible and imidized prior to bonding, LARC-TPI shows much potential as a high-temperature adhesive for laminating large areas of polyimide film.

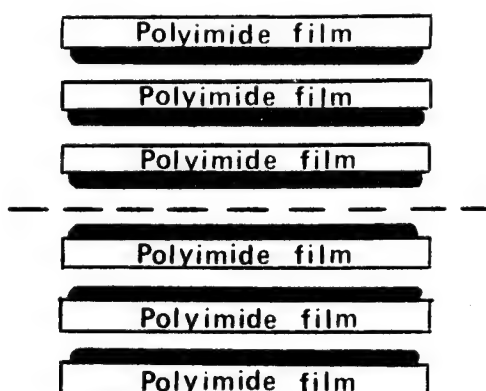
A film-laminating process has been developed whereby films primed with a thin coat of LARC-TPI adhesive are bonded together using temperature and pressure. As an alternate process, LARC-TPI polyamic acid adhesive film may be imidized by heating prior to being sandwiched between polyimide film. When using either process to produce flexible circuits, a conductive metal may be interposed between layers of the polyimide film. Metal-containing laminates have been made using aluminum, brass, copper and stainless steel sheets or foils (ref. 16).



METAL-CONTAINING LAMINATES (Al, Cu, Steel, Brass)



MULTI-PLY LAMINATES



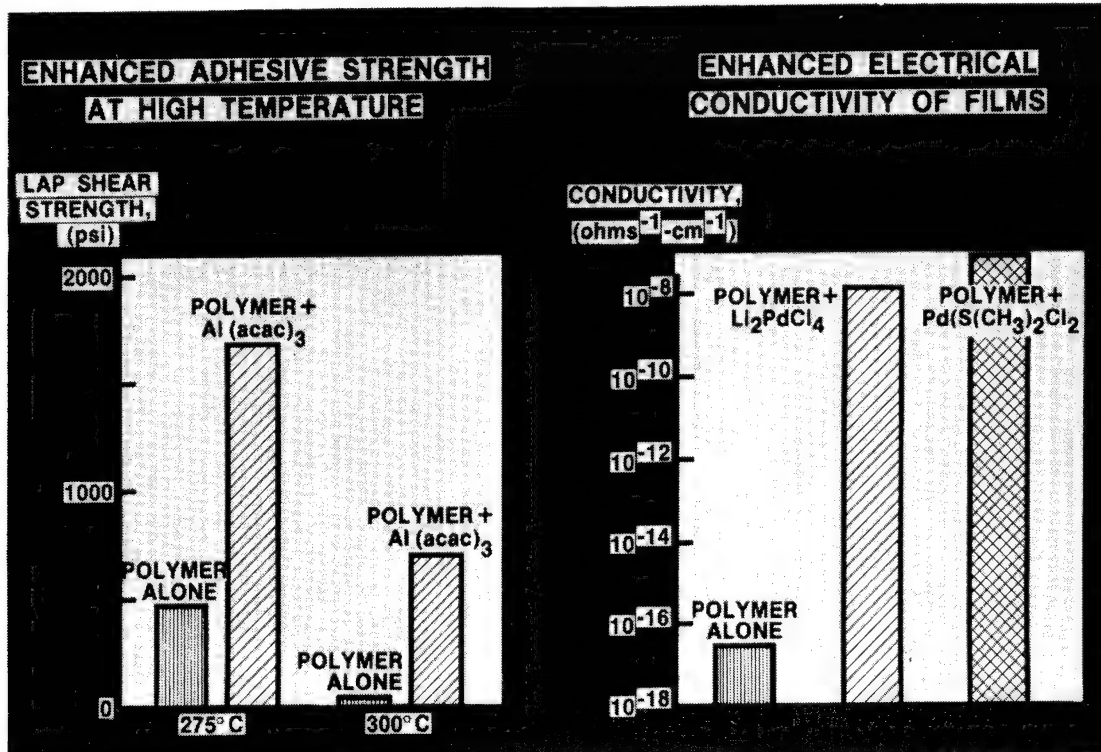
METAL IONS IMPROVE POLYIMIDE PROPERTIES

Polymer films are attractive for various aerospace applications such as antenna surfaces, adhesives, coatings, etc. However, covalently bonded polymers inherently lack the electrical conductivity desirable to resist spacecraft charging or to act as a Faraday Cage and even the most stable polymers developed to date have limited temperature capability.

Several options are available to increase electrical conductivity in a polymer film: (1) mix metallic flakes or powders into the formulation; (2) laminate metallic/polymer films; and (3) add complex metallic ions to the backbone of the polymer structure. The latter is a very attractive option because the potential for conductivity increases with less increase in the characteristically low polymer film density than is experienced with the other options, but this application has had relatively little attention until recently.

Recent research activity has demonstrated the potential of certain selected metallic ion additions to a polyimide to increase electrical conductivity in a film and high-temperature performance in an adhesive. The addition of the aluminum-ion complex increased adhesive shear strength significantly at 275°C and 300°C. Even more dramatic was the increased electrical conductivity of polyimide films when palladium- and palladium/lithium-ion complexes were added. Electrical conductivity at room temperature was increased by 8 orders of magnitude.

This research is now directed towards elucidation of the mechanisms of electrical (and thermal) conductivity in these metallic ion containing polymers to provide a rational basis for the selection of the most effective ion additions for specific property improvements (ref. 17).



A STUDY OF THE MUTAGENICITY OF AROMATIC DIAMINES

Aromatic diamines are a class of chemicals that are vital for the preparation of high-performance polymers, including the polyurethanes, epoxies, polyamides, and polyimides. However, a number of them are toxic to humans. During the past decade Langley's polymer research has resulted in the synthesis of a broad collection of aromatic diamines with systematic variations in their chemical structures. Although the main reason for acquiring these chemicals was for polymer research, they were also used for a study to learn if any aspects of their chemical structures could be used to predict the mutagenic tendencies of diamines. Mutagenicity is a toxic feature of chemicals that is related to the carcinogenicity of the chemicals.

This comprehensive study has been performed by the Monsanto Research Corporation of Dayton, Ohio on Langley-supplied amines. The investigation disclosed that steric and chemical structural characteristics could be useful in predicting which of the diamines might be mutagenic. The chart below summarizes those results for the steric or spatial isomers (horizontal) of four chemical series (vertical) of aromatic diamines. For example, in general, the electronegative chemical groupings (C = O and especially SO₂) that join the two aniline functions cause the resulting diamines to be less mutagenic (a smaller number or absence of '+'s). Conversely, the electropositive coupling groups (CH₂ and especially O) cause the diamines to be more mutagenic. Also, the first three steric isomers on the left tend to be more mutagenic than the three on the right. Unfortunately, many of Langley's accomplishments in polyimide structure-property studies have been achieved using the meta, meta' diamine isomers (third from the left) which are quite mutagenic. But this study also showed that the meta, para' isomers (second from the right) are generally nonmutagenic, so they might be used for polyimides since they give polymers with properties not very different from those made with the meta, meta' diamines.

It is expected that this investigation will extend the usefulness of this novel group of diamine starting materials beyond the original polymer-oriented objectives by providing toxicologists with the means to predict the mutagenic tendencies inherent in aromatic diamines.

Z						
CH ₂	+++++	+++	++	++	-	-
C=O	+++. .	++++	+++	-	-	-
SO ₂	+	NT	+	-	-	-
O	NT	+++	++++	++++	+++	NT

CODE: +++++ = VERY STRONG MUTAGEN; ++++ = STRONG; +++ = MODERATE;
++ = LOW; + = VERY LOW; - = NONMUTAGENIC, NT = NOT TESTED

SUMMARY

The polymer program at LaRC involves exploratory studies in polymer science. These include the synthesis of novel polymers and their characterization.

Polymer synthesis programs involve the development of novel thermoplastics, pseudothermoplastics, and thermosets. These systems are prepared to elucidate structure-property relationships involving thermal capabilities, toughness, processability and environmental stability. Recent investigations have led to the development of more easily processable polyimides, solvent-resistant polysulfones and polyphenylquinoxalines, and tougher high- and intermediate-temperature polymers.

Characterization efforts have included high-pressure liquid chromatography methodology, the development of toughness tests for fiber-reinforced composites, a study of electrical properties of metal-ion-filled polyimides, and a study of the mutagenicity of aromatic diamines. Also the mechanism of cure/ degradation of experimental polymers has been studied by rheology, mechanical behavior, separation techniques and spectroscopy. Some of these programs have involved the degradative crosslinking of alkyl-containing polyimides, the separation and identification of crosslinked phenylquinoxalines, the rheological behavior of hot-melt polyimides, and the elucidation of the cure of norbornene endcapped imides.

- o Synthesis Program for Polymers
- o Characterization of Monomers and Polymers
- o Development of Polymers for specific applications
 - Matrix Resins
 - Adhesives
 - Films

REFERENCES

1. St. Clair, T. L.; St. Clair, A. K.; and Smith, E. N.: Structure-Solubility Relationships in Polymers, Academic Press, Chapter 15, pp. 199-215, 1977.
2. Hergenrother, P. M.: Am. Chem. Soc. Div. Org. Coat. and Plastics, 46, 1982, p. 165.
3. Greenwood, T. D.; Armistead, D. M.; Wolfe, J. F.; St. Clair, A. K; St. Clair, T. L.; and Barrick, J. D.: Polymer, 23, Apr. 1982, pp. 621-625.
4. Burks, H. D.; and St. Clair, T. L.: NASA TM-84494, 1982.
5. Hergenrother, P. M.: Macromolecules, 14, 1981. pp. 891, 898.
6. Hergenrother, P. M.: Polymer Eng. and Sci., 21 (16), 1981, p. 1072.
7. St. Clair, A. K.; and St. Clair, T. L.: Polymer Eng. and Sci., 22 (1), 1982, pp. 9-14.
8. St. Clair, T. L.; and Yamaki, D. A.: A Thermoplastic Polyimidesulfone, to be presented at First Technical Conference on Polyimides, Society of Plastics Engineers, Inc. (Ellenville, NY), Nov. 10-12, 1982.
9. St. Clair, A. K.; and St. Clair, T. L.; SAMPE Quarterly, 13 (1), 1981, pp. 20-25.
10. Bascom, W. D.; Bitner, J. L.; Moulton, R. J.; and Siebert, A. R.: Composites, Jan. 1980, p. 9.
11. O'Brien, T. K.; Johnston, N. J.; Morris, D. H.; and Simonds, R. A.: SAMPE Journal, 18 (4), 1982.
12. St. Clair, A. K.; and St. Clair, T. L.: International J. of Adhesion and Adhesives, 1 (5), 1981, pp. 249-255.
13. Dexter, H. B.; and Davis, J. G. (Eds.): Graphite/Polyimide Composites, NASA CP-2079, 1979.
14. Young, P. R.: NASA TM-83192, 1981.
15. Jensen, B. J.; and Young, P. R.: Polyimide Characterization Studies: Effect of Pendent Alkyl Groups, to be presented at First Technical Conference on Polyimides, Society of Plastics Engineers, Inc. (Ellenville, NY), Nov. 10-12, 1982.
16. St. Clair, A. K.; and St. Clair, T. L.: U.S. Patent Application, serial no. 189,234, Sept. 22, 1980.
17. Taylor, L. T.; St. Clair, A. K.; Carver, V. C.; and Furtsch, T. A.: U.S. Patent 4,311,615, Jan. 19, 1982.

BISMALEIMIDES AND RELATED MALEIMIDO POLYMERS AS MATRIX RESINS
FOR HIGH TEMPERATURE ENVIRONMENTS

John A. Parker, Demitrius A. Kourtides, and George M. Fohlen
National Aeronautics and Space Administration
Ames Research Center

Bismaleimides are being increasingly used as matrix resins for graphite-reinforced composites. The monomers are cured by a thermally-induced addition reaction to give highly cross-linked, void-free network polymers having good physical properties with higher thermal stability, higher char yield, better fire resistance, and lower water absorption than currently used epoxy systems.

There are problems with maleimides, however, such as solvent retention in the prepgs, high temperature often needed for curing, and the brittleness of the polymers due to the high cross-link density obtained in network polymers.

The monomeric bismaleimides are relatively easy to make with a wide variety of structural variation available for property modification. The structural modifications to be described will include a variety of aromatic diamines. Phosphorous-containing aromatic di- and triamines have been made into bis- and trismaleimides to give polymers that will not burn, even in pure oxygen. Some maleimides based on the cyclotriphosphazene nucleus give good polymers having excellent thermo-oxidative stability as measured by high char yields in air at 700 °C.

Other modifications that will be described are those that are designed to improve the fracture toughness. The diamines, for instance, can be extended by reactive dianhydrides to give lengthened bismaleimides. By decreasing the cross-link density, the brittleness is expected to be reduced. Some of the systems described have also been modified by reactive elastomers to impart toughening.

Coreaction of bismaleimides with other thermostable reactive monomers such as vinylstyrylpyridines or stilbazole combine the good properties of both types of resins with a lowering of the curing temperature required. Among some of the maleimide resins it is possible to find systems that will be useful for continuous service at 300 °C (570 °F).

INTRODUCTION

This paper reviews some of the important structure-property relationships that exist for bismaleimides and related polymers as they influence the potential application of this class of polymers when used as matrix resins for fibrous composites in high-temperature environments. Of special interest is the use of these polymers as binders for fire-resistant secondary lightweight composites for aerospace application. Some consideration is given to the potential application of this class of resins for long-time use as secondary structures and as elastomeric-toughened primary structures at temperatures in excess of 300 °C. The advantages and limitations of state-of-the-art bisimides with respect to high-temperature use, fireworthiness, processability, and environmental stability are described.

Polymers have been prepared by modification of the basic maleimido structures and by polymerization mechanisms which eliminate thermally-weak bonding units. Easily thermally degraded aliphatic linkages (also contributing to brittleness) and pivotal groups such as methylene and isopropylidene have been replaced with phosphonates and cyclotriphosphazenes. Virtually completely fire-resistant polymers with limiting oxygen indices of 100 have been obtained. The effect of microstructural changes on the pyrolysis mechanisms in both inert and air environments has been demonstrated. Polymers have been found with residue weights in excess of 80 percent in air at 700 °C. Substantial retention of mechanical properties suggests a new upper limit for polymer application. The role of residual solvent on high-temperature properties of bismaleimides has been found to be extremely deleterious. Hot-melt systems have been devised by chain extension and copolymerization with reactive oligomers to eliminate the use of solvent and to reduce the cure temperature and internal strains.

A key objective of this paper is to introduce a new class of bisimide copolymers derived from the polymerization of vinyl stilbazole oligomers which can be processed without solvent, cured under somewhat lower temperature conditions than standard epoxides (165 °C), and gives a resulting matrix resin with a glass-transition temperature and polymer decomposition temperature in excess of 400 °C. It appears that the stilbazole chain unit provides a thermally-stabilizing effect on the aliphatic linkage resulting from the vinyl addition polymerization as well as a "buried" or thermally-reactive functionality to cross-link the polymer at temperatures in excess of 500 °C. This results in the high char yield (50 percent or greater) needed for fire resistance but allows for greater chain flexibility at use temperatures. This unique combination of bismaleimide and vinyl stilbazole as addition copolymers provides a wide range of formulation possibilities to tailor the matrix resin to a variety of high-temperature and fire-resistant applications.

Bismaleimides

Generically, these polymers refer to those matrix resins for application in fibrous composites which contain at least two maleimido groups prepared through the reaction of maleic anhydride. Generally this is a two-step reaction involving the formation of an amide acid intermediate followed by ring closure to give maleimido end groups. Primary aromatic diamines are shown in figure 1. The resulting oligomers are soluble in acetone, tetrahydrofuran, and N-methylpyrrolidone. As simple bisimide derivatives of aromatic diamines they are generally high-melting solids of low viscosity which polymerize rapidly at temperatures slightly above their melting point. When fully cured these simple bisimides exhibit high glass temperatures in excess of 350 °C, and anaerobic char yields greater than 60 percent, but are extremely brittle due to their high cross-link density.

These polymers made a brief appearance in the late sixties for applications requiring somewhat higher-temperature resins than conventional epoxides for glass-fiber reinforced composites. There is a very limited need for matrix resins, with modest improvements in thermal stability when compared with epoxy resins. Simple bisimides, such as those derived from methylenedianiline with a melting point of 202 °C, are soluble in polar solvents and are extremely difficult to process as mentioned above. For these reasons they found no significant application. However, these simple bisimides exhibit high char yields of 60 to 70 percent as measured anaerobically at 600 °C with very little thermoplasticity in the fire environment. It has been a major objective of current research to overcome the limitations of processing and brittleness of bisimides and at the same time retain the excellent fireworthiness and high-temperature stability of the basic bisimide system.

Several modifications of bisimide structure have appeared commercially. The Keramide resin systems presumably take advantage of the opportunity of adding an aromatic amine across the maleimido double bond to introduce an aliphatic secondary amine bridge, as shown in figure 2. This reaction increases the molecular weight of the bisimide precursor and introduces a point of chain flexibility. One observes easier processability, lower melting point, better solubility, more controlled viscosity, and reduced cure rate (better reaction control). The chain extension also reduces the glass temperature and inherent brittleness to some degree. Keramide 601, which is typical of this class of bisimide modification in fiber-glass composites, is probably good for continuous application at 150 °C for 50 000 hr with good electrical properties. It has found wide use in circuit board applications and in some cases may be preferred over epoxy resins. The presence of the Michael addition product introduces a point of thermal instability in the imide chain which suppresses the char yield and thermal stability, thus impairing the use of this class of resins in high-temperature and fire-resistance applications.

A second modification of the microstructure of bisimide matrix resins is found in M-751, as shown in figure 3. There the bisimide prepolymer has been chain extended by increasing the chain length of the diamine by the reaction of p-phenylene diamine with m-aminobenzoid acid, giving the bisimide shown as B. In addition, the prepolymer is further chain extended by including an equal molar amount of an amine-terminated maleimide which also reacts *in situ* by Michael addition. This so called "eutectic" mixture increases molecular weight, reduces the melting point, increases viscosity, and moderates the reactivity of the maleimido double bond during processing. As will be seen, this molecule still has several points of thermal instability; the Michael product and the phenylene-methylene bridge. Although the aromatic amide reacts at high temperature to eliminate water and hydrogen, it appears that the carbon-nitrogen bond is retained. As a consequence, M-751 is characterized by a high anaerobic char yield of greater than 60 percent.

This class of polymers has two specific limitations for use as easily processable high temperature resins. In figure 4, the results of the differential scanning calorimeter, DSC, are shown. An endotherm at 125 °C characterizes the melting point and an exotherm at 275 °C displays the DSC curing temperature. The melting point and viscosity of the melt taken together do not permit hot-melt processing as solvent is required. The high temperature needed to fully cure M-751 (275 °C) limits its use in conventional composite processing where cures at 160 °C are more appropriate.

In 1976 Kourtides et al. (ref. 1) demonstrated the unusual fire resistance of M-751 in secondary composite structures intended for application as interior panels for mass transportation. Parker (ref. 2) showed that the anaerobic char yield in the range of 45 to 65 percent accounted for a unique and optimized combination of flammability and ablation properties. This optimized combination of properties in secondary structures such as interior panels gave rise to a maximum time to flash-over and minimum smoke and toxic gas emissions, as well as good fire-retardant properties.

Table 1 compares the relative ranking of the flammability characteristics, the limited oxygen index, and the percent optical transmission with the measured anaerobic char yields of M-751, H-795, and other matrix resin polymers. It can be seen that the improvement of bismaleimides is some two to three times better than the epoxide-based composite system. The same relative ranking of flammability is seen in both glass and graphite compositions.

The high-temperature pyrolysis reactions occurring in one flaming combustion mode have been found to correlate rather well with the anaerobic char yield at 600 to 800 °C. As will be seen, there are parallel correlations with polymer decomposition temperatures and glass temperatures of some systems. Anaerobic char yield alone should not be used as a criterion for high temperature thermo-oxidative stability. The general quantitative pyrolysis reactions of simple bisimides can be simply accounted for by ring coalescence of the aromatic and bisimide rings with the elimination of water and hydrogen. The resulting carbon-nitrogen ring system is usually stable in air up to 400 °C and is rapidly oxidized to zero char yield at temperatures greater than 500 °C. Fortunately, in the fire case the rate controlling pyrolysis reactions take place in an essentially anaerobic environment where the effect of thermo-oxidative stability is minimal.

As will be seen, phosphorous modification of the maleimido matrix resins provides both thermal and thermo-oxidative stabilities. The only factor which limits the general acceptance of M-751 and H-795 bismaleimides for superior fireworthy composite structures is the high temperature required for curing compared with standard epoxy systems.

Structural Composites from Maleimido Matrix Resins

Bismaleimides cure without the evolution of small volatile molecules by the thermal polymerization of the maleimide double bond. This feature of these molecules is a significant advantage in obtaining void-free composites. Thermal degradation induced by "backbiting" reactions of unreacted amino and carboxylic acid groups is virtually eliminated.

Unfortunately, as pointed out above, the poly-addition reaction exhibits a DSC curing reaction at 275 °C. In curing 9-ply satin-weave graphite composites, this reaction temperature extrapolates to temperatures of 220 to 240 °C for 2 to 3 hr and still may require further postcure to realize the potential mechanical properties.

In addition to causing higher processing costs than standard graphite epoxides, these higher cure temperatures can produce large internal strains in standard bisimide composites. It has been observed that these high internal strains encountered in large graphite composites can induce the formation of intolerable concentrations of microcracks with catastrophic loss of impact properties uncharacteristic of small laboratory samples. It has been found that addition of small amounts of liquid elastomer of the order of 2 to 3 percent (not conventional rubber toughening) gives acceptable composites free of microcracks, resulting in nominal impact resistance.

What is needed is an alternative curing mechanism for bisimide structures which will permit lower-temperature processing and still not interfere with the inherent thermal stability of the aromatic bisimide ring system. This question will be taken up in detail in the next section.

Processing Conventional Bisimides

Up to this point, bismaleimides made processable by chain extension through thermally-weak links and requiring solvent-based varnishes to prepare prepgs have been considered for fire resistant secondary structures used under ambient conditions. It has been found that under normal processing conditions it is virtually impossible to remove the last traces of solvent (between 1 to 3 percent) from the

cured graphite composite, as shown in figure 5. Here it can be seen that the steady-state concentration of solvent, in this case NMP, decreases with increasing temperature but is never completely eliminated (ref. 3).

The effect of this residue of solvent, which appears to plasticize the M-751 (shown as bismaleimide A in figure 6), is catastrophic. Here the loss in modulus is plotted as a function of test temperature. It can be seen that the compressive modulus (also true of ultimate strength) decreases very rapidly with temperatures from room temperature to 300 °C. Here the bisimide A composite has lost better than 60 percent of its initial properties.

Initially the graphite composite is equivalent to the epoxy resin. At elevated temperatures, however, it is no better than the epoxide. This result is compared with the phenolic resin which shows no loss in properties over the entire temperature range. In fact, the phenolic resin shows an upward turn in the compressive modulus due to further curing above 250 °C.

It can be concluded from these results that although the bisimide A is thermally and oxidatively stable to 250 to 300 °C (unlike the epoxide which is thermally degrading in this temperature range), bisimide A has no better performance than the epoxide due to adventitious solvent. It is clear from the foregoing result that primary structural composites for use at temperatures around 300 °C cannot easily be formulated from useful solvent systems.

What is needed is a processable bismaleimide in the form of a hot-melt system to eliminate both the need for solvent application and chain extension by a more thermally-stable chain extension mechanism than the Michael addition product. Bisimide H-795 fulfills these requirements. The general structure for this hot-melt bisimide is shown in figure 7. Here the simple aromatic bisimide has been chain extended to double the molecular weight by eliminating the thermally-weak chain links present in M-751, thus reducing the comparable melt viscosity and providing an easily processable melt at 120 °C.

The compressive moduli for comparable structural graphite composites are plotted as a function of temperature in figure 8. Here it can be seen that the hot-melt bisimide H-795 (bisimide B composite) retains its mechanical properties without change to 300 °C at which point both epoxy and bisimide A have completely degraded.

From these data alone it is not possible to distinguish between solvent effects and chain degradation. Both degradation processes and plasticization are involved in the failure of bisimide A to perform at high temperatures. It is clear from the foregoing that high-temperature structural composites from bisimide systems will probably evolve from hot-melt systems containing no common aliphatic bridging units.

Recently it has been observed that bismaleimides in general have been found to exhibit significantly better hot-wet strength than comparable graphite epoxy systems. The effect of bisimide structure on moisture absorption was examined by simple immersion tests of both neat resins and graphite composites formulated from the neat resins. The room temperature water absorption data is plotted in figure 9. Here it can be seen that the water absorption for bisimides is much slower initially than that of standard epoxides, but eventually they attain values quite comparable to the epoxy resin. This is not true for the formulated composite. The rate of water absorption for bisimide B, the more polar hot-melt

bisimide, is comparable to the rate of absorption of the epoxide. The more aliphatic bisimide has a very low water absorption and equilibrium value. It is conjectured that the reported excellent hot-wet strength for current bisimides is determined in large measure by the polarity of the bisimide molecular unit, low initial rate of water absorption, and the fact that water may be less effective as a plasticizer for bisimide structures.

Even with the advantages of the hot-melt bisimide B (H-795), it still exhibits a DSC cure temperature of 275 °C and all the limitations these cure conditions impose. Matrix resins are desirable as alternatives to epoxide polymers for advanced aerospace composite structures. These are known by NASA as the second generation matrix resins. With the limitations previously outlined, it is clear that contemporary bisimides do not meet these needs.

It is well known that vinyl monomers such as styrene and divinylbenzene readily copolymerize with maleic and fumaric acid derivatives at low temperatures from 120 to 150 °C. Peroxide catalysis of this reaction forms the basis for polyester laminate technology. It has also been found that styrene, for example, readily polymerizes with phenylmaleimide to give high molecular weight linear polymers which are initiated thermally or with peroxides. It is reasonable to expect that vinyl monomers and a wide variety of vinyl-terminated oligomers would be expected to act as reactive diluents or comonomers for maleimido oligomers.

The objectives for an optimum liquid oligomer and bismaleimide copolymer are outlined in table 2. Processing as a hot melt and curability with a vinyl oligomer theoretically should present no particular difficulty. However, simple vinyl monomers should be expected to give difficulties as a result of volatility; that is, microvoid formation and volatile losses. The simple aliphatic vinyl linkage should be expected to degrade the high-temperature performance by depolymerization and scission, thus limiting high-temperature stability and substantially reducing the anaerobic char yield, which reduces flammability. It is extremely unlikely that any simple vinyl-hydrocarbon monomer can be found as a copolymer reactant which can meet the objective criteria set forth in table 2.

Earlier (ref. 3) it was shown that graphite composites formulated from poly-styrylpyridine matrix resins, obtained from the condensation reaction of collidine and aromatic dialdehydes, give the best fire endurance and high-temperature stability of any matrix resin yet evaluated. Unfortunately, because of the elimination of water in condensation curing reactions, void-free composites are difficult to obtain. Also, extremely vigorous curing temperatures above 250 °C are required. Short-term high-temperature stability at temperatures in excess of 400 °C have been observed. It is believed that the matrix resin is stabilized by the presence and persistence of the double bond of the conjugated stilbazole group at temperatures up to 400 °C. From model compound studies (ref. 4), it appears that the stilbazole group reacts in situ to give a highly cross-linked ring system, characterized by char yields of 70 to 80 percent at 600 to 800 °C in nitrogen.

The special thermal properties of the stilbazole double bond have been taken advantage of in the design and synthesis of the two types of liquid oligomers shown in figure 10. Earlier attempts (ref. 5) to synthesize vinyl-terminated linear stilbazoles from dimethylpyridines such as lutidine did not meet the criteria for epoxide resin replacement.

The two types of oligomers shown in figure 10, however, seem to meet these needs. 5-vinyl-2-methylpyridine gives a low melting (40 °C) oligomer, suitable for copolymerization with a wide variety of maleimido prepolymers. A chain-extended

version obtained with collidine is also shown in figure 10. Vinylstyrylpyridine, VPSP, has been prepared from collidine, terphthaldehyde, and 5-vinyl-2-methylpyridine. Both comonomers have been easily thermally polymerized with the hot-melt bisimide, H-795, over a wide range of comonomer ratios.

Typical thermal processes occurring during these copolymerizations are shown for the case of VST and H-795 in the differential scanning calorimeter traces in figure 11. Here the heat flow is plotted as a function of temperature. It can be seen that the VST oligomer exhibits a DSC melting temperature of 50 to 60 °C with a slow and weak exothermic curing reaction occurring over a temperature range from 160 to 240 °C, due to the thermal polymerization of the vinyl double bond. In separate thin-film IR studies it has been shown that the stilbazole double bond does not participate in this reaction. Another mild exotherm becomes apparent above 322 °C, probably associated with limited polymerization of the stilbazole double bond.

A similar thermal history is shown in figure 11 for the bismaleimide hot melt, H-795. The DSC shows an endothermic melting point around 118 °C and a DSC cure temperature of 282.4 °C, typical of aromatic bismaleimides. It can be seen that the copolymer formulated from a mole ratio of 3:7 of VST to H-795 begins to melt around 50 °C and then polymerizes rapidly at 164 °C, a cure temperature some 120 °C less than pure bismaleimide. Similar reductions in melting points and cure temperatures are seen with VPSP/H-795 copolymers.

The results obtained from the thermochemical-physical characterization of this new family of copolymers are compared in table 3. It can be seen that in all of the copolymer ratios investigated, the cure temperatures are significantly reduced below those required for the bisimides and in most cases less than those required for aerospace-grade epoxides (MY-720-DDS). As might have been anticipated, the degree of cure temperature reduction changes monotonically with the concentration of vinyl double bonds contributed by the VSP or VPSP in the bismaleimide copolymer. It is interesting to note that the glass temperatures of these copolymers, as measured by dynamic mechanical analysis, is 380 °C or higher in all cases; that is, several hundred degrees higher than the cure temperature of 160 to 200 °C. The anaerobic and high temperature stability in all cases is at least equivalent or better than the bisimide alone, as indicated with polymer decomposition temperatures in excess of 400 °C. As predicted from studies on other stilbazole polymers, the anaerobic char yields are significantly higher than those possible from aerospace-grade epoxides.

With the exception of the high VST ratio of 3:7, all the measured char yields of these copolymers are substantially higher than the H-795 bismaleimide alone. It is probable that the 3:7 copolymer has too low a cross-link density to effect optimum char yield.

As mentioned previously, the parallelism that exists among char yield, glass temperature, and thermoplasticity at 300 °C is clearly apparent in the results shown in table 3. It can be seen that the dynamic modulus from DMA measurements of the low-temperature cured copolymers in typical graphite-composite formulations remains unchanged from room temperature to 300 °C. The long-term thermo-oxidative stability of these new graphite composites remains to be examined.

A preliminary evaluation of the mechanical properties of these new copolymers as matrix resins for graphite composites was performed on simple 8-ply satin-weave graphite fabrics with resin contents from 26 to 32 percent. The results are shown

in table 4, compared with an H-795 control. It can be seen that the flammability of the composites based on the copolymers is better than the bisimide alone. It is also obvious that the copolymers give both short-beam shear and strength values two to three times greater than the bisimide alone. No attention has been given to optimizing the fiber sizing or polyphase matrix toughening to improve damage tolerance or impact strength.

It should also be noted that the use of vinyl-terminated stilbazole oligomers may be applied generally to a variety of heretofore difficult bisimides. The values for water absorption after 2 hr in boiling water are also given in table 4. The absorption amounts to 1 percent or less. It has been found that comparable epoxy-graphite composites usually absorb 2 to 3 percent under similar conditions. One may expect substantial improvement in the hot-wet strength of these composites.

Here, then, is a nonpolar (no oxygen), low-temperature curing oligomer which reduces water absorption, gives a threefold improvement in mechanical properties, requires no solvent, gives char yield consistent with optimum fire resistance, and has service temperatures of 300 °C or better. It is believed that the vinyl stilbazole copolymers described in this paper represent a significant advance in matrix resins for graphite secondary structures, where ease of processing, fireworthiness, and high-temperature stability are product requirements. Further research is necessary to evaluate the toughness and impact resistance of these copolymers as matrix resins for primary structure.

In the case of high-temperature, speciality graphite-composite structures, where economic considerations of materials and processing can be relaxed for performance, maleimido matrix resins can be modified to give very thermally-stable polymers. These polymers are good for continuous service at 300 °C or better and have complete fire resistance, limiting oxygen index of 100, and mechanical properties superior to the best graphite-epoxy composites.

Two structural changes in state-of-the-art bisimides must be met. First, the bond strength of the pivotal aliphatic carbon bridge must be replaced with a more thermal-oxidative resistant group than an aliphatic carbon. Secondly, the cross-link density must be reduced by chain extension to overcome the brittleness of the matrix resin.

As shown in figure 12, two bismaleimide matrix resins have been prepared by replacing the usual methylene bridge with phosphonate linkages (ref. 6). In resin 1 the methylene bridge has been replaced by an aminophenylphosphonate and in resin 2 it has been replaced with methylphosphonate. These two polymers were rubber modified with ATBN and the perfluoroalkylene diamine shown in figure 12. Resin 1 was formulated with ATBN between 3.9 and 18 percent. Even small additions of ATBN degrade the fire resistance and high-temperature stability of the neat resin. Thermogravimetric analysis of all of these modifications gave polymer decomposition temperatures above 350 °C and anaerobic char yields between 47 and 71 percent. Addition of 6.4 percent of the perfluoroalkylene diamine (3F), shown as g in table 6, had little or no effect on the neat resin char yield and still resulted in polymers with an LOI of 100.

The effect of the perfluoroalkylene ether modification on the mechanical properties of bisimide II are shown in table 7. It can be seen that with exception of the LOI and flexural modulus, this chain extension reaction gave a substantial improvement in all the mechanical properties as compared with the control, and substantially better properties than the composite derived from MY-720 cured with DDS.

An alternative scheme for enhancing the stability of maleimido matrix resins involves replacing the connecting atoms with a thermally stable moiety, in this case the tricyclophosphazene shown in figure 13. Here the resulting hexamine is capped with three maleimido groups leaving three amino groups for chain extension. Other variations of this modification are shown in figure 14 (ref. 7).

As shown in figure 15, all of the maleimido tricyclophosphazenes show polymer decomposition temperatures well over 350 °C in air. High char yields (greater than 80 percent) are again observed with these phosphorous comodified polymers. Both resins I and II gave residue polymer weights between 40 and 70 percent in air up to 800 °C. All organic matrix resin systems examined to this point gave essentially zero char yields in air at temperatures between 500 to 600 °C. These results suggest unexpected thermo-oxidative stabilization of the bisimide system by these phosphazene modifications and may provide a matrix resin for short-term use under rather severe thermo-oxidative conditions. The details of these thermo-chemical reactions of phosphate bisimides remain to be resolved.

What is again remarkable, as in the case of polymer VI which is readily soluble in methylethylketone and gives tough polymer films when polymerized at 250 °C, is the fact that the polymer shows a char yield of 80 percent; a new pyropolymer relatively stable in air at 800 °C is formed. This film, although somewhat brittle, exhibits good semiconducting properties with resistivities in the range of 10 ohm-cm.

The char yields of these tricyclophosphazenes in nitrogen at 800 °C and in air at 700 °C illustrate the unusual thermo-oxidative stability of this new class of maleimide resins. Figure 16 compares these resins with various state-of-the-art bisimides and other aromatic matrix resin polymers with anaerobic char yields in excess of 40 percent. Only the phosphorous-modified polymers give substantial pyrolysis residue weights in air at 700 °C. One may speculate at this point that it may be practical for some purposes to posture composites derived from silicon carbide fibers at temperatures between 600 and 700 °C to obtain composites suitable for continuous service in air at temperatures above 500 °C.

Finally, figure 17 shows the results obtained by isothermally aging thin films of resin VI in air and nitrogen. These films were cast from MEK and cured at 220 °C. Even with this limited degree of cure there is no weight loss in N₂ up to 72 hr at 350 °C. These data suggest that this polymer may provide continuous service in air at 300 °C. For compositions which can tolerate up to 10 percent weight loss this temperature might be extended to 350 °C.

Concluding Remarks

It has been shown that significant processing and property improvements can be achieved by copolymerization of state-of-the-art bisimides with various vinyl stilbazole derivatives to give both fire resistance and high-temperature properties from hot-melt compositions. Significant improvement in mechanical properties has been achieved through these modifications which may make these new matrix resins ideal candidates for fireworthy secondary graphite composite structures. Phosphorous modifications of maleimido polymers through phosphonate structure and tricyclophosphazene derivatives have provided families of new matrix resins for short-time applications in severe thermo-oxidative environments. With further research these may provide matrix resins for long-term thermo-oxidative stability of advanced composites at temperatures up to 400 to 500 °C.

The authors wish to acknowledge the contributions of Dr. M.T. Hsu for the characterization studies conducted on some of the resins discussed.

Notice

Reference to a company or product name does not imply approval or recommendation of any of the products stated in this paper by the National Aeronautics and Space Administration to the exclusion of others that may be suitable.

References

1. Kourtides, D.A., Parker, J.A., Gilwee, W.J., Lerner, N.R., Hilado, C.J., LaBossiere, L.A., and Hsu, M.T., A Composite System Approach to Aircraft Fire Safety. NASA TMX-73126, April 1976.
2. Parker, J.A., Fish, R.H., Kourtides, D.A., and Gilwee, W.J.: Fire Dynamics of Modern Aircraft From a Materials Point of View. Journal of Fire and Flammability, October 1975.
3. Malasine, B., "PSP 6022 Resin, A Solution For The Electrical Problem Posed by Potential Release of Free Carbon/Graphite Fibers into The Environment." Proceedings of the 24th National SAMPE Symposium, Vol. 24, Book 1, p. 1 (1979).
4. Heimbuch, A.H., and Parker, J.A., "Polystyrylpyridine (PSP)", Chemistry and Technology Presentation at Polymers/West, Gordon Research Conferences, Ventura, CA (1982).
5. Hamermesh, C.L., "Development of Synthesis Specifications and Curing Process for Modified Polystyryl Pyridine," Final Report NAS2-10709 (Dec. 1981).
6. Varma, I.K., Fohlen, G.M., Hsu, M.T., and Parker, J.A., "New Phosphorus-Containing Bisimide Resins," Paper presented at U.S.-Japan Polymer Symposium, Palm Springs, CA, Nov. 22-26 (1980). Published in Contemporary Topics in Polymer Science, Vol. 4, (1981).
7. Varma, I.K., Fohlen, G.M., Parker, J.A., and Varma, D.S., "Phosphorous Containing Imide Resins: Modification By Elastomers", presented at the Symposium on Fiber-Reinforced Composites, Dec. 2-3, 1981 at Charlotte, North Carolina.

TABLE 1. - RELATIVE RANKING OF GRAPHITE FABRIC
(W-133) COMPOSITES BASED ON
FLAMMABILITY PROPERTIES

Resin	LOI	%T	Resin γ_c 800 C, N ₂	Average, %
Polyphenylsulfone (RADEL 5000)	52	92	47	90.4
Phenolic-Novolak (MXG-6070)	50	92	46	88.7
Benzyl (WRF-1200)	49	81	53	88.1
Polyethersulfone (P-300)	54	74	40	81.4
Bismaleimide B (H795)	56	54	49	80.3
Bismaleimide A (M-751)	47	23	50	64.4
Phenolic-Xylok (Xylok 210)	46	1.5	46	53.5
Epoxy (Control) Fiberite 934	41	1.8	21	36.7

$$\text{AVERAGE \%} = \left(\frac{\text{LOI}}{\text{LOI}_{\text{max}}} \right) 100 + \frac{100}{10} \left(\frac{D_s}{132} \right) + \frac{\gamma_c}{\gamma_{c_{\text{max}}}} ,$$

%T = % Optical
Transmission

γ_c = % Char Yield

TABLE 2. - OBJECTIVE FOR SECOND GENERATION COMPOSITE-LIQUID OLIGOMER AND BISMALEIMIDE COPOLYMERS

Processability	Hot melt (melting point is less than 130°C) Soluble in low boiling solvent Low gel temperature (<120°C) and time (1/2 hr)
Easy to cure	Low cure temperature (350°F) and time (less than 4 hr)
Impact resistance	Less than 10% shear strength loss after impact with 10 in-lb
High temperature stability	Decomposition temperature is higher than 300°C
Fire resistance	LOI is greater than 40

TABLE 3. - COMPARISON STATE OF THE ART MATRIX RESINS WITH VST/BMI AND VPSP/BMI COPOLYMERS

Resin System	Cure temperature (DSC Peak), °C	T _g °C	PDT (N ₂) °C	Char yield %	Composite modulus GPa	
					25°C	300°C
Epoxy (MY720)	255	250	300	30	13.5	2
Bismaleimide (H795)	282	>400	400	42	15	14
Copolymers:						
VST:H795 = 1:4	197	380	400	43	13	12
VST:H795 = 3:7	164	----	400	36	----	---
VPSP:H795 = 1:9	245	>400	400	43	17	16
VPSP:H795 = 1:4	230	>400	400	50	15.5	15
VPSP:H795 = 3:7	226	----	400	55	----	---

TABLE 4. - PRELIMINARY MECHANICAL PROPERTIES ASSESSMENT OF VST, VPSP/BMI COPOLYMER COMPARED WITH H 795 IN GRAPHITE FIBER COMPOSITES

Physical and mechanical properties	Resin system with 9ply satin weave graphite fiber				
	H 795	VPSP/H795 1:4	VST/H795 1:4	VST/H795 3:7	VPSP
Resin content %	30.5	26	30	31.5	26
Density, g/cc	1.55	1.43	1.39	1.38	1.44
LOI	52	62	46	-----	57
Water absorption, % 2 hrs boiling water	0.72	1.17	0.99	0.86	1.36
Short beam shear R.T. ksi	1.7	2.95	2.96	2.89	3.15
R.T. flexural: modulus, msi	7.7	7.3	7.3	7.4	7.6
Strength, ksi	24	41	46	41	49
Flexural, 100 °C modulus, msi hot-wet	-----	-----	-----	-----	-----
Strength, ksi hot-wet	-----	-----	-----	-----	-----

TABLE 5. - PROPERTIES OF LIQUID OLIGOMER-BISMALEIMIDE SYSTEMS

Low cure temperature	170 °C
Low gel temperature	110 °C
Low gel time	15 min
Long pot life at room temperature	3 months
High glass transition temperature	>350 °C
High stiffness modulus	>13 GPa at room temperature
High fire resistance	LOI is above 45
Use no solvent (hot melt) or low boiling solvent (THF) for prepreg	-----

TABLE 6. - THERMAL CHARACTERISTICS OF MODIFIED
BISIMIDE RESINS

Sample	Resin and elastomer	Char yield, %* neat resin	LOI, % O ₂ laminate
a	I (control)	61	100
b	II (control)	71	100
c	I + 3.9 % ATBN	58	---
e	I + 18 % ATBN	47	85
f	I + 6.4 % 3F	56.5	100
g	II + 6.4 % 3F	68	100

*In N₂, at 800°C.

TABLE 7. - PROPERTIES OF PHOSPHORYLATED BISIMIDE II MODIFIED WITH
ELASTOMER 3F

Property	Bisimide II		Epoxy*	Percent improvement	
	Control	+6.4% 3F		Over control	Over epoxy
Flexural strength x10 ³ , psi	109.45	138.64	92.26	+26.7	+50.3
Flexural modulus x10 ⁶ , psi	19.4	20.04	7.1	No change	+182
Energy, ft-lb	28.3	41.3	---	+45.9	-----
Tensile strength, x10 ³ , psi	59.8	76.9	82.6	+28.6	-6.9
Shear strength x10 ³ , psi	5.38	10.2	7.74	+89.6	+32.5
LOI, % O ₂	100	100	36	No change	+++
Resin content, %	18-20	22.5	25.3	-----	-----
Resin char yield, %	71	68	20	-4.2	-----

*MY 720 cured with DDS

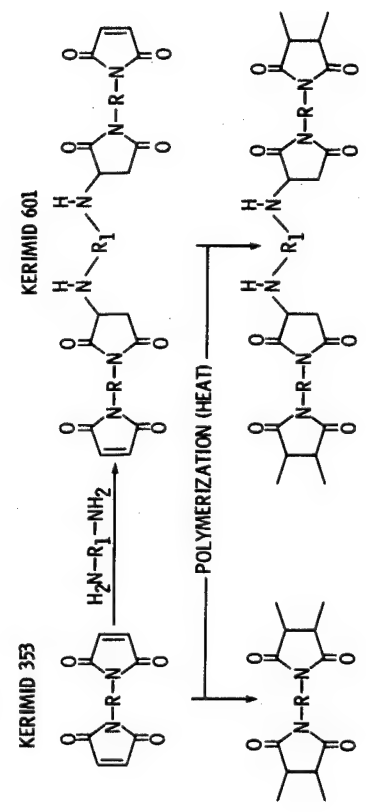
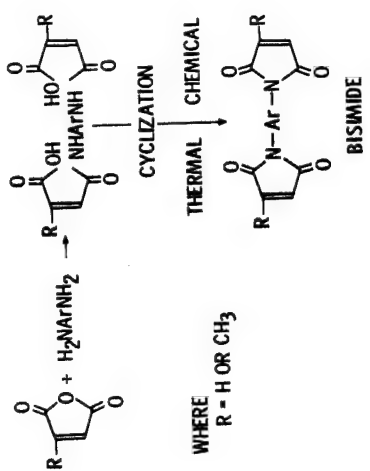


Figure 1. - General synthesis of an aromatic bisimide.

Figure 2. - Chain extension of bisimide by amine addition to double bond (Michael addition).

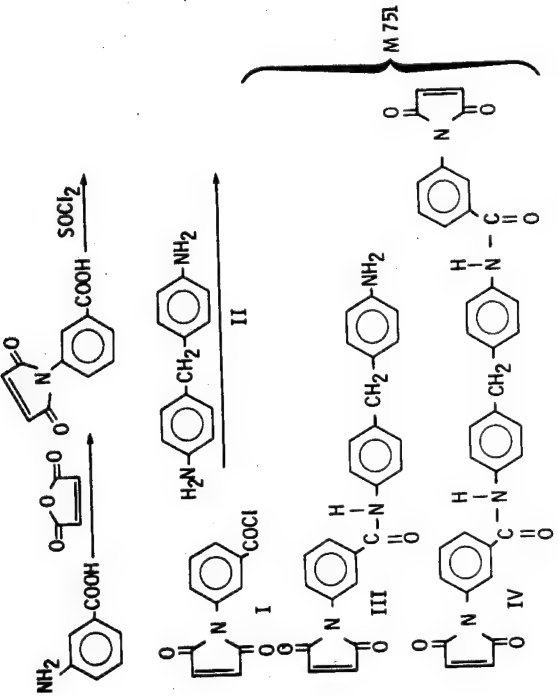


Figure 3. - Chemistry of M 751 resin.

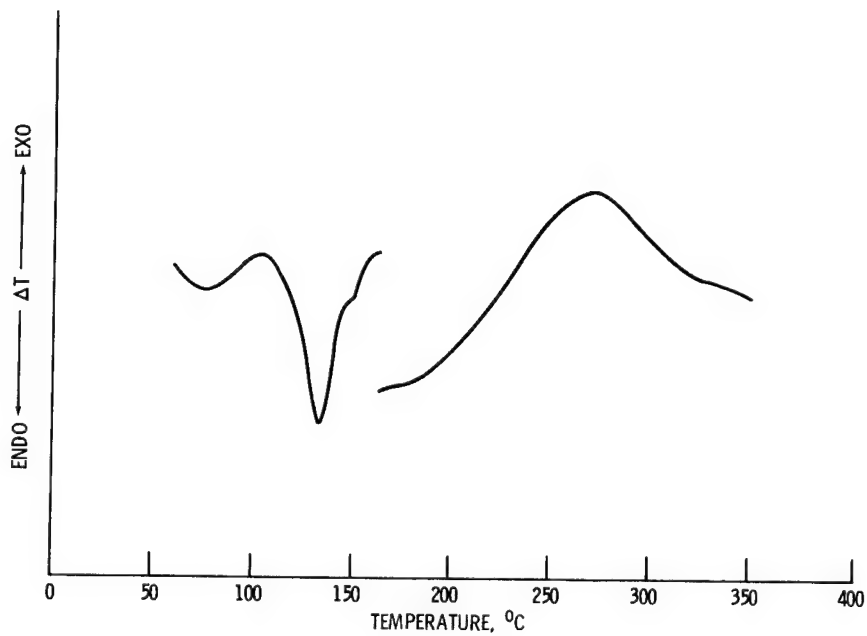


Figure 4. - Melting and polymerization behavior of bismaleimide resin M 751.

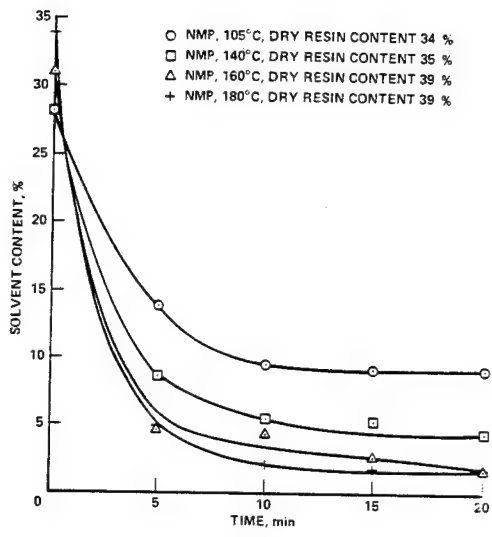


Figure 5. - Plot of solvent content as function of time showing remaining traces of solvent.

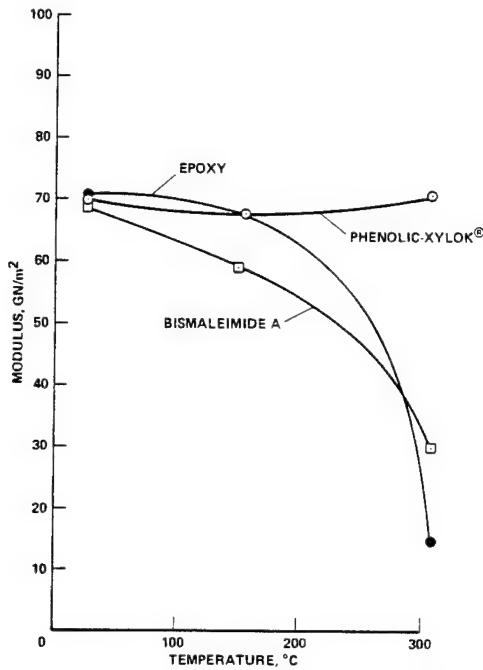


Figure 6. - Plot of modulus as function of temperature showing the decrease in modulus from room temperature to 300 °C.

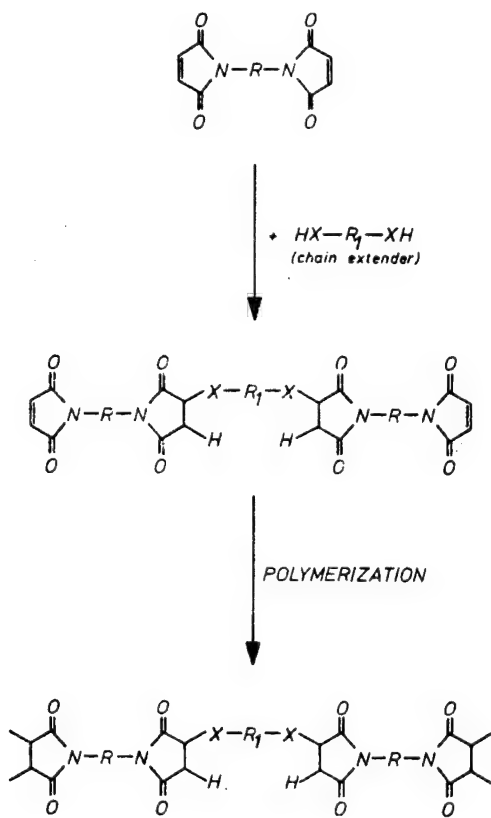


Figure 7. - Chemistry of H 795 resin.

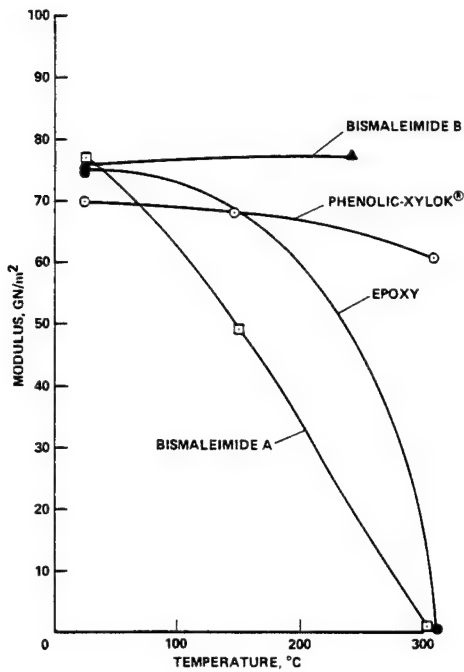


Figure 8. - Plot of modulus as function of temperature showing stability of bisimide B composite at temperatures which degrade both epoxy and bisimide A.

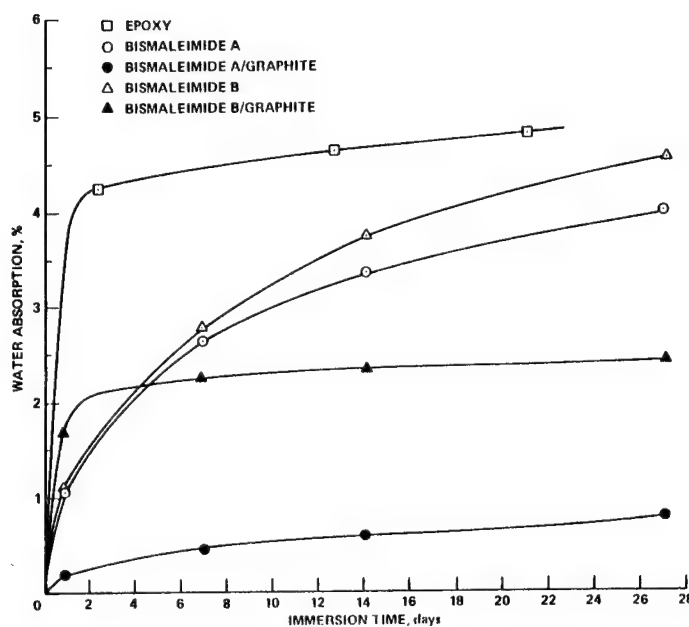


Figure 9. - Plot of water absorption as function of immersion time for bisimides and standard epoxides.

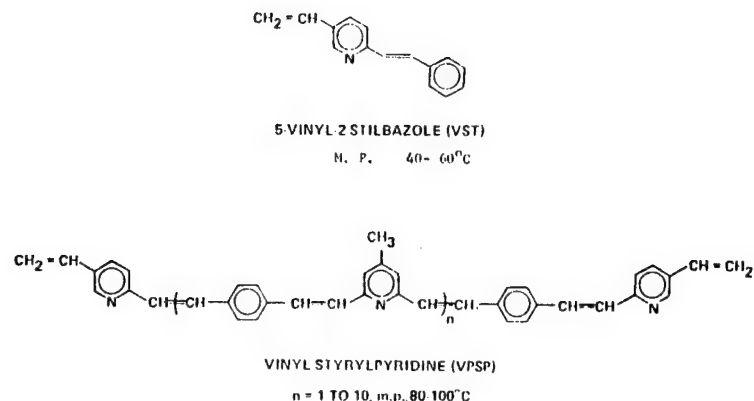


Figure 10. - Chemical structure of liquid oligomers.

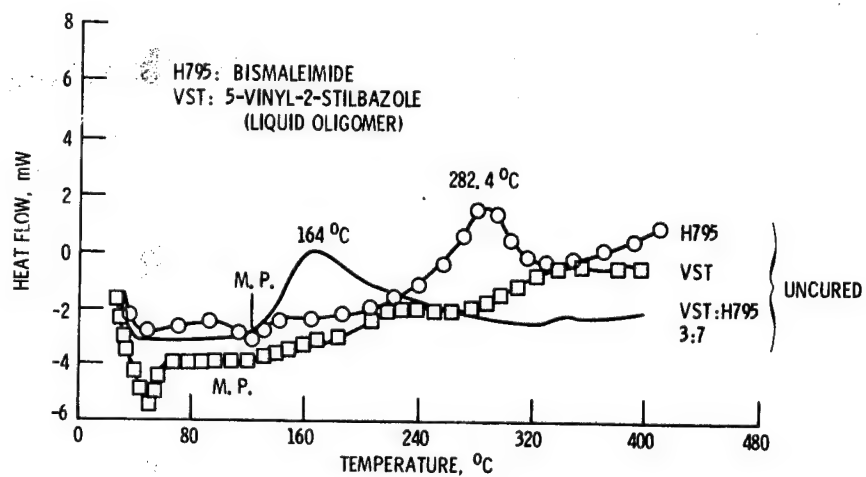


Figure 11. - DSC of bismaleimide (H 795) and VST/H 795 copolymers.

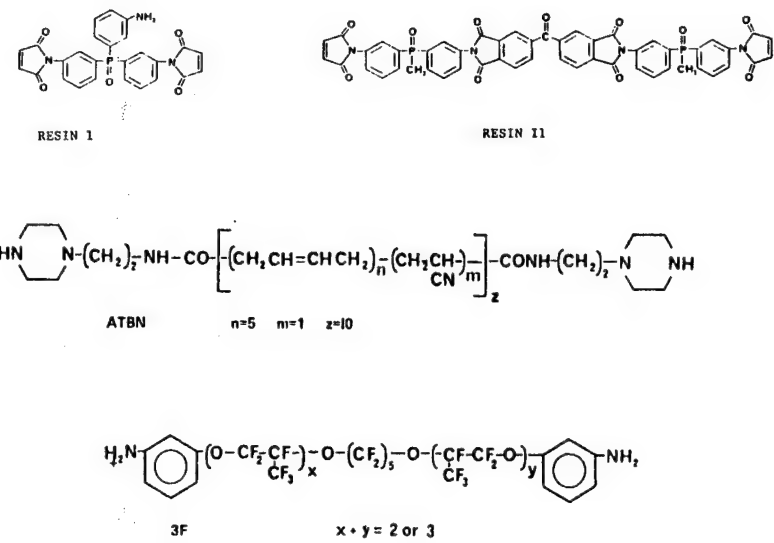


Figure 12. - Molecular structure of bismaleimide matrix resins prepared by replacing the methylene bridge with phosphonate linkages.

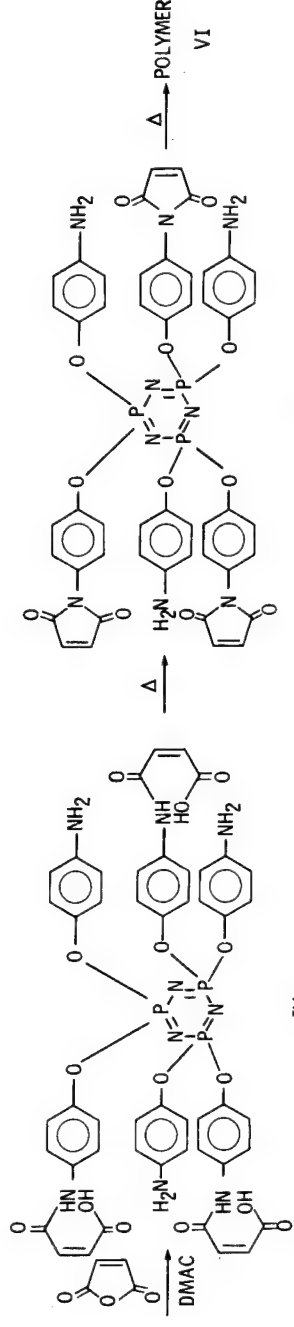
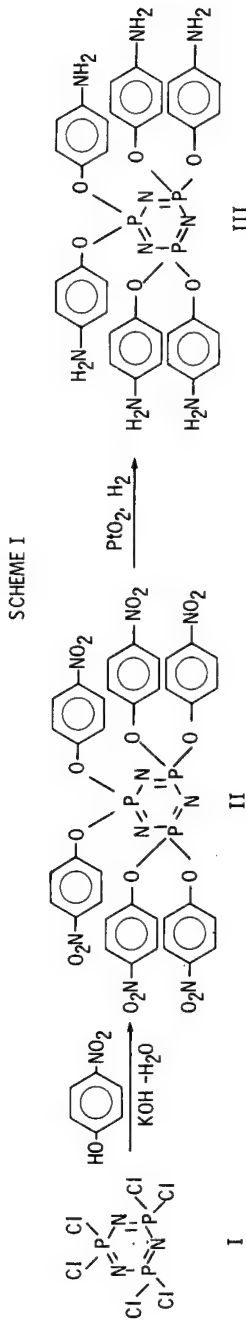


Figure 13. - Schematic showing the method for enhancing the stability of maleimido matrix resins with a thermally-stable tricyclic phosphazene moiety.

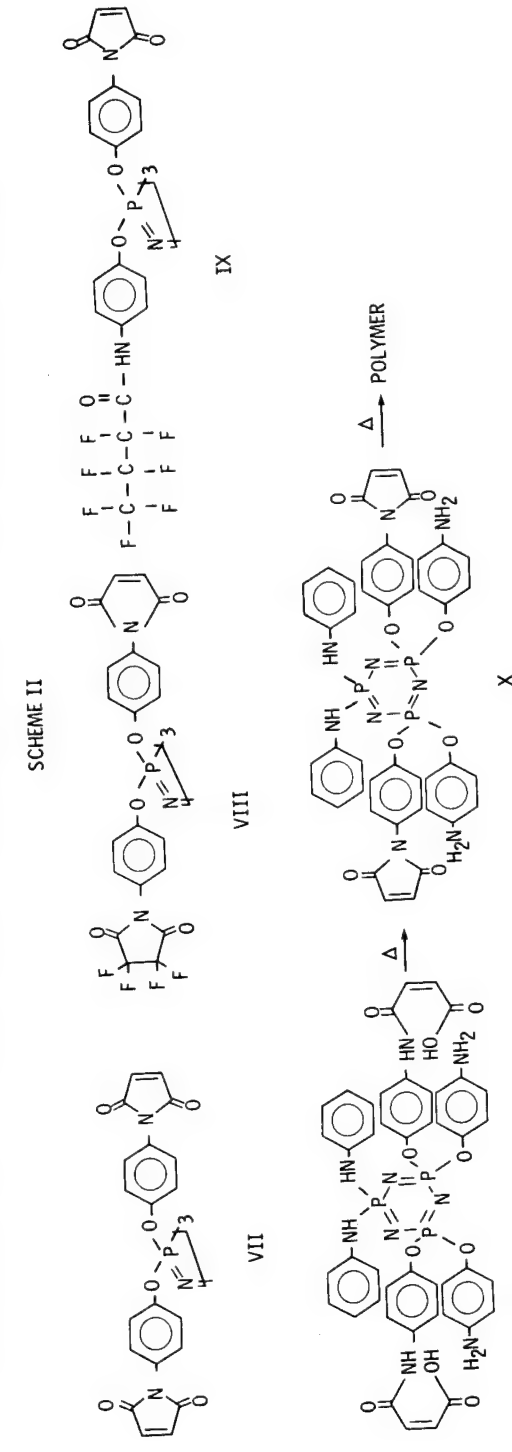


Figure 14. - Schematic showing additional variations of maleimido matrix resins.

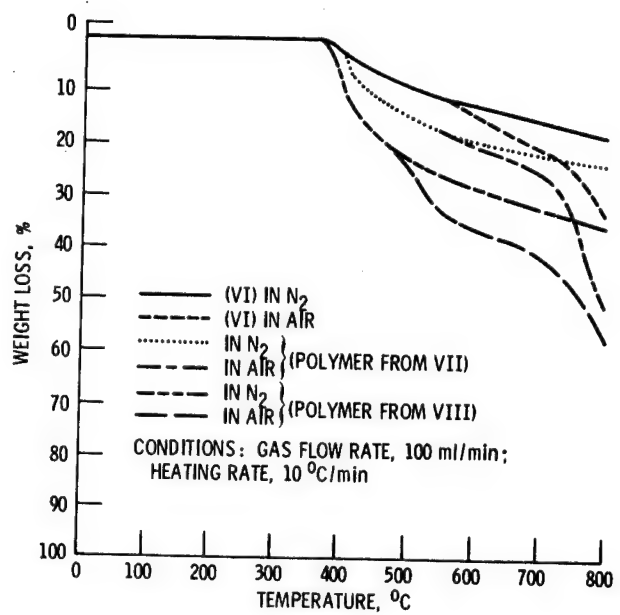


Figure 15. - Thermogravimetric analysis of cyclophosphazene polymers.

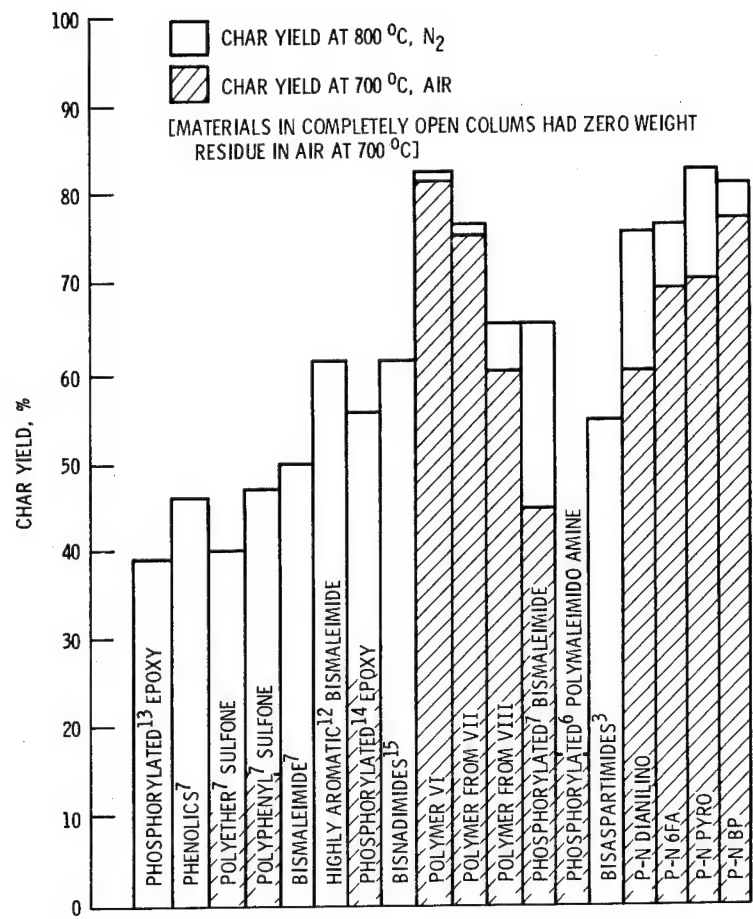


Figure 16. - Histogram comparing the thermal oxidative stability of tricyclophosphazenes with state-of-the-art bisimides and aromatic matrix resin polymers.

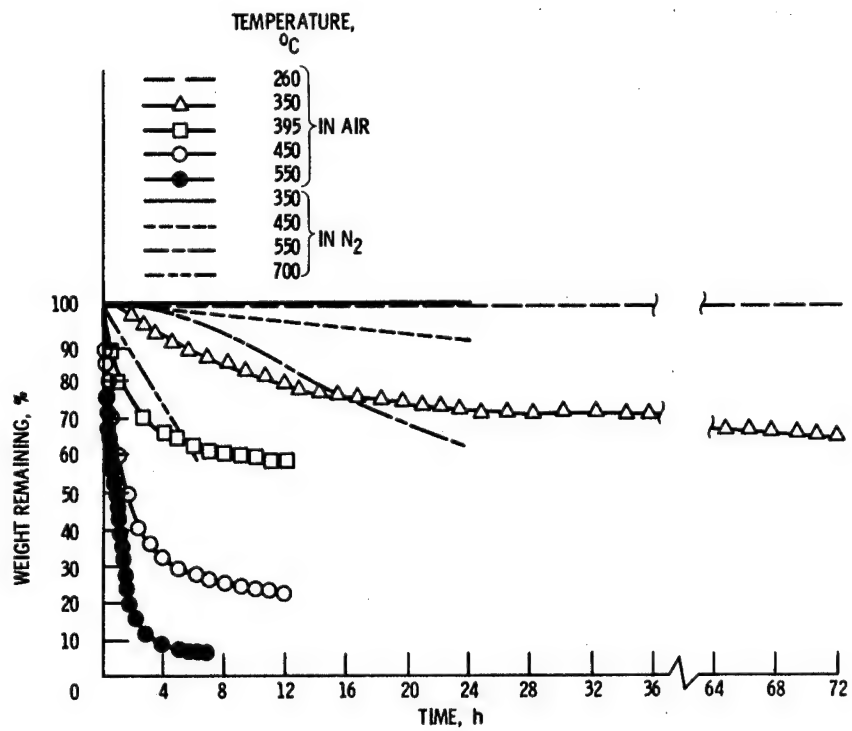


Figure 17. - Isothermal weight loss of (VI) at various temperatures.

THE SYNTHESIS, CHARACTERIZATION AND THERMAL CHEMISTRY
OF MODIFIED NORBORNEYL PMR ENDCAPS*

Chaim N. Sukenik, William M. Ritchey,
Vinay Malhotra and Uday Varde
Department of Chemistry
Case Western Reserve University

As part of a program to further our understanding of the polymerization of Nadic-Endcapped PMR systems, we have synthesized a series of model Norbornenyl-Imides and explored their thermal behavior. We report herein their syntheses and characterizations as well as their rearrangement and polymerization chemistry. Monomer isomerization at temperatures as low as 125°C and oligomer formation at somewhat higher temperatures have been observed. Approximate relative rates for competing isomerization pathways have been established and some information has been obtained about the details of oligomer formation. The relationship of this data to current PMR systems is briefly discussed.

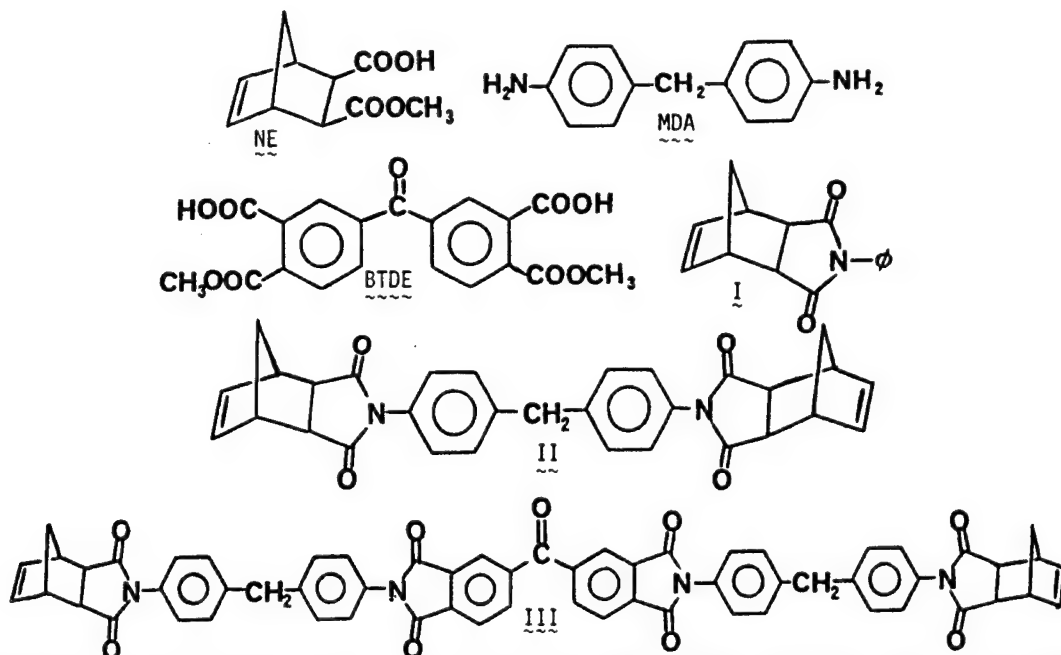
INTRODUCTION

While there are already many successful applications of polyimides in high temperature polymer matrix composites, the search still continues for materials with better performance and/or processing properties. The specific focus of our work is on understanding and ultimately improving the current PMR-15 polyimide system. This thermally cured resin consists of a mixture of 2-carbomethoxy-3-carboxy-5-norbornene (NE), 4,4'-methylene dianaline (MDA), and 3,3'-dicarbomethoxy-4,4'-dicarboxybenzophenone (BTDE). It has been modeled effectively by monoimide I, diimide II, and polyimide III. This is consistent with the notion that thermal imide formation dominates the early stages of the curing process.

Interestingly, the later stages in the curing of PMR systems remain a mystery. It is assumed that the heavily crosslinked polymer products result from a thermal vinyl polymerization of species like II and III. However, neither the mechanism of this polymerization nor the structural details of the crosslink network have been established. It is this aspect of PMR-15 that we intend to probe.

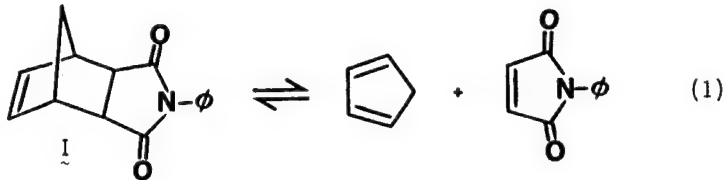
The plan of our research has been to design new, modified, model PMR monomers by making appropriate changes in the structure of I (the "parent" model compound). These modified monomers are chosen with an eye toward their potential for elucidating the mechanism of the PMR cure. The new model monomers are then studied

* This work was supported by NAG 3-163.

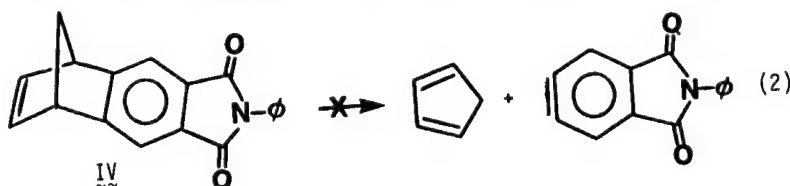


under cure-like conditions. It is hoped that these studies will provide a better understanding of PMR chemistry and will also lead to the development of new PMR resins with lower curing temperatures than are required by current PMR. Ideally, these new resins would also have improved structural and oxidative integrity.

The specific mechanistic questions that we are considering require that we first establish the relevance of any retro Diels Alder reaction of the norbornene to the polymerization process. We would then be able to begin to study the presumed vinyl polymerization of the double bond in the norbornene endcap. The fact that the kind of retro Diels Alder shown in equation (1) does occur in norbornene derivatives and even for imide I itself has been demonstrated (vide infra). However, the significance of this process to the thermal polymerization is as yet unclear.



We therefore designed two kinds of modified monomers. The benzonorbornadiene imide, IV, was suggested as a compound with a vinyl group comparable to that in I, II and III but which cannot undergo retro Diels Alder reaction (equation 2). If the polymerization of I were occurring by a simple addition type vinyl polymerization, then IV should behave similarly. Furthermore, the possibility that IV might polymerize to yield a new resin type with higher aromatic content might add an interesting dimension to its performance properties. If, however, the cyclo-



pentadiene or maleimide generated by equation (1) are crucial to the polymerization of I, then IV might not polymerize at all.

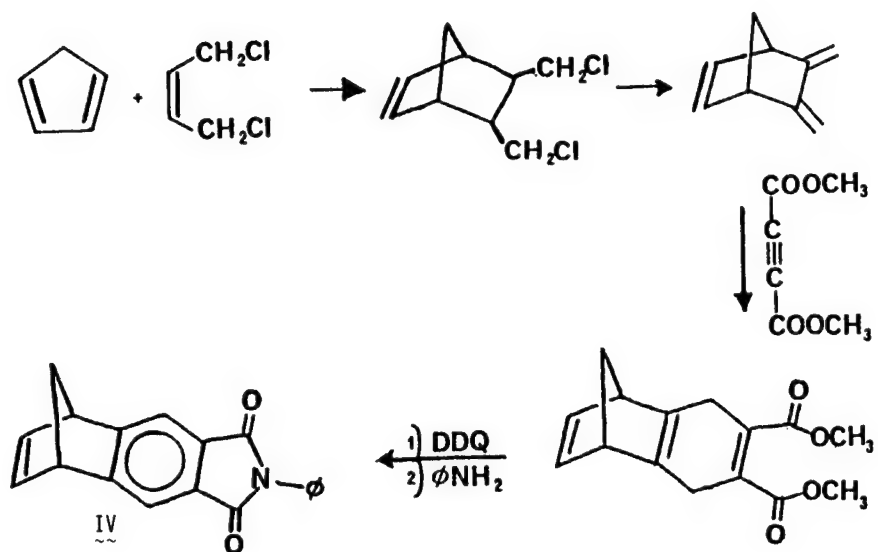
The second kind of modified monomer involved selective functionalization of I with various X groups at either a bridgehead (V) or vinyl (VI) position. This would allow an investigation of the effect of various X groups on both the ease of polymer formation and the properties of the new resins. The specific X groups that we initially chose were X = \emptyset and X = COOMe. These were suggested based on the known thermal polymerization of both styrene and methyl methacrylate and the analogy between the vinyl substituted norbornenes (VI) and these materials.



MONOMER SYNTHESIS

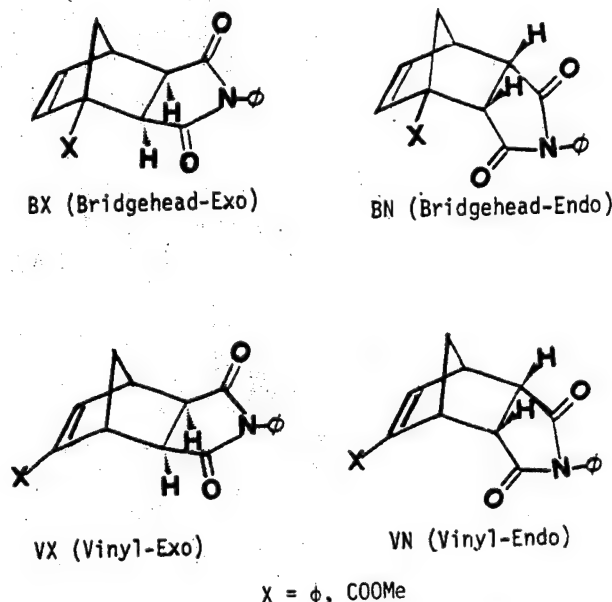
The synthesis of IV was modeled after the route to related benzonorbornadienes used by Paquette et al (ref. 1). This route, which is shown in Scheme I, has been used to produce gram quantities of IV. This compound is a pale yellow crystalline substance with M.P. = 149°-150°C. It has been thoroughly characterized by H^1 NMR, C^{13} NMR, MS and IR.

SCHEME I



The selective synthesis of V and VI is complicated by the fact that V and VI each represent two compounds, i.e. each of them can exist with the imide ring either exo or endo to the norbornene skeleton (as is also the case for I itself). This means that, for each X group, we must prepare and characterize four distinct compounds (Scheme II).

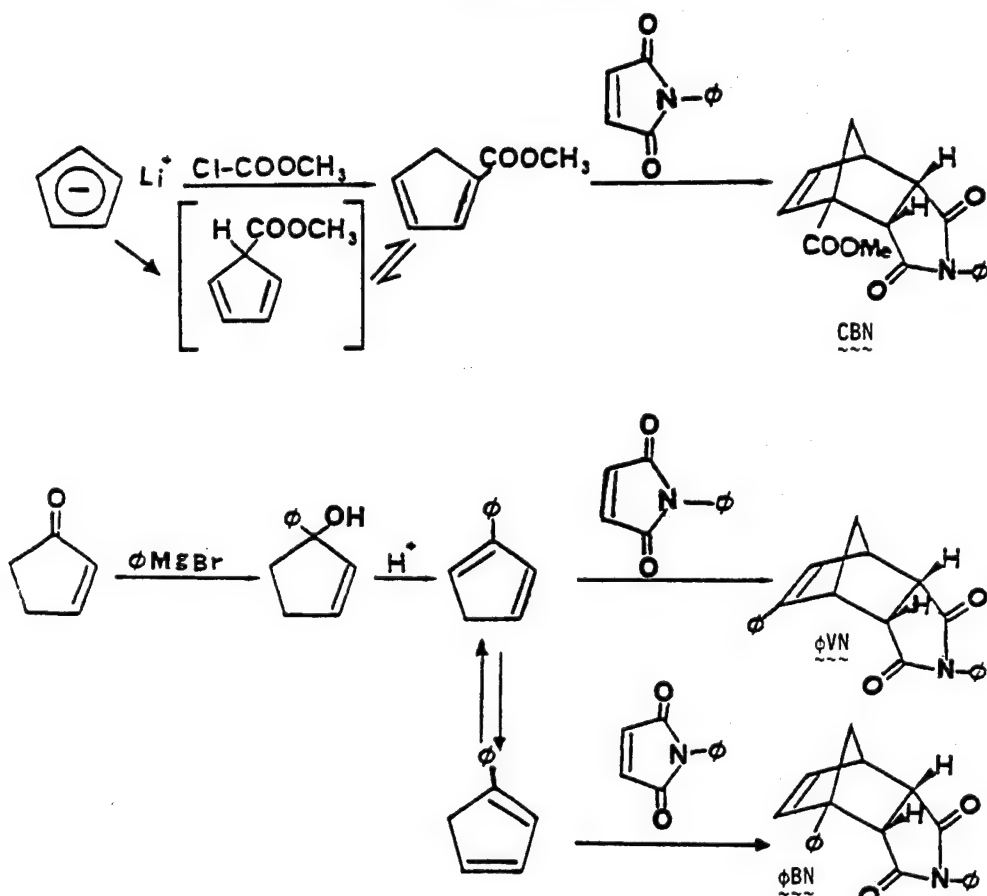
SCHEME II



While a number of attempts were made to functionalize either exo or endo I and specifically obtain one of the isomers of V or VI, these were all unsuccessful. We instead chose an approach which made our functionalized monomer in much the same way as I itself is made, the Diels Alder reaction of cyclopentadiene with N-phenyl-maleimide. We used either phenylcyclopentadiene (ref. 2) or carbomethoxycyclopentadiene (ref. 3) and allowed it to react with N-phenyl-maleimide. The synthetic routes and the specific isomers that were produced are shown in Scheme III. The notation used to identify these compounds is based on a three-letter code where the carbomethoxy derivatives of V are called CBN (Carbomethoxy-Bridgehead-Endo) and CBX (Carbomethoxy-Bridgehead-Exo) and the derivatives of VI are labeled as CVN and CVX, respectively, to identify the vinyl substituent. Phenyl compounds are similarly named ϕ BN, ϕ BX, ϕ VN, and ϕ VX. The two isomers of the parent model compound I will also be referred to by the same convention as PN (parent-endo) and PX (parent-exo).

It should be noted that these routes lead only to endo ring-fused products, as expected for Diels Alder reactions. It is also important to point out that with carbomethoxycyclopentadiene only the 1-substituted isomer, the thermodynamically preferred isomer, could be trapped. Thus only CBN could be synthesized directly. However, in-situ trapping of phenylcyclopentadiene generated as the 2-substituted isomer was possible and allowed direct synthesis of ϕ VN. As was the case with carbomethoxy, if the phenylcyclopentadiene is allowed to equilibrate to the 1-substituted isomer, only ϕ BN is obtained.

SCHEME III

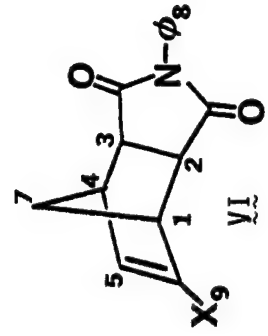
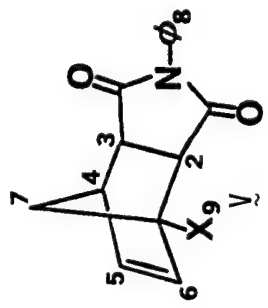
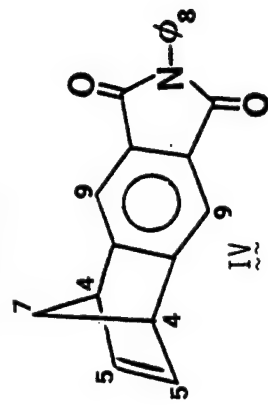


While the above routes led us directly to only three of our desired eight compounds (four phenyl and four carbomethoxy isomers), we found that low temperature thermolysis allows isomer interconversion within each substituent set. It was this isomerization that was used to obtain most of the remaining compounds. The results and interpretation of these isomerization experiments are presented in the following section. At this point we need only note that CBN, CVN, CVX, φBN, φVN, and φVX have all been obtained as pure crystalline materials and have been fully characterized by H^1 NMR, C^{13} NMR, MS and IR. A tabulation of physical and spectral data for these six compounds, as well as for the benzo model (IV), is shown in Tables I and II. Both CBX and φBX have been difficult to obtain in

TABLE I: Melting Point, Infrared, and Ultraviolet Data

	M.P. (°C)	IR: C=O (cm ⁻¹)	UV (CH ₃ CN) : log ε (λ254nm)
Benzo (IV)	149-150°	1710	4.11 (λ_{max} = 240nm, log ε = 4.60)
CBN	173-174°	1712	2.40
CVN	98-99°	1712	2.80
CVX	135-136°	1711	2.84
φBN	172-173°	1708	2.51
φVN	152-153°	1702	3.87 (λ_{max} = 264nm, log ε = 4.19)
φVX	195-197°	1706	3.91 (λ_{max} = 264nm, log ε = 4.05)

TABLE II. Nuclear Magnetic Resonance Data



a) ^1H NMR: (200MHz; CDCl_3 [^3J Benzene-d₆]); chemical shift in units δ ; multiplicity:singlet(s), doublet(t), triplet(t), doublet of doublets(dd), doublet of triplets(dt), multiplet(m).

Compound	H ₁	H ₂	H ₃	H ₄	H ₅	H ₆	H _{7a}	H _{7b}	H ₈	H ₉
Benzo VI	—	—	—	3.97(m)	5.74(t)	—	2.24(d)	2.38(d)	7.22-7.44	7.62(s)
CBN, V X=COOMe	—	3.86(d) *3.84(d)	3.58(d) *3.16(dd)	*3.22(m) *3.30(m)	*6.25(d) *6.22(dd)	*1.72(d) *6.66(d)	*1.93(d) *1.80(d)	*6.86-7.34 *1.94(dd)	*7.24-7.72	*7.35(s) *3.80(s)
CVN, VI X=COOMe	3.52(m) *3.00(m)	3.88(m) *4.00(m)	3.62(m) *3.28(m)	3.52(m) *3.00(m)	7.12(d) *7.24(d)	—	1.70(d) *1.06(d)	1.94(dt) *1.58(dt)	6.96-7.44 *7.12-8.00	3.68(s) *3.70(s)
CVX, VI X=COOMe	3.72(s) *4.06(s)	2.92(m) *2.50(d)	2.92(m) *2.78(d)	3.50(m) *3.30(m)	7.14(d) *7.05(d)	—	1.52(d) *1.14(d)	1.72(dt) *1.56(dd)	7.18-7.38 *7.30-7.66	3.74(s) *3.72(s)
ΦBN, V X=Φ	—	3.65(m) *2.97(d)	3.65(m) *2.87(dd)	3.65(m) *3.05(m)	6.40(dd) *5.94(dd)	6.44(d) *6.07(d)	2.09(m) *1.29(dd)	2.09(m) *1.59(dd)	7.16-7.64 *7.01-7.56	7.16-7.64 *7.01-7.56
ΦVN, VI X=Φ	3.99(m) *3.02(m)	3.56(m) *2.30(m)	3.56(m) *2.30(m)	3.56(m) *2.65(m)	6.50(d) *5.71(d)	—	1.72(d) *0.45(d)	1.95(dt) *0.92(dt)	6.63-7.52 *6.36-6.94	6.63-7.52 *6.36-6.94
ΦVX, VI X=Φ	3.85(d) *3.60(m)	3.01(d) *2.38(m)	3.01(d) *2.38(m)	3.56(dd) *3.16(m)	6.57(d) *5.97(d)	—	1.64(d) *1.30(s)	1.82(dt) *1.30(s)	7.26-7.54 *7.08-7.37	7.26-7.54 *7.08-7.37

TABLE II (continued) Nuclear Magnetic Resonance Data

b) C¹³NMR: (50 MHz, CDCl₃, Proton Decoupled, chemical shift δ (#attached H)).

Benzo(IV): 164.71(0), 160.05(0), 143.14(1), 132.16(0), 129.41(0), 128.63(1), 127.84(1), 127.06(1), 116.47(1), 70.20(1), 49.80(2).

CBN: 176.97(0), 175.93(0), 172.67(0), 136.17(1), 135.13(1), 132.73(0), 130.28(1), 129.89(1), 127.67(1), 62.19(0), 57.99(2), 53.84(3), 50.07(1), 48.17(1), 47.34(1).

CVN: 177.11(0), 176.58(0), 164.58(1), 146.02(1), 141.33(0), 132.80(0), 130.42(1), 130.01(1), 129.89(1), 53.85(1), 53.12(3), 47.75(2), 47.24(1), 46.74(1), 46.69(1).

CVX: 173.73(0), 173.43(0), 161.57(0), 145.49(1), 141.18(0), 129.80(0), 127.06(1), 126.67(1), 124.71(1), 50.59(3), 46.51(1), 46.31(1), 46.27(1), 44.71(1), 42.35(2).

ΦBN: 176.28(0), 175.78(0), 139.52(0), 138.23(1), 134.34(1), 131.77(0), 129.01(1), 128.54(1), 128.51(1), 127.32(1), 126.26(1), 126.55(1), 62.1(0), 57.93(2), 49.51(1), 47.96(1), 45.25(1).

ΦVN: 176.66(0), 176.09(0), 146.98(0), 133.29(0), 131.55(0), 128.86(1), 128.54(1), 128.30(1), 128.10(1), 126.69(1), 126.38(1), 125.55(1), 51.86(2), 47.76(1), 46.98(1), 46.09(1), 45.80(1).

ΦVX: 176.92(0), 176.74(0), 150.29(0), 133.56(0), 131.82(0), 130.50(1), 129.20(1), 128.78(1), 128.71(1), 128.11(1), 126.38(1), 125.07(1), 49.42(1), 47.59(1), 47.18(1), 47.03(1), 42.26(2).

significant quantities from either direct synthesis or isomerization studies. While this has been a disappointment, the discussion of the thermal chemistry of our model monomers will suggest that both of these compounds are of little consequence for our polymerization work.

THERMAL REARRANGEMENTS IN SOLUTION

As a means of first understanding any unimolecular thermal chemistry that might be occurring under pre-cure or cure conditions, we have looked at the behavior of all of our model monomers in solution between 100°-200°C. In general, we see no dependence of this chemistry on the choice of solvent (e.g. benzene, diphenylmethane, decalin). Since all of our reactions are done in sealed glass tubes, we have no problems with loss of material or solvent. And finally, since these reactions are done as dilute solutions of monomer in inert solvent, there is no problem with competing intermolecular (polymer forming) reactions. It was our intent to, first, clearly define the unimolecular thermal behavior of our substrates, and then be in a better position to deal with the behavior of neat samples and of polymer forming cures. These neat samples, presumably, have their intramolecular chemistry superimposed on the polymerization process itself.

The study of monomer isomerization in solution led to a number of conclusions. The benzo compound, IV, undergoes no unimolecular chemistry in solution up to 250°C and will thus not be considered any further in this section. Secondly, the parent compound I and its ϕ and COOMe derivatives each undergo isomerization in solution

to a bonafide equilibrium mixture. This equilibrium mix may be reached at different rates depending on the starting isomer, but regardless of the isomer initially used, the final mixture is the same ($\pm 2\%$; as measured by NMR). A summary of this equilibration data is given in Table III. Suffice it to say that dilute solutions of any of our monomers show no polymer formation even after a day at 200° and that such samples are fully equilibrated. The approach to equilibrium was, predictably, more rapid at higher temperatures, but this was not investigated in detail.

TABLE III: Isomer Composition at Equilibrium

Conditions: $200^\circ \pm 5^\circ \text{C}/15 \pm 5 \text{ hr}$ Solvents: $\phi\text{H}, \phi_2\text{CH}_2$, decalin

Parent: 44% PN% 56% PX

ϕ : 1% BN/?% BX/37% VN/62% VX

COOMe: 2% BN/1% BX/27% VN/71% VX

To probe the isomerization threshold of the various monomers, we looked at the thermal reactivity of each monomer in solution at temperatures as low as 110° and for times up to 24 hrs. Due to their greater availability, the bulk of these studies were done on endo isomers only. However, adequate confirmation was obtained that nothing unusual occurred in the exo compounds of both the parent and vinyl substituted monomers. A representative set of data from isomerization experiments in benzene solution are shown in Table IV.

TABLE IV: Low Temperature Isomerization in Benzene Solution

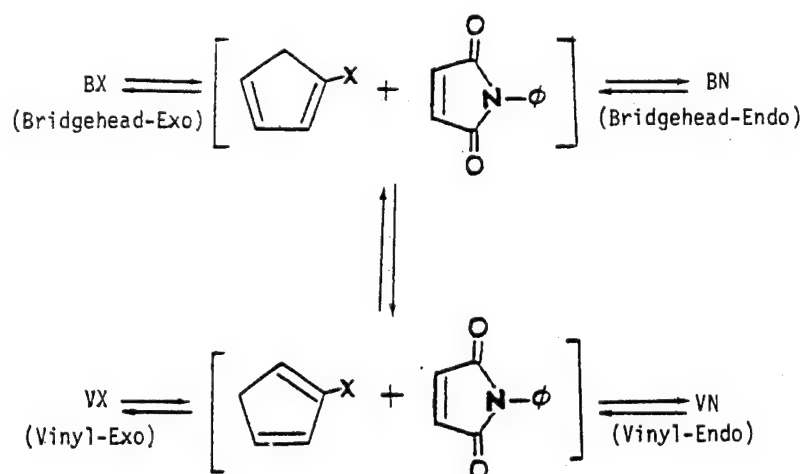
Substrate	Temp (24 hr)	BN	BX	VN	VX
CBN	125°	49	4	44	4
CVN	155°	4	2	88	6
ϕBN	125°	17	-	74	9
ϕVN	155°	-	-	92	8
PN	155°	PN:88		PX:12	

Both the parent and vinyl substituted isomers are largely thermally stable at temperatures up to 150°C ($10 \pm 2\%$ isomerization after 24 hrs). However, those isomers with bridgehead substitution (either ϕ or COOMe) are substantially rearranged at even lower temperatures (125°C). In this context we also note that the activation provided for these bridgehead substituted monomers is somewhat greater for ϕ substituents than for COOMe. Lastly, we should point out that while 155°C for 24 hrs barely affects ϕVN , three hrs at 155°C (experiment not shown in Table IV) almost totally ($>90\%$) isomerizes ϕBN .

A second observation concerns the fate of these more labile bridgehead substituted compounds under conditions where little or no isomerization of vinyl substituted compounds is seen. Both ϕBN and CBN go to a mix of vinyl substituted isomers with very little bridgehead endo/exo isomerization. For the ϕ system the bridgehead-exo isomer has yet to be detected, while in carbomethoxy case it is seen by NMR, but never to an extent of greater than 10%. Interestingly, the vinyl-endo to vinyl-exo ratio formed on isomerization of either the ϕ or COOMe bridgehead

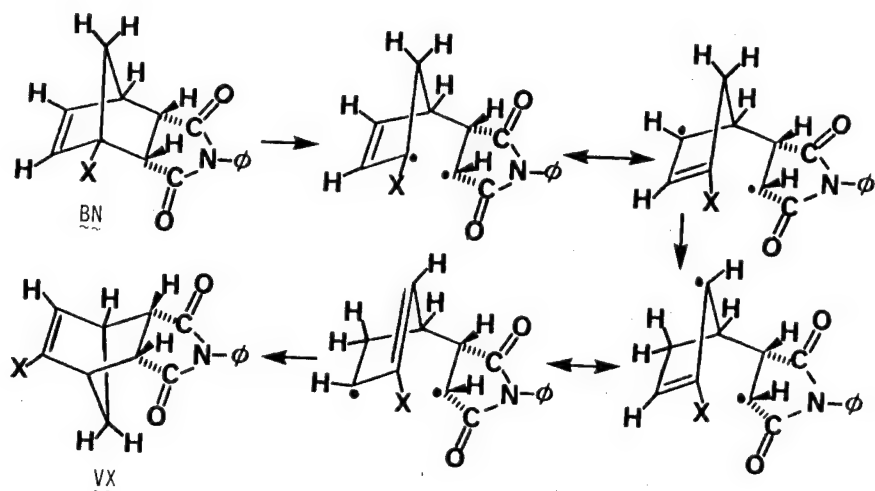
compound heavily favors the vinyl-endo isomer. This preference for isomerization of the bridgehead-endo, preferentially, to the vinyl-endo is completely consistent with an isomerization process (Scheme IV) that proceeds via a) retro-Diels Alder of the bridgehead compound; b) isomerization of the substituted cyclopentadiene from the 1-substituted isomer to the 2-substituted cyclopentadiene; and c) Diels Alder cycloaddition of the 2-substituted cyclopentadiene with the N-phenyl maleimide that had been generated. This last Diels Alder would be expected to show the same, high, endo selectivity we observed in our initial syntheses. Interestingly, this is precisely the opposite conclusion that one would expect to reach if the isomerization did not involve a bona fide retro Diels Alder. If the isomerization of either ϕ BN or CBN were proceeding by a series of one-bond cleavage and H shift steps, then the expectation would be for BN to go selectively

SCHEME IV



to VX and not to VN at all. This is shown in an alternate hypothetical mechanism in Scheme V. Thus, our isomerization is clearly proceeding by a retro Diels Alder, consistent with literature precedent in related systems (ref. 4).

SCHEME V



An important conclusion from the above studies is that not only do all of our norbornenyl imides undergo retro Diels Alder reaction, but that this reaction pathway is greatly facilitated by bridgehead substitution. However, vinyl substitution has little or no effect on the ease of retro Diels Alder reaction as evidenced by its lack of effect on isomerization rates of VN and VX relative to parent, I.

POLYMERIZATION STUDIES

The first point to be addressed in our discussion of the polymerization of our model monomers is to consider the relevance of the "low temperature" isomerization to the actual polymerization process. That is, we must assess the extent to which isomerization of a substituted monomer has occurred relative to the degree of polymerization of monomer under comparable conditions of time and temperature. To answer this question, we took neat samples of each of our endo substrates (parent, vinyl, and bridgehead) and heated them in sealed glass tubes. At 195°C for 15 hrs, neither parent (I) nor the benzo analog (IV), showed any significant degree of polymerization. In fact, parent shows only small amounts of polymer even after 96 hrs at 195°C. It thus seems clear that, at moderate temperatures (~200°C), parent (I) achieves exo/endo equilibration much more easily than it polymerizes. While we suggest that this will translate into our obtaining comparable polymer structures, at comparable rates, whether we start from pure PN or pure PX, this remains to be confirmed.

The isomerization of our substituted monomers (V and VI) under cure-like conditions leads to a somewhat more complicated situation. Some of the results obtained from the carbomethoxy substituted compounds are shown in Table V. This data provides convincing evidence that under conditions where only small amounts of polymer are detected by Gel Permeation Chromatography (GPC), the composition of neat samples of monomers are nearly the same whether they started as pure CBN or pure CVN.

TABLE V: Isomer Distribution During 195°C Cure (neat sample, sealed glass tube)

Substrate	1 hr	4 hr	15 hr
	VN:VX:BN+BX	VN:VX:BN+BX	VN:VX:BN+BX
CBN	71:21:7	34:57:9	30:68:2
CVN	72:24:4	33:59:6	25:74:1

When this isomerization data is combined with a measure of extent of polymerization that we have obtained by GPC analysis of these same samples the picture that emerges is as follows. If the thermal cure of a neat carbomethoxy sample is done at <200°C, isomer interconversion proceeds well ahead of polymerization. That is, there is less than 50% polymerization of the carbomethoxy sample even after 96 hrs, yet isomer equilibration is complete in less than a day. More specifically, in the approximately 15 hrs required for isomer equilibration at 195°C, there is <10% polymerization.

In a higher temperature cure, the situation is less clear. When neat samples of the carbomethoxy compounds were heated at 250°C they were 50%-80% polymerized even after 2 hrs. We therefore looked at isomer distribution after 0.5 hr and 1 hr

at 250°C, full well realizing that our isomerization was proceeding in competition with polymerization. We now see evidence for two phenomena that still require further investigation. First of all, inspection of these samples at 0.5 hr and 1.0 hr suggests that complete isomer equilibration is not achieved before these higher temperature samples are polymerized. Secondly, we now start to see some evidence of different polymerization rates from our different substituted monomers. These observations suggest that polymer structure and properties may also vary as a function of starting isomer mix in these higher temperature cures, but this is yet to be studied.

The situation in the curing of the ϕ substituted versions of V and VI is even more complex than for the COOMe substitution, since the ϕ substituted compounds show appreciable polymerization even under our lower temperature cure conditions. Specifically, whereas 195°C for 15 hrs showed full COOMe equilibration and <10% polymer, the ϕ substituted monomers are all more than half polymerized after 15 hrs at 195° and were already showing significant amounts of polymer after only 8 hrs. Isomer equilibration seems to still run ahead of polymerization but the delineation is no longer as clear.

The higher temperature (250°C) cure for the ϕ isomers is also somewhat less tractable. After 2 hrs all of these samples showed no residual monomer, yet the approach to equilibrium after 1 hr was still incomplete. However, it is clear that the initial conversion of ϕ BN to (largely) ϕ VN has made samples arising from either of these two isomers have similar composition (analogous to Table V above). Other than this observation, there is still a great deal of ambiguity about the details of this polymerization vs isomerization question at 250°C.

The one point that does seem clear about our substituted monomers in general, is that both ϕ and COOMe substitution do substantially facilitate thermal polymerization. A qualitative summary of the data at 195°C indicates that after 15 hrs, parent(I) is less than 10% polymerized, while ϕ substitution results in greater than 2/3 polymer. At 250°C, parent is less than 1/3 polymerized in two hrs., while COOMe is 50%-80% polymer and ϕ is >90% polymer. These numbers are all very crude and are currently being refined, but they do represent clear trends.

While only preliminary results are available on the curing of the benzo compound (IV), a comment on those experiments is in order. Differential Scanning Calorimetry of IV (ref. 5) gives strong indication of significant thermal activity above 250°C. We find that our crude measures of polymerization activity both by NMR and GPC are consistent with the contention that IV polymerizes about as readily as I both in the 200°C and 250°C experiments. The nature of the polymers formed from IV in experiments at both 250°C and 282°C are currently under investigation.

It should be pointed out that while a great deal of current work reinforces the notion that the retro Diels Alder of norbornenyl endcaps is crucial to the behavior of PMR-15 (ref 6), our data seems not to require such chemistry for polymerization to occur. Two facts support this conclusion. Firstly, the benzo system (IV) which is incapable of retro Diels Alder chemistry seems to polymerize as readily as the parent model compound. Secondly, while we know that our vinyl substituted monomers undergo isomerization by retro Diels Alder with comparable ease to the isomerization of the parent compound, they still polymerize significantly more easily. Both these observations suggest that while retro Diels Alder is certainly occurring in PMR solutions, it may not be at the heart of the polymerization activity of these systems. We are continuing to explore this question.

REFERENCES

- (1) Paquette, L. A.; Cottrell, D. M.; Snow, R. A.; J. Am. Chem. Soc. (1977) 99, 3723.
- (2) Riemschneider, R.; Nehrin, R. Monatsh. Chem. (1960), 91, 829.
- (3) Grunewald, G. L.; Davis, D. P.; J. Org. Chem. (1978), 43 3074.
- (4) Ganter, C.; Scheidegger, W.; Roberts, J. D. J. Am. Chem. Soc. (1965), 87, 2771.
- (5) The assistance of Dr. Richard Lauver, NASA Lewis Research Center, in obtaining these and other DSC measurements, is gratefully acknowledged.
- (6) Wong, A. C.; PhD Thesis, Case Western Reserve University (1979) and references therein.

- 07

ALL-AROMATIC BIPHENYLENE END-CAPPED POLYQUINOLINE AND POLYIMIDE MATRIX RESINS

John P. Droske[†] and John K. Stille
Colorado State University

William B. Alston
National Aeronautics and Space Administration
Lewis Research Center

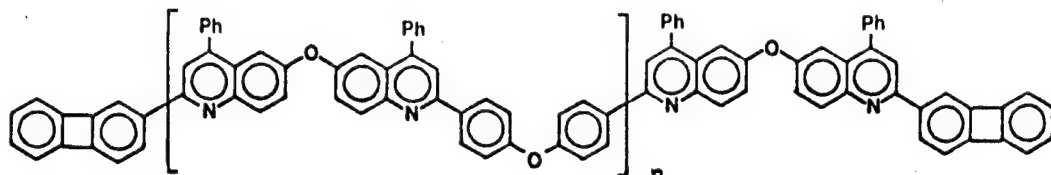
A promising approach to the processing of thermally stable polymers is the use of oligomeric pre-polymers containing reactive end-groups which undergo crosslinking/chain extension during processing and post-cure. Unfortunately, end-capped pre-polymers generally afford processed materials which show lower retention of properties for extended periods at high temperatures than would be expected had an all-aromatic, high molecular weight polymer been employed. Since the decreased thermo-oxidative stability is partly attributable, in some cases, to the use of aliphatic reactive end-groups (ref. 1), end-groups which afford more thermally stable structures are desired.

Biphenylene is an especially attractive reactive end-cap for high performance composite resins due to its all-aromatic structure. Biphenylene undergoes thermolysis above 350°C to afford tetrabenzocylooctatetraene (tetraphenylene), aromatic polymer, or stable aromatic compounds depending on the reaction conditions (ref. 2 and fig. 1). Thus, any structure formed as a result of the thermolysis of a biphenylene unit in a thermally stable polymer would be expected to maintain the all-aromatic character and high temperature performance of the polymer. The temperature necessary for the ring opening reaction can be lowered by the addition of appropriate transition metal catalysts, such as (NBD Rh Cl)₂ and (PPh₃)₂ Ni(CO)₂ which are known to open strained cyclic hydrocarbons by an oxidative addition mechanism (ref. 3).

RESULTS AND DISCUSSION

Neat Resin Properties

Of the various polyquinolines that have been prepared (ref. 4), the ether-ether linked polyquinoline showed the greatest promise as a laminating resin due to its good solubility in common organic solvents (e.g. CHCl₃) and its relatively low



[†]Present Address: Department of Chemistry
University of Wisconsin-Stevens Point

Tg (266°C). We envisioned that the use of an oligomeric ether-ether linked poly-quinoline would give a most processable thermoplastic resin, which could be converted to a thermosetting resin with a high Tg after processing by reaction of the biphenylene end-groups. Since it is desirable to use the least amount of the biphenylene end-cap possible (functionalized biphenylenes are only prepared with considerable difficulty), a series of biphenylene end-capped oligomeric polyquinolines having various degrees of polymerization were prepared.

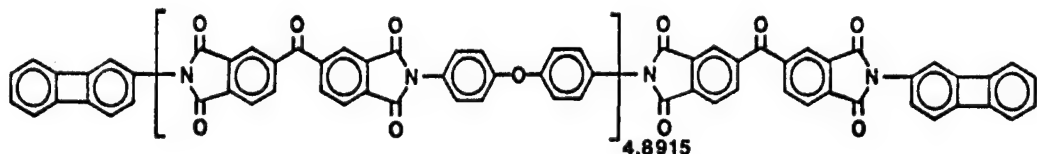
The neat resins, containing 2.5 wt% $(Ph_3P)_2Ni(CO)_2$, were melt pressed into thin films at 325° under 5000 lb. load for 15 minutes. All films after processing were insoluble (24 hours in $CHCl_3$) and had Tg's of 235°- 243°C. Young's modulus above Tg increased by an order of magnitude due to the crosslinking (Table 1). It was surprising that the Tg as well as the mechanical properties above Tg after processing were independent of the degree of polymerization and thus, the concentration of biphenylene end-caps. The results suggested that a limited and approximately equal amount of crosslinking was occurring in each of the three samples. As a control, phenyl end-capped polyquinolines of $\overline{DP} = 11$ and $\overline{DP} = 22$ were prepared and melt processed in the presence of the Ni° catalyst under the same conditions. The $\overline{DP} = 11$ material had very poor film qualities whereas the $\overline{DP} = 22$ material processed into a good quality, transparent film. However, both samples after processing were completely soluble in $CHCl_3$ and showed no increase in Tg indicating that no cross-linking/chain extension occurred in the absence of the biphenylene end-cap.

Thermal gravimetric analysis of melt pressed film samples of biphenylene end-capped polyquinoline ($\overline{DP} = 22$) containing 2.5 wt% $(PPh_3)_2 Ni(CO)_2$ showed breaks in air and nitrogen of 535°C and 570°C, respectively. These values are comparable to those obtained with film samples of high molecular weight polyquinolines cast from solution. However, oxidative isothermal aging at 300°C for 100 h showed 3% weight loss for the melt pressed film of biphenylene end-capped polyquinoline whereas the high molecular weight polyquinoline film showed 0% weight loss during the same aging.

Composite Properties

Graphite-reinforced composites were prepared from biphenylene end-capped poly-quinoline of $\overline{DP} = 22$. This degree of polymerization was considered to be an optimum of processability with a minimum incorporation of the biphenylene end-cap since no gains were realized when a lower degree of polymerization polyquinoline (containing a corresponding higher concentration of the biphenylene end-cap) was used. Pre-pregs were prepared by brush-coating a chloroform solution of the polymer onto either unidirectional Celion^R - 6000 graphite fiber or Celion^R - 3000 graphite cloth. When the Ni° catalyst was used, processing was effected at 625°F (330°C) under 1500 psi for 2 hours. The uncatalyzed laminates were processed at 735°F (391°C) under 2000 psi for 3 hours, the higher temperature being necessary to effect the uncatalyzed ring opening of biphenylene. In both cases high quality void-free laminates were prepared but due to the relatively flexible polymer backbone and the moderate degree of crosslinking attributable to the biphenylene end-cap, thermoplastic breaks during room temperature interlaminar shear were observed. Furthermore, only 25% of the initial room temperature interlaminar shear strength was retained after oxidative aging at 650°F (343°C) for 50 h, even though the composite weight loss was only two percent during the aging.

Using the PMR (polymerization of monomer reactants) approach (ref. 5), unidirectional Celion^R - 6000 graphite fiber was impregnated with a methanolic solution of the diester of 3, 3', 4, 4' - benzophenonetetracarboxylic dianhydride, oxydianiline, and 2-aminobiphenylene in a calculated stoichiometry to give DP = 4.8915 (FMW = 3000). The pre-preg showed desirable tack and drape. The pre-preg was staged at



400°F (204°C) for 1 hour and processed at 735°F (391°C) under 1500 psi for 3 hours. (The Ni° catalyst was not used since it was insoluble in the methanolic monomer solution.) The resultant 9-ply laminates were of high quality and had low void content but showed thermoplastic breaks during interlaminar shear testing even though the Tg of the composite (337°C) was well above the test temperature (316°C). In an effort to increase the crosslink density, 3, 5 and 10 mole % of the oxydianiline monomer was replaced with the appropriate amount of the triamine, 3, 3', 5' - triaminobenzophenone. Composites in which 3 and 5 mole % of the diamine was replaced with the triamine showed sufficient crosslink density as evidenced by true thermoset breaks during interlaminar shear testing at 600°F (316°C, Table 2). However, photomicrographs of the composites after oxidative isothermal aging at 600°F for 50 h showed the presence of voids. Polyimide composites isothermally aged at 650°F (343°C) under a nitrogen atmosphere for 71 h did not show degradative void formation.

CONCLUSION

Biphenylene end-capped polyquinoline and polyimide resins afforded low void content graphite-reinforced composites with good initial properties. However, with both resins, rapid degradation occurred during oxidative isothermal aging at elevated temperatures. The degradation was not observed during isothermal aging under a nitrogen atmosphere which suggests that the biphenylene end-cap (or the resulting crosslink/chain extension structures) are not particularly thermooxidatively stable. The nature of the thermooxidative instability is currently under investigation.

REFERENCES

1. Alston, W. B.: Characterization of PMR-15 Polyimide Resin Composition in Thermooxidatively Exposed Graphite Fiber Composites. NASA TM-81565, 1980 and Proc. of the 12th SAMPE National Technical Conference, October, 1980.
2. a. Lindow, D. F.; Friedman, L. J. Am. Chem. Soc. 1967, 89, 1271.
b. Friedman, L.; Rabideau, P. W. J. Org. Chem. 1968, 33, 451.
c. Friedman, L.; Lindow, D. F. J. Am. Chem. Soc. 1968, 90, 2324.
3. a. Cassar, L.; Eaton, P. E.; Halpern, J. J. Am. Chem. Soc. 1970, 92, 3515.
b. Gassman, P. G.; Reitz, R. R. J. Am. Chem. Soc. 1973, 95, 3057.
c. Bishop, K. C. Chem. Rev. 1976, 76, 461.
d. Stille, J. K.; Lau, K.S.Y. Accounts of Chemical Research 1977, 10, 434.
4. Stille, J. K. Macromolecules 1981, 14, 870.
5. Serafini, T. T.; Delvigs, P.; Alston, W. B.: PMR Polyimides - Review and Update. NASA TM-82821, 1982 and Proc. of the 27th National SAMPE Symposium and Exhibition, May, 1982.

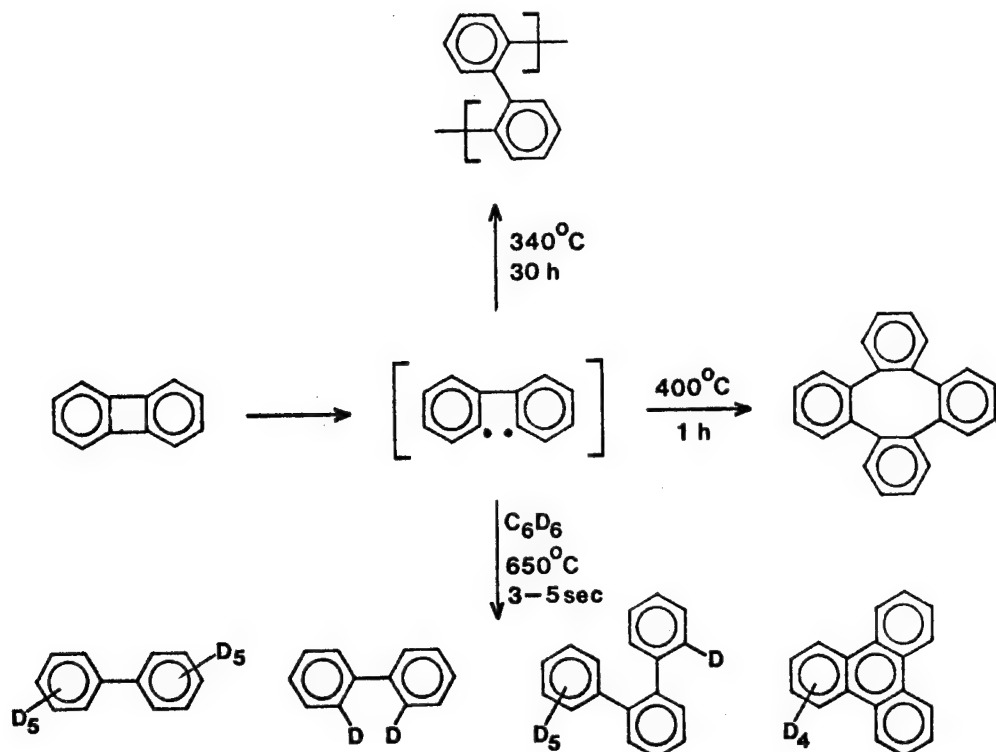


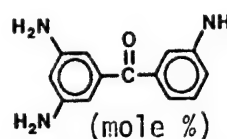
Figure 1. The products of the pyrolysis of biphenylene under various conditions.

Table 1. Biphenylene End-Capped Polyquinoline.

Neat Resin Processing						
325°C, 500 psi, 15 min; (Ph ₃ P) ₂ Ni(CO) ₂						
DP	Wt % biphenylene	Tg (°C) before processing	Tg (°C) after processing	ΔTg	Solubility (CHCl ₃ , 24h)	E' above Tg (dynes/cm ² @ T° ^o C)
3	23	153	235	+82	26%	-----
11	7.5	212	243	+31	i	1.4 x 10 ⁸ (285-335°C)
22	3.6	232	243	+11	i	1.0 x 10 ⁸ (291-330°C)
22*	0	232	232	0	s	-----

*phenyl end-cap

Table 2. Biphenylene End-Capped Polyimide/Celion^R-6000 Unidirectional Graphite Composite.

 (mole %)	POST-CURE	Tg (°C, TMA) after pc	RT	ILSS 600°F (psi)	% wt loss 48 h/600°F
0	150 h/600°F	337	14370	7098 pc*	1.4
3	14 h / 650°F	325	12261	7316 pc	-
5	47h / 600°F	328	13294 pc	6842 pc	1.2
10	43h / 600°F	310	9628 pc*	5422 pc*	1.7

* Thermoplastic break

-08

EVALUATION OF A HIGH TEMPERATURE ADHESIVE FOR FABRICATING
GRAPHITE/PMR-15 POLYIMIDE STRUCTURES

S.G. Hill and J.B. Cushman
Boeing Aerospace Company

Tests were conducted to measure shear strength, shear modulus and flatwise tensile strength of A7F (amide-imide modified LARC-13) adhesive system. An investigation was also conducted to determine the effect of geometric material parameters, and elevated temperature on the static strength of "standard" joints. Single-lap and double-lap composite joints, and single, double and step lap composite to metal joints were characterized. A series of advanced joints consisting of preformed adherends, adherends with scalloped edges and joints with hybrid interface plies were tested and compared to baseline single and double-lap designs.

INTRODUCTION

Graphite/polyimide composites have shown potential for use as a structural material at elevated temperatures on advanced aerospace vehicles. Unlike typical graphite/epoxy systems which are limited to 300° - 350°F operating range, graphite/polyimide systems can operate in the 500 - 600°F range. This characteristic makes graphite/polyimide systems attractive for use in high Mach number missiles and space shuttle type transportation systems where, depending on configuration, location, and thermal protection system, temperatures greater than 500°F could be experienced.

To evaluate a high temperature adhesive for fabricating graphite/PMR-15 polyimide structures, a test program was conducted to evaluate A7F polyimide adhesive for bonding metal-to-metal, metal to composite, and composite-to-composite joints. The A7F adhesive was formulated by Boeing using LARC-13 adhesive furnished by NASA Langley. U.S. Polymeric, Inc. coated the A7F adhesive on 112 E-glass/A-1100 scrim to make film adhesive. Three environmental conditions for the adhesive tests were examined: 1) as cured/past cured, 2) soaked for 125 hours at 589°K (600°F) in a one (1) atmosphere environment (air), and thermally cycled 125 times in a temperature range from 116°K to 589°K (-250 - 600°F). Test for the standard joints and advanced joints ranged from 116K - 561K (-250°F - 550°F).

MATERIAL

The high temperature adhesive characterized in this study is designated A7F. A7F is a 50:50 resin solids copolymer blend of LARC-13 adhesive (supplied by NASA, Langley) (Ref. 1) and AMOCO's AI 1130 Amide-Imide. Sixty percent by weight aluminum powder and 5% by weight Cab-O-sil are added. The adhesive was applied to 112E glass/A-1100 scrim to form a .25mm (.01 in.) thick adhesive film.

The high temperature composite materials characterized under the study were laminates of graphite/polyimide tape materials. Based on previous experience from the CASTS* program research, Boeing and NASA chose the celion/PMR-15 material system. The graphite fiber was CE 3000, with NR150B2G polyimide sizing. Preimpregnated tape was procured from U.S. Polymeric, Inc. to a material specification contained in Reference 2. Gr/PI and S-glass/PI fabric used in the advance joints were preimpregnated in the Boeing Materials Technology Laboratory utilizing resin from the same batch that was used to impregnate the tape material. The titanium used was Ti-6Al-4V (standard) per MIL-T-9046, Type III, Composition C.

SPECIMEN FABRICATION - ADHESIVE TESTS

Specimens for the adhesive test were fabricated in the laboratory using standard laboratory practices. Titanium surfaces were chromic acid anodized and primed with a dilute solution of the A7F adhesive. Specimens were assembled to the configurations in Figures 1-3 using A7F film adhesive and cured using the procedures in Reference 2.

SPECIMEN FABRICATION - BONDED JOINT TESTS

The composite adherends were laminates of graphite fibers impregnated with PMR-15 resin. The fibers were sized with NR150B2G. Special requirements were imposed upon the prepreg supplier (U.S. Polymeric, Inc.) that limited the size of resin batches mixed to 24 lb. maximum. This was to limit the exothermic reaction during mixing. Prepreg was fabricated from one fiber lot. Because of limits on resin batch size, more than one batch of resin was needed to make the required amount of prepreg; therefore, quality control tests were conducted on any prepreg roll that was made from a different resin batch. Chemical characterization tests were also conducted using high pressure liquid chromatography, gas chromatography, mass spectroscopy, infrared spectroscopy, and thermal gravametric analysis.

Panels fabricated from the prepreg were cured according to the cure cycle in Reference 2. All panels were non-destructively inspected. The procedure used was C-scan at 5-6 MHz sweep at 4 db loss above the water path. Laminates containing voids or other defects greater than .06 in² were rejected for use in this study. Once the panel had passed C-scan, the panels were ready for preparation for bonding. The panels were primed and bonded with A7F adhesive per the procedure in Reference 2.

Effect of Conditioning on Specimens

Three environmental conditioning cycles were used in this study. Conditioning code numbers were assigned to the specimens as follows:

Condition 1 As cured/post cured

*Composites for Advanced Space Transportation Systems (Contract NAS1-15009 & NAS1-15644).

Condition 2 Aged for 125 hrs and at 589K (600°F) in a 1 atm environment (air)

Condition 3 Thermally cycled 125 times -116K (-250°F) -- 589K (600°F) in an one (1) atmosphere environment (air). The cryogenic temperature of -250°F was held for one half (1/2) hr and the maximum temperature was held for one (1) hour per cycle.

The conditioning cycles did not exhibit a significant effect on the specimens. The specimens tested at the 561K (550°F) displayed better properties than specimens tested at 116K (-250°F).

Adhesive Test Results

Average test results for the 12.7 mm (0.5 in.) single lap shear, "thick adherend" shear and flatwise tension tests are shown in Table 6-1 for the various conditionings and test temperatures.

Since the "thick adherend" test specimen has lower peel stresses than the standard single lap specimens, it was expected that the shear strengths from this test would be higher than those from the titanium lap shear (ASTM D 1002) tests. Results for cured/post-cured specimens at 294K (70°F) and 561K (550°F) are higher for the ASTM D 1002 procedure than for the "thick adherend" procedure. ASTM D 1002 results for aged specimens were slightly higher than "thick adherend" results at 561K (550°F).

There is no known explanation for these anomalies other than possible material and processing variations. C-scans of the bond lines showed no defects. Adhesive thicknesses could have been different for the two specimen configurations. Also there may have been some edge effects during the curing or aging. The thick adherend specimens were conditioned as a single plate approximately 508 mm (20 in.) wide and then cut into specimens. The ASTM D 1002 specimens were made from standard titanium "finger" blanks 25.4 mm (1.0 in.) wide which may have contributed to edge effects.

The average shear modulus from the "thick adherend" tests was 58 MPa (8000 psi) with the data showing drops in moduli at both cryogenic and elevated temperature with respect to room temperature. The room temperature aged specimens exhibited a bimodulus behavior. Results from the same tests show a decrease in ultimate shear strain with increasing temperature.

Flatwise (out-of-plane) tension tests were conducted on cured/post-cured specimens that had stainless steel rods, while the aged specimens had titanium rods. All specimens failed cohesively. Test results show a drop in strength with an increase in temperature. On the average, flatwise tension strength for A7F adhesive are twice that for a Celion 3000/PMR-15 laminate (Ref. 3). This indicates that joints with strengths governed by peel failures will fail in the laminate rather than in the adhesive.

Results of coefficient of thermal expansion (CTE) tests on A7F adhesive conducted under contract TASK 1.2.1 (Ref. 3) are shown in Figure 4. Data show a significant drop in CTE due to aging.

Standard Joint Test Results

Test results obtained for the single- and double-lap joints had a significant amount of data scatter. Therefore, comparisons between joint types are based on average failure loads only.

In most cases the "Gr/PI-Gr/PI" joints exhibited an intralamina failure mode caused by peel stresses in the composite adherends as shown in Figure 5. This failure mode consists of a failure within a ply, as opposed to an interlamina mode where the failure occurs between plies. For both single- and double-lap joints, the intralamina failure occurred in the ply nearest the joint interface, with the failure occurring for the double-lap joint in the inner adherends.

The "Gr/PI-titanium" specimens also exhibited intralamina and/or interlamina failures in the plies near the joint interface; however, some specimens also had adhesive failures over a portion of the joint. Evidence of partial adhesive failure occurred at all test temperatures but was predominant at the elevated temperature.

Failure loads versus lap length for single- and double-lap "Gr/PI-Gr/PI" and "Gr/PI-titanium" joints are shown in Figures 5 and 6 respectively. As expected there was a general increase in failure load with increasing lap length, with the loads appearing to approach asymptotes.

Results for the "3-step" symmetric step-lap joints are shown in Figure 8. As was expected there is a strong temperature dependence in the strength of these joints. This is attributable to the difference in coefficients of thermal expansion between the Gr/PI and titanium adherends and the elevated cure temperature, which result in residual thermal stresses in the joint and thus decreased strength at lower temperatures.

A comparison of "Gr/PI-titanium" double lap joints with the "3-step" symmetric step-lap joint shows them to be about equal in strength for the lap lengths tested. At these load levels a double-lap joint would be the better design solution because of simplicity in manufacturing (other design constraints such as fatigue resistance, surface smoothness or weight may not allow this). Higher loads would dictate a symmetric step-lap (with more than 3 steps) or a scarf joint since increasing the lap length of a double-lap joint would not result in any significant additional strength.

In general, failure loads for the standard joints increased with increasing temperature, with the change in loads from cryogenic to room temperature being less than the change in loads from room to elevated temperature.

The maximum joint loads achieved in the standard joint test program are summarized in Figure _____. The maximum load achieved for a single-lap joint (25.4 mm (1.0 in.) wide) was 9.71 kN (2184 lb) while for the double-lap and step-lap joints (25.4 mm (1.0 in.) wide) it was 24.64 kN (5540 lb) and 22.89 kN (5147 lb) respectively. All three maximums occurred at a test temperature of 561K (550°F). Maximum loads shown should not be construed to be the maximum obtainable. Other layups or joint configurations for a particular joint type could have resulted in higher failure loads.

Advanced Joint Test Results

Results of the preformed adherend tests demonstrate that preforming the adherends of a single-lap joint gives a significant increase in load carrying capability. Figures 11 and 12 show the effect of preforming for temperatures of 294K (70°F) and 561K (550°F). The average failure load for each lap length is normalized by the average failure load for the baseline (straight adherends) configuration (from the advanced joint test matrix) with the same lap length. In all cases, preforming the adherends increased the average failure load. Increases ranged from 92% to 262% at 294K (70°F) and from 46% to 234% at 561K (550°F). No comparisons were made at 116K (-250°F) because there was no baseline data at this temperature; however, results similar to the 294K (70°F) tests would be expected.

In contrast to the standard joints, the preformed adherend specimens had failure loads at elevated temperature which were in all cases lower than those at room temperature. The results for the 116K (-250°F) specimens were not as consistent; with some values falling above the room temperature loads, some values between the room and elevated temperature loads and in some values below the elevated temperature failure loads. These results may be in part due to the large scatter in the failure load data.

Several failure modes were exhibited by the preformed adherend specimens as outlined in Table 2. The failure modes changed from a purely intralaminar peel failure in the ply next to the joint interface, to severe delaminations and peel failures through the adherend thickness, to a failure outside of the joint at the preform bend as the lap lengths and preform angles increased. This change in failure modes may explain why the longer lap length specimens showed smaller improvements in strength over the baseline joints than the shorter lap length specimens (see Figs. 11 and 12). This result was the reverse of that expected from the results of testing by Sawyer and Cooper (Ref. 4).

Scalloping the single-lap joints gave a slight drop in failure load while scalloping the double-lap joints resulted in an average increase of 17% in failure load. The difference between these two cases can be attributed to the different failure mechanisms of a single versus double-lap joint. The failure in a single-lap joint is governed by both the moment introduced in the joint and by peel stresses. The failure in the double-lap joints is governed primarily by the peel stresses in the inner adherend at the end of the lap. Since scalloping the ends of the adherends was designed to reduce the peel stresses at the end of the lap, it would be expected that the double-lap joints would be more affected by scalloping than single-lap joints.

Failure loads versus lap length for the Gr/PI fabric interface, and S-glass fabric interface specimens tested at room and elevated temperature are compared to baseline data in Figures 13 and 14. Placing fabric interfaces, S-glass/PI and Gr/PI, between the single-lap joint adherends resulted in 28% to 76% increases in average failure load (see Table 8-2) except for the 25.4 mm (1.0 in.) lap length S-glass/PI specimens, which showed no significant change in strength. The increase in strength can be attributed to a reduction in peak shear and peel stresses due to the "softer" interface materials. Most of the fabric interface specimens delaminated between the two fabric plies, as opposed to delaminating in the adherends as was the case for the standard joints.

The temperature dependence of the joint strengths for the scalloped adherend and fabric interface joints was less than that for the standard joints. In general, there was no significant difference between the failure loads for the room and elevated temperature cases for these joints, with the average difference being a 5% increase from room to elevated temperature. For the few cases where there was a significant difference the elevated temperature loads were greater than the corresponding room temperature failure loads.

CONCLUSIONS

1. A7F maintains shear strength of 8.3 MPa (1200 psi) after exposure to environmental conditions.
2. A7F maintain flatwise tension strength above 11.0 MPa (1600 psi) at 561K (550°F).
3. CTE data for A7F adhesive shows a significant drop after aging.
4. Single-lap joints with preformed adherends showed a large increase in strength.
5. Adding a fabric interface between single-lap joint adherends, either S-glass/PI or Gr/PI, results in a significant increase in joint strength.
6. Scalloping the adherends of a single-lap joint does not significantly improve joint strength.
7. Graphite polyimide joints will carry loads of the magnitude expected for advanced aerospace vehicles at temperatures from 116K (-250°F) to 561K (550°F).
8. The weak link in joint strength was the low transverse tension strength of the composite.

REFERENCES

1. St. Clair, T. L.; and Progar, B. J.: LARC-13 Polyimide Adhesive Bonding. SAMPLE Series Volume 24--The Enigma of the Eighties: Environment, Economics, Energy. San Francisco. May 1979, pp. 1081-1092.
2. Sheppard, C. H.; Hoggatt, J. T.; and Symonds, W. A.: Quality Control Development for Graphite/PMR-14 Polyimide Composite Materials. NASA CR-159182, 1979.
3. Cushman, J. B.; and McCleskey, S. F.: Design Allowables Test Program, Celion 3000/PMR-15 and Celion 6000/PMR-15, Graphite/Polyimide Composites. NASA CR-165840, 1982.
4. Sawyer, James Wayne; and Cooper, Paul A.: Analysis and Test of Bonded Single Lap Joints with Preformed Adherends. AIAA/ASME/ASCE/AHS 21st Structures, Structural Dynamics and Materials Conference. May 1980, pp. 664-673.

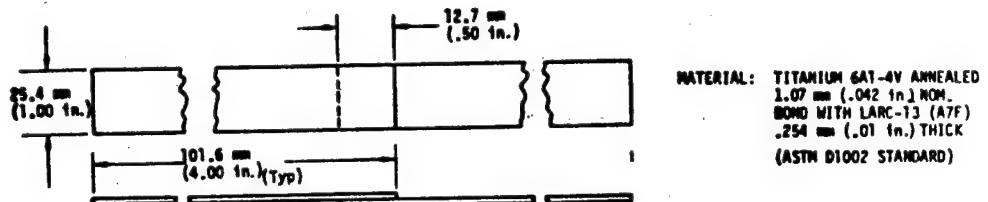


Figure 1: Titanium Single Lap Shear Specimen

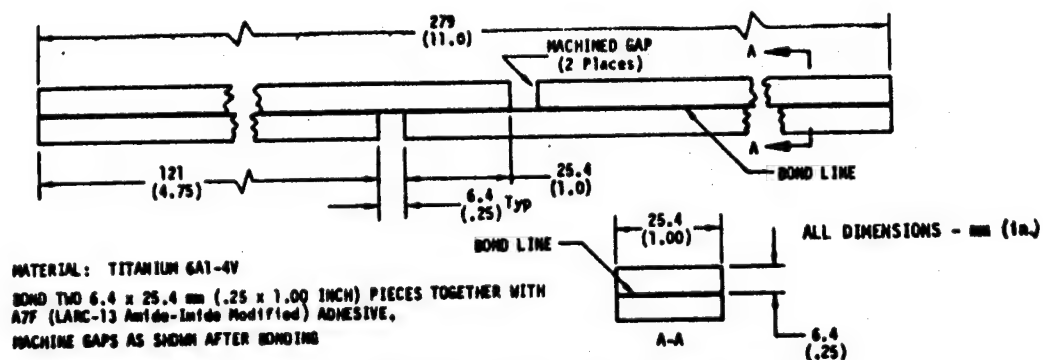


Figure 2: Thick Adherend Shear Test Specimen

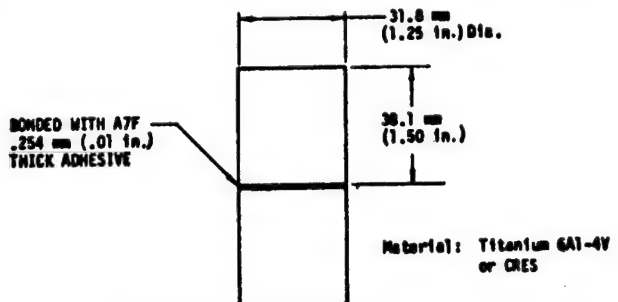


Figure 3: Flatwise Tension Adhesive Test Specimen

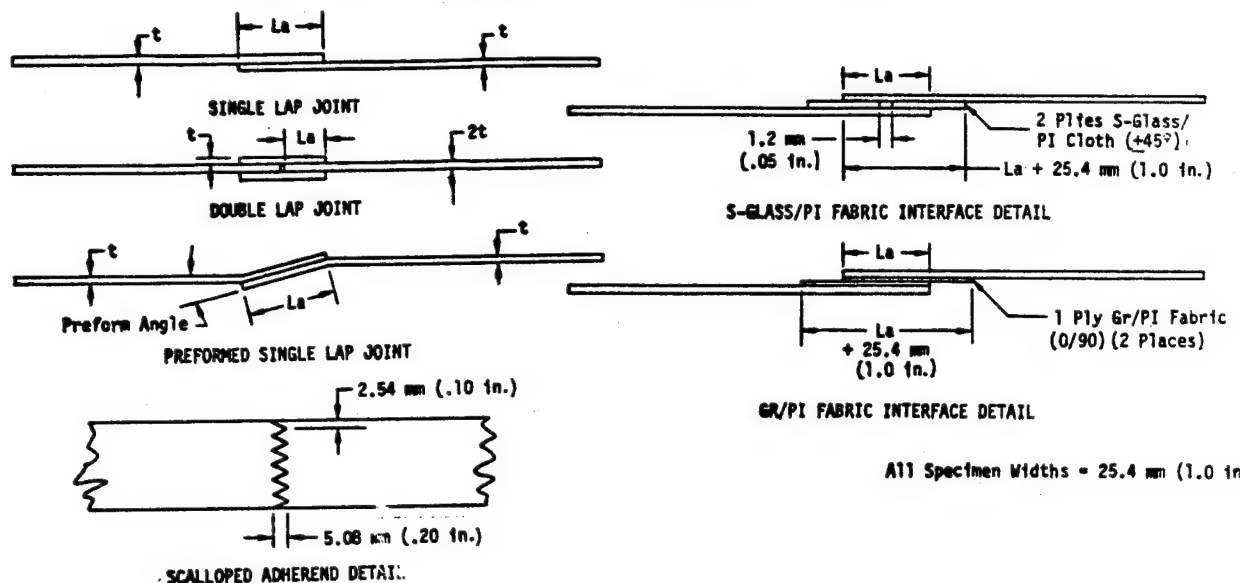


Figure 4: Advanced Joint Configurations

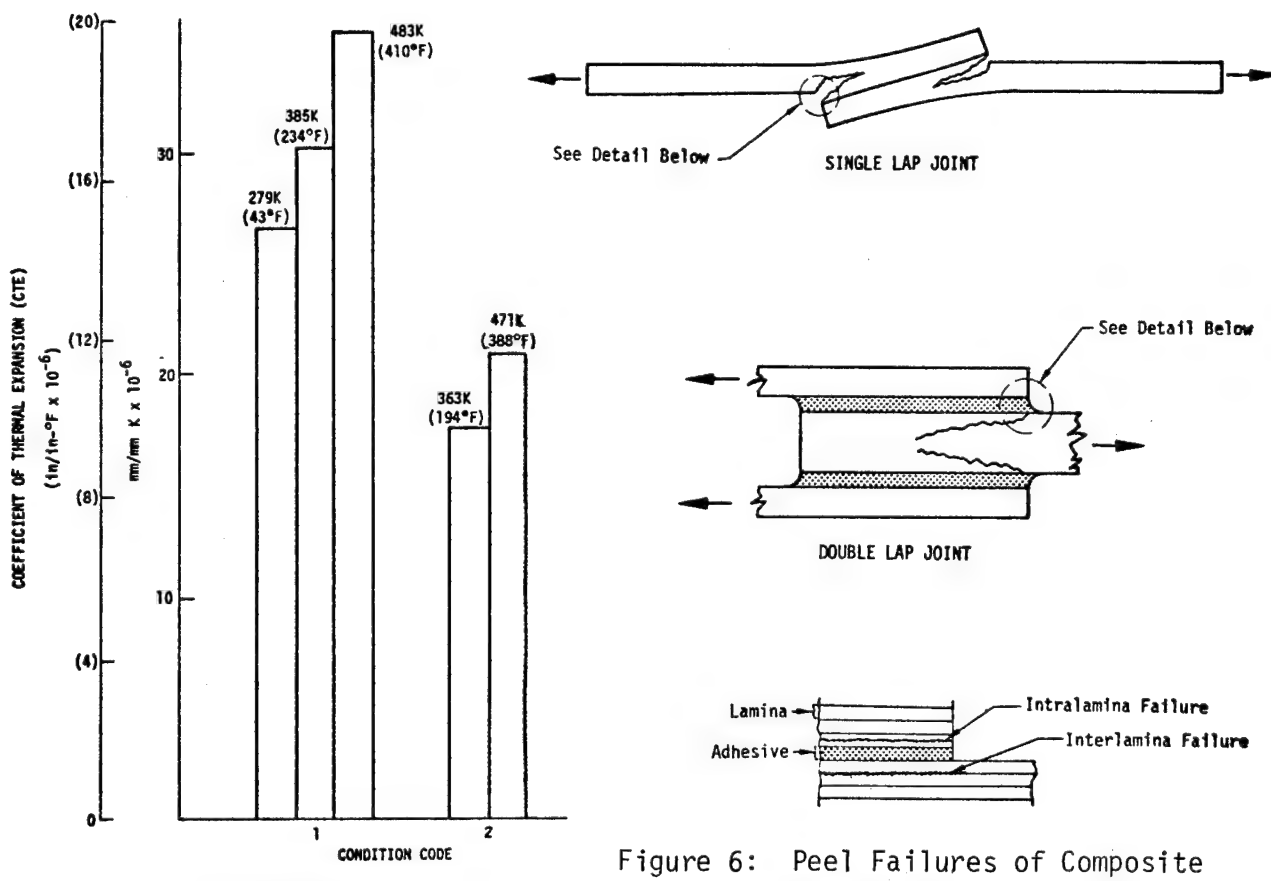


Figure 6: Peel Failures of Composite Bonded Joints

Figure 5: Coefficient of Thermal Expansion--"A7F" Adhesive

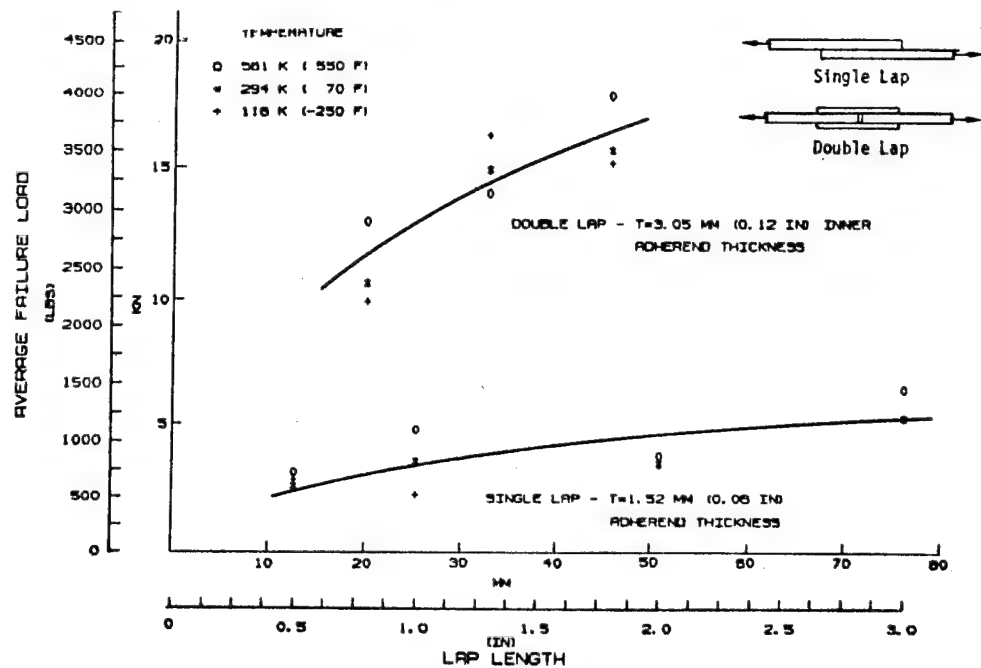


Figure 7: Comparison of Single- and Double-Lap Joints GR/PI to GR/PI Joints

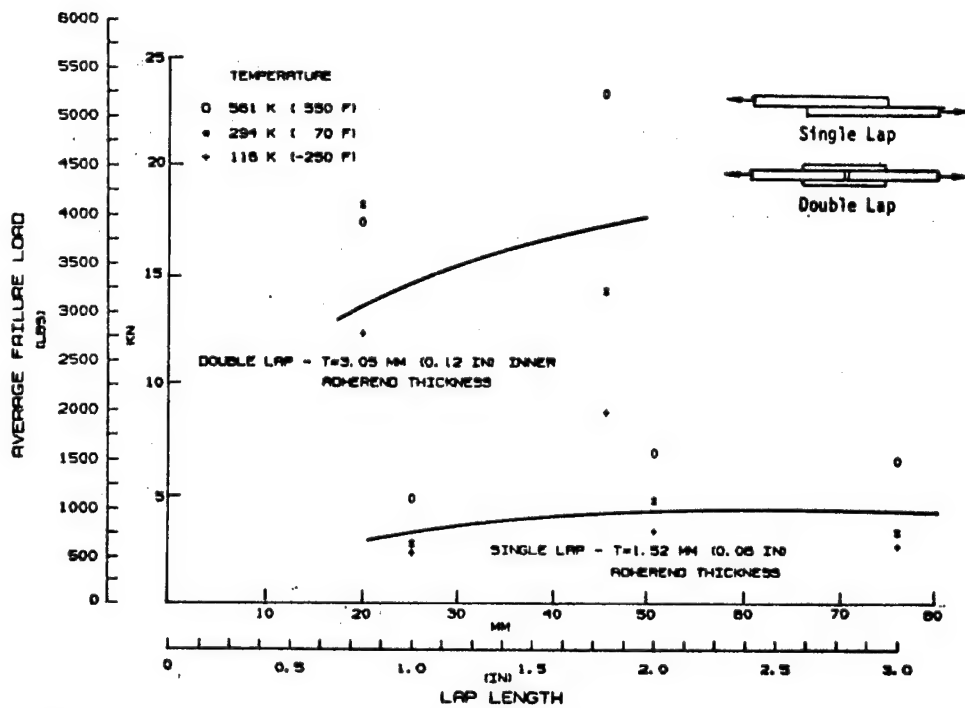


Figure 8: Comparison of Single- and Double-Lap Joints
GR/PI to Titanium Joints

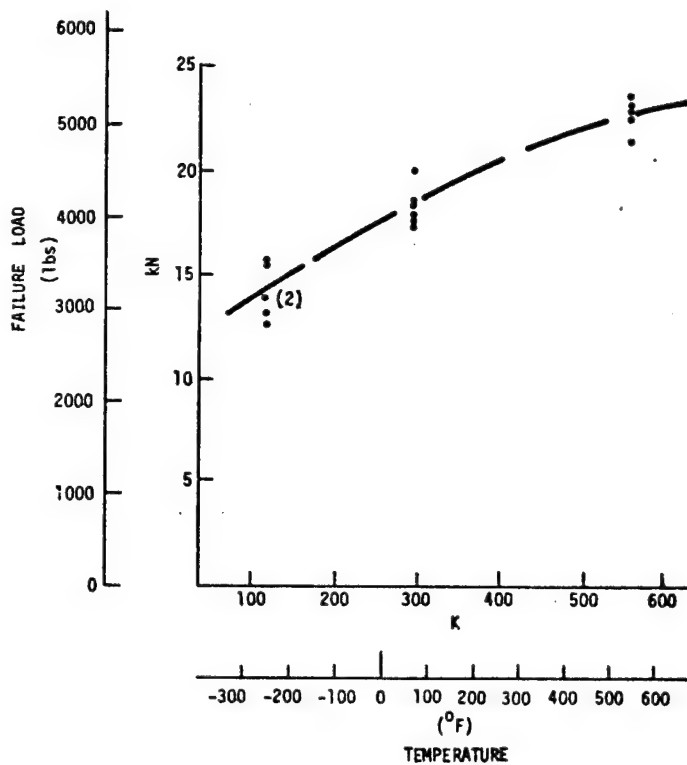


Figure 9: "3 Step" Symmetric Step-Lap Joint, GR/PI to Titanium

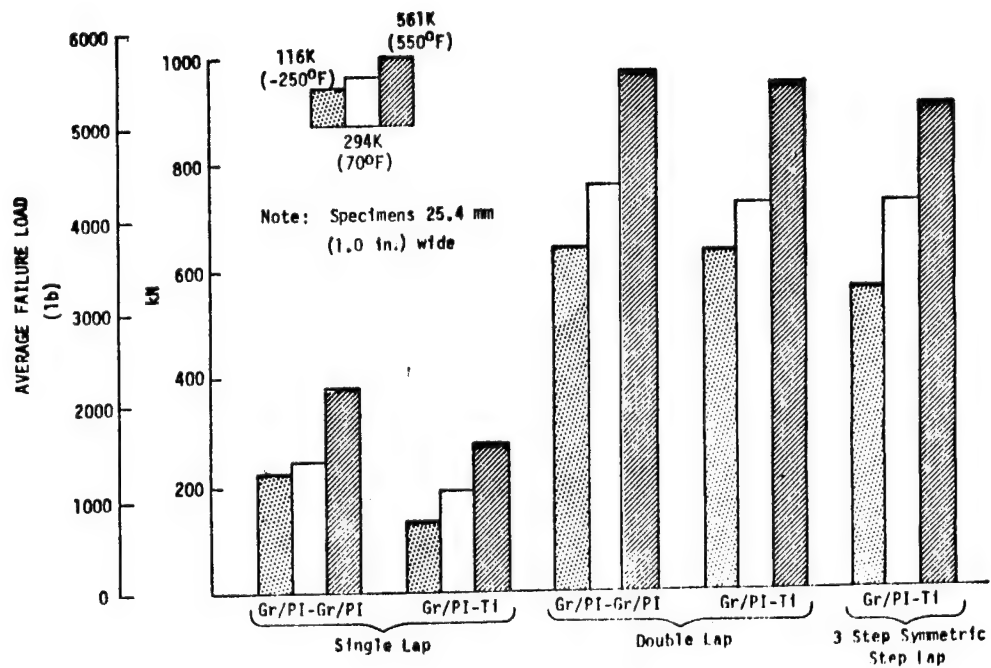


Figure 10: Maximum Joint Loads Achieved

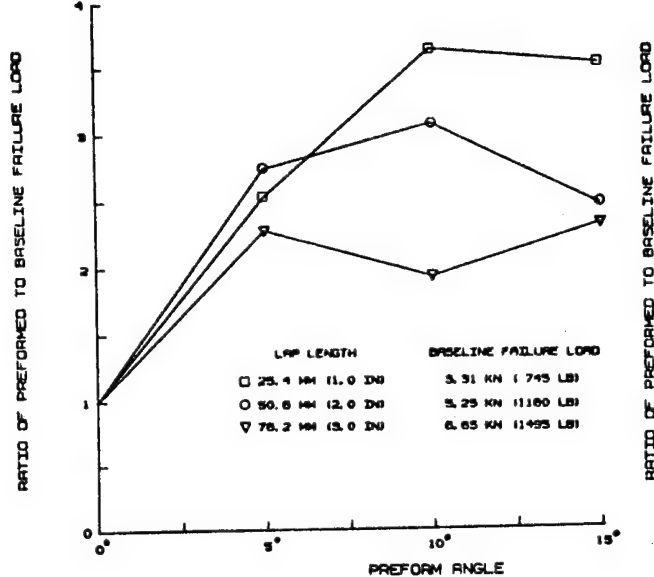


Figure 11: Effect of Preformed Adherends

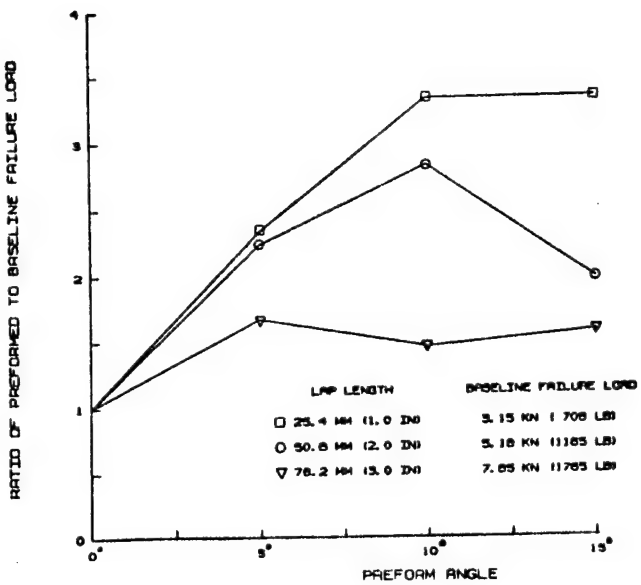


Figure 12: Effect of Preformed Adherends

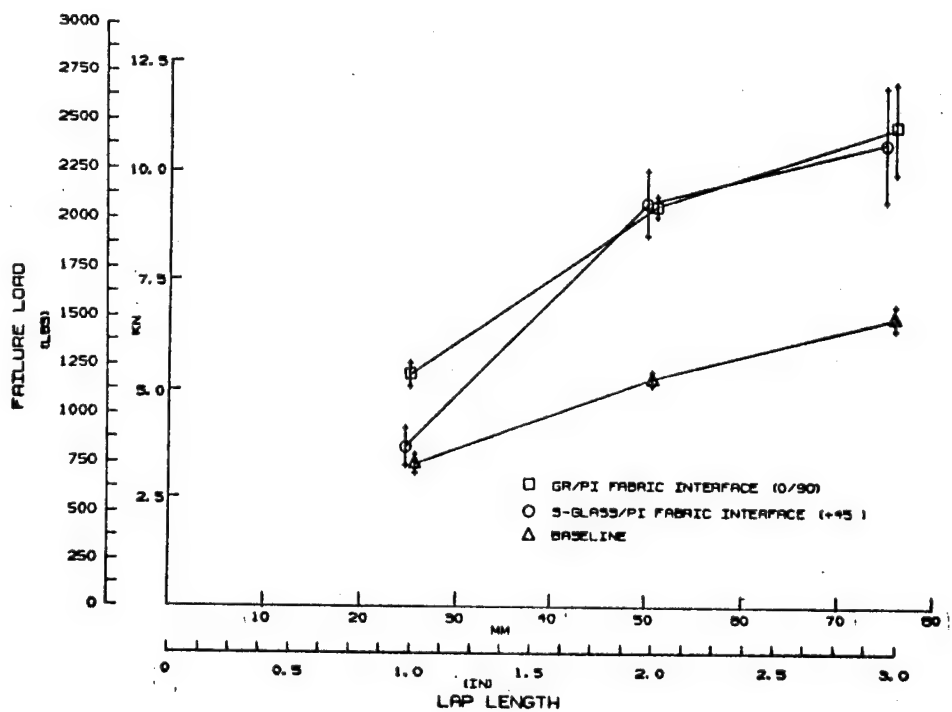


Figure 13: Effect of Fabric Interfaces - Single-Lap Joints

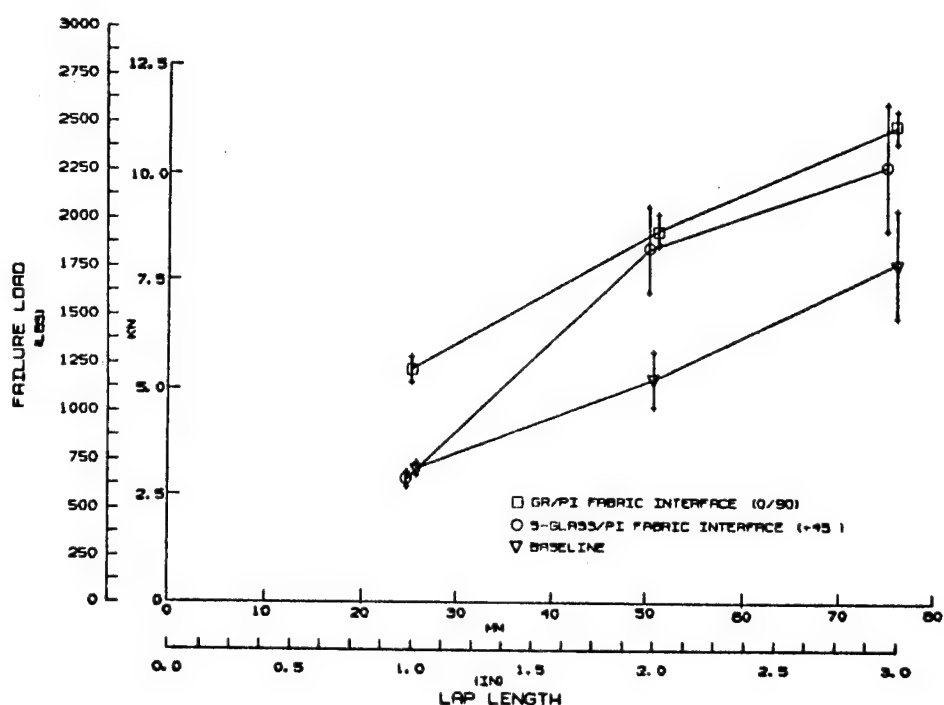


Figure 14: Effect of Fabric Interfaces - Single-Lap Joints

CONDITIONING	TEMPERATURE K	LAP SHEAR ASTM D 1002 SHEAR STRENGTH MPa	"THICK ADHEREND" TESTS			FLATWISE TENSION STRENGTH MPa
			SHEAR STRENGTH MPa	SHEAR MODULUS MPa	SHEAR STRAIN	
Cured/ Post Cured	116 294 561	20.7 19.67 13.53	22.57 16.72 8.79	61.83 70.37 45.82	.7085 .4000 .4276	55.01 22.58 11.65
Aged 125 hrs @ 589K (600°F)	116 294 561	14.75 14.11 14.34	21.21 16.09 13.33	40.72 79.92 Inft. 53.53 Sec. 52.70	.6305 .5263 .4459	45.15 27.37 22.10
Cycled 125 Times -116K (-250°F to 589K (600°F)	116 294 561	11.56 12.18 15.03	— — —	— — —	— — —	— — —

CONDITIONING	TEMPERATURE F	LAP SHEAR ASTM D1002 SHEAR STRENGTH psi	"THICK ADHEREND" TESTS			FLATWISE TENSION STRENGTH psi
			SHEAR STRENGTH psi	SHEAR MODULUS psi	SHEAR STRAIN	
Cured/ Post-Cured	-250 70 550	3003 2853 1963	3274 2425 1275	8968 10206 6645	.7085 .4000 .4276	7978 3275 1690
Aged 125 hrs @ 589K (600°F)	-250 70 550	2140 2047 2080	3076 2333 1933	5906 11592 Inft. 7764 Sec. 7643	.6305 .5263 .4459	6549 3970 3205
Cycled 125 Times - 116K (-250°F) to 589K (600°F)	-250 70 550	1676 1767 2180	— — —	— — —	— — —	— — —

Table 1: Average Test Results For A7F Adhesive

SPECIMEN CONFIGURATION	TEST NO.	LAP LENGTH mm (in.)	FAILURE MODE NUMBERS		
			116K (-250°F)	294K (70°F)	561K (550°F)
5° Preformed	1a 1b 1c	25.4 (1.0) 50.8 (2.0) 76.2 (3.0)	1 1 2	1 1 1	1 1 1
10° Preformed	2a 2b 2c	25.4 (1.0) 50.8 (2.0) 76.2 (3.0)	1 3 3	1 2 2, 3	1 2 3
15° Preformed	3a 3b 3c	25.4 (1.0) 50.8 (2.0) 76.2 (3.0)	1, 2 3, 4 4	1 3 4	1 3 1, 4

Failure
Mode No. Failure Mode

1. Intralamina failure in adherend first ply + adherend-adhesive interface failure
2. Interlamina failure in adherend + some tensile failures of individual plies
3. Interlamina failure through adherend + tensile failures of individual plies
4. Tensile failure of adherend at preformed bend

Table 2: Preformed Adherend Failure Modes

-09

NEW PROCESSABLE MODIFIED POLYIMIDE RESINS FOR
ADHESIVE AND MATRIX APPLICATIONS

David Landman
Hysen Division
The Dexter Corporation

A broad product line of bismaleimide modified epoxy adhesives which are cured by conventional addition curing methods are described. These products fill a market need for 232°C (450°F) service adhesives which are cured in a manner similar to conventional 177°C (350°F) epoxy adhesives. The products described include film adhesives, pastes and a primer. Subsequent development work has resulted in a new bismaleimide modified epoxy resin which uses an unique addition curing mechanism. This has resulted in products with improved thermomechanical properties compared to conventional bismaleimide epoxy resins. A film adhesive, paste and matrix resin for composites using this new technology is described. In all cases the products developed are heat cured by using typical epoxy cure cycles viz. 1 hour at 177°C (350°F) followed by 2 hours postcure at 246°C (475°F).

INTRODUCTION

Last year a broad product line of 232°-288°C (450-550°F) adhesives was described (ref. 1). These products process very easily using conventional epoxy curing conditions viz. 1 hour at 177°C (350°F) using minimum pressure (clamp or autoclave) followed by 2 hour postcure at 246°C (475°F). Two different chemistries have been used to develop these products although the base resin technology is bismaleimide modified epoxy. Table 1 summarizes some of the products which have been developed.

The "conventional BMI technology" in Table 1 refers to bismaleimide modified epoxy resins which are cured by addition methods as described in the literature (ref. 2). The "unique new BMI technology" in Table 1 refers to an addition curing mechanism which is not described in the literature and results in products with improved thermomechanical performance compared to other bismaleimide modified resins. We are still early in the development of a data base for these products, but from their neat resin properties, it is obvious that the unique new BMI technology has applicability to matrix resin for composites without attendant short out-life and volatiles/odor problems, as well as to adhesive applications.

The measurements and calculations were made in U.S. Customary Units.

RESULTS AND DISCUSSION

1. Hysol's Conventional BMI Technology Adhesives

The first film adhesive supported on a glass scrim fabric is EA9655. Table 2 shows some of its adhesive properties on various substrates. Some indication of thermal stability at 232°C (450°F) can be inferred from the tensile shear strength performance of EA9655 on aluminum substrates after 3000 hours at 232°C (450°F) as shown in Table 2. EA9655 has applicability in bonding honeycomb core materials and shows a moderate amount of peel strength (see Table 2).

The paste adhesives, EA9351 and EA9367 were developed for edge-filling and potting applications. EA9351 handles like a conventional epoxy paste which requires warming to about 49°C (120°F) for easy troweling. EA9367 is a syntactic paste version of EA9351 with a density of approximately 0.92 gm/cc. Table 3 shows some of the adhesive properties of these materials. Note that even with a cure of 2 hours at 177°C (350°F), EA9351 develops quite acceptable adhesive strength.

LR 100-581 was developed primarily as a protective coating which is applied by spraying. It is 20% by weight solids content, and is compatible with EA9655. Table 4 shows some of the properties of aluminum adherends treated with LR 100-581.

2. Hysol's Unique BMI Technology Adhesives

EA9673 is the designation for a film adhesive supported on a glass scrim fabric that is the unique bismaleimide modified epoxy which leads to improved thermomechanical properties. Table 5 shows some adhesive properties for EA9673 using different substrates. Basically, it gives good performance through the range 25°-287°C (77°-550°F). There also appears to be some limited strength characteristics at 360°C (680°F). In terms of thermal stability at 260°C (500°F) we have generated only one datum point after 700 hours. Further work on more suitable substrates is in progress. EA9673 also has remarkable outlife characteristics as shown in Table 6. A sample of the film adhesive was accidentally left out on a benchtop and showed no loss of tack after 27 days in the open environment. Testing was carried out to 48 days with no loss of tack and retention of adhesive properties (Table 6).

A paste adhesive based on the unique bismaleimide modified epoxy chemistry has also been developed. LR 100-637 is a room temperature trowelable paste which has low slump during cure. Table 7 shows the adhesive properties of this material which should have similar outlife characteristics as for EA9673. In addition, a core splice (LR 100-633) material which expands 2.5 to 3.0 :1 during cure has been developed. The room temperature tube shear strength for LR 100-633 is 11.0 MPa (1.6 ksi) when tested at room temperature. It would be anticipated that this strength would be maintained to 260°-287°C (500-550°F) based on results for EA9673 and LR 100-637.

3. Bulk Resin Properties of EA9655 and EA9673

The Tg values for both EA9655 and EA9673 are shown in Table 8. These values were determined by thermomechanical analysis (TMA) on a Perkin-Elmer analyzer and by dynamic mechanical analysis (DMA) using a DuPont 981 DMA. Experience has shown that the DMA data is usually more reliable than TMA. Wet data refers to boiling castings of EA9655 and EA9673 in water for two days, and then rapidly carrying out the appropriate test.

Figures 1 and 2 show rheometrics plots for EA9655 and EA9673. EA9655 has a minimum viscosity of 41.6 poise at 177°C (350°F) and EA9673 has a minimum viscosity of 1.9 poise at 143°C (290°F). A lower viscosity version of EA9655 can be formulated, depending on application requirements. From this rheometrics data it is evident that EA9673 resin would be suitable for making prepreg materials.

Dog bone specimens for bulk tensile properties of EA9655 and EA9673 using the ASTM D638 testing procedure were prepared. Table 9 shows ultimate tensile strengths, modulus and elongation for these materials. As further confirmation of the EA9673 tensile property data, the variation of Young's modulus with temperature, both dry and wet, is shown in Figures 3 and 4. EA9673 appears to have dry properties suitable to at least 260°C (500°F) and wet properties to 210°C (410°F).

4. Matrix Resins

The resin used to make prepreg materials from EA9673 film adhesive is designated EA9102 as shown in Table 1. The chemistry of EA9102 is bismaleimide modified epoxy with the unique addition curing mechanism as noted earlier.

Table 10 shows short beam shear data obtained on unidirectional and woven graphite as well as Kevlar with EA9102 resin. The resin contents are a little high, but the main point is that the values obtained are consistent with use conditions as expressed for bulk castings. The 177°C (350°F) wet data on unidirectional graphite is lower than more recent data that has been generated at 32% resin content. This data suggest the short beam shear strength is closer to 63.4 MPa (9.2 ksi). The woven graphite data shows little decrease in short beam shear strength in going from 177°C (350°F) dry to wet conditions.

Table 11 shows compressive data for EA9102 resin on woven Kevlar^R. We believe that this data is very conservative due to difficulties in making good specimens for compressive tests. In addition, our compressive specimen jig was not absolutely true, so that some buckling deformation could occur. Nevertheless, the data probably represent the best compressive strengths reported for woven Kevlar^R to date. We have reason to believe that our resin actually reacts with the surface of Kevlar^R and therefore results in these improved compressive values.

A resin has also been developed for potential filament winding applications. This resin is still in preliminary evaluation and is denoted LR 100-617. The TMA data suggests that LR 100-617 has a Tg of approximately 274°C (525°F). Figure 5 shows a rheometrics profile for LR 100-617, and Figure 6 shows a time at temperature study for this material. This data suggests a reasonable winding temperature for LR 100-617 would be approximately 82°C (180°F). Further work on this resin is still in progress.

CONCLUDING REMARKS

A broad line of adhesives and resins which perform in the range of 232-287°C (450-550°F) have been developed. The new bismaleimide modified epoxy resin with the unique curing mechanism shows great promise for improved thermomechanical properties in such resins. This material is applicable to adhesive and matrix applications. Further work to define the long term thermal performance of these materials is in progress.

REFERENCES

1. Landman, D., "New Processable Polyimide Based Adhesives", First Technical Conference on Polyimides, SPE, Inc., Ellenville, NY (1982)
2. See for example: F. P. Darmory, "Processable Polyimides" in New Industrial Polymers, ACS Symposium, pp 124-44 (1974)

TABLE 1: Hysol's Bismaleimide Modified Epoxy Product Line

Conventional BMI Technology	New BMI Technology	Type of Product
EA9655	EA9673	Film Adhesive
EA9351	LR 100-637	Paste Adhesive
EA9367	—	Syntactic Paste Adhesive
—	LR 100-633	Core Splice
LR 100-581	—	Primer/Paint
—	EA9102	Matrix Resin
—	LR 100-617	Filament Winding Resin

TABLE 2: Some Adhesive Properties of EA9655 Film Adhesive
at 488 gm/m² (0.1 psf) Weight

A. Tensile Shear Strength

<u>Temperature/Condition, °C (°F)</u>	<u>Substrate</u>	<u>Tensile Shear Strength, MPa (Ksi)</u>
25 (77)	Aluminum	18.6 (2.7)
232 (450)	"	20.2 (2.9)
232°C/aged 3000 hours @232°C	"	8.3 (1.2)
	b V378/graphite	
25 (77)		14.5 (2.1)
232 (450)	" "	13.0-16.5 (1.9-2.4)
	c PMR-15/graphite	
25 (75)		12.1 (1.8)
260 (500)	" "	10.3 (1.5)

B. Flatwise Tensile Strength

<u>Temperature, °C (°F)</u>	<u>Substrate</u>	<u>Flatwise Tensile Strength, MPa (Ksi)</u>
25 (77)	Aluminum	6.9 (1.0)
177 (350)	"	5.5 (0.8)
	d F178/graphite	
25 (77)		4.7 (0.7)
177 (350)	" "	4.8 (0.7)
	F178/graphite	
25 (77)		4.8 (0.7)
149 (300)	" "	4.8 (0.7)

C. Honeycomb Climbing Drum Peel at 25°C (77°F) on 2024 T3 aluminum face sheets (bare, FPL etched) and 5052 aluminum honeycomb core of 4.8 mm (3/16 in.) and 128 Kg/m³ (8pcf) density: 19 N·m/m (13.0 in. lbs./3 in. width)

NOTES: (a) Adherends: 2024 T3 bare, FPL etched
 (b) Product from U. S. Polymeric
 (c) Product from NASA (Lewis)
 (d) Product from Hexcel Corp.
 (e) Cure cycle is 1 hour @177°C (350°F) with 0.17 to 0.34 MPa (25-50 psi) applied pressure, followed by postcure of 2 hours @246°C (475°F) with no applied pressure.

TABLE 3: Some adhesive properties of EA9351 and EA9367 on 2024 T3 bare FPL etched aluminum

<u>Adhesive</u>	<u>Temperature, °C (°F)</u>	<u>Tensile Shear Strength, MPa (Ksi)</u>	
		<u>Cure A</u>	<u>Cure B</u>
EA9351	25 (77)	16.0 (2.3)	13.8 (2.0)
"	177 (350)	-----	-----
"	232 (450)	14.0 (2.0)	-----
"	260 (500)	9.6 (1.4)	6.9 (1.0)
EA9367	25 (77)	13.8 (2.0)	-----
"	260 (500)	8.3 (1.2)	-----

NOTES: Cure A is 1 hour @177°C (350°F) with 0.17 MPa (25 psi) pressure, followed by 2 hours @246°C (475°F) postcure.

Cure B is 2 hours @177°C (350°F) with no postcure.

TABLE 4: Adhesive Properties of 2024 T3 bare FPL etched aluminum substrates primed with LR 100-581 and bonded with EA9655 at 488 gm/m² (0.1 psf) weight

<u>Temperature, °C (°F)</u>	<u>Tensile Shear Strength, MPa (Ksi)</u>		
	Primed		Unprimed
	<u>Cure A</u>	<u>Cure B</u>	
25 (77)	16.3 (2.4)	9.4 (1.4)	13.4 (1.9)
260 (500)	13.0 (1.9)	14.7 (2.1)	14.4 (2.1)

NOTES: Cure A - primer is cured 1 hour @177°C (350°F)

Cure B - primer is cured 1 hour @177°C (350°F) followed by 1 hour @246°C (475°F)

In both cases EA9655 is cured as shown in Table 2.

TABLE 5: Some Adhesive Properties of EA9673 Film Adhesive
at 488 gm/m² (0.1 psf) Weight

A. Tensile Shear Strength

Temperature/Condition, °C (°F)	Substrate	Tensile Shear Strength, MPa (Ksi)
25 (77) 232 (450) 232°C/aged 700 hours @260°C 260 (500) 288 (550) 316 (600)	Aluminum	13.8 (2.0)
	"	13.1 (1.9)
	"	12.4 (1.8)
	"	15.2 (2.2)
	"	13.1 (1.9)
	"	3.4 (0.5)
25 (77) 232 (450) 288 (550)	V378/graphite	12.4 (1.8)
	" "	12.4 (1.8)
	" "	12.4 (1.8)
22 (72) 204 (400) 260 (500) 316 (600) 360 (680)	PMR-15/graphite	11.0 (1.6)
	" "	11.0 (1.6)
	" "	10.3 (1.5)
	" "	2.1 (0.3)
	" "	1.1 (0.16)

B. Honeycomb Climbing Drum Peel @25°C (77°F) on 2024 T3 aluminum face sheets (bare, FPL etched) and 5052 aluminum honeycomb core of 4.8 mm (3/16 in.) cell size and 128 Kg/m³ (8 pcf) density:

19.4 N-m/m (13.3 in. lbs./3 in. width)

NOTES: (a) Adherends: 2024 T3 bare, FPL etched
 (b) Product from U.S. Polymeric
 (c) Product from NASA, Lewis; postcure cycle in this
 case was 2 hours @288°C (550°F)
 (d) Cure cycle is as shown in Table 2

TABLE 6: Outlife as a function of Tensile Shear Strength for EA9673

<u>Conditions*</u>	<u>Tensile Shear Strength, MPa (Ksi)</u>	
	<u>25°C (77°F)</u>	<u>260°C (500°F)</u>
Initial	13.8 (2.0)	15.8 (2.3)
After 27 Days	11.6 (1.7)	15.8 (2.3)
After 48 Days	15.0 (2.2)	15.8 (2.3)

* NOTES: Samples of tape left on bench at prevalent atmospheric conditions.
 Substrates are FPL etched bare 2024 T3 aluminum.
 Cure is as shown in Table 2.

TABLE 7: Some Adhesive Properties of LR 100-637 on
 2024 T3 FPL etched bare aluminum

<u>Temperature, °C (°F)</u>	<u>Tensile Shear Strength, MPa (Ksi)</u>
25 (77)	11.7 (1.7)
232 (450)	15.8 (2.3)
260 (500)	13.8 (2.0)
287 (550)	11.0 (1.6)

NOTE: Cure is 1 hour @177°C (350°F) with 0.17 MPa (25 psi) pressure,
 followed by 2 hours @246°C (475°F)

TABLE 8: Bulk Resin Tg Data for EA9655 and EA9673

<u>Method</u>	<u>Tg, °C (°F)</u>	
	<u>EA9655</u>	<u>EA9673</u>
TMA, Dry	253 (487)	299 (570)
TMA, Wet	109-118 (228-244)	
DMA, Dry	267 (512)	300 (572)
DMA, Wet		210 (410)

NOTES: TMA = Thermomechanical Analysis

DMA = Dynamic Mechanical Analysis

Wet = Casting immersed in boiling water for 2 days

TABLE 9: Tensile Properties for Bulk Casting of EA9655 and EA9673

<u>Temperature, °C (°F)</u>	<u>EA9655</u>	<u>EA9673</u>
Ultimate Strength, MPa, (Ksi)		
23 (75), dry	51.7 (7.5)	58.6 (8.5)
23 (75), wet	39.3 (5.7)	ND
177 (350), dry	26.9 (3.9)	43.4 (6.3)
260 (500), dry	ND	26.9 (3.9)
Modulus, GPa (Ksi)		
23 (75), dry	3.4 (493)	3.4 (493)
23 (75), wet	1.7 (247)	ND
177 (350), dry	1.6 (232)	1.8 (261)
Elongation (%)		
23 (75), dry	1.6	2.2
23 (75), wet	2.5	ND
177 (350), dry	2.2	3.3

NOTES: ND = Not Determined

Wet = 4 weeks @71°C (160°F) immersed in water.

TABLE 10: Short Beam Shear Data for Prepregs of EA9102 on unidirectional and woven graphite, as well as Kevlar^R

<u>Temperature, °C (°F)</u>	<u>Short Beam Shear Strength, MPa (Ksi)</u>		
	<u>Unidirectional Graphite</u>	<u>Woven Graphite</u>	<u>Woven Kevlar</u>
23 (75)	130.2 (18.9)	55.1 (8.0)	37.9 (5.5)
177 (350), dry	91.6 (13.3)	40.7 (5.9)	22.7 (3.3)
177 (350), wet	55.1 (8.0)	35.1 (5.1)	ND

NOTES: (a) Unidirectional graphite is Courtaulds E/XA-S, 6K high strain fiber with resin content 39.5%; void content, 0%; lay-up, (0°) 15

(b) Woven graphite is Celion 3K/8HS with resin content, 37.4%; void content, 1.0%; lay-up, (0°) 8.

(c) Woven Kevlar^R is style 285 Kevlar^R 49 with resin content, 45.0%; void content, 1.0%; lay-up, (0°) 8.

(d) Cure cycle: Heat up at 1-3°C (2-5°F) per minute to 113°C (235°F) with pressure of 0.7 MPa (100 psi); hold 1 hour @113°C (235°F); heat up at 1-3°C per minute to 177°C (350°F); hold for 1 hour at 177°C; cool to 66°C (150°F) and postcure in an oven at 246°C (475°F) for 2 hours.

(e) Wet = Sample immersed in boiling water for 2 days.

(f) ND = Not Determined.

TABLE 11: Compressive Strengths for EA9102 on woven Kevlar^R

<u>Temperature, °C (°F)</u>	<u>Compressive Strength, MPa (Ksi)</u>
23 (75)	229.4 (33.3)
177 (350)	148.1 (21.5)

NOTES: (a) Woven Kevlar^R as noted in (c) of Table 10

(b) Cure cycle as noted in (d) of Table 10

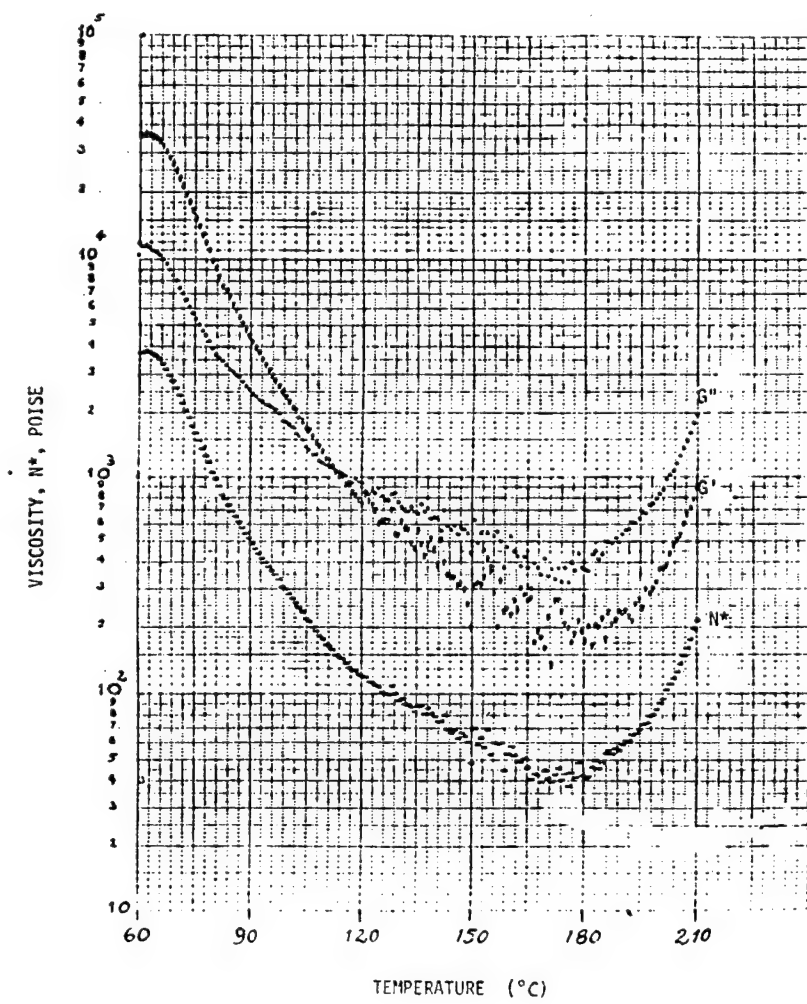


Figure 1. Rheometrics plot for EA9655 resin.

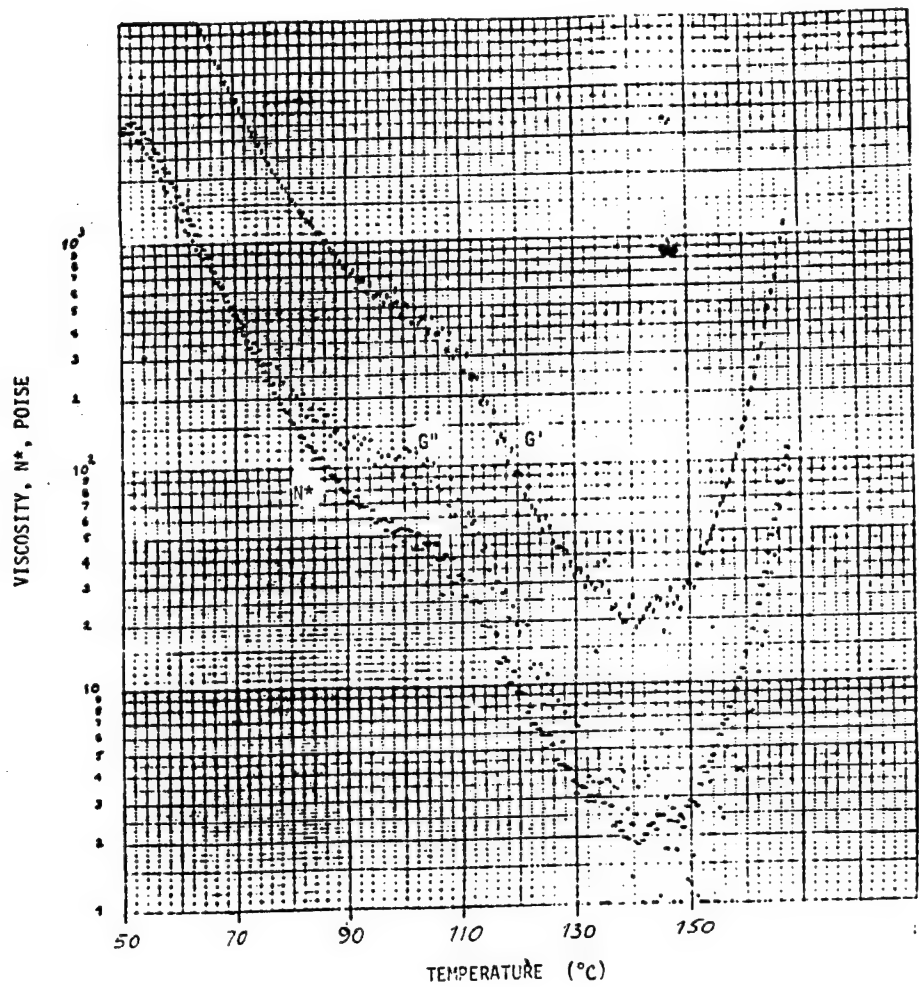


Figure 2. Rheometrics plot for EA9673 resin.

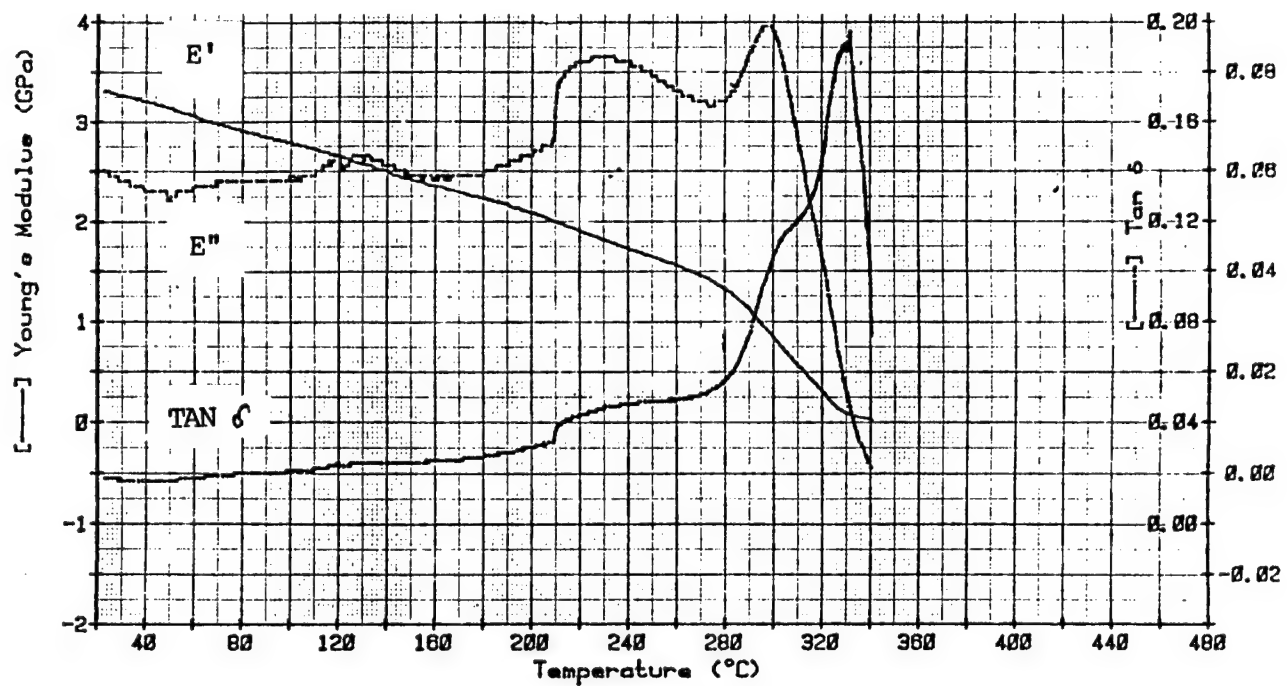


Figure 3. Dynamic mechanical analysis of EA9673, dry.

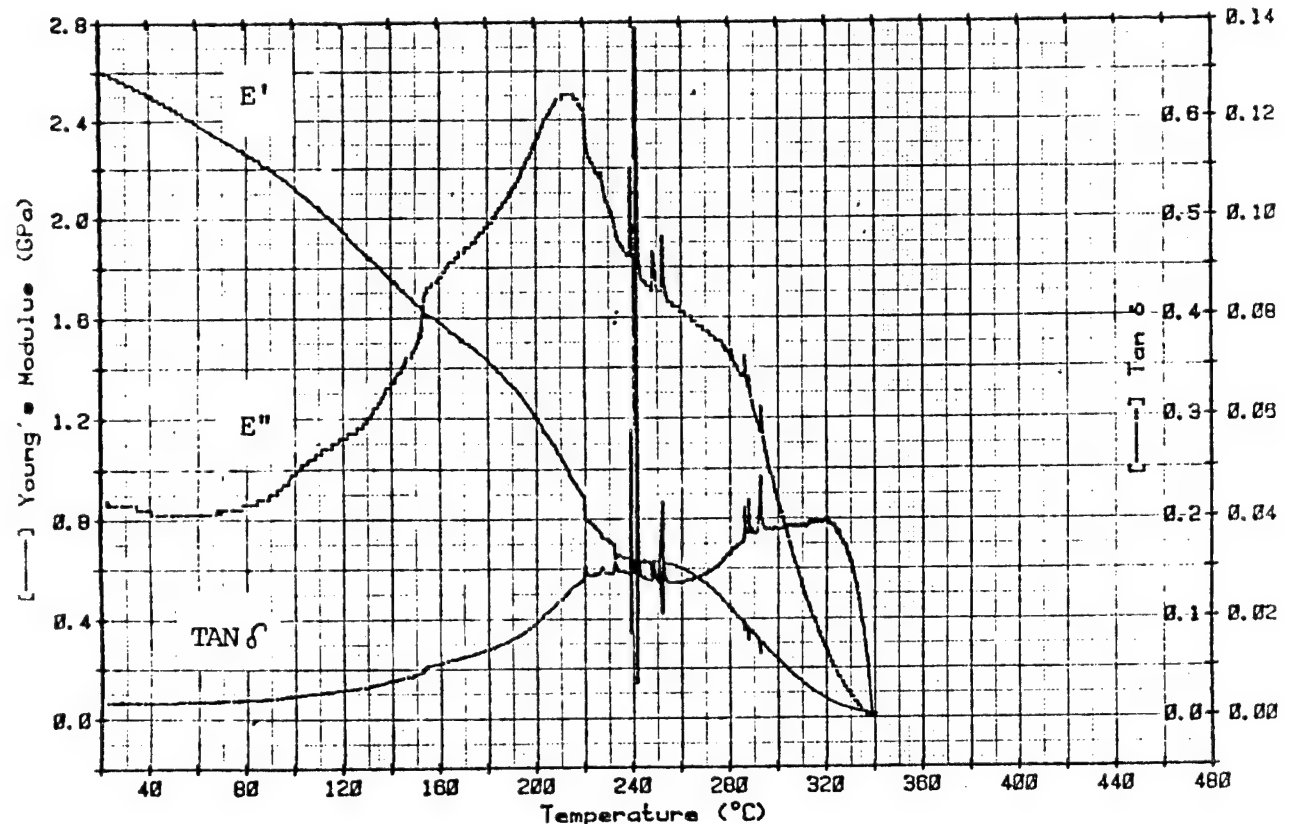


Figure 4. Dynamic mechanical analysis of EA9673, wet. Note, there is a scale difference for Young's modulus compared to Figure 1.

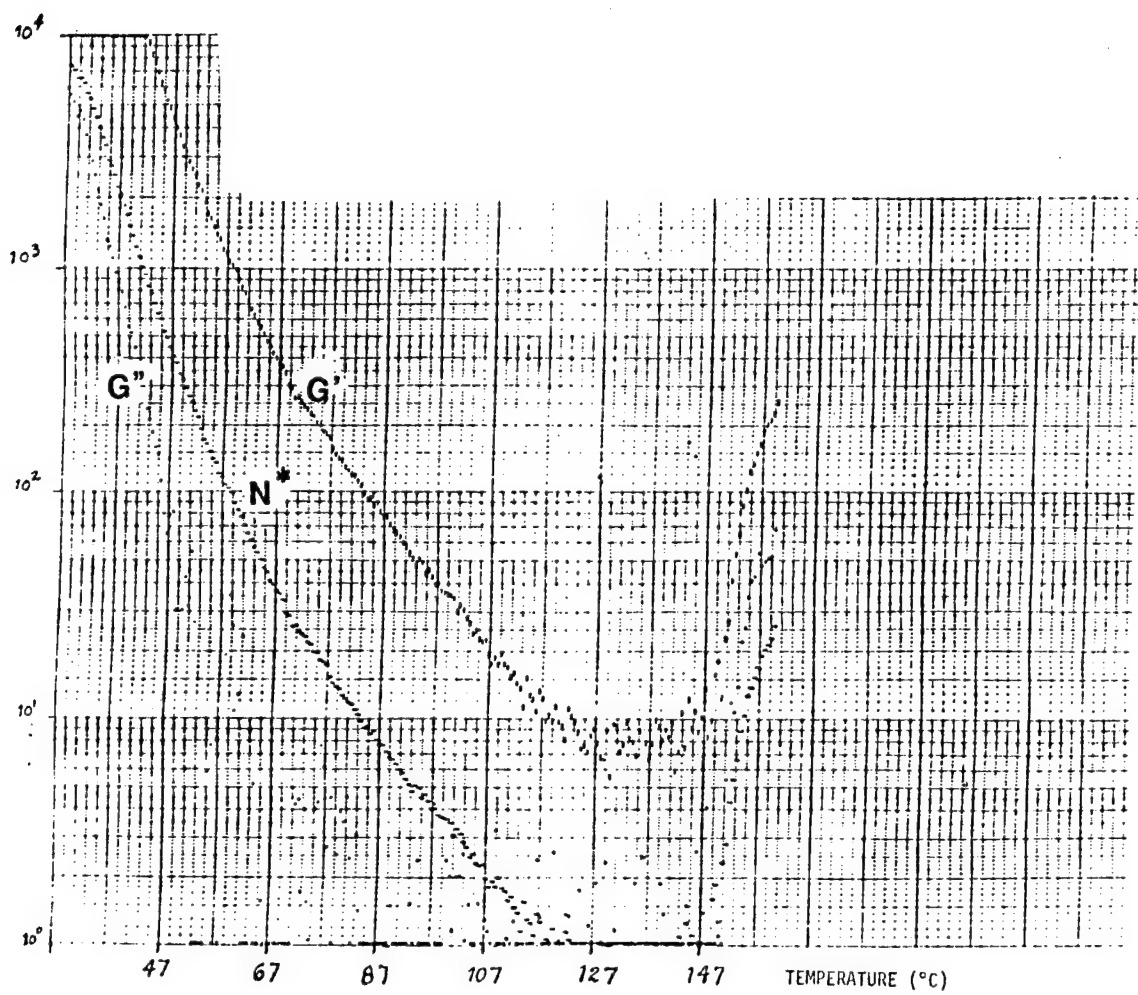


Figure 5. Rheometrics profile as function of temperature for LR100-617.

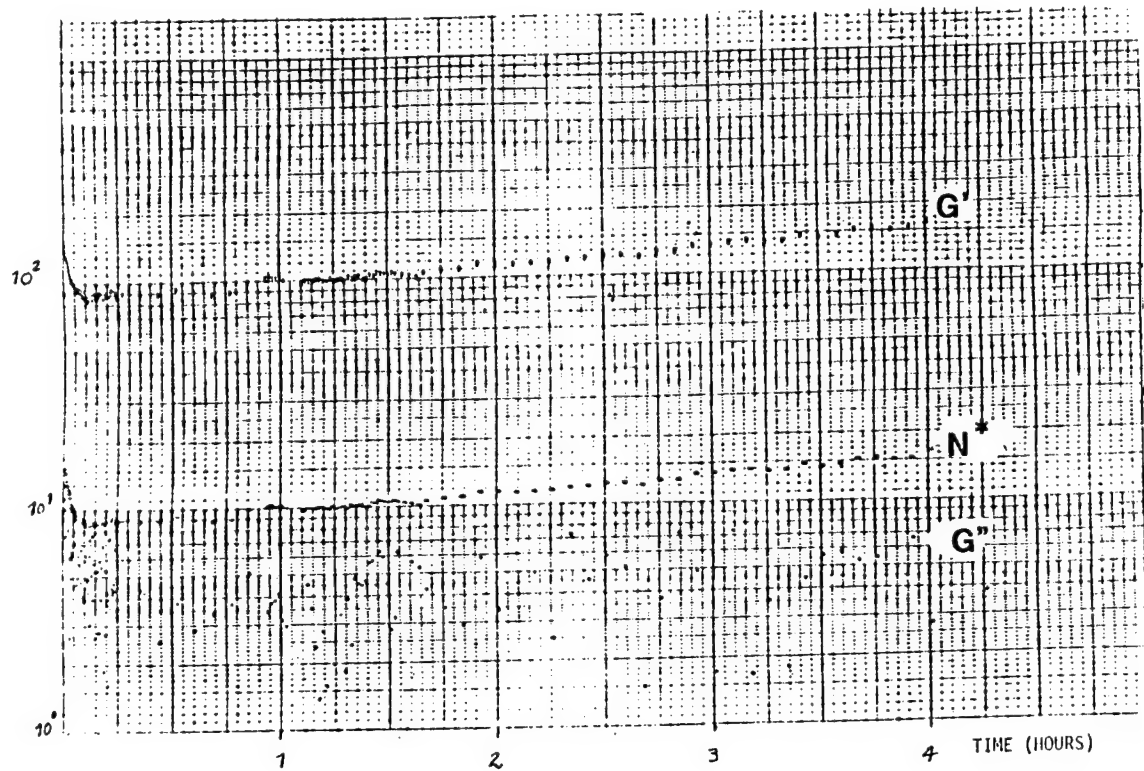


Figure 6. Rheometrics profile for LR100-617 kept at 82 °C.

RECENT DEVELOPMENTS IN POLYIMIDE AND
BISMALEIMIDE ADHESIVES

Robert E. Politi
Chemical Research Division
American Cyanamid Company

Research on high temperature resin systems has intensified during the past few years. In the Aerospace Industry, much of the motivation for this increased activity has been to replace heat resistant alloys of aluminum, stainless steel and titanium by lighter weight glass and carbon fiber reinforced composites. Applications for these structures include: (1) engine nacelles involving long time exposure (thousands of hours) to temperatures in the 150 to 300°C range, (2) supersonic military aircraft involving moderately long exposure (hundreds of hours) to temperatures of 150 to 200°C, and (3) missile applications involving only brief exposure (seconds or minutes) to temperatures up to 500°C and above.

Because of fatigue considerations, whenever possible, it is preferable to bond rather than mechanically fasten composite structures. For this reason, the increased usage of high temperature resin matrix systems for composites has necessitated the development of compatible and equally heat stable adhesive systems.

This paper briefly reviews the performance of high temperature epoxy, epoxy-phenolic and condensation polyimide adhesives. This review is followed by a discussion of three recently developed types of adhesives: (1) condensation reaction polyimides having improved processing characteristics, (2) addition reaction polyimides, and (3) bismaleimides.

All of the adhesives discussed in this paper are suitable for bonding honeycomb to skin sandwich structure. However, in the interest of brevity, with few exceptions I have chosen to use lap shear strength as the criteria for comparing performance of the various types of adhesive.

Epoxy Adhesives

Epoxy adhesives based on multifunctional resins are available which exhibit excellent strength retention at temperatures up to about 225°C. Where long term aging is required, epoxies are generally limited to applications requiring continuous service at temperatures no higher than 175°C. The adherends involved are most commonly aluminum alloys and epoxy matrix composite structures.

Epoxies are comparatively low in cost and are by far the simplest and most economical adhesives to process. Full cures may be accomplished at moderate temperatures (150 to 200°C). Furthermore, because curing is accomplished by addition reactions, no volatiles are evolved and dense, non-porous glue lines are easily obtained with low pressure bonding.

Figure 1 shows the lap shear strength of FM® 400 at various temperatures. This adhesive was designed for use on supersonic military aircraft and has excellent strength retention at temperatures up to 215°C. Strength then drops rather sharply to 6.9 MPa (1000 psi) at 260°C. The effect of heat aging on FM® 400 is shown in Figure 2. After 3000 hours aging at 215°C, the adhesive retains approximately 80% of its original lap shear strength. This is more than sufficient for most military aircraft.

Other multifunctional epoxy adhesives are available for use in applications such as engine nacelles, where resistance to heat aging for very long periods of time is required. Figure 3 shows the performance of an epoxy adhesive of this type when heat aged at 175°C.

It can be seen that there is no significant drop in lap shear strength after 20,000 hours at 175°C. It is interesting to note that the configuration of the bond line has a pronounced effect on the ability of the adhesive to withstand heat aging. In the lap shear configuration, the adhesive is protected from oxidation by solid metal skins. In the sandwich panel constructed of solid aluminum skins to aluminum honeycomb, there is a substantial quantity of air trapped in the panel which initiates oxidative degradation. As a result, this structure shows a 50% drop in flatwise tensile strength after 10,000 hours aging. Degradation is most rapid in the quiet nacelle type of sandwich panel constructed with perforated skins. In this configuration, the bond line is completely exposed to oxygen in the atmosphere and a 50% drop in lap shear strength occurs after about 5000 hours heat aging.

Epoxy-Phenolic Adhesives

Epoxy-phenolics rival the polyimide adhesives in their ability to withstand short time exposure to extremely high temperatures. For this reason, they are admirably suited for use on missiles, and are generally preferred to polyimides because of their lower cost and ease of processing. Bond pressures of 28 MPa (40 psi) and cure temperatures of 150°C are usually adequate for most applications.

Figure 4 shows the effect of temperature on the bond strength of an aluminum powder filled epoxy-phenolic adhesive. This adhesive (HT® 424) retains 6.9 MPa (1000 psi) lap shear strength at 540°C.

Figure 5 shows the effect that oxidation has on the life of the adhesive at 260°C. On a 17-7 PH steel substrate, the adhesive shows excellent strength retention after 500 hours when heat aged in a nitrogen atmosphere. On the same steel substrates, lap shear strength drops to zero after only 100 hours heat aging in air. It is interesting to note that degradation is much slower in an air atmosphere on an aluminum substrate. This illustrates the role of transition metals such as iron in catalytically promoting oxidative degradation of organic adhesives.

Condensation Reaction Polyimides

High temperature adhesives based on condensation reaction polyimide precursors have been marketed for over 15 years. Adhesives of this type are supplied in both liquid form and as solid films. In addition, they may be filled or unfilled. Aluminum powder filled adhesives have proved to be superior in strength to unfilled adhesives and are generally used for metal bonding applications. Unfilled adhesives are primarily used for radomes and other applications where radar transparency is required.

Condensation reaction polyimides require high cure temperatures; 260°C or even higher depending on the expected service temperature. Processing is further complicated by the high volatile content of these adhesives (about 12% for aluminum filled adhesives and 30% for unfilled adhesives). One processing advantage that they have over addition reaction polyimides is that they can be cured under pressure at 175°C and then post cured without pressure at higher temperatures. This permits the use of low temperature autoclaves and conventional bagging materials. Inexpensive ovens can be used for postcuring the bonded panels. A typical cure cycle for condensation reaction polyimides consists of heating the panel from room temperature to 175°C in 2 hours or less under full vacuum plus .28 MPa (40 psi) air pressure. Vacuum and air pressure are maintained while the panel is held at 175°C for 2 hours. Post curing of small panels may be carried out by placing them in a 175°C oven and raising the temperature to about 290°C and holding at 290°C for 2 hours. For large panels with impermeable skins, it may be necessary to very slowly raise the temperature to 290°C over a period of several hours to prevent blister formations in the glue line.

FM® 34 was perhaps the first polyimide adhesive developed that gained any significant commercial acceptance. Its performance at temperatures up to 540°C is depicted in Figure 6. It will be noted that its strength retention at 540°C does not significantly differ from that of the more easily processed epoxy phenolic adhesive (HT® 424). However, as can be seen from Figure 7, FM® 34 was far superior in thermal stability showing no significant drop in strength after 40,000 hours at 260°C.

FM® 34 contained an arsenic compound which inhibited catalytic decomposition by transition metal substrates such as titanium and steel. FM® 34 is no longer supplied and has been replaced with FM® 34B-18. FM® 34B-18 which is free of arsenic shows excellent strength retention after 1200 hours heat aging at 260°C, but degrades rapidly during the next 2000 hours. In applications where transition metals are not involved (for example, in bonding to polyimide composites) FM® 34B-18 is fully as resistant to long time heat aging as FM® 34.

Processing Condensation Polyimides to Minimize Volatile Problems

The volatiles released during the cure of condensation PI adhesives come from two sources: (1) volatilization of retained solvent and (2) water released during imidization of the precursor resin. The polyimide precursor resin is very high melting and very brittle and for this reason, solvent is left in the adhesive film as a plasticizer to impart drape and tack to the adhesive film as well as to insure flow during bonding.

As the temperature is raised during the bond cycle imidization occurs. Water is released as a result of this condensation reaction. If the retained solvent is not released soon enough in the bond cycle, sufficient imidization occurs to make the resin insoluble in the solvent and it precipitates. When the solvent is subsequently released later in the bond cycle, a weak porous bond results because the resin is incapable of flow.

The solvent most commonly used in PI adhesives is N-methyl-2-pyrrolidone (NMP) which boils at about 200°C at atmospheric pressure. Since considerable imidization occurs long before the adhesive reaches even 175°C, precipitation of the resin would occur if processing were carried out at atmospheric pressure. For this reason, bonding is carried out under vacuum to insure release of the solvent earlier in the bond cycle. Figure 8 shows the boiling point of NMP at various degrees of vacuum. At

about 13 psi vacuum, the boiling point is depressed to about 140°C. With a 13 psi or higher vacuum and a heat up rate of 1.5°C per minute or faster, volatile release occurs early enough in the bond cycle to minimize precipitation.

Improved Condensation Reaction Polyimides

The previous section has shown how good quality bonds can be obtained with the FM® 34 series of adhesives by carefully controlling processing conditions. However, this problem becomes particularly severe when wide area bonds with impermeable metal skins as adherends are involved. Under these conditions, volatile release is retarded and occurs later in the bond cycle resulting in excessive resin precipitation.

A new condensation reaction polyimide adhesive designated as FM® 36 was developed to overcome this problem. It is based on a more soluble precursor resin that remains soluble in the NMP solvent even after substantial imidization has occurred. FM® 36 is an unfilled adhesive designed for applications requiring radar transparency. Figure 9 compares its performance in a wide area lap shear panel to that of FXM 34B-32 (a radar transparent version of FM® 34). It can be seen that the lap shear strength of the two adhesives is comparable with a 2.5 cm width bond line. The lap shear strength of FM® 34B-32 drops to nearly zero with a 15 cm wide bond line, while the FM® 36 shows no drop in strength with a 22.5 cm wide bond line.

Figure 10 shows that FM® 36 has good strength retention up to 290°C. We have not as yet run lap shear tests at higher temperatures. Figure 11 shows that this adhesive retains about 60% of its original strength after 1000 hours aging at 290°C on a titanium substrate. We have previously noted that titanium accelerates the decomposition of adhesives. Therefore, we expect better strength retention after heat aging on composite substrates. Preliminary results substantiate this expectation, but we do not yet have a reliable data base because of sporadic interlaminar shear failures in the PI laminate substrates.

Addition Reaction Polyimides

Addition reaction polyimides make it possible to obtain bond lines with extremely low void contents. Adhesives of this type are generally supplied as supported film containing sufficient alcohol to impart tack and drape to the adhesive. A typical bond cycle is as follows:

1. RT to 205°C in 1 hour under 5 psi vacuum pressure.
2. Hold 15 minutes at 205°C maintaining 5 psi vacuum.
3. Apply full vacuum plus 100 psi air pressure for remainder of cycle.
4. Raise temperature to 290°C in about 40 minutes.
5. Hold 2 hours at 290°C.
6. Cool to 100°C before releasing pressure.

Unlike the condensation reaction type, addition reaction polyimides remain thermoplastic after imidization and solvent removal has occurred. Hence, when pressure is applied after solvent removal at 205°C, a dense non-porous glue line results. Upon heating to 290°C, further curing occurs via an addition reaction involving unsaturated end groups such as nadic anhydride.

Unlike the condensation reaction PI's which can be processed using the post cure concept, addition reaction PI's must be held under pressure throughout the cure cycle. Therefore, relatively costly high temperature presses or autoclaves are required to fabricate panels with addition PI adhesives.

FM® 35 is an addition PI adhesive containing an aluminum powder filler. As is shown in Figure 12, it is comparable in strength retention to the condensation PI's at temperatures up to 290°C. Figure 13 demonstrates that good quality large area bonds can be made with this adhesive.

Composites made from addition reaction PI's are generally fabricated using 200 psi pressure to insure low void content in the laminate. There is no significant difference in the lap shear strength of FM® 35 when bonding pressure is varied from .28 MPa (40 psi) to 1.38 MPa (200 psi). We have not, however, measured the void content of bond lines made at different pressures or the possible effect of variations in void content on strength retention after heat aging. This work is now in progress.

Bismaleimide Adhesives

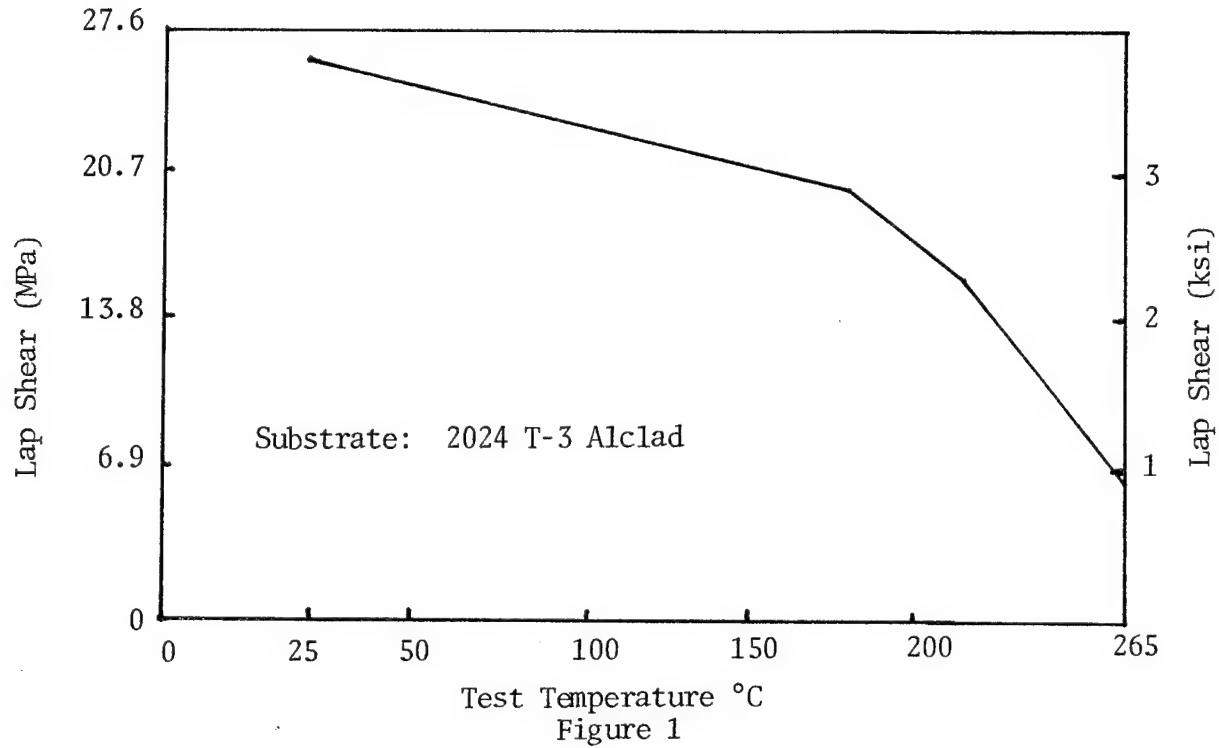
Bismaleimide adhesives fill a niche between high temperature epoxy and PI adhesives. Unmodified BMI resins are hard, brittle solids. In order to impart drape to adhesive films based on these resins, they must be plasticized. However, unlike the PI resins, plasticization may be accomplished without resorting to the use of solvents. Volatile-free adhesive films having drape can be formulated through the use of reactive liquid monomers as plasticizers. Since cross linking occurs via an addition reaction, no volatiles are evolved during the cure of these adhesives.

Cure temperature requirements vary depending on the particular BMI resin employed and the specific monomeric plasticizers selected. In general, good results can be obtained using a cure of 2 hours at 175°C under .28 MPa (40 psi) pressure followed by a 2 to 4 hour post cure at 200 to 225°C.

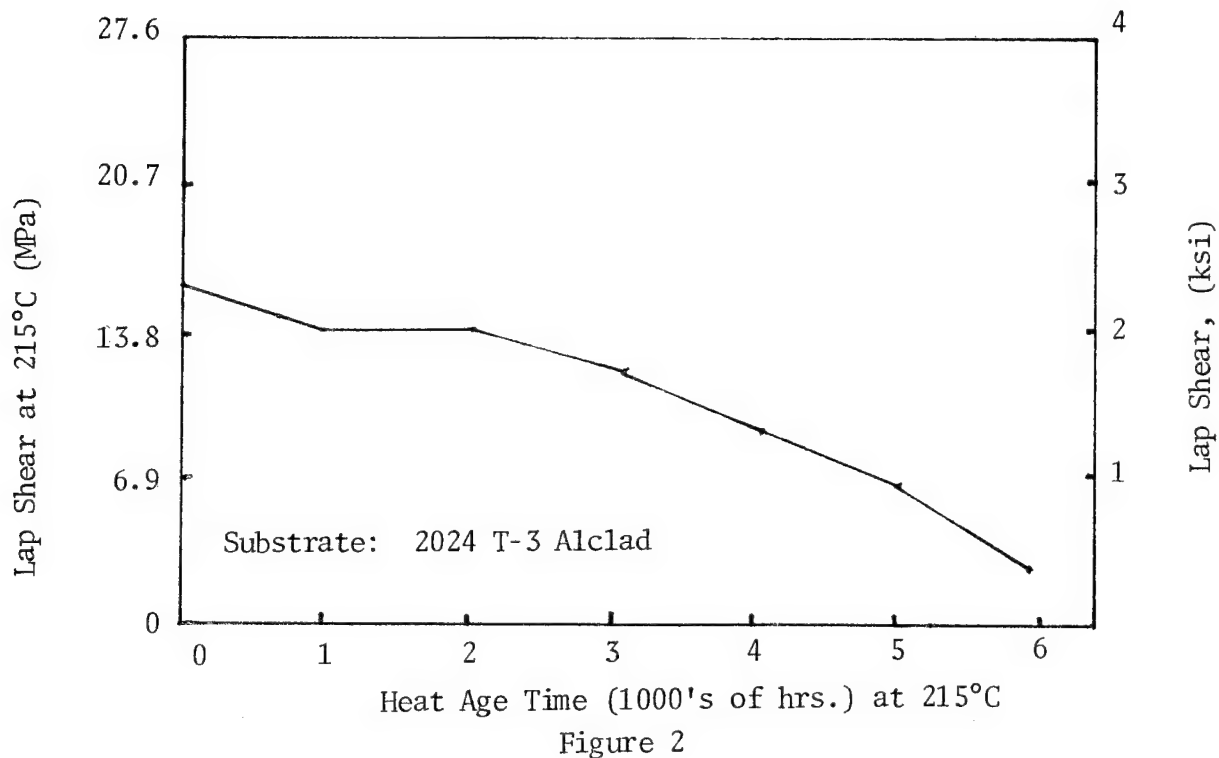
Figure 14 shows the performance of an experimental BMI adhesive over a range of temperatures. Strength retention is surprisingly good up to about 300°C. However, in applications where long term exposure to high temperatures is involved, BMI adhesives are not expected to be durable beyond 200 to 225°C.

Almost limitless variations in formulation are possible with BMI adhesives. The experimental BMI on which data is presented in Figure 14 contains no toughener and as a result, has quite low lap shear strength. Considerable work is now in progress to formulate BMI's having optimum balance between toughness and heat resistance.

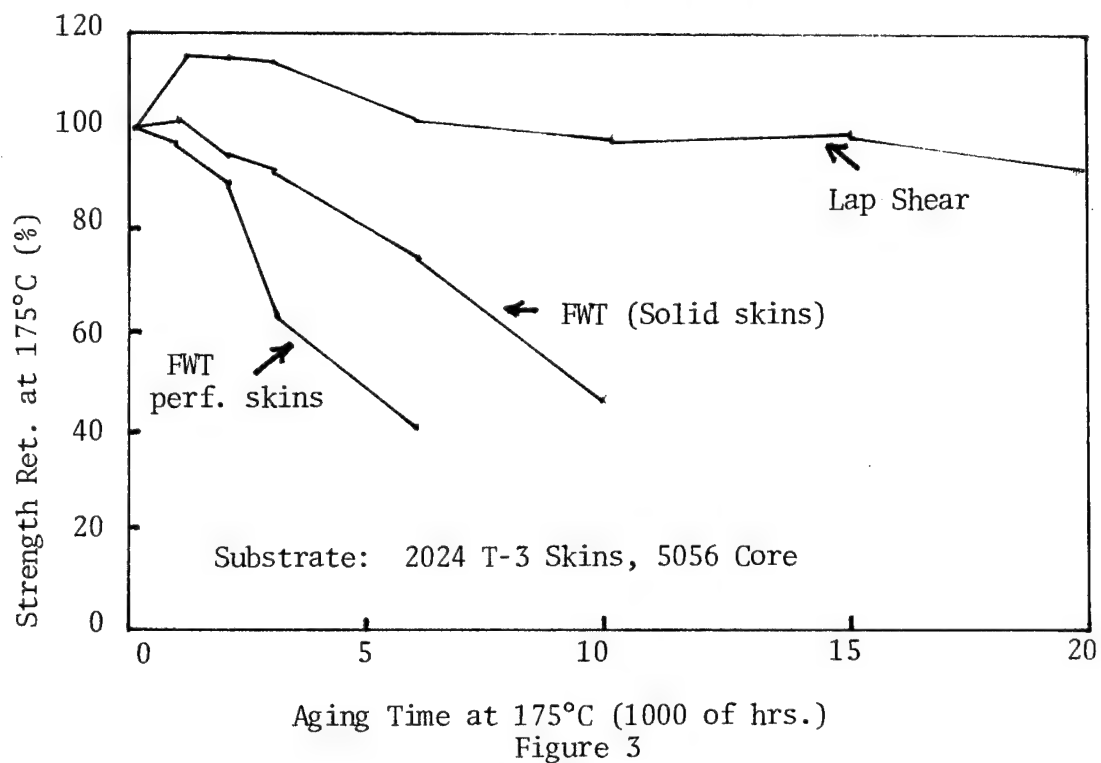
EFFECT OF TEMPERATURE ON EPOXY ADHESIVE (FM® 400)



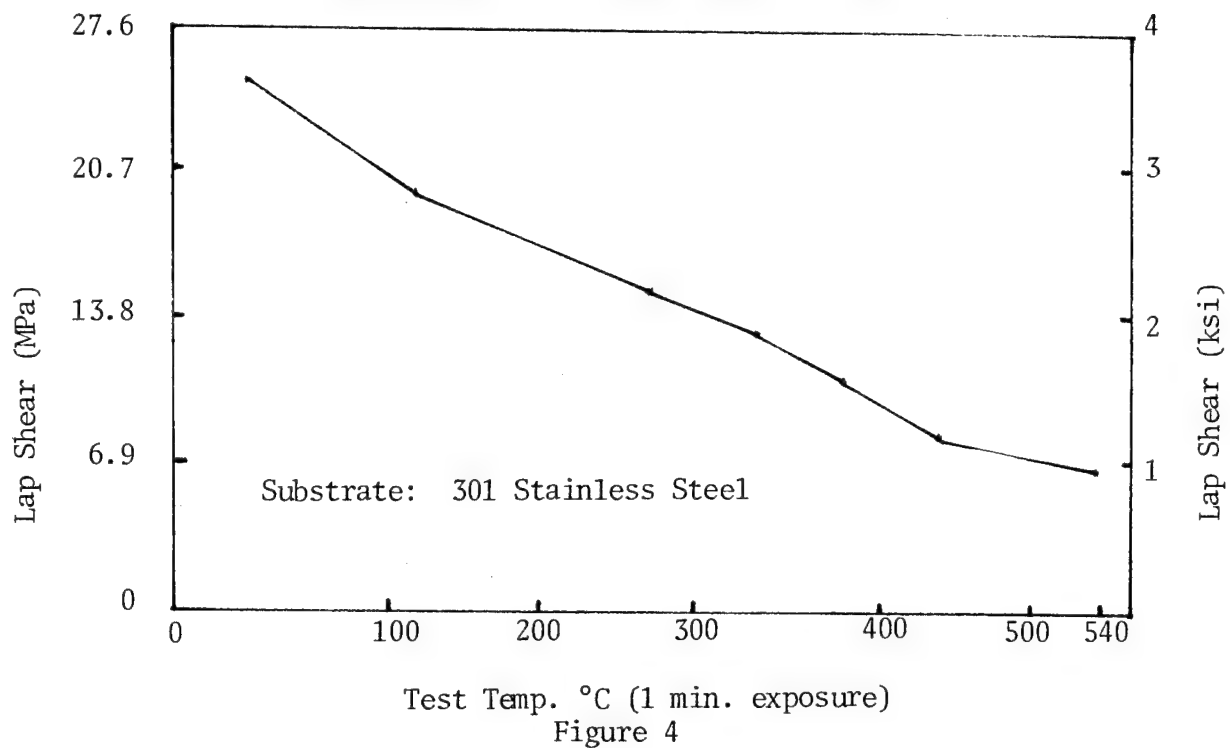
EFFECT OF HEAT AGING ON AN EPOXY ADHESIVE (FM® 400)



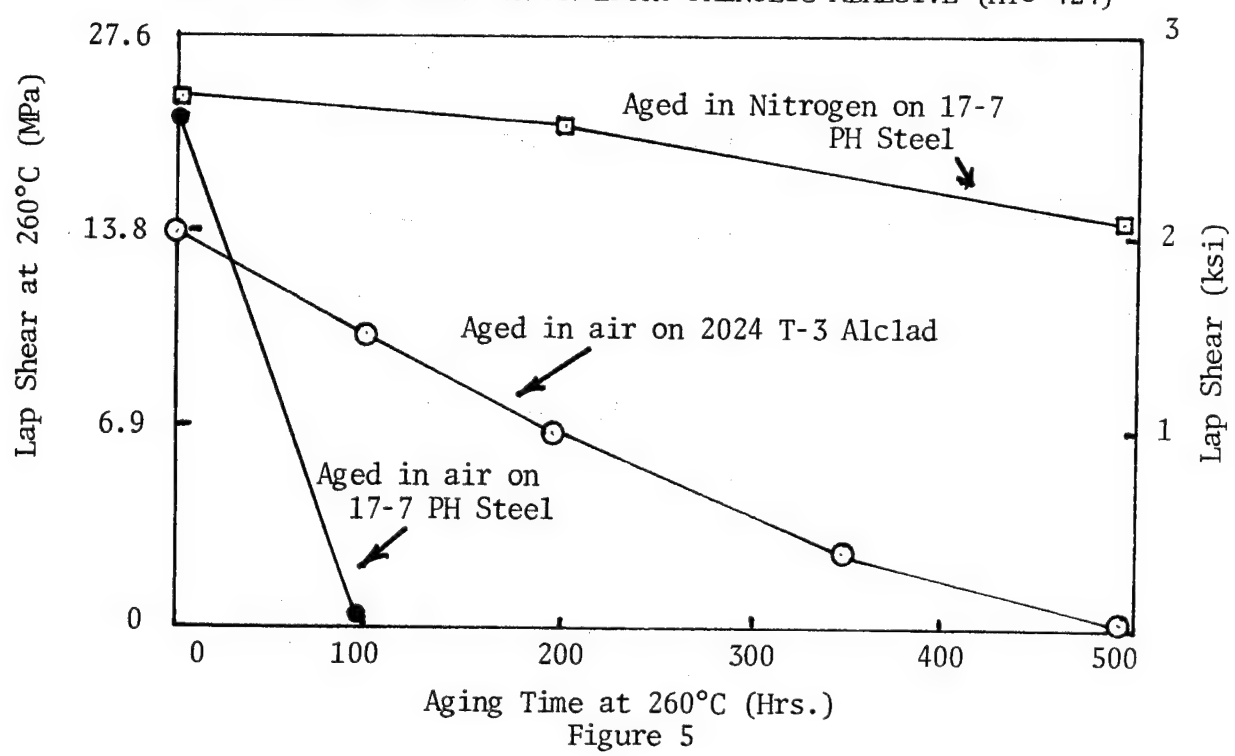
EFFECT OF BOND CONFIGURATION ON HEAT AGING



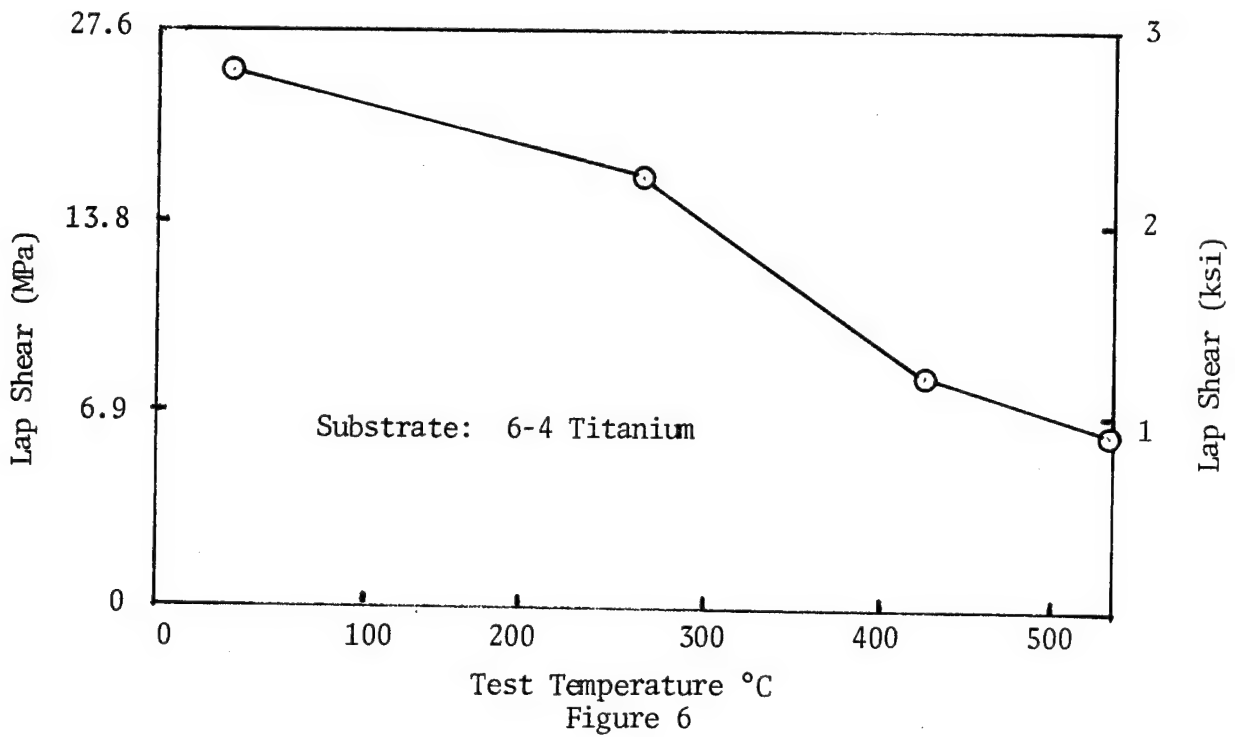
EFFECT OF TEMPERATURE ON AN EPOXY-PHENOLIC ADHESIVE (HT® 424)



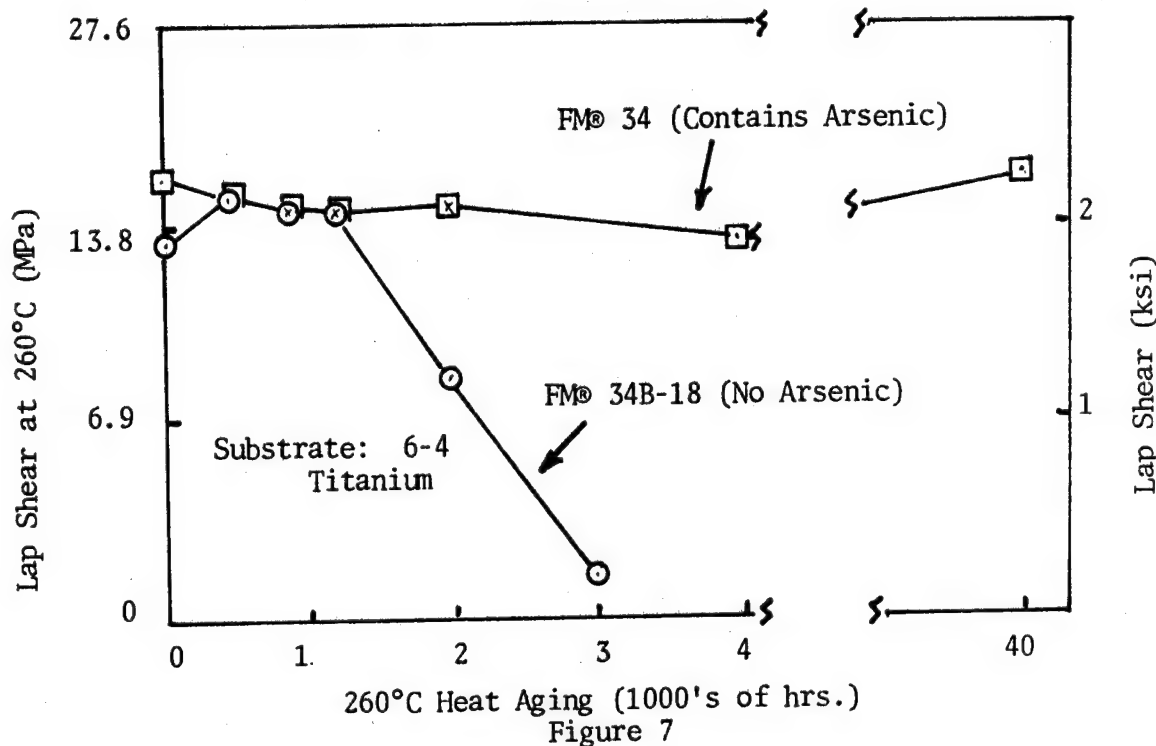
EFFECT OF HEAT AGING ON AN EPOXY-PHENOLIC ADHESIVE (HT® 424)



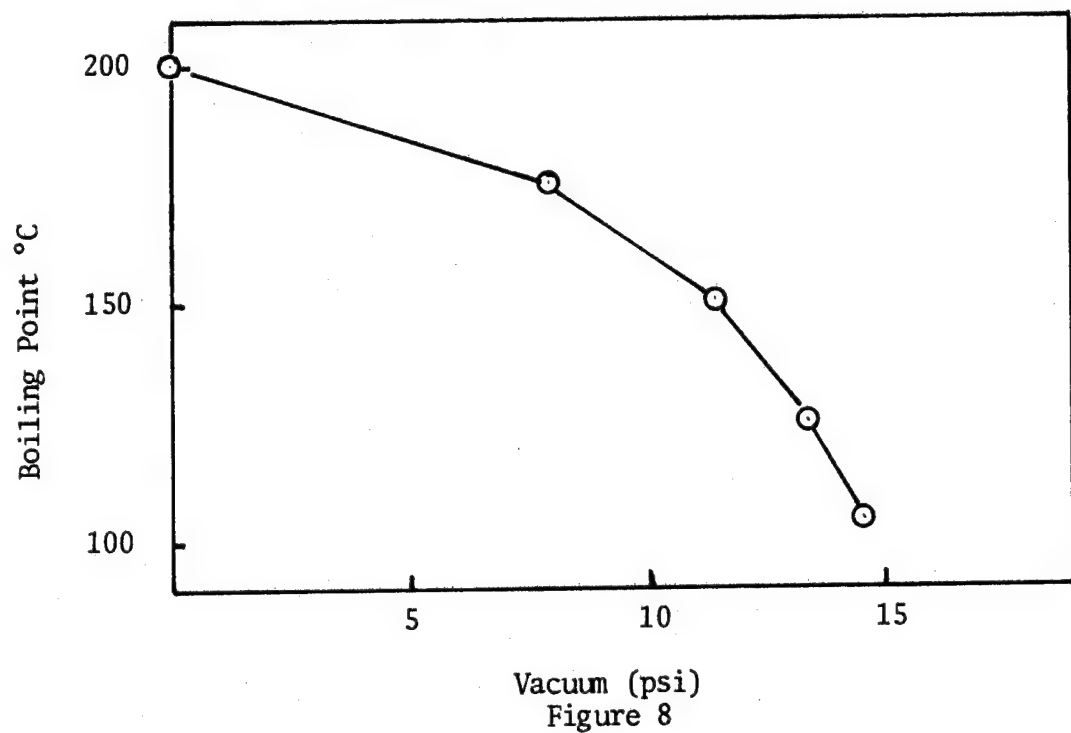
EFFECT OF TEMPERATURE ON FM® 34 (POLYIMIDE ADHESIVE)



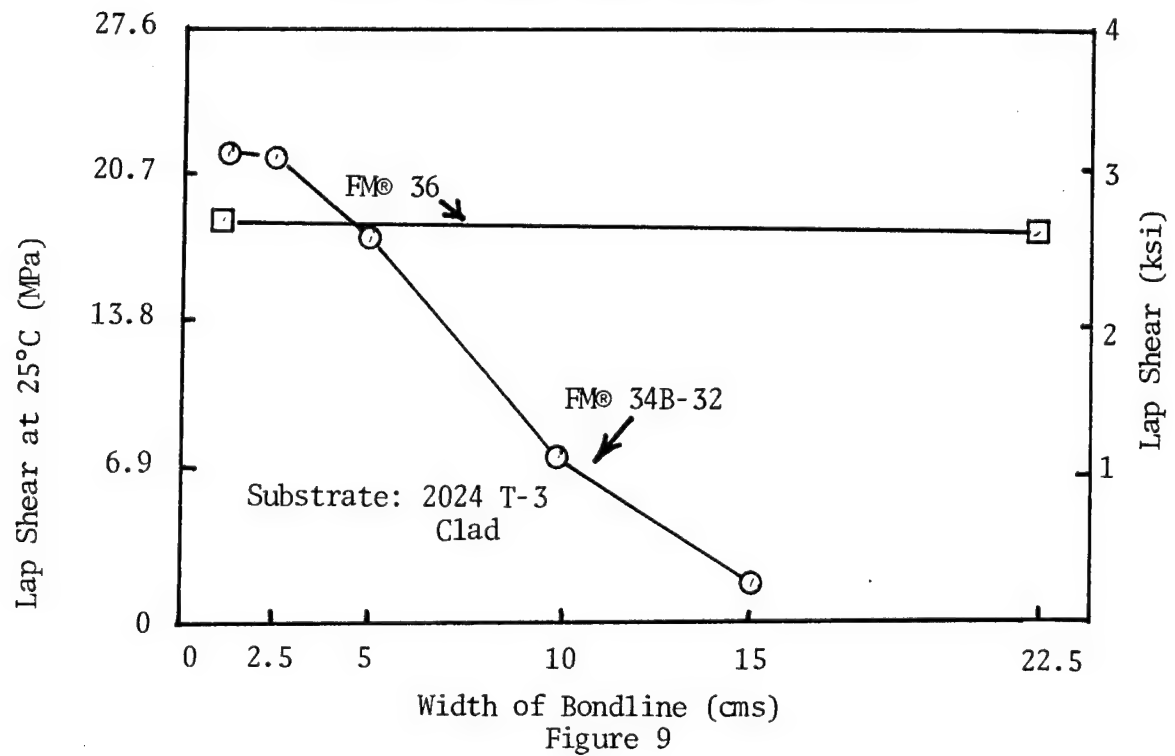
EFFECT OF ARSENIC COMPOUND ON THERMAL STABILITY



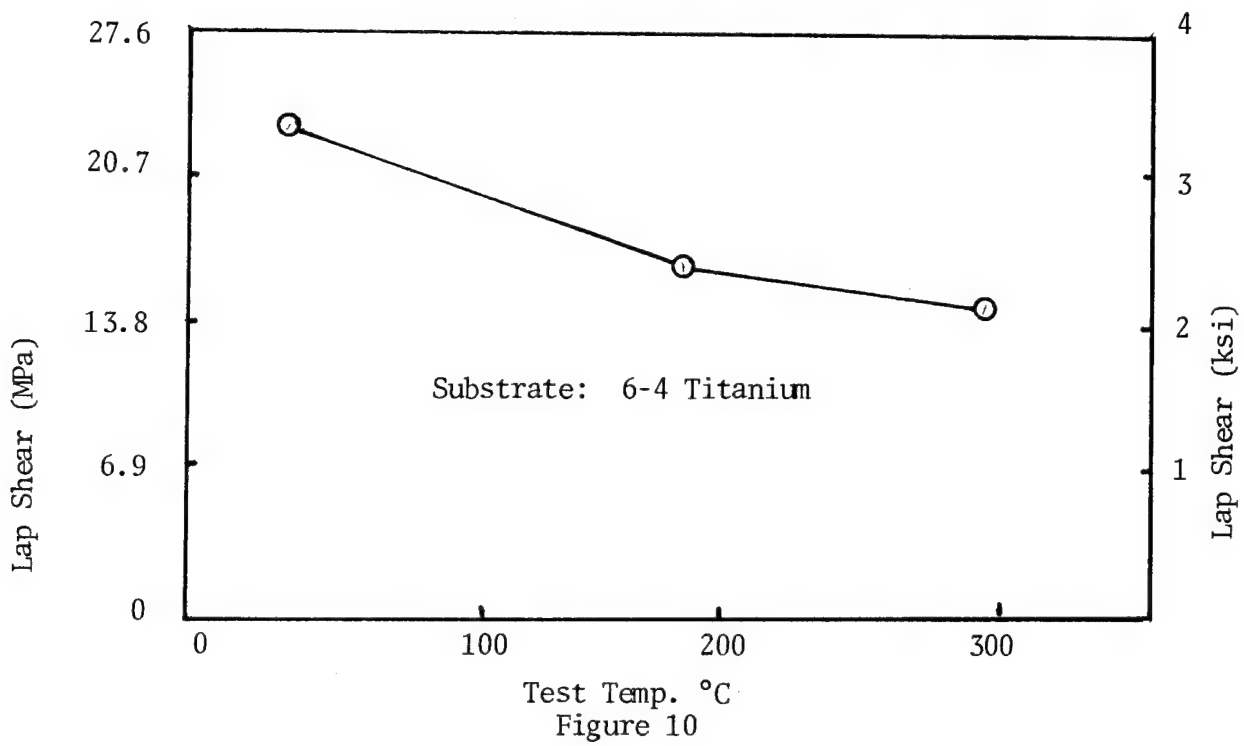
Boiling Point Curve of NMP



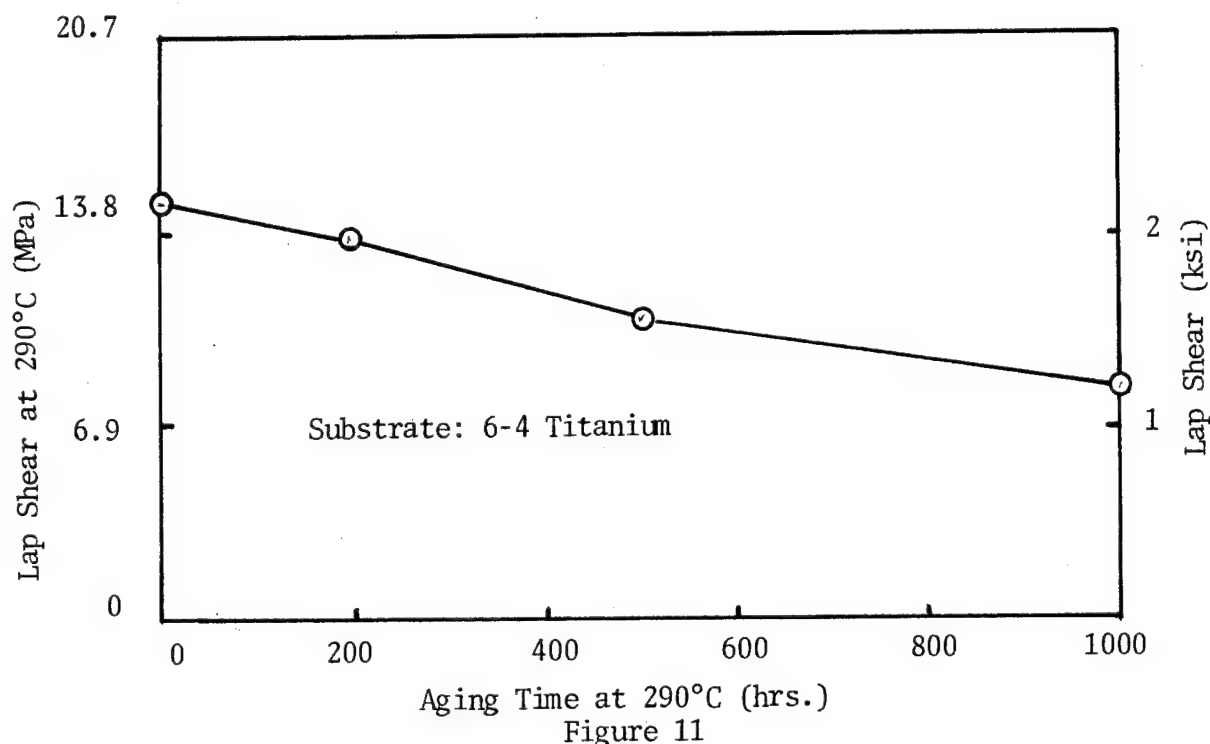
EFFECT OF PANEL WIDTH ON BOND STRENGTH



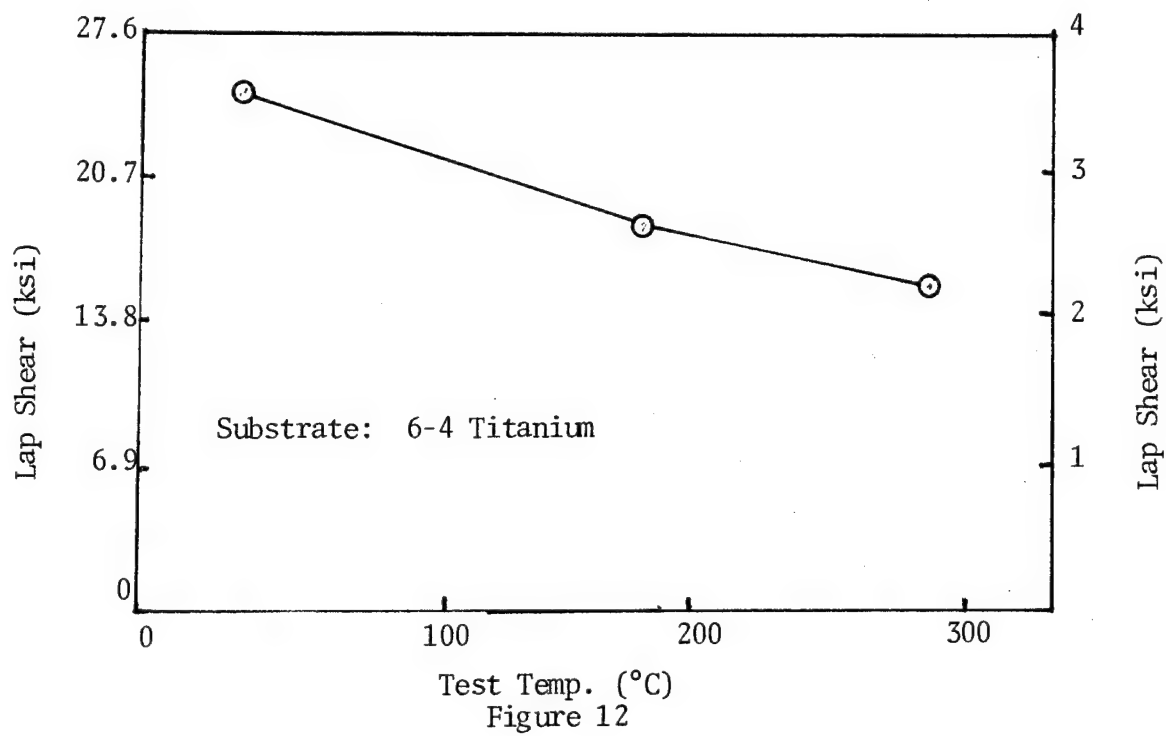
EFFECT OF TEMPERATURE ON FM® 36 (POLYIMIDE ADHESIVE)



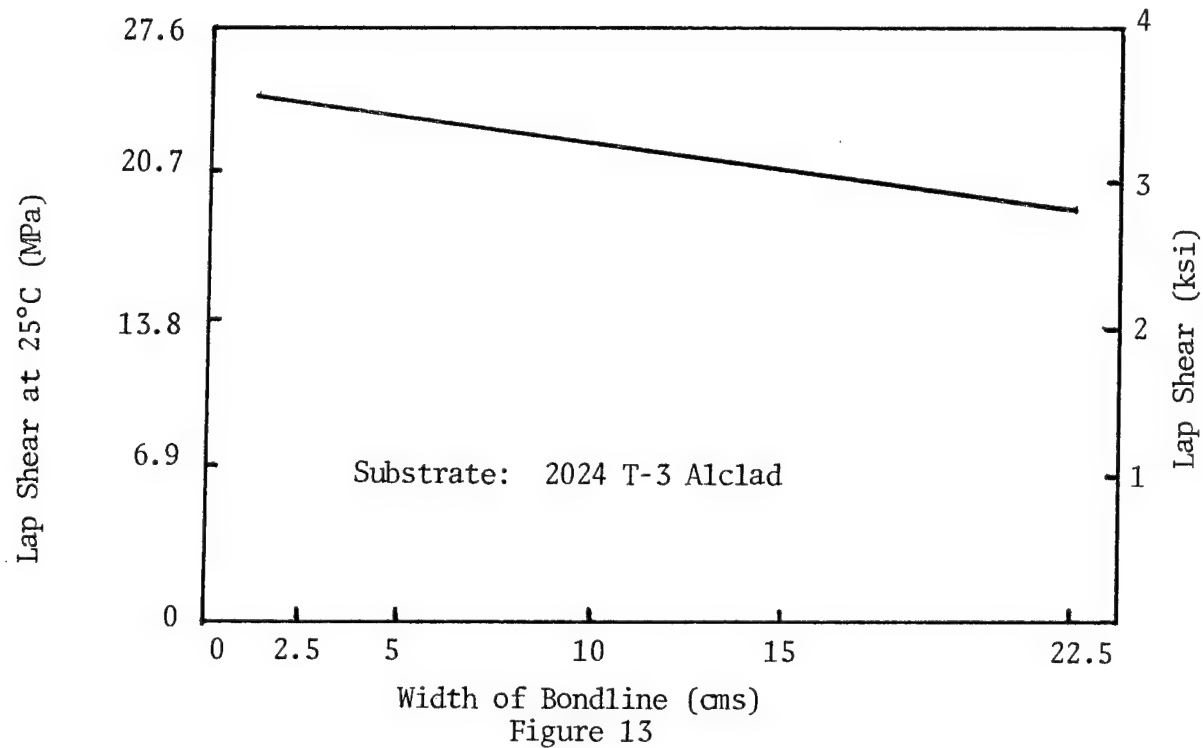
EFFECT OF HEAT AGING ON FM® 36 (PI ADHESIVE)



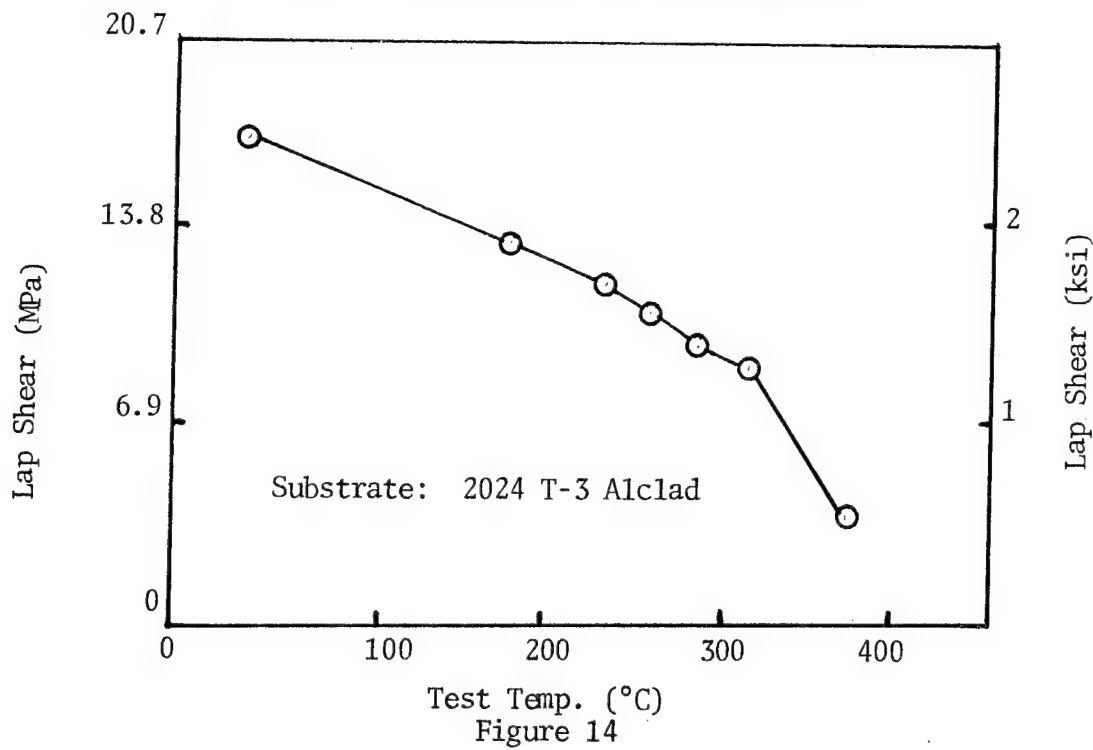
EFFECT OF TEMPERATURE ON AN
ADDITION REACTION PI ADHESIVE (FM® 35)



EFFECT OF PANEL WIDTH ON
BOND STRENGTH OF FM® 35



EFFECT OF TEMPERATURE ON A BMI ADHESIVE



CHEMICAL CONTROL OF RATE AND ONSET TEMPERATURE
OF NADIMIDE POLYMERIZATION

Richard W. Lauver
National Aeronautics and Space Administration
Lewis Research Center

The chemistry of norbornenyl capped imide compounds (nadimides) is briefly reviewed with emphasis on the contribution of Diels-Alder reversion in controlling the rate and onset of the thermal polymerization reaction. Control of onset temperature of the cure exotherm by adjusting the concentration of maleimide is demonstrated using selected model compounds. The effects of nitrophenyl compounds as free radical retarders on nadimide reactivity are discussed. A simple copolymerization model is proposed for the overall nadimide cure reaction. An approximate numerical analysis is carried out to demonstrate the ability of the model to simulate the trends observed for both maleimide and nitrophenyl additions.

INTRODUCTION

Norbornenyl-capped polyimide resins have been investigated as matrix resins since the early seventies (refs. 1 and 2). The application of composites employing matrix resins utilizing this addition chemistry has increased substantially in recent years (ref. 3). Engineering interest in these resin systems has outpaced the chemical understanding of the cross-link chemistry. Improved understanding would place the current technology on firmer chemical grounds, and would provide a basis for defining the potential for improvements in processability and thermo-oxidative stability. There have been several studies of nadimide thermal chemistry (refs. 4 to 6) since the initial mechanistic arguments of Jones, et al. (refs. 1 and 7), however, the reaction mechanism of the cross-link reaction has not been fully elucidated.

The principal purpose of this study was to evaluate chemical approaches for control of the onset temperature and rate of cure in nadimide resins. Two approaches are presented which provide such control. Another major aspect of this paper is the evaluation of a proposed copolymerization model for the mechanism of nadimide cure. The model is numerically evaluated to demonstrate that the major trends observed experimentally can be simulated by the model.

Experimental - The differential calorimeter scans (DSC) were run (typically) on approximately 2 mg of sample in aluminum pans (covered but not sealed) under 100 psi of nitrogen (static) at a heating rate of 10 °C/min.

Calculations - Calculations were performed on a microcomputer using a Basic language program (listing is available on request). The inherent limitations in speed, as well as the preliminary state of the model, prompted the utilization of a relatively coarse time interval (30 seconds) in the simulations.

RESULTS AND DISCUSSION

Background

Several thermal reactions of nadimide groups can be postulated. Figure 1 summarizes four processes which have been identified during nadimide thermal cures. It is not implied that this is the comprehensive set of reactions, but rather those which have been well documented.

The isomerization of nadic groups is well known, and the extent of this endo-to exo-rearrangement has recently been studied for nadimide oligomers (refs. 5, 8, and 9). The isomerization appears to occur rapidly even at moderate temperatures, and apparent equilibrium endo/exo mixtures can be attained in a few hours in the oligomeric and monomeric systems studied. It is not evident, however, that this activity contributes significantly to the overall cure chemistry for the usual high temperature conditions (relatively rapid rise to 316 °C), even though some differences in reactivity of the isomers has been postulated (ref. 5).

Diels-Alder reversion (reaction 2 of fig. 1) of the nadimide to form cyclopentadiene and maleimide is an element of nearly all mechanistic descriptions of nadimide thermal chemistry. Nondissociative mechanisms have been proposed to account for both polymerization and isomerization (ref. 8). However, even one of the proponents of nondissociative mechanisms for describing norbornenyl chemistry invokes reversion to account for the high-temperature reactions of nadimides (ref. 10). Cyclopentadiene has been monitored as a volatile by-product during thermal polymerization of nadimides (refs. 4 and 11), however, the amount of cyclopentadiene actually evolved is difficult to quantify and has not been fully documented. Consequently, the predominant evidence for reversion (mostly unreported in the literature) arises in materials engineering studies and in the fabrication of components where the odor of dicyclopentadiene can be detected in traps or inappropriately cured parts. The kinetics of the net cross-link reaction appear pseudo first order as determined calorimetrically (ref. 6). This observation and the magnitude of the rate constant are consistent with Diels-Alder reversion being the rate limiting step in the net reaction. It is this observation, and the chemical rationale discussed below that are the basis for the mechanistic model utilized in this paper.

Double Diels-Alder adducts (reaction 3 of fig. 1) have been observed as by-products of the thermal reaction of selected nadimide monomers (ref. 5). This product provides a statistically favorable mode of consuming cyclopentadiene. It is not presumed to have a major effect on the cure reaction since its reactivity should be essentially equivalent to the parent nadimide.

The desired polymerization reaction is presumed to be free radical vinyl addition of all the species present at any instant as the system evolves as a function of time and temperature as noted above. It is presumed that the reaction is thermally initiated, and that the polymer composition and rate of polymerization are determined by the relative reactivities and concentrations of each component. For simplicity in the current model, it is presumed that all the cyclopentadiene is consumed in the double adduct noted earlier and that all the nadimide compounds have the same reactivity. These assumptions reduce the model to a classical binary copolymerization reaction of nadimide and maleimide with thermal initiation. The most unique aspect of the model is the Diels-Alder interrelation of the comonomers. This constraint requires that the concentration of the maleimide is defined by concentration of nadimide and the rate of Diels-Alder reversion at each time and temperature.

Experimental Observations

Two chemical approaches have recently been observed (ref. 12) which can be employed to promote the onset of nadimide cure, as defined by the cross-link exotherm, at significantly lower temperatures than observed for the unmodified materials.

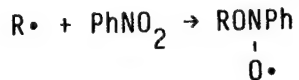
The first approach requires addition of maleimide oligomers to preimidized nadic oligomers or resins. The rationale for this chemical approach is based on the copolymerization model described above and is simply: an increase in the initial concentration of one of the principal coreactants should increase the rate of the net reaction. Figure 2 shows a series of differential calorimeter scans for mixtures of the bismaleimide and the bisnadimide of methylenedianiline. With increasing maleimide concentration, the cross-link exotherm progresses from a temperature characteristic of most nadimide oligomers (peak maximum near 360 °C) to lower temperatures, and, ultimately to that characteristic of the bismaleimide (peak maximum near 250 °C). Figure 3 shows the overall trend. The shape of this curve is not easily rationalized. In particular, the exotherm appears to exhibit significant sensitivity to quite low concentrations (near 0.1 mole fraction) of nadimide in maleimide. This chemical approach for decreasing cure temperature is most appealing since it permits continuous adjustment of the cure temperature over a range of about 100 °C as the composition changes from pure nadimide to pure maleimide. Unfortunately, the reactivity of the maleic double bond toward free amine (Michael addition) does not permit the utilization of this approach in monomeric precursor solutions for composite fabrication. The approach could be useful in applications currently using preimidized molding powders. However, it has not been fully evaluated.

The second approach requires addition of aromatic nitro compounds to a nadimide mixture. This approach evolved from a study of the reactivity of a large number of substituted phenyl nadimides (ref. 12) which showed the nitro-containing compounds to have exceptional low temperature reactivity. Figure 4 compares the cross-link exotherms for two nitro-containing systems with that for the bisnadimide of methylenedianiline. The principal observations for nadimide thermal cures in the presence of nitrophenyl additives were as follows: (1) Each nitro compound exhibits a unique cure temperature. (2) The cure temperature is related to (a) the number of nitro groups in the additive, and (b) the extent of electron withdrawal in the phenyl ring containing the nitro group. Table I summarizes the peak exotherm temperatures for several nadimide systems incorporating nitrophenyl groups. (3) The predominant cure exotherm shows little sensitivity to the concentration of the nitro additive. Even when the nitro groups are limited by concentration or mobility (in particular, nitrophenyl nadimides which will be restrained once the nadic moiety has been incorporated into the polymer), the systems exhibit initial exothermic activity at the temperature characteristic of the nitrophenyl additive and subsequently complete the cure at the temperature characteristic of unmodified nadimide.

The effect of nitrophenyl additives on the homopolymerization of maleimides was also examined. Nitrophenyl additives with bismaleimides retard the cure reaction in the classical sense (the cure exotherm moves to higher temperatures). The peak exotherm temperatures for mixtures of the bismaleimide of methylenedianiline with selected nitrophenyl additives are given in table II.

Overall, these nitrophenyl effects are rationalized on the basis of: (a) efficient retardation (i.e., inhibition) of the free radical reactions at low

temperatures (<200 °C), and (b) thermal regeneration of reactive radicals at temperatures characteristic of the monomer/retarder combination. A possible mechanism is the addition of radicals, $R\cdot$, to the nitrophenyl compound, $PhNO_2$, to form inorganic ester radicals



Any reaction of this type interrupts the propagation of radicals in the system by forming a more stable, slower-reacting intermediate (the inorganic radical). However, such species would have relatively low stability because the R-O-N bond energies of analogous nonradical esters are known to be small (in the range 30 to 35 kcal/mole, ref. 13). Hence, at some temperature in the dynamic thermal cure, the accumulation of radical esters will thermally decompose to regenerate more highly reactive species ($R\cdot$ or, possibly, $RO\cdot$). This decomposition will necessarily be a simple first order disproportionation which will generate in relatively short time (compared to the other initiation reactions) a large concentration of radicals. Such a dramatic increase in radical concentration appears adequate to initiate substantial cure of the vinyl compounds of concern near the dissociation temperature of the retarding intermediate even when the parent compound (nadimide or phenylmaleimide) normally cures at higher temperatures.

This chemical approach for controlling the onset of nadimide cure is compatible with normal processing procedures. PMR resins with selected nitrophenyl additives are being evaluated as matrix resins.

Rate Equation and Numerical Model

The classical binary copolymerization rate equation was utilized for the model.

$$RATE = \frac{(r_1 [NI]^2 + 2[NI][MI] + r_2[MI]^2) (\sqrt{RI}/\gamma_1)}{(r_1^2 [NI]^2 + 2(\phi r_1 r_2 \gamma_2/\gamma_1) [NI][MI] + (r_2 \gamma_2/\gamma_1)^2 [MI]^2)^{1/2}}$$

where

- [NI] concentration of nadimide (monomer 1)
- [MI] concentration of maleimide (monomer 2)
- r_1 reactivity ratio
- $\gamma_1 = \sqrt{k_{T11}/k_{P11}}$
- ϕ cross termination factor = $k_{I12}/\sqrt{k_{T11}k_{T22}}$
- RI initiation rate = $k_{I11}[NI]^2 + C[NI][MI] + k_{I22}[MI]^2$
- C cross initiation factor = $k_{I12}/\sqrt{k_{I11}k_{I22}}$

Imposing the Diels-Alder relationship on the concentrations adds the requirements that NI decrease and MI increase due to reversion at the specified temperature

$$[MI] = [MI]_0 + k_R [NI]_0 \Delta t$$

$$[NI] = [NI]_0 - k_R [NI]_0 \Delta t$$

where

k_R reversion rate constant
 Δt time interval of the summation

and the subscripted terms are the concentrations after the previous iteration.

The effect of the retarder is introduced in a form suggested by Schultz and Strassberger (ref. 14):

$$\text{Rate}' = \text{Rate}/(1 + k_I [I])$$

where

[I] concentration of retarder
 k_I rate constant for reaction with retarder

and the initiation rate becomes

$$RI' = RI + k_D [I^\bullet]$$

where

[I^\bullet] concentration of reacted retarder
 k_D rate constant for regeneration of radicals

and the concentrations are modified as

$$[I] = [I]_0 - RI_0 \Delta t + k_D [I^\bullet] \Delta t$$

$$[I^\bullet] = [I^\bullet]_0 + RI_0 \Delta t$$

to account for the variation with time and temperature.

Choice of Rate Constants

The Arrhenius activation energies and pre-exponential factors employed in the calculations are summarized in table III. The primary rationale for choosing these parameters was to utilize values typical of condensed phase, thermally-initiated vinyl polymerizations. Such data are limited; however, the well documented discussions of styrene and methylmethacrylate were chosen as guidelines. Specific rationale are noted below and summarized in table III. The Arrhenius parameters for the initiation rate constants were chosen to reflect literature values for thermally-initiated vinyl polymerization. The activation energies (25 kcal/mole) are considered to be reasonable estimates since they are typical of many vinyl monomers. The pre-exponential factor for maleimide (10^6 sec^{-1}) is analogous to that found for styrene and reflects a moderately reactive monomer. The factor for nadimide (10 sec^{-1}) reflects a very slowly reacting monomer similar to (but not as slow as) methylmethacrylate (ref. 15). The Arrhenius parameters for the propagation rate constants ($A = 10^7 \text{ sec}^{-1}$ and $E_a = 7 \text{ kcal/mole}$) are typical of most vinyl polymerizations. The termination rate parameters were again based on the reported data for styrene and methylmethacrylate. The activation energies (3 kcal/mole) are typical of many vinyl monomers. However, the pre-exponential factors are adjusted to reflect a termination frequency for maleimide (10^9 sec^{-1}) analogous to styrene, but increased efficiency for nadimide ($2 \times 10^{11} \text{ sec}^{-1}$).

Overall, the rate constants defined by these parameters are considered to be conservative choices for this model. The accessible homopolymerization reaction, polymerization of bismaleimide, is well fit by the chosen parameters. The Diels-Alder reversion rate is defined by the Arrhenius parameters previously observed (ref. 5) for the net cross-link reaction ($A = 4 \times 10^{13}$ and $E_a = 44$ kcal/mole). These values appear consistent with published rate constants for such reactions (ref. 16). The choice of parameters for nadimide and the magnitude of the cross terms were strongly influenced by the necessity of simulating the elevated temperature exotherm of the bisnadimide. Within the scope of this model, the suppression of the nadimide cure exotherm to temperatures above 300 °C required both low reactivity of the nadimide (as defined above) and predominant cross termination. It should be noted that there are other kinetic factors (not included in this simple model) which may contribute to the late reaction exotherm of the nadimides. For example, chain transfer reactions could contribute to this effect.

The cross terms are, overall, rationalized by analogy of published data for maleic anhydride copolymerizations with norbornene or related vinyl monomers (ref. 17). The reactivity ratios were set equal and held constant ($r_1 = r_2 = .01$). The cross initiation and cross termination terms were used as fitting factors in adjusting the calculated nadimide exotherm. A range of values was tested for the cross initiation factor ($C = 1$ to 10) and a small value ($C = 2$) appeared most useful. A large range of values was tested for the cross termination factor ($O = 1$ to 10^4) and a large value ($O = 10^3$) was found necessary, as discussed above, to simulate the nadimide data.

The additional parameters required for the model incorporating retardation were chosen using very simplistic assumptions. The rate constant, k_I , for reaction of retarder was presumed very large for all temperatures and simply set at unity. The dissociation or transfer rate constant was presumed to have classical vibrational activation and the pre-exponential was chosen accordingly ($A = 4 \times 10^{13}$). A range of activation energies (30 to 40 kcal/mole) was evaluated. This energy range is consistent with the bond energy of inorganic esters of the type proposed above (ref. 13). This range of activation energies provided a reasonable simulation of the experimental trends as shown below.

It is emphasized that these rate parameters were used without change for all the calculations described below. The only variables explored in the calculated results were the activation energy for dissociation of the retarding intermediate (discussed above) and the initial concentrations: nadimide ($[NI] = 0$ to 5 mole/liter), maleimide ($[MI] = 0$ to 5 mole/liter), and retarder ($[I] = 0$ to 5 mole/liter).

Calculated Results

It should be kept in mind that these are intended to be "order of magnitude" approximations of the reaction scheme. The principal desire is to demonstrate that the observed trends in the experimental data can be reproduced with this simple model.

Figure 5 shows the calculated concentration dependence of the temperature of maximum rate of polymerization for the mixed bismaleimide/bisnadimide systems. The general shape of the curve compares favorably with the experimental data (fig. 3). Although some of the initial parameters of the numerical model might be debated, it should be noted that all the rate parameters are the same in each calculation and hence the only variable reflected in this curve is the relative concentrations of

bismaleimide and bisnadimide. It is of particular interest that the sensitivity at low nadimide concentrations appears to be reproduced in this simple model. It seems that, for this model, the cross termination term predominates for even small concentrations of nadimide. Recall that the large cross termination factor was introduced to reproduce the high temperature cure of the nadimide system; thus, it is implied that the nadimide (or the cyclopentadiene evolved) has a net retarding effect on the free radical reactions of the cure.

The calculated effect of retarder on the rate of polymerization of nadimide is demonstrated in figures 6 and 7. Figure 6 shows, for $E_a (I) = 33$ kcal/mole and a 1 mole/liter concentration of the retarder, a peak reaction rate near 250°C rather than approximately 325°C calculated for the unmodified nadimide system. Varying the concentration, $[I]$, from 1 to 5 mole/liter in the calculation changed the peak temperature less than 20°C , which simulates the observed small concentration dependence moderately well. The effect of increasing the activation energy for dissociation of the retarded intermediate, $E_a (I)$, from 30 to 38 kcal/mole at constant concentration is shown in figure 7. This range of activation energies covers the desired range noted above, and produces a span of peak polymerization temperatures which is consistent with the experimental data. Calculated data for bismaleimide with retarder is shown in figure 8 and, again the general trend can be reproduced. These calculations require activation energies slightly higher than for the nadimides, however, and the calculations, overall, appear to be more sensitive to the nitrophenyl parameters for the retardation effect and possibly reflects limitations in the simple model.

CONCLUDING REMARKS

Two chemical approaches were described which provide control of the onset and rate of polymerization of nadimides:

(1) Addition of bismaleimide to nadimides. This approach provides a continuous range of cure temperatures between the two extremes of the monomers.

(2) Addition of nitrophenyl compounds. This approach provides specific onset temperatures characteristic of the additive chosen.

A simple copolymerization model was chosen to describe the net polymerization of nadimides and to account for the trends in thermal reactivity observed with the two concepts described above. An approximate numerical analysis was carried out which successfully reproduced the major experimental trends.

From this analysis it was concluded that the rate of polymerization of nadimide was dominated by (1) the inherent low reactivity of nadimide toward homopolymerization, (2) the Diels-Alder reversion to form maleimide (the comonomer), and (3) a large cross termination rate.

From this analysis it was concluded that nitrophenyl additives affect nadimide cures in two ways: (1) as a free radical retarder at low temperatures ($<200^\circ\text{C}$), and (2) as free radical generators at temperatures where the retarded intermediates dissociate.

REFERENCES

1. Burns, E.A.; Jones, R.T.; Vaughn, R.W.; and Kendrick, W.P.: Thermally Stable Laminating Resins, NASA CR-72633, 1970.

2. Serafini, T.T.; Delvigs, P.; and Lightsey, G.R.: Thermally Stable Polyimides from Solutions of Monomeric Reactants, *J. Appl. Polym. Sci.*, 16, 905 (1971).
3. Serafini, T.T.; Delvigs, P.; and Alston, W.B.: PMR Polyimides - Review and Update, *NASA TM-82821*, 1982, and also *Proc. of 27th SAMPE National Tech. Conf.*, May 1982.
4. Wereta, A.; and Hadad, D.K.: Analytical Techniques Applied to the Optimization of LARC-160 Composite Laminates, in *Resins for Aerospace*, Ed. C.A. May, Am. Chem. Soc. Symposium Series no. 132, 1980, p. 225.
5. (a) Wong, A.C.; and Ritchey, W.M.: *Macromolecules*, 14, 825 (1981). (b) Wong, A.C.; Garroway, A.N.; and Ritchey, W.M.: *Macromolecules*, 14, 832 (1981).
6. Lauver, R.W.: Kinetics of Imidization and Crosslinking in PMR Polyimide, *J. Polym. Sci., Polymer Chem. Ed.*, 17, 2529 (1979).
7. Jones, R.J.; Vaughn, R.W.; and Burns, E.A.: Thermally Stable Laminating Resins, *NASA CR-72984*, 1972.
8. Wong, A.C.; and Ritchey, W.M.: *Spectroscopy Letters*, 13, 503 (1980).
9. Sukenik, C.N.; Ritchey, W.M.; Malhotra, V.; and Varde, U.: The Synthesis, Characterization, and Thermal Chemistry of Modified Norbornenyl PMR Endcaps, this volume.
10. Gaylord, N.G.; Martan, M.; and Deshpande, A.B.: *J. Macromol. Sci. Chem.*, A19, 537 (1983).
11. Lindenmeyer, P.H.; and Sheppard, C.: Characterization of PMR Polyimide Resin and Prepreg, *NASA CR-168217*, 1984.
12. Lauver, R.W.; and Alston, W.B.: Reactivity of Substituted Phenylnadiimides, 23rd Rocky Mt. Conf. (Soc. of Appl. Spectroscopy and Chromatography Disc. Grp.), Aug. 1980.
13. Wiberg, K.B.: *Physical Organic Chemistry*, John Wiley and Sons, New York, NY (1964), pp. 242-243.
14. Schultz, G.V.; and Strassberger, M.: *Chem. Ber.*, 80, 232 (1947), as discussed in *Ency. of Polym. Sci.*, vol. 7, pp. 644-647.
15. Walling, C.; and Briggs, E.R.: *J. Am. Soc.*, 68, 1141 (1946), as discussed in Flory, P.J.: *Principals of Polymer Chemistry*, Cornell Un. Press, Ithaca, NY (1953), pp. 131-132 and 158.
16. Wasserman, A.: *Diels-Alder Reactions*, Elsevier, Amsterdam (1965), p. 61.
17. Trivedi, B.C.; and Culbertson, B.O.: *Maleic Anhydride*, Plenum Press, New York, NY (1982), p. 301.

TABLE I - PEAK EXOTHERM TEMPERATURE OF BISNADIMIDE
OF METHYLENEDIANILINE WITH SELECTED
NITRO PHENYL ADDITIVES

Additive	Concentration (mole fraction)	Exotherm maximum (C°)
nil	--	350
3, 5-NO ₂ Benzonitrile	.15	233, 330 (minor)
	.38	233
	.51	233
3, 4-NO ₂ Toluene	.17	255, 335 (minor)
	.27	255
	.42	255
3-NO ₂ Phenylnadicimide	.20	287, 360 (minor)
	1.0	287, 360 (minor)

TABLE II - CORRELATION OF MAXIMUM CURE EXOTHERM
TEMPERATURES FOR VINYL MONOMERS WITH
NITRO PHENYL ADDITIVES

Additive	Temperature of maximum exotherm (C°) for	
	Bisnadicimide ^a	Bismaleimide ^a
nil	350	250
3, 5-NO ₂ Benzonitrile	233	235
3, 4-NO ₂ Toluene	255	305
4-NO ₂ Chlorobenzene	297	265

^aBisimides of methylenedianiline.

TABLE III - ASSUMED ARRHENIUS PARAMETERS

Rate constant	A (1/sec)	E _a (kcal)	Rationale
Initiation: k _{I11}	10	25	Slow; similar to MMA
	10 ⁶	25	Moderate; similar to styrene
Propagation: k _{P11}	10 ⁷	7	Typical for vinyl
	10 ⁷	7	Typical for vinyl
Termination: k _{T11}	2x10 ¹¹	3	~Efficient for vinyl
	10 ⁹	3	Typical for vinyl
Thermal: k _R	4x10 ¹³	44	Experimental
	4x10 ¹³	33-44	Reasonable bond energies
Cross terms: r ₁ = r ₂ = .01, ϕ = 1000, C = 2			

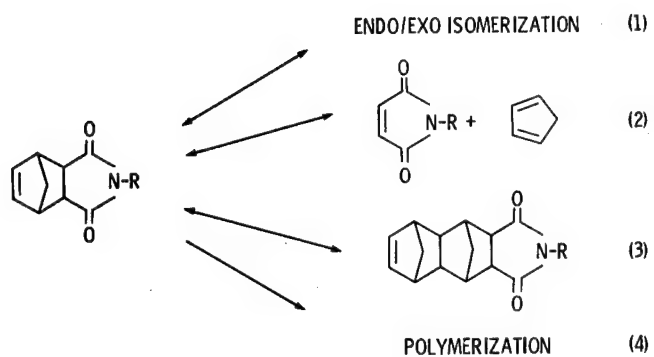


Figure 1. - Four possible thermal reactions of nadimides.

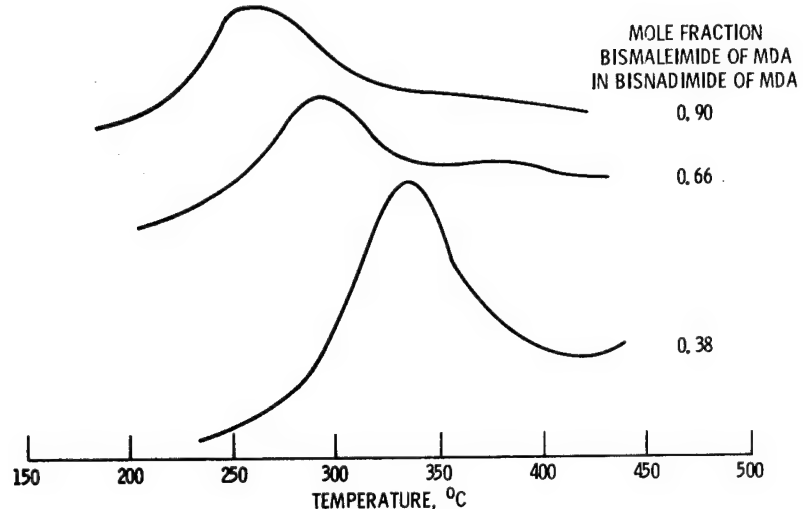


Figure 2. - The effect of bismaleimide concentration variations on the cure exotherm of bisnadicimide.

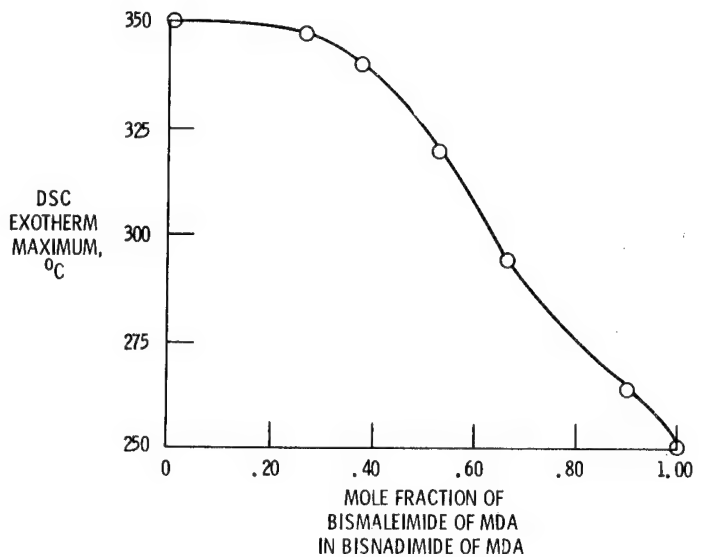


Figure 3. - Variation of cure exotherm maximum with concentration of bismaleimide in nadimide.

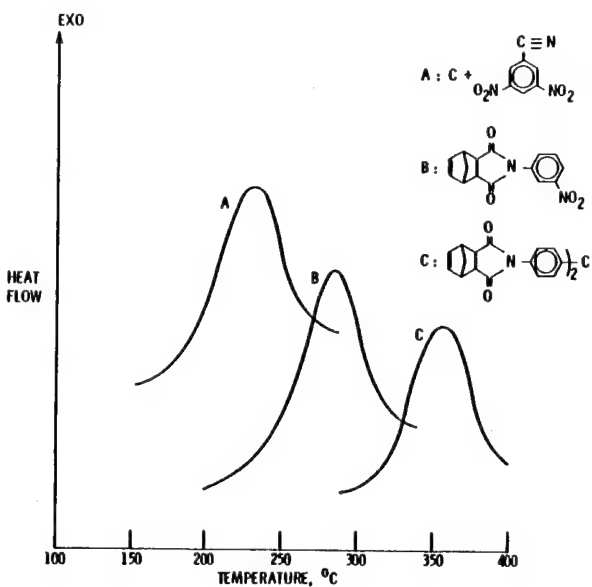


Figure 4. - Decrease in temperature of cure exotherm for nadimide in the presence of nitro phenyl groups.

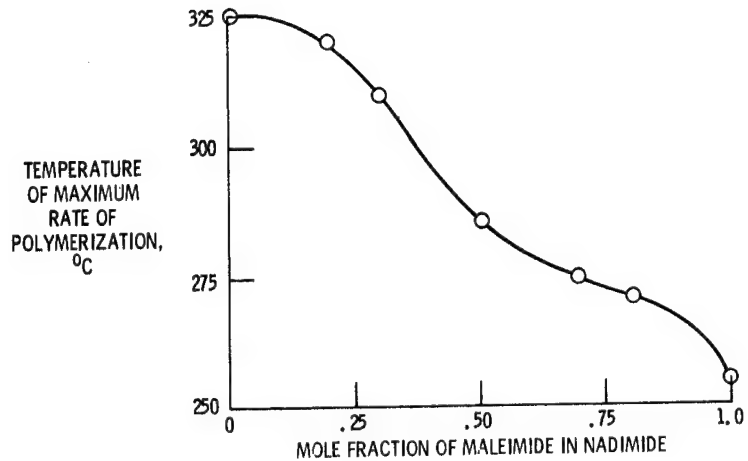


Figure 5. - Calculated dependence of maximum polymerization rate on concentration of maleimide in nadimide.

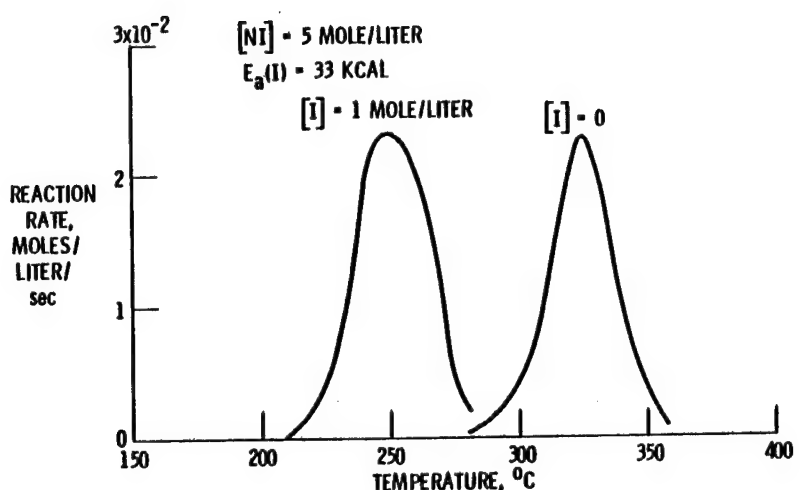


Figure 6. - Calculated effect of retarder on nadimide reaction rate.

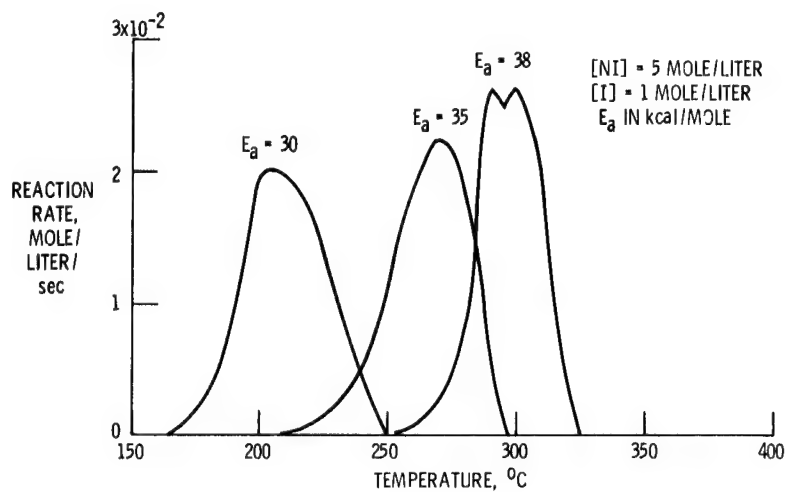


Figure 7. - Calculated effect of activation energy, E_a , for regeneration of retarder on nadimide reaction rate.

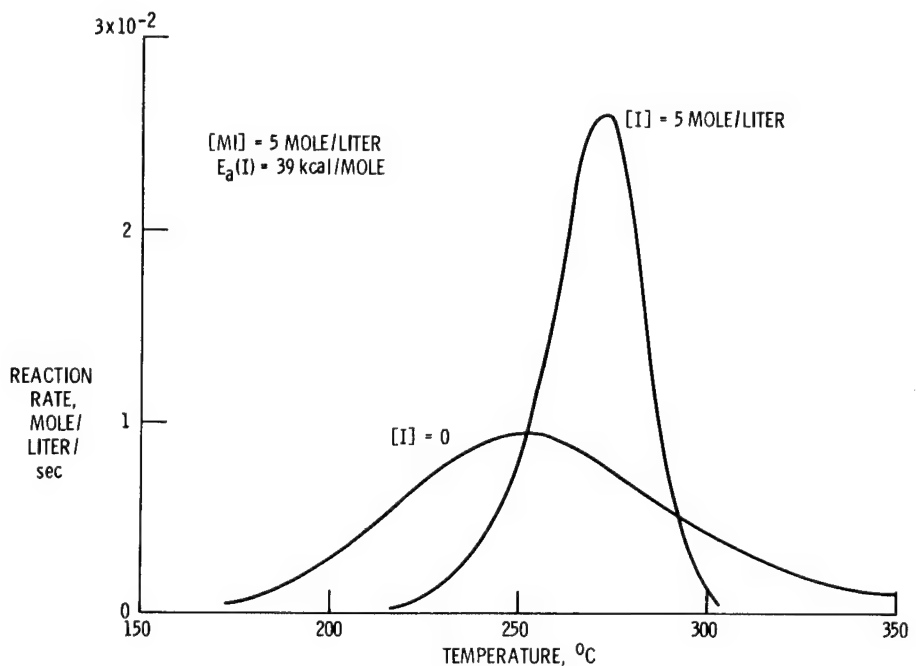


Figure 8. - Calculated effect of retardation on rate of polymerization of bismaleimide.

CHARACTERIZATION METHODOLOGY

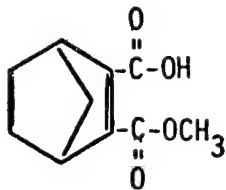
FOR PMR-15*

A. B. Hunter
Boeing Aerospace Company

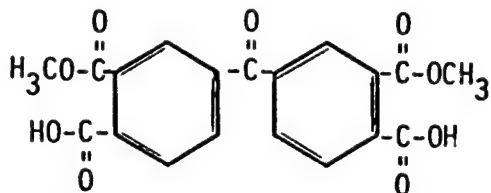
Characterization of model compounds, monomers, resin solutions and cure cycles of PMR-15 polyimide were performed. Successful separation of various reaction products were also accomplished by liquid chromatography. The PMR-15 cure analysis was performed by fourier transform spectroscopy and gas chromatograph - mass spectrometry. Characterization receiving inspection tests for Quality Control are recommended.

INTRODUCTION

Within the aerospace industry polyimides are becoming increasingly important. One particular polyimide being developed for various uses is PMR-15 as developed by NASA-Lewis. PMR-15 consists of three monomers

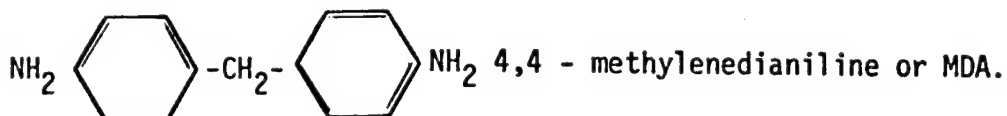


A monomethyl ester referred to as NE;



a dimethyl ester referred to as BTDE;

and



*Work performed under contract NAS 3-22523.

The monomers polymerize under heat by the combining of BTDE and MDA with NE being an end cap. Final crosslinking occurs through the end cap. The material is usually received as a graphite prepreg and is then molded into part configuration under heat and pressure.

DEVELOPMENT OF METHODOLOGY

The starting materials for this polymer are 1) monomethyl ester of 5-norbornene -2, 3-dicarboxylic acid (NE), 2) Dimethyl ester of 3, 3', 4, 4' -benzophenone-tetracarboxylic acid (BTDE) and 3) 4, 4' - methylenedianiline (MDA). The two esters are synthesized from their respective anhydrides which are purchased commercially. The MDA is also purchased commercially. The starting products are then combined in a methanol solution to form the PMR resin. A suggested route for the polymerization of the resin system through the cure cycle is the formation of polyamide acid then polyimidization and finally the material becomes thermally crosslinked. Through the course of the reaction, water, methanol, and cyclopentadiene are evolved as reaction products.

The resin and starting materials were evaluated by liquid chromatography. Two modes were used as described below:

Mode	Adsorption	Reverse Phase
Columns	2 DuPont PSM60	Varian RP MCH10
Mobile Phase	1: THF:H ₂ O with 0.01% Acetic Acid	Methanol Water
Program	Isocratic	Gradient 40:60 to 80:20 15 Min.
Detector	UV @ 210 and 254 NM	UV @ 210 and 254 NM

The isocratic method separates the esters their isomers and reaction products. (See Figure 1). One difficulty with this method is the MDA remains on the column and needs to be flushed out periodically to restore baseline. Another difficulty of the method is during the synthesis of the BTDE a small amount of triester is formed. The triester elution peak is sometimes poorly resolved with the NE peak. However, a quantitation can be made because the NE absorbs at 210 NM whereas the triester absorbs at both 254 and 210 NM. Figure 2 illustrates two batches of BTDE comparing a normal cook to one that has been overcooked. Figure 3 illustrates PMR resin with the formation of tetraester. The presence of tetraester has been correlated with a fall off in mechanical properties. The gradient method illustrated in Figure 4 separates the MDA from the esters. Although it does not show the detail of the isocratic method, it does permit quantification of the MDA. Also with this method a reaction product is detected as the resin ages, See Figure 5. Thermal analysis studies were also performed. Figure 6 illustrates a typical differential scanning calorimeter analysis performed in a pressure cell. One area of interest in the scan is the high temperature exotherm occurring at 587K denoting crosslinking taking place. The cure was also followed by infrared analysis which readily detects the disappearance of the MDA and formation of imide groups. In addition, the outgassing reaction products were monitored by

gas chromatography. Water, methanol and cyclopentadiene were all detected. Cyclopentadiene was first detected at 423K and as the sample reaches 573K a discontinuity occurs in the outgassing of cyclopentadiene that seems to correlate with the exotherm detected by DSC.

A number of methods were investigated to characterize the chemical and physical changes which occur during this cure cycle. The physical changes were found to be best characterized by dynamic mechanical analysis (DMA) using the DuPont compound pendulum method. Typical results are shown in Figure 7. The first three damping peaks occur at 373K (212⁰F), 423K (302⁰F) and 503K (446⁰F) and correspond very nicely with (1) the melting of the monomers, (2) the imidization reaction, and (3) the glass transition of softening and flow of the polyimide. The frequency curve, which is a measure of modulus, clearly shows that the first damping peak corresponds to a decrease in modulus (melting) while the second corresponds to the increase in modulus due to the imidization reaction. The third peak shows a frequency and damping relationship typical of the glass transition in a thermoplastic polymer. During the 30 minute holding period at 522K (480⁰F) both the damping and the frequency increase slightly which would be consistent with the completion of the ring closing imidization reaction and the continued flow of the thermoplastic polyimide. With the resumption of heating at the end of the 30 minute hold period, both the damping and the frequency decrease to a minimum at about 563K (554⁰F) and then increases as the crosslinking reaction caused by the thermal decomposition of the nadic ring begins to influence the flow properties of thermoplastic polyimide. Clearly the 30 minute hold period at 522K (480⁰F) is the proper point to apply pressure to effect the best possible consolidation of a composite material since it is just above the glass transition of the essentially complete polyimide and below the activation temperature for the crosslinking reaction.

Based on the characterization studies we have identified certain Receiving Inspection tests for Quality Control. The starting materials are controlled by liquid chromatography. The resin and prepreg are controlled by liquid chromatography, infrared analysis and gas chromatography. These tests have successfully identified non-processable material and materials with low mechanical properties during this contract.

LIQUID CHROMATOGRAPHY

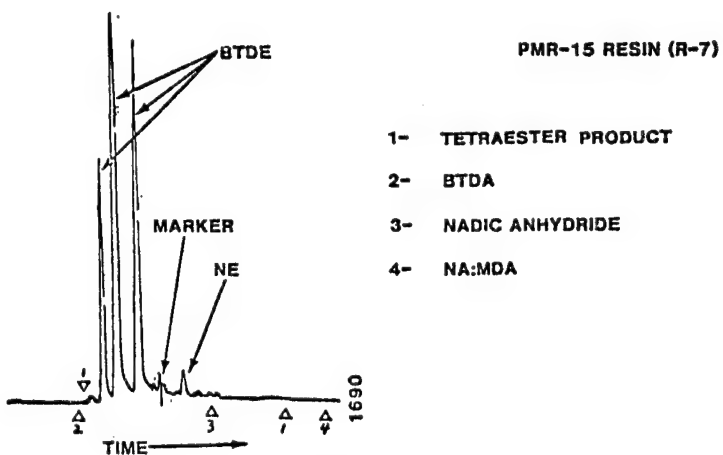


Figure 1

LIQUID CHROMATOGRAPH
BTDE

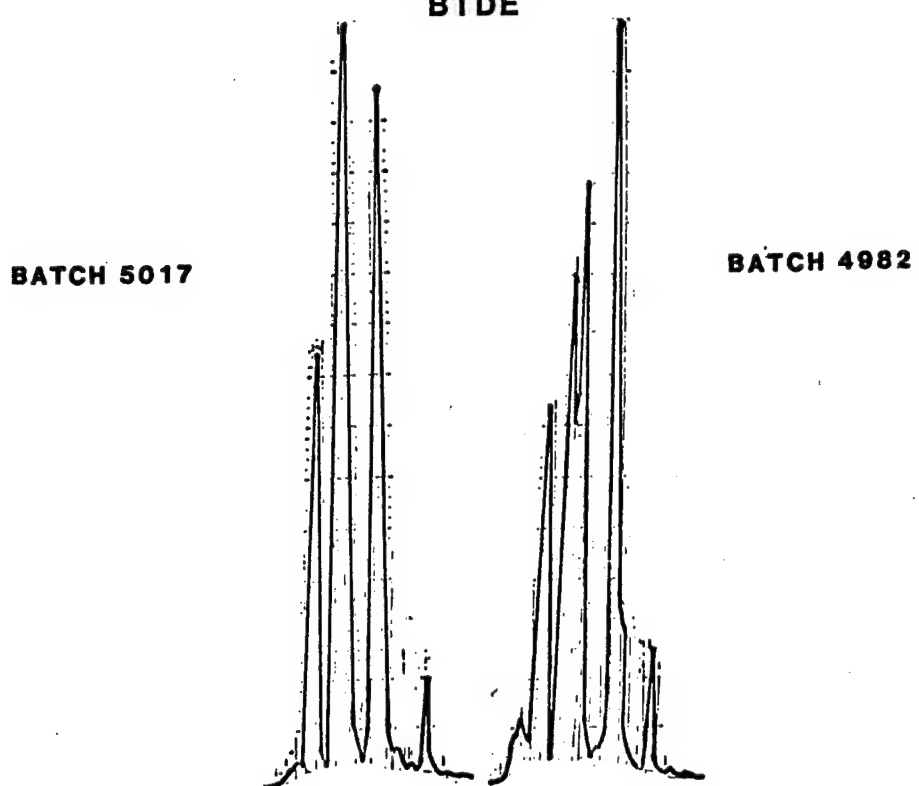


Figure 2

LIQUID CHROMATOGRAPHY

PMR-15

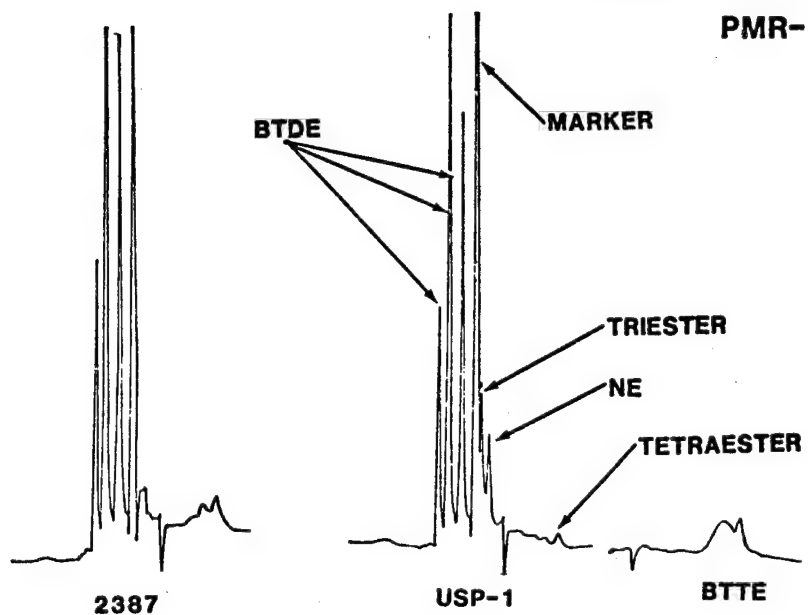
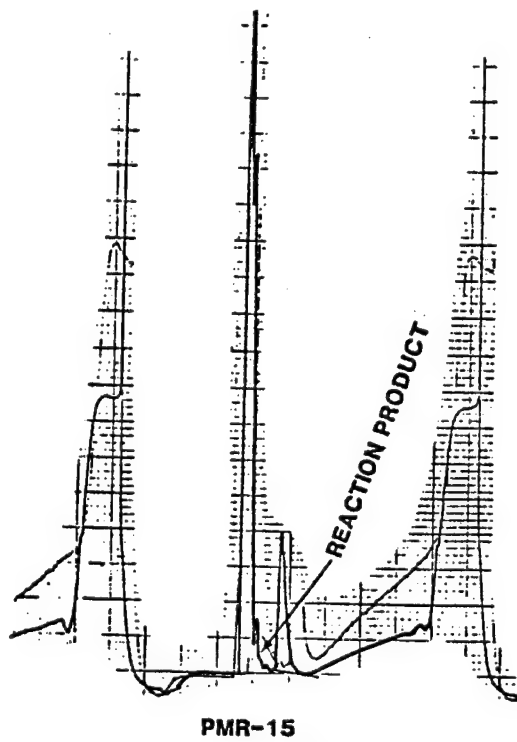
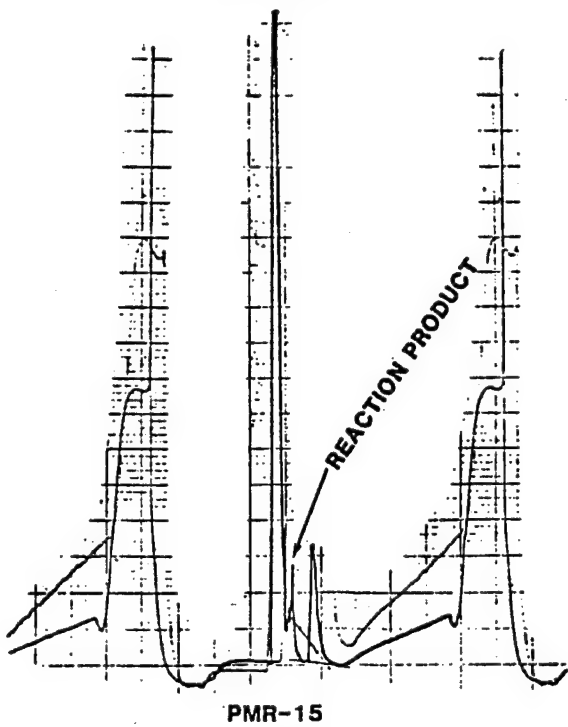


Figure 3



HPLC OF 67% SOLUTION RESIN - FRESH - UNAGED

Figure 4



HPLC SOLUTION RESIN AFTER 24 HOURS AT 316K(110°F)

Figure 5

Sample: PMR-15 LOT-G05244 R-2
Size: 13.22 AS RECD
Rate: 10C/MIN

DSC

Date: 7-Dec-82

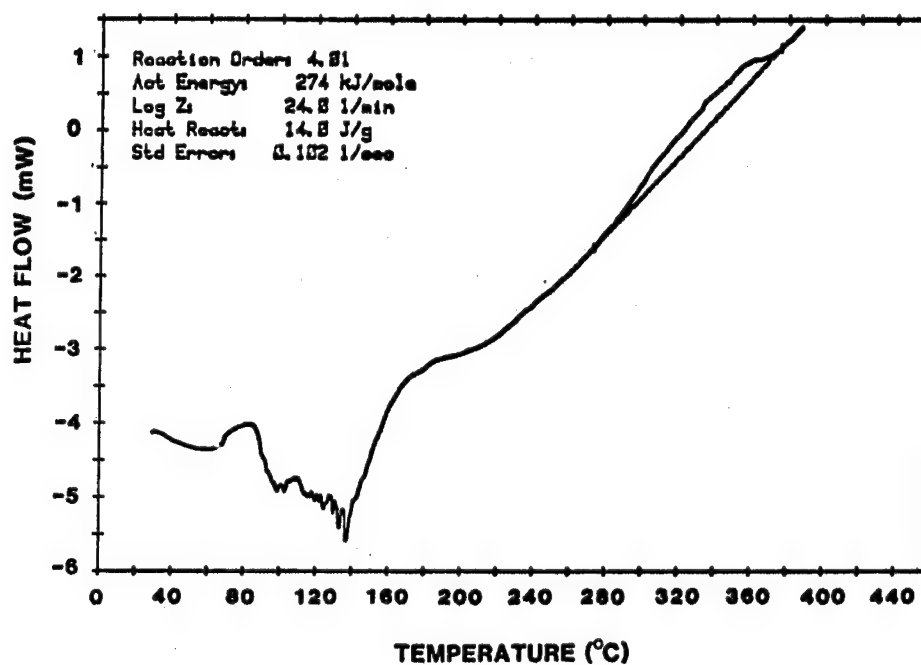


Figure 6

Sample: PMR-15 2187 3-PLY
Size: 10.7 X 6.35 X .33
Rate: 1.7

DMA

Date: 28-Oct-82

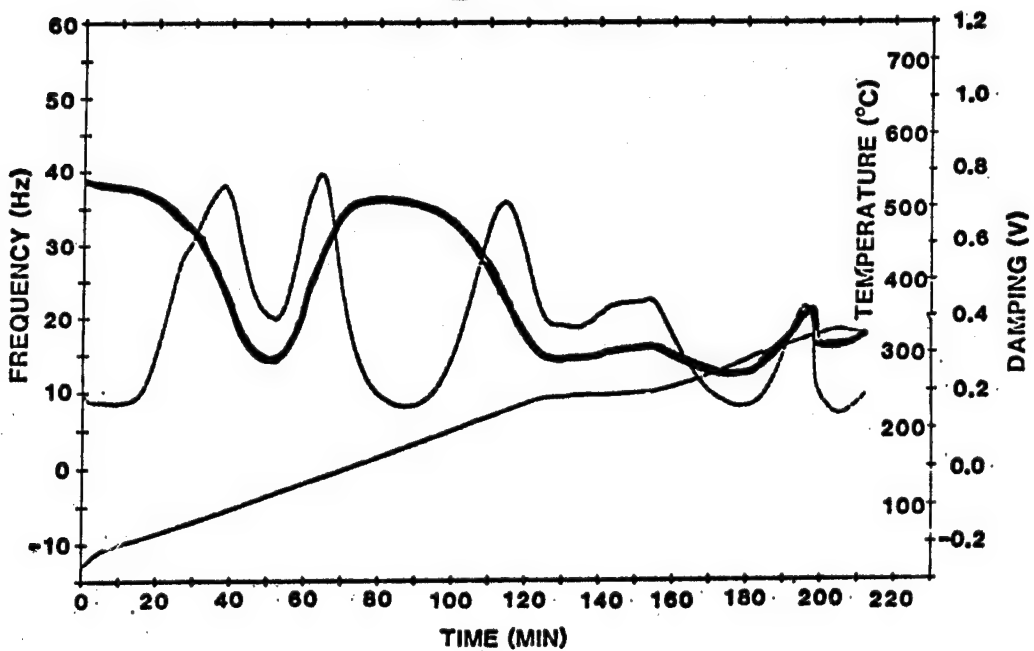


Figure 7

CHARACTERIZATION OF POLYIMIDE

MATRIX RESINS AND PREPREGS

M. G. Maximovich and R. M. Galeos
Lockheed Missiles and Space Company (LMSC)

Graphite/polyimide composite materials are attractive candidates for a wide range of aerospace applications. They have many of the virtues of graphite/epoxies, i.e. high specific strengths and stiffness, and also outstanding thermal/oxidative stability. Yet they are not widely used in the aerospace industry due to problems of processability.

By their nature, modern addition PI resins and prepregs are more complex than epoxies; the key to processing lies in characterizing and understanding the materials.

Chemical and rheological characterizations were carried out on several addition polyimide resins and graphite reinforced prepregs, including those based on PMR-15, LARC 160 (AP 22), LARC 160 (Curithane 103) and V378A. The use of a high range torque transducer with a Rheometrics mechanical spectrometer allowed rheological data to be generated on prepreg materials as well as neat resins. The use of prepreg samples instead of neat resins eliminated the need for pre-imidization of the samples and the date correlates well with processing behavior found in the shop. Rheological characterization of the resins and preprep found significant differences not readily detected by conventional chemical characterization techniques.

INTRODUCTION

A great deal of interest has been expressed in graphite/polyimide composite materials for applications where outstanding thermal/oxidative stability is a prime requirement. These materials also exhibit excellent mechanical properties, low specific gravities, and other attractive properties, yet they are only occasionally used in actual production programs.

The factor limiting the use of G/PI composites is processability. High quality, reproducible hardware is difficult to fabricate, due to lack of understanding and control of the various physical and chemical changes that occur during the processing of these materials. Many modern addition PIs, such as PMR-15 and LARC 160, are based on the Ciba-Geigy P-13N chemistry. Figure 1 shows the temperature ranges over which several different phenomena occur during the processing of P-13N. Small changes in structure can shift these temperature ranges and so alter the processing window for these materials. By understanding the chemistry and rheology of these materials, we hope to define and optimize the processing windows for the reliable, reproducible fabrication of high quality composite hardware. The purpose of this work was to further identify and develop techniques to chemically and rheologically

characterize and understand the behavior of G/PI prepreg material during processing.

Experimental

1. Materials. The prepgs based on LARC 160 (AP-22) and PMR-15 were obtained from Fiberite Corp. The V378 prepreg material were obtained from U.S. Polymeric, Inc. PMR-15 and LARC 160 (AP-22) neat resins were prepared at LMSC using the procedures well documented in the literature (1,2). The Curithane 103 version of LARC 160 was prepared using a simple one-to-one substitution of Curithane 103 for Jeffamine AP-22 in the LARC 160 procedure. The LARC-160 (Curithane 103) based prepreg was prepared from the resin synthesized at LMSC.

2. Chemical Characterization.

2.1 I.R. Studies

As previously reported, (3) IR spectroscopy and liquid chromatography were employed. Samples of both LARC 160 batches appear to show no significant differences in IR absorption peaks.

As synthesized, the volatile content of each LARC 160 batch was running about 48%. This was determined by inserting a resin sample into a preheated oven at 316°C for 30 minutes and then calculating the sample weight loss. This figure includes both solvent and condensation by-products. In order to be more representative of resin found in a prepreg, it was decided that a realistic volatile to resin ratio should be determined and also that the as-synthesized resin should be dried to this level. The dry resin content (after 30 minutes at 316°C) and volatile content (same conditions) of fabric LARC 160 prepreg used at LMSC runs around 36% and 12%, respectively. This gives a ratio of 1:3 or in other words 25% of the net resin weight is volatile. Drying conditions of 50°C for 2 to 3 hours in a vacuum oven seem to be appropriate and IR data shows no side reaction products. The infrared spectra of the three synthesized resins are shown in Figures 2-4.

2.2 HPLC Studies

HPLC traces were run using established test procedures (4). In our case the aqueous portion of the gradient mobile phase was not buffered with KH₂PO₄. However, the change did not appear to affect the quality of the component separations. Figures 5-7 show the chromatograms of the LARC on IMR resins.

General identification of specific peaks is made in a few instances. Lack of chromatogram complexity as compared to that obtained by Rockwell (5) may be attributed to two factors. First, our syntheses were carried out in fairly pure ethanol whereas Rockwell's esterification was conducted using an industrial alcohol mixture. Second, our resins were prepared under dilute solvent conditions. According to the 9th Quarterly Report (June - September 1980) from Rockwell (6), high viscosity during the co-esterification of the starting anhydride materials results in incomplete conversion of BTDA to the BTDE diester and, thus, the presence of the BTDA tetra-acid (BTA) and BTDE monoester will be evident.

To determine the effects of staging on the separated peaks, staged resins were analyzed by HPLC. The chromatogram comparison is shown in Figure 8. Keep in mind that the resin staged 1 hour at 121°C was not completely soluble in acetonitrile. Thus, the curve represents resin that was soluble and prefiltered through a 0.45 fluoromembrane filter. As can be seen, there are obvious effects on all peaks as the result of staging. Slight changes are evident even for the resin drying period of 2 hours at 50°C. The significance of these differences is not known at this time. Radical variations are seen in the extreme case of 1 hour staging at 121°C. The main reaction peak predominates in this curve.

2.3 DSC Characterization

DSC studies were carried out on both unstaged resin and resin staged $\frac{1}{2}$ hour at 120°C. Only minor differences were noted between the two LARC 160 versions. A set of curves was also run on a PMR-15 batch prepared at LMSC and is included for comparative purposes. Figure 9 through 14 show this data.

As noted previously (3), the main conclusion to be drawn from the chemical characterization studies were the little difference found between the two versions of LARC 160, which, in turn, differed significantly from the PMR-15 resin.

2.4 Rheological Characterization

2.4.1 Resin Studies

The first attempt to generate rheological data on the LARC 160 and PMR-15 resins were not entirely satisfactory. Although samples could be dried 2 hours at 50°C to remove solvent without significantly changing the resins, excessive volatiles were evolved during the cure. These volatiles, with condensation products and residual solvent, caused bubble formation in the Rheometrics mechanical spectrometer (RMS) sample cavity. The bubble formation led to excessive scatter in both the apparent viscosity (η^*) and the $\tan \delta$ data.

In order to avoid the problem, a pressure cell transducer was obtained from Rheometrics. The cell had 500 psi pressure capability and was designed for use with resin systems that outgas during cure. Unfortunately, little improvement was found in the data generated while using the pressure cell. Inspection of the samples showed bubbling still occurred within the samples and the resin was forced out from between the parallel plates. An extensive effort was made to overcome the problem, including modifications of the plates, the fixtures and the test geometry. When these efforts proved unsuccessful, work with the pressure cell was discontinued.

Our next approach was to use preimidized samples of PMR and LARC resins in our study. This greatly reduced the amount of volatile material to be eliminated during the rheological testing.

Data was gathered on samples which were oven imidized at 121°C for 60 minutes prior to characterization. After imidization, samples were pulverized and desiccated. Prior to measurement, samples were further dried in a desiccated vacuum oven (RT/380-510 mm Hg) overnight.

In order to form a sample in the environmental chamber of the rheometer, the chamber was preheated to 200°C and a pre-weighted amount of imidized resin (fine powder) was introduced between opened parallel plates. The chamber was then closed and

when the indicated temperature again reached 200°C, a sample was formed by closing the plates to a predetermined gap (0.6 mm). The chamber was then again opened and excess resin was removed from the edges of the plate. The chamber was reclosed and heating was resumed when the chamber reached 200°C.

Complex viscosity as a function of temperature is shown in Figure 15 for LARC 160 (AP 22 and Curithane 103 versions) and PMR 15 (ethanol solution) at heating rates of 2 and 4°C/min. There appear to be distinct differences between all of the resins. The greatest difference was between the two types of LARC 160. Because of the greater amount of 4,4'-MDA in Curithane 103, one might logically expect this version of LARC 160 to have a higher minimum viscosity than its AP-22 counterpart. However, the data shows the opposite. Furthermore, if the AP-22 version of LARC 160 is compared to earlier data obtained from preimidized LARC 160 prepreg the viscosity profiles of the two resins are significantly different. The resin from the prepreg reaches a minimum viscosity in the neighborhood of 400 poise at 292°C as compared to around 7,000 poise at 250°C for freshly synthesized resin. Although the heating rates were the same, i.e., 4°C/min, the prepreg resin was scanned and started at 239°C while the current material resin was scanned from 200°C. The additional time at higher temperatures tends to explain the observed differences and also presents another problem. The viscosity measured in a characterization run might not reflect the true viscosity during a process. It clearly points out the need for parallel heat histories of samples being compared.

Note that an improved viscosity characterization procedure would be desirable to eliminate the initial peak in complex viscosity during the first 10-20 minutes of a run. The resin is not very fluid at 200°C. The lower temperature was used to minimize any reactions during sample formation and hence give better reproducibility. This higher initial viscosity requires a low shear stress and low shear rate because of the transducer limitations. However, the deflection of the transducer shaft must exceed 0.001 of the radius in order to give reliable results. The shear strain of 3 used to generate the data in Figure 15 was later found to be slightly less than required by calculation ($\gamma = 5$). The data is thus questionable. The effect of shear strain was examined in subsequent tests and the data appears in Figure 16.

For the AP-22 version of LARC 160, shear strains of 3, 5, 10 and 50 were examined. A starting temperature of 230°C was required to get the initial viscosity low enough to accept the higher shear strains. The data shows a scatter band but no systematic variation as a function of shear strain. The only large difference occurs in the case of $\gamma = 3$. Similar data for the Curithane 103 version of LARC 160 at shear strains of 3, 10 and 50 are also shown in Figure 16. In this case, the largest difference occurs in the case of $\gamma = 50$. It would appear that a shear strain of 10 might be the best choice. Despite the scatter, it is clear that in all cases the Curithane 103 version of LARC 160 has a lower minimum viscosity in the process critical range as compared to AP-22.

Note also that the curves for PMR-15 and AP-22 based LARC 160 resemble each other far more than they resemble that of the Curithane 103 based LARC 160.

2.4.2 Prepreg Viscosity Studies

A problem encountered throughout the work with the addition polyimide systems was that of sample preparation. Almost any technique for preparing a neat resin sample from prepreg can significantly change the nature of the resin. Solvent techniques

can pose serious problems in removing residual polar solvents that interact strongly with the polymer. Small amounts of such solvents, if not removed, act as plasticizers and reduce T_g of the resin. Heating to remove solvent will stage or alter the resin. Even physically scraping or grinding off resin flash can result in a sample contaminated with fiber or debris.

Another serious question must also be addressed. Laminates are fabricated from prepreg, not resin. How does the rheological response of the resin in the presence of the reinforcement differ from that of the neat resin? The presence of the fiber with its large surface area and the presence of active chemical species on the fiber surface can certainly affect the resin, both physically and chemically.

It was therefore decided to attempt to develop techniques for determining the rheological characteristics of reinforced prepreg samples on the Rheometrics mechanical spectrometer. Techniques were successfully developed, using well characterized graphite/epoxy materials and are reported elsewhere. (7) LARC 160/woven T300 prepreg samples were investigated, but initial efforts proved unsuccessful. The imidized systems were too high in viscosity to study with the torque transducers available to us at the time.

A high range torque transducer was obtained from Rheometrics. Prepreg samples were next pre-imidized using a 2 hour, 121°C hold, as for the neat resin samples. Unfortunately no additional LARC 160 (Curithane) prepreg was available. Figures 17 and 18 show the curves generated as preimidized LARC 160 (AP-22) and PMR-15 prepreg, and compare the dates with that generated on the neat resin. Note the significant difference in minimum viscosity (nearly an order of magnitude) of resin vs. prepreg samples. Minimum viscosity also occurs at a higher temperature for the prepreg than for the neat resin specimens.

Recent work on epoxy systems by Brown (8) has shown that volatiles in laminates escape out the sides of the layup rather than diffuse through the top and bottom. The bubbles follow the fibers to the edge of the panel, rather than working their way through the plies. It seemed possible that the RMS prepreg samples would behave in a similar manner, allowing good data to be obtained on prepreg without the need for an imidization step.

Samples were dried at 50°C, then placed in the RMS cavity. The runs were started at 60°C and cured to over 380°C. Little or no problems were encountered with bubble formation and data scatter and good, reproducible curves were obtained. Figure 19 compares the apparent viscosity curves of LARC 160 (AP-22) prepreg and PMR-15 prepreg, imidized versions, while Figure 20 shows the same data for samples run without imidization. The curves on the non-imidized versions appear to agree best with laboratory experience, as the low temperature, low viscosity behavior of the PMR is seen. The imidized and non-imidized data is consistent at higher temperatures as one would expect. LARC 160 shows lower viscosity (higher flow) at the usual processing temperatures (i.e. 270 - 320°C) for these systems.

Samples of another commercial addition polyimide, U.S. Polymeric V378A, were available. Rheometrics curves were successfully run on V378A resin reinforced with Celion 3000 and T300 fibers. Although rheological curve of the neat resin from each batch showed little difference, a significant difference in the prepreg viscosity curves were observed as can be seen in Figure 21. The Celion reinforced prepreg has a significantly lower minimum apparent viscosity, and therefore higher flow. This is consistent with the processing characteristics for these prepgs

observed in the LMSC shop and elsewhere in the industry.

2.4.3 Solid State Rheometrics Studies

In order to run solid state rheological studies on the two LARC 160 resins, it was necessary to prepare neat resin moldings. This was not an insignificant task, as a staging cycle was required that allowed the powdered resin to be cured under pressure. Simple casting and curing or pressing to stops resulted in high void moldings or moldings with incomplete consolidation. After several attempts, we developed cycles for both resin systems. The Curithane based LARC 160, however, required significantly more staging than the AP-22 version to achieve the low flow characteristics required to produce satisfactory moldings. The staging cycles shown in Table 1 were used. The staged powders were then molded at 320°C, 0.83 MPa pressure for 1 hour. Satisfactory moldings were produced, samples were machined for rheological testing. Figures 22 and 23 give the solid state curves for the two LARC 160 polymers. The peak in $\tan \delta$ occurred at 367°C for the AP-22 LARC 160, while the curve went off-scale (at 397°C) for the Curithane 103 version. This data is consistent with TMA results that indicate a possibly higher T_g for Curithane LARC 160.

2.5 Laminate Fabrication

Prior to obtaining our high range torque transducer for polyimide prepreg studies, data generated on the neat resin systems was used as a basis for fabricating LARC 160 matrix laminates.

Standard commercial Fiberite prepreg was used in the AP-22 based laminate. Here LARC 160 is used to impregnate woven T-300 (8 harness satin) epoxy finish graphite cloth. The following cure schedule was used:

- (1) Heat at 2°C/minute to a temperature of 121°C.
- (2) Hold 90 min at 121°C, then heat at 2°C/min.
- (3) Pressurize to 1.2 MPa at 260°C.
- (4) Continue heating at 2°C/min to 330°C.
- (5) Hold 90 min at 330°C, 1.2 MPa, then cool under pressure to below 100°C.

A well consolidated laminate was made by this procedure.

From the rheological data generated on the LARC resin it was apparent that the AP-22 cycle would need to be modified to successfully produce a Curithane based laminate. If the η^* curves are compared, the Curithane LARC 160 must be heated to 290°C to achieve a viscosity equivalent to that of the AP-22 LARC 160 at 260°C (pressurization point). It was, therefore, decided to use the AP-22 LARC 160 cure schedule listed above, but to pressurize at 290°C rather than 260°C.

A sample of Curithane 160 was applied to woven T-300 (8 HS), epoxy finish cloth reinforcement by a "dip and squee-gee" technique. The prepreg was air dried at ambient temperature overnight, followed by 4 hours at 93°C in a circulating air oven. The purpose of this bake was to eliminate solvent and thereby minimize plasticization and flow during cure. The resulting prepreg has a resin content of 46.8%. The laminate was laid up in a matched metal mold and press cured using the standard LARC 160 (AP-22) cycle, but applying pressure at 290°C. An apparently

high quality laminate was successfully molded by this procedure.

CONCLUSIONS AND RECOMMENDATIONS

Several important results were obtained and conclusions reached during the course of the work:

- o Although only small differences were found between LARC 160 (AP-22) and LARC 160 (Curithane 103) by conventional chemical characterization techniques, major differences were found during rheological characterization.
- o Imidized Curithane 103 based LARC 160 has significantly lower viscosity and therefore higher flow than AP-22 based LARC 160 during processing. PMR-15 behaves much more like LARC 160 (AP-22) than does LARC 160 (Curithane 103).
- o Rheological studies can be used to develop processing cycles for Curithane 103 based LARC 160 resin and prepreg.
- o Techniques were successfully developed to generate rheological data on LARC 160 and PMR-15 prepreg samples. Pre-imidization is not required with prepreg samples, but is necessary with neat resin samples.
- o Rheometrics rheological data was generated on V378A prepreg systems. The type of woven graphite was found to significantly affect the rheological characteristics of the prepreg and was consistent with their observed processing behavior.
- o Fully cured Curithane based LARC 160 may have a Tg that is higher than that of AP-22 based LARC 160.

REFERENCES

1. St. Clair, T. L.; Jewell, R. A., National SAMPE Tech. Conf. Series, 1976, 8, 82; Sci. Adv. Mat'l & Proc. Eng. Ser., 1978, 23, 520.
2. Serafini, T. T., Processable High Temperature Resistant Polymer Matrix Materials, NASA TM X-71682, 1975.
3. Maximovich, M. G.; Galeos, R. M., "Polyimides: Synthesis, Characterization and Applications", K. L. Mittal, Editor, Plenum Press, New York, October 1983.
4. Leaky, J. D., "Development and Demonstration of Manufacturing Processes for Fabricating Graphite/LARC 160 Polyimide Structural Elements", Contact NAS1-15371, 5th Quarterly Report, June through September 1979.
5. Young, Philip R., and Sykes, George F., "Analysis of Aromatic Polyamine Mixtures for Formulation of LARC-160 Resin".

6. Leaky, J. D., "Development and Demonstration of Manufacturing Processes for Fabricating Graphite/LARC 160 Polyimide Structural Elements", Contract NAS1-15371, 9th Quarterly Report, June through September, 1980.
7. Maximovich, M. G. and Galeos, R. M., "Rheological Characterization of Advanced Composite Prepreg Materials", 28th National SAMPE Symposium, Anaheim, Calif., April, 1983.
8. Brown, G. G. and McKague, G. L., "Processing Science of Epoxy Resin Composites", AFML Contract F 33615-80-C-5021, Fifth Quarterly Report, February, 1982.

TABLE 1 LARC 160 STAGING FOR MOLDING COMPOUNDS

AP-22 LARC 160 CYCLE	CURITHANE LARC 160 CYCLE
STEP: I. 140°C - 90 MIN.	I. 140°C - 90 MIN.
2. 140°C - 30 MIN.	2. 140°C - 30 MIN.
3. 180°C - 60 MIN.	3. 180°C - 60 MIN.
4. 210°C - 30 MIN.	4. 210°C - 60 MIN.
5. 250°C - 60 MIN.	5. 220°C - 60 MIN.
<u>4.5 HOURS TOTAL</u>	<u>6.25 HOURS TOTAL</u>

* RESIN WAS GROUNDED BETWEEN STAGING STEPS TO FACILITATE VOLATILE REMOVAL.

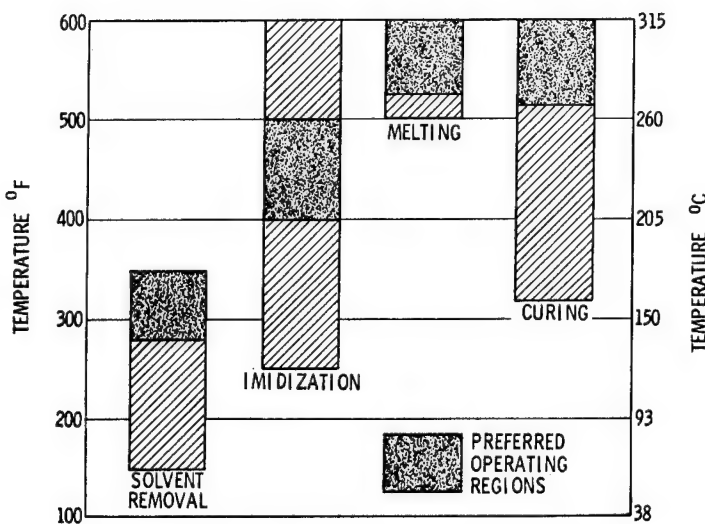


FIGURE 1 PROCESSING PARAMETERS FOR TYPICAL ADDITION PI

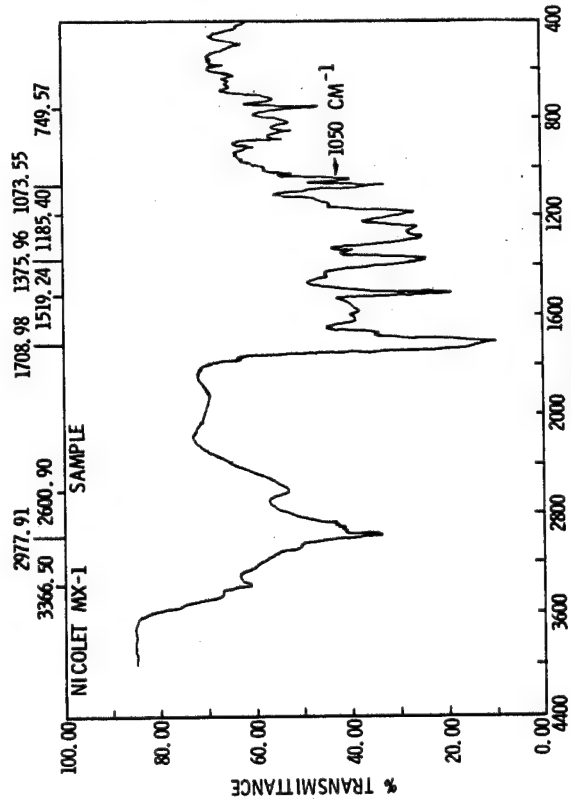


FIGURE 2 IR OF SYNTHESIZED LARC 160 WITH JEFFAMINE AP-22

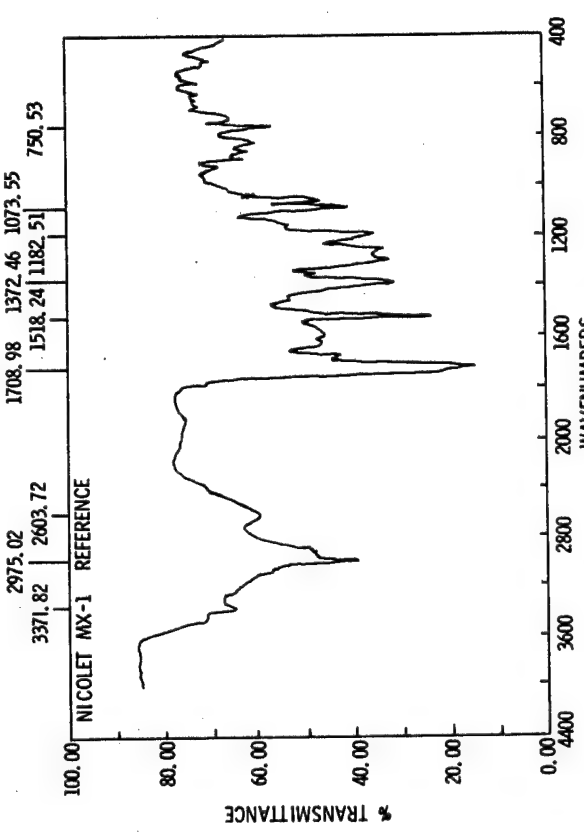


FIGURE 3 IR OF SYNTHESIZED LARC 160 WITH CURITHANE 103

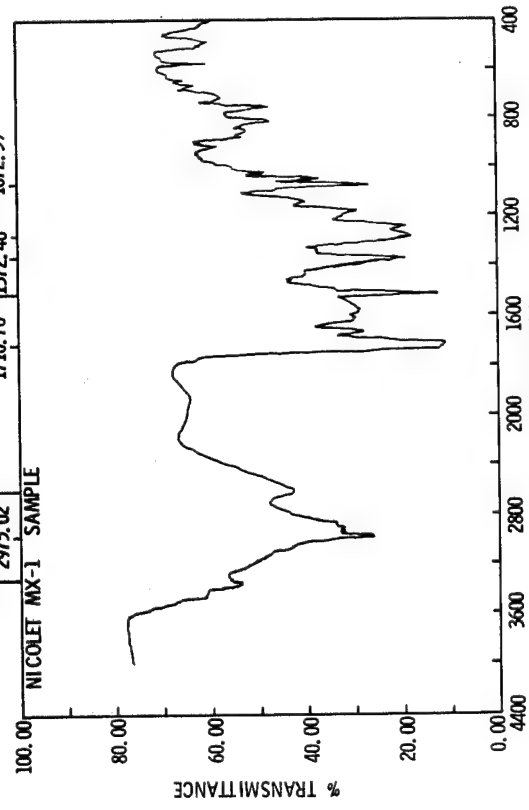


FIGURE 4 IR OF SYNTHESIZED PMR-15

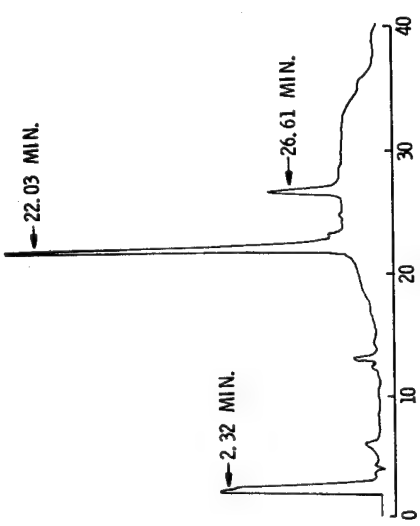


FIGURE 5 CHROMATOGRAM OF PMR-15

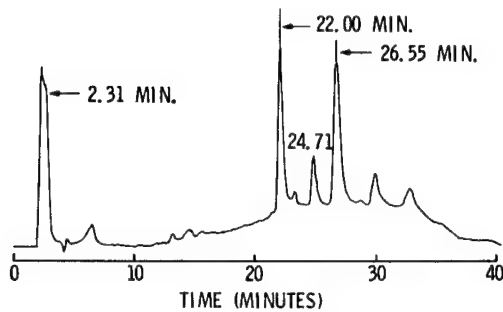


FIGURE 6 CHROMATOGRAM OF LARC 160 WITH AP-22

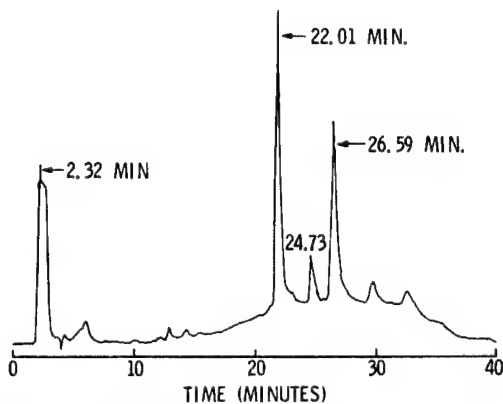


FIGURE 7 CHROMATOGRAM OF LARC 160 WITH CURITHANE 103

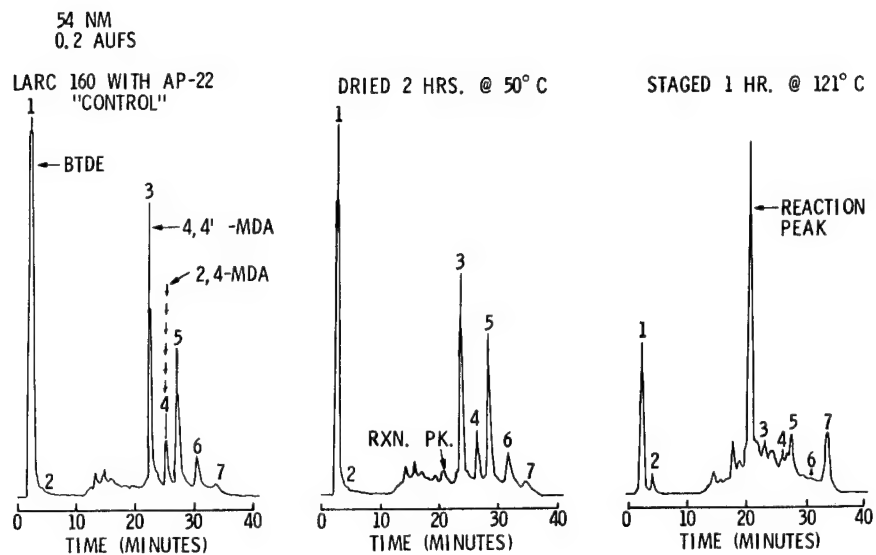


FIGURE 8 EFFECTS OF STAGING ON HPLC CHROMATOGRAMS

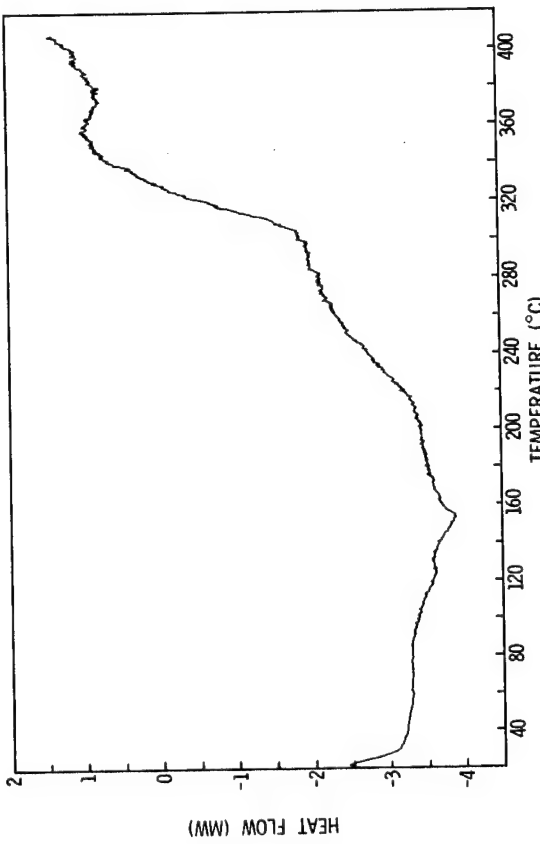


FIGURE 9 DSC OF PMR-15 UNSTAGED

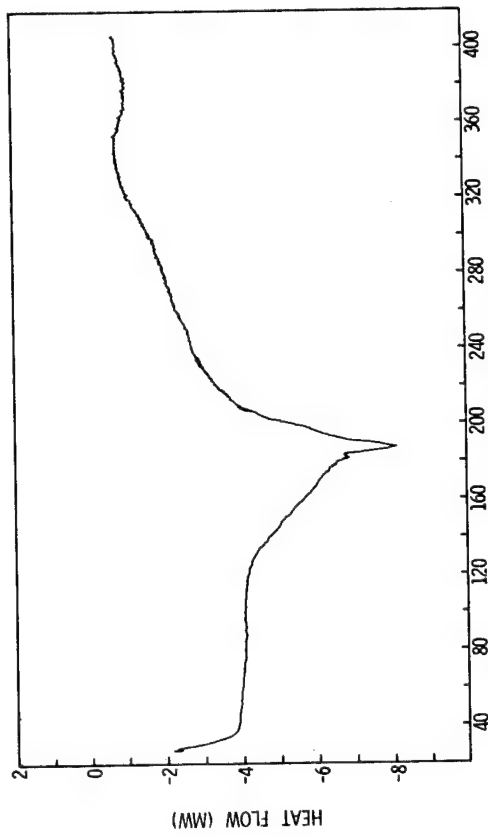


FIGURE 10 DSC OF PMR-15 STAGED .5 HR/120 C

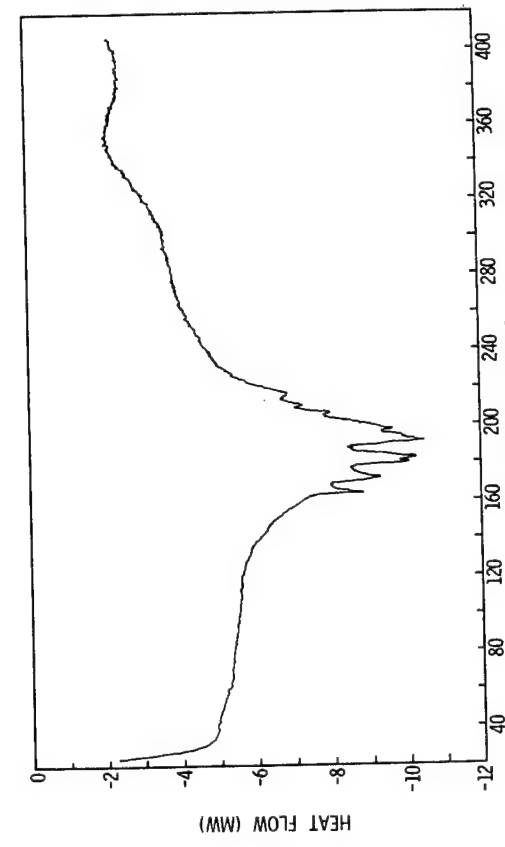


FIGURE 11 DSC OF LARC 160/22 UNSTAGED

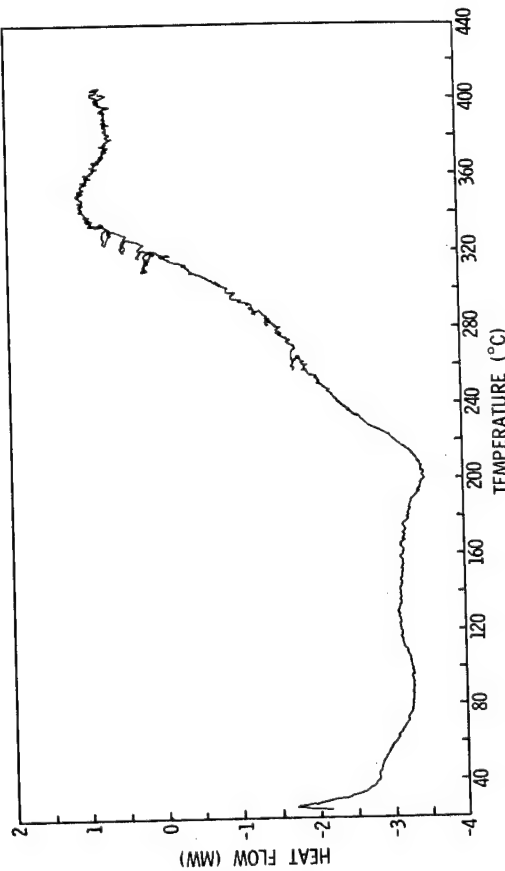


FIGURE 12 DSC OF LARC 160/22 STAGED .5 HR/120 C

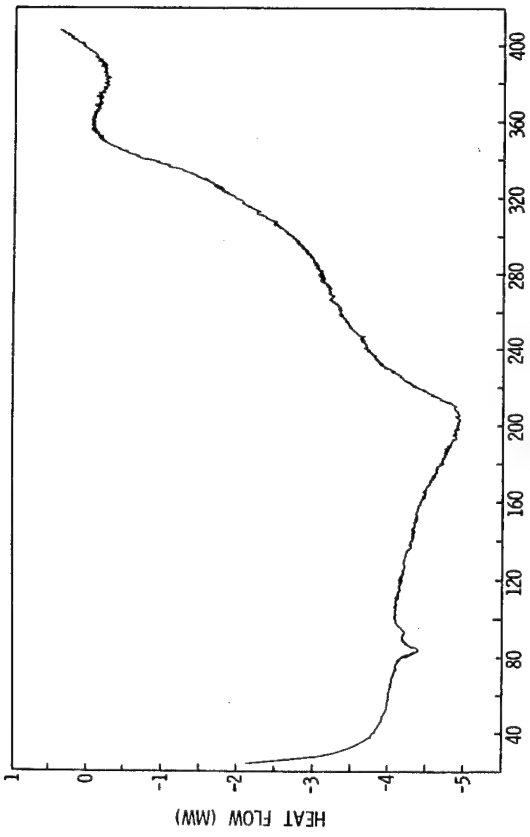


FIGURE 13 DSC OF LARC 160/103 UNSTAGED

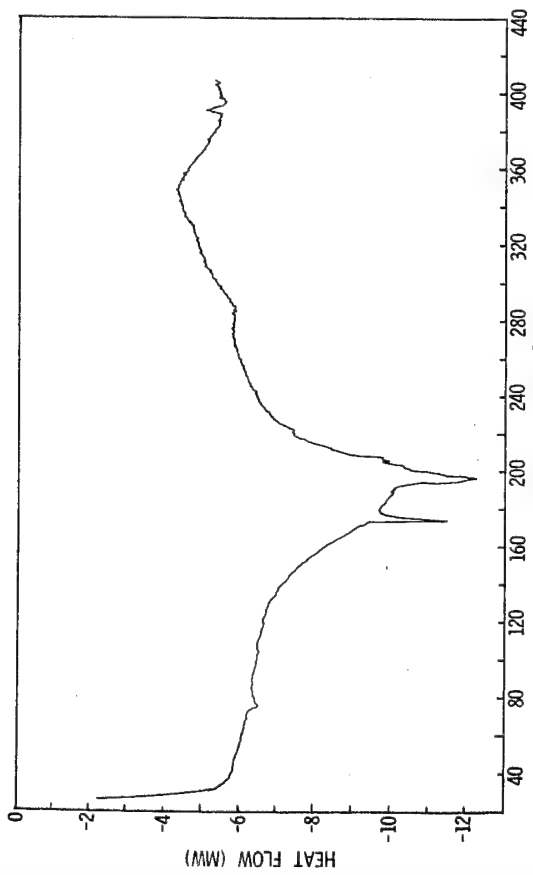


FIGURE 14 DSC OF LARC 160/103 STAGED .5 HR/120 C

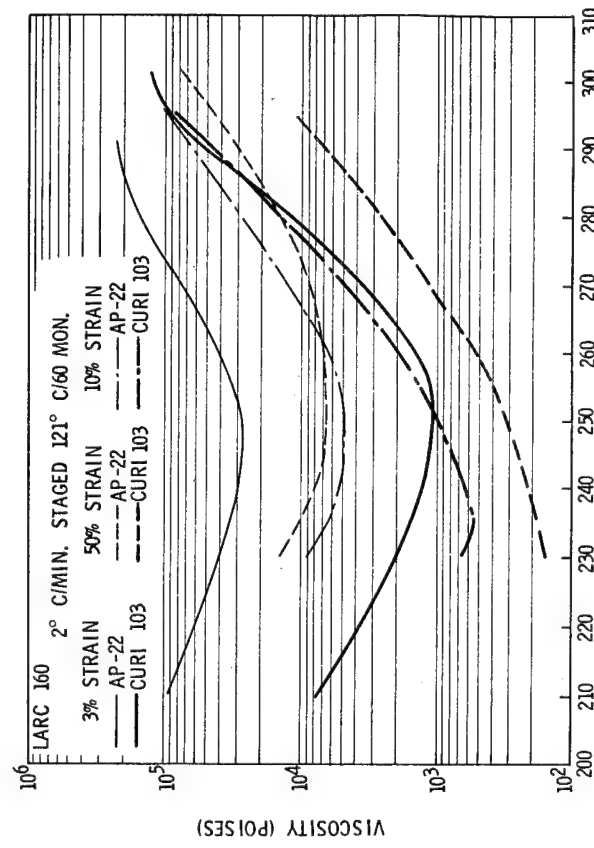


FIGURE 16 EFFECT & OF SHEAR STRAIN

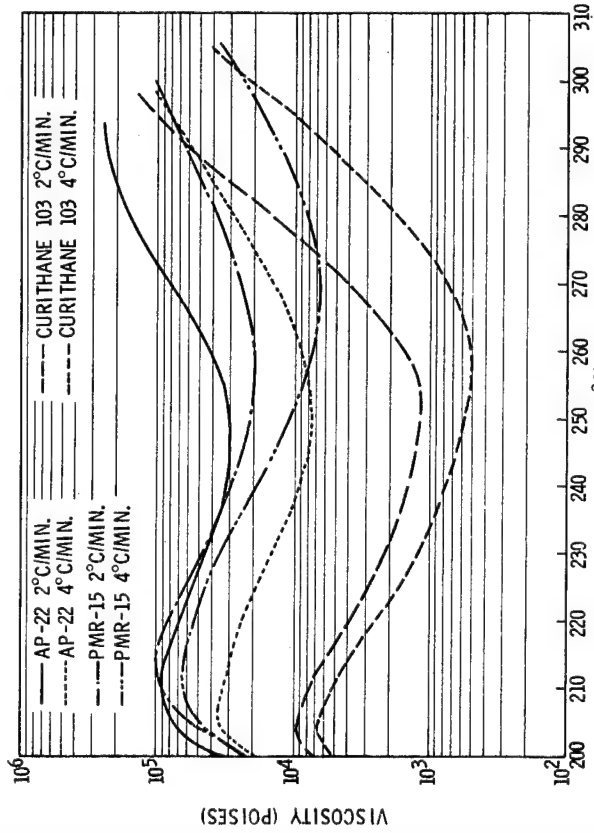
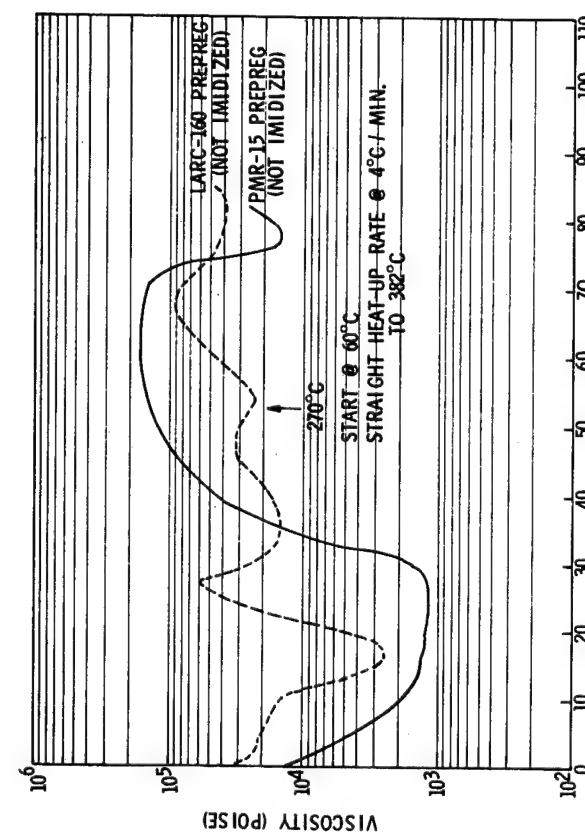
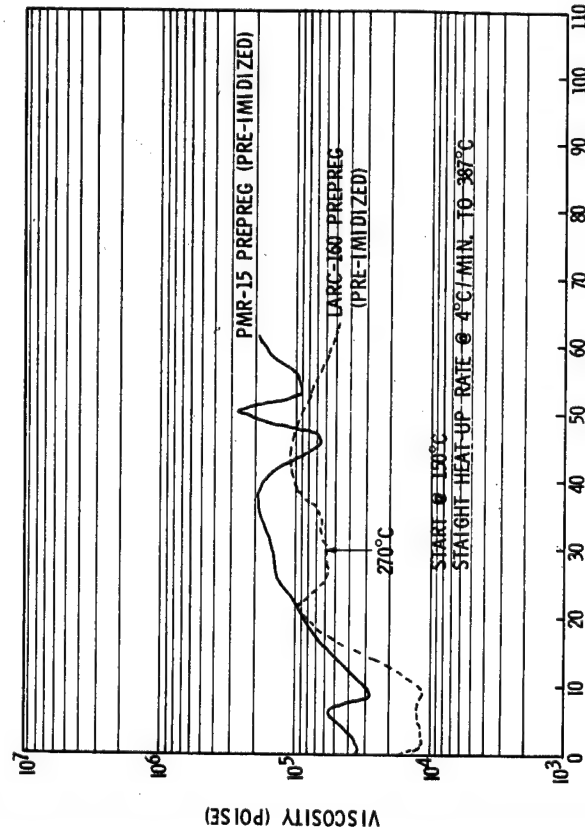
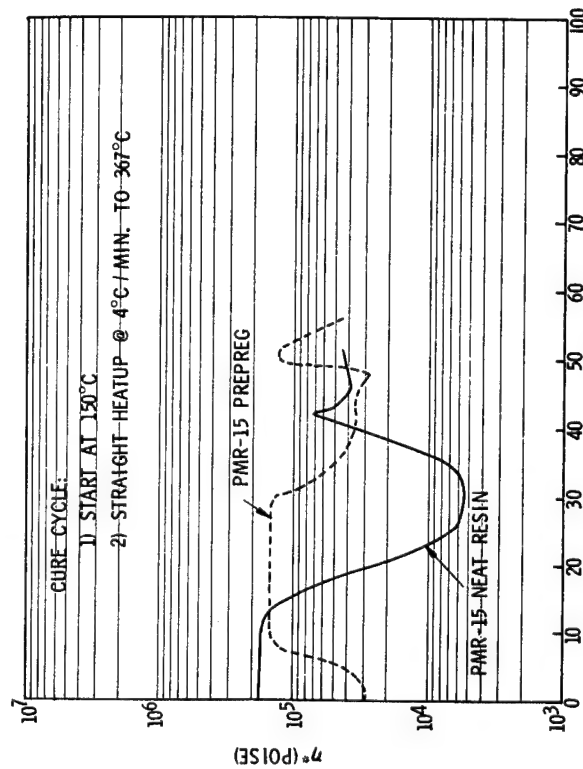
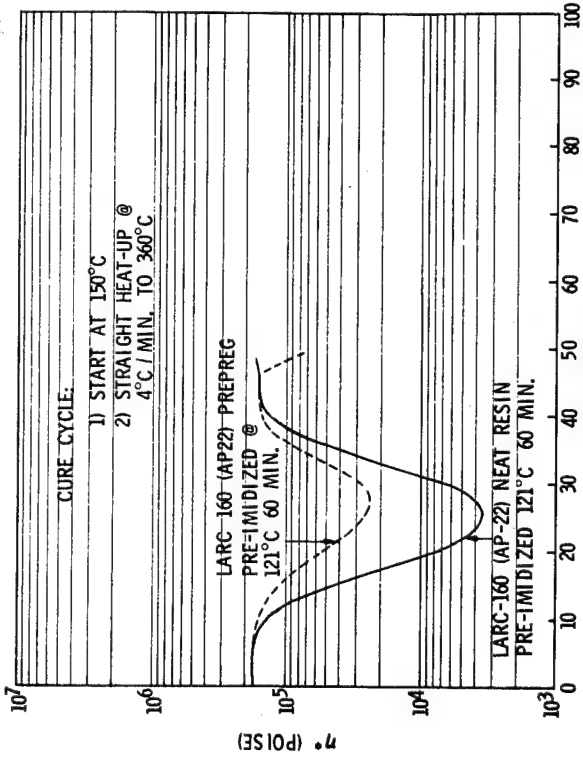


FIGURE 15 COMPLEX VISCOSITY VS TEMPERATURE



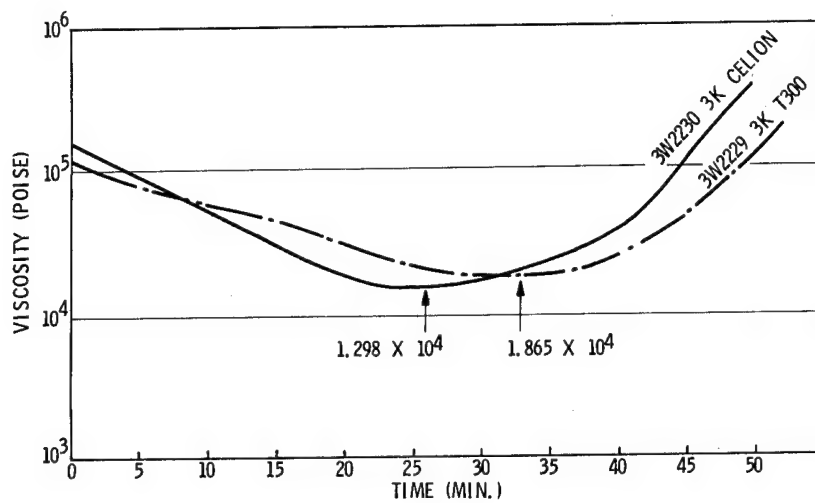


FIGURE 21 V378 PREPREG VISCOSITY VS TIME

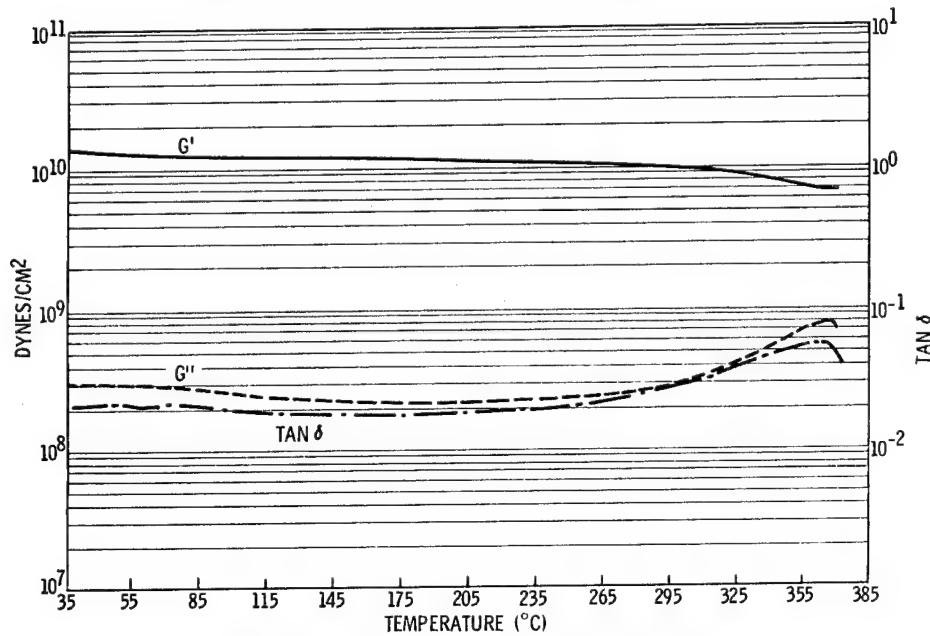


FIGURE 22 LARC 160, AP-22 (NEAT RESIN CASTING)

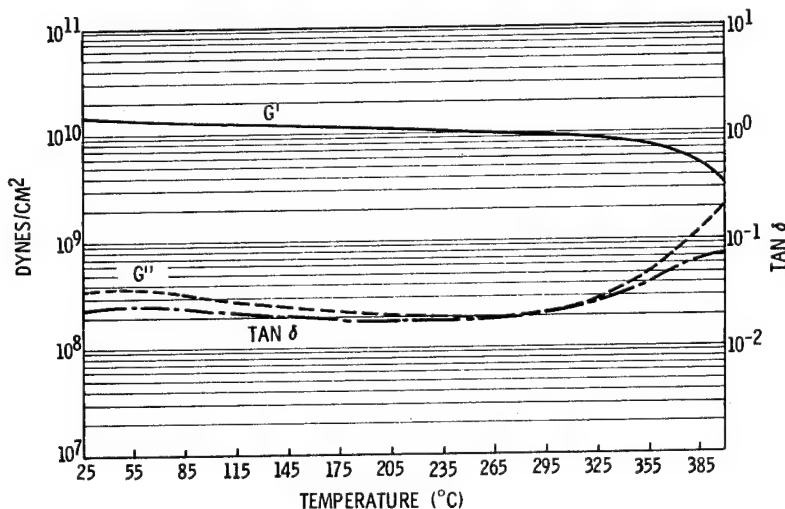


FIGURE 23 LARC 160, CURITHANE 103 (NEAT RESIN CASTING)

QUALITY ASSURANCE PROCEDURES FOR V378A MATRIX RESIN*

Charles L. Hamermesh and Paul J. Dynes
Rockwell International Science Center

A characterization methodology has been developed on which to base quality assurance procedures for U.S. Polymeric V378A bismaleimide matrix resin. Chemical composition was established by partition reverse-phase and size exclusion liquid chromatography. Cure rheology behavior was quantitatively characterized by dynamic viscoelastic analysis using the parallel-plate technique. The overall cure process was characterized by differential scanning calorimetry. The sensitivity of the procedures was evaluated by studying the effects of ambient out-time on the chemical and behavioral properties of the resin.

INTRODUCTION

The use of composites in aerospace applications has grown substantially in recent years and it appears that this upsurge will continue into the foreseeable future. Composites, however, are only useful if their performance is both reliable and reproducible. With the state-of-the-art composite materials, the epoxy resins, a considerable effort was undertaken a number of years ago to define the chemical nature and behavior of such material so that quality of composites could be assured.

Bismaleimides, although not new, are being reexamined as potential candidates for the next generation of matrix resins for intermediate temperature usage in the 450-505 K (350-450°F) range. As a class, bismaleimides show generally higher cured glass transition temperatures and less environmental sensitivity than state-of-the-art epoxies. They have suffered, however, from too much brittleness and difficult processibility.

These problems have been alleviated to a large degree in V378A, a modified bismaleimide developed by U.S. Polymeric (ref. 1). This system possesses the easy processibility characteristics of epoxies but shows improved retention of mechanical properties at 450 K (350°F) under moisture saturation conditions. Its rapid development and testing in primary aircraft structures have prompted the need for a characterization methodology upon which to base quality assurance procedures. V378A, like most matrix resins, with the exceptions of the PMR type systems developed by the Government owned laboratories, is a proprietary formulation. Thus, the specific composition and exact nature of the ingredients which make up the system are not likely to be divulged by its owners beyond such general descriptions as "a formulation of a modified bismaleimide and at least two volatile components." As

*This work was performed under the auspices of the Materials Laboratory, Air Force Wright Aeronautical Laboratories, Wright-Patterson AFB, OH 45433.

this paper shows, this need not be a deterrent to the development of the characterization procedures for quality assurance of the material. With a good understanding of the underlying chemistry of bismaleimide resins and the inferences which can be drawn as to the general nature and purpose of the volatile components, a strong base can be established for the characterization of such a system despite its proprietary nature and without jeopardizing the rights of its owner.

SYMBOLS

G^*	dynamic shear modulus, N/m ² (dynes/cm ²)
G'	storage shear modulus, N/m ² (dynes/cm ²)
G''	loss shear modulus, N/m ² (dynes/cm ²)
ω	oscillating shear frequency rad/s
η^*	dynamic viscosity, N.s/m ² (poise)
E_a	activation energy, J/mole (kcal/mole)
dH/dT	differential heat input, J/s (mcal/s)
ΔH	heat of polymerization, J/g (cal/g)
ϕ	heating rate, K/min
T_{OS}	DSC exotherm onset temperature, K
T_{IP}	DSC exotherm inflection temperature, K
T_{EXO}	DSC exotherm peak temperature, K

HIGH PERFORMANCE LIQUID CHROMATOGRAPHY

The primary goal of the liquid chromatographic study was to develop a quantitative procedure capable of separating the primary ingredients present in V378A resin. These included the major resin, which is composed of several fractions, and the two volatile components in the formulation.

The liquid chromatography method chosen was a partition reverse-phase separation utilizing a water/acetonitrile solvent gradient. This type of analysis has proven to be the most successful for prepolymer resins containing a broad range of component polarities and oligomer molecular weights. Detection of components was made by ultraviolet spectrophotometry. A detection wavelength of 200 nm was chosen to enhance the analysis of Volatile Component 2 in the resin. In order to completely dissolve the resin for analysis a minimum of 25% dimethylformamide in tetrahydrofuran was required. A summary of the chromatographic conditions used for the analysis of V378A resin is given in table 1.

The separation of V378A resin using this procedure is shown in figure 1. A total of approximately eighteen components are resolved. Eight of these have been identified as belonging to one of the three major ingredients of V378A resin. Identification was based on peak elution times verified by spiking of V378A resin with individual ingredients. The liquid chromatographic separations of the three major components of V378A resin are shown in figure 2.

Although a large number of components are separated by the partition liquid chromatographic technique, it was found that the acetonitrile or tetrahydrofuran insoluble fractions of V378A resin did not elute during the water/acetonitrile solvent gradient. Moreover, the fractions soluble in tetrahydrofuran or acetonitrile gave the same chromatographic peaks and peak area distributions as did totally solubilized samples. The V378A resin system thus appears to be comprised of two fractions. One is of relatively low molecular weight consisting of the two volatile components and bismaleimide resin oligomers. The insoluble fraction is presumably composed of products formed by reactions among these starting ingredients.

Characterization of the insoluble fraction of V378A resin was made by size exclusion liquid chromatography. With tetrahydrofuran as solvent, the once solubilized resin remains in solution during size exclusion analysis. The experimental details of this technique are given in table 2. The size exclusion separation of V378A resin is shown in figure 3. The first and therefore highest molecular weight component to elute was determined to correspond to the insoluble fraction of the resin not detected by partition liquid chromatography. The remaining ingredients, however, are not resolved as well as with the partition method. Partition and size exclusion liquid chromatography thus complement each other and together provide the means for a comprehensive analysis of the chemical constituents of V378A resin.

CURE RHEOLOGY

The rheological behavior of V378A neat resin during cure was studied with the Rheometrics Visco-Elastic Tester. The experimental conditions used to analyze the resin are given in table 3. The instrument calculates the dynamic shear modulus G^* and its two components, the dynamic storage or elastic modulus G' and the dynamic loss or viscous modulus G'' . A dynamic viscosity is defined from the dynamic modulus as, $\eta^* = G^*/\omega$, where ω is the oscillatory shear frequency. The variation in the dynamic viscoelastic properties of V378A resin during a 2 K/min heating cycle is plotted in figure 4.

Several factors critical to a matrix resin's processibility can be derived from these data. One is the initial value of the dynamic viscosity. V378A has a room temperature value of $\sim 6 \times 10^2$ N·s/m² (6×10^3 poise) which imparts satisfactory drape in the prepreg. Resin dynamic viscosity decreases with increasing temperature until around 383 K where it reaches a minimum of $\sim 5 \times 10^{-1}$ N·s/m² (5 poise). Above this temperature, polymerization reactions bring about a rapid rise in dynamic viscosity. At a specific temperature the shear storage and loss moduli are equal. This midway point between viscous liquid behavior and solid state elastic response has been found to correlate with resin gelation as measured by standards methods (ref. 2).

The dynamic viscosity profiles for several cure cycle heating rates are shown in figure 5. Faster heating rates tend to reduce the minimum dynamic viscosity reached during cure. This effect can be of value for controlling the amount of flow desired during processing. The temperatures at which gelation occurs for four heating rates are given in table 4. By analogy to differential scanning calorimetry, the dependence of the temperature at gelation on heating rate can be plotted in a modified Arrhenius equation (ref. 3). The data are plotted in figure 6 where a good fit to the Arrhenius equation is found. An activation energy to gelation of 89.5 J/mole (21.4 kcal/mole) is calculated from the slope of the curve.

The rheological behavior of V378A resin was also explored under isothermal cure conditions. The dynamic viscoelastic properties of V378A resin at 393 K are shown in figure 7. Initially, the resin displays a very low viscosity with almost no elastic character ($G' \approx 0$). At longer times G' increases rapidly and surpasses G'' . Again gelation is associated with the crossover of the two dynamic moduli. The gel times determined by this method are given in table 5 for several temperatures. These data are plotted in figure 8 according to the Arrhenius equation. A linear relationship is found and from the slope of the curve an activation energy of 89.7 J/mole (21.4 kcal/mole) to gelation is derived.

DIFFERENTIAL SCANNING CALORIMETRY

The differential scanning calorimetry (DSC) behavior of V378A resin is shown in figure 9 for a heating rate of 1.25 K/min. Curing is characterized by two exotherms. The major exotherm is centered at 415 K (142°C) while a second much smaller one occurs about 70 K higher. The major exotherm is related to reactions involving Volatile Component 1. The exotherm at higher temperature appears to result primarily from additional polymerization of bismaleimide groups.

Several DSC parameters were evaluated for quality assurance purposes. They include the reaction onset temperature T_{OS} , the peak inflection temperature T_{IP} , the peak exotherm temperature T_{EXO} and the heats of polymerization ΔH associated with the two reaction exotherms. A summary of such data for four heating rate experiments is given in table 6.

Heats of polymerization were not sufficiently reproducible to use as quality assurance parameters. The characteristic thermogram temperatures, however, can be determined more precisely. The peak exotherm temperature T_{EXO} , in particular, is very reproducible. The inflection point temperature T_{IP} was also investigated, as it has been shown to coincide with gelation in epoxy resin systems (ref. 3). The heating rate dependence of T_{IP} and T_{EXO} are plotted in figure 10 according to the modified Arrhenius relation discussed previously. Linear relationships are obtained which define activation energies of 78.9 J/mole (18.7 kcal/mole), 69.1 J/mole (16.5 kcal/mole) from T_{EXO} and T_{IP} , respectively. The inflection point temperature data in table 6 are in fairly good agreement with the rheologically determined gel temperatures given in table 4. Experimentally, gel times determined from rheological data are more accurate and reproducible than can be derived from DSC measurements.

RESIN OUT-TIME EVALUATION

It was of interest to examine the effects of ambient aging on the properties of V378A neat resin. Film samples of resin were exposed to 296 K and 30-60% RH conditions for periods up to three weeks. At ambient the resin loses its tack within one day. It has, however, a twenty-one day recommended out-time in terms of processibility.

Partition liquid chromatographic analysis of resin aging revealed only one significant change to be taking place. The concentration of Volatile Component 1 decreases as shown in figure 11. The decrease in Volatile Component 1 occurs as a result of both B-staging and evaporation. Weight loss measurements indicate approximately one-third loss due to evaporation and the remainder cause by resin advancement. Evidence of resin advancement is shown by size exclusion chromatography in figure 12 where the concentration of early eluting highr molecular weight species increases with resin aging.

Two rheological tests were used to characterize the effects of ambient aging on V378A resin. They were a linear 2 K/min heating rate cure and a 398 K isothermal gel time test. The results of the 2 K/min cure cycle experiments are shown in figure 13. The dynamic viscosity profiles show a significant increase with ambient aging time. A plot of the gel times determined from the isothermal rheology data are plotted in figure 14. For short aging times the gel time increases and then drops markedly around the fourth day of aging.

DSC is a sensitive tool for analyzing the effect of aging on V378A resin. Thermograms for resin aged up to 20 days are plotted in figure 15. The primary result of out-time is a reduction in the major DSC exotherm which is associated with the reactions of Volatile Component 1. The smaller high temperature exotherm appears to be unaffected by ambient aging. The major exotherm has a slight shoulder located at 370-390 K. After about 1 week of aging, this shoulder begins to resolve itself into a new exotherm peak centered near 395 K. These changes are indicative of a resin in which more than one path of cure is available. In such cases, the cure temperature and kinetic parameters of the various reaction paths control which path predominates.

REFERENCES

1. McKague, L: V378A Polyimide Resin - A New Composite Matrix for the 80's. Proceedings of ASTM Symposium on Composites for Extreme Environments, Bal Harbour, FL, November 11, 1980.
2. Tung, M.C.; Dynes, P.J: Relationship Between Viscoelastic Properties and Gelation in Thermosetting Systems. *J. Appl. Polym. Sci.*, 27, 569 (1982).
3. Carpenter, J.F: Instrumental Techniques for Developing Epoxy Cure Cycles. Proceedings of 21st National SAMPE Symposium and Exhibition, Los Angeles, CA, April 6-8, 1976.

Table 1
Experimental Conditions for Separation of
U.S. Polymeric V378A Resin by Partition
Liquid Chromatography

Column:	Spectra-Physics Sperisorb 10 ODS
Solvent:	Baker Liquid Chromatographic Water Burdick and Jackson Acetonitrile
Gradient:	10-80% $\text{CH}_3\text{CH}/\text{H}_2\text{O}$, Linear in 50 min
Flow:	Ultraviolet at 200 nm
Sample:	10 μl of a 1.5 mg/ml solution in 25/75 DMF/THF

Table 2
Experimental Conditions for Separation of
U.S. Polymeric V378A Resin by Size
Exclusion Chromatography

Column:	Waters Associates μ -Styragel 1 (500 \AA) + 2 (100 \AA)
Solvent:	Burdick and Jackson Tetrahydrofuran (Unstabilized UV Grade)
Flow:	1 ml/min
Detection:	Ultraviolet at 254 nm
Sample:	100 μl of a 2 mg/ml solution in 25/75 DMF/THF

Table 3
Rheometrics Visco-Elastic Tester
Experimental Parameters

Geometry	25 mm Parallel plates
Frequency	10 rad/s
Gap	0.5 mm
Percent Strain	< 10%
Environment	Dry nitrogen

Table 4
 Variation in Temperature at
 Gelation According to $G' = G''$
 Criterion of U.S. Polymeric
 V378A Resin

ϕ K/min	T ($G' = G''$) K
2	401
3	408
4	412
5	415

Table 5
 Variation in Time to Gelation
 According to $G' = G''$ Criterion
 of U.S. Polymeric V378A Resin

Temperature K	Gel Time min
388	18.6
393	11.3
398	8.2
413	3.2

Table 6
 Differential Scanning Calorimetry Analysis
 of U.S. Polymeric V378A Resin

ϕ K/min	T_{OS} K	T_{IP} K	T_{EXO}	ΔH_1 J/g	ΔH_2
1.25	363	388	402	235	18
2.50	345	403	415	214	15
5.00	366	418	429	264	10
10.0	367	429	442	205	10

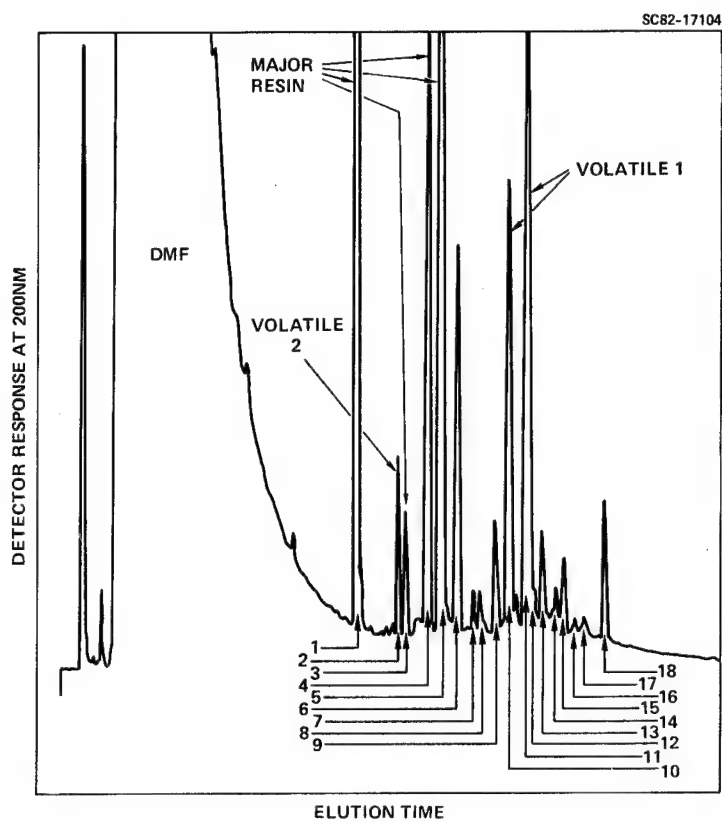


Figure 1.
Partition liquid chromatographic analysis of U.S. Polymeric V378A resin.

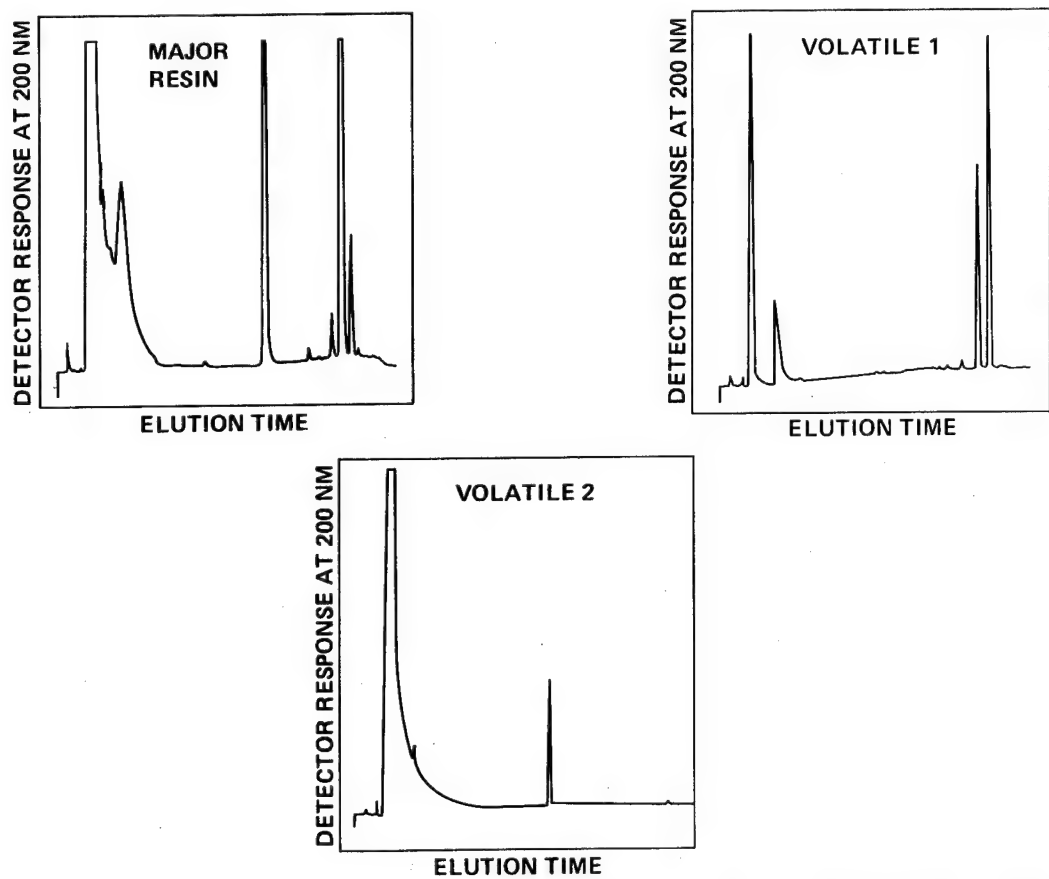


Figure 2. Partition liquid chromatographic analysis of U.S. Polymeric V378A resin ingredients.

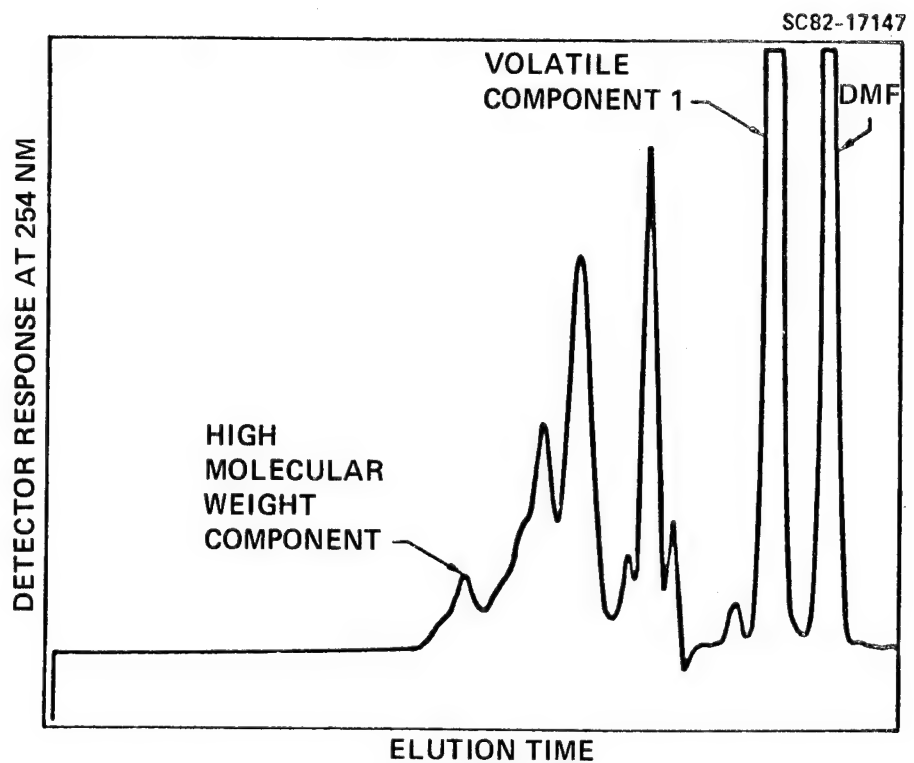


Figure 3. Size exclusion liquid chromatographic analysis of U.S. Polymeric V378A resin.

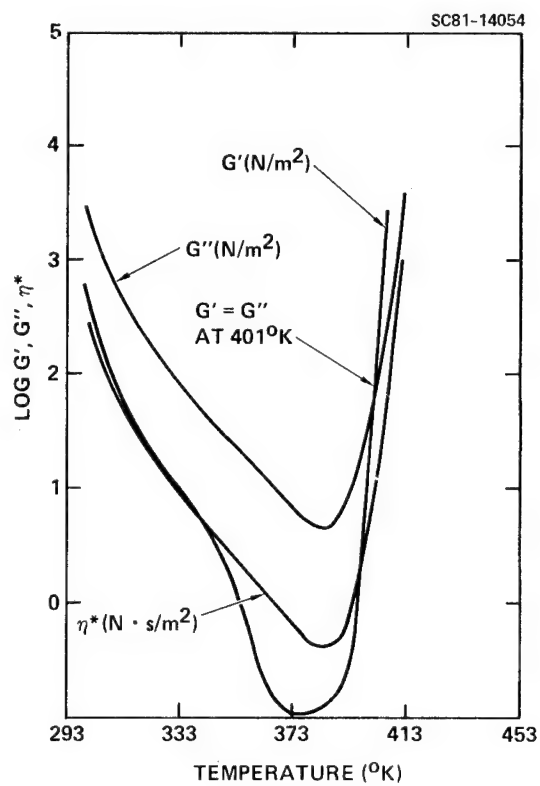


Figure 4.
Dynamic viscoelastic behavior of
U.S. Polymeric V378A resin at a
2 K/min heating rate.

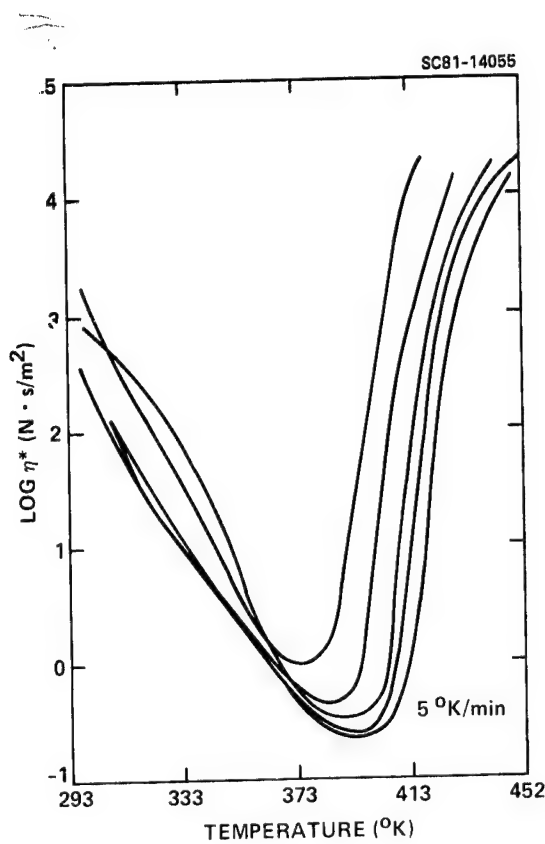


Figure 5.
Effect of heating rate on the cure rheology of U.S. Polymeric V378A resin.

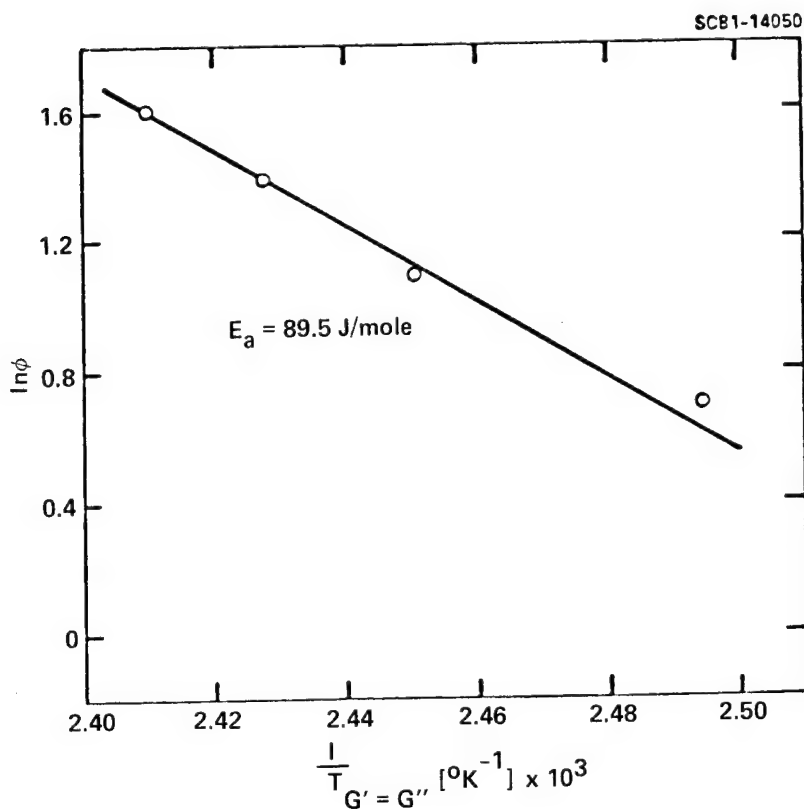


Figure 6.
Dependence of the dynamic moduli crossover temperature with heating rate for the cure of U.S. Polymeric V378A resin.

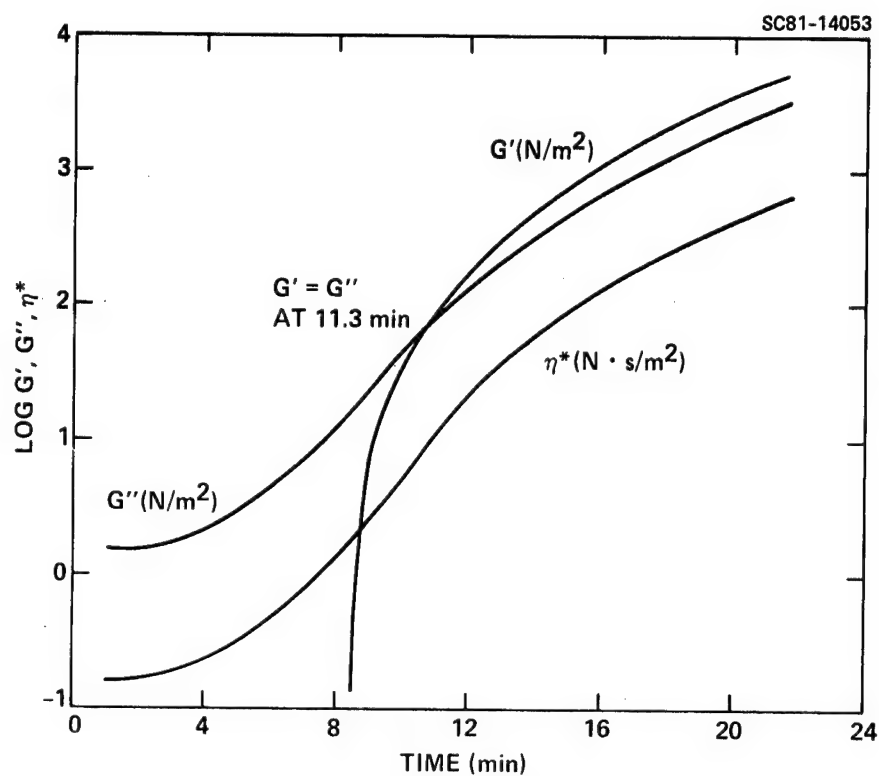


Figure 7.
Dynamic viscoelastic behavior of U.S. Polymeric V378A resin at 393 K.

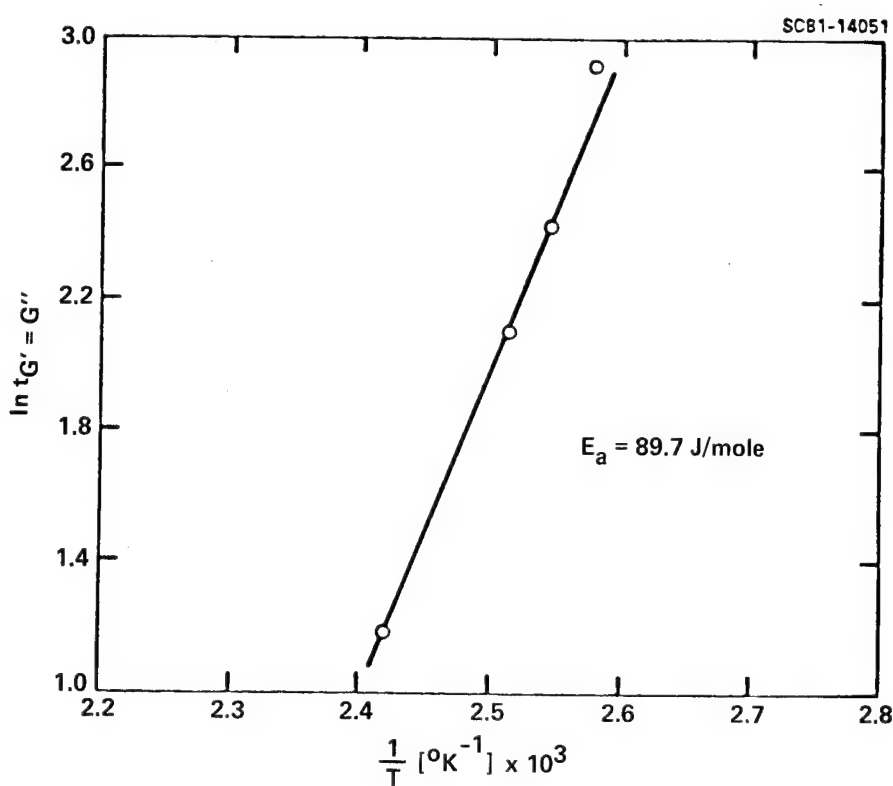


Figure 8.
Dependence of the dynamic moduli crossover time with isothermal cure temperature for U.S. Polymeric V378A resin.

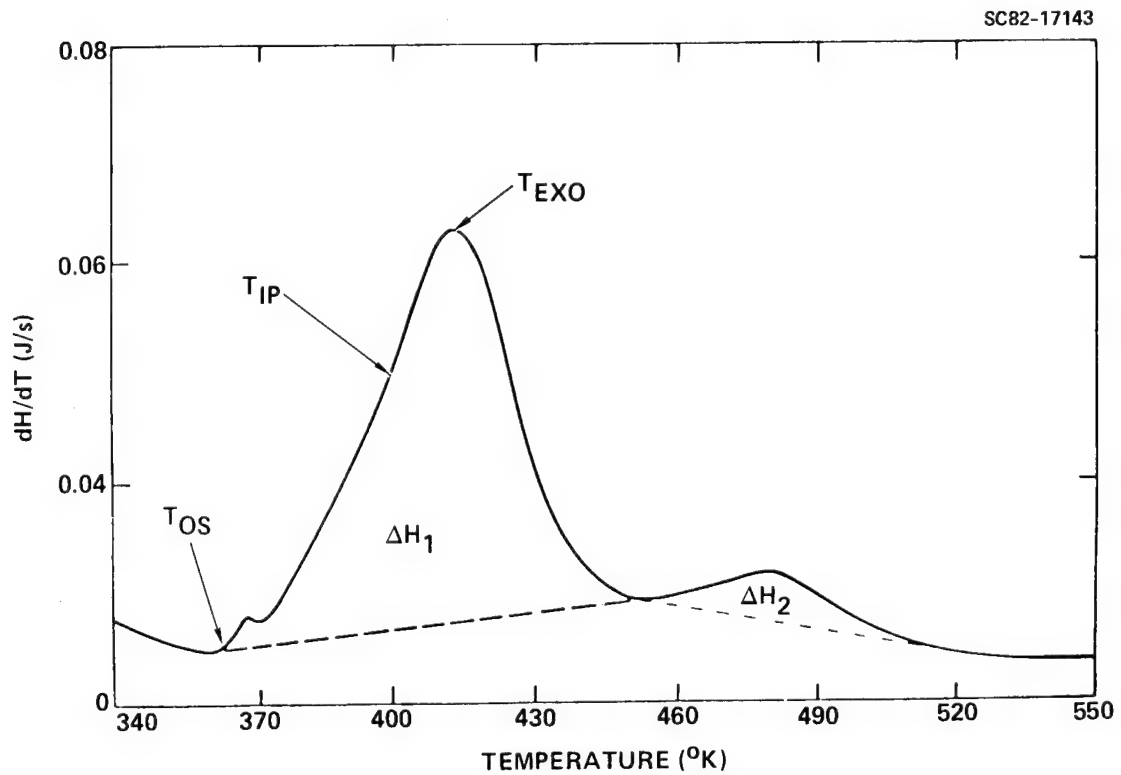


Figure 9. DSC thermogram for the curing of U.S. Polymeric V378A resin.

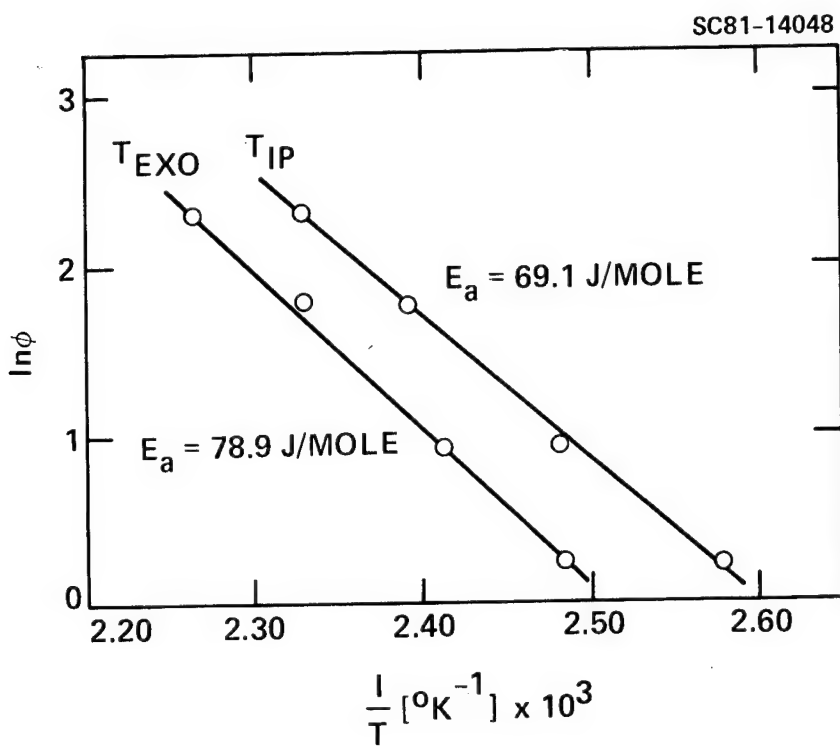


Figure 10.
Dependence of DSC exotherm peak and inflection point temperature with heating rate for U.S. Polymeric V378A resin.

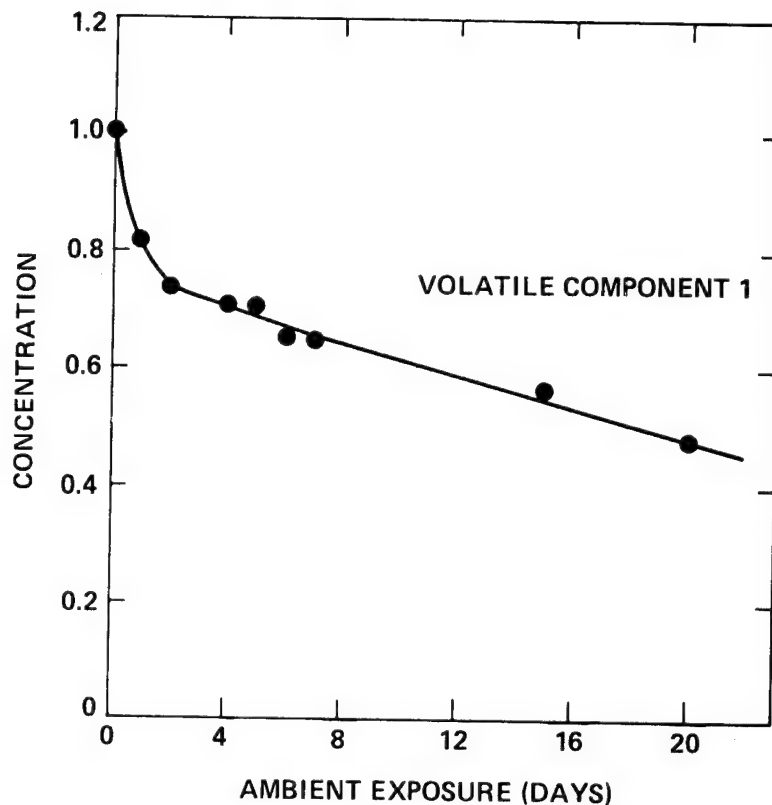


Figure 11.
Effect of ambient aging on the concentration of Volatile Component 1 in U.S. Polymeric V378A resin.

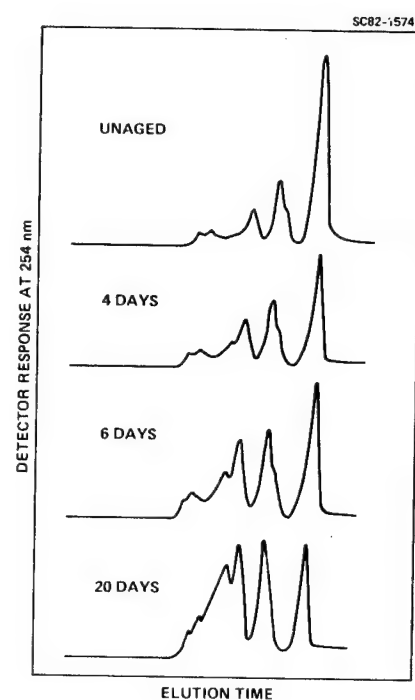


Figure 12.
Effect of ambient aging on the size exclusion liquid chromatographic separation of U.S. Polymeric V378A resin.

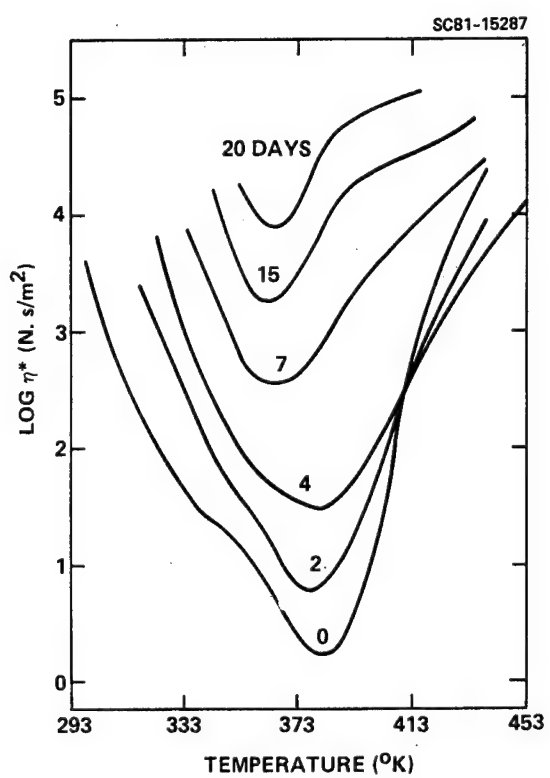


Figure 13.
Effect of ambient aging on the
cure rheology of U.S. Polymeric
V378A resin.

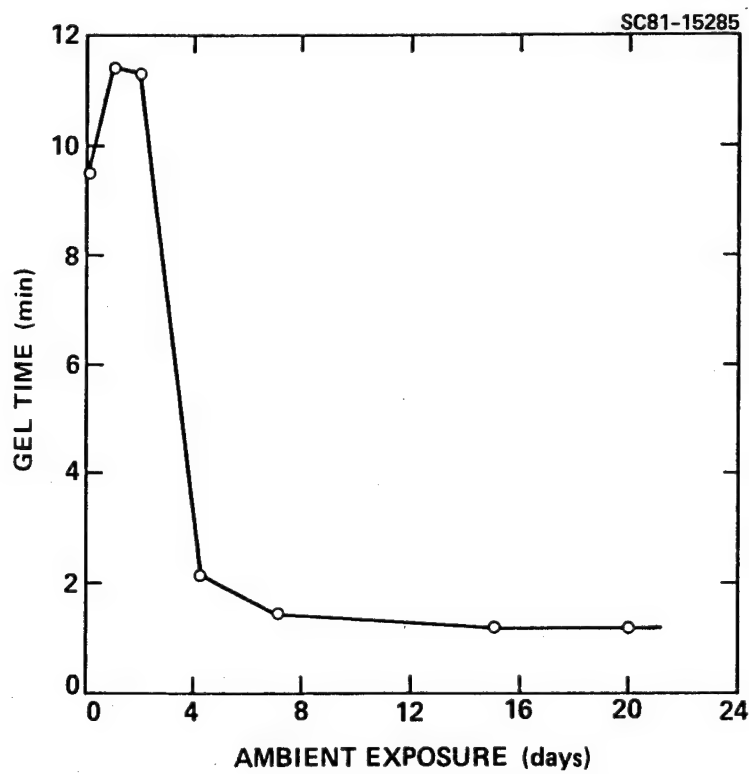


Figure 14.
Effect of ambient aging on the
time of gelation at 398K for
U.S. Polymeric V378A resin.

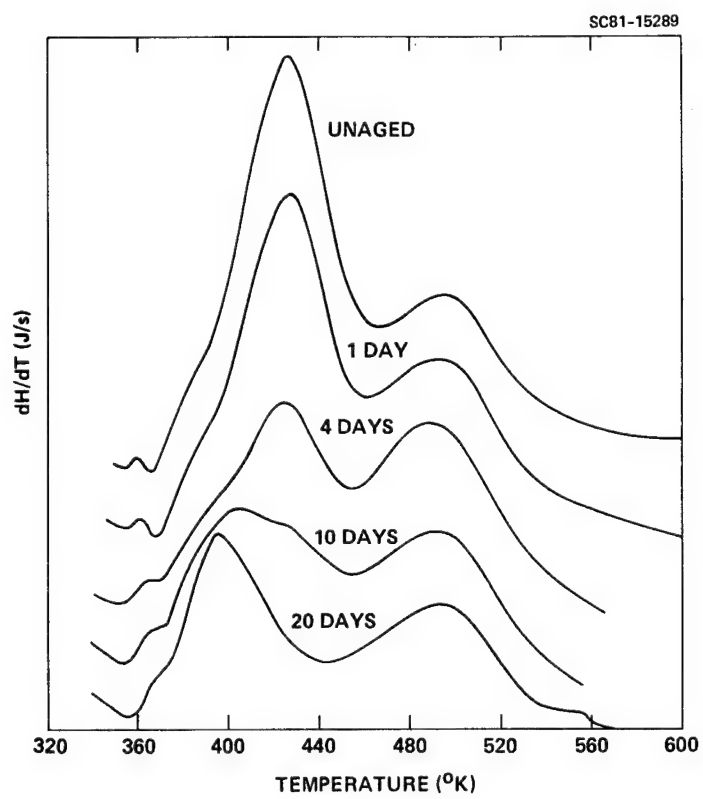


Figure 15. Ambient aging effect on the DSC behavior of U.S. Polymeric V378A resin.

REPLACEMENT OF MDA WITH MORE OXIDATIVELY STABLE DIAMINES IN PMR-POLYIMIDES

William B. Alston
Propulsion Laboratory
U. S. Army AVSCOM Research and Technology Laboratories
NASA Lewis Research Center

Studies were performed to investigate the effect of substituting 4,4'-oxydianiline and 1,1-bis(4-aminophenyl)-1-phenyl-2,2,2-trifluoroethane for the 4,4'-methylenedianiline in PMR polyimide matrix resin. Graphite fiber reinforced composites were fabricated from unsized Celion 6000 and PMR-polyimide matrix resins having formulated molecular weights in the range of 1500 to 2400. The composite processing characteristics were investigated and the initial room temperature and 316 °C (600 °F) composite mechanical properties were determined. Comparative 316 °C composite weight losses and 316 °C mechanical properties retention after prolonged 316 °C air exposure were also determined.

INTRODUCTION

The development of in situ polymerization of monomeric reactants (PMR) polyimides was first reported by investigators at the NASA Lewis Research Center (ref. 1). They reported that a methanol solution of 2.08 moles of the dimethyl ester of 3,3',4,4'-benzophenonetetracarboxylic acid (BTDE), 3.08 moles of 4,4'-methylenedianiline (MDA), and 2 moles of the monomethyl ester of endo-5-norbornene-2,3-dicarboxylic acid (NE) provided a highly processable matrix resin. This resin solution, designated PMR-15, when polymerized in situ on the fiber, provided an optimum balance of desirable composite processing characteristics, composite thermo-oxidative stability, and retention of composite mechanical properties after long-term high-temperature aging. The in situ polymerization from monomeric reactants (PMR) represented a new technology of addition-cured polyimide matrix resins. Today, PMR-15 is commercially available from the major suppliers of prepreg materials and is being used in a wide range of aerospace components (ref. 2). A recent study (ref. 3) concluded that degradation of the MDA monomer is the major contributor to observed weight loss of PMR-15 composites in a 316 °C (600 °F) air environment. The purpose of this study was to determine the effects of replacing the MDA monomer in PMR-15 with two different, more thermo-oxidatively stable diamine monomers, 4,4'-oxydianiline (ODA) and 1,1-bis(4-aminophenyl)-1-phenyl-2,2,2-trifluoroethane (3FDA), on composite weight losses and retention of composite high-temperature mechanical properties.

Throughout this paper, interpretative descriptions will refer to more oxidatively stable diamines compared to the less oxidatively stable methylene-containing MDA diamine (used in PMR-15). This is to be understood in the context of meaning addition-cured polyimides containing more oxidatively stable connecting linkages such as those traditionally used in thermo-oxidatively stable condensation polyimides. Examples of these more oxidatively stable connecting linkages are the oxygen linkage (used in all ODA-based condensation polyimides), the carbonyl linkage in BTDE (used in all 3,3',4,4'-benzophenonetetracarboxylic dianhydride (BTDA)-based condensation polyimides), and the phenyl trifluoroethane linkage (3F) in 3FDA (similar in structure to the very thermo-oxidatively stable hexafluoroisopropylidene (6F) connecting linkage used in all 6F based condensation polyimides). The 3F

linkage has been shown to be slightly superior thermally to the 6F linkage when compared in polyarylates using thermal gravimetric analysis (TGA) in a nitrogen environment (ref. 4). A slight increase was observed for 3F linkage polyarylate incipient decomposition temperature to 446 from 438 °C for the 6F linkage polyarylate. Similar comparative TGA data (ref. 5) ranked the 3F and 6F connecting linkages as being of the same relative thermal stability. However, neither study (ref. 4 or 5) reported any thermo-oxidative comparisons of the 3F and 6F linkages in an air environment. In contrast, the less oxidatively stable MDA diamine monomer in PMR-15 is to be understood in the context of containing an oxidizable methylene connecting group which kinetically is as much as two orders of magnitude more oxidizable than primary, secondary, and tertiary aliphatic hydrocarbons (ref. 6) such as in the nadimide crosslinker endcaps in PMR-15. Hydrocarbon-containing addition-curing polymers such as PMR-15 are generally considered to be of poorer thermo-oxidative stability than their nonhydrocarbon-containing counterparts, the thermo-oxidatively stable condensation polymers containing connecting linkages such as oxygen, carbonyl, and 6F groups. Thus, based on traditional relative thermal and thermo-oxidative stabilities of connecting linkages and textbook comparative hydrocarbon oxidative reactivities, the predicted order of oxidative stability of the monomeric components within the PMR polyimide polymers in this study would be as follows:

BTDA ~ ODA ~ 3FDA >> Aliphatic Nadic Endcaps >> MDA

EXPERIMENTAL PROCEDURES

Monomer and PMR Solution Preparation

The monomers used in the study are shown in table I. The NE, ODA, and BTDA were obtained as reagent grade chemicals from commercial sources and used in as-received form after verifying the melting points (m.p.). The 3FDA was synthesized by the literature procedure (ref. 7) as shown in row 1 of table II except that the reaction was scaled up five- and tenfold and the 3FDA was purified to a white powder (m.p. 217 to 217.5 °C) in 70 to 79% yields by multiple recrystallizations from chloroform. Table II also shows in row 1 that the purification in reference 7 was done by a chromatographic separation which provided an 88% yield of rose-colored 3FDA (m.p. 201 to 204 °C) in contrast to the improved purification of this study done by recrystallization from chloroform. The BTDE was synthesized by heating at the reflux temperature a suspension of BTDA in a calculated amount of methanol until the BTDA dissolved and then by continued heating for an additional 2 hr to result in a 50 weight percent (wt %) solution of BTDE in methanol. The PMR solutions were prepared at room temperature by adding, all at once to the BTDE solution, the NE, the diamine monomer (MDA, ODA, or 3FDA), and an equivalent weight of methanol to maintain 50 wt % solids. In the ODA and 3FDA formulations, additional methanol and a mixed solvent consisting of methanol and acetonitrile, respectively, were added to provide 35 wt % solids. The use of additional methanol and the mixed solvent were required along with gentle heating to dissolve the ODA and 3FDA in the PMR solution. The monomer combinations, abbreviations, formulated molecular weights, molar ratio value, and alicyclic weight percent of the PMR matrix resins used in this study are shown in table III.

Model Compounds and Instrumental Analysis

Bisnadicimide derivatives of MDA, ODA, 3FDA, and 4,4'-diaminobenzophenone (DABP) were prepared by imidization in hot acetic acid followed by addition of acetic anhydride to complete the imidization. The bisnadicimide derivatives were isolated in 80 to 90% yields by cooling the acetic acid reaction solution and suction filtration of the precipitated white solids. Recrystallizations were done in acetic acid except for the 3FDA bisnadicimide which was recrystallized from acetonitrile. The m.p. of the bisnadicimides were: MDA = 255 to 256 °C, ODA = 258 to 260 °C, 3FDA = 245 to 246 °C, and DABP = 320 to 321 °C. Thermal gravimetric analysis (TGA) of the bisnadicimide model compounds was done on Perkin Elmer TGS-2, infrared analysis on a Nicolet FT-IR 7199, carbon and hydrogen NMR analysis on a Varian FT-80A, and differential scanning calorimeter (DSC) analysis on a DuPont 990 equipped with a pressure DSC cell. The glass transition temperature (T_g) of the matrix resins was determined at a heating rate of 20 °C (36 °F)/min on a DuPont 942 thermo-mechanical analyzer.

Composite Fabrication

Prepreg tapes were made by drum winding at 4.72 turns/cm (12 turns/in) and impregnating unsized Celion 6000 graphite fiber with the various PMR solutions listed in table III to yield prepgs containing 40 to 41 wt % monomers. (This is calculated to provide cured laminates of 63 wt % fiber when resin flow is about 3%). The prepgs were air dried on the rotating drum at room temperature for 3 to 6 hr and then allowed to stand without rotation overnight. The prepg tapes were removed from the drum, cut into 7.6 by 20.3 cm (3 by 8 in) plies, and stacked unidirectionally 12 plies thick. The prepg stack was placed in a pre-forming mold and staged at 204 °C (400 °F) for 1 hr under a pressure of approximately 0.5 kPa (0.067 psi). A typical plystack lost 4 to 6 g of volatiles and weighed 48 to 52 g after staging. Composites were molded by placing the staged prepg stack into a matched metal die at room temperature. The die was inserted into a 316 °C (600 °F) press. When the die thermocouple read 232 °C (450 °F), a pressure of 3.45 MPa (500 psi) was applied. After the mold reached 316 °C (600 °F), the temperature and pressure were maintained for 2 hr. The mold was then allowed to cool to at least 177 °C (350 °F) before releasing the pressure and disassembling. The weight of the laminate plus flash was typically 0.5 to 1.0 g less than the staged prepg. The weight of the flash divided by the composite plus flash weight was called the resin flow and ranged from 0.3% for ODAPMR-15 to 7% for 3FDAPMR-15 with a 2 to 4% range for the other composites. The laminates were postcured by heating in air from 24 to 316 °C (75 to 600 °F) over 2 hr, holding at 316 °C for 16 hr, and then slowly cooling to 24 °C. Postcure weight losses were all between 0.3 and 0.6%.

Composite Testing

All laminates were inspected for acceptability by an ultrasonic C-scan technique and then cut into nine 2.5 by 6.7 cm (1 by 2-5/8 in) pieces. Two pieces of each laminate were used to prepare triplicate flexural and interlaminar shear strength (ILSS) test specimens for room temperature and 316 °C (600 °F) tests. All the laminates were then inspected by obtaining photomicrographs of the composite cross sections to assure the composites were void free and of even resin/fiber distribution. Flexural strength tests were performed in accordance with ASTM Test for Flexural Properties of Plastics and Electrical Insulating Materials (D790-71).

Tests were made on a three-point load fixture with fixed span of 5.1 cm (2 in). The thickness of the Celion 6000 composite specimens ranged from 1.93 to 1.98 mm (0.076 to 0.078 in) for 3FDAPMR-15 and ODAPMR-15 to 2.06 to 2.16 mm (0.081 to 0.085 in) for all the other laminates resulting in a span/depth ratio ranging from 26.3 to 23.5, respectively. ILSS tests were performed essentially in accordance with ASTM Tests for Apparent Interlaminar Shear Strength of Parallel Fiber Composites by Short Beam Method (D2344-76) using a constant span/depth ratio of five. The rate of center loading for flexural and ILSS tests was 1.27 mm/min (0.05 in/min). Flexural and ILSS tests were conducted in an environmental heating chamber following a 15-min equilibration time at the test temperature. The mechanical property values reported are averages of three tests at each condition. Fiber content was determined for all laminates before aging by using a H_2SO_4/H_2O_2 digestion procedure. The flexural data were not normalized to a common fiber volume percent because of the small range of the fiber weight percents found by digestion and the insignificant effect of normalization on the raw flexural data (as shown later). The remaining seven 2.5 by 6.7 cm (1 by 2-5/8 in) test coupons were used for long-term isothermal exposure in a 316 °C (600 °F) circulating air oven having an air change rate of 100 cm³/min (6.1 in³/min). Composite weight loss measurements were made throughout the exposure period. Every 300 hr one test coupon was removed for 316 °C mechanical testing as described previously. Thus, the number of specimens for the weight loss measurements decreased sequentially from seven to one. Photomicrographs of the cross sections of aged composites were also obtained to visually investigate the manner in which the composites thermo-oxidatively degraded.

RESULTS AND DISCUSSION

Weight Loss Investigations

The thermal and thermo-oxidative stability of the bisnadiimide model compounds of ODA, MDA, 3FDA, and DABP (described in the Model Compounds and Instrumental Analysis section) were investigated by dynamic thermal gravimetric analysis (TGA) in nitrogen and air atmospheres. The TGA curves presented in figure 1 show that the bisnadiimide model compounds provided a char yield in nitrogen at 800 °C ranging between 28 and 42% weight retention. The amount of char yield at 800 °C appeared to be proportional to the molecular weight of the diamine. However, the intermediate weight retention plateaus (in the 300 to 500 °C region) in air or nitrogen tended to exhibit an inverse relationship to the molecular weight of the diamine. The MDA bisnadiimide, containing the lowest molecular weight diamine, provided an intermediate weight retention plateau in air or nitrogen that was greater than or equal to the weight retentions of the higher molecular weight bisnadiimides prepared from the more oxidatively stable diamines, ODA, DABP, and 3FDA. This suggested a greater amount of favorable weight retaining reactions occurred in the MDA bisnadiimide compared to the other three bisnadiimides.

It should also be noted that the intermediate plateau weight retentions were always greater for all four bisnadiimides in air than in nitrogen. This suggests complex weight gaining oxidation reactions occur in all four bisnadiimides. Unfortunately, these differences were too inconclusive to use dynamic TGA as a routine technique to screen the bisnadiimide binary monomer combinations for decisive conclusions about long-term stability of various connecting groups in matrix resins. For example, even though an oxidation product of MDA would be DABP, the TGA weight retentions in air of the MDA and DABP bisnadiimides were not identical. Thus, it would be highly desirable to include DABP (as a higher oxidation state of MDA) along with the three diamines (MDA, 3FDA, and ODA) used in this composite study.

Unfortunately, a small test laminate prepared with BTDE/DABP/NE PMR polyimide at $N = 2.0$ (FMW = 1500) did not exhibit sufficient resin flow to fabricate a comparable quality composite to the other laminates in this study (as listed in table III). Consequently, a DABP PMR-15 laminate was not included in this study even though it represents an oxidation product of PMR-15 and could also be considered as a PMR resin prepared with a diamine containing a more thermo-oxidatively stable connecting linkage such as carbonyl (DABP), oxygen (ODA), or phenyltrifluoroethane (3FDA). In retrospect, the unprocessability of BTDE/DABP/NE is due to the lack of a sufficient melt flow region on a 316°C (600°F) processing cycle. This might have been predicted from the approximately 60°C higher m.p. of the DABP bisnadiimide compared to the m.p. of the 3FDA, ODA, and MDA bisnadiimides (see the Model Compounds and Instrument Analysis section). Thus, only the processable PMR monomer combinations given in table III were used to prepare graphite fiber composites with the following unsized Celion 6000 fibers: original experimental Celion 6000 of lot number HTA-7-6Y11 (hereafter designated old Celion (OC)), production grade Celion 6000 of lot number HTA-7-1231 (2760 MPa (400 ksi) tensile strength; hereafter designated intermediate Celion (IC)), and improved production Celion 6000 of lot number HTA-7-2531 (3590 MPa (520 ksi) tensile strength; hereafter designated new Celion (NC)).

The weight losses of the Celion 6000/PMR composites after extended 316°C (600°F) air exposure are plotted in figure 2. At a common alicyclic weight percent (FMW = 1500) on OC fiber the PMR-15 exhibited a lower weight loss than either 3FDAPMR-15 or 3FDAPMR-24. A 37.5% reduction in the amount of aliphatic NE (by increasing FMW to 2400) did not reduce the composite weight loss of OC/3FDAPMR-24 below the composite weight loss of OC/PMR-15.

The photomicrographic cross sections shown in figure 3 (and the IC and NC/PMR composites not shown) and the ultrasonic scans of all of the postcured OC, IC, and NC/PMR composites in this study were of comparable quality, thus eliminating void content, or composite processability, as a possible cause of the differing weight loss behavior observed in the OC/MDA, 3FDA, and ODA PMR composite systems and in the IC and NC/PMR composite weight loss comparisons to follow. Figure 2 also shows that the NC/PMR-15 composite provided a lower weight loss than either IC/3FDAPMR-19.5 or NC/3FDAPMR-24; the same trend was observed in comparing PMR-15 to 3FDAPMR-24, both on OC fiber.

It is important to note that all the composites in this study were aged at the same sample size and geometry, at the same time, and in the same 316°C (600°C) oven to minimize the effect of oven temperature fluctuations on composite weight loss results. The only exception was the IC/3FDAPMR-19.5, which was aged at a different time. The fact that the IC/3FDAPMR-19.5 and NC/3FDAPMR-24 weight loss measurements were conducted at different times using a different fiber lot and possibly under slightly different temperature conditions could account for the almost identical weight loss behavior exhibited by IC/3FDAPMR-19.5 and NC/3FDAPMR-24. A higher weight loss had been predicted for IC/3FDAPMR-19.5 because it has a higher aliphatic nadimide content than NC/3FDAPMR-24.

The use of two different fibers could also contribute to the similarity in the 3FDAPMR-19.5 and 24 weight losses in figure 2. Composite weight losses are sensitive to fiber type as shown by the comparison of PMR-15 on OC and NC fiber (shown in fig. 2). This suggests that the lower weight loss with NC fiber may result from a lower level of deleterious resin/fiber thermo-oxidative interactions with PMR-15 resin compared to the OC fiber. Differences in thermo-oxidative weight loss of PMR-15 resin on different fibers have been reported previously and discussed as due

to deleterious resin/fiber thermo-oxidative interactions, presumably due to differences in the contaminants of the fiber surfaces (ref. 8).

The OC, IC, and NC fibers used in this study lost 5 to 7% of their weight after 900 hr of air exposure at 316 °C (600 °F). Graphite fiber weight losses after a similar exposure can range from virtually 0% for high-modulus graphite fiber types to virtually 100% for high-strength high-sodium-content graphite fiber types (ref. 8). Therefore, the narrow range of 5 to 7% fiber weight loss in this study indicates the thermo-oxidative stability of the OC, IC, and NC fibers are quite comparable, thus leaving differences in the resin/fiber thermo-oxidative interactions as the probable cause of lower composite weight loss of NC/PMR-15 compared to OC/PMR-15. Thus, the major cause of the observed differences in the composite weight losses shown in figure 2 has to be due to the different diamines used in formulating the PMR matrix resin because variances due to void content, composite processability, sample aging size and geometry, sample aging temperature/time, and fiber thermo-oxidative stability have been eliminated, minimized, or accounted for.

The significantly greater level of weight loss of the ODAPMR-15 and 3FDAPMR-15 composites prepared with the more oxidatively stable diamines, compared to PMR-15 with the oxidizable MDA diamine, seems to be the reverse of what would be predicted based on the general concept that improved thermo-oxidative stability comes from preparing polymers with improved thermally and thermo-oxidatively stable monomers. A similar result was found in previous nadimide cured polymer studies. Neat resins prepared from BTDA/ODA/NE and pyromellitic dianhydride (PMDA)/ODA/NE (ref. 9) and composites fabricated from PMR solutions of BTDE/ODA/NE in N-methyl pyrrolidinone solvent (ref. 1) were of poorer 316 °C (600 °F) thermo-oxidative stability than when MDA was used instead of ODA as the diamine monomer.

In contrast, classical thermo-oxidative stability studies of condensation polyimides have shown that MDA/PMDA (ref. 10) and MDA/BTDA (refs. 10 and 11) provide only comparable or greater weight loss, but never significantly less, than PMDA on BTDA condensation polymers prepared with more oxidatively stable diamines, such as ODA and DABP. However, the level of weight loss reported for MDA condensation polyimides would have been slightly greater had it not been for the weight gaining oxidation reactions of the benzylic methylene connecting linkage oxidizing to a carbonyl linkage and the thermo-oxidative crosslinking reactions of the benzylic methylene linkage as identified in the literature (refs. 10 to 12). In this study of nadimide terminated polyimides the converse result was found: the MDAPMR-polyimide (PMR-15) consistently provided less weight loss than the PMR polyimides containing the more oxidatively stable diamines, ODA and 3FDA. It might be possible to account for the lower weight loss in the same manner as is done in the literature (refs. 10 to 12) for condensation polyimides containing MDA; that is, by oxidation of the benzylic methylene to a carbonyl connecting group and thermo-oxidative benzylic crosslinking reactions. However, these reactions would have to proceed with greater efficiency to provide less weight loss in PMR-15 (compared to ODAPMR-15 and 3FDAPMR-15) than the same benzylic connecting group thermo-oxidative reactions occurring in MDA condensation polyimides. These polyimides provide, at best, only comparable weight loss when compared to oxidatively stable diamines in non-MDA condensation polyimides.

Because the concentration of methylene connecting groups in condensation polyimides is greater than in the nadimide terminated PMR-15 (endcapping dilutes the molar concentration of the "within the chain" species), the same favorable benzylic weight gaining oxidations to a carbonyl connecting group and benzylic thermo-oxidative crosslinking can not kinetically occur to a greater extent in PMR-15 than

in the MDA condensation polyimide. Thus, the lower weight loss of PMR-15 compared to non-MDA PMR resins (ODAPMR-15 and 3FDAPMR-15) is not due solely to the use of the MDA monomer. Instead, the introduction of a second species, the polymerized nadimide endcap in cured PMR-15, in combination with the MDA benzylic linkage must account for a greater efficiency of thermo-oxidative crosslinking reactions such as those between benzylic methylene and polymerized nadimide endcap. This provides an oxidatively crosslinkable polymer exhibiting significantly lower weight loss than polymerized nadimide endcapped polyimides without the benzylic site (ODAPMR-15 and 3FDAPMR-15).

In summary, without both the polymerized nadimide endcap and the benzylic connecting linkage being present simultaneously, the weight loss of condensation or of low molecular weight addition polymers increases. This is the case with MDA condensation polyimides versus oxidatively stable diamine condensation polyimides (refs. 10 to 12) and in this study of PMR-15 versus ODAPMR-15 and 3FDAPMR-15 to 24. Thus, the presence of two easily oxidizable sites (polymerized nadimide and benzylic linkage) in PMR-15 results in a synergistic increase in thermo-oxidative weight retention due to favorable weight gaining oxidations and thermo-oxidative crosslinking reactions of benzylic methylene connecting linkages with polymerized nadimide endcaps.

Elimination of this synergistic effect can be accomplished with comparable weight losses resulting; however, the important point to understand is that the polymers with the synergism will exhibit less weight loss than that predicted, and polymers without the synergism will exhibit weight losses determined solely by the concentration and relative reactivities of the remaining oxidizable species. One example of this is the comparable weight loss observed for NC/3FDAPMR-24 and OC/PMR-15 (fig. 2), obtained by reducing the NE content 37.5% (increase to FMW = 2400) and by reducing the deleterious resin/fiber thermo-oxidative interactions by using NC fiber with the 3FDAPMR-24 resin (without the synergism). Another example (ref. 13) is the identical composite weight loss observed for PMR-II composites (without the synergism effect) and MDA-containing analogous composites (with the synergism), obtained by using a very oxidatively stable diamine monomer without any connecting linkage in PMR-II. In this case the weight loss comparison was done using composite samples that had not been aged together and using a fiber which, at that time period, exhibited deleterious resin/fiber thermo-oxidative interactions. These conditions combine to possibly nullify comparisons of the overall degradation rate of the more easily oxidizable MDA-containing analog and PMR-II. However, if the comparison is done on the same fiber (OC or NC), the PMR-15 composites (with the synergism) exhibited less weight loss than the 3FDAPMR-24 composite (without the synergism). In the PMR-II case (ref. 13) the study would have to be redone either as neat resins or with a fiber that exhibits a reduced level of deleterious resin/fiber thermo-oxidative interactions in order to determine if the weight loss of the MDA analog of PMR-II (with the synergism) would be less than, or only remained equal to, the weight loss of PMR-II (without the synergism).

A more indepth analysis of PMR-15 thermo-oxidative degradation mechanisms (ref. 3) has shown the oxidation of the benzylic connecting linkage to a carbonyl linkage does occur in PMR-15. An infrared analysis using a bulk sampling technique showed the oxidation to be limited (<0.8%). The oxidation to a carbonyl has been more clearly identified (ref. 14) as occurring on the thermo-oxidatively exposed resin surface by infrared analysis using a surface sampling technique; however, the extent of the surface carbonyl formation was not determined. The oxidative crosslinking reaction in PMR-15 has also been observed, but not structurally characterized, by infrared analysis as an oxidation found in the polymerized nadimide

component of PMR-15 (ref. 3). This nadimide thermo-oxidative reaction may be speculated as being the cause of an observed shift in the infrared band pattern related to the nadimide band variations adjacent to a benzylic group that has been oxidized to the carbonyl. This shift was observed in investigations of samples taken from the surface region of oxidatively exposed resin (ref. 14). The net overall effect of the multiple oxidation reactions occurring in PMR-15 (with the synergism) and in ODAPMR-15 or 3FDAPMR-15 or 24 (with the benzylic site for the synergism not present) can be best understood visually. Figure 4 contains photomicrographs of cross sections of composites of ODAPMR-15, PMR-15, 3FDAPMR-15, and 3FDAPMR-24. All the photomicrographs were taken when levels of composite weight loss were comparable or bracketed the weight loss of OC/PMR-15 after 2100 hr of 316 °C (600 °F) air exposure. The pictures in figure 4 show that the synergistic combination of benzylic methylene linkages and polymerized nadimide endcaps in PMR-15 limits the thermo-oxidative behavior to favorable surface oxidation reactions (carbonyl formation) and nadimide-benzylic thermo-oxidative crosslinking (as described above in this interpretation of ref. 14). In contrast, the increased depth of degradative void and crack formation with the PMR resins using more oxidatively stable diamines (without the synergism as in ODAPMR-15 and 3FDAPMR-15 and 24) is the result of unfavorable hydrocarbon thermo-oxidation of the polymerized nadimide crosslinker (being the next most oxidizable species when the benzylic methylene connecting linkage is not present).

Mechanical Property Investigations

The initial room temperature interlaminar shear strength (ILSS) of the seven composites ranged between 108 and 128 MPa (15.6 and 18.5 ksi). The 316 °C (600 °F) ILSS of the seven composites are shown in figure 5 as a function of 316 °C exposure time. The initial 316 °C ILSS ranged from 35 to 63 MPa (5.1 to 9.1 ksi). The initial 316 °C ILSS of composites made with 3FDAPMR-24 exhibited a thermoplastic failure mode which changed to a normal thermoset ILSS failure mode after 300 hr of 316 °C air aging. After 2100 hr of 316 °C air exposure a clear trend was apparent in the ILSS data: the only composites that exhibited excellent retention of 316 °C ILSS were the OC/PMR-15 and NC/PMR-15 composites. The OC/3FDAPMR-19.5 and NC/3FDAPMR-24 composites, which exhibited similar weight loss behavior compared to OC/PMR-15, failed to retain their initial 316 °C (600 °F) ILSS to the extent of the OC/PMR-15 composite. Even the OC/ODAPMR-15 composite which displayed the highest initial 316 °C ILSS fell below the OC/PMR-15 and NC/PMR-15 ILSS after only approximately 700 hr of 316 °C exposure. After 900 hr of 316 °C air exposure, the OC/3FDAPMR-15 composite had formed so much loose surface fiber due to the high rate of weight loss that the test interval was decreased to 150 hr and testing was performed to only 1500 hr of exposure. The OC/ODAPMR-15 had an identical rate of weight loss to OC/3FDAPMR-15 but did not exhibit as much loose surface fiber probably because of the lower fiber weight percent/higher resin weight percent (56.1%/43.9%) of OC/ODAPMR-15 compared to the higher fiber weight percent/lower resin weight percent (70.2%/29.8%) of OC/3FDAPMR-15. Thus, testing was done on the ODAPMR-15 composites for up to 2100 hr of 316 °C exposure. However, both OC/ODAPMR-15 and OC/3FDAPMR-15 composites exhibited a severe decrease in the ILSS after 900 hr of 316 °C air exposure.

The 316 °C (600 °F) flexural strength retention of the composites is shown in figure 6. The initial room temperature flexural strengths were in the range of 1566 to 1973 MPa (227 to 286 ksi). The initial 316 °C flexural strengths ranged from 752 to 1056 MPa (109 to 153 ksi). The flexural data shown have not been normalized to a common fiber weight or volume percent because all the laminates except OC/ODAPMR-15 and OC/3FDAPMR-15 were of very similar fiber weight percents ranging

between 63.9 and 65.7 percent, thus having no visible normalization effect on figure 6. The fiber weight percent for OC/3FDAPMR-15 was 70.2%. Thus, if OC/3FDAPMR-15 was normalized down to a 64% range, it would only further lower by about 10% the curve that was already the lowest of the set of seven curves after long-term exposure. The fiber weight percent for OC/ODAPMR-15 was 56.9%. If it was normalized up to a 64% range, it would only further raise by about 11% the curve that was the highest initially but dropped to the second lowest after long term exposure, hence not causing any changes in the relative position of the curve related to the other six curves in figure 6. Thus, a comparison of these curves shows that after much less than 2100 hr of 316 °C air exposure a similar trend to that seen in the ILSS retention (fig. 5) was again apparent. Only the OC and NC/PMR-15 composites exhibited excellent retention of 316 °C flexural strength; all the composites prepared with PMR monomer combinations using more oxidatively stable diamines exhibited severe decreases in flexural strength after 900 hr of 316 °C exposure. Even the OC/ODAPMR-15 composite, which displayed the highest initial 316 °C (600 °F) flexural strength, fell below the OC/PMR-15 and NC/PMR-15 flexural strengths after only 600 hr of 316 °C air exposure. Also, just as was observed in the ILSS data, the composites IC/3FDAPMR-19.5 and NC/3FDAPMR-24 which had exhibited weight loss behavior similar to that exhibited by OC/PMR-15 failed to display the same high level of flexural strength retention as did the OC/PMR-15 composite. The failure to provide comparable properties at comparable weight losses should not be surprising. PMR polyimide literature cites as an example MDA-containing composites prepared with varying dianhydride monomers (thus all containing the synergism) in which the retention of mechanical properties and extent of composite weight loss were not closely correlated (ref. 1). However, in this study it should be noted that, whether comparisons of mechanical property retention are done on the basis of equal composite weight loss or equal composite exposure time, the retention of ILSS and flexural strength was consistently and significantly better for PMR-15 (containing MDA with the thermo-oxidative synergism) than for PMR composites prepared with resins containing more oxidatively stable diamines (not containing MDA with its synergistic effect).

The flexural moduli of the seven composites are plotted in figure 7. The initial room temperature flexural moduli ranged between 117 300 and 132 480 MPa (17.0 and 19.2 ms¹). The initial 600 °F flexural moduli ranged from 93 150 to 120 060 MPa (13.5 to 17.4 ms¹). Unlike the ILSS (fig. 5) and flexural strength (fig. 6) a clear trend is not readily apparent in the retention of 316 °C (600 °F) flexural moduli. However, the flexural moduli after prolonged 316 °C exposure did exhibit the same overall order as the composite weight loss curves in figure 3. Perhaps more important, an examination of the flexural strength load curves uncovered a secondary slope. Recalculation of the flexural moduli with the secondary slopes did again exhibit a trend similar to the trends observed for ILSS and flexural strength retention. Figure 8 shows the retention of secondary moduli of the seven composites during prolonged air exposure. The solid symbols at the 0-, 300-, and 600-hr exposure times are the primary moduli at the exposure time when the primary moduli no longer were the same as the secondary moduli (the resin had started to exhibit a nonelastic response to applied load). The solid symbols at later exposure times (>1500 hr) are the final primary moduli from figure 7. Again the OC and NC/PMR-15 composites exhibited the highest retention of secondary flexural moduli as shown by the least decrease from the initial and final primary moduli values. The PMR-15 composites also took the longest exposure time to exhibit the least decrease in primary moduli to secondary moduli compared to the 3FDA composites which showed a moderate decrease in primary moduli at 0 hr and the ODAPMR-15 which exhibited a large decrease from its 600-hr primary moduli. Just as observed in the ILSS and flexural strength data, even the IC/3FDAPMR-19.5 and NC/3FDAPMR-24 composites which

exhibited similar weight losses when compared to OC/PMR-15 failed to retain their secondary moduli at comparable 316 °C (600 °F) exposure times to the extent the OC/PMR-15 composite retains the 316 °C secondary moduli. Indeed, there exists a large decrease to the secondary moduli at the final exposure times in all the 3FDAPMR composite primary moduli and also in the ODAPMR composite primary moduli compared to OC and NC/PMR-15 composite primary moduli.

Thus, the retention of all three composite 316 °C (600 °F) mechanical properties (ILSS, flexural strength, and flexural modulus) has been shown to be considerably poorer for PMR resin formulations containing the more oxidatively stable ODA and 3FDA compared to PMR-15 containing oxidizable MDA. The poor retention of composite mechanical properties of the OC/ODAPMR-15 and OC/3FDAPMR-15 was not unexpected in view of their greater weight losses compared to PMR-15 (fig. 2). However, when the long-term 316 °C mechanical properties are compared at equal composite weight losses (using later composite exposure times for PMR-15 compared to earlier exposure times for other PMR resins) the retention of mechanical properties of OC/ODAPMR-15 and OC/3FDAPMR-15 was still considerably poorer compared to OC/PMR-15. Reduction in the aliphatic nadimide content and use of the more oxidatively stable 3FDA on NC fiber (NC/3FDAPMR-24) provided a closely comparable rate of weight loss to OC/PMR-15, but even at the identical extended exposure times (and identical weight loss), the long-term retention of NC/3FDAPMR-24 composite mechanical properties was still considerably inferior to the mechanical property retention of OC/PMR-15.

A reason for the inferior mechanical property retention of NC/3FDAPMR-24 may be seen in the photomicrograph cross sections of the ODAPMR-15, 3FDAPMR-15 and 24, and PMR-15 composites shown in figure 4. The photographs were taken after long-term exposure times when composite weight losses were similar or bracketed the weight loss of OC/PMR-15 after 2100 hr of exposure (used as the comparative standard in fig. 4). The ODAPMR-15 and 3FDAPMR-15 and 24 composites show a much greater depth of void and crack formation, due to thermo-oxidative degradation, than PMR-15, thus visually accounting for the reduced level of composite mechanical property retention compared to PMR-15. When the thermo-oxidative reactions (carbonyl formation and thermo-oxidative crosslinking) are confined to the exterior polymer surface by using two easily oxidizable sites in PMR-15 (the synergism of the benzylic methylene of MDA and polymerized nadimide endcap), an undamaged PMR-15 interior results, as shown in figure 4. This would account for the high retention of PMR-15 composite mechanical properties. With the favorable weight gaining benzylic site thermo-oxidation and thermo-oxidative crosslinking of benzylic site with polymerized nadimide endcaps in the PMR-15 surface region (as discussed in the Weight Loss Investigations section), the thermo-oxidatively crosslinked network polymer structure would be maintained to account for the retention of composite mechanical properties of PMR-15.

In contrast, without the favorable synergistic thermo-oxidative reactions, such as occurs in ODAPMR-15 and 3FDAPMR-15 and 24 without the benzylic site of MDA, the thermo-oxidative degradation pathways can only proceed by using the next most easily oxidizable site, the polymerized, aliphatic nadimide crosslinker. The thermo-oxidative degradation rate would then be solely dependent on the reactivity and concentration of the remaining oxidizable species. This nonsynergistic situation provides a thermo-oxidative degradation pathway which would propagate with only limited termination ability (thermo-oxidative crosslinking) leading eventually to a breakdown of crosslink density and molecular weight of the polymerized nadimide structure. The nadimide hydrocarbon thermo-oxidative degradation pathway (in the absence of the benzylic methylene group) would then account for the increased rate of weight loss and inferior retention of mechanical properties, compared to PMR-15.

This is what was observed in this study when doing comparisons where the oxidizable concentration of hydrocarbon endcap was determined by the 1500 to 2400 formulated molecular weight of the PMR resins containing more oxidatively stable diamines.

CONCLUSIONS

Based on the results of this investigation the following may be concluded:

1. The use of 4,4'-methylenedianiline in nadimide-cured PMR-15 matrix resin appears to be essential for obtaining low composite weight loss. The use of more thermo-oxidatively stable diamine monomers such as ODA and 3FDA results in increased composite weight loss of the 1500 to 2400 formulated molecular weight nadimide cured matrix resins in this study.
2. The use of 4,4'-methylenedianiline in nadimide-cured PMR-15 matrix resin also appears to be essential for obtaining high retention of initial composite high-temperature (316 °C) mechanical properties. The use of more thermo-oxidatively stable diamine monomers such as ODA and 3FDA results in a deleterious effect on retention of composite high-temperature (316 °C) mechanical properties of the 1500 to 2400 formulated molecular weight nadimide-cured matrix resins in this study.
3. The lower composite weight loss and higher retention of composite mechanical properties of PMR-15 compared to PMR resins formulated with more oxidatively stable ODA or 3FDA was interpreted to be due to the synergistic combination of two easily oxidizable sites (benzylidic methylene of MDA and polymerized nadimide endcap). This interactive site combination confines the thermo-oxidative reactions to favorable weight gaining reactions (such as carbonyl formation) and thermo-oxidative cross-linking in the air exposed surface regions of PMR-15. The synergistic combination reduces the rate of thermo-oxidative degradative weight loss and increases the retention of composite mechanical properties of PMR-15 compared to other nadimide-cured resins without the benzylidic methylene group, such as the 1500 to 2400 formulated molecular weight ODAPMR and 3FDAPMR polyimides in this study.
4. The use of new Celion 6000 fiber (NC) might contribute to longer PMR-15 composite 316 °C (600 °F) lifetime than previously obtainable with old Celion (OC) fiber, probably due to a reduced level of deleterious resin/fiber thermo-oxidative interactions with NC than OC fiber.

REFERENCES

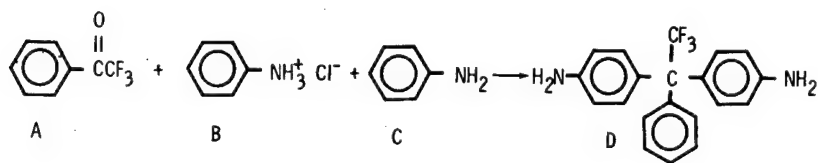
1. Delvigs, P., Serafini, T. T., and Lightsey, G. R.: Addition-Type Polyimides from Solutions of Monomeric Reactants, NASA TN D-6877, August 1972 and also Proc. of 17th SAMPE National Symposium, April 1972.
2. Serafini, T. T., Delvigs, P., and Alston, W. B.: PMR Polyimides - Review and Update, NASA TM 82821/AVRADCOM TR 82-C-3, May 1982 and also Proc. of 27th SAMPE National Symposium, May 1982.
3. Alston, W. B.: Characterization of PMR-15 Polyimide Resin Composition in Thermo-Oxidatively Exposed Graphite Fiber Composites, NASA TM 81565/AVRADCOM TR 80-C-10 Oct. 1980, and also Proc. of 12th SAMPE National Technical Conference, Oct. 1980.

4. Korshak, V. V.: Heat-Resistant Polymers, Israel Program for Scientific Translations, Ltd. Jerusalem, Israel, 1971, pp. 170-171.
5. Arnold, C., Jr.: Stability of High Temperature Polymers, J. Polymer Science, Macromolecular Reviews, Vol. 14, p. 289 (1979).
6. Gould, Edwin S.: Mechanism and Structure in Organic Chemistry, Holt, Rinehart and Winston, Inc., New York, NY, 1959, pp. 705-707.
7. Kray, W. D. and Rosser, R. W.: Synthesis of Multifunctional Triarylfluoroethanes. I. Condensation of Fluoro Ketones, J. Org. Chem., Vol. 42, No. 7, pp. 1186-1189, 1977.
8. Alston, W. B.: Resin/Fiber Thermo-Oxidative Interactions in PMR Polyimide/Graphite Composites, NASA TM 79093/AVRADCOM TR 79-6 and also Proc. of 24th SAMPE Symposium, May 1979.
9. Burns, E. A., Jones, R. J., Vaughan, R. W., and Kendrick, W. P.: Thermally Stable Laminating Resins, NASA CR-72633, pp. 29-31, January 1970.
10. Dine-Hart, R. A. and Wright, W. W.: Effect of Structural Variations on the Thermo-Oxidative Stability of Aromatic Polyimides, Die Makromolekulare Chemie, Vol. 153, 277 (1972).
11. Bell, V. L., Stump, B. L., and Gager, H.: Polyimide Structure-Property Relationships. II. Polymers from Isomeric Diamines, J. Polymer Science, Vol. 14, 2275 (1976).
12. Jewell, R. A. and Sykes, G. F.: Thermo-oxidation of Methylene Bridging Groups in Polyimides in, "Chemistry and Properties of Crosslinked Polymers", S. S. Labana, Editor, Academic Press, New York, p. 97 (1977).
13. Serafini, T. T., Vannucci, R. D., and Alston, W. B.: Second Generation PMR Polyimides, NASA TMX-71894, April 1976.
14. Young, P. R., Stein, B. A., and Chang, A. C.: Resin Characterization in Cured Graphite Fiber Reinforced Composites Using Diffuse Reflectance - FTIR, in "Materials and Processes - Continuing Innovations," Proc. of 28th National SAMPE Symposium and Exhibition, p. 284, April 1983.

TABLE I. - MONOMERS USED IN POLYIMIDE SYNTHESIS

STRUCTURE	NAME	ABBREVIATION
	Monomethyl Ester of Endo-5-Norbornene-2,3-Dicarboxylic Acid	NE
	Dimethyl Ester of 3,3',4,4'-Benzophenonetetracarboxylic Acid	BTDE
	4,4'-Methylenedianiline	MDA
	4,4'-Oxydianiline	ODA
	1,1-Bis(4-Aminophenyl)-1-Phenyl-2,2,2-Trifluoroethane	3FDA

TABLE II. - 3FDA MONOMER SYNTHESIS



TIME/TEMP hr/°C	MOLAR RATIO A:B:C	SCALE GRAMS OF A	D, AS SYNTHESIZED			D, AS PURIFIED			
			YIELD, %	MP, °C	COLOR	PROCEDURE	YIELD, %	MP, °C	COLOR
24/REFLUX	1:1.4:7.5	10	-	-	-	SILICA GEL CHROMATOGRAPHY WITH BENZENE, THEN BENZENE/HEPTANE RECRYSTALLIZATION	88*	201-204	ROSE
30/185	1:1.4:7.0	12.5	103.1	191-196	PURPLE		41.0	214-215	LAVENDER
16/185		12.5	103.3	180-190			32.6	213-214	LAVENDER
22/180		12.5	96.2	202-207			78.3	215.5- 216	WHITE
20/160		50	97.4	200-205			78.8	216.5- 217.5	
17/165	1:1:5.2	100	94.9	190-198			69.8	217- 217.5	

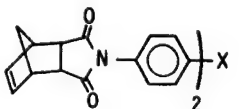
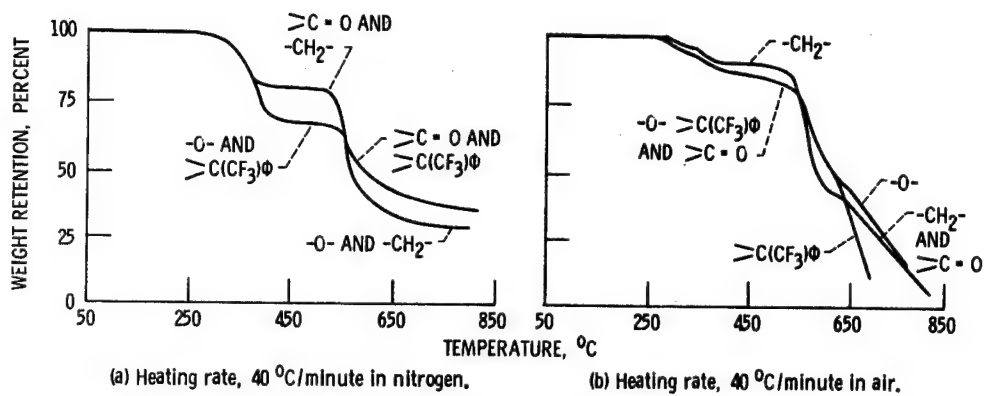
* J. ORG. CHEM., 42, 1186 (1977).

TABLE III. MONOMER STOICHIOMETRY FOR PMR SOLUTIONS

REACTANTS, Molar ratio N/N+1/2	ABBREVIATION	N	FORMULATED MOLECULAR WEIGHT ^a (FMW)	WEIGHT PERCENT ALICYCLIC ^b
BTDE/MDA/NE	PMR-15	2.083	1500	12.27
BTDE/ODA/NE	ODAPMR-15	2.083	1505	12.22
BTDE/3FDA/NE	3FDAPMR-15	1.377	1500	12.27
BTDE/3FDA/NE	3FDAPMR-19.5	2.083	1943	9.44
BTDE/3FDA/NE	3FDAPMR-24	2.808	2400	7.67

^aWhere FMW = N(m.w.BTDE)+(N+1)(m.w.Diamine)+2(m.w.NE)-2(N+1)
(m.w.H₂O+MeOH)

^bWhere percent alicyclic = 100 x 2(m.w.C₇H₈)/FMW



$X = -\text{CH}_2-$, $-\text{O}-$, $>\text{C}(\text{CF}_3)\Phi$ OR $>\text{C}=\text{O}$

ENDO, ENDO BISNADIMIDES

Figure 1. - Model compound thermogravimetric analysis.

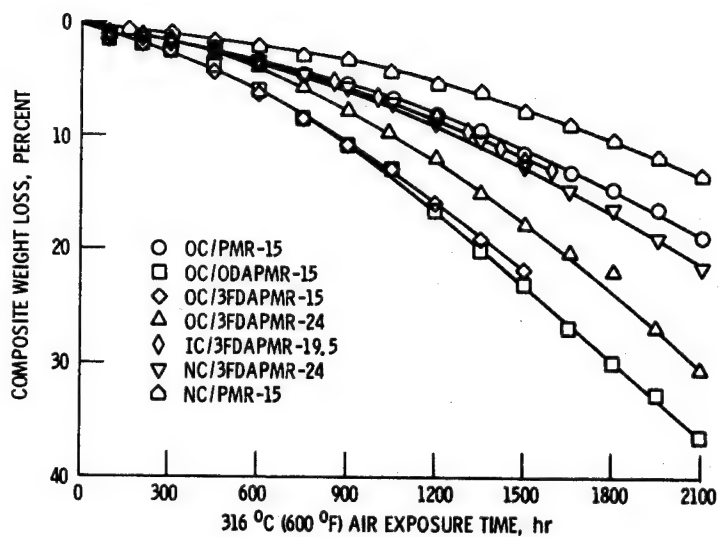
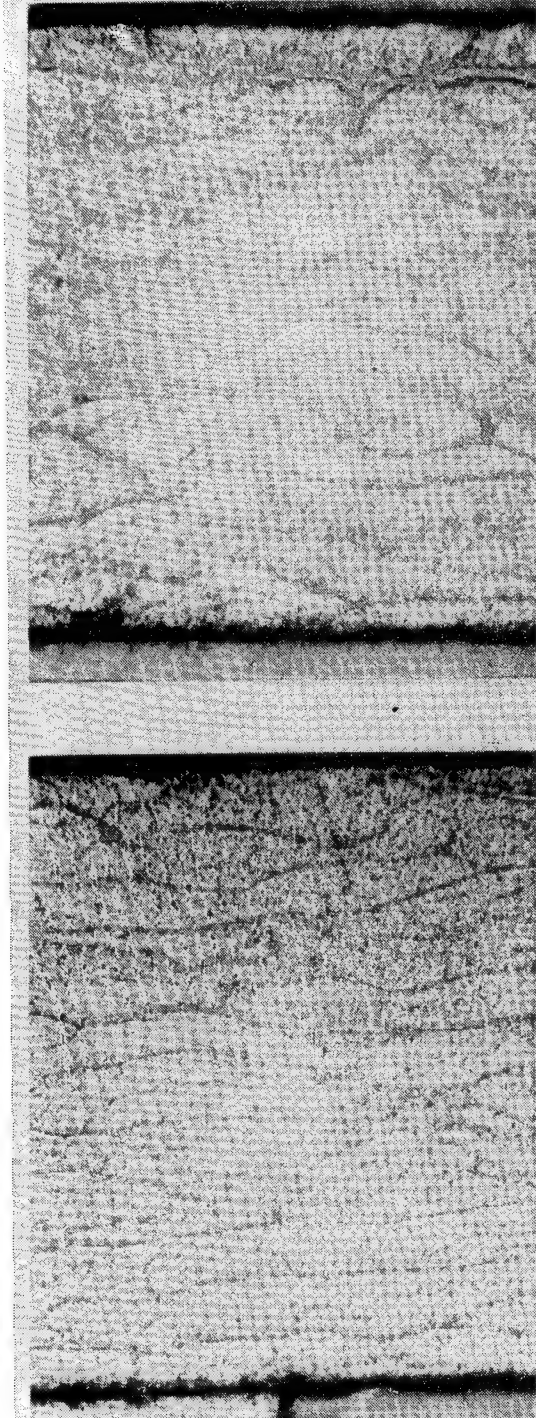


Figure 2. - Composite weight loss of Celion 6000/PMR polyimide composites as function of 316 °C (600 °F) air exposure time.



PMR-15

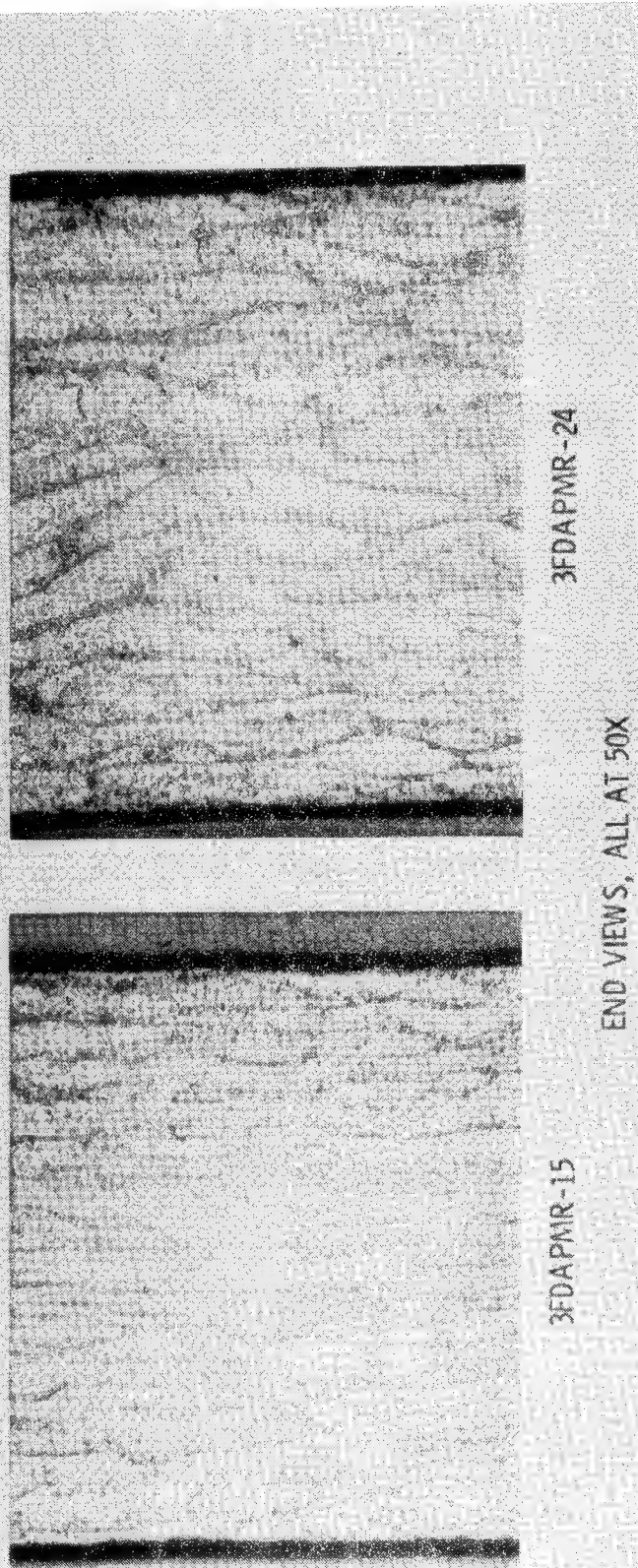


Figure 3. - Cross sections of original Celion (OC) 6000/PMR-polyimide composites.
END VIEWS, ALL AT 50X

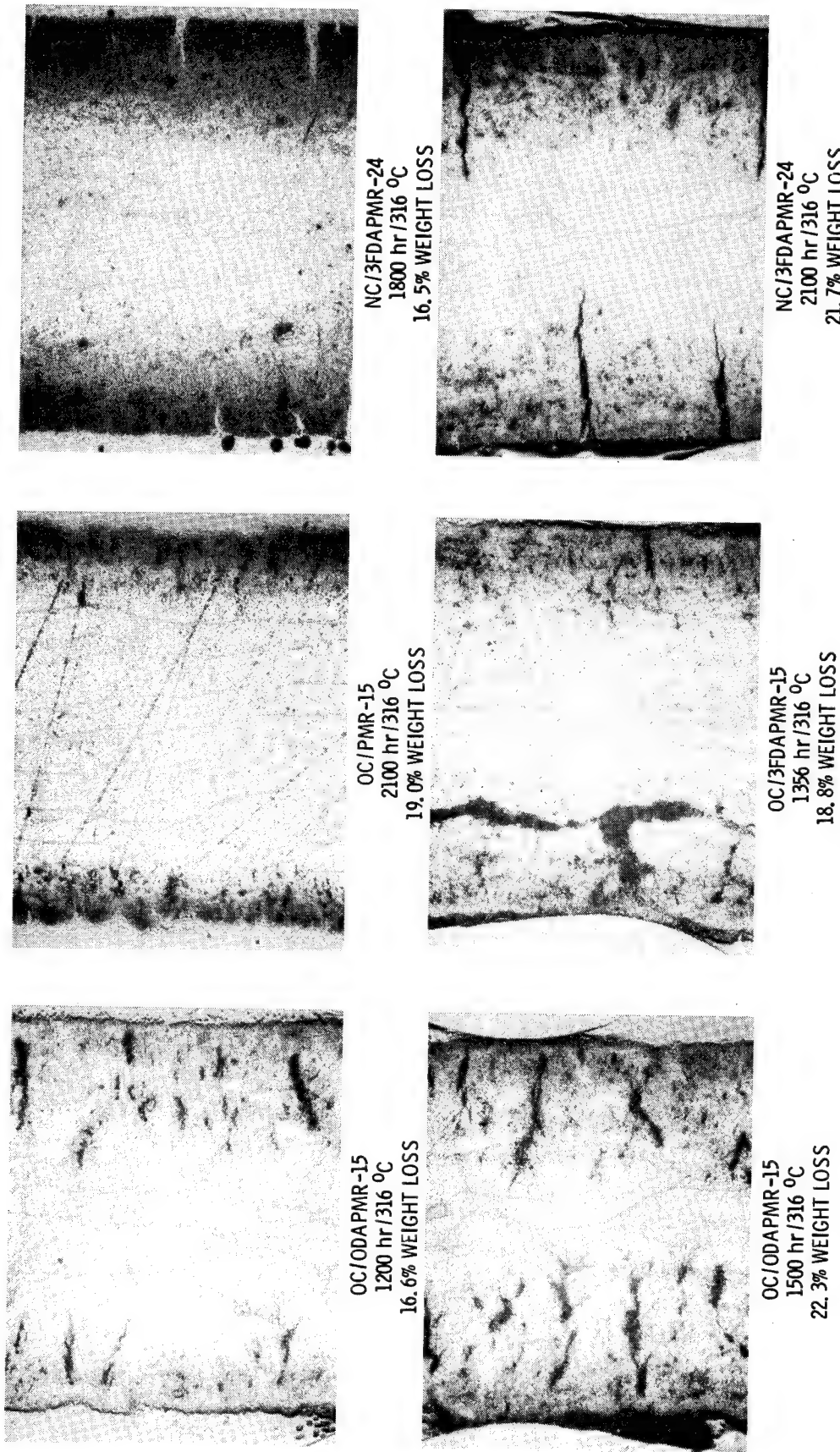


Figure 4. - Physical appearance of Celion 6000/PMR-polyimides at comparable composite weight loss.

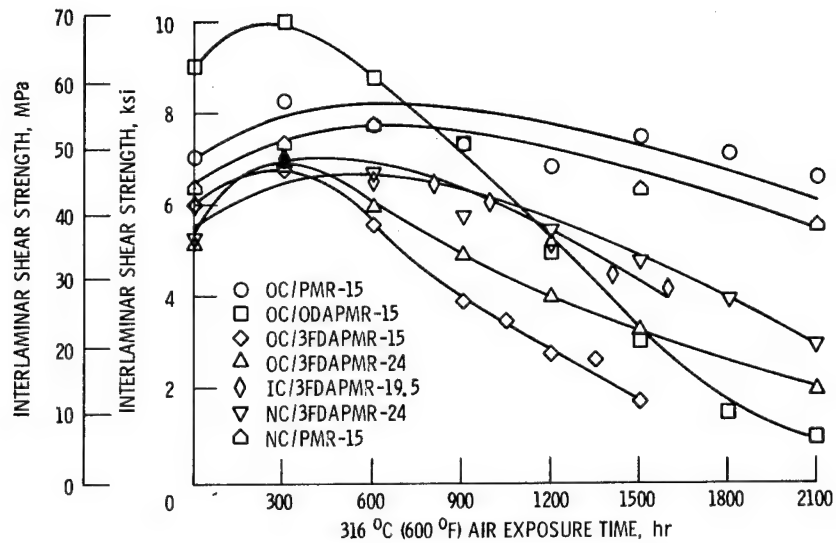


Figure 5. - 316 °C (600 °F) interlaminar shear strength of Celion 6000/PMR polyimide composites as function of 316 °C (600 °F) air exposure time.

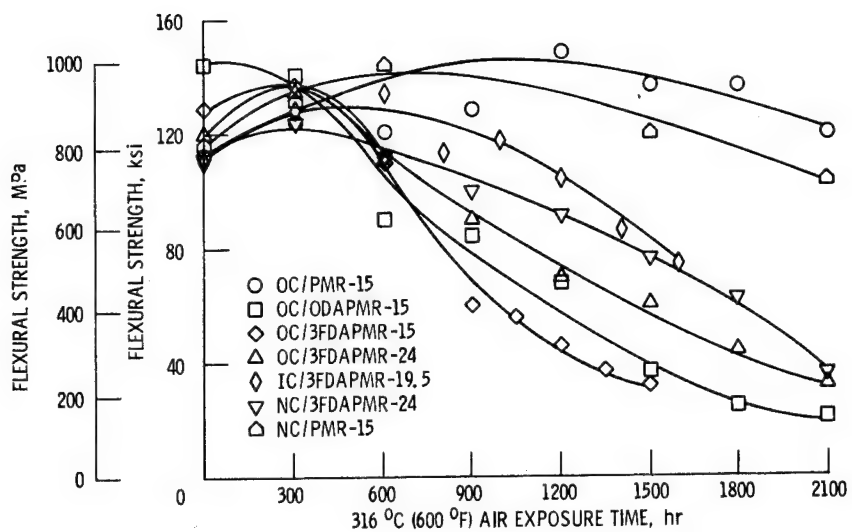


Figure 6. - 316 °C (600 °F) flexural strength of Celion 6000/PMR polyimide composites as function of 316 °C (600 °F) air exposure time.

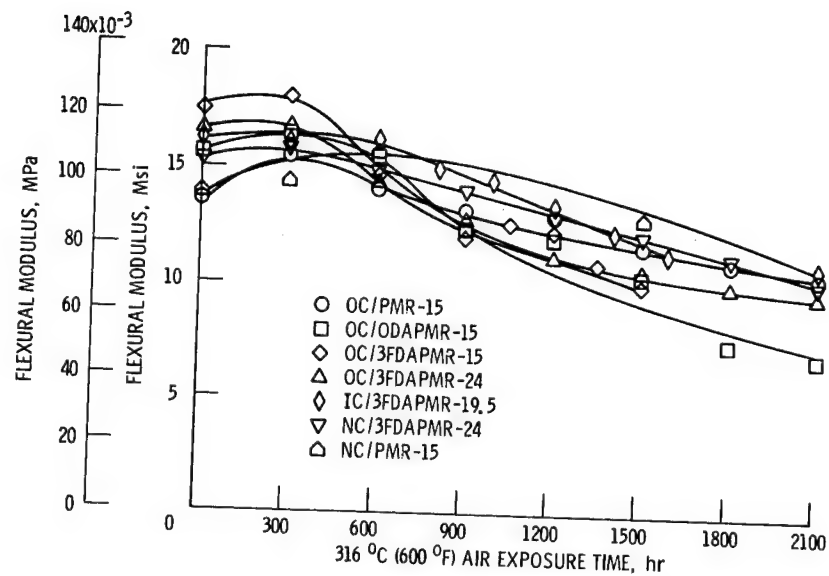


Figure 7. - 316 °C (600 °C) flexural modulus of Celion 6000/PMR polyimide composites as function of 316 °C (600 °F) air exposure time.

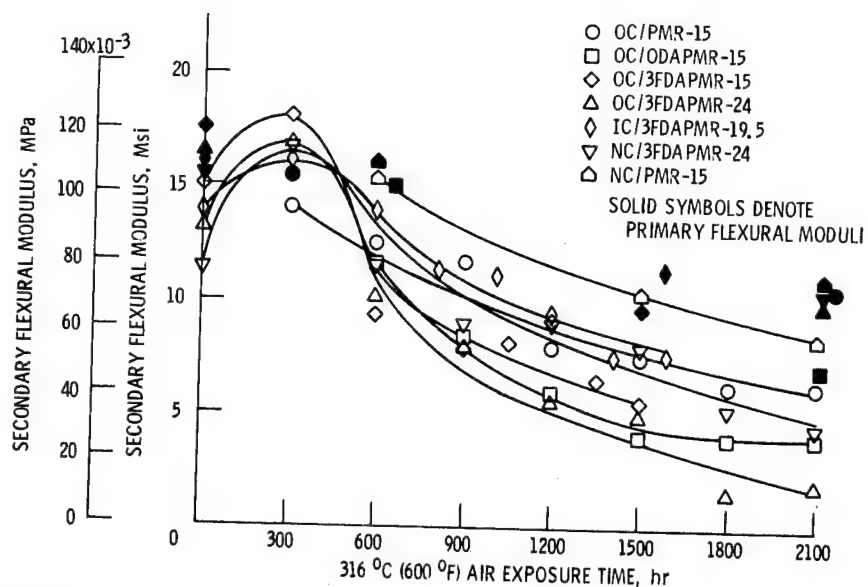


Figure 8. - 316 °C (600 °F) secondary flexural modulus of Celion 6000/PMR polyimide composites as function of 316 °C (600 °F) air exposure time.

PROPERTIES OF AUTOCLAVED Gr/PI COMPOSITES

MADE FROM IMPROVED TACK PMR-15 PREPREG

Raymond D. Vannucci
National Aeronautics and Space Administration
Lewis Research Center

Autoclave processing studies were conducted, using improved tack PMR-15 prepreg, to determine the effect of tack enhancing PMR resin modifications on composite processability and mechanical properties.

Improved tack graphite fiber reinforced PMR-15 prepgs were prepared and exposed to ambient conditions for various times and then autoclave molded into composites. Composite specimens were prepared and tested for flexural and interlaminar shear strengths at room temperature and 316 °C. The retention of flexural and interlaminar shear strength as a function of exposure in air at 316 °C was also determined.

The results show that the modified PMR resin solutions provide prepreg with improved tack and drape retention characteristics without adversely affecting processability or mechanical properties of autoclave-molded graphite fiber reinforced PMR-15 composites.

INTRODUCTION

Composites made with PMR-15 polyimide are now gaining acceptance as viable engineering materials for high-use-temperature applications. This acceptance is due to both the thermo-oxidative stability of PMR-15 and the ease with which PMR-15 prepreg materials can be processed into composite structures. An important factor contributing to the processability of PMR-15 materials is the volatility of the alcoholic solvents used in preparing prepregging solutions. These low-boiling-point solvents (methanol or ethanol) are easily removed during fabrication, making it possible to obtain void-free or low-void composites. However, the volatility of these solvents does limit the tack and drape retention of PMR-15 prepreg exposed to the ambient. Retention of these two important material handling properties is essential for consistent performance during layup of composite structures, particularly large composite structures which may require long layup times.

In the past, efforts to improve the tack and drape retention of PMR-15 prepreg materials involved the use of reactive diluents (ref. 1) or higher boiling point solvents (ref. 2). The use of reactive diluents provided only slight improvements in tack and drape retention. Higher boiling point solvents, while providing significantly improved tack and drape retention, are difficult to remove during processing and severely affect the processability of PMR-15 materials.

In a more recent study (ref. 3), PMR resin compositions were identified which offer potential for improving the tack and drape retention of PMR prepreg materials without affecting the processability or elevated temperature mechanical properties of compression-molded graphite fiber reinforced PMR-15 composites. This was accomplished by utilizing mixtures of low-boiling alcoholic solvents, which are easily

removed during processing, and modified monomer reactants which do not alter PMR resin cure chemistry.

The purpose of this investigation was to determine the effect of improved tack PMR-15 prepreg on the processability and mechanical properties of graphite fiber reinforced autoclave-molded PMR-15 composites.

EXPERIMENTAL PROCEDURE

Prepreg Fabrication and Testing

The monomer reactants used to prepare the resins used in this study are shown in table I. The monomer reactants and PMR-15 prepregging solutions were prepared as described in reference 3. Style 182 fabric woven from epoxy sized T-300 graphite fiber and unsized Celion 6000 unidirectional graphite fiber tows were used as reinforcing materials. Prepreg was prepared by brush application of the PMR solution onto flat 45.7 by 30.5 cm sections of fabric and onto drum wound (4.72 turns/cm) unidirectional tows to yield composites having 58 vol % fiber. Silicone coated paper was used as the peel ply for both prepreg materials.

Prepreg tack was determined on simple lap shear specimens having a length of 12.7 cm, a width of 2.54 cm, and an overlap of 2.54 cm. The test specimens were prepared from prepreg exposed for various times under ambient conditions by removing the peel ply and joining the unexposed side to the exposed side. The force to separate the prepreg was then measured at a loading rate of 12.7 cm/min. All tack values reported are averages of three or more tests. A qualitative assessment of prepreg drape, or deformability, was obtained by supporting a prepreg strip (30.5 by 2.54 cm) at its center and observing the deformation of the prepreg under its own weight.

Composite Fabrication and Testing

Composites were autoclave molded from both T-300 graphite fabric prepreg and from Celion 6000 graphite fiber tape prepreg. The schematic for vacuum bag layup of the unidirectional tape prepreg is shown in figure 1. The prepreg tapes were cut into 15.2 by 20.3 cm plies, fiber axis parallel to the long direction, and stacked unidirectionally to produce 12-ply composites. The fabric prepreg was cut into 15.2 by 15.2 cm plies and stacked 6 plies thick, with the warp aligned in the zero degree direction. The vacuum bag layup for fabric reinforced prepreg was identical to that shown in figure 1, except that no side containment or pressure plate was employed. The autoclave cure cycle used for fabricating composites from both tape and fabric prepreg materials is shown in figure 2. After curing, all composites were given a free-standing postcure in a forced-air oven by heating at 5 °C/min to 316 °C followed by a 24-hour hold at 316 °C.

Prior to test specimen preparation, all composites were inspected using the ultrasonic C-scan technique. Composite flexural strength tests were performed in accordance with ASTM D-790 at a fixed span of 5.08 cm. Specimen thicknesses ranged from 0.191 to 0.216 cm. The resultant span/depth ratios ranged from 27 to 23.5. Interlaminar shear strength tests were performed essentially in accordance with ASTM D-2344 at a constant span/depth of 5. Elevated temperature tests were conducted on specimens after isothermal exposure in air, for various times, at the

test temperature. Flexural and interlaminar shear strength values reported are averages of three or more tests.

RESULTS AND DISCUSSION

Resin Selection

The commercially available PMR polyimide, designated PMR-15, consists of a methanol solution of the monomethyl ester of 5-norbornene-2, 3-dicarboxylic acid (NE), the dimethyl ester of 3,3',4,4'-benzophenonetetracarboxylic acid (BTDE), and 4,4'-methylenedianiline (MDA). In a previous study (ref. 3), it was found that the substitution of higher alkyl ester monomers for methyl ester monomers in PMR-15 resins, as well as the use of a mixture of low-boiling-point alcoholic solvents, provided PMR-15 prepreg with improved tack and drape retention.

Table II lists the various modified PMR-15 resin systems investigated in the earlier study (ref. 3). The table lists the alkyl ester monomers and solvent used for each resin system and the designated abbreviation for each resin system.

Table III summarizes the results obtained in the earlier study from the tack and drape tests performed on graphite fiber prepreg made from each of the resin systems listed in table II. The results show that the substitution of a 3:1 methanol/1-propanol (M/P) solvent mixture for methanol in the resin system containing methyl esters (C_1) extended the prepreg tack retention from 2 to 3 days to 6 to 7 days for T-300 fabric prepreg and to 7 to 8 days for Celion 6000 reinforced tape prepreg. The results also show that the prepgs containing the higher alkyl esters in the mixed solvents exhibited more pronounced improvements in tack and drape retention than the methyl ester mixed solvent system. The best overall tack and drape retention was obtained from prepreg containing propyl ester (C_3) monomers, even in a solvent mixture of 9:1 M/P.

However, this system exhibited excessive resin flow during imidization. The 1-propanol produced as a by-product during imidization, together with 1-propanol present in the solvent mixture causes a significant reduction in the resin melt viscosity during the early stages of the imidization reaction and results in increased resin flow.

Based on the results from the earlier study (ref. 3), the PMR resin systems selected for study in this investigation included the systems containing C_1 and C_2 esters in solvent mixtures of 3:1 M/P, the control resin system C_1 -M, and two resin systems which were not previously studied, C_1 -4:1 M/P and C_2 -5:1 M/P. In the present study, it was found that these two resin systems, containing a reduced level of 1-propanol, provided prepgs with tack retention comparable to those made using a 3:1 M/P solvent mixture (5 to 6 days versus 6 to 7 days for C_1 -3:1 M/P and 10 days for C_2 -5:1 M/P versus 12 days for C_2 -3:1 M/P using T-300 reinforcement).

Composite Processing Studies

In the earlier study (ref. 3), it was found that the resin modifications employed to improve prepreg tack did not necessitate altering the parameters previously established for compression molding PMR-15 composites. In this investigation, studies were conducted to establish autoclave cure parameters for the

selected resin systems using T-300 fabric reinforced and unidirectionally reinforced Celion 6000 graphite fiber prepreg materials.

A commonly used autoclave cure cycle for state-of-the-art PMR-15 prepreg material is shown in figure 3. During this study, it was found that the improved tack prepreg exhibited excessive resin flow when using the cure cycle shown in figure 3. As discussed earlier, the 1-propanol added to the carrier solvent significantly reduced the melt viscosity of the resin during the early stages of the imidization reaction. Therefore, to minimize resin flow, initial imidization was conducted at a lower heating rate (0.6 °C/min) and a reduced vacuum level (5 cmHg). When a temperature of 137 °C was reached, sufficient resin advancement had occurred to permit the use of a faster heating rate and increased vacuum level (3 °C/min and 60 cmHg, respectively). The recommended cure cycle for autoclave curing improved tack graphite fiber reinforced PMR-15 prepreg is shown in figure 2. Low-void (1.3 vol %) composites were fabricated from each of the prepreg materials by employing this cure cycle.

Composite Properties

The mechanical properties of autoclave-molded PMR-15/Celion 6000 composites made from the control resin and the selected modified resin systems are shown in table IV. Also shown in the table are the prepreg storage conditions, prepreg volatile content, and the percent fiber volume for each composite. It can be seen that after 5 days exposure at ambient conditions, the C₂ prepreg containing a 3:1 M/P solvent exhibited a volatile content 1.2 percent higher than that of the C₂ prepreg prepared with a 5:1 M/P solvent. The 3 percent difference in fiber volume between the composites prepared by the C₂-3:1 M/P and C₂-5:1 M/P prepreg systems can be attributed to the higher concentration of 1-propanol present in the C₂-3:1 M/P system. Therefore, a 5:1 M/P solvent mixture is recommended for prepared improved tack prepreg with ethyl esters (C₂). Furthermore, comparison of the fiber content data shows that by employing the modified autoclave cure cycle shown in figure 3, it was possible to control the resin flow of improved tack prepreg having a volatile content of 12.4 percent or less to yield composites having a fiber volume of close to 63 percent. In order to achieve resin flow comparable to state-of-the-art PMR-15 prepreg material, it is recommended that the volatile of improved tack prepreg not exceed 12.4 percent prior to autoclave molding.

A comparison of the composite mechanical properties data of table IV shows that the room temperature and 316 °C flexural and interlaminar shear strengths of composites prepared from the improved tack prepreg, which had been exposed for 5 days, compare very favorably to the properties of the control composite prepared from freshly made prepreg.

Figures 4 and 5 show the retention of 316 °C composite flexural and interlaminar shear strengths, respectively, as a function of isothermal exposure in air at 316 °C for the autoclave-molded Celion 6000 graphite fiber composites.

Figure 4 shows that the 316 °C flexural strength retention of the composites prepared from the improved tack prepgs is equivalent to the flexural strength retention of the composite prepared from the control prepreg. In figure 5 it can be seen that the 316 °C interlaminar shear strength retention of the composites made from the improved tack prepgs is nearly identical to that exhibited by the composite made from the control prepreg.

The mechanical properties of autoclave-molded PMR-15/T-300 graphite fabric reinforced composites are shown in table V. Data are shown for composites prepared from the control resin and the modified resin systems (C_1 -3:1 M/P, C_1 -4:1 M/P, and C_2 -5:1 M/P) which exhibit resin flow comparable to that of the control resin system during autoclave molding. The data show that the room-temperature and short-term 316 °C flexural and interlaminar shear strengths of the composites prepared from the improved tack prepreg are in close agreement with the flexural and interlaminar shear strengths of the composites made from the control system.

CONCLUSIONS

Based on the results of this investigation, the following conclusions may be drawn:

1. By employing a modified autoclave cure cycle, it is possible to fabricate high-quality, low-void composites from improved tack graphite fiber reinforced PMR-15 prepreg materials.
2. Autoclave-molded composites fabricated from improved tack graphite fiber reinforced PMR-15 prepreg exhibit mechanical properties which are essentially equivalent to the mechanical properties of composites autoclave molded from state-of-the-art graphite fiber reinforced PMR-15 prepreg.

REFERENCES

1. T. T. Serafini and P. Delvigs, ICCM/2, Proc. of 1978 Conf. on Composite Materials, B. Norton, ed., AIME, New York, 1978, pp. 1320-1329.
2. R. A. Buyny, NASA CR-165432, Oct. 1981.
3. R. D. Vannucci, Proc. of 1982 Nat. Tech. Conf. of Society of Plastics Engineers, Bal Harbour, FL., pp. 131-133.

Table I.-MONOMERS USED FOR PMR-15 POLYIMIDE SYNTHESIS

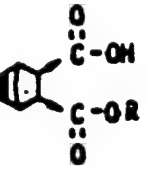
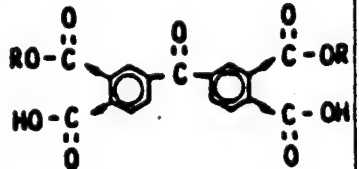
Structure	Name	Abbreviation
	Monoalkyl ester of 5-norbornene-2,3-dicarboxylic acid	NE
	4,4'-Methylenedianiline	MDA
	Dialkyl ester of 3,3',4,4'-benzophenonetetracarboxylic acid	BTDE
$R = \text{CH}_3, \text{C}_2\text{H}_5, \text{C}_3\text{H}_7$		

TABLE II. - ESTER AND SOLVENT
MODIFIED PMR-15 RESIN SYSTEMS^a

Ester ^b	Solvent ^c	System abbreviation
C ₁ (Control)	M	C ₁ -M
C ₁	3:1 M/P	C ₁ -3:1 M/P
C ₂	E	C ₂ -E
C ₂	3:1 M/P	C ₂ -3:1 M/P
C ₃	9:1 M/P	C ₃ -9:1 M/P
C ₃	3:1 M/P	C ₃ -3:1 M/P

^aReference 3.

^bC₁ = methyl, C₂ = ethyl,
C₃ = propyl.

^cM = methanol, E = ethanol,
P = 1-propanol.

TABLE III. - TACK AND DRAPE
RETENTION OF MODIFIED
PMR-15 PREPREG^a

Prepreg system	Tack limit ^b fabric/tape	Drape limit ^b fabric/tape
C ₁ -M	2-3/2-3	2/2
C ₁ -3:1 M/P	6-7/7-8	5/6
C ₂ -E	3-4/-	2/-
C ₂ -3:1 M/P	12/15	7/8
C ₃ -9:1 M/P	12/15	12/15
C ₃ -3:1 M/P	12/21	12/21

^aPMR-15/T-300 graphite fabric and
PMR-15/Celion 6000 graphite fiber tape,
reference 3.

^bDays at ambient conditions.

TABLE IV. - MECHANICAL PROPERTIES OF AUTOCLAVE-CURED MODIFIED PMR-15/CELION
6000 GRAPHITE FIBER COMPOSITES

Prepreg system	Prepreg exposure, days ^a	Prepreg percent volatile content	Composite fiber, vol %	Interlaminar shear strength, MPa		Flexural strength, MPa	
				R.T.	316 °C	R.T.	316 °C
C ₁ -M (Control)	1	11.7	62.7	103	44.8	1532	834
C ₁ -3:1 M/P	1	13.5	65.0	90	42.7	1632	861
C ₁ -3:1 M/P	5	12.4	63.0	100	46.2	1639	841
C ₁ -4:1 M/P	5	12.0	63.0	107	41.3	1570	896
C ₂ -3:1 M/P	5	13.2	66.0	96	46.1	1612	875
C ₂ -5:1 M/P	5	12.0	63.0	106	42.0	1557	875

^aDays exposed to ambient conditions.

TABLE V. - MECHANICAL PROPERTIES OF AUTOCLAVE-CURED MODIFIED
PMR-15/T-300 GRAPHITE FABRIC COMPOSITES

Prepreg system	Prepreg exposure, days ^a	Prepreg fiber, vol %	Interlaminar shear strength, MPa		Flexural strength, MPa	
			R.T.	316 °C	R.T.	316 °C
C ₁ -M (Control)	3	64.0	50.3	36.5	1337	682
C ₁ -3:1 M/P	3	65.5	49.6	35.8	1268	689
C ₁ -4:1 M/P	3	64.0	54.1	36.5	1337	709
C ₂ -5:1 M/P	3	65.0	54.4	35.8	1280	662

^aDays at ambient conditions.

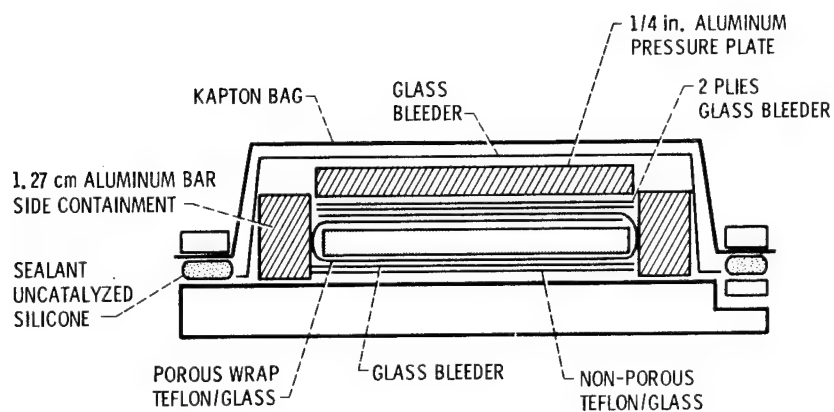


Figure 1. - Vacuum bag layup for unidirectional reinforced PMR-15/Celion 6000.

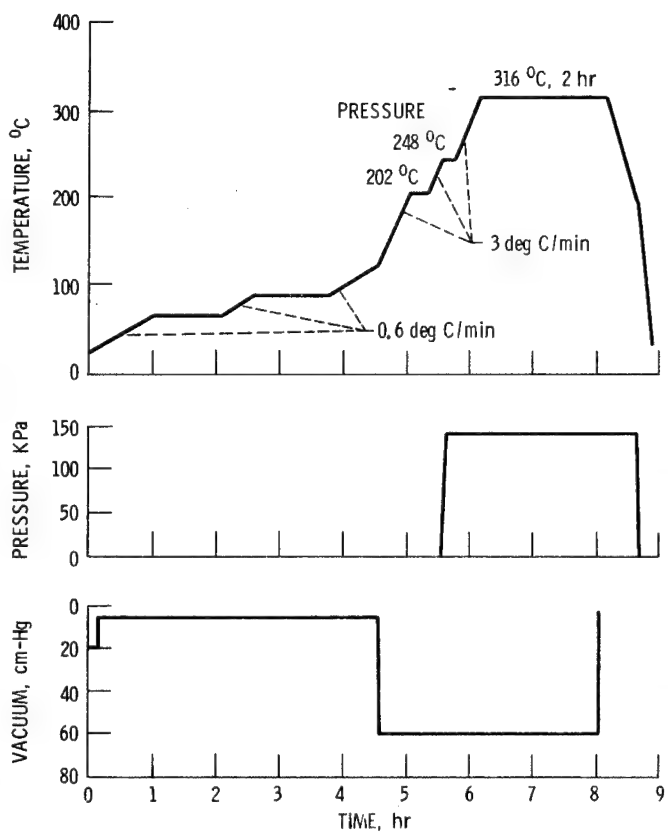


Figure 2. - Autoclave cure cycle for improved tack PMR-15/graphite fiber prepeg.

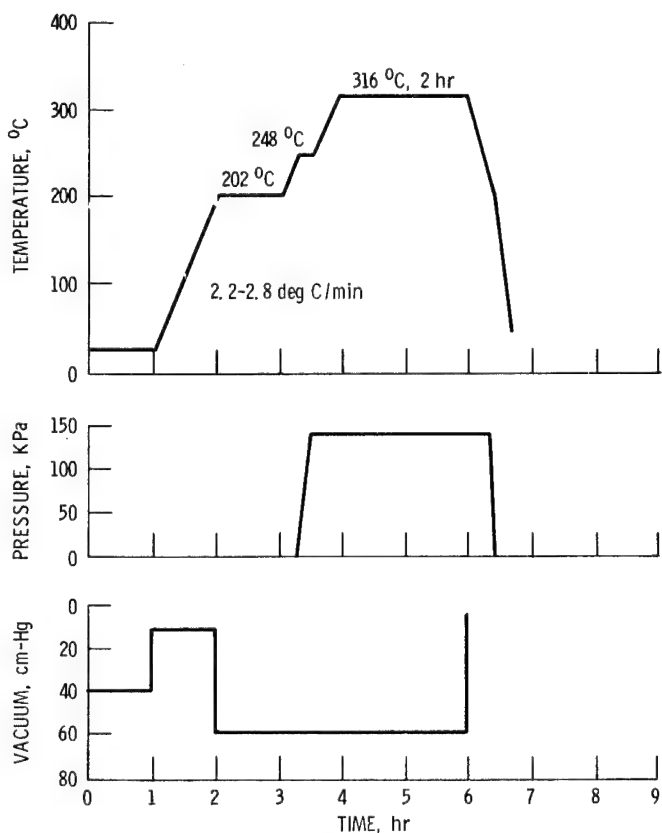


Figure 3. - Typical autoclave cure cycle for PMR-15 materials.

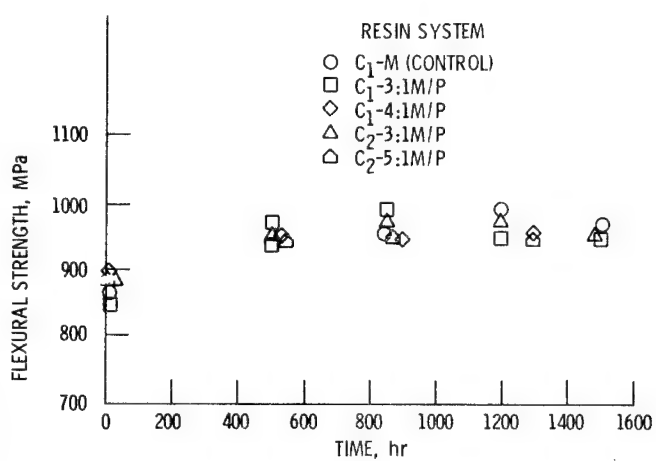


Figure 4. - Flexural strength of autoclave molded modified PMR-15/Celion 6000 graphite fiber composites exposed and tested at 316 °C.

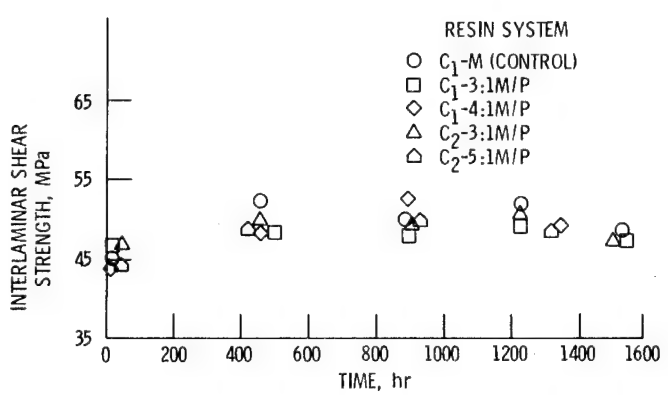


Figure 5. - Interlaminar shear strength of autoclave molded PMR-15/Celion 6000 graphite fiber composites exposed and tested in air at 600 °C.

THERMO-OXIDATIVE STABILITY OF GRAPHITE FIBER/PMR-15

POLYIMIDE COMPOSITES AT 350°C

Daniel A. Scola
United Technologies Research Center

A series of graphite fiber/PMR-15 polyimide composites were subjected to isothermal aging at 350°C in flowing air (100 cc/min and 1000 cc/min) over a 520 hr time period. The graphite fibers were analyzed by ISS/SIMS techniques before composite fabrication. Fibers exposed at the surface of the composite due to the isothermal aging process were also analyzed by the ISS/SIMS method. Component and composite weight loss studies were also conducted for similarly exposed materials. Optical micrograph investigations of composites to follow the progress of the thermo-oxidative process were also conducted. Flexural and interlaminar shear strengths of the unaged and aged composites were measured. The relationship of component and composite properties as they relate to the thermo-oxidative behavior of the materials was discussed.

INTRODUCTION

The long term durability of graphite fiber reinforced PMR-15 polyimide composites at 316°C and above, is dependent on the two major aspects of these composite systems. These are (1) the thermal and thermo-oxidative stability of the individual components and (2) the influence of the interface region between fibers and matrix on matrix stability. In studies carried out at 316°C (600°F) on several fiber/PMR-11 and PMR-15 polyimide systems, in flowing air, it has been demonstrated that the thermo-oxidative stability of these systems is effected by fiber surface impurities, such as the alkali metal ions, sodium and potassium (ref. 1). Gibbs et al. (ref. 2) have shown that HTS graphite fibers contain a large concentration of sodium ions on the surface, while Dryzal and Hammer (ref. 3) have demonstrated that AS graphite fibers also contain large concentrations of sodium ions relative to other graphite fibers. The overall objectives of this investigation are (1) to determine the mechanism of the thermo-oxidative process in flowing air of several composite systems consisting of the addition polyimide PMR-15 in combination with the graphite fiber reinforcements, and (2) to determine the upper temperature limit of these composite systems.

In the present paper the surface composition of several graphite fibers as determined by ISS/SIMS analysis and the relationship of the surface composition to component properties and composite thermo-oxidative stability will be discussed. Thus, the surfaces of the neat fibers and fibers from composites exposed as a result of the thermo-oxidative process were analyzed. Weight loss studies of the component materials and each graphite/PMR-15 composite system were conducted. Optical microscopy and mechanical property measurements of the "as fabricated" and isothermally exposed composites were also carried out.

EXPERIMENTAL

Fiber Materials

Fiber materials were obtained commercially; AS from Hercules Inc., Thorne 300 from Union Carbide Corp., Celion 6000 from Celanese Corp., Fortafil 5 from Great Lakes Carbon Corp., and Panex 30 from Stackpole Carbon Corp. The following fibers were investigated: Panex 30 (unsized) (Roll #18-00506), Fortafil 5 (unsized) (Lot #SeRS-1528-B), Fortafil 5 (P.I. compatible size, not PI) (Lot #2237-29-15), Celanese 6000 (unsized) (Lot #HTA-7-8422), Celanese 6000 (NR150B2 size) (Lot #HTA-7-9821), Thorne 300 (water sized) WYP 30 1/0, AS4W6 (water size) (Lot #205-1), and Celion 6000 (Celanese PI size) (Lot #HTA-7-2832).

PMR-15 Polyimide Resin

The polyimide resin system used in this study was prepared and processed from a methanol solution of monomers as described previously (refs. 4,5).

ISS/SIMS Analysis of Fiber Surfaces

The equipment and procedures used in the surface analysis by Ion Scattering Spectroscopy (ISS) and Secondary Ion Mass Spectroscopy (SIMS) have been described previously (ref. 6). Table 1 lists the conditions for the analysis. For the ISS analysis, samples were bombarded by a primary ion beam of $^3\text{He}^+$ at an energy of 2.5 keV and a beam current density of $1.3\mu\text{amps}/\text{cm}^2$. For the SIMS analysis, samples were bombarded by a primary ion beam of $^{20}\text{Ne}^+$ for a near surface analysis (5-10 \AA) and again at the approximate sputtered depth of 100 \AA , at a beam energy of 2.5 keV and a beam current density of $1.3\mu\text{amps}/\text{cm}^2$. Surfaces were sputtered using a Perkin Elmer PHI sputter ion gun at a beam energy of 5 keV and a current density of $14.3\mu\text{amps}/\text{cm}^2$. The sputter rate was approximately 5 $\text{\AA}/\text{min}$. The SIMS data for each fiber are reported in relative atomic ratios. These were calculated as follows: the values of counts per second (c/s) of each element on the fiber surface were adjusted to relative atomic values by dividing each c/s value by the sensitivity factor for that element. These relative atomic values were then normalized by dividing the relative atomic value of each element on a given fiber surface by the relative atomic value of

each element on a given fiber surface by the relative atomic value of the element present in the smallest amount. For the data at the 5-10 \AA level, hydrogen atomic ratios were calculated but not reported since the hydrogen ratios are high for all fibers, as expected. In addition, since high levels of C^+ , CH^+ , CH_2^+ , CH_3^+ and C_2H^+ species were observed in most fibers, these were not considered in the atomic ratio calculation. Moreover for species other than ^{12}C , correction factors do not exist. The data can be considered as relative atomic ratios of elements on a carbonaceous substrate.

To compare the elemental surface compositions between fibers, the relative atomic values for each element determined as described above were divided by the smallest relative atomic value observed for that element in the series of fibers analyzed. Such comparisons assume that substrate effects on the sputtering of easily ionized elements are negligible.

PMR-15 composites of each fiber were fabricated and subjected to isothermal aging at 350°C in flowing air, 100 cc/min or 1000 cc/min for time periods up to 700 hrs. The surfaces of the fibers, exposed as a result of this thermo-oxidative process, were also examined by the ISS/SIMS technique.

Isothermal Weight Loss Measurements

Fibers, neat PMR-15 resin and composites were weighed at various time periods to determine weight changes due to the 350°C, air flow (100 cc/min or 1000 cc/min) exposure.

Isothermal Aging Procedure

Component materials and precut flexural and interlaminar shear composite specimens were placed in the center 20 cm portion of a ceramic tube 5.0 cm diameter x 61 cm in length. A constant temperature of 350°C was maintained in the 20 cm zone area where the specimens were being aged. Air was passed into the tube at a rate of 100 cc/min or 1000 cc/min depending on the study.

Composite Fabrication

Graphite fiber/PMR-15 composites were fabricated from PMR-15 impregnated fiber tape. The tape was prepared by brush coating a 50 wt% of PMR-15 resin components in methanol onto a dry wound tape 11.3 cm (4.5") wide x 43.2 cm (17") in diameter. The impregnated tape was cut into the appropriate lengths, 25.4 cm (~10"), then 19 layers were stacked one over the other in a mold. The mold was subjected to a heat treatment at 200°C for 1 hour to form an imide prepolymer. The female portion was positioned into the mold and the assembly was placed in a preheated press (232°C). Pressure (6.9 MPa, 1000 psi) was applied immediately to consolidate the layers, released at 232°C, then reapplied. The temperature was raised to 316°C, and the system

was maintained at these conditions (316°C, 6.9 MPa, 1000 psi) for 1 hour. The composite was cooled to RT under pressure and postcured in air in the free state by a graduated increase in temperature to 316°C over an 8 hour period, followed by a hold at this temperature for 12 hours.

The nominal dimensions of each composite were 11.4 cm x 25.4 cm x 0.254 cm (4.5" x 10" x 0.10"). Interlaminar shear specimens 0.64 cm wide x (4 x thickness + 0.25 cm) and flexure specimens (0.64 cm wide x (20 x thickness + 0.25 cm)) were cut from each composite for mechanical tests and isothermal aging studies.

Mechanical Property Measurements

Flexural strength measurements were made by the 3 point bend method at a span-to-depth ratio of 20/1 (ASTM-D-790) and crosshead speed of 0.127 cm/min (0.05 in/min). The interlaminar shear strength measurements were made by the 3 point bend method at a span-to-depth ratio of 4/1 and crosshead speed of 0.127 cm/min (0.05 in/min) (ASTM D-2344).

RESULTS AND DISCUSSION

ISS/SIMS Analysis of Fibers

Typical ISS spectra are shown in Figs. 1b, 2b and 3b. ISS spectra for the other samples are not shown. All samples reveal the presence of carbon, oxygen, sodium, and potassium within 5-10Å of the surface. In addition to these elements, unsized Fortafil 5 shows a high concentration of chromium (Fig. 1b) whereas the sized Fortafil 5 fiber shows the complete absence of the chromium ion (Fig. 2b). Celion 6000 NR-150B2 sized shows a high concentration of fluorine (Fig. 3b) as expected since the NR-150B size is a fluorinated material. The high chromium and fluorine levels for these fibers are also revealed in the SIMS spectra (Figs. 1a and 2a). Data from the ISS analysis were not used semi-quantitatively in this study, but were used to corroborate the SIMS results.

The relative atomic ratios of the elements present on the fiber surfaces at near surface (5-10Å) and after sputtering to a depth of ~100Å are listed in Tables 2 and 3. Typical SIMS spectra are shown in Figs. 1a, 2a and 3a. It should be mentioned that all fiber surfaces at 5-10Å show the presence of organic species, based on masses corresponding to C⁺, CH⁺, CH₂⁺, CH₃⁺, C₂⁺ and C₂H⁺ which sputtered from the surface. In addition, all show a high concentration of hydrogen which is a reflection of the presence of hydrocarbons, water, and hydrogen-containing graphite fibers. The carbon and hydrogen concentrations were not considered in the calculation of atomic ratios for the 5-10 and ~100Å levels. The ions of special interest at both the 5-10Å and 100Å levels are sodium, potassium, calcium, chromium and iron. At the 5-10Å level (Table 2), sodium is present at a very high concentration on the Panex 30 (unsized) fibers, (relative atomic ratio 110), and on the unsized Celion 6000,

Thornel 300, and AS graphite fibers at relative atomic ratios of 8.4, 3.1 and 2.8 respectively. The potassium concentrations on all fibers are lower than the sodium concentrations and much lower than the iron concentrations, except for AS fibers, which do not contain iron. A high chromium concentration is noted for unsized Fortafil 5, Panex 30 (unsized) and Celion 6000 unsized and PI sized. The ISS spectrum (Fig. 1b) for Fortafil (unsized) also shows the presence of chromium. Except for Magnamite AS4(u) fibers, all fibers contained considerable quantities of iron. The presence of fluorine on AS4(u) is noted. This element is also present at the 100 \AA level. The high concentration of calcium on unsized and PI sized Celion 6000 is also noted. This element persists at the ~100 \AA level, but at much lower concentrations.

At the ~100 \AA level (Table 3), all but Panex 30(u) and Fortafil 5(u) contain calcium. AS4(u) is the only fiber which shows the presence of fluorine. It should be noted that there is a significant reduction of the sodium content at the ~100 \AA level (Table 3) on all fiber surfaces, except for AS4(u) where an approximate two-fold increase is found. Iron persists in all fibers at approximately one-third to one-quarter the levels exhibited at the ~10 \AA level. Chromium is now detected on Thornel 300(u), AS4(u) and Celion 6000 PI size, whereas this element was not detected at the 10 \AA level in these fibers.

In comparing elements present on each fiber surface from fiber to fiber, the relative atomic ratios based on counts/sec of a given element were calculated as described in the experimental section. The results are listed in Tables 4 and 5 for near surface ~10 \AA and ~100 \AA depths respectively. At the ~10 \AA level, a high relative atomic ratio of sodium is noted on Panex 30(u) and Celion 6000(u); a high atomic ratio of calcium is also noted for Celion 6000(u). The potassium atomic ratio for Celion 6000 PI size is high relative to the other fibers. The high atomic ratio of chromium on Fortafil 5(u) and Panex 30(u) should be recognized. With these exceptions, the relative atomic ratio of elements listed are essentially equivalent. At the 100 \AA depth (Table 5), two fibers, Panex 30(u) and AS4(u), show very high relative atomic ratios of sodium compared to the other fibers. Moreover, AS4 fiber also contains a very high level of potassium, calcium, chromium and iron relative to the other fibers. The high relative atomic ratio of calcium on Celion 6000 unsized and sized is also apparent. With these exceptions the levels of elements present on the surface in comparing fiber to fiber are essentially equivalent.

ISS/SIMS Analysis of Fibers from Isothermally Aged Graphite Fiber/PMR-15 Composites

Exposure of the graphite fiber/PMR-15 polyimide composite to flowing air (100 cc/min) or (1000 cc/min) at 350°C for time periods of 250 hrs or longer caused surface oxidation of the polyimide resin, thereby exposing graphite fibers on the periphery of the composite in the process. The exposed fibers were then analyzed by the ISS/SIMS technique in the same manner as described for the neat fibers. Composite samples from each series were handled with care in order to prevent contamination of the fiber on the top surface of each sample.

Examples of ISS spectra of fibers from two isothermally aged composites, Celion 6000(u)/PMR-15 and Panex 30(u)/PMR-15 are shown in Fig. 4. Of significance in these spectra is the large peak (counts/sec) due to sodium on the Panex 30(u) fiber relative to the Celion 6000(u) fiber. A high concentration of sodium was also found in Panex 30 fibers before composite fabrication. Examples of SIMS spectra of fibers from Celion 6000(u)/T300(u)/AS4(u) composites at the 10 \AA level are shown in Fig. 5. The high counts/sec of sodium on T300(u) and AS4(u) relative to Celion 6000(u) and Fortafil 5(u) should be noted. The ISS/SIMS analyses were conducted after 250 hrs at 350°C in an air flow of 1000 cc/min. The relative atomic ratios of elements present on each fiber surface are compared at two depths of penetration, near surface ~10 \AA and at ~100 \AA and are listed in Tables 6 and 7 respectively. For an appreciation of the actual atomic counts/sec which these numbers represent, the actual counts/sec for each specific element, for example sodium, present in the lowest atomic count/sec from fiber-to-fiber is given as a footnote to the tables. Therefore, it can be seen that a high value for a relative atomic ratio for a specific element does not necessarily mean that the fiber or composite contains a high concentration of that element on the surface. However, it is clear that at near surface ~10 \AA and at ~100 \AA , sodium is by far the element present in the greatest concentration; approximately 5 times potassium, 30-60 times calcium, 200-800 times chromium, 200-400 times iron. Fluorine was found to be present in only AS4(u) fiber.

The relative atomic ratios of sodium for each fiber and composite material are compared in Table 8. Of particular interest is the significant change in sodium concentration from the near surface ~10 \AA , to the 100 \AA level in the AS4(u) neat fiber and in the Panex 30(u) fiber from the composite. Also, the higher concentration of sodium is noted on the T300(u), and Fortafil 5(u) fibers from the composite than was observed on the neat fiber at the 10 \AA and 100 \AA levels.

Optical Micrographs of Unaged and Isothermally Aged Composites

Optical micrographs of cross sections, transverse to the fiber direction, of the "as fabricated" isothermally aged composites after 250 and 520 hrs at 350°C in flowing air (1000 cc/min) are shown in Figs. 6 through 11. With the exception of the Fortafil 5(u)/PMR-15 composite, each composite after 250 hrs exposure developed surface cracks on the ends of the composite. Furthermore, oxidation of the surface resin on the periphery of each composite generates a covering of loose fibers. The cracks are not apparent after the 520 hr exposure, but considerably more surface fibers appear. This is true for all composites, with the extent of the cracking and quantity of surface fibers dependent on the graphite fiber/PMR-15 composite system.

Component and Composite Weight Loss

The fiber, resin and composite weight losses after exposure at 350°C in an air flow (1000 cc/min) for several hours are listed in Table 9. Composite weight losses

at 350°C in an air flow of 100 cc/min were almost identical to the 1000 cc/min air flow weight losses. The component and composite weight losses over approximately 700 hrs are shown graphically in Figs. 12 and 13. The high weight loss (78%) of the PMR-15 neat resin after 385 hrs is particularly revealing since several of the composites show very low weight loss after 520 hrs. This suggests that after the surface polyimide resin is oxidized, the fiber forms a protective blanket over the composite, acting as a scavenger for the oxygen present. The formation of a passive layer on the resin from components of the fiber thereby inhibiting oxidation of the matrix is also a possibility. The poor thermo-oxidative stability of the Thorne 300(u) and Panex 30(u) relative to the other fiber is also noted. Moreover, the poor thermo-oxidative stability of the Fortafil 5/PMR-15 composite relative to the excellent thermo-oxidative stability of the Fortafil 5(u) fiber itself suggests that the interface region in this system is the weak link and the point at which the composite system is thermo-oxidatively degraded. The higher weight loss of the AS4(u)/PMR-15 composite system relative to the neat AS4(u) fiber itself also suggests that interaction effects in the interface region of the composite may be responsible for this behavior. The relatively good agreement in weight losses of the Celion 6000 unsized and PI sized composites with weight losses of the neat fibers indicates that this interface region is not being degraded and, as mentioned above, that the exposed fiber is protecting the underlying composite system.

Optical Micrographs of Polished Cross Sections of Isothermally Aged Composites

In order to determine the extent of cracking in the composite due to isothermal aging, a shear specimen from each series was ground and polished. The total grinding and polishing depth required before any evidence of cracking was eliminated from each composite was determined.

Optical micrographs of the polished cross sections (Figs. 14-18) reveal that after grinding and polishing to a depth of 0.19 cm (0.075 in.), into the Celion 6000(u)/PMR-15 composite, a crack and void-free composite was found. Surface cracks which develop at the ends of the Celion 6000(u)/PMR-15 composite during aging do not penetrate the composite. In the other composites, after grinding to a depth of 1.1 cm (0.45 in.), each still showed the presence of at least one major flaw or crack and the presence of voids in the interface region of the composite. It should be noted that even though most of the composites contained one large flaw or crack area, the remainder of the composite was essentially free of voids and cracks. This is strong evidence that the PMR-15 polyimide resin matrix does not undergo thermo-oxidative or pyrolytic degradation in the internal regions of the composite. The major thermo-oxidative degradation process occurs on the external surface. The evidence for this is (1) the weight losses, (2) size reduction of cross sections (Figs. 14-18) of each composite, and (3) void-free regions in the matrix of the aged composites.

Mechanical Properties of Isothermally Exposed Composites

Elevated temperature flexural and shear strengths of these composite systems after aging at 350°C for several hours in flowing air are listed in Tables 10 and 11 respectively. The "as fabricated" properties are listed for comparison.

The higher flexural properties after aging at 350°C for 250 hrs is due to a postcure effect (ref. 7), which causes an improvement in the properties over the initial unaged composite. Inspection of Table 10 shows that only two composites retain a reasonable fraction of the unaged or 250 hr aged properties. These are the Celion 6000 unsized and PI sized fiber/composite systems. The behavior of these composites in shear (Table 11) is similar to that observed with the flexural properties. There is an improvement in the shear strength for most composite systems after 250 hrs exposure at 350°C, due to the postcure effect. However, only two composite systems retain a reasonable fraction of the unaged and 250 hr aged properties. These are the Celion 6000 unsized and PI sized composites, with the unsized fiber system displaying superior thermo-oxidative resistance relative to the PI sized Celion 6000 composite, and vastly superior oxidation resistance to the Thornel 300(u), AS4(u), Fortafil 5(u) and Panex 30(u) composite systems. A comparison of the component and composite weight loss rates, the sodium content on fiber/composite systems and 350°C flexural strength after 520 hrs is listed in Table 12. The stability of the Celion 6000(u)/PMR-15 composite, and by inference, the apparent stability of the fiber-matrix interface region is clearly shown when the rate of oxidation of the fiber, resin and composite and the flexural strength of the aged composite are considered. The protective effect of the fiber on the surface of the composite is illustrated by the strength of the aged composite, and is further illustrated by the photomicrograph of the cross section (transverse to the fiber direction) of the Celion 6000(u)/PMR-15 composite (Fig. 14). The photomicrograph of a shear specimen 1.52 cm (0.6 in.) in length reveals that no degradation occurs at the interface, and that there is no apparent pyrolysis or thermo-oxidative degradation of the matrix in the bulk of the composite. Surface cracks which develop at the ends of the composite during aging do not penetrate the composite. This was illustrated by the observation that after grinding and polishing the aged composite to a depth of 0.19 cm (0.075 in.), all evidence of surface cracks was removed (Fig. 14). Micrographs of shear specimens of the other composites (Figs. 15-18) reveal the presence of at least one major flaw or crack through the entire composite and the presence of voids in the interface regions of the composites.

CONCLUSIONS

The surfaces of commercial graphite fibers contain sodium, potassium, calcium, chromium and iron in varying relative atomic ratios. For 350°C applications in flowing air (100 cc or 1000 cc/min), the fiber rating in PMR-15 composites is as follows: Celion 6000(u) > Celion 6000 (PI Celanese size) > Fortafil 5(u) > AS4(u) > Thornel 300(u) > Panex 30(u). The thermo-oxidative stability of the above fibers in

the neat form and the PMR-15 resin under the same conditions is as follows: Fortafil 5(u) >> Celion 6000(u) > AS4(u) > Celion 6000 (PI Celanese size) > PMR-15 > Thornel 300(u) > Panex 30(u). The greater thermo-oxidative stability of composites relative to the fiber and polyimide matrix can be attributed to an overall protective blanket provided by the fiber after the resin is oxidized. The formation of a passive layer on the matrix due to deposition of components from the fiber can also be the method by which thermo-oxidative process is retarded. The formation of these protective barriers appears to be the mechanism of degradation for composites which exhibit internal thermo-oxidative stability and no internal pyrolysis of the matrix, namely the Celion 6000(u) and Celion 6000 (PI)/PMR-15 systems. For composites which show good fiber thermo-oxidative stability, such as Fortafil 5(u) and AS4(u), two factors may be responsible for the poor thermo-oxidative stability of the composite and subsequent poor mechanical properties. The first is (1) the aging process may generate poor bonding at the fiber/matrix interface, and (2) impurity components on the fiber, such as sodium or potassium ions, may accelerate thermo-oxidation of the resin and fiber in the interface region. Those composite systems which exhibited the poorest thermo-oxidative stability contain substantial quantities of sodium and potassium on the fiber, relative to the more thermo-oxidatively stable composite systems.

The fiber degradation rate appears to have a significant influence on the thermo-oxidative stability of the PMR-15 composite. The major degradation process occurs via thermo-oxidation of the surface of the composite. There is no evidence of internal oxidation or pyrolysis of the polyimide matrix under these conditions.

REFERENCES

1. Scola, D. A.: A Study of the Thermo-oxidative Process and Stability of Graphite and Glass/PMR Polyimide Composite. SAMPE, 27th National SAMPE Symposium and Exhibition, San Diego, CA, Vol. 27, 923-939 (1982).
2. Gibbs, H. H.; Wendt, R. C.; and Wilson, F. C.: SPI, 33rd Annual Technical Conference, Reinforced Plastics/Composites Institute, Section 24-F (1978).
3. Drzal, L. T.; and Hammer, G. E.: ALWAL-TR-80-4143, April 1981.
4. Serafini, T. T.; Delvigs, P.; and Lightsey, G. R.: U.S. Patent 3,745,149, July 1973.
5. Serafini, T. T.; Delvigs, P.; and Lightsey, G.R.: J. Poly. Sci., Vol. 16, No. 4, pp 905-915 (1972).
6. DiBenedetto, A. T.; and Scola, D. A.: J. Colloid & Interface Science, Vol. 64, No. 3, pp 480-500 (1978).
7. Pater, R. H.: Novel Improved PMR Polyimides. 13th National SAMPE Technical Conference, 13, 38-52 (1981).

TABLE 1. - ISS/SIMS ANALYSIS

Conditions:

Energy of primary ion beam	2.5 keV
Beam current	40 nAmps
Current density	1.3 μ amps/cm ²
Rastered area	(1x3) mm ²
Gated area	70% of rastered area
Sputter rate	~2 Å/min

Analysis:

ISS - First scan with ^3He (2 scans, 3 minutes each) to detect scattered $^3\text{He}^+$ ions only; sensitive to low atomic no. elements

SIMS- Second scan with ^{20}Ne (2 scans) to detect $+$ and $-$ secondary ions; sensitive to higher atomic no. elements and molecular fragments

TABLE 2. - SIMS ANALYSIS OF GRAPHITE FIBER SURFACES

Fiber	Relative Atomic Ratio ~10 Å ^{20}Ne					
	Na	K	Ca	Cr	Fe	F
Panex 30(u)	110	1.0	-	7.9	23	-
Fortafil 5(u)	2.0	1.0	-	9.4	21	-
Celion 6000(u)	8.4	1.0	33	4.4	15	-
Thornel 300(u)	3.1	1.0	1.7	-	18	-
AS4(u)	2.8	1.0	3.2	-	-	17
Celion 6000(PI)	3.5	1.0	20	-	15	-

TABLE 3. - SIMS ANALYSIS OF GRAPHITE FIBER SURFACES

Fiber	Relative Atomic Ratio ~100Å 20Ne					
	Na	K	Ca	Cr	Fe	F
Panex 30(u)	11	1.0	-	3.2	5.2	-
Fortafil 5(u)	1.6	1.0	-	5.1	3.7	-
Celion 6000(u)	2.2	1.0	5.3	4.8	6	-
Thornel 300(u)	1.7	1.0	1.7	5.2	7.5	-
AS4(u)	6.0	2.6	3.2	2.7	5.3	1.0
Celion 6000(new PI)	2.0	1.0	1.4	2.4	5.1	-

TABLE 4. - SIMS ANALYSIS OF GRAPHITE FIBERS

Fiber	Relative Atomic Ratio (Counts/sec ¹) 10Å Ne					
	Na	K	Ca	Cr	Fe	F
Panex 30(u)	43	1.0	-	2.0	1.0	-
Fortafil 5(u)	1.0	1.3	-	3.2	1.3	-
Celion 6000(u)	5.2	1.6	18	1.8	1.1	-
T300(u)	1.9	1.6	1.0	-	1.4	-
AS4(u)	1.5	1.4	1.6	-	1.6	1.0
Celion 6000(PI)	1.5	3.8	1.3	1.0	-	-

¹ actual counts/sec for element in lowest count/sec

Fortafil 5(u)	Na 1348	Celion 6000(PI)	Cr 37
Panex 30(u)	K 475	Panex 30(u)	Fe 127
T300(u)	Ca 186	AS4(u)	F 492

TABLE 5. - SIMS ANALYSIS OF GRAPHITE FIBERS

Fiber	Relative Atomic Ratio (Counts/sec ¹)					
	100Å	Ne	Ca	Cr	Fe	F
Panex 30(u)	28.0	6.1	-	1.7	2.0	-
Fortafil 5(u)	2.5	3.9	-	1.7	1.1	-
Celion 6000(u)	2.2	2.4	2.4	1.0	1.1	-
T300(u)	2.1	3.2	1.0	1.3	1.3	-
AS4(u)	71	75	18	6.5	9.2	-
Celion 6000(PI)	1.0	1.0	4.6	-	1.0	1.0

¹actual counts/sec for element in lowest count/sec

Celion 6000(PI)	Na 1814	Celion 6000(u)	Cr 161
Celion 6000(PI)	K 670	Celion 6000(PI)	Fe 127
T300(u)	Ca 500	Celion 6000(PI)	F 866

TABLE 6. - SIMS ANALYSIS OF GRAPHITE FIBER/PMR-15 COMPOSITES
AFTER 250 HRS AT 350°C, 1000 CC/MIN (AIRFLOW)

Fiber	Relative Atomic Ratio (Counts/sec ¹)					
	10Å	Ne	Ca	Cr	Fe	F
Panex 30(u)	9.5	5.4	1.0	4.4	1.0	-
Fortafil 5(u)	5.4	10	11	1.0	29	1.7
Celion 6000(u)	1.0	1.9	18	8.0	17	1.0
Thornel 300(u)	4.2	1.0	2.4	3.4	33	-
AS4(u)	3.5	2.0	6.3	3.1	59	1.1
Celion 6000 (Celanese PI size)	1.0	4.0	17	16	127	-

¹actual counts/sec for element in lowest count/sec from fiber to fiber

Celion 6000(PI)	Na 21,958	Fortafil 5(u)	Cr 25
T300(u)	K 4,076	Panex 30(u)	Fe 51
Panex 30(u)	Ca 37.3	Celion 6000(u)	F 652

TABLE 7. - SIMS ANALYSIS OF GRAPHITE FIBER/PMR-15 COMPOSITES
AFTER 250 HRS AT 350°C, 1000 CC/MIN (AIRFLOW)

Fiber	Relative Atomic Ratio (counts/sec ¹)					
	Na	K	Ca	Cr	Fe	F
Panex 30(u)	30	1.1	1.0	1.0	1.0	-
Fortafil 5(u)	8.8	6.6	26	3.1	13	3.3
Celion 6000(u)	1.0	1.0	30	5.4	19	1.0
Thornel 300(u)	10	1.1	11	5.0	15	-
AS4(u)	5.4	1.6	14	4.7	12	7.6
Celion 6000 (Celanese PI size)	1.5	2.7	29	9.7	24	-

¹actual counts/sec for element in lowest counts/sec from fiber to fiber

Celion 6000(u)	Na 4839	Panex 30(u)	Cr 25
Celion 6000(u)	K 1686	Panex 30(u)	Fe 25
Panex 30(u)	Ca 152	Celion 6000(u)	F 136

TABLE 8. - SIMS ANALYSIS OF FIBERS AND AGED COMPOSITES FOR SODIUM

Fiber/PMR-15 Composite	Relative Atomic Ratio (Counts/sec ¹)				
	Fiber		Composites 250 hrs at 350°C 1000 cc/min (airflow)		
	10Å	100Å	10Å	100Å	
Celion 6000(u)	5.2	2.2	1.02	1.0	
Celion 6000(PI)	1.5	1.0	1.0	1.5	
Thornel 300(u)	1.9	2.1	4.2	10	
AS4(u)	1.5	71	3.5	5.5	
Fortafil 5(u)	1.0	2.5	5.4	8.8	
Panex 30(u)	43	28	9.5	30	

¹See Tables 4, 5, 6, and 7 for actual counts/sec

TABLE 9. - COMPONENT AND COMPOSITE WEIGHT LOSSES AT 350°C
(1000 cc/min airflow)

Fiber/PMR-15 Composite	Fiber ¹ Wt% Loss after 450 hrs	Composite Wt% Loss after 520 hrs
Celion 6000(u)	11.2	12.5
Celion 6000(PI)	16.0	12.0
Thornel 300(u)	94.2	40.0
AS4(u)	10.4	21.1
Fortafil 5(u)	0.43	24.3
Panex 30(u)	99.5	95
PMR-15 resin ¹	77.8 ¹	-

¹PMR-15 resin is listed in this column (after 385 hrs)

TABLE 10. - FLEXURAL PROPERTIES OF ISOTHERMALLY AGED PMR-15 COMPOSITES
(350°C, 1000 cc/min airflow)

Composite System	350°C Flexural Properties					
	Unaged		After 250 hrs		After 520 hrs	
	Strength MPa (ksi)	Modulus GPa (10 ⁶ psi)	Strength MPa (ksi)	Modulus GPa (10 ⁶ psi)	Strength MPa (ksi)	Modulus GPa (10 ⁶ psi)
Celion 6000(u)	269 (39)	49.7 (7.2)	373 (54)	58.7 (8.5)	421 (61)	87.6 (12.7)
Thornel T300(u)	366 (53)	42.8 (6.2)	366 (53)	96.6 (14)	82.8 (12)	11.0 (1.6)
Celion 6000(PI)	276 (40)	39.3 (5.7)	656 (95)	159 (23)	297 (43)	60.7 (8.8)
AS4(u)	297 (43)	46.9 (6.8)	469 (68)	145 (21)	124 (18)	65.5 (3.7)
Fortafil 5(u)	379 (55)	48.9 (7.1)	814 (118)	138 (20)	221 (32)	82.8 (12)
Panex 30(u)	393 (57)	69.0 (10)	173 (25)	19.3 (2.8)	completely degraded	-

TABLE 11. - INTERLAMINAR SHORT BEAM SHEAR STRENGTH OF
ISOTHERMALLY AGED PRM-15 COMPOSITES
(350°C, 1000 cc/min airflow)

Composite System	350°C Shear Strength, MPa (ksi)		
	Unaged	After 250 hrs	After 520 hrs
Celion 6000(u)	19.3 (2.8)	34.3 (4.97)	33.1 (4.8)
Thornel 300(u)	28.9 (4.2)	28.3 (4.10)	6.76 (0.98)
Celion 6000(PI)	26.9 (3.9)	29.7 (4.3)	13.4 (1.94)
AS4(u)	12.4 (1.8)	23.8 (3.45)	2.85 (0.413)
Fortafil 5(u)	13.1 (1.9)	23.5 (3.40)	4.41 (0.64)
Panex 30(u)	20.0 (2.9)	mostly fiber remaining	mostly fiber remaining

TABLE 12. - COMPARISON OF COMPONENT AND COMPOSITE PROPERTIES
(after 350°C, 1000 cc/min airflow)
520 hrs

Fiber/Composite Systems	Fiber Wt Loss Rate 10^{-4} g/hr	Composite Wt Loss Rate 10^{-4} g/hr	Fiber Composite Sodium Content Rel. Atomic Ratio ¹ $\sim 100\text{\AA}$	350°C Flexural Strength ksi
Celion 6000(u)	11.0	3.1	1.0	61
Celion 6000(PI)	15.5	3.7	1.5	43
Fortafil 5(u)	0.40	3.9	8.8	32
AS4(u)	11.0	5.4	5.5	18
Thornel 300(u)	86	10.9	10	12
Panex 30(u)	140	25	30	
PMR-15 resin	5.7	-	-	completely degraded

¹ where 1.0 = 4839 counts/sec of sodium

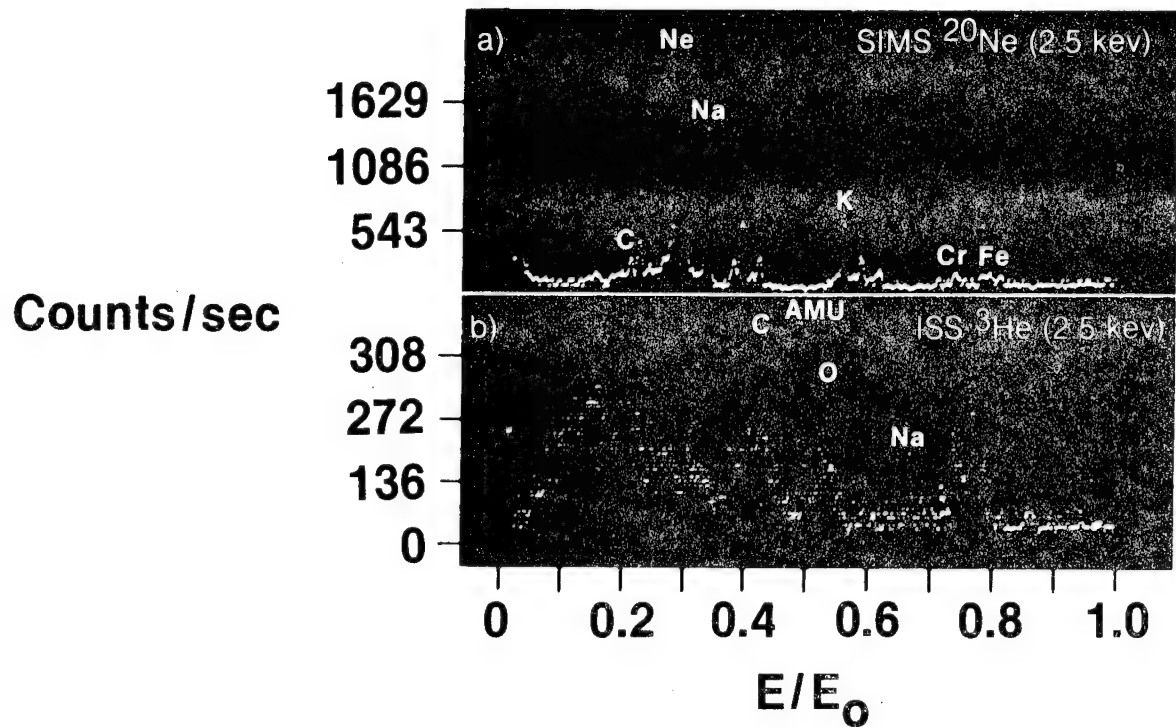


Figure 1. - ISS/SIMS spectra of Fortafil 5 unsized fiber $\sim 10\text{\AA}$.

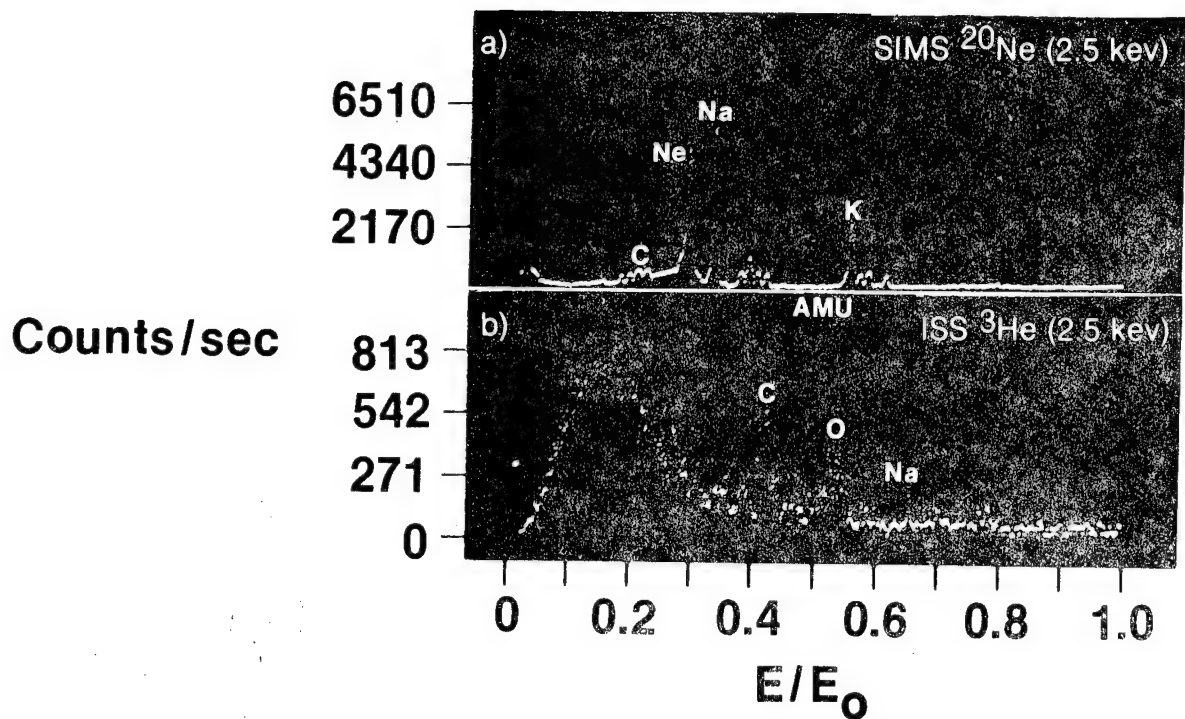


Figure 2. - ISS/SIMS spectra of Fortafil 5 sized fiber $\sim 10\text{\AA}$.

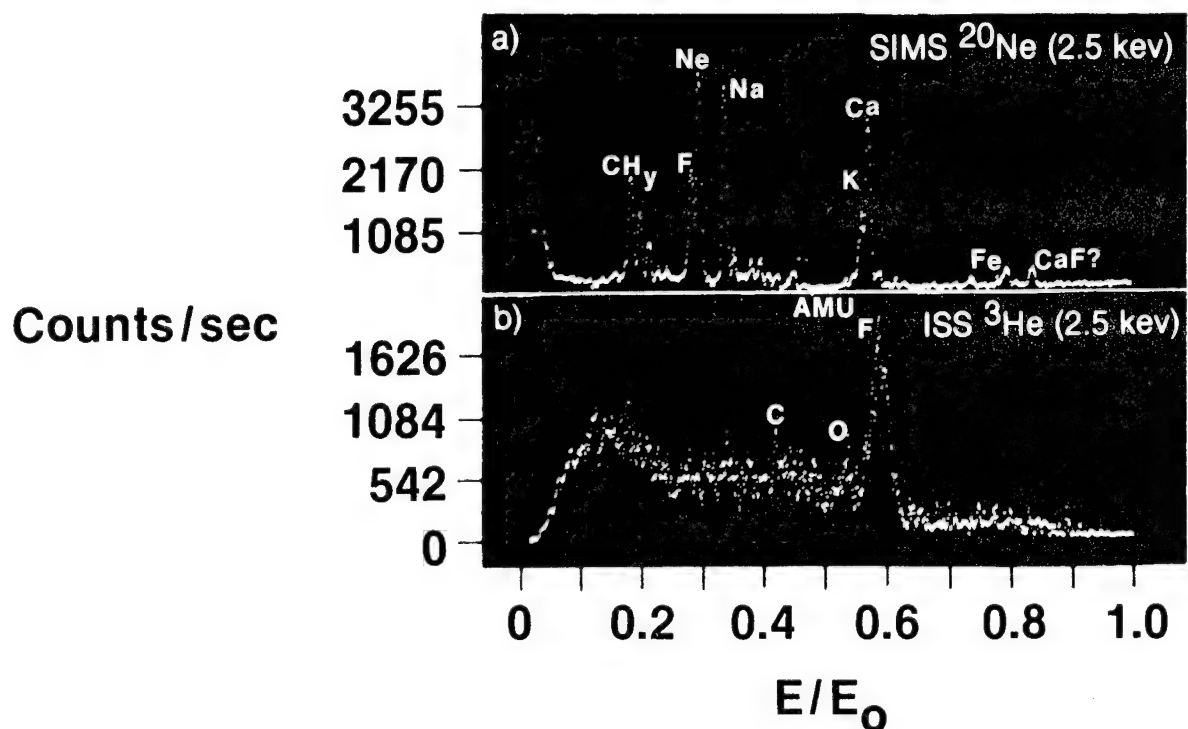


Figure 3. - ISS/SIMS spectra of Celion 6000 NR150B2 sized fiber $\sim 10\text{\AA}$.

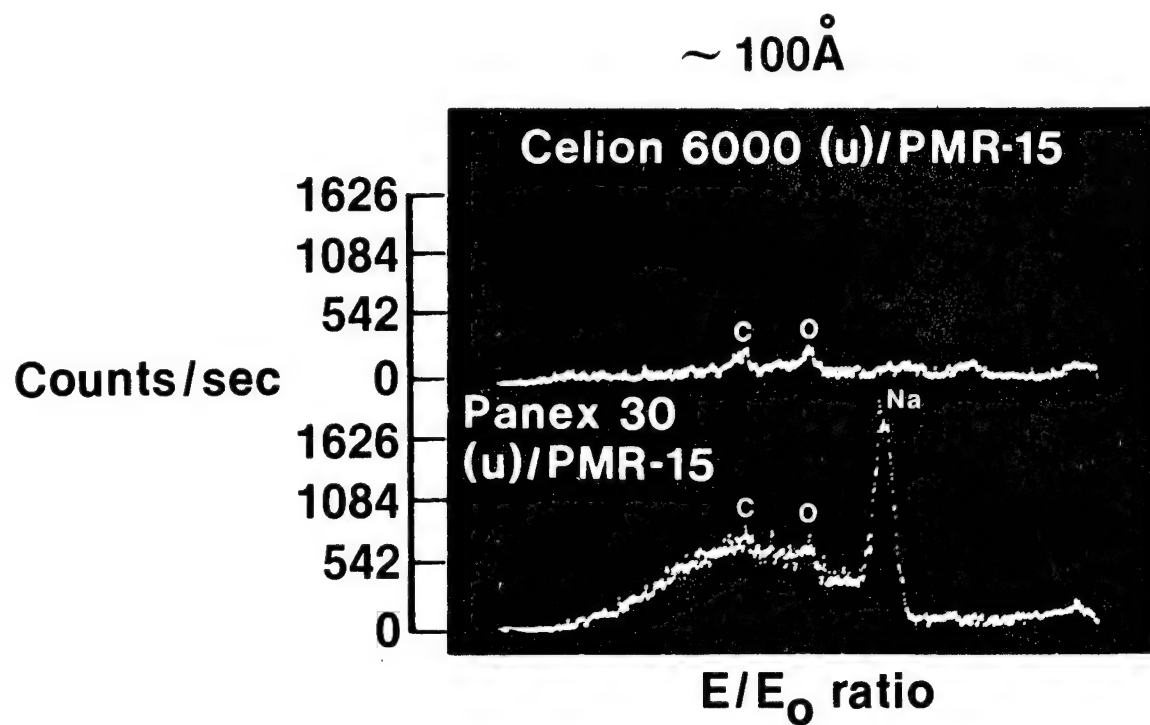


Figure 4. - ISS spectra of isothermally aged composites.
(350 °C, 220 hrs, 1000 cc/min airflow)

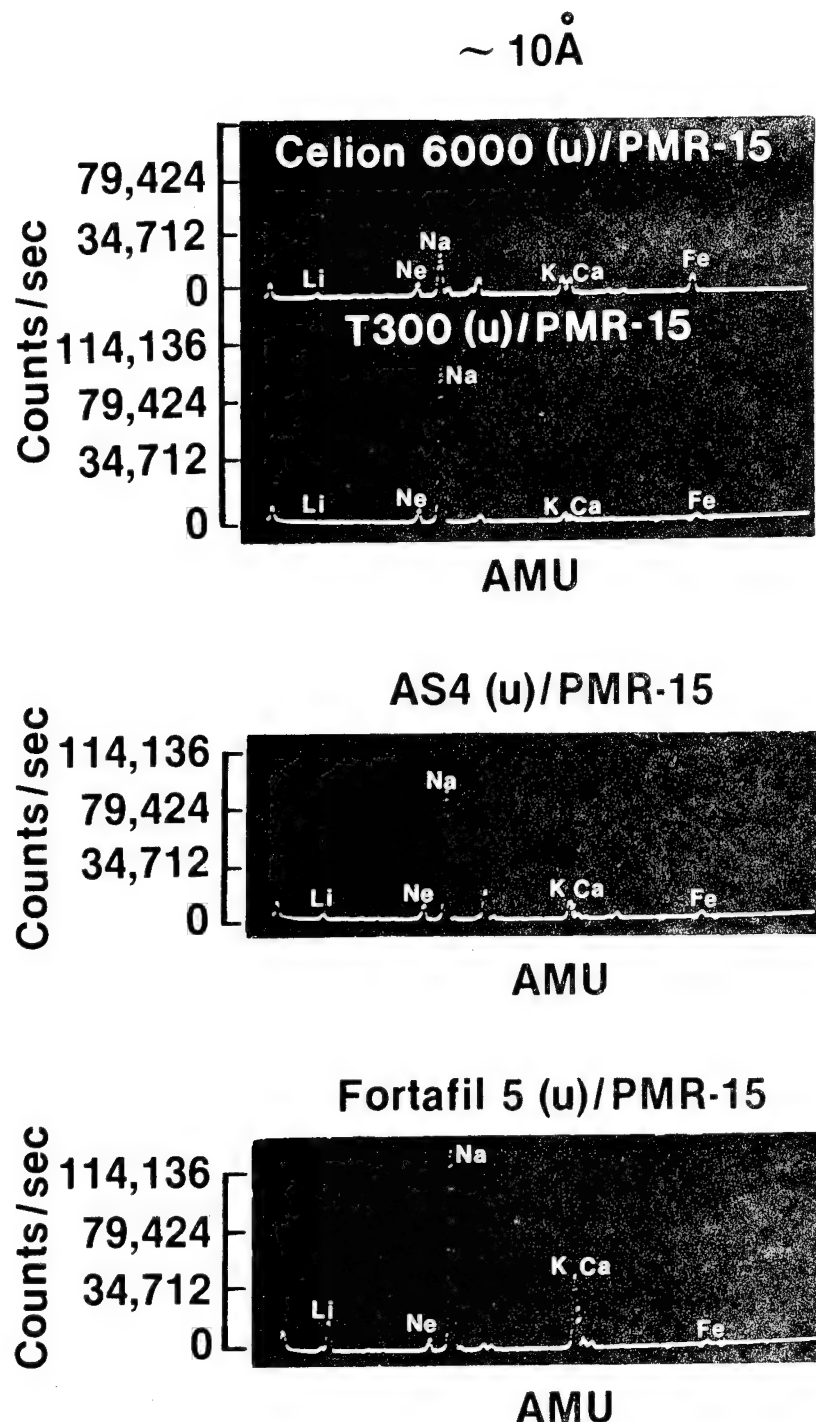
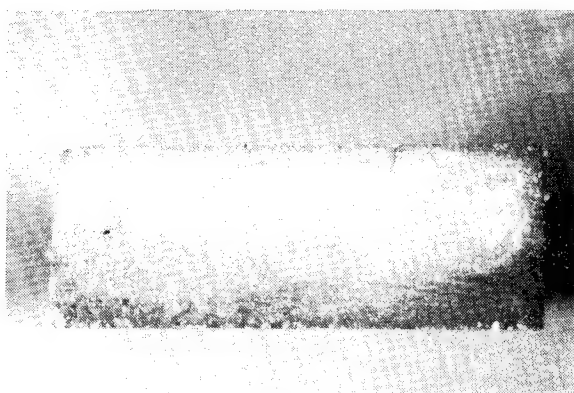
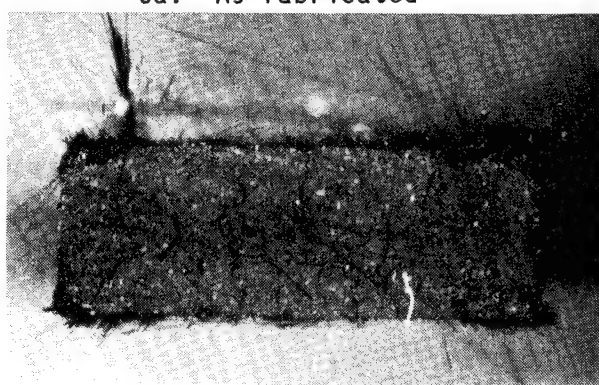


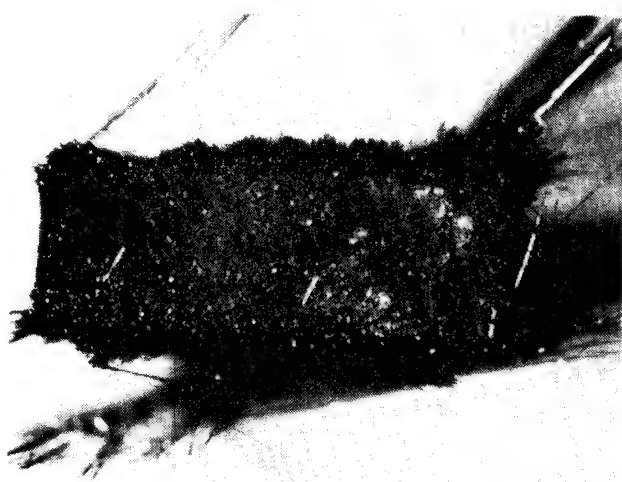
Figure 5. - SIMS spectra of isothermally aged composites.
(350 °C, 220 hrs, 1000 cc/min airflow)



6a. As fabricated



6b. After 250 hrs

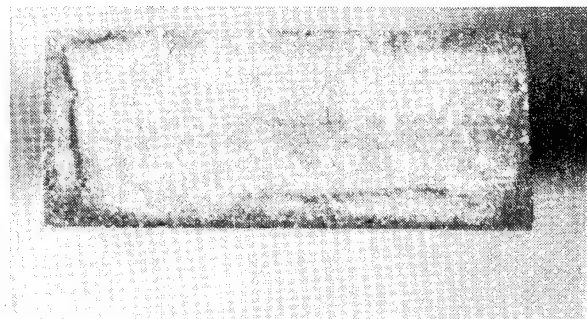


6c. After 520 hrs

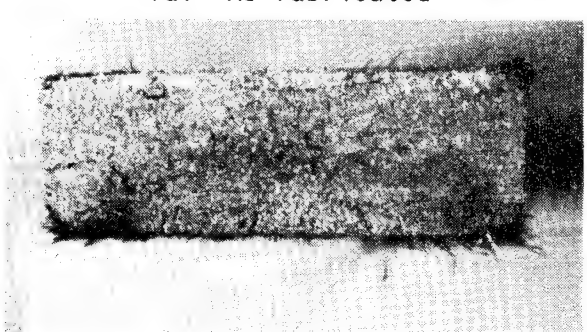
Figure 6. - Thermo-oxidation process of graphite fiber/PMR-15 composites.

(350 °C, 1000 cc/min airflow)

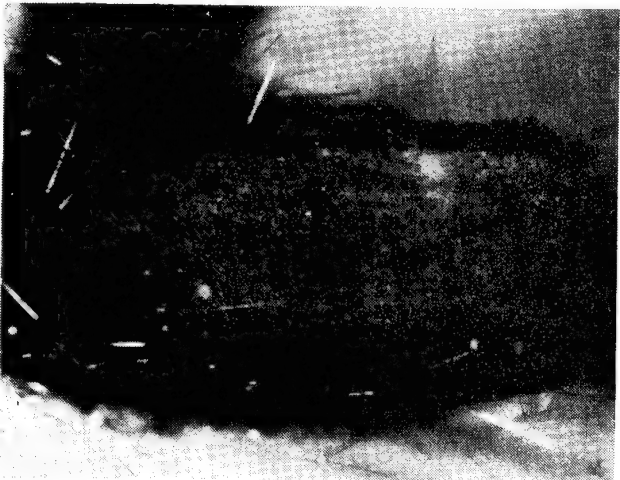
Celion 6000 (u)/PMR-15



7a. As fabricated



7b. After 250 hrs



7c. After 520 hrs

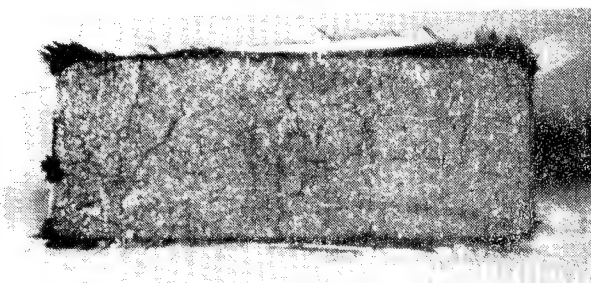
Figure 7. - Thermo-oxidation process of graphite fiber/PMR-15 composites.

(350 °C, 1000 cc/min airflow)

Celion 6000 (PI sized)/PMR-15



8a. As fabricated



8b. After 250 hrs

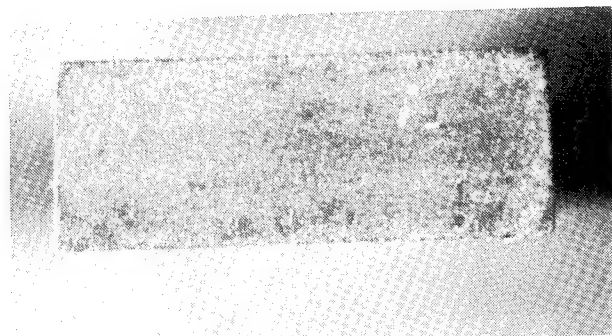


8c. After 520 hrs

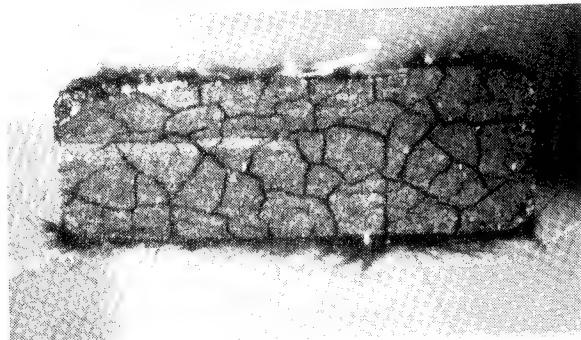
Figure 8. - Thermo-oxidation process of graphite fiber/PMR-15 composites.

(350 °C, 1000 cc/min airflow)

AS4 (u)/PMR-15



9a. As fabricated



9b. After 250 hrs

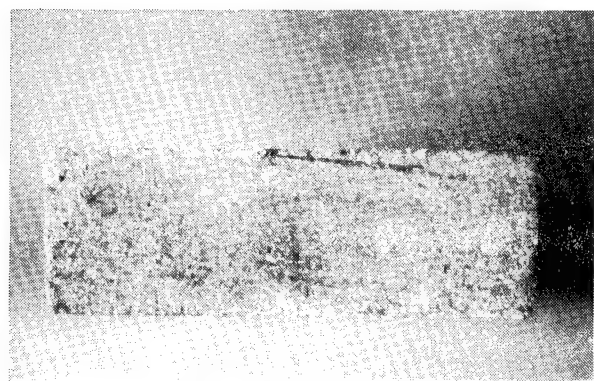


9c. After 520 hrs

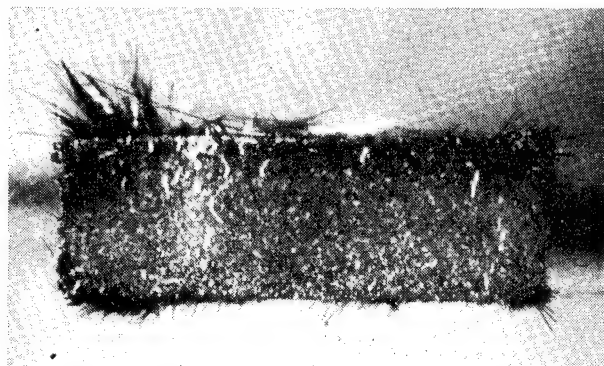
Figure 9. - Thermo-oxidation process of graphite fiber/PMR-15 composites.

(350 °C, 1000 cc/min airflow)

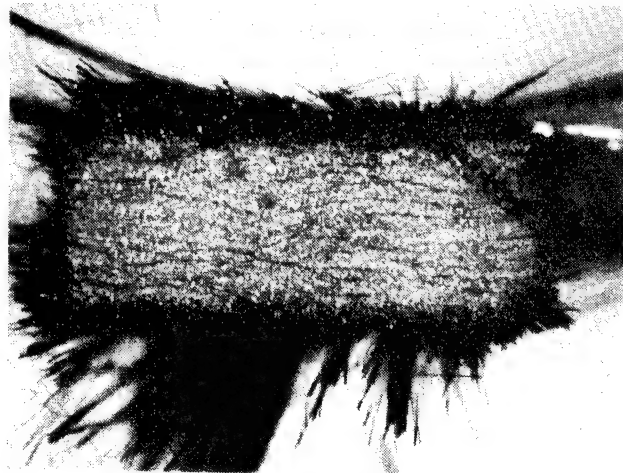
ThorneL 300 (u)/PMR-15



10a. As fabricated



10b. After 250 hrs



10c. After 520 hrs

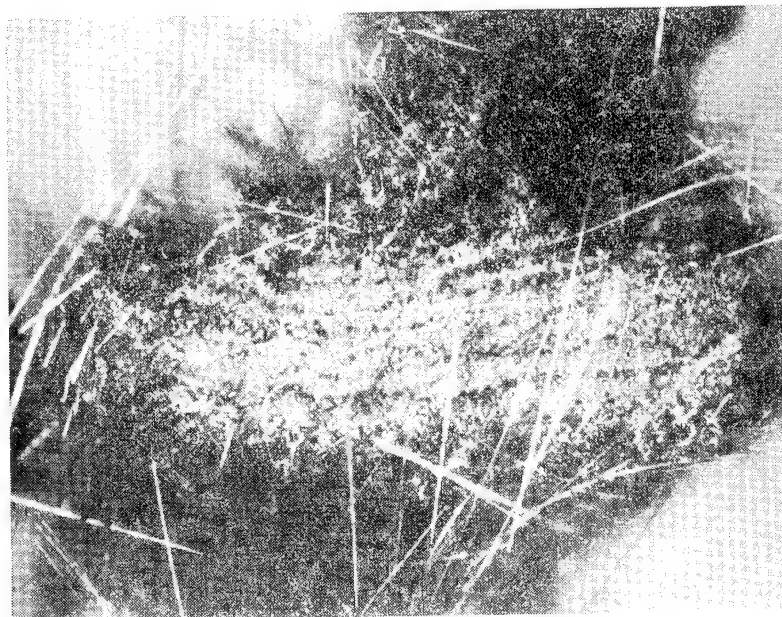
Figure 10. - Thermo-oxidation process of
graphite fiber/PMR-15 composites.

(350 °C, 1000 cc/min airflow)

Fortafil 5 (u)/PMR-15



11a. As fabricated



11b. After 250 hrs

Figure 11. - Thermo-oxidation process of graphite fiber/PMR-15 composites.
(350 °C, 1000 cc/min airflow)
Panex 30 (u)/PMR-15

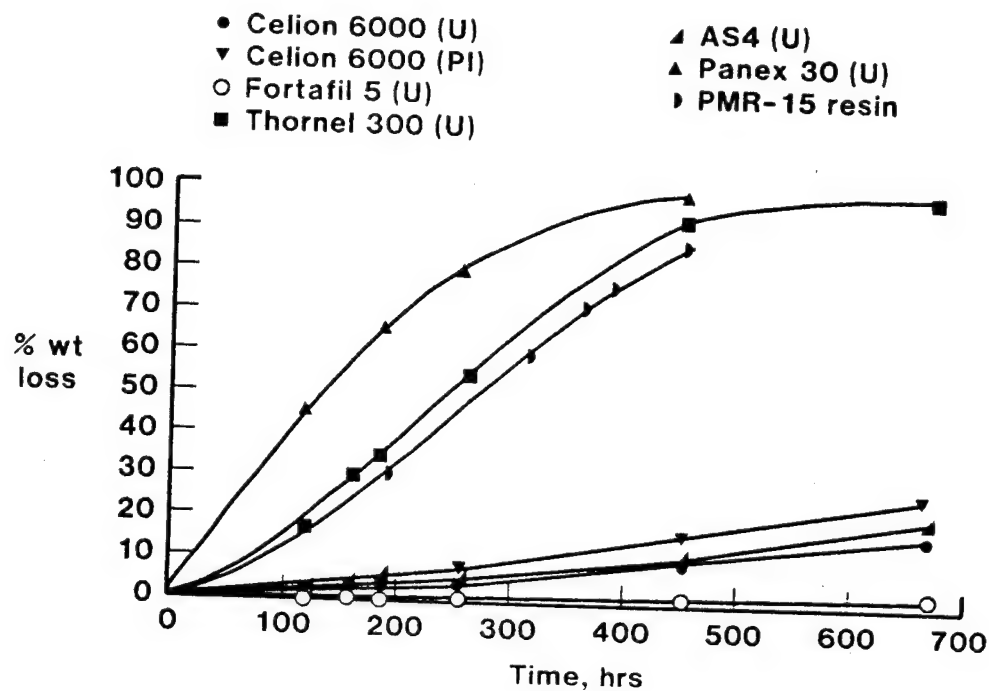


Figure 12. - Weight loss of component materials.
(350 °C, 1000 cc/min airflow)

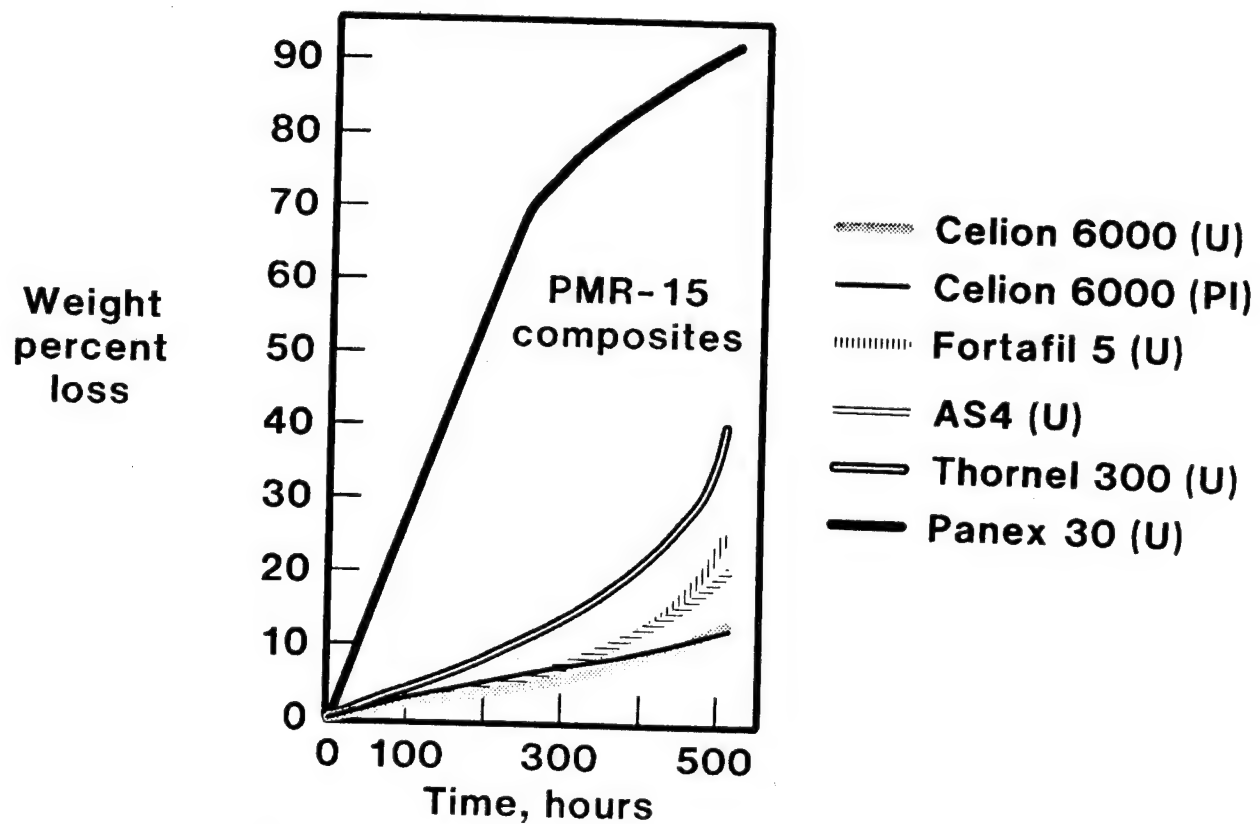
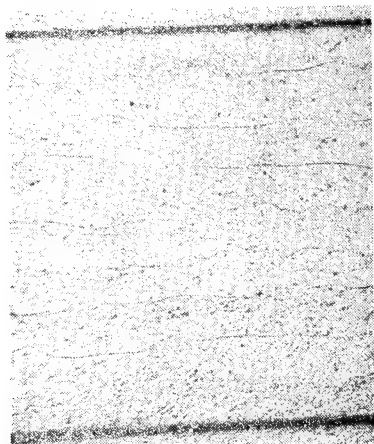
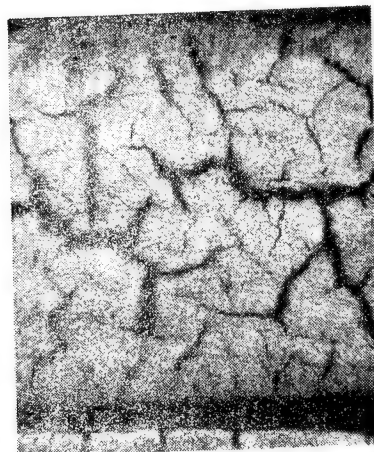


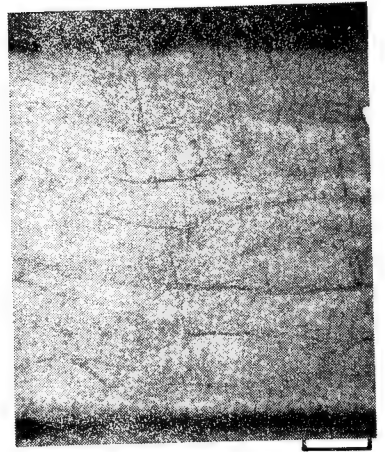
Figure 13. - Composite weight loss.
(350 °C, 1000 cc/min airflow)



14a. As fabricated

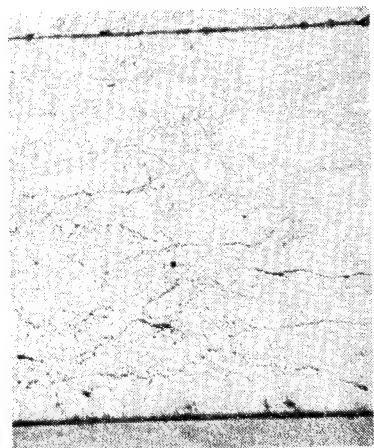


14b. After 250 hrs

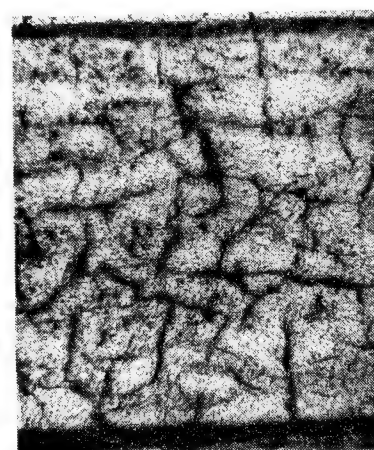


14c. After polishing 0.075 in.
(depth of crack)

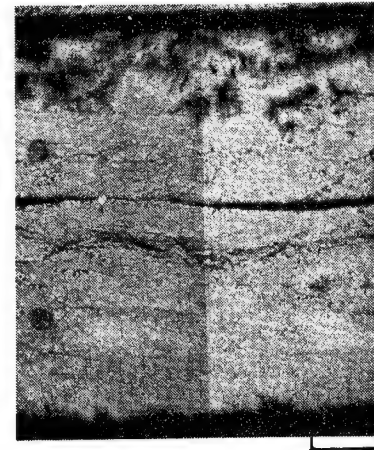
Figure 14. - Cross section of Celion 6000 (u)/PMR-15 composite.
(350 °C, 1000 cc/min airflow)



15a. As fabricated



15b. After 250 hrs

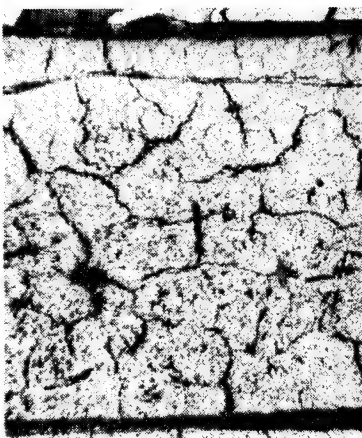


15c. After polishing 0.45 in.

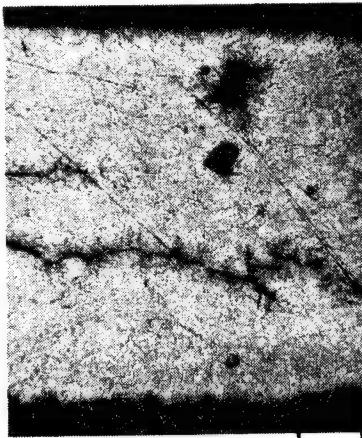
Figure 15. - Cross section of Celion 6000 (PI)/PMR-15 composite.



16a. As fabricated

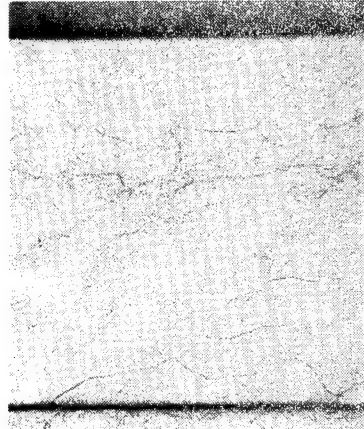


16b. After 250 hrs



16c. After polishing 0.45 in.

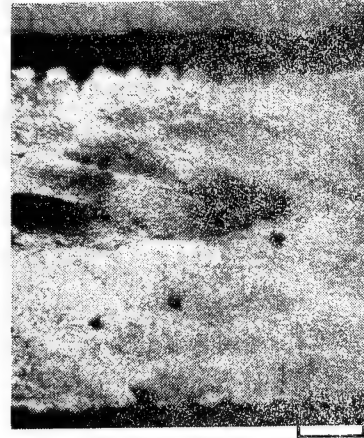
Figure 16. - Cross section of AS4 (u)/PMR-15 composite.
(350 °C, 1000 cc/min airflow)



17a. As fabricated

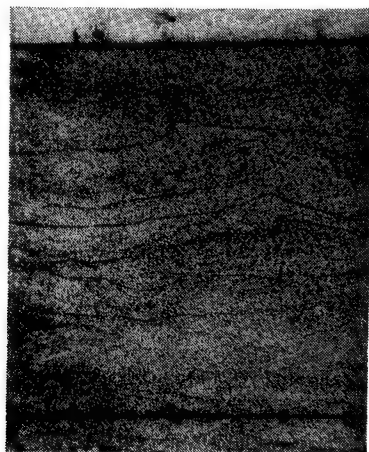


17b. After 250 hrs

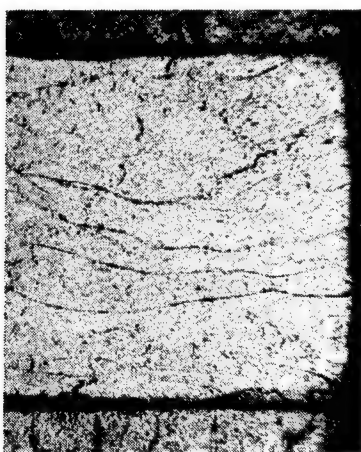


17c. After polishing 0.45 in.

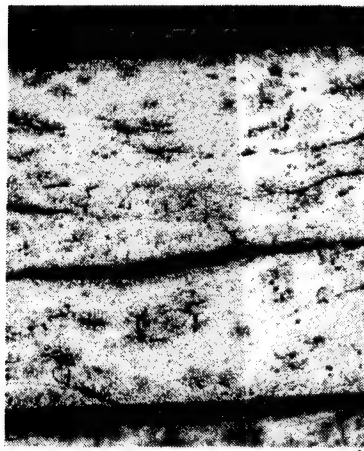
Figure 17. - Cross section of Thorne 300 (u)/PMR-15 composite.
(350 °C, 1000 cc/min airflow)



18a. As fabricated



18b. After 250 hrs



400 μ m

18c. After polishing 0.45 in.

Figure 18. - Cross section of Fortafil 5 (u)/PMR-15 composite.

RHEOLOGICAL, PROCESSING, AND 371 °C MECHANICAL PROPERTIES
OF CELION 6000/N-PHENYLNADIMIDE MODIFIED PMR COMPOSITES

Ruth H. Pater
National Aeronautics and Space Administration
Lewis Research Center

The rheology, processing, and chemistry of newly developed N-phenylnadimide modified PMR (PMR-PN) polyimide resins are reviewed. The 371 °C performance of their composites reinforced with Celion 6000 graphite fibers is also reviewed, along with the state-of-the-art Celion 6000/PMR-15 composite. The effects of the 371 °C exposure in air for up to 300 hr on the composite glass transition temperatures, weight loss characteristics, and dimensional stability are presented. The changes in the composite 371 °C interlaminar shear and flexural properties are also presented. In addition, composite interfacial degradation as a function of exposure time at 371 °C was followed by scanning electron microscopy. The results suggest that the composite materials can be used at 371 °C for at least 100 hr.

INTRODUCTION

High-performance polymer matrix composites constitute a class of engineering materials that have significant potential for application in advanced aircraft engines. In the past 10 years considerable effort has been made toward the design and fabrication of a variety of advanced composite components which operate at a temperature range of 260 to 316 °C (ref. 1). A significant improvement in engine efficiency could be achieved by extending the use temperature of advanced composites up to 371 °C. Thus far, most high-temperature polymer matrix composite studies have been conducted at temperatures of 316 °C and below. Composite performance above 316 °C, however, has not been extensively investigated (refs. 2 and 3). Because of this lack of property data at temperatures above 316 °C, composite applications at higher temperatures, such as 371 °C, cannot be assessed realistically at the present time.

In 1981, a new series of N-phenylnadimide (PN) modified PMR polyimides (ref. 4) was reported. These are designated as PMR-P1, -P2, etc., where P1, P2, etc., refer to a formulation containing a given quantity of PN. Collectively, they are designated as PMR-PN. Initial studies revealed that the composites prepared from these matrices and Celion 6000 graphite fibers exhibited excellent processability and thermo-oxidative stability at 316 °C in air for up to 1500 hr (ref. 4). Composite dynamic mechanical properties were also investigated from the viewpoint of clarifying the resin chemistry (ref. 5).

This paper reviews the rheology, processing, chemistry, and 371 °C properties of PMR-PN resins and their composites reinforced with Celion 6000 graphite fibers. Data are presented on the physical, thermal, and mechanical properties of the composites aged at 371 °C in air.

RESULTS AND DISCUSSION

Rheological and Processing Characteristics

Resin rheology. - The modified resins are prepared from in-situ thermal polymerization of four monomer reactants: the monomethyl ester of 5-norbornene-2,3-dicarboxylic acid (NE), 4,4'-methylenedianiline (MDA), the dimethyl ester of 3,3'4,4'-benzophenonetetracarboxylic acid (BTDE), and N-phenylnadimide (PN). Their chemical structures along with the idealized cross-linked polyimide structure are shown in figure 1. Table I gives the chemical compositions of the modified (PMR-PN) and unmodified (PMR-15) PMR polyimides investigated. This table shows that the PN contents in the four PMR-PN formulations are relatively low compared to the amounts of the other three monomers.

Despite relatively low quantities of PN employed, PN exerts a significant influence on the rheological properties of PMR-PN resins and composites as explained below. Further, the flow properties of the modified resins exhibited a strong dependence on the stereochemistry of PN which exists in two isomeric forms: endo and exo. As seen in figure 2, the use of endo-N-phenylnadimide in PMR-P1 formulation (curve c) causes a decrease while the use of exo-N-phenylnadimide in the same formulation (curve a) causes an increase in the minimum viscosity of PMR-15 (curve b). This behavior can be attributed to the melting-point difference between these two isomers as shown in figure 3. The endo-isomer shows a sharp endotherm at 145 °C due to melting, while the exo-isomer shows a considerably higher melting temperature (195 °C). The exotherms at 360 and 367 °C for exo- and endo-PN, respectively, are due to their polymerization reaction.

Therefore, to obtain improved flow, the use of the endo-form of PN, rather than the exo-isomer, is recommended. For this reason, PMR-PN resins reported hereafter use the endo-form of PN to improve their flow characteristics.

Figure 4 shows the influence of endo-PN concentration on the dynamic shear viscosity of the imidized molding powders (ref. 4). In comparing curves b through g with curve a, it can be seen that the PMR-PN samples exhibited lower shear viscosities than PMR-15 over the temperature range of 238 to 303 °C. The minimum viscosities for the PMR-PN samples ranged from 1769 dyne/cm² for PMR-P1 to 884 dyne/cm² for PMR-P5, compared with a value of 2940 dyne/cm² for the control PMR-15. This represents a decrease of 40 to 70 percent in the minimum viscosity of PMR-15. Figure 5 shows that the addition of the first 4 mole percent of PN (PMR-P1) to PMR-15 causes a significant and disproportionate reduction in the minimum shear viscosity. A linear correlation between the minimum viscosity and PN concentration appears to exist in the PN concentration range of 4 to 20 mole percent.

Processing characteristics. - The resin flow characteristics in composites are known to have significant effects on composite processing and properties. A plot of the resin flow in Celion 6000/PMR-PN composites as a function of the PN concentration is shown in figure 6. Note that, in order to provide a valid basis for comparing resin flow behavior, all of the composites were molded using the same cure cycle (ref. 4). From figure 6, it is evident that the PMR-PN composites, like the PMR-PN molding powders discussed previously, exhibited improved resin flow compared to PMR-15 composite. These results indicate that PN is an effective flow-modifying agent. This can be attributed to the fact that PN exists in the liquid

state up to the cure temperature (316 °C). These results also suggest that the flow properties of PMR-PN resins and composites can be tailored to meet specific processing requirements by adding small quantities of PN.

Studies reported in reference 4 showed that resin flow in compression-molded PMR-PN composites could also be controlled by varying the pressurization temperature in the cure cycle. For example, increasing the pressurization temperature from 232 °C for PMR-15 to 282, 288, 293, and 299 °C for PMR-P1, -P2, -P3, and -P4 composite systems, respectively, reduced the composite resin flow to about 3 percent, which is equivalent to the resin flow of PMR-15 composite.

Postulated Structure of PMR-PN Polyimides

As mentioned previously, figure 1 shows the chemical structures of four monomer reactants, PN, NE, MDA, and BTDE, used in the synthesis of PMR-PN polyimides. It is postulated that the three monomers, NE, MDA, and BTDE, first react to form a PMR-15 imide prepolymer through an amic acid intermediate. It is further postulated that the imide prepolymer can undergo a crosslinking reaction with itself and with PN to give a crosslinked homopolymer or copolymer system. The presence of a copolymer as an integral part of the polymer system is supported by the dynamic mechanical properties reported previously (ref. 5).

The incorporation of PN into the PMR-15 polymer network could result in a change in the basic structure of PMR-15 which, in turn, could alter the chemical properties of PMR-15. The idealized structures of PMR-15 and PMR-PN polyimides are shown in figures 7 and 8, respectively. In PMR-15 the molecular structure between the crosslinking sites consists of several aromatic and imide functionalities. A molecular model (not shown) of the idealized structure of PMR-15 demonstrated that there is considerable steric crowding and interaction between neighboring chains. This steric crowding can be substantially reduced, when some of the PMR-15 chain groups are replaced with the pendant phenyl group from PN. With such a replacement, not only would the steric crowding be reduced, the crosslinking density would also be reduced because there are only two crosslinking sites in each PN, while there are four in each PMR-15 structural unit. Thus, the replacement would lead to a copolymer having increased flexibility due to decreased crosslinking density and possibly increased free volume. This hypothesis is consistent with the physical and mechanical properties determined in the previous studies (refs. 4 and 5).

Effects of 371 °C Postcure and Aging on Physical, Thermal, and Mechanical Properties of Celion 6000/PMR-PN Composites

Physical properties. - The effects of 16- and 30-hr postcures at 371 °C on composite weight loss and dimensional changes of the composite systems are listed in table II. Approximately 2 percent weight loss was experienced by all composites after 30 hr of postcure. All composites exhibited 1 percent shrinkage in the transverse direction to the fibers, and as expected, nondetectable dimensional change in the longitudinal direction for either 16- or 30-hr postcure. Weight losses at 371 °C for exposure times up to 300 hr are shown in figure 9. After 300 hr, PMR-P1 and PMR-P2 exhibited the lowest weight losses (~5.7) compared to the control system PMR-15 (7.2).

Thermal properties (T_g). - Figure 10 shows the effects of 371 °C exposure in air on the glass transition temperature (T_g) of the composites. The lower initial T_g for PMR-PN systems compared to the T_g of PMR-15 system may be explained on the basis of a lower crosslink density for PMR-PN relative to PMR-15 as discussed previously. The attainment of maximum T_g for the PMR-PN and PMR-15 composites follows a stepwise process and occurs in two distinct stages: (a) stage one occurs within the first 30 hr of postcure in which a rapid increase in T_g occurs. The rate constant (k_1) for this step varied from 2.0 °C/hr for the control (PMR-15) to 1.5 °C/hr for the P-4 specimen; (b) stage two occurs between 30 to ~160 hr; the rate constant k_2 was found to be 0.11 °C/hr, which is approximately 14 times slower than k_1 . This may be explained by a decrease in concentration of crosslinkable groups with time and/or by a quenching effect due to molecular immobility. The dependence of T_g on the exposure time can be expressed by the following equation:

$$T_g = k_1 \ln t + C \quad (1)$$

where k_1 is the rate constant for either stage one or stage two, t is time, and C is a constant. Normally, a postcure time of 10 hr at 316 °C is employed for PMR composite materials intended for use at 316 °C. The results presented in figure 10 and equation (1) suggest that longer postcure times at 371 °C are required, if the materials are to be used at 371 °C. The composites attained a T_g of 371 °C after a postcure time of 50 hr or longer at 371 °C.

Mechanical properties. - Figures 11 and 12 show the 371 °C mechanical properties of the composites, after a 30-hr 371 °C postcure, followed by exposure up to 100 hr in air at 371 °C. Even though testing temperature (371 °C) was above or close to the glass transition temperatures, most of the composite materials exhibited good mechanical properties at 371 °C during the first 100 hr of exposure. Thus, a 30-hr postcure time appears to be adequate for attaining a useful level of mechanical properties at 371 °C. Prior to exposure at 371 °C, PMR-PN composites exhibited lower flexural strengths (fig. 11), but somewhat higher interlaminar shear strengths (fig. 12), compared to the control. After the 100-hr exposure, all PMR-PN composites exhibited higher flexural and interlaminar shear strengths than the control specimen PMR-15, particularly the PMR-P1 and PMR-P2 composite systems. The increase in the 371 °C flexural and interlaminar shear properties during the 50-hr exposure interval from 50 to 100 hr indicates that the useful lifetime of PMR-PN composite materials may be greater than 100 hr. This is supported by the thermogravimetric analysis (TGA) data of PMR-P1 resin shown in figure 13 which shows that PMR-P1 resin aged for 100 hr at 371 °C in air is more thermo-oxidatively stable than both the unaged and 371 °C, 200-hr aged samples.

In addition to the mechanical properties presented previously, the trend for the higher thermo-oxidative stability of PMR-P1 and PMR-P2 composite systems at 371 °C is further supported by the weight loss data presented in figure 9 and the fiber retention comparison illustrated in figure 14. Thus, the thermo-oxidative stability of the PMR-PN composite systems follows the order (from ref. 4)

$$\text{PMR-P1} \sim \text{PMR-P2} > \text{PMR-P3} \sim \text{PMR-15} > \text{PMR-P4}$$

Scola reported that the thermo-oxidative degradation of Celion 6000/PMR-15 at 335 °C occurs only at exposed composite surfaces and that oxidative degradation and pyrolysis do not occur within the bulk of the composite system (ref. 3). Figure 15 shows the SEM micrographs of PMR-P1 composites aged at 371 °C for time periods up to 200 hr. The micrographs shown were taken near the exposed surfaces of the

composites. No matrix or interfacial degradation was observed as a result of the 30-hr postcure at 371 °C in air (fig. 15(a)). However, some matrix degradation occurred between 0 and 120 hr at 371 °C in air (fig. 15(b)). Continued exposure to 200 hr resulted in extensive matrix and interfacial degradation (figs. 15(c) and (d)). The other PMR-PN composite systems exhibited similar interfacial characteristics as that of PMR-P1 during the thermo-oxidative treatment.

The minimal degradation as assessed by SEM analysis and the high level of mechanical properties of the composites after 100 hr at 371 °C in air suggest that the 371 °C useful life of the PMR-PN composites is at least 100 hr.

CONCLUSIONS

PMR-PN resins exhibit higher resin flow characteristics than the unmodified PMR-15 system. Addition of PN does not compromise the elevated temperature properties of PMR-15; in fact, the results indicate that the 371 °C shear and flexural properties of the PMR-P1 and PMR-P2 modified systems after 100 hr aging at 371 °C are superior to those of PMR-15. The addition of PN appears to be a technically sound approach for attaining PMR-polyimide formulations with improved processing characteristics without sacrificing the thermo-oxidative stability of the resin and composite systems.

REFERENCES

1. Serafini, Tito T.; Delvigs, Peter; and Alston, William B.: PMR Polyimides - Review and Update. NASA TM-82821, 1982.
2. Pike, R.A.; and DeCrescente, M.A.: Elevated Temperature Characteristics of Borsic and Graphite Fiber/Polyphenylquinoxaline Resin Composites. The Wide World of Reinforced Plastics. Society of the Plastics Industry, New York, 1974, Section 18F.
3. Scola, Daniel A.: A Study of the Thermo-Oxidative Process and Stability of Graphite and Glass/PMR Polyimide Composites. 27th National SAMPE Symposium and Exhibition, SAMPE, Azusa, CA, 1982, pp. 923-939.
4. Pater, Ruth H.: Novel Improved PMR Polyimides. Technology Transfer, SAMPE, Azusa, CA, 1981, pp. 38-52.
5. Pater, Ruth H.: Dynamic Mechanical Properties of N-Phenylnadicimide Modified PMR Polyimide Composites. NASA TM-83051, 1983.

TABLE I. - COMPOSITIONS OF PMR-PN POLYIMIDES

Resin system	Monomer (mole)				PN mole percent ^a
	NE	MDA	BTDE	PN	
PMR-15 (control)	2	3.087	2.087	0.0	0.00
PMR-P1				.041	0.57
PMR-P2				.099	1.36
PMR-P3				.136	1.87
PMR-P4				.177	2.41

^aPN mole percent = moles of PN/moles of
(NE+MDA+BTDE+PN).

TABLE II. - EFFECTS OF 317 °C POSTCURE ON PHYSICAL PROPERTIES
OF CELION 6000/PMR-PN POLYIMIDE COMPOSITES

Composite property	Postcure time, hr	Resin system				
		PMR-15 (control)	PMR-P1	PMR-P2	PMR-P3	PMR-P4
Weight loss, percent	16	1.6	1.6	1.6	1.6	1.7
	30	2.1	2.0	2.1	2.2	2.3
Transverse shrinkage, percent	16	0.9	0.9	1.0	1.0	1.0
	30	0.9	1.0	1.1	1.1	1.1

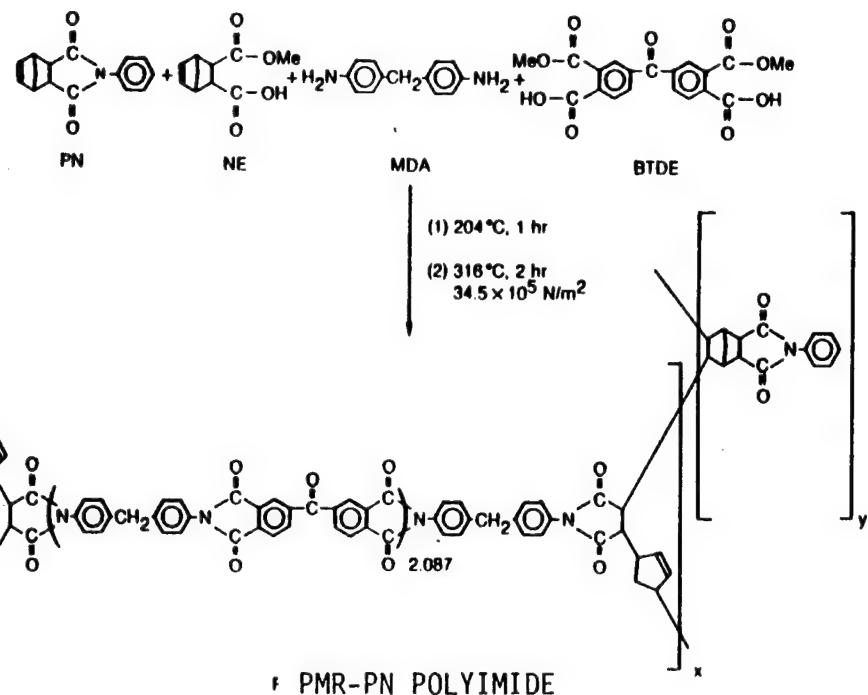


Figure 1. - Synthetic reaction for PMR-PN polyimides.

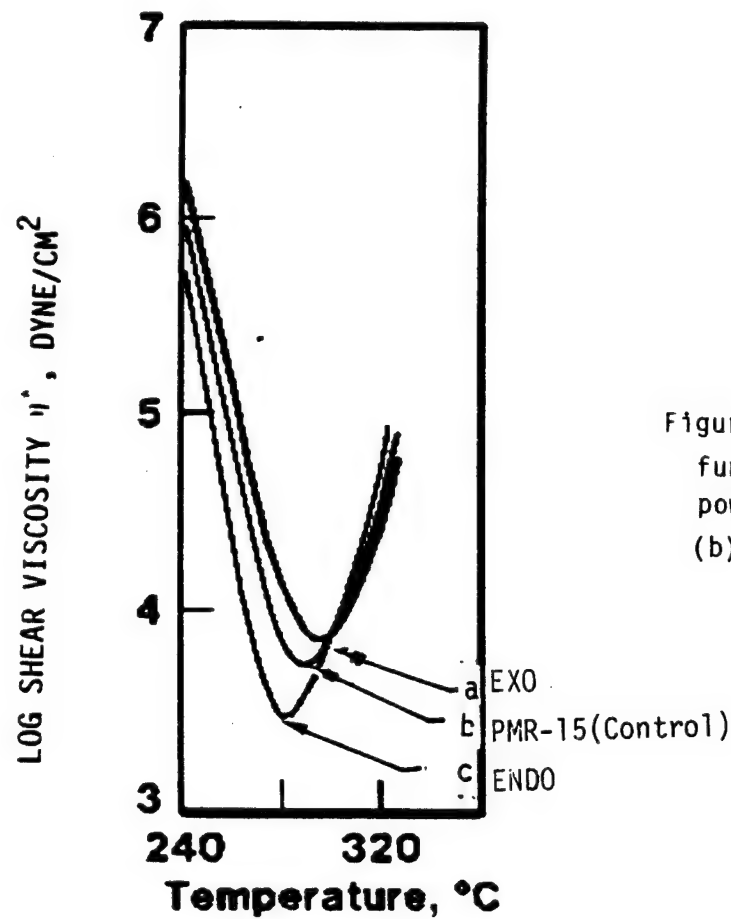


Figure 2. - Log shear viscosity as function of temperature for molding powders. (a) PMR-P1 using exo-PN. (b) PMR-15. (c) PMR-P1 using endo-PN.

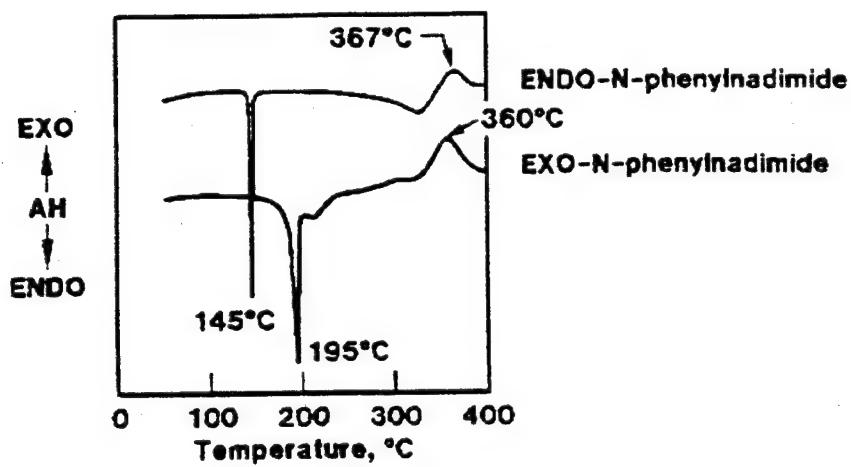


Figure 3.- Differential scanning calorimetry scans of endo- and exo-PN.

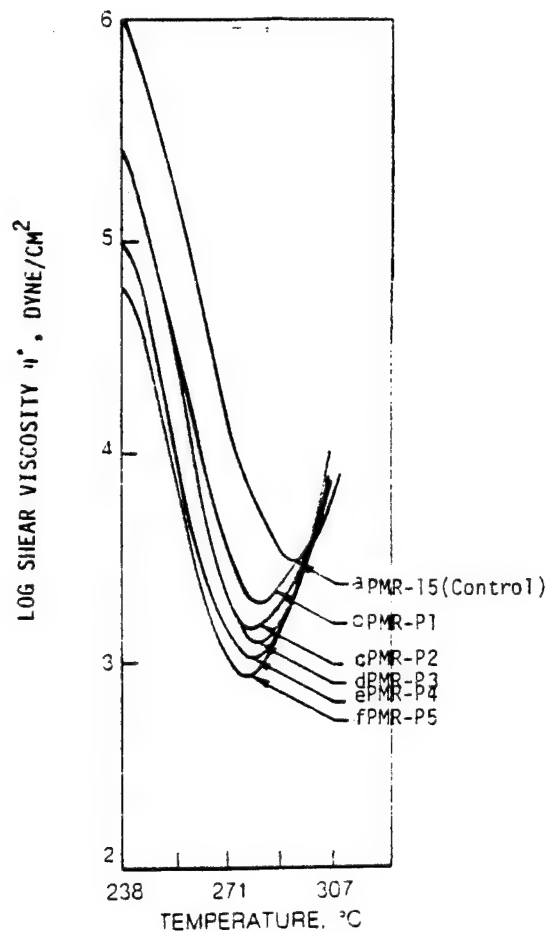


Figure 4. - Log shear viscosity as function of temperature for PMR-PN molding powders.

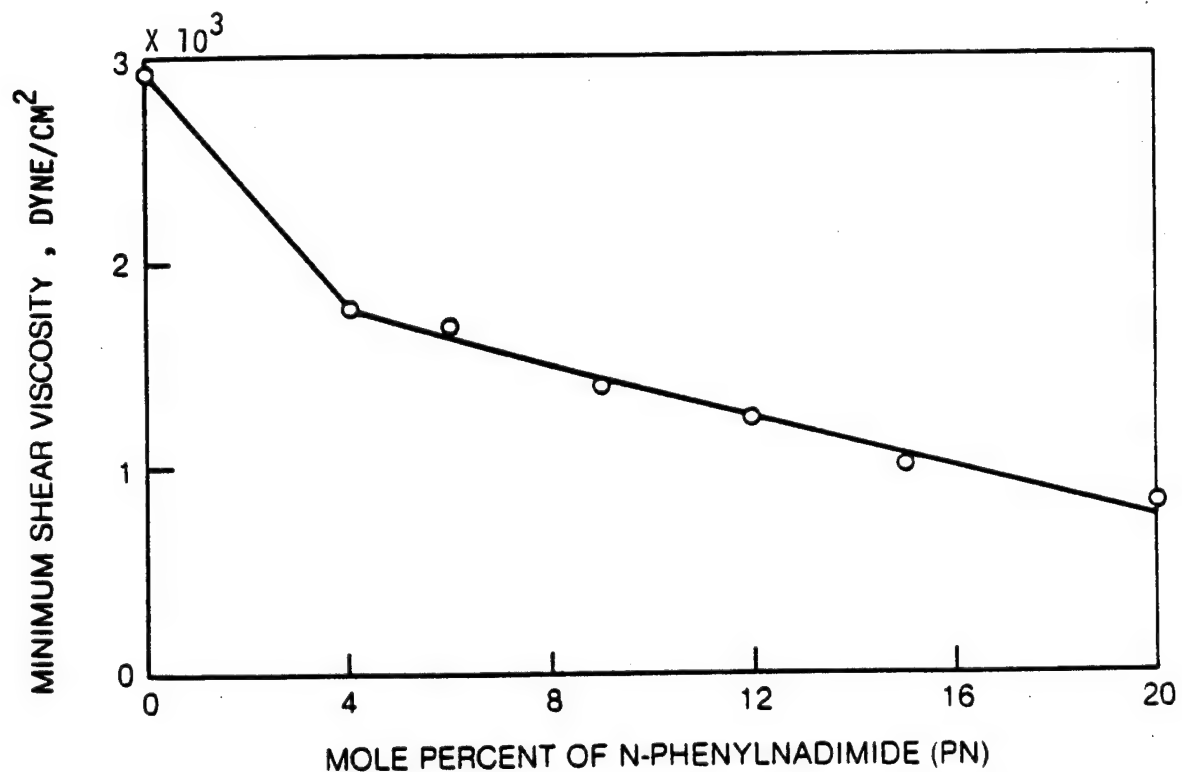


Figure 5. - Minimum shear viscosity as function of PN concentration for PMR-PN molding powders.

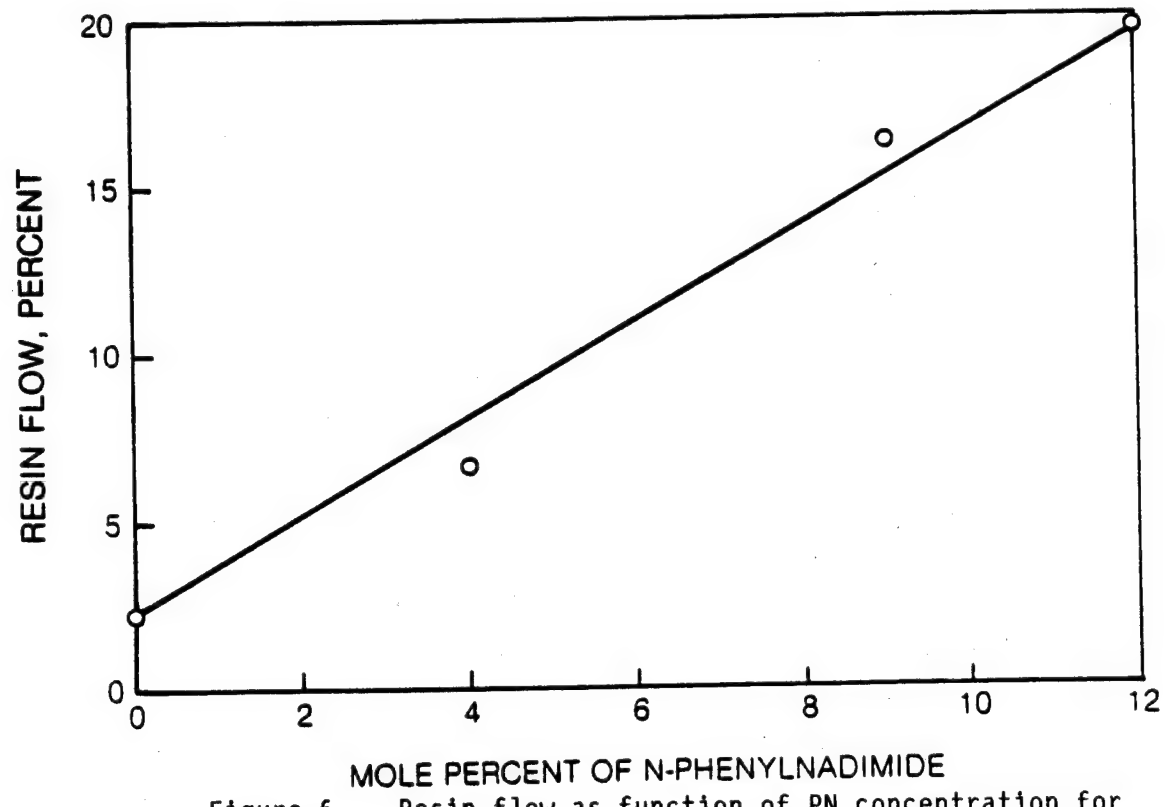


Figure 6. - Resin flow as function of PN concentration for Celion 6000/PMR-PN composites.

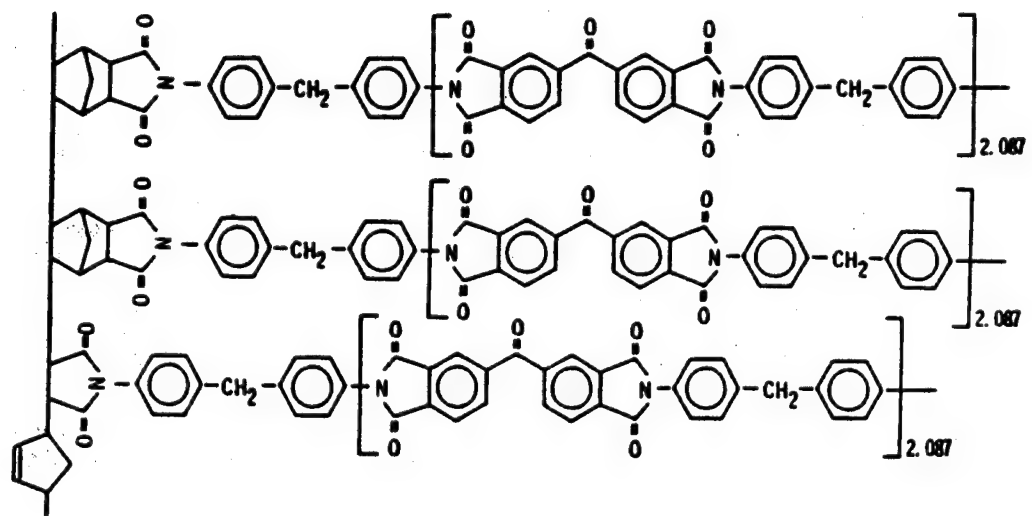


Figure 7. - Idealized structure for PMR-15.

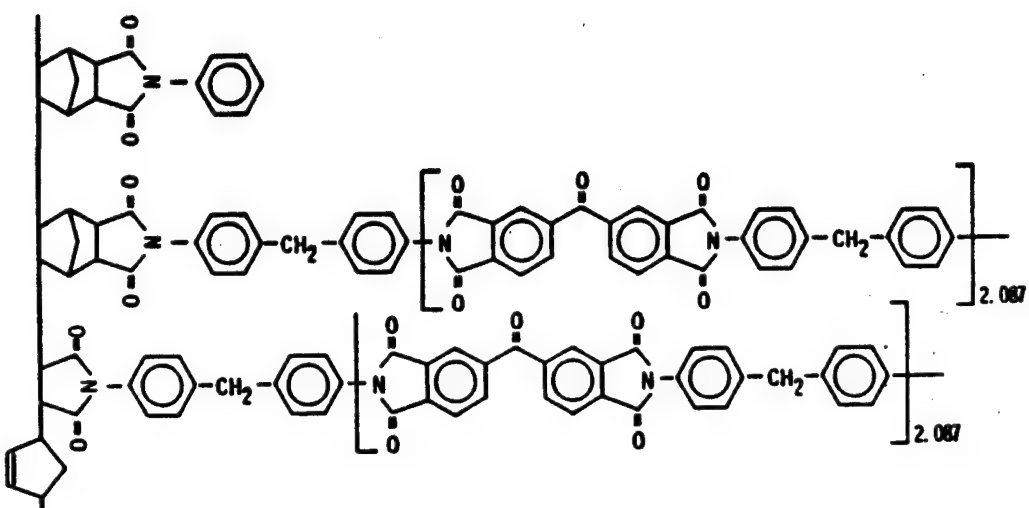


Figure 8. - Idealized structure for PMR-PN polyimide.

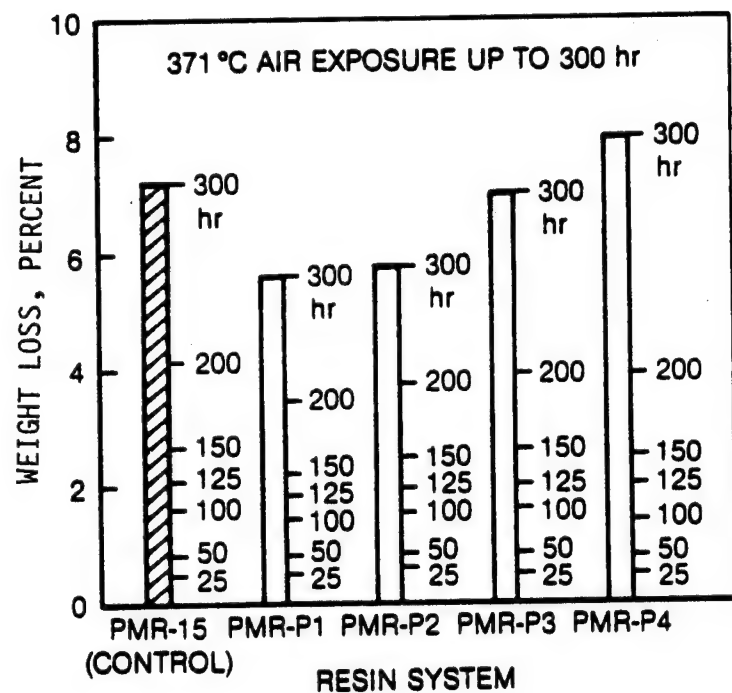


Figure 9. - Weight loss of postcured Celion 6000/PMR-PN composites.

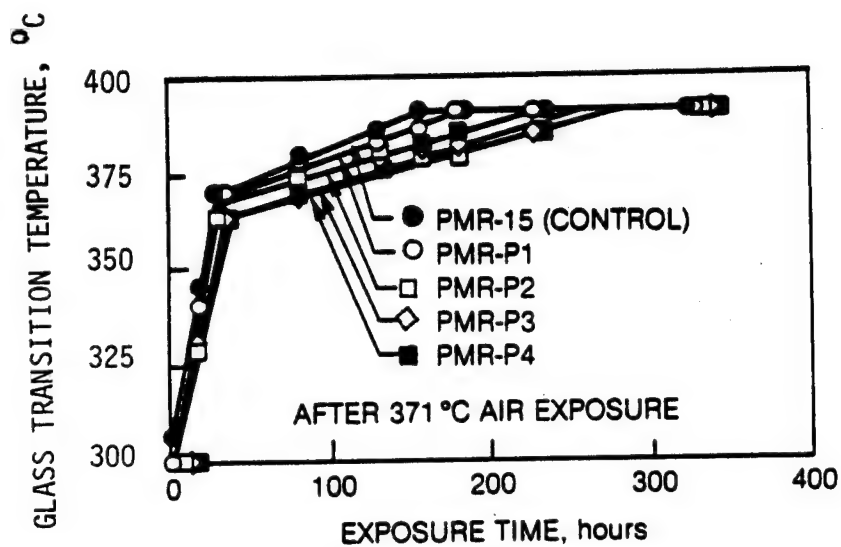


Figure 10. - Glass transition temperature as function of exposure time for as fabricated Celion 6000/PMR-PN composites.

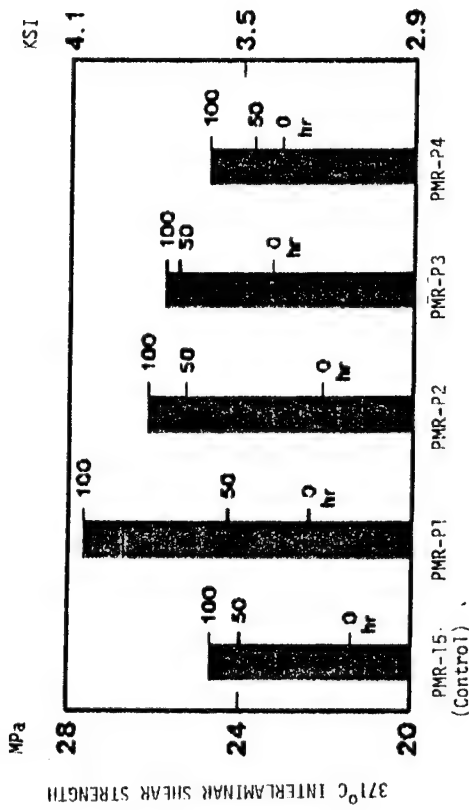


Figure 11. - Flexural strength of postcured Celion 6000/PMR-PN composites at 371 °C.

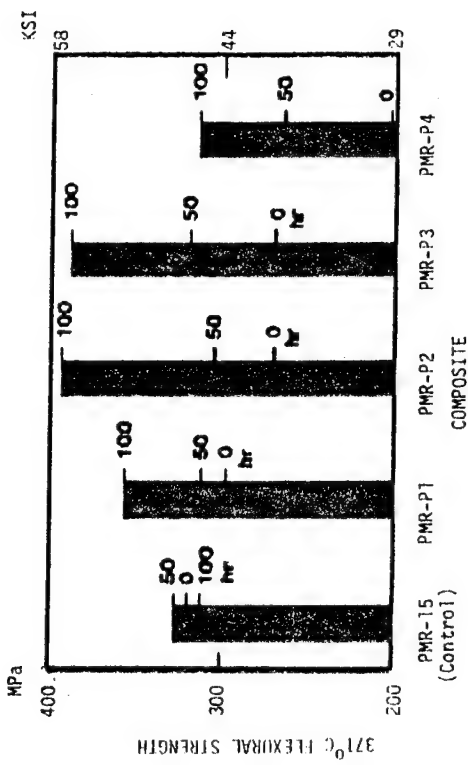


Figure 11. - Flexural strength of postcured Celion 6000/PMR-PN composites at 371 °C.

Figure 11. - Flexural strength of postcured Celion 6000/PMR-PN composites at 371 °C.

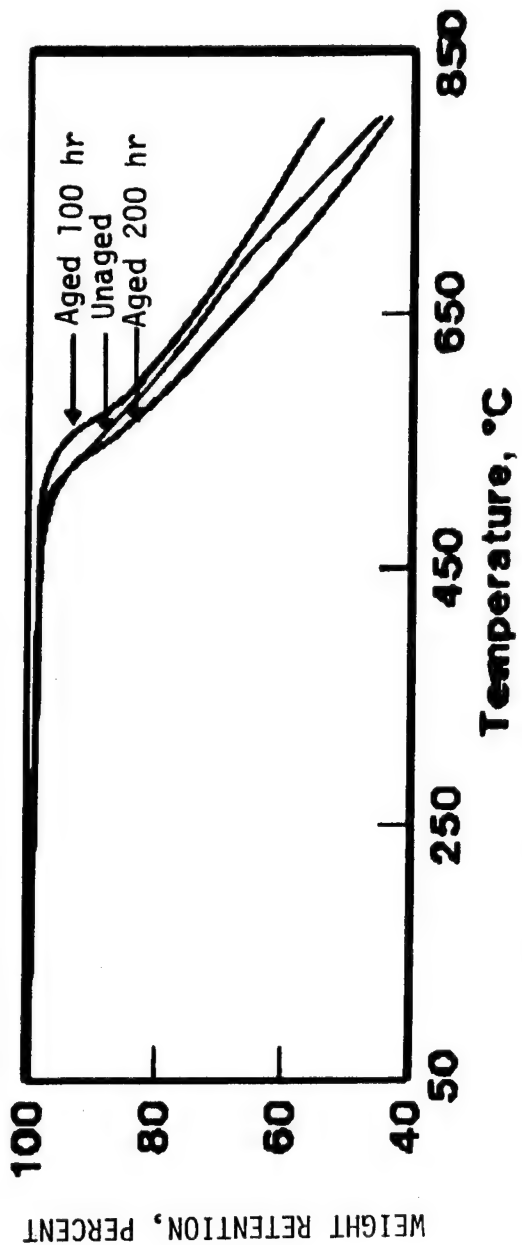


Figure 12. - Interlaminar shear strength of postcured Celion 6000/PMR-PN composites at 371 °C.

Figure 13. - Thermogravimetric analysis curves for PMR-P1 resin exposed in air at 371 °C.

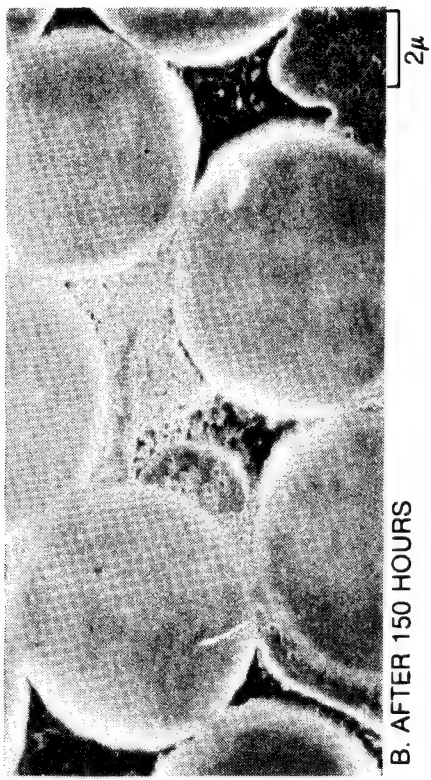


A. CELION 6000/PMR-P1

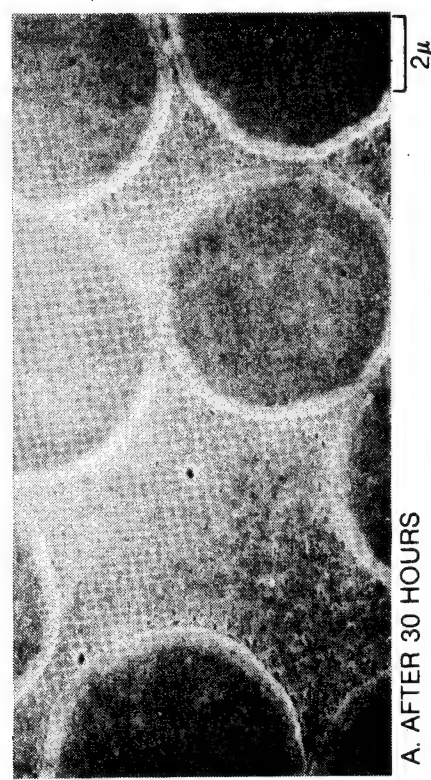


B. CONTROL CELION 6000/PMR-15

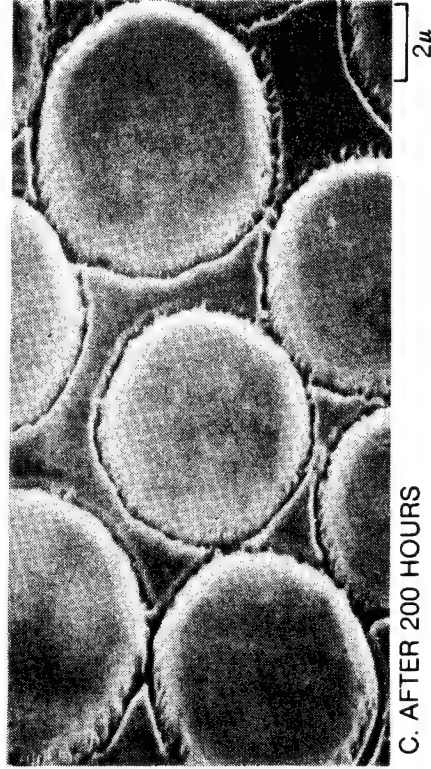
Figure 14. - Comparison of fiber retention characteristics for Celion 6000/PMR-P1 and control PMR-15 composites after a 30 hr postcure followed by a 200 hr exposure in air at 371 °C.



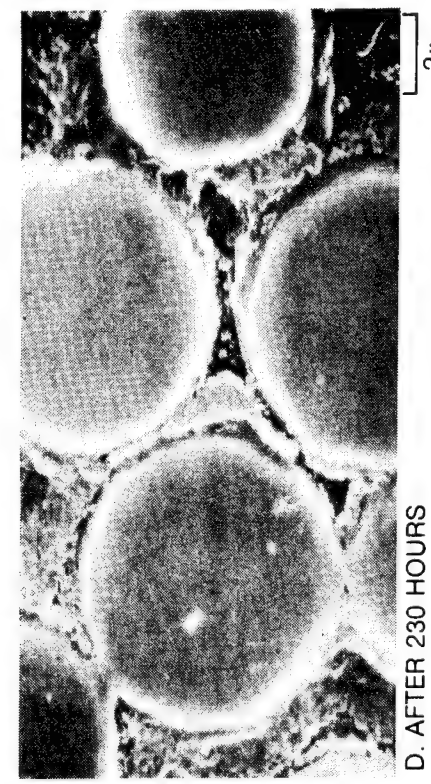
A. AFTER 30 HOURS



B. AFTER 150 HOURS



C. AFTER 200 HOURS



D. AFTER 230 HOURS

Figure 15. - SEM photomicrographs of Celion 6000/PMR-P1 composites after a 30 hr postcure followed by exposure in air at 317 °C for 120, 170, and 200 hr, respectively.

HIGH TEMPERATURE, SHORT TERM TENSILE STRENGTH OF C6000/PMR-15 COMPOSITES

P.R. DiGiovanni and D. Paterson
Raytheon Company
Missile Systems Division

Tensile tests were conducted on 0° unidirectionally reinforced Celion 6000 graphite fibers in PMR 15 polyimide matrix. Tensile strengths for coupons subjected to short and long term uniform temperatures were obtained. Thick coupons, heated on one side to produce significant transient through thickness temperature gradients, were tested and compared to the strength of specimens with uniform temperature distributions.

All coupons were radiantly heated and reached maximum test temperatures within 15 sec. Tensile loads were applied to the coupons after 15 sec of elevated temperature exposure. Loading rates were selected so that specimen failures occurred within a maximum of 45 sec after reaching the test temperature. Results indicate that significant tensile strength remains beyond the material post cure temperature.

BACKGROUND

Medium range tactical missile airframe components have historically been designed with low cost metallic materials insulated by a variety of thermal protection coatings when flight regimes cause excessive aerodynamic heating of the structure. The major design considerations for missile body shells are strength, stiffness, weight, minimum thickness to permit maximum internal packaging volume, and minimum unit cost in production. Aluminum airframe structures are limited to moderate free flight Mach numbers due to the rapid reduction in strength at temperatures above 600°F. High strength metallic airframe structures are more difficult to manufacture and are subject to increasing material and fabrication costs. Ablation or subliming thermal protection systems are costly, increase the net thickness of components thereby resulting in constricted internal volume, and are susceptible to damage during handling operations and aircraft captive-carry.

The development of advanced continuous filament composite materials over the past two decades has been mainly restricted to applications in the aircraft and space technology areas and has used epoxy matrices which are limited to 250°F - 300°F for long term use. Polyimide matrix materials have recently been developed which can sustain temperatures up to 600°F for long durations. The maturation of graphite/polyimide composites, due to improved manufacturing technology and increasing filament production, has continuously reduced hardware cost, stimulating increasing applications.

The unique aspects of graphite/polyimide materials such as tailor able thermal expansions, stiffness and strength by appropriate selection of laminate orientation are several characteristics important to the missile airframe designer. The strength data at elevated temperatures of most advanced composite materials has been developed for aircraft applications which assume long term exposure at elevated temperature environments. Since many tactical missiles are characterized by flight times of less than two minutes duration at higher than cure temperature, advanced composite strength data obtained for long term high temperature exposure

is potentially conservative for missile airframe applications. Therefore, a test program was conducted to determine if the strength of graphite/polyimide could be extended to temperatures up to 900°F for short durations.

Two issues are being addressed as part of the short time high temperature strength evaluation of advanced composites. First, the evaluation of tensile strengths of 0° unidirectional six ply thick graphite/polyimide coupons when subjected to uniform through thickness transient temperatures for exposure times of one minute or less. Second, the tensile strength evaluation of 20 ply thick 0° graphite/polyimide coupons wherein significant through thickness temperature gradients existed. For the latter case, high temperature exposure was limited to one minute and maximum temperatures reached were the same as for the thin (six ply) test cases. The purpose of tests conducted during the existence of thermal gradients across the thick test coupon was to determine whether higher tensile strengths could be achieved in those cases than for the uniform temperature case. When comparing strengths for both transient uniform and transient non-uniform coupon temperature histories, strengths for the non-uniform case were based on maximum face temperatures, not average through thickness temperatures.

Shown in figure 1, for tactical missiles, are typical ranges of maximum external surface structural component temperature ranges, maximum through thickness temperature differences, time to reach and time to maximum temperature, and total flight times.

Ranges shown in figure 1 represented the bases for the tensile coupon tests conducted during the presently reported experimental study.

TEST SPECIMEN PREPARATION, INSTRUMENTATION, AND TEST PROCEDURE

Tensile test, straight edged, 0° unidirectional tabbed coupons were cut from Celion 6000/PMR-15 panels fabricated by the Hamilton Standard Division of United Technologies Corp., Windsor Locks, Ct. Six ply and twenty ply panels, 9 in. x 10 3/4 in., were press-cured in heated ceramic platens. The six ply laminated panels were used to provide uniform through thickness transient temperature test coupons, while the thicker twenty ply laminated panels provided test coupons used for through thickness transient temperature gradient tensile tests. The unidirectional panels were fabricated from Fiberite prepreg HY-E 1666AE, Lot C1-467. The laminated panels were imidized and cured following a procedure developed by Hamilton Standard for fabrication of C6000/PMR-15 F100 engine nozzle flaps. The panels were postcured at 600°F for 12 hrs. in an air circulating oven.

Test coupon tab materials were fabricated using seven plies of 0°/90° 7781 fiberglass cloth/PMR-15 laminate for the six ply 0° coupons and twenty plies of 0° C6000/PMR-15 laminate for the thick twenty ply coupons. For the latter case, an additional twenty ply C6000/PMR-15 panel was specifically fabricated to provide tab material for the thick coupons. Tab lengths were 1 1/2 in. for both thin and thick coupons and were bonded to the panels using PMR-15 adhesive for subsequent cutting into straight edged tensile coupon shape. Tab angles for all test coupons were 90°. Coupon widths were 0.5 in. nominal for thin (six ply) and thick (20 ply) coupons. Panel cutting was performed with diamond blades to ensure high finishes on coupon edge faces.

Thermocouples were bonded back-to-back at the center of each coupon, using M Bond-610 adhesive. The thermocouple adhesive was cured at 325° for 30 min. Thermocouple wires were perpendicular to the specimen axis to minimize shadowing of the radiant flux. Details of the thin and thick test coupons and thermocouple locations are shown in figure 2.

A modular radiant heating reflecting assembly, using a bank of quartz lamps on each side of the test coupon, was adapted to an MTS series 810 Material Testing System. Thermocouple output was fed back to a temperature controller which regulated power to the lamps in order to obtain desired transient temperature responses on each side of the Gr/Pt test coupons. Temperature rise times, temperature hold times, and temperature gradients as measured by the center located thermocouples could be controlled. A schematic of the controlled radiant heating apparatus and instrumented tensile test coupon affixed to the tensile tester is depicted in figure 3. The grips were insulated during all elevated temperature tests.

Temperature response tests were conducted on a six ply tension coupon to determine the ability to control transient through thickness temperature nonuniformity as well as to measure axial temperature variations which existed during transient heating.

To determine both these coupon temperature responses, one of the standard six ply coupons was instrumented with eight thermocouples distributed axially along the mid-center line on one side and four thermocouples on the opposite side. The thermocouples located at the axial center position were back to back. The remaining four opposite side thermocouples were axially offset from 0.10 in. to 0.45 in. Three thermocouples were embedded 0.40 in. in the tab. The location of the thermocouples is shown in figure 4. The thermocoupled coupon was placed in the tensile tester with grips locked on the tabs. A negligible mechanical load was applied sufficient to maintain the coupon in a fixed position during the application of heat. The most severe heating condition was one wherein the temperature of the center of the coupon, initially at 77°F, reached 800°F within 15 sec. Between 20 sec and 80 sec the measured temperature was controlled to monotonically increase from 845°F to 865°F. At 80 sec into the experiment the heat lamps were turned off. The maximum temperature difference between each side of center of the six ply coupon did not exceed 25°F and occurred when coupon center temperatures exceeded 850°F. Maximum temperature within the tab, adjacent to the bond line, reached 210°F after 88 sec. The results obtained from the previously described experiment were used to determine the effect of axial temperature variation on the test coupon stresses. A three dimensional finite element stress analysis was performed on a typical six ply tabbed Gr/Pt coupon, and the results will subsequently be discussed.

TEST RESULTS

Having established repeatability and ability to control transient prescribed temperature histories at the center of the coupon, as well as maintaining a uniform axial temperature distribution about the major axial portion of the test coupon gage length, tension tests during long term steady state heating and transient heating conditions were conducted. Steady state heating in the present context refers to 10 min. exposure to heating, at the end of which time coupon temperatures over the coupon gage length were uniform. Shown in figure 5 are the ultimate tensile strengths after 10 min. exposure to temperatures measured at the test coupon center. Because of the need to conserve test coupons for transient temperature tests, only one test at each steady state temperature was performed. However,

while the initial set of six ply 0° coupons had observable tab offset (each side of different length) due to initial fabrication problems, four were tested at room temperature conditions. Three of these four tests resulted in an average ultimate stress 203 ksi with a spread of 4 ksi. The fourth coupon, with significant damage in the six ply region at the edge of the tab, resulted in failure at the tab at a stress of 172 ksi. An additional six ply panel was fabricated and the tab problem corrected. No data from coupons obtained from the problem tab panels is presented. While the test data from the C6000/PMR-15 coupons exceeds that in reference 1, it is important to note that two different Gr/P1 systems are compared in the results shown in figure 5. Also, the test coupon of (ref. 1) has a 4 in. gage section and 2.5 in. bevelled tabs. The increase in strength from 750°F and 850°F may be illusory because of the minimum specimens tested, and/or post curing effects. The former seems more likely since the 0° tensile strengths are fiber dominated.

In order to determine transient short term tensile strengths with uniform through thickness temperature distributions, six ply coupons were subjected to temperature histories as shown in figure 6. Loading was applied at a constant load rate at 15 sec following start up of heating, and all coupons failed within 40 sec. Assuming that the 0° tensile modulus is never reduced below 5×10^6 psi for all short term temperatures to 850°F. max., this results in maximum strain rate during the tests of 0.05 in/in-min.

The corresponding ultimate tensile strengths for short term uniform through thickness elevated temperatures are shown in figure 7.

Three tensile tests at each temperature were conducted as shown in figure 7. The primary results indicate that up to 850°F, approximately 70 percent of room temperature strength is maintained for up to 40 sec. Failure stresses for the six ply coupons were between 199-205 ksi at room temperature and between 125 and 165 ksi when subjected to short term 850°F transient temperatures. Relatively smooth strength decreases were obtained for coupons subjected to temperatures between R.T. and 850°F. Unlike the steady state ultimate strength behavior, significant strength decrease is apparent at 450°F, well below the post cure temperature of 600°F. Strength continues to decrease with temperature to 750°F and then remains constant but with increasing scatter to 850°F. This differs significantly from the steady state 0° tensile strength variation up to matrix post cure temperature experienced by graphite/epoxies (ref. 1) and graphite/polyimides (ref. 2).

In order to determine whether significant strength increases occur when high transient temperatures occur on only the external structural surfaces and large through thickness thermal gradients exist due to low transverse thermal conductivity, transient temperature histories were produced in thick, [0°]20, coupons as shown in figure 8.

As in the case of [0°]6 coupons, tensile loads were applied to the thick coupons following 15 sec of heating. After 20 sec of heating the maximum temperature on one side of the coupon was held constant while the temperature on the cooler side continued to increase. At 50 sec heating ceased and temperatures on both sides of the coupon instantaneously decreased. For the thermal gradient test, ultimate tensile stresses obtained for maximum coupon surface temperature of 650°, 750°, 850° and 950°F are shown in figure 9.

No significant increase in strength for coupons subjected to short term thermal gradients were observed when compared to the coupons subjected to short term uniform temperatures for the same maximum temperatures. Even when the short term thermal gradient strength data is compared to strengths obtained for long term temperature subjected coupons (figure 5), no significant increase in tensile strength is observed. (However, sufficient analysis has not been conducted to determine whether longer end tabs should be used for 20 ply straight coupons and if a uniform uniaxial state of stress exists in the gage section of 9 in. thick coupons.) The low value of room temperature ultimate stress, as shown in figure 9, for the $[0^\circ]_{20}$ tensile specimen compared to the $[0^\circ]_6$ specimen suggests at least a further investigation into the stress state in thick tensile coupons. Also, it should be noted that 5 percent less fiber volume was measured in the thick 20 ply panel than in the thin six ply panel from which the test coupons providing the data in question were obtained (both fiber volume measurements were obtained from one random sample of each panel).

THREE DIMENSIONAL FINITE ELEMENT IDEALIZATION OF THERMAL STRESS EFFECTS

To better understand the effect of axial thermal gradients in the $[0^\circ]_6$ Gr/Pi test coupon, the test coupon including end tabs and adhesive were analyzed using the finite element idealization.

Symmetry of the test coupon enables the stress analysis to be performed using one-eighth of the coupon. The analysis is based on a 20 node isoparametric orthotropic brick element using the SAPV Structural Analysis Program (ref. 3). The finite element model represents a 6 laminae 0° unidirectional Gr/Pi end tab, a 0.002 in. PMR-15 adhesive layer, and a 6 laminae 0° unidirectional Gr/Pi specimen.

The end tab was modeled using three elements (two laminae) in the thickness direction, the adhesive layer by one element in the thickness direction, and the test specimen by 6 elements in the thickness direction, one for each lamina. The width of the elements was reduced in the tab end region in the axial direction of the center of the test coupon. It is assumed that the test coupon is stress free at the post cure temperature of 600°F. The detailed finite element geometrical model is shown in figure 10. The tab and adhesive element widths are 0.05 in. in the tab/specimen region and increase to 0.25 in. for the remainder of the tab. The specimen element width is 0.1 in. and increases to 0.5 in. for the remainder of the specimen length.

The measured temperature distribution for the $[0^\circ]_6$ ply coupon at 25 sec after heating is shown in figure 11. Through thickness variations were small and neglected in the finite element analysis.

Material properties used in the finite element analysis are given below:

Graphite/Polyimide Specimen (refs. 4 and 5)

$$E_{11} = 20 \times 10^6 \text{ psi} \quad E_{22} = E_{33} = 1.2 \times 10^6 \text{ psi}$$

$$G_{12} = G_{13} = G_{23} = 1 \times 10^6 \text{ psi}$$

$$\nu_{12} = \nu_{13} = \nu_{23} = 0.33$$

$$\alpha_{11} = 1 \times 10^{-7} \text{ in/in-}^{\circ}\text{F}$$

$$\alpha_{22} = \alpha_{33} = 1.44 \times 10^{-5} \text{ in/in-}^{\circ}\text{F at } 70^{\circ}\text{F}$$

$$\alpha_{22} = \alpha_{33} = 1.58 \times 10^{-5} \text{ in/in-}^{\circ}\text{F at } 300^{\circ}\text{F}$$

$$\alpha_{22} = \alpha_{33} = 1.15 \times 10^{-5} \text{ in/in-}^{\circ}\text{F at } 900^{\circ}\text{F}$$

PRM-15 Adhesive (ref. 6)

$$E = 0.47 \times 10^6 \text{ psi}$$

$$G = 0.17 \times 10^6 \text{ psi}$$

$$\nu = 0.36$$

$$\alpha = 28 \times 10^{-6} \text{ in/in-}^{\circ}\text{F}$$

The important results for calculated stresses are shown in figure 12. Recall that the stresses calculated are due solely to steady temperature distribution measured experimentally. The stress free state was assumed to exist at the post cure temperature of 600°F.

The maximum transverse coupon normal stress distribution indicates failure of the matrix between fibers in the tab region. Examination of the temperature distribution (figure 11) shows that coupon temperatures are below 200°F. Since the tab is fixed on the outer face, the large transverse tensile stress is in response to constraining the coupon contraction. At the stress level predicted severe microcracking would have been initiated leading to a redistribution of transverse stress. Since the tensile tests are fiber dominated, no significant effect of the transverse cracking on the 0° tensile would be expected if damage between the matrix and fiber surface also does not result. The early strength decrease with temperature as shown in figure 7 may be an indication of early fiber/matrix interface failure. Further experimentation and photomicrographic examination of sectioned tab region is indicated to better understand the failure mechanism under elevated temperature highly transient environments.

CONCLUDING REMARKS

Tensile tests at transient elevated temperatures on [0°]₆ Celion 6000/PMR-15 graphite polyimide material for maximum temperatures up to 850°F were conducted. It was shown that controlled quartz heat lamps can provide near uniform through thickness temperature distributions for 60-70 sec for six ply coupons. Thick, 20 ply 0° coupons were used to provide controlled maximum surface temperature and prescribed transient temperature gradients.

During uniform through thickness transient temperature tests, 0° strength decreased moderately at 450°F, while 70 percent of the room temperature strength existed for peak transient temperature up to 850°F. Tensile strengths up to 115 ksi were obtained for 20 ply 0° coupons when the outer surface maximum temperature reached 950°F in less than one minute. A three dimensional finite element analysis of a [0°]₆ heated coupon, exhibiting a significant axial thermal gradient, indicated high transverse tensile normal stress in the tab region of the tensile coupon. Finally, in order to better understand failure of thick unidirectional

coupons subjected to short term through thickness and axial temperature gradients, a detailed stress and thermal analysis should be further studied to determine edge and thickness effects and to establish an optimum tensile coupon configuration.

REFERENCES

1. Hofer, K.E., Jr.; Larsen, D.; Humphreys, V.E.: Development of Engineering Data on the Mechanical and Physical Properties of Advanced Composite Materials. AFML-TR-74-266, 1975.
2. Kerr, J.R.; Haskins, J.F.: Time-Temperature-Stress Capabilities of Composite Materials for Advanced Supersonic Technology Application - Phase I. NASA CR-159267, 1980.
3. SAPV2: A Structural Analysis Program for Static and Dynamic Response of Linear System USC, Dept. of Civil Eng'g. Los Angeles, 1977.
4. Campbell, M.D.; Burleigh, D.D.: Thermophysical Properties Data on Graphite/Polyimide Composite Materials: NASA CR-159164, 1979.
5. McCleskey, S.F.; Cushman, J.B.; Skoumal, D.E.: High Temperature Composites for Advanced Missiles and Space Transportation Systems. AIAA Paper No. 82-0707, 1982. Also in Proc. AIAA/ASME/ASCE/AHS 23rd Structures, Structural Dynamics and Materials Conf., May 1982, pp. 212-222.
6. Hanson, M.P.; Chamis, C.C.: Graphite Polyimide Composite for Application to Aircraft Engines. NASA TN-D-7698, 1974.

- MAX SURFACE TEMP – 750°F – 1000°F
- ΔT AT MAX TEMP – 100°F – 175°F
- TIME TO MAX TEMP – 15 sec – 30 sec
- TIME AT MAX TEMP – 0 sec – 10 sec
- TOTAL FLIGHT TIME – 24 sec – 70 sec

Figure 1 Typical medium range tactical missile temperature response.

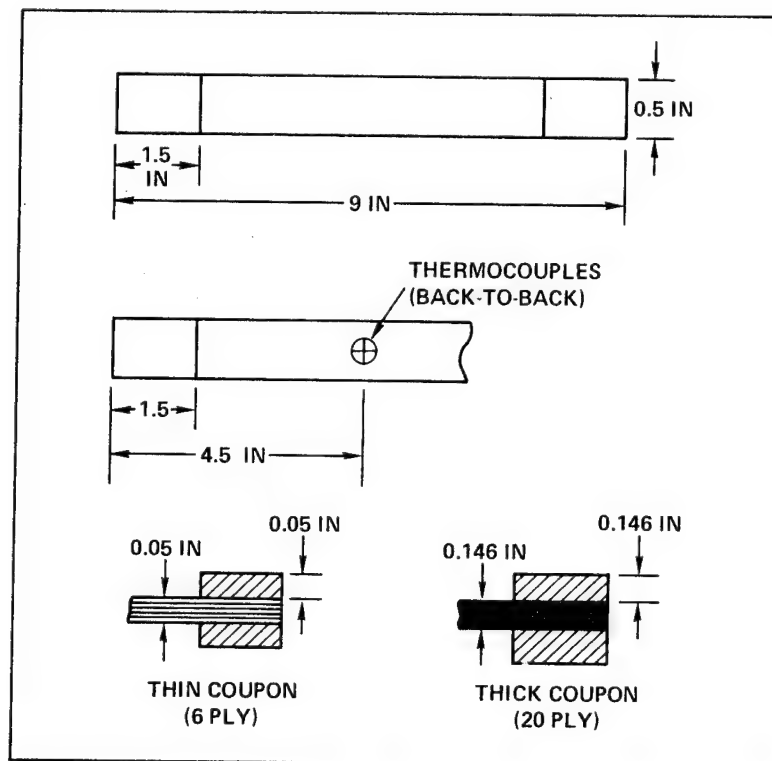


Figure 2 Test coupon and instrumentation details.

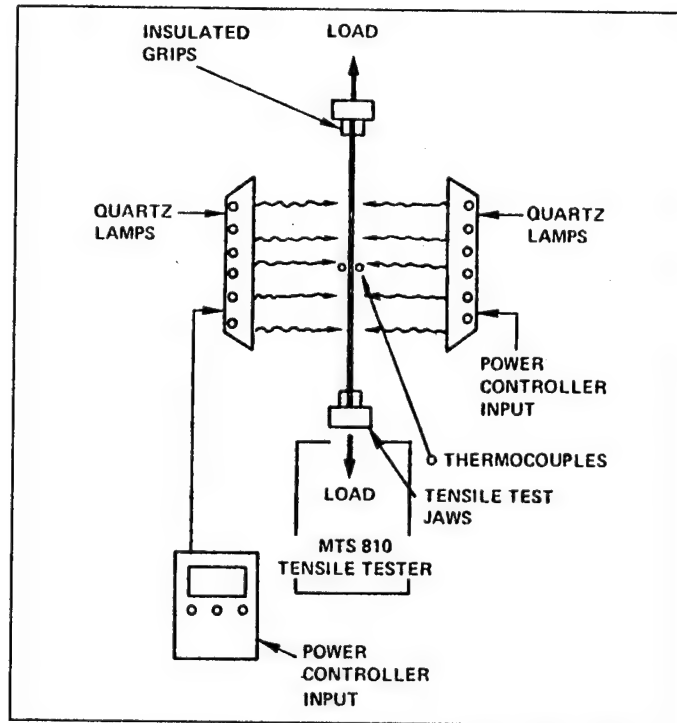


Figure 3 Transient heating/tensile loading schematic.

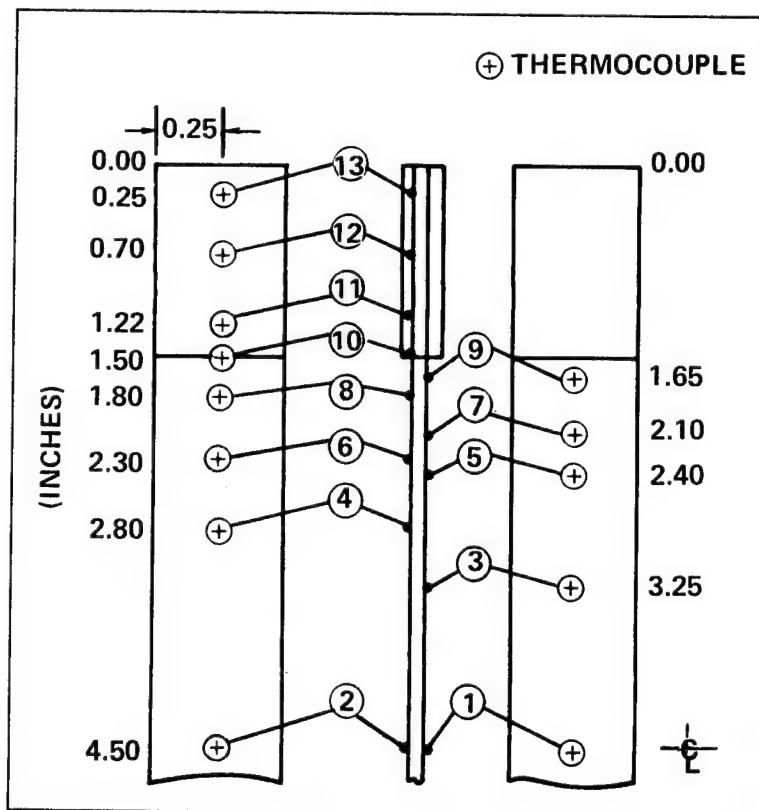


Figure 4 Thermocoupled test coupon (6 ply - 0°).

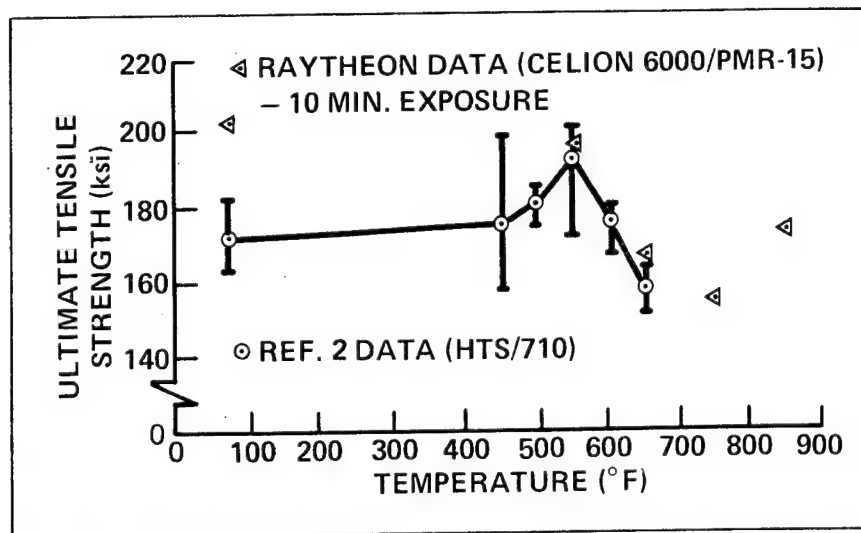


Figure 5 Long term uniform temperature tensile strength of 0° Gr/Pi.

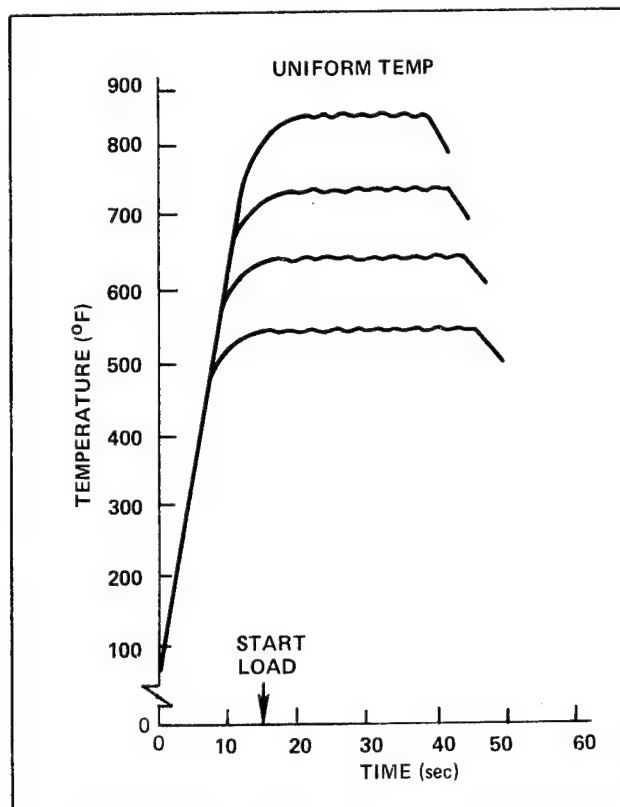


Figure 6 Transient temperature histories for 0° 6 ply tensile coupons.

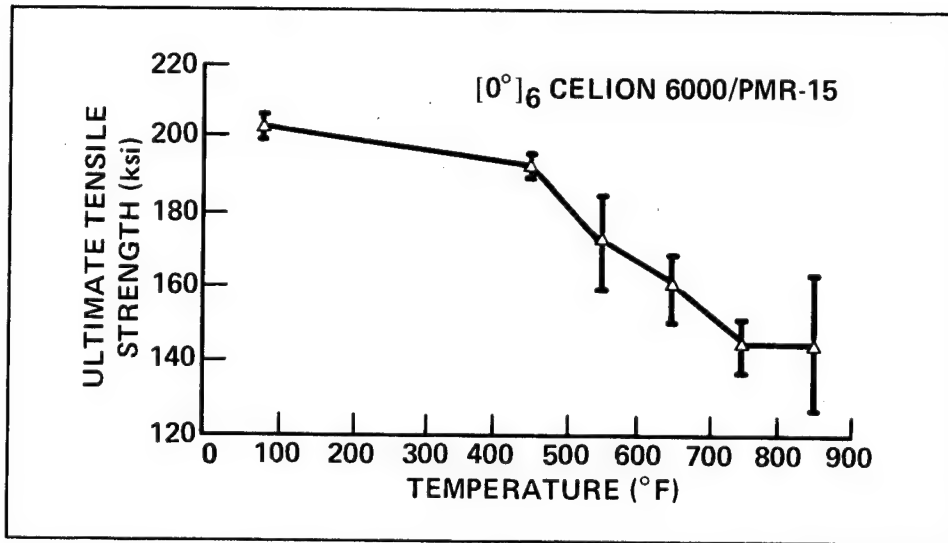


Figure 7 Short term uniform temperature tensile strength.

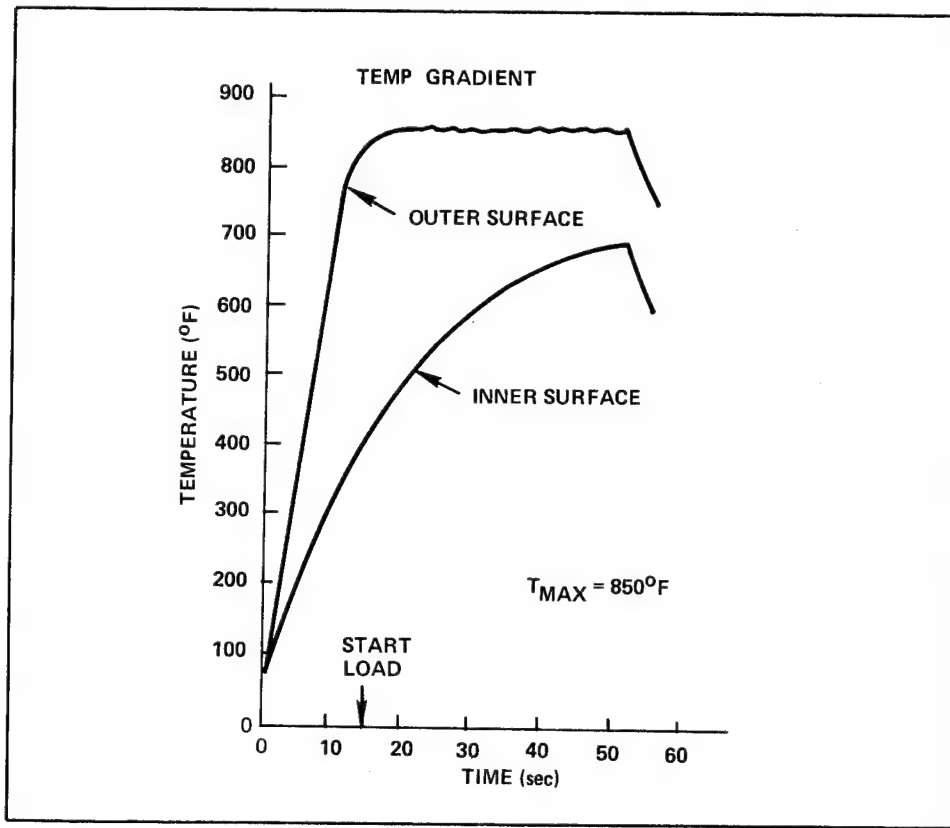


Figure 8 Transient temperature history for [0°]₂₀ coupons.

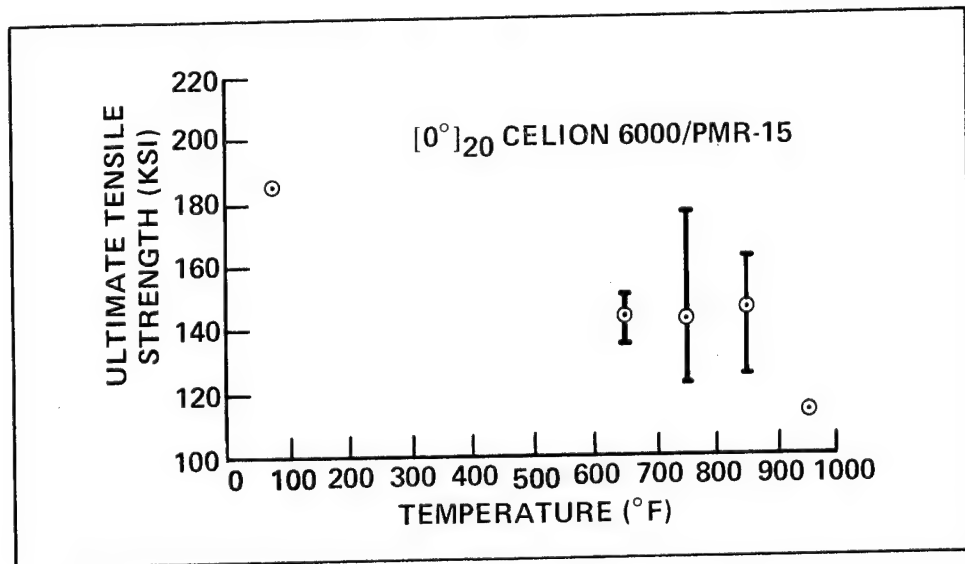


Figure 9 Short term thermal gradient tensile strength.

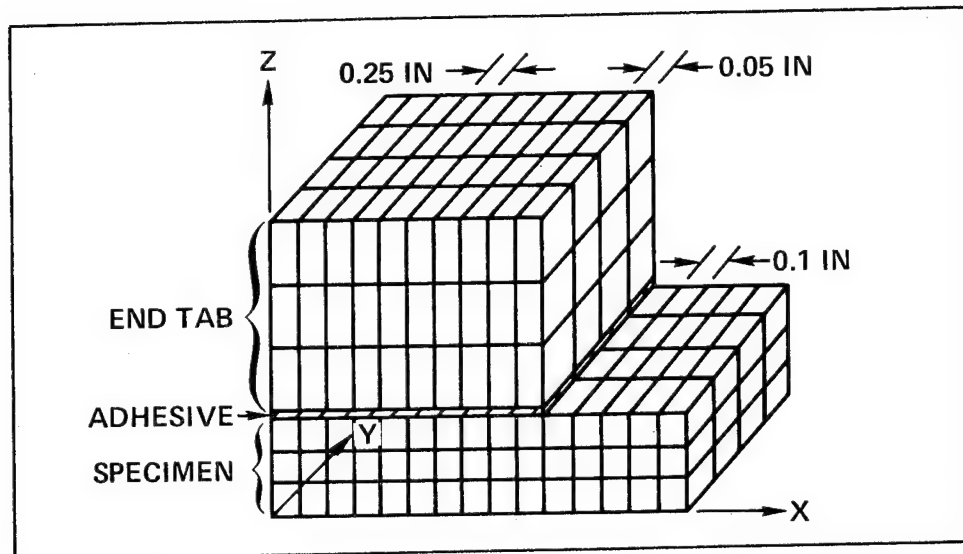


Figure 10 F.E. idealization of test coupon.

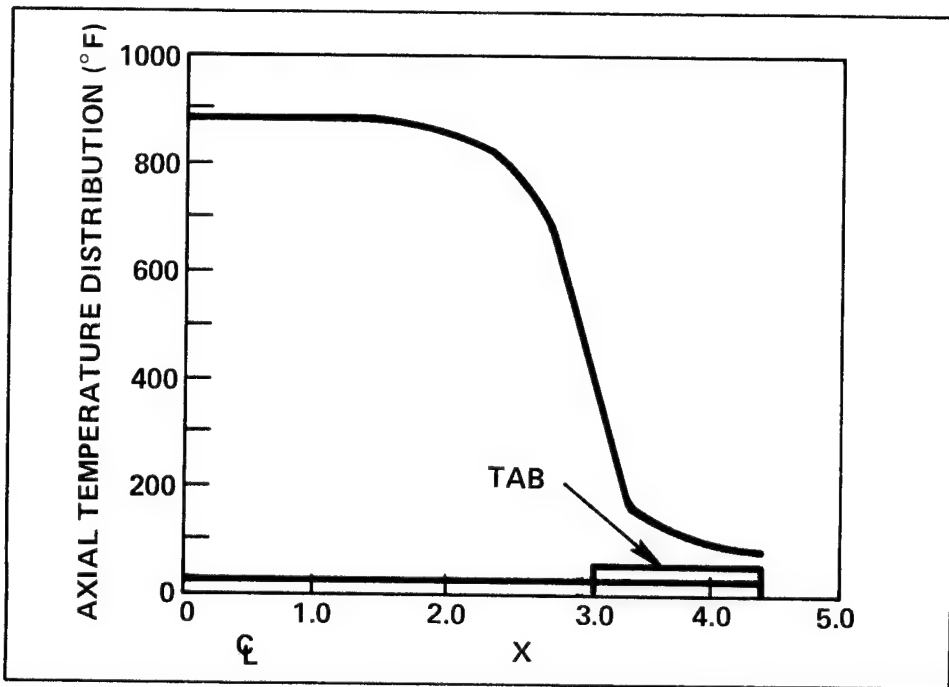


Figure 11 Temperature versus axial position along $[0^\circ]_6$ for maximum axial temperature gradient.

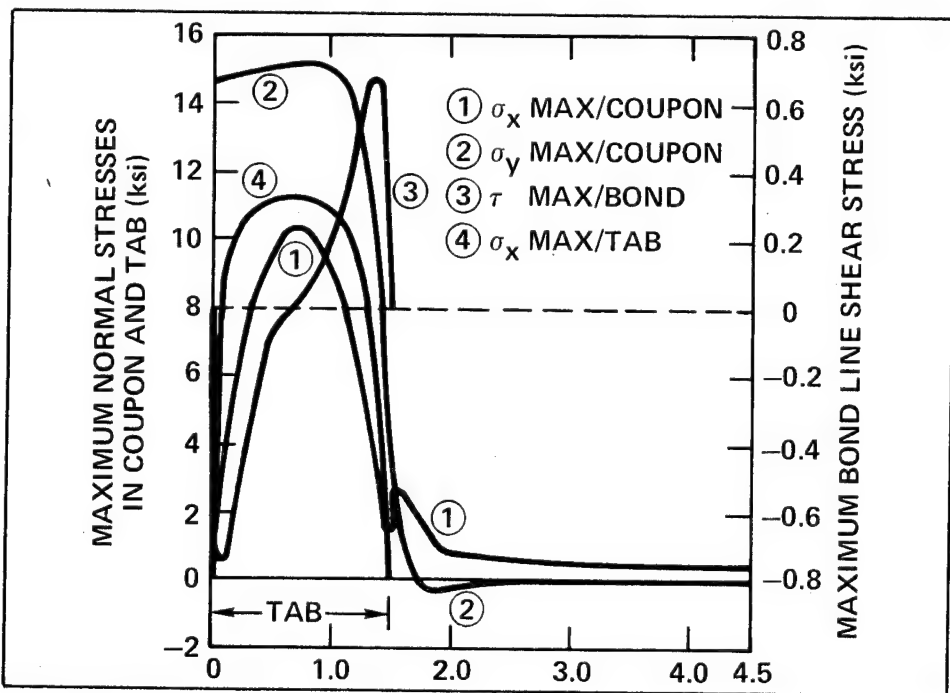


Figure 12 Maximum stress distributions in coupon, bond line, and end tab due to heating (stress free temperature = 600°F).

POLYIMIDE MATRIX RESINS FOR UP TO 700°F SERVICE

R. J. Jones, G. E. Chang, S. H. Powell and H. E. Green
TRW Energy Development Group

1.0 INTRODUCTION

Linear aromatic/heterocyclic condensation polyimides were the first candidates of this generic type of polymer to find acceptance as an item of commerce. Different types of the linear condensation polyimides have been qualified for many aerospace applications including matrices for high performance seals, bushings, bearings and radomes as well as wire coatings and other applications. Upper use temperatures in air normally employed for the first generation linear condensation polyimides were 316°C (600°F) and below.

A series of linear condensation polyimides have appeared on the market beginning in the 1960's for high performance resin applications. The polymer systems that have endured as viable commercial systems include such resins as Skybond polyimides from Monsanto (Reference 1) and the Vespel and Kapton polyimide products available from Du Pont (References 2 and 3).

In the mid-1960's, when requirements began to emerge for high performance, large airframe structures fabricated from polyimides, key deficiencies inherent with linear condensation polyimides began to manifest themselves. Upon attempts to compression mold thick reinforced laminates and/or autoclave fabricate composite structures, the continual evolution of residual solvent and aqueous condensation volatiles consistently led to high void content products which were unsuitable for most structural applications. Also, the normally existing high molecular weight state of the linear condensation polyimides required processing parameters, particularly high pressures, which continue to be beyond the capability of state-of-the-art autoclave fabrication hardware. These deficiencies prompted the trade to investigate alternative polyimide approaches to the linear condensation materials.

The quest for alternative high performance resins to linear condensation polyimides began in the mid-1960's. The major thrust in this work

emphasized research on technology which minimized evolution of volatiles during fabrication and cure as well as alteration of resin molecular weight to promote facile autoclavability at pressures of 1.3 MPa (200 psi) or less. The two most successful alternative polyimide approaches which give resins suitable for longer-term service at temperatures up to 316°C (600°F) are the norbornene and acetylene terminated polymers.

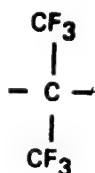
In 1966, TRW discovered that low molecular weight (e.g., 1000 g/mol to 2000 g/mol) polyimide prepolymers terminated by nadic anhydride processed in a significantly easier fashion than the linear condensation polyimides. Addition cure through the elements formed from the nadic moiety at 316°C gave essentially void free composite structures. This work led to introduction of a commercial product designated P13N (Reference 4). Significant ingredient formulary improvements at NASA Lewis Research and NASA Langley Research Centers have led to new polyimide products designated PMR-15 and LARC-160 resins, respectively (References 5 and 6, respectively). Each of the improved products are finding wide trade acceptance as autoclavable, high performance polyimides and have essentially replaced P13N.

While TRW was investigating the technology that led to P13N, research at Hughes Aircraft Company discovered that polyimide prepolymers, terminated in aromatic acetylene derivatives, gave cured polymers possessing processability, low void content and high temperature use characteristics very similar to P13N. These acetylene terminated resins have been designated HR-600-type polyimides (Reference 7). Development work on improved polyimide modifications is continuing at Hughes Aircraft Company (Reference 8).

During the late-1960's, the addition-type polyimides discussed above fulfilled most requirements for high performance resins. This was primarily as a result that needs did not exist for resins that required stability at 316°C (600°F) to 371°C (700°F) in air for hundreds to thousands of hour service lives. However, beginning in the mid-1970's, advanced jet engine development (e.g., Pratt and Whitney's F-100 and GE's F-101) sought matrix resins suitable for use at > 316°F in air atmospheres ranging up to 0.4 MPa (60 psia). These engine requirements prompted additional polyimide

development which has led to identification of second generation, very thermo-oxidatively stable linear condensation polyimides which possess a new type of backbone linkage in the aromatic polyimide backbone.

The initial second generation linear condensation polyimide to be developed were resins containing a perfluoroisopropylidene linkage shown below in either the two ring dianhydride and/or diamine constituent of the



polymers. These polyimides were discovered by Du Pont and introduced to the trade as the NR-150B series of resin products (Reference 9). Although these high performance linear polymers demonstrated significant promise to meet several jet engine composite applications, general sale of the materials to the trade has been recently terminated.

Because of the unavailability of polyimide matrix resins for use at temperatures up to 371°C in air as dictated by the removal of NR-150B resins from the marketplace, TRW initiated development studies in 1980 to assess whether another second generation family of linear resins may be suitable for service at temperatures > 316°C. The new TRW polyimide resins, designated partially fluorinated polyimides, have given data which suggest they do indeed possess thermo-mechanical characteristics making them suitable for service in the temperature range of 316°C to 371°C in air. Ongoing development of the partially fluorinated polyimides as high performance composites matrix resins constitute the topic of this paper. Evaluation studies completed to date are presented and discussed in Section 2.

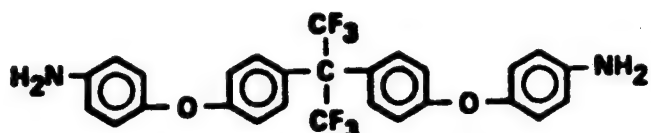
2.0 TECHNICAL DISCUSSION

TRW is in the process of data accumulation that strongly indicates that incorporation of the perfluoroisopropylidene linkage in molecular structures other than those employed in Du Pont's NR-150B polyimides likewise yield polymers demonstrating extremely high thermo-oxidative stability. Polyimide synthetic and characterization studies conducted to

date on new polymers incorporating the perfluoroisopropylidene linkage are presented and discussed below.

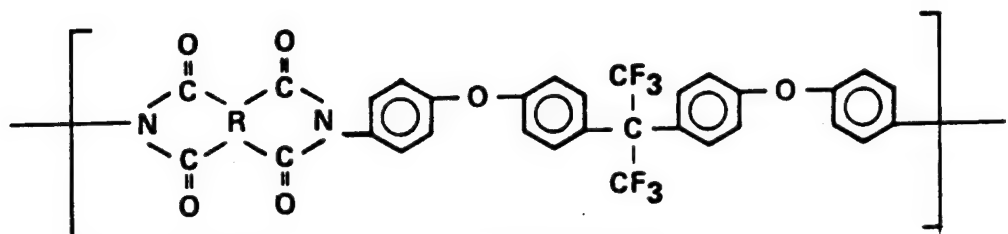
2.1 PARTIALLY FLUORINATED POLYIMIDE CHEMISTRY

TRW has discovered that use of a partially fluorinated aromatic diamine 2,2-bis[4-aminophenoxy)phenyl]hexafluoropropane (4-BDAF, see structure below) yield linear condensation polyimides possessing con-



4-BDAF

siderable promise for long term service in highly oxidative environments at temperatures up to 371°C. The 4-BDAF monomer and polyimides therefrom were discovered in 1975 on NASA Lewis Research Center Contract NAS3-17824 (Reference 10). The diamine monomer and polyimide resins are described and claimed in U.S. Patent Numbers 4,203,922 and 4,111,906 (Reference 11 and 12), respectively. A general structure for polyimides prepared from 4-BDAF diamine is presented below.



WHERE R = AROMATIC RING STRUCTURE

The promise shown in 1980 and 1981 for the 4-BDAF diamine as a key starting ingredient for high performance polyimides prompted Morton Chemical Company to express interest to become a qualified source of supply for the material. After two years of synthesis process and purity

assessment, Morton has recently obtained an exclusive license from TRW to commercially produce and sell the diamine under the art taught in U.S. Patent Number 4,203,922. Limited availability of the product to the trade is anticipated to occur in 1983.

2.2 INVESTIGATION OF PARTIALLY FLUORINATED POLYIMIDES AS A MATRIX FOR 357°C (675°F) SERVICE

Although, as previously stated, the linear condensation polyimides from 4-BDAF diamine were discovered in 1975, directed research and development activities on the diamine and polyimides therefrom was not undertaken at that time due to lack of clearly identifiable markets for products. In 1980, in response to urging by the jet engine primes and government agencies, TRW initiated studies to determine whether the partially fluorinated polyimides produced from 4-BDAF diamine could serve to replace currently available condensation polyimides as well as serve as a potential substitute for the very high performance linear resins offered by Du Pont as the NR-150B family of polyimides.

The 1980 studies on the TRW partially fluorinated polyimides were structured to assess basic thermo-oxidative stability, glass transition temperature and processability characteristics related to potential use as a jet engine compressor stage stator vane bushing at a service life temperature of 357°C (675°F). This effort was jointly sponsored by the GE Aircraft Engine Group, Evendale, Ohio and the Bearings and Applied Technology Divisions of TRW. In this study, a number of significant discoveries were made as summarized below.

Two candidate polyimide polymers were prepared from pyromellitic dianhydride (PMDA) and benzophenonetetracarboxylic acid dianhydride (BTDA) employing TRW's 4-BDAF as the diamine ingredient at the Redondo Beach, California facility. Solutions of the amide-acid precursor were supplied to the TRW Bearings Division, Jamestown, New York for processing studies. The amide-acid solutions were converted into polyimide molding compounds employing Celanese's GY-70 high modulus chopped graphite at a 50% by weight level as the reinforcement. The two candidate materials were compression molded into resin discs of dimensions approximately one-inch in diameter by one-inch thick. Prototype jet engine compressor stator vane bushings

were machined from the discs to 0.001-inch tolerances. A photograph of the prototype bushings is provided as Figure 1.

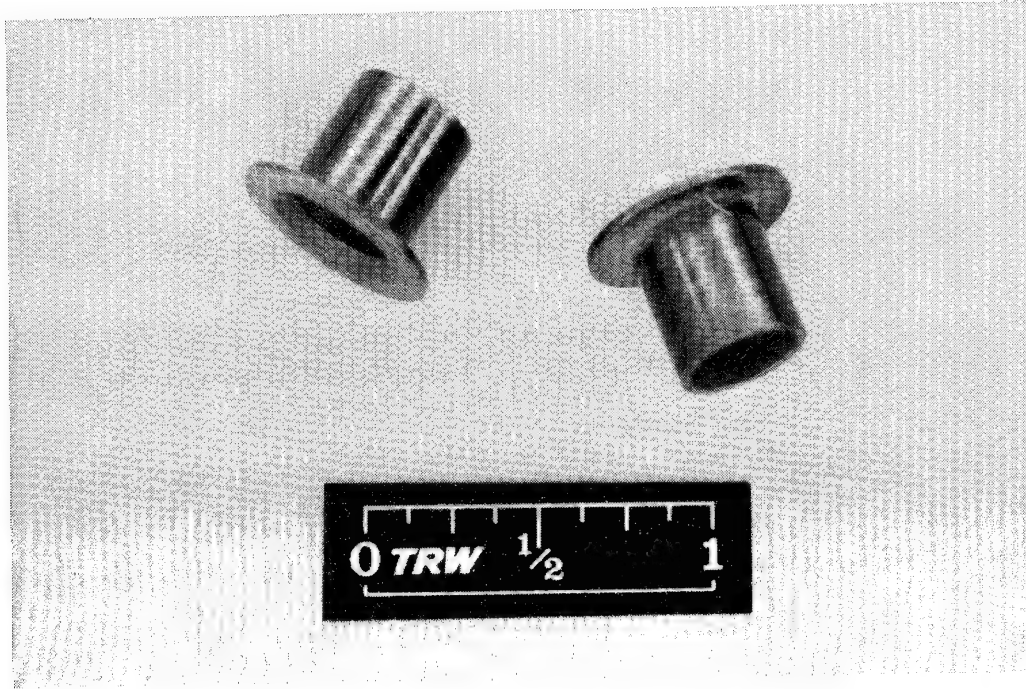


Figure 1. Prototype Jet Engine Stator Vane Bushings

Resin disc samples of each of the two candidate polyimides were provided to GE for oxidative and thermo-mechanical testing. The two polyimide candidates were subjected to the GE oxidative screening test which consists of a one hundred hour exposure at 357°C under a four atmosphere flow of compressed air. The results from this test and related thermal measurements are presented in Table 1. For the purposes of GE product interests, the 4-BDAF/BTDA formulation was definitely unsuitable for further consideration due to its weight loss at 675°F and the surprisingly low glass transition temperature of $\sim 310^{\circ}\text{C}$. Conversely, although the weight loss was relatively high for the 4-BDAF/PMDA formulation, the highly desirable T_g of this candidate of $\sim 390^{\circ}\text{C}$ was held to be very promising and the material was deemed worthy of further study.

Subsequent joint GE/TRW studies on polymer development have yielded neat molded 4-BDAF/PMDA specimens which give a weight loss of only 8% at 357°C. A key factor in this significant product improvement is thought to be the current high quality of the 4-BDAF diamine produced by Morton Chemical on up to 50-lb/run batches. The initial work employed

diamine synthesized at TRW on a much smaller scale. The stator vane bushing development effort is continuing employing diamine produced by Morton Chemical.

TABLE 1
PARTIALLY FLUORINATED POLYIMIDE THERMAL ANALYSIS PROPERTIES

Property Measurement	Experimental Results 4-BDAF/PMDA	Experimental Results 4-BDAF/BTDA
Glass Transition temperature (Tg) ^a)	390°C (734°F)	310°C (590°F)
Onset temperature of oxidative degradation ^b)	495°C (923°F)	490°C (914°F)
Isothermal aging in air (% weight loss) ^c)	20	34

^a) Determined on a Du Pont Model 990 thermalmechanical analysis attachment operating in a penetration mode.
^b) Determined on a Du Pont Model 990 thermalgravimetric analysis attachment employing a 3°C/minute heat-up rate and 100cc/minute air flow.
^c) Determined on composite discs containing 50% by weight GY-70 chopped fiber reinforcement; aging conditions consisted of a 675°F temperature for 100 hours employing a four atmosphere compressed air flow.

The initial promise of the GE/TRW study on the partially fluorinated polyimide prompted TRW to initiate investigation of other resin matrix applications. Initial lubricity and wear test results are the subject of a NASA Lewis Research Center technical publication (Reference 13). Additional tribological property evaluations are being conducted by TRW on NASA Lewis Research Center Contract NAS3-23054 (Reference 14). Assessment of the partially fluorinated polyimides as a matrix for high performance hydraulic seal back-up rings is planned for study at TRW on USAF Contracts F33615-81-C-5092 and F33615-82-C-5021 (Reference 15 and 16, respectively). A summary of properties other than thermal measurements determined in these and related property assessment studies is provided in Table 2.

TABLE 2
REPRESENTATIVE PARTIALLY FLUORINATED POLYIMIDE PROPERTIES

Property Measurement	Results
Specific Gravity	~ 1.4 ^a)
Hydrolytic Stability	No degradation observed in two hours water boil ^b)
Solvent Resistance	No degradation noted in methyl-ethyl ketone and jet reference fuel soak ^b)
Filler Compatibility	Amenable to fibrous and powder filling to at least 50% by weight ^a)
Filler Wetting	Excellent (photomicroscopy) ^a)
Machinability	Excellent (0.001 to 0.002-inch tolerance) ^a)

a) Determined on compression molded discs.
b) Determined on films of nominal 0.005-inch thickness.

2.3 INVESTIGATION OF PARTIALLY FLUORINATED POLYIMIDES AS A MATRIX FOR 371°C (700°F) SERVICE

In 1982, TRW initiated studies on NASA Contract NAS3-23274 to investigate monomer ingredient modifications intended to upgrade the baseline 4-BDAF/PMDA polyimide (see Section 2.2) to render the partially fluorinated polyimides suitable for \geq 371°C service in highly oxidative environments. The requirement for 371°C matrix resins has been stated by jet engine primes for future advanced jet engine systems.

A total of five new linear condensation polyimides were prepared and characterized in Contract NAS3-23274. Specifically, each of the following polyimides were synthesized (please see Table 3 for monomer structures):

- 2-C1-4-BDAF/PMDA,
- 2-C1-4-BDAF/6-FDA,
- 4-BPDA/PMDA,
- 4-BPDA/6-FDA and
- 4-BDAF/6-FDA.

TABLE 3
MONOMERS SELECTED FOR STUDY ON CONTRACT NAS3-23274

Monomer Name/Abbreviation	Monomer Structure
Pyromellitic Dianhydride (PMDA)	
2,2-Bis(3,4-dicarboxyphenyl)hexafluoropropane dianhydride (6-FDA)	
2,2-Bis[4-(3-Halo-4-aminophenoxy)-phenyl]hexafluoropropane a) (3-H-4-BDAF)	

TABLE 3 (CONTINUED)
MONOMERS SELECTED FOR STUDY ON CONTRACT NAS3-23274

Monomer Name/Abbreviation	Monomer Structure
2,2-Bis[4-(2-halo-4-aminophenoxy)phenyl]-hexafluoropropane a) (2-H-4-BDAF)	
4,4'-Bis(4-aminophenoxy)biphenyl (4-BPDA)	
2,2-Bis[4-(4-aminophenoxy)phenyl]-hexafluoropropane (4-BDAF)	

a) Chlorine has been selected as the halogen atom to be initially introduced.

The synthesis, characterization, processing and evaluation of these new polyimides is described below.

The resins were synthesized as their polyimide-precursors in dimethyl acetamide employing a resin varnish solids loading of twenty-five percent by weight. The polyimides were prepared by solvent removal and imidization in the temperature range of 100°C to 200°C. The resins were then post-cured at 371°C. Each polyimide demonstrated an initial weight loss by thermalgravimetric analysis (TGA) in air at a minimum of 490°C. The TGA results were deemed encouraging towards a goal isothermal stability of 371°C. A representative thermogram is presented in Figure 2.

The five new polyimides were isothermally aged as powders (nominal twenty-five mesh particles) for two hundred and forty hours at 371°C employing an ambient atmospheric air flow of ten cubic centimeters per minute. Both 4-BDAF/PMDA powder and a neat resin molded disc were included in the aging study to serve as control specimens.

The results of this 371°C aging study are plotted in Figure 3. The 371°C isothermal stability of 2-Cl-4-BDAF/PMDA, 2-Cl-4-BDAF/6-FDA and

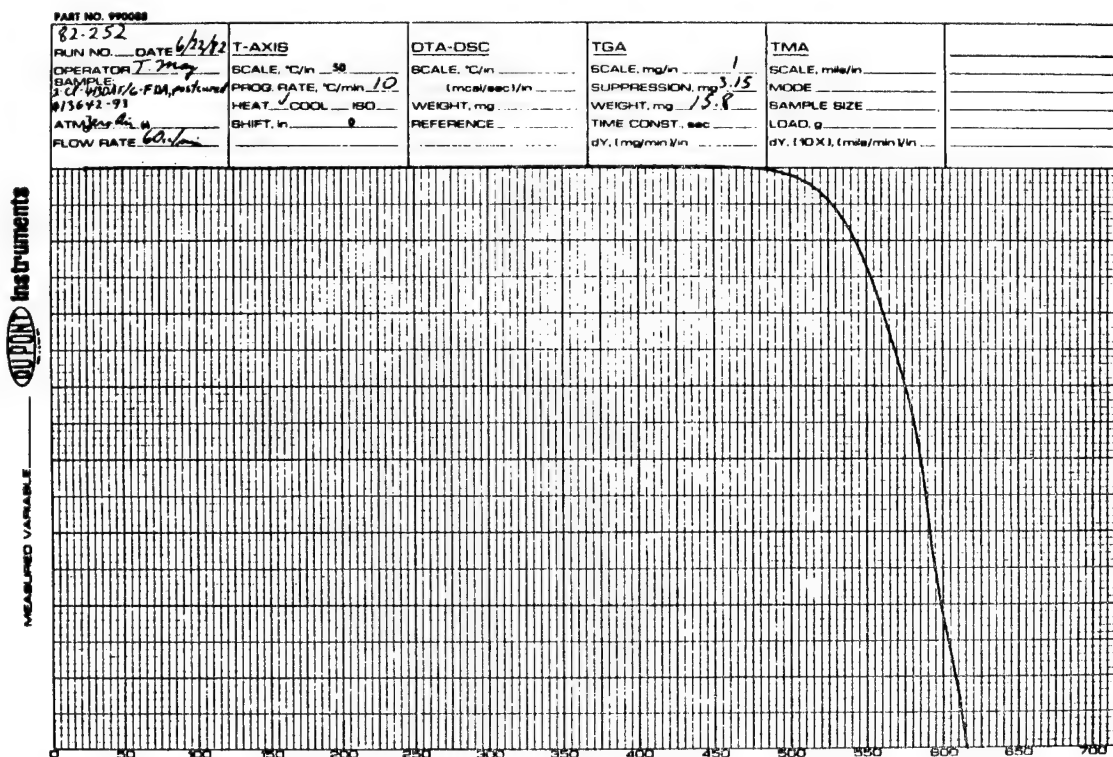


Figure 2. Thermogram of 2-CL-4-BDAF/6-FDA.

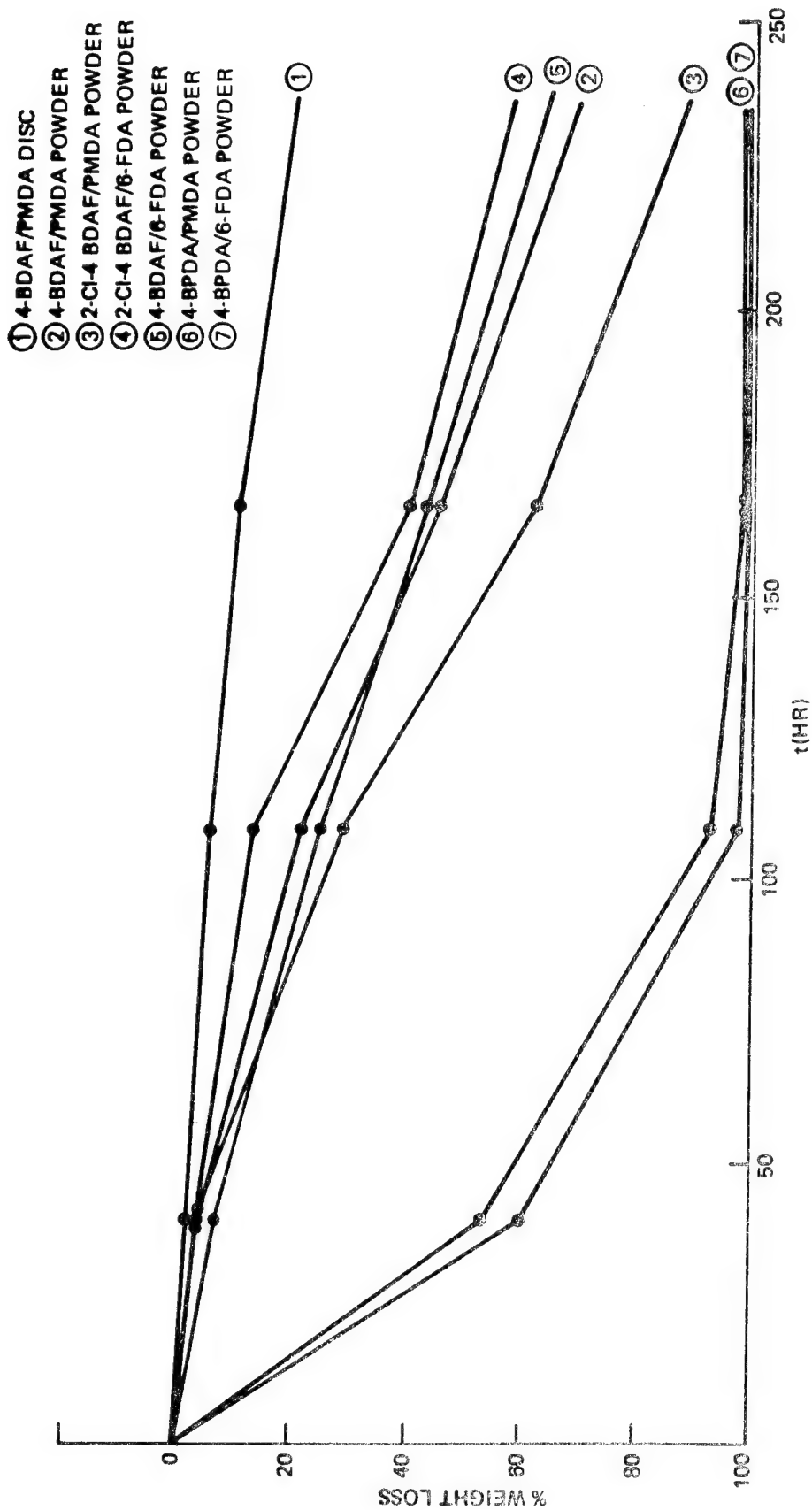


Figure 3. Isothermal Aging Results at 371°C for Partially Fluorinated Polyimide Candidates.

4-BDAF/6-FDA were judged to be promising. Comparison of the weight loss of these polyimides and the 4-BDAF/PMDA controls as powders of up to approximately thirty percent with the 4-BDAF/PMDA disc weight loss of six percent after one hundred hours (the minimum goal for jet engine performance) gave promise that each new resin had the potential as an excellent candidate for 371°C service. Conversely, the 4-BPDA/PMDA and 4-BPDA/6-FDA resins demonstrated surprisingly poor thermo-oxidative stability at 371°C and were eliminated from further consideration as high performance matrix resin candidates.

Neat resin fabrication studies were conducted on the promising new polyimide candidates and the 4-BDAF/PMDA control. It was determined that compression molding temperatures and pressures up to 450°C (850°F) and 408 MPa (6000 psi), respectively, are required for the polyimides. These processing parameters yielded neat resin discs of up to 6.35-cm (2.5-inch) diameter discs which were essentially void-free and possessed specific gravities in the desired range of 1.40 to 1.45. A representative compression molding cycle is presented in Table 4.

Completion of the processing studies, thermalmechanical analysis (TMA) determination of glass transition temperatures and isothermal aging of molded discs at 371°C and compressed air pressures up to 0.4 MPa (60 psia) for durations of up to two hundred and forty hours is in progress. The results of these key tests will be presented.

3.0 CONCLUSIONS

Based upon the test results completed to date, TRW offers the following conclusions concerning partially fluorinated polyimides as matrix resins for up to 371°C (700°F) service in air:

- The polymers can be easily prepared by conventional linear condensation methodology
- Neat resin glass transition temperatures of a minimum of 390°C are achievable
- Several polymer candidates have demonstrated promising thermo-oxidative stability at 371°C for a minimum of one hundred hours in flowing air at ambient atmospheric pressure

TABLE 4
SUMMARY OF A REPRESENTATIVE MOLDING CYCLE EMPLOYED
TO FABRICATE NEAT RESIN FORMULATION 4-BDAF/PMDA

Time at Temperature (minutes)	Bumping Cycles Performed (0 to 3408 MPa/6000 psi)	Mold Temperature (°C/°F) ^a
0 to 30	8	284°C/544°F to 334°C/633°F
31 to 60	9	334°C/633°F to 385°C/725°F
61 to 100	8	385°C/725°F to 416°C/780°F
101 to 120	0 ^b)	416°C/780°F to 452°C/846°F
121 to 150	0 ^b)	452°C/846°F to 456°C/853°F

^aAverage of three thermocouple measurements.

^bPressure was applied constantly at 408 MPa.

- Several polymer candidates are amenable to compression molding into defect-free neat resin parts

It is believed that synthesis and fabrication process optimization, coupled with fibrous reinforcement, will yield partially fluorinated polyimide matrices suitable for a minimum of one hundred hour service at 371°C under 0.4 MPa compressed air pressures.

4.0 ACKNOWLEDGEMENT

The authors wish to express their appreciation to Dr. T. T. Serafini and his associates at NASA Lewis Research Center and Mr. Stanley Harrier, General Electric Aircraft Engine Group for their encouragement and assistance in the development of partially fluorinated polyimides as high performance matrix resins.

5.0 REFERENCES

1. Technical Bulletin No. 6236A, Skybond 703, High Heat Resistant Resins, Monsanto.
2. Exploring Vespel Territory, The Properties of Du Pont Vespel Parts, Du Pont Company.
3. Kapton Polyimide Film, Summary of Properties, Du Pont Company.
4. E. A. Burns, H. R. Lubowitz and J. F. Jones, Final Report Contract NAS3-7949, NASA CR-72460.
5. T. T. Serafini, P. Delvigs and G. R. Lightsey, *J. Appl. Polym. Sci.*, 16, 905 (1972).
6. T. L. St. Clair and R. A. Jewell, 23rd National SAMPE Symp., 23, 520 (1978).
7. A. Landis and R. Andres, "High Temperature Laminating Resins," Summary Report, AFML-TR-70-250, December 1970.
8. Hughes Aircraft Company, Unpublished results.
9. H. H. Gibbs, 17th National SAMPE Symp., 17, III-B-6 (1972).
10. G. Zakrezewski, M. K. O'Rell, R. W. Vaughan and R. J. Jones, Final Report Contract NAS3-17824, NASA CR-134900.
11. R. J. Jones, M. K. O'Rell and J. M. Hom, U.S. Patent 4,203,922 (1980).
12. R. J. Jones, M. K. O'Rell and J. M. Hom, U.S. Patent 4,111,906 (1978).
13. R. L. Fusaro, Tribological Evaluation of Composite Materials Made from a Partially Fluorinated Polyimide, NASA Technical Memorandum 82832, April, 1982.
14. Contract NAS3-23054, Unpublished Results.
15. Contract F33615-81-C-5092, Unpublished Results.
16. Contract F33615-82-C-5021, Unpublished Results.

SURFACE PROTECTION OF GRAPHITE FABRIC/PMR-15

COMPOSITES SUBJECTED TO THERMAL OXIDATION

M. P. Hanson and T. T. Serafini
National Aeronautics and Space Administration
Lewis Research Center

Graphite fabric/PMR-15 laminates develop matrix cracks during long-term exposure in air at temperatures in the range of 500 to 600 °F. This study was performed to demonstrate the effectiveness of incorporating graphite mat surface plies as a means of reducing the development of matrix cracks. Celion 3000 graphite fabric/PMR-15 laminates were fabricated with graphite or graphite mat/-325-mesh boron powder surface plies. Laminates without mat surface plies were also fabricated for control purposes. Composite flexural strength, flexural modulus, and interlaminar shear strength were determined at 288 °C before and after long-term exposure (up to 1500 hr) in air at 316 °C. The results of this study showed that the incorporation of graphite mat surface plies reduces matrix cracking and improves the elevated temperature mechanical property retention characteristics of the composites.

INTRODUCTION

In many instances graphite fabric is being selected as the fiber reinforcement material in structural composites intended for high-performance aerospace applications. For example, a graphite fabric/PMR-15 polyimide composite material has been selected for replacement of the current bill-of-materials titanium outer duct used on the General Electric F404 engine (ref. 1). The unique bidirectional properties of graphite fabric laminates enable designers to design composite structures having simplified laminate configurations which not only meet design requirements but are also less costly to fabricate than structural components made from unidirectional tape.

All polymer matrix composites subjected to long-term exposure in air at elevated temperatures, even those employing the so-called high-temperature polymers, exhibit weight loss and degradation of mechanical properties. Composite weight loss and concomitant property degradation have been attributed to diffusion-controlled oxidative degradation of the matrix (ref. 2). However, a recent study (ref. 3) on the effects of long-term, elevated-temperature exposure on the properties of T300/PMR-15 fabric laminates also identified matrix cracking as a contributing factor to weight loss and property degradation. Crack initiation is likely due to stresses in the matrix resulting from the local, nonuniform fiber distribution in woven fabrics.

Recently developed graphite mat (ref. 4) has potential for providing a more uniform fiber distribution. Thus, it was postulated that incorporation of a ply of graphite mat on the surface of fabric laminates would minimize cracking and thereby improve the property retention characteristics of graphite fabric laminates exposed to an elevated temperature oxidative environment.

The results of a study to improve the char-forming characteristics of matrix resins (ref. 5) suggested that boron powder might be an effective antioxidant for high-temperature resins. It was further postulated that a surface layer consisting

of both graphite mat and boron powder would significantly improve the elevated-temperature performance of graphite fabric/PMR-15 laminates.

The purpose of this investigation was to determine the effectiveness of surface plies of either graphite mat or graphite mat with boron powder as a means of protecting graphite fabric/PMR-15 laminates exposed to thermo-oxidative environments. Celion 3000 graphite fabric laminates with and without mat or mat/boron powder surface plies were fabricated using PMR-15 polyimide. Composite flexural strength, flexural modulus, and interlaminar shear strength were determined at 288 °C before and after long-term exposure (up to 1500 hr) in air at 316 °C. Composite weight loss at 316 °C was also determined.

EXPERIMENTAL PROCEDURE

Materials

Style W1133 8 harness satin-woven fabric from Celion 3000 graphite yarn was used as the primary reinforcing material. The yarn was sized with an epoxy compatible sizing. The mat material was a commercial product consisting of 1.9-cm-long Celion carbon fibers with a polyester binder. The mat weight was 112 gm/m². The boron additive used was an amorphous -325-mesh powder.

The polyimide resin used in this investigation was the high-temperature polyimide designated as PMR-15. The monomers used to formulate PMR-15 are shown in table 1. The monomethyl ester of 5-norbornene-2,3-dicarboxylic acid (NE) and 4,4'-methylenedianiline (MDA) were obtained from commercial sources. The dimethyl ester of 3,3', 4,4'-benzophenonetetracarboxylic acid (BTDE) was prepared as a 50 weight percent solution by refluxing a suspension of the corresponding dianhydride in anhydrous methanol for ~2.75 hr. The monomer stoichiometry for the PMR-15 solution was 2 NE/3.087 MDA/2.087 BTDE. The PMR-15 solution was prepared by dissolving the monomers in a calculated amount of anhydrous methanol to yield a 50 weight percent solution.

Composite Fabrication and Specimen Preparation

The woven fabric was impregnated with a predetermined quantity of the PMR-15 resin solution to provide cured laminates having a fiber content of ~55 volume percent. The prepgs were air dried to reduce the volatile content to ~10 percent prior to cutting into plies.

Prior to impregnating the mat material, the polyester binder was burned-off by placing the as-received mat between perforated steel sheets and heating the steel/mat sandwich at 450 °C in an air-convection oven for 2 hr. The binder-free mat was allowed to cool to room temperature, placed between 0.625 cm mesh screens, and then impregnated with the PMR-15 resin solution. The mat containing the boron additive was impregnated with a PMR-15 solution to which 5-percent-by-weight boron powder had been added. Both mat preparations were air dried to reduce the volatile content to ~10 percent prior to cutting into plies. The impregnated fabric and mat materials were cut into 7.6 by 20.3 cm plies. The warp yarns of the fabric plies were parallel to the 20.3 cm dimension. The basic laminate consisted of a 6-ply layup of the woven fabric; laminates with mat surfaces consisted of the basic laminate with 1 ply of mat on each side. All of the fabric plies were stacked with their warp yarns in the 0° direction. Each layup was then stacked between a porous release fabric in a preforming mold and imidized at 204 °C for 1 hr under a pressure of ~0.07 N/cm². Compression molding was accomplished by placing the

staged layup into a matched metal die and heating to 232 °C at essentially zero pressure. A pressure of 345 N/cm² was applied and the mold temperature was increased to 316 °C at a rate of 5.6 °C/min. Pressure and temperature were maintained for 2 hr followed by cooling to 204 °C before releasing the pressure and removing the laminate for the mold. The cured laminates were postcured in an air-circulating oven in which the temperature was raised from ambient temperature to 316 °C at a rate of 2.2 °C/min and then held at 316 °C for 16 hr.

Composite Environmental Exposure

Coupons (approximately half of a 7.6 by 20.3 cm laminate) were subjected to thermo-oxidative exposure. All of the coupons were cut from essentially void-free laminates as assessed by ultrasonic C-scan. The thermo-oxidative environments were provided by an air circulating oven. Air was metered into the oven at a rate of 100 cm³/min. Coupons were periodically removed from the oven and allowed to cool to room temperature in a desiccator before reweighing to determine weight loss.

Composite Testing

Flexural tests conformed essentially to the ASTM standard method D790. Tests were made on a 3-point loading fixture with a variable span. Tests were performed using a span-to-thickness ratio of ~32. The rate of center loading for flexural testing was 0.127 cm/min. Interlaminar shear strength tests were conducted in accordance to ASTM D2344 using a constant span-to-thickness ratio of 4. For the elevated temperature tests, the load was applied to the specimens after the chamber had equilibrated at the test temperature for 10 min.

RESULTS AND DISCUSSION

Figure 1 shows the variation of 316 °C weight loss with exposure time in air at 316 °C for all of the Celion 3000 graphite fabric/PMR-15 composites investigated in this study. Also shown in the figure is the 316 °C weight loss of unidirectional Celion 6000 (unsized)/PMR-15 composites (ref. 6). As can be seen in the figure, all of the composites exhibited about the same level of thermo-oxidative stability. These results indicate the surface plies of mat or mat/boron powder had neither a beneficial or adverse effect on composite thermo-oxidative stability (TOS) as assessed by weight-loss measurements. The data also show that the presence of the epoxy sizing, used in weaving the fabric, did not cause increased degradation of the fabric composites. While an improvement in thermo-oxidative stability would have been desirable, the absence of a detrimental effect encouraged further investigation of the concept of using surface plies of mat material to reduce internal cracking.

Retention of composite mechanical properties after prolonged exposure at elevated temperature is a more meaningful assessment of composite TOS than composite weight loss. Figure 2 shows the 288 °C flexural property retention characteristics of the various laminates exposed at 316 °C as a function of exposure time in air at 316 °C. It can be seen that the property retention of the all-fabric laminates is lower than the property retention of laminates surface protected with mat or mat/boron. After 1500 hr of exposure at 316 °C, the unprotected fabric composite flexural strength retention was 56 percent, compared to ~74 percent retention of flexural strength for both the mat and mat/boron protected materials. The retention of modulus was 66 percent for unprotected fabric composites as compared to 88 and 104 percent retention for mat and mat/boron protected fabric/PMR-15 composites,

respectively. These results show that the surface protection is effective and that the improved retention of modulus is particularly significant.

The foregoing flexural strength comparisons were based on the ultimate properties of the laminates tested. However, the load-deflection characteristics of the isothermally-exposed, unprotected fabric/PMR-15 laminates revealed severely degraded structural integrity. Figure 3 shows typical flexural load-deflection curves for unprotected laminates tested after postcure (fig. 3(a)) and after 624 hr of isothermal exposure at 316 °C (fig. 3(b)). It can be seen that the postcured, but not exposed, laminate (fig. 3(a)) exhibited a load-deflection curve that is essentially linear to the ultimate load. In contrast, exposed, unprotected composites showed a quasi-yield point, or discontinuity, in the load-deflection curve (fig. 3(b)) that occurred at a relatively low load depending upon the duration of exposure. The average retention level as a function of time at which the yield occurred is indicated by the tailed symbols in figure 2. In marked contrast, the load-deflection characteristics of either graphite mat or graphite mat/boron surface plies had load-deflection characteristics similar to that of the postcured, but not exposed, fabric laminates. Using the discontinuity in the load-deflection curve instead of ultimate properties as the basis for flexural strength retention, the useful flexural strength retention is 45 percent after 624 hr and 22 percent after 1500 hr.

Figure 4 shows the 288 °C interlaminar shear strength retention of the laminates as a function of exposure time in air at 316 °C. It can be seen that the shear strength retention after long-term exposure has been improved by the mat and mat/boron surface plies. After 624 hr of exposure the shear strength retention varied ~5 percent among the three laminate constructions. After 1500 hr of exposure the interlaminar shear strength retention was 69 and 73 percent for the all-fabric laminates and mat-protected laminates, respectively. The mat/boron surface-modified laminates exhibited 87 percent retention of interlaminar shear strength after 1500 hr exposure in air at 316 °C. As is known, interlaminar shear specimens fail close to the specimen neutral plane. Thus, the higher interlaminar shear strength retention level for the mat/boron protected laminates suggests that the addition of boron to the mat increased the effectiveness of the mat in preventing interior cracking.

To ascertain the changes in structural features which might have resulted from elevated temperature exposure, cross sections of as-fabricated (postcured) laminates and exposed laminates were examined metallographically. Figure 5 shows representative photomicrographs of specimens from graphite fabric/PMR-15 as-fabricated laminates and from laminates that had been exposed for 624 hr at 316 °C. Figure 5(a) shows that the as-fabricated laminates were defect free. In figure 5(b) it can be seen that numerous through-the-surface-ply cracks had developed after 624 hr of exposure. Because specimens subjected to flexural testing fail at one of the surfaces by either a tensile or compressive failure mode, the presence of numerous surface cracks in the exposed composites accounts for the severe reduction in the flexural strength retention of the unprotected laminates (fig. 3).

Figure 6 shows representative photomicrographs of graphite fabric laminates with graphite mat surface plies. As can be seen in figure 6(a), the as-fabricated laminate was essentially defect free. Figure 6(b) shows the same laminate after 624 hr at 316 °C. It can be seen that the thermal-oxidative exposure has caused some internal cracking. Also, the surface cracking of the protected laminate was negligible compared to the surface cracking of the unprotected laminate (compare figs. 5(b) and 6(b)).

Figure 7 shows representative photomicrographs of graphite fabric laminates with graphite mat impregnated with PMR-15 and boron powder. It can be seen that the as-fabricated laminate (fig. 7(a)) as well as the exposed laminate (fig. 7(b)) were essentially free of surface and interior cracking. The absence of interior cracks in the mat/boron protected laminates accounts for their higher interlaminar shear strength retention compared to the other two laminate constructions. The important point to be noted, however, is that the incorporation of a surface ply of mat material was essential for the achievement of improved properties after elevated temperature exposure.

Although no attempt was made in this investigation to optimize the physical performance of the mat as a surface protection for graphite fabric/PMR-15 composites, variables such as mat thickness and density undoubtedly influence properties. If optimized, these variables would lead to significantly enhanced performance.

CONCLUSIONS

Based on the results obtained in this investigation, the following conclusions can be drawn:

(1) Isothermally exposed Celion-3000 graphite fabric/PMR-15 composites with graphite mat surface protection have greater flexural strength, flexural modulus, and interlaminar shear strength retention than fabric laminates without mat protection.

(2) Isothermally exposed graphite composites with mat surface protection exhibit essentially a linear flexural load-deflection relationship to failure whereas composites without mat protection exhibit a pronounced quasi-yield significantly below the failure load.

(3) Adding boron powder to the mat had essentially no effect on the flexural strength retention. However, flexural modulus and interlaminar shear strength retention were significantly improved.

(4) Mat protected composites did not exhibit improved thermo-oxidative stability in isothermal weight loss as compared to unprotected graphite fabric composites.

REFERENCES

1. Serafini, Tito T.: PMR Polyimide Composites for Aerospace Applications. NASA TM-83047, 1982.
2. Alston, William B.: Characterization of PMR-15 Polyimide Resin Composition in Thermo-Oxidatively Exposed Graphite Fiber Composites. NASA TM-81565, 1980.
3. Serafini, T. T. and Hanson, M. P.: Environmental Effects on Graphite Fiber Reinforced PMR-15 Polyimide. Composites for Extreme Environments. ASTM STP 768, N. P. Adsit, ed., American Society for Testing and Materials, 1982, pp. 5-19.
4. New Nonwoven Fiber Mats Finding Multiple Uses In Plastics. Plastics Design Forum, Sept./Oct. 1980, pp. 82, 84, 86.

5. Gluyas, R. E. and Bowles, K. J.: Improved Fiber Retention by the Use of Fillers in Graphite Fiber/Resin Matrix Composites. NASA TM-79288, 1980.
6. Vannucci, Raymond D.: Properties of PMR Polyimide Composites Made with Improved High Strength Graphite Fibers. NASA TM-81557, 1980.

TABLE 1. - MONOMERS USED FOR PMR 15 POLYIMIDE

STRUCTURE	NAME	ABBREVIATION
	MONOMETHYL ESTER OF 5-NORBORNENE-2,3-DICARBOXYLIC ACID	NE
	DIMETHYL ESTER OF 3,3',4,4'-BENZOPHENONETETRACARBOXYLIC ACID	BTDE
	4,4'-METHYLENEDIANILINE	MDA

CS-71803

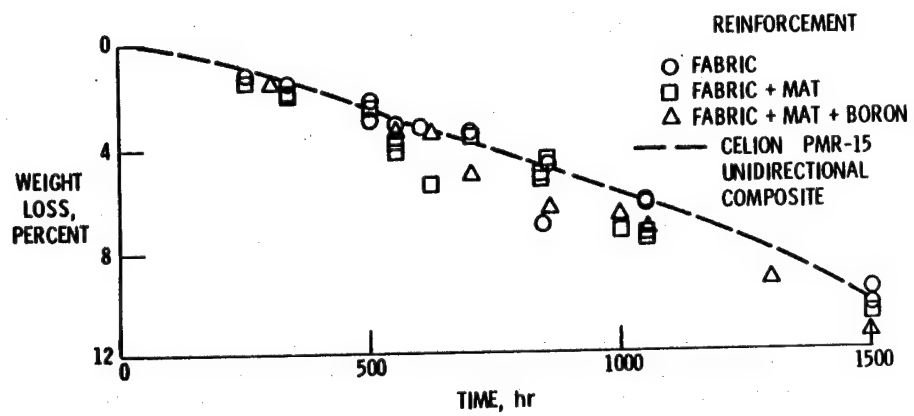


Figure 1. - Weight loss of Celion 3000 graphite fabric/PMR-15 laminates exposed in air at 316 °C.

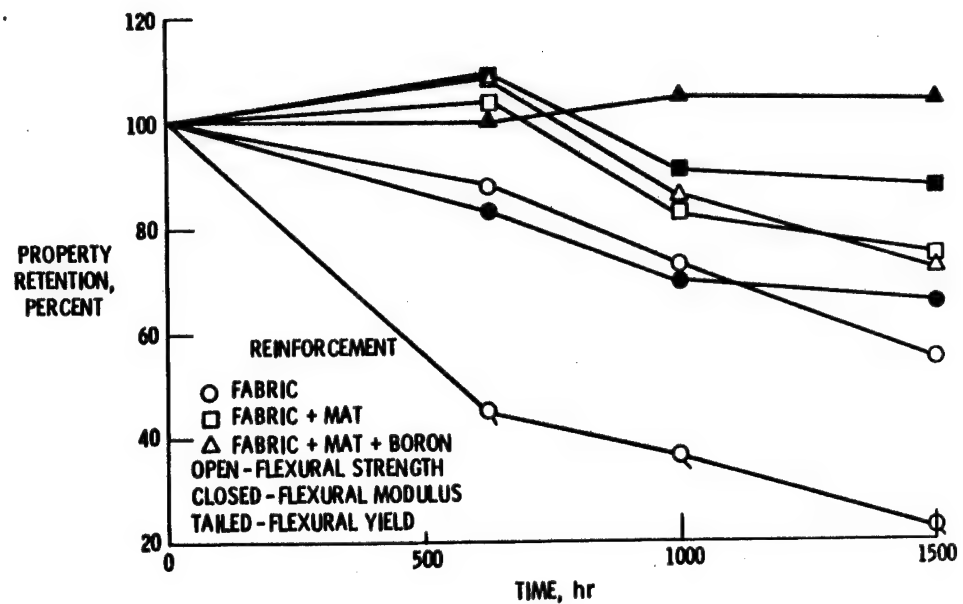


Figure 2. - Flexural properties of Celion 3000 graphite fabric/PMR-15 laminates exposed in air at 316 °C and tested at 288 °C.

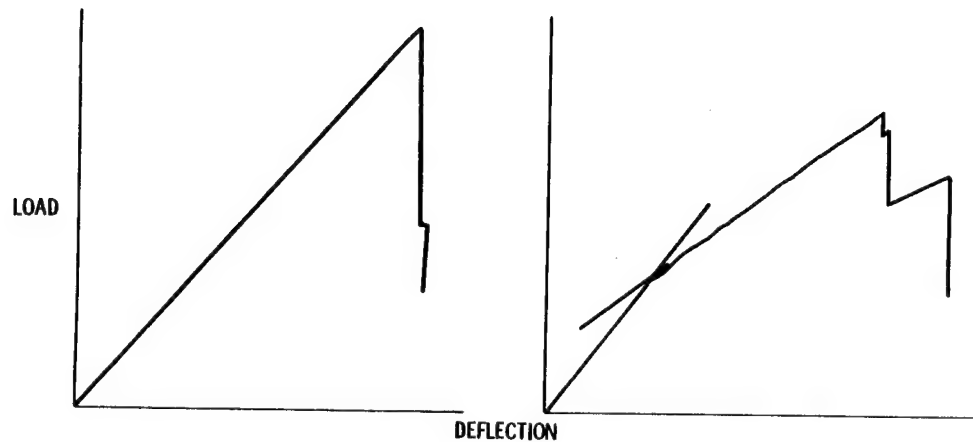


Figure 3. - Typical flexural load - deflection curves of Celion 3000 graphite fabric/PMR-15 laminates; (a) tested at 288 °C after postcure (b) tested at 288 °C after 624 hr exposure in air at 316 °C.

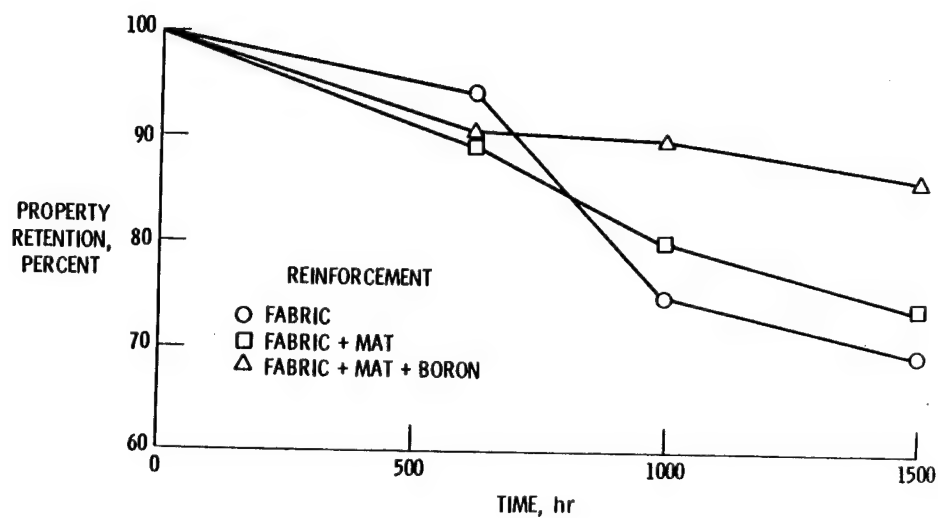


Figure 4. - Shear property retention of Celion 3000 graphite fabric/PMR-15 laminates exposed in air at 316 °C and tested at 288 °C.

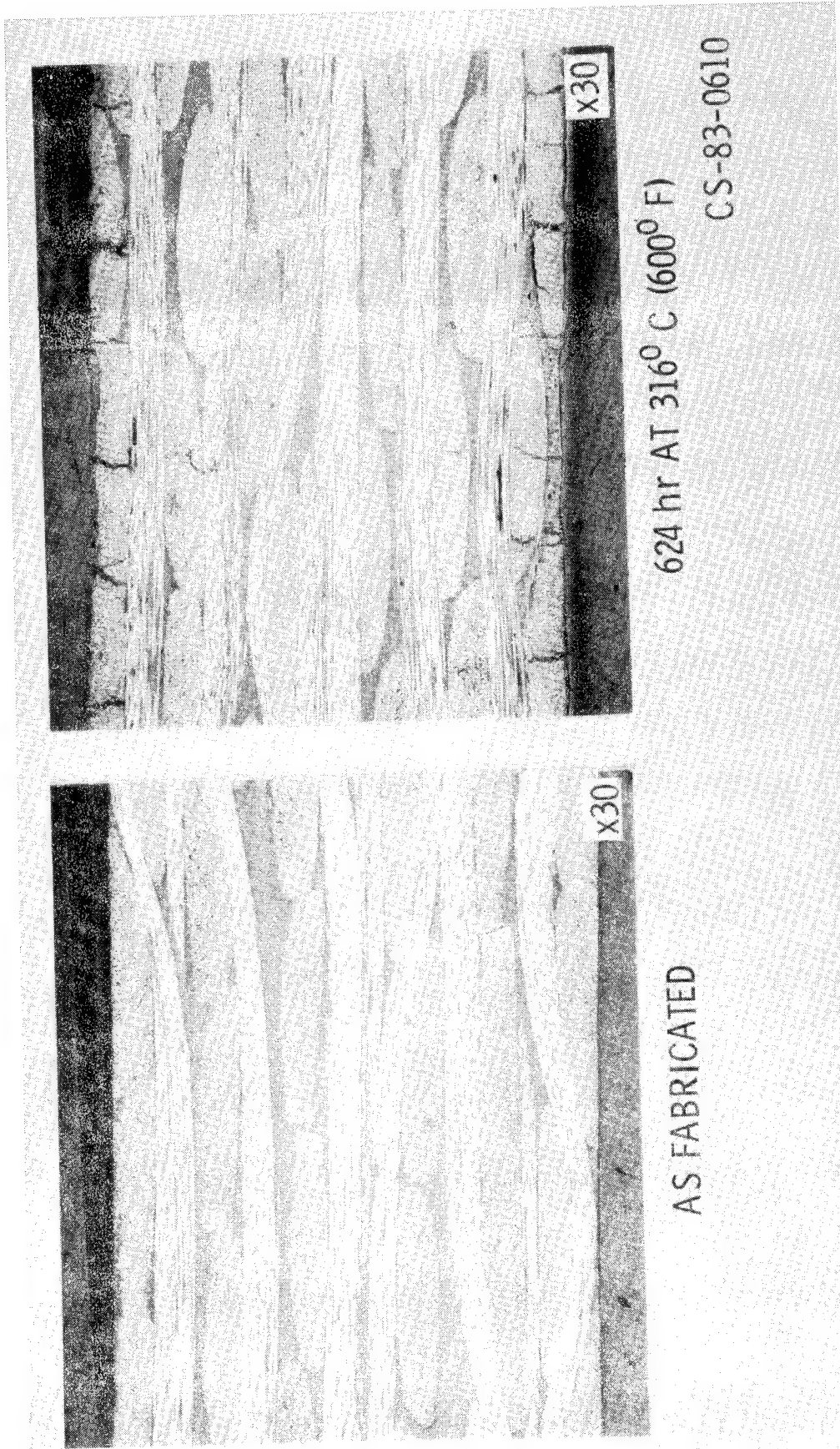


Figure 5. - Typical photomicrographs of Celion 3000 graphite fabric/PMR-15 laminates before and after elevated temperature exposure in air.

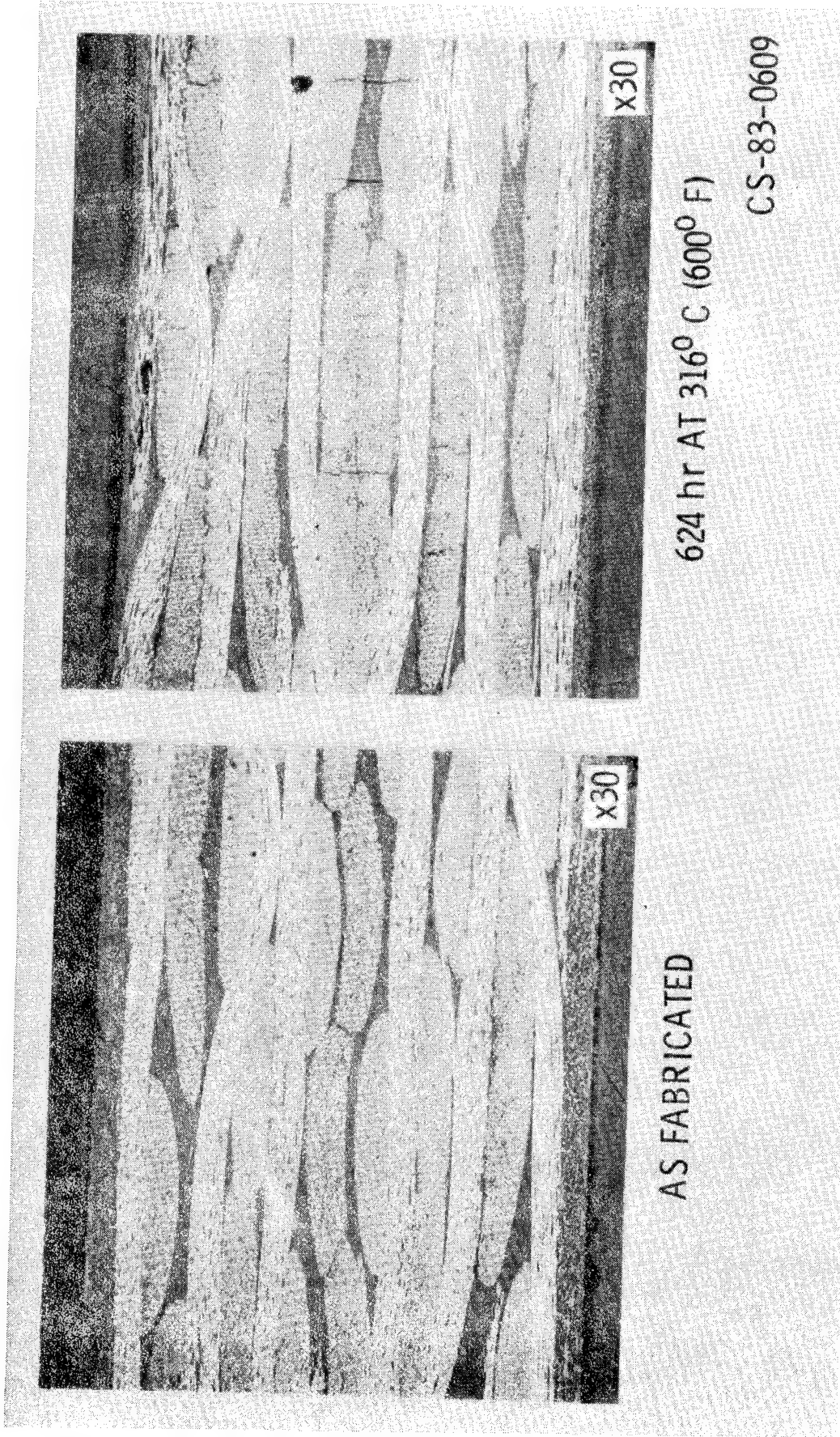


Figure 6. - Typical photomicrographs of Cellofan 3000 graphite fabric/PMR-15 laminates made with graphite mat surface plies, before and after elevated temperature exposure in air.

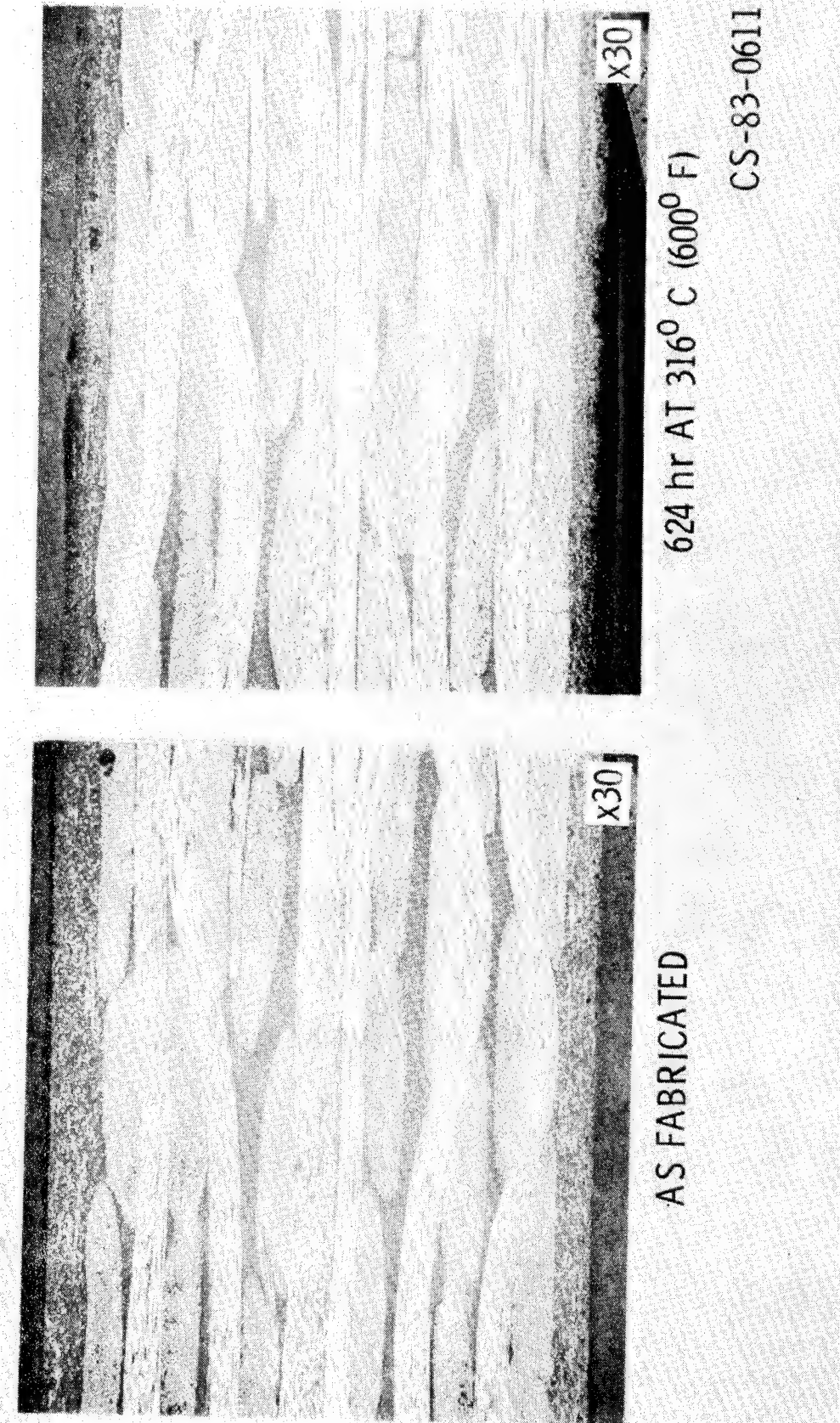


Figure 7. - Typical photomicrographs of Celion 3000 graphite fabric/PMR-15 laminates, made with graphite mat/boron powder surface plies, before and after elevated temperature exposure in air.

MICROSCOPIC EVALUATION OF A POLYIMIDE (PMR15)-GRAPHITE COMPOSITE

Jeffry J. Fedderly and Joseph M. Augl
Naval Surface Weapons Center

This work is part of an effort to evaluate the high temperature performance of a polyimide (PMR15)-graphite composite which consists of several plies of woven strands of carbon fibers (see fig. 1). Further details of the material are given in the background section. The longterm effect of high temperature on the dry material was studied by exposing polished test specimens of 473°F in a oven for nearly 400 hours. Periodically the specimens were removed and observed microscopically. Gradually surface cracks began to appear and the number of cracks increased over time. At the conclusion of the exposure the specimens were gradually ground down and observed in order to determine the depth of the cracks into the interior of the material. This procedure was repeated at an exposure temperature of 550°F.

The effect of absorbed moisture in the material being rapidly driven off by a sharp temperature gradient was studied by equilibrating polished specimens to an 80% R.H. environment, then thermally cycling them between room temperature and 473°F. Microscopic observations of the specimens were made following the cycling process.

Optical microscopy was used for the majority of the material observations made during this study. Since repeated observations of the same areas of composite specimens were to be made following various exposure intervals, the gold surface coating required for scanning election microscopy was not desirable for it may have interfered with the composite's surface properties during exposure. Some observations were made using a scanning election microscope, following the conclusion of the exposure periods.

BACKGROUND

The carbon fiber-polyimide composite materials studied are comprised of several plies. Each ply consists of woven structure of carbon fiber strands. In the weave pattern, strands which are oriented in one direction, interlock with only every eighth bundle oriented in the perpendicular direction.

Thus, each ply consists of two distinct layers. One layer is dominated by fiber strands oriented in one direction, while the other layer is dominated by strands oriented perpendicular to the strands of the first layers (see Fig. 2). With this structure, observations of the cross section reveal that for each ply there are two distinct rows of fibers with only an occasional crossover which indicates an interlocking of strands.

Composite specimens with two different ply sequences were investigated. One was a 2.90mm. thick, 8 ply material consisting of plies whose fibers were oriented only in 0° and 90° directions. The other composite was a 1.35mm. thick, 4 ply material consisting of two outer plies whose fibers are oriented in the 0° and 90° directions and two inner plies whose fibers are oriented in the ± 45° directions. The 8 ply composite has essentially zero void volume, whereas the 4 ply composite has nearly a 3% void volume fraction.

Most of the observations of the specimen's surfaces were along the cross section oriented in the 0° direction. Upon observing this cross section, the fibers oriented in the 0° direction (running the length of the cross section) appear as long thin strands. The cross section of the fibers oriented in the 90° direction are observed from this surface and appear roughly as hexagons (circular at low magnification). Fibers oriented in the ± 45° directions appear as elongated hexagons (ovals at low magnification) with the length in the 0° direction being 1.4 times the width in the transverse direction.

EXPERIMENTAL

Sample Preparation

Composite specimens which were observed microscopically were cut from a panel into pieces approximately 1.5cm in length by 1.2cm in height. The lengths of the pieces were oriented along the 0° fiber direction. In order to microscopically observe a given surface of the specimen, that surface had to be highly polished. Polishing was accomplished by rough grading the surface using a series of SiC abrasive papers (320, 400, and 600 grit), then fine polishing the surface with alumina powders on a motorized polishing wheel. Using the larger powders first, the specimens polished with 9.5μ, 1.0μ, 0.3μ, and 0.05μ powders.

Thermal Exposure

The subjection of specimens to 400 hours of either 473°F or 550°F was accomplished by placing them on an aluminum block in a preheated oven. An iron-constantan thermocouple was taped to the surface of the block in order to accurately monitor the temperature. When a specimen was removed from the oven for periodic observations it was placed on a cool aluminum block in order to facilitate rapid cooling.

Specimens equilibrated to 80% R.H. and thermally cycled, were cycled by being placed for a given period of time on an aluminum block in an oven heated to 473°F. The cycle was then completed by removing the specimens from the oven and cooling them on an aluminum block for a time equal to the exposure time. The 4 ply pieces were exposed for periods of 2 minutes, and the thicker 8 ply pieces for periods of 4 minutes. This cycle was repeated 50 times, except occasionally specimens were removed for longer periods of time in order to make microscopic observations.

Microscopy

Microscopic observations were made with a Zeiss universal microscope. Photographs were taken with the aid of a Polaroid camera attachment. Polaroid Type 52 medium contrast black and white film was used.

RESULTS AND DISCUSSION

Initial Specimen Condition

The initial condition of both sets of specimens (4 and 8 ply) appeared to be good. Only a few hairline cracks were observed prior to exposure. The 8 ply material has virtually no voids. The rare voids that were found were always located in resin pockets, between bundles. The 4 ply material has nearly a 3% void content. In addition to the larger voids found in resin pockets, areas within the fiber bundles were found which contained many small voids (see fig. 3).

400 Hour Exposure at 473°F

Specimens from both composite materials were subjected to 473°F exposure for 391 hours. The specimens were removed 7 times during the exposure in order to examine the extent of the damage to the material as a function of time. The behavior of the 8 ply material will be discussed first.

8 Ply Test Panel Two material samples were observed and photographed along the cross section oriented in the 0° direction. The first observation of the material after the beginning the exposure was made after 17 hours of exposure. The couple of very thin cracks which had been present initially had now widened slightly. The only other noticeable change was that in the regions between 90° fibers (perpendicular to the surface) very shallow depressions in the resin could be seen (see fig. 4a) indicating a slight degradation and loss of resin. After 38 hours of exposure no other change or damage was observed except for a slight increase in the loss of resin from the surface. The first new crack in one sample did not appear until after 169 hours. Only after 258 hours of exposure did several cracks appear in both specimens (see fig. 5). In every case the cracks are located in the 90° fiber areas and run transverse to the 0° direction, never along it. The lengths of the cracks are dictated by the width of the 90° fibers bundles. In most every case the crack runs the entire width of the 90° fiber areas (about 0.35mm. maximum), but never beyond into 0° fiber areas where cracks would have to cut through carbon fibers in order to propagate. The few cracks which had developed earlier had now widened noticeably. The loss of resin from the surface still appeared to be continuing slowly. After 324 hours of exposure many more cracks had formed and there was continued lengthening and widening of old cracks. The maximum widths of the cracks was approximately 13μ. The depressing which were due to resin loss were only a few microns deep (see fig. 4d) and thus this damage seems minimal.

After 391 hours of exposure or at 473°F the cross section appears to be heavily cracked and damaged (see fig. 6), but the real extent of the damage was not known until the depth of the cracks into the interior was determined. In order to determine the depth of the cracks into the material, the cross section of the specimen was gradually ground down and periodically examined for the extent of cracking.

After about 0.1mm. had been ground down most of the cracks, which had formed during the exposure, had been removed. Thus most all the cracks observed along the cross section were less than 0.1mm. deep. After 0.3mm had been ground down from the surface only a couple of cracks still remained and these were two cracks which were present in the material before exposure began.

4 Ply Test Panel: These specimens were first cut and observed along the 0° cross section as were the 8 ply specimens. During exposure, the loss of resin from the surface was similar to the behavior of the 8 ply material. Depressions in the resin, as observed in the areas between 90° fibers, are easily observable, but after 391 hours of exposure at 473°F are only a few microns deep.

The cracking behavior of the 4 ply material was different than that of the 8 ply material in several ways. First, the onset of surface cracking appeared sooner in the 4 ply panel than in the 8 ply panel. After only 50 hours of exposure a couple of cracks were observed in 90° fiber areas. From 50 to 313 hours of exposure there was a slow, steady increase in the number of surface cracks that did not appear in the 8 ply material until after 108 to 170 hours of exposure. As in the 8 ply material, cracks started as being short and thin and grew with additional exposure. In this material the maximum width of the 90° areas is smaller than in the 8 ply composite thus the maximum length of cracks, which run transverse to the 0° direction in the 90° fiber regions, are shorter (0.20mm) than in the 8 ply composite (0.35mm). The cracks grew to maximum widths of about 7 μ . Also the cracks generated in the 4 ply material, almost without exception, originated in areas containing a high concentration of small voids intermixed in between the 90° fibers (see fig. 7). The 8 ply composite did not have void filled areas such as this.

Another difference between the two materials is that, although the 4 ply composite began crack formation earlier in the exposure period than did the 8 ply material, the 4 ply specimens do have a noticeably smaller final crack density than do the 8 ply specimens (see fig. 8). Also noticeable in figure 8, is that the cracks in the 4 ply material have formed only in the 90° fiber strand areas, which are in the outer two plies. As with the 8 ply material, one would not expect to crack formation in the 0° strands at the 0° cross section. Yet, it might be expected that cracks would form in the $\pm 45^\circ$ fiber regions. Cracks could form and propagate between fibers in the transverse direction and still be observed along the 0° cross section, yet no cracks are found in these areas.

In order to determine whether the stresses as a whole are significantly less in the interior plies of the 4 ply material than in the 8 ply material or whether the stresses which produce cracks are governed by the orientation of the fibers with respect to the cross section, a new specimen was cut which had 4 cross-sectional surfaces prepared for observation. One side was cut along the 0° axis and perpendicular to the 90° fibers (as before), another was cut along the +45° axis and perpendicular to the -45° fibers, another was cut along the 90° axis and perpendicular to the 0° fibers, and the last surface was cut along the -45° axis and perpendicular to the +45° fibers. As this specimen was subject to 473°F exposure, it became evident that cracking occurred only in regions where the fibers were perpendicular to the exposed cross-sectional surface. Areas with fibers in the -45° direction, now produced cracking behavior when the cross section was cut in the +45° direction (see fig. 9). Like, this occurred in areas of +45° fibers with a -45° cross-sectional surface (see fig. 10).

The cross section which was cut along the + 45° direction showed the greatest amount of cracking. In this cross section the -45° fiber areas from both of the inner plies are adjacent to each other and perpendicular to the surface. Many of the cracks extended across the full width of the combined -45° fiber area (see fig. 9). The -45° area is bounded on both sides by the +45° strands whose fibers run perpendicular to the -45° fibers and only the axis of the cross section. The cross section with the least number of cracks is the one cut along the 90° direction. Here the 0° fiber regions are perpendicular to the surface and are in the outermost regions of the specimen. The other side of the 0° fiber area is bounded by a 90° fiber region (see fig. 9). The only cracks found during the exposure were located in 0° fiber areas where the 0° and 90° fiber strands had crossed over, resulting in the 0° bundle being shifted from the outside of the specimen to the interior and vice-versa for the 90° bundle. No cracks were formed during exposure in the areas where the 0° fibers were in the outermost portions of the material. The couple of cracks in this region, as seen in figure 9, were present before exposure began. The cross sections which were oriented along the 0° and -45° directions and which had 90° and +45° fibers perpendicular to their respective surfaces exhibited an intermediate amount of crack formation. The strands, in which cracking occurred were bounded on one side by fibers running perpendicular to them along the axis of the cross section and on the other side by bundles oriented 45° from the axis of the cross section (see fig. 10).

From the study of this 4 cross-section specimen, it is clear that cross-sectional surface cracking occurred only in areas where the fibers were perpendicular to the cross section. The extent of cracking appears to be dependent on the orientation of the adjacent fiber strands. Areas of cracking which are bounded on both sides by fibers oriented perpendicular to them along the cross section have a greater extent of cracking than areas in which one side is bounded by fibers perpendicular to them and the other side is bounded by fibers oriented 45° from them. On the surfaces where the perpendicular fibers were on the outside of the specimen and bounded only on one side by fibers perpendicular to them, virtually no cracking occurred. The 8 ply material consists of only perpendicular fiber regions bounded on both sides by 0° fibers, thus the crack density of this material was greater than that of the 4 ply material where this pattern never occurs then the specimen is cut along the 0° axis.

After the exposure was completed it was also noticed that cracks had formed along the outside surfaces of the 4 ply specimen as well as the cracks observed along the cross sections. Since these cracks were more difficult to observe and less prevalent than the cross-sectional ones, they were at first unnoticed. These cracks run along the length of the fibers found on the outside of the material. These cracks are long compared to the cracks in the cross section, whose lengths are limited by the widths of the perpendicular fiber bundles. The longest cracks observed were only about 3mm. long. Close-ups of a few of these cracks can be seen in figure 11. A sketch of the crack arrangement on the outer surface is shown in figure 12. At the outer surface the 0° fibers are dominant so most of the cracks are also oriented in that direction. Cracks are also found perpendicular to these in the regions where the 90° strands have crossed over in the weave and are on the outside.

Although it appears as if the material is significantly damaged, a grinding down of the material was necessary to determine if any damage occurred to the interior of the material.

One of the outer surfaces of the specimen which was initially 1.3mm. thick was gradually ground down and periodic examinations of the surface were made. The cracks from the outermost surface were observed on the ground surface until 0.15mm. had been removed. The midpoint of the outer ply had been reached. Beyond this point, going deeper into the specimen, the orientation of the fibers shifts 90°. The 90° fiber strands at the outer surface, instead of being present at an occasional cross-over are now the dominant fibers, and the 0° strands are now the occasional cross-over fibers. At this depth into the interior of the material, no cracks were found covering the outer surface as had been observed in the outer half of the outer ply. The only cracks found on this surface originated at the intersection of the 0° cross section and ran along the direction of the 90° fibers. The cracks were all short, less than 0.5mm. in length. From figure 13, it can be seen that the cracks observed from the 0° cross section penetrate very little into the material and that the vast majority of the interior has remained undamaged.

The grinding down of the sample was continued through the next ply to the midpoint of the specimen. Similar to the 0°, 90° ply mentioned above, the $\pm 45^\circ$ ply showed only short cracks along the +45° fibers at the -45° cross section when the +45° strands were dominant and along the -45° fibers at the +45° cross section when the -45° strands were dominant.

In the interior of the material, cavities were observed running along the axis of the fibers, but these are due to the voids present in the material. An unexposed sample was ground down and its interior possessed the same cavity structure. Thus the only damage to the material appears to be cracks in the outer half of the outer plies and along the exposed cross section. The cracks in the cross section are all less than 0.5mm. deep and most are approximately 0.1mm. deep.

400 Hour 550°F Exposure

8 Ply Test Panel A specimen was cut and polished for observation along the 0° cross section as had been done for the 473° exposure. A couple of cracks were initially present along the 15mm. length of material. Another specimen was prepared and polished along one of the outer surfaces. During the course of the exposure, observations and photographs were made of a localized area of this outer surface, but due to the fact that there is a smaller crack density on the outer surface than on the cross section, no cracks happened to form in this area. Following the exposure the entire outer surface was scanned carefully and the crack pattern sketched. The results will be discussed later.

The cross section of the 8 ply material responded very similarly to the 550°F exposure as it had to the 473°F exposure. After only 16 hours there was a slight but noticeable loss of resin from the surface. After 240 hours of exposure the loss of resin from the surface appeared to have stopped. The depressions left in the surface appear to be no deeper than those formed during the 473°F exposure. Cracks began to appear in the 90° fiber areas after 98 hours of exposure. This is somewhat accelerated from the 473° exposure in which several cracks did not form until after approximately 160 hours of exposure. The number of cracks increased over time until 300 hours of exposure when no additional cracking occurred. The final crack density of the 550°F exposed material appears virtually indistinguishable from that of the 473°F exposed material. The lengths and widths of the cracks in both specimens also appeared identical.

The entire polished outer surface of the other specimen exposed to 550°F was examined and its crack pattern carefully sketched (see fig. 14). The surface appears very similar to the 4-ply material following 473° exposure. The longest of the cracks are approximately 3.5mm. long and the crack density is comparable to that of the 4 ply specimen. As with the 4 ply material, the surface was ground down in order to determine the extent of damage to the interior of the material. Once approximately 0.18mm. had been removed from the original thickness of the material (at the midpoint of the outer ply) all of the cracks had been removed except the short cracks at the cross-sectional surface. Along with the 4 ply material, this shows that crack formation is a surface phenomenon and does not effect the interior of the composite. Many cracks were formed on the outer surfaces, but were limited to just the outer half of the outside plies. The cross-sectional surface was also heavily cracked, but as can be observed from grinding down the specimens, most of the cracks are only about 0.3mm. deep into the material, with an occasional crack extending about 0.7mm. into the interior. These cracks are somewhat longer than the cracks formed during the 473°F exposure, yet the majority of the interior of the composite has been undamaged due to the 550°F exposure.

Thermal Cycling

Both 4 and 8 ply specimens which had been equilibrated to an 80% R.H. environment were thermally cycled between room temperature and 473°F as described in the experimental section. The 8 ply material was subjected to 50 cycles of 4 minutes heating time and 4 minutes of cooling time. The thinner 4 ply material was subjected to 50 cycles of 2 minutes heating time and 2 minutes of cooling time. Due to the cycling process the absorbed moisture near the outer surface was quickly driven off while the interior of the specimens retained a significant fraction of its original moisture content (see fig. 15).

During the cycling process of the 8 ply specimen, the specimen is removed after 1,5,10,20 and 50 cycles for microscopic observation. It was thought that if any cracking or other damage was to occur, it would occur early in the cycling process when the surface moisture was being rapidly driven off. Yet no signs of damage were observed either early in the process or after the 50 cycles exposure. The only noticeable change occurring at the surface was the condensation of what appeared to be moisture into small beads at the ends of the specimen where dirt particles had collected. These (water beads?) were observed after 5, 10, and 20 cycles of exposure, but not after the full 50 cycles.

The 4 ply specimen was removed after only 20 and 50 cycles for observation since no damage occurred to the 8 ply material. As with the 8 ply material, no cracking or other damage was observed on the surface of the specimen. Thermal cycling of specimens equilibrated to 80% R.H. apparently has no noticeable effect on the appearance of the composite surface.

CONCLUSIONS

The 400 hour exposure of the polyimide-graphite composite to 473°F did result in considerable surface cracking, both at the cross-sectional surfaces of the specimen and at the outer surfaces of the material. On the cross-sectional surfaces the cracks appeared only within the strands which were oriented perpendicular to the surface. The 4 ply composite exhibited crack formation somewhat earlier in the exposure process than the 8 ply material, yet its final crack density along the cross section was less than that of the 8 ply composite.

There was also considerable cracking along the outside surfaces of the specimens. Although the amount of cracking appears to be considerable, the extent of damage to the interior of the material was shown to be minimal. Most of the cracks from the cross-sectional surface extended only about 0.1mm. into the interior, while a few cracks did extend about 0.5mm deep. The cracks from the outer surfaces extended only to the midpoint of the outer plies. Thus, for the 4 ply material, 75% of the interior contains no cracking behavior, and for the 8 ply material, 88% of the interior is crack free. There was also a slight loss of resin from the surface which was noticed from the depressions that were formed between the fibers perpendicular to the surface. These depressions (observed with the aid of an election microscope) are only a couple of microns deep, thus the loss of resin appears to be minimal.

The 400 hour exposure at 550°F produced similar results as with the 473°F exposure. The amount of cracking on both the cross-sectional and outer surfaces was comparable to that of the 473°F exposure. The only noticeable differences were that the initial cracking occurred somewhat sooner during the 550°F exposure and that the depth of the cracks from the cross section into the interior were slightly greater than those formed during the 473°F exposure. Yet, as with the 473°F exposed specimens, the only observable damage occurred at the outer portions of the material and the majority of the interior remained undamaged.

Thermally cycling composite materials, equilibrated at 80% R.H., from room temperature to 473°F produced no observable damage. During this period, moisture is rapidly driven from the outer regions of the composite while the center of the material still retains a large portion of its original moisture content. If any significant damage was to be produced due to thermal cycling, it would have been expected to occur within the first portion of this cycling process when the rate of moisture loss was at its greatest.

From the observations made during this study, the PMR15-graphite composite material in question appears to be satisfactory for operations at these temperatures (up to 550°F). This study has shown that for these given exposure times and temperatures, cracking is entirely a surface phenomenon and that the damage due to cracking will be minimal. Cracks can be expected to develop in the outer surfaces of the material, but these cracks will penetrate only to the midpoint of the outer ply. Since this cracking behavior, along with the slight loss of resin from the surface were only forms of damage observed (no evidence of debonding, delamination, or other damage were found), it would be expected that there would be some loss of material properties following thermal exposure, but that these losses would be quite small.

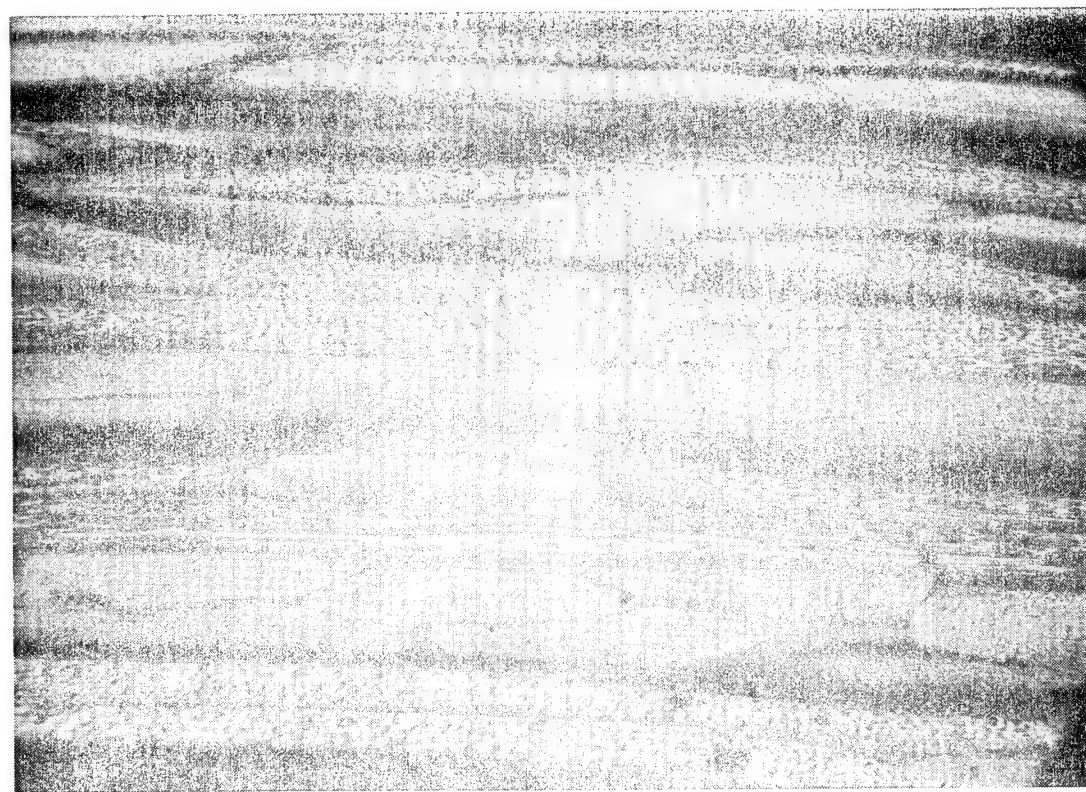


Figure 1. - Cross section of 8 ply material.

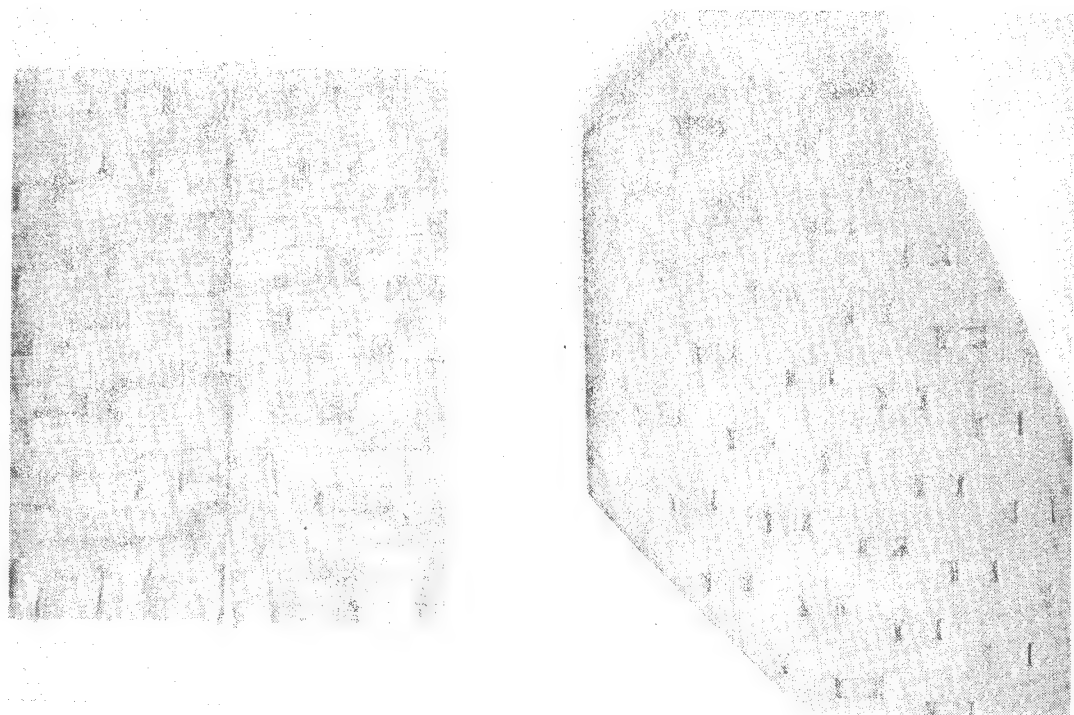
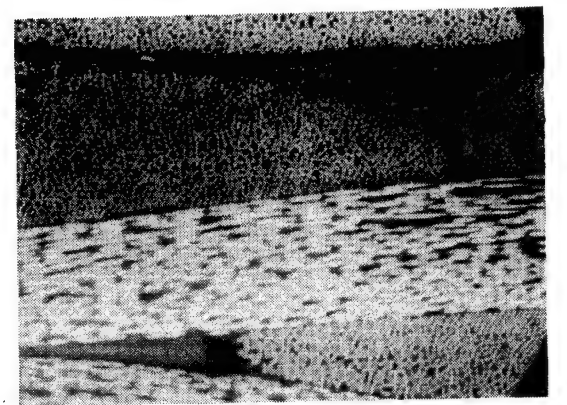
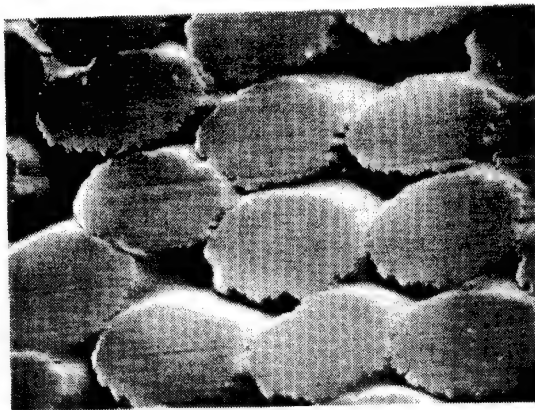


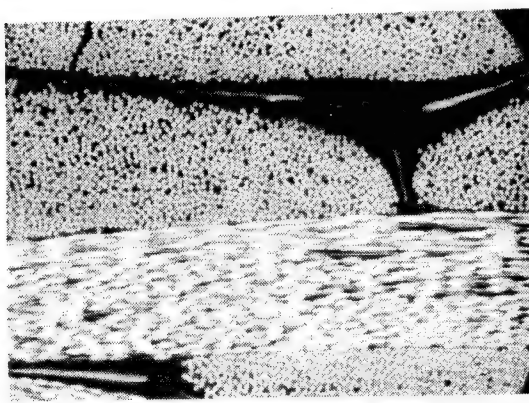
Figure 2. - Weave pattern in composite.



a



b



c

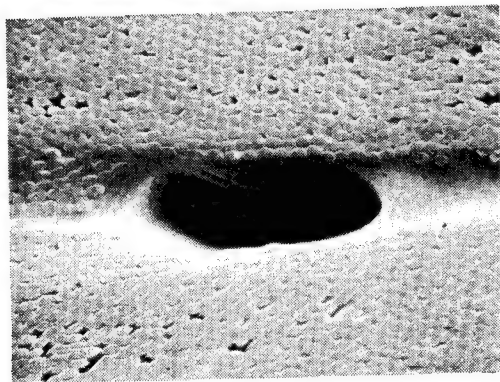
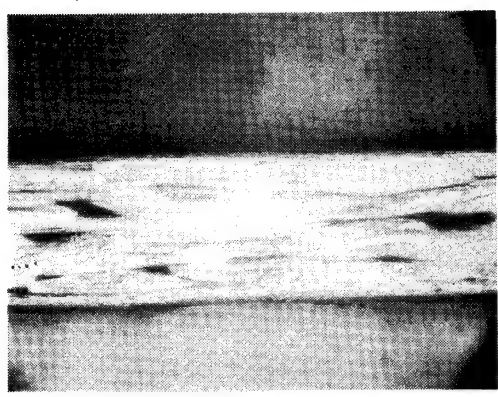
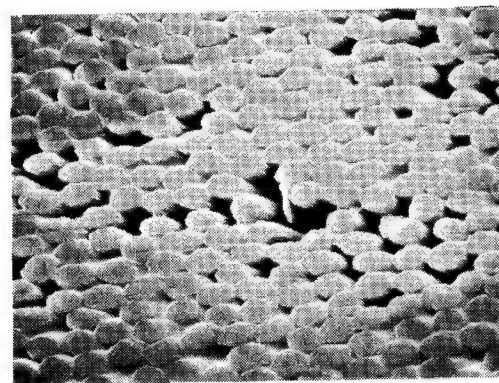


Figure 3. - Initial condition of 4 ply material.

Figure 4. - Loss of resin from composite surface.

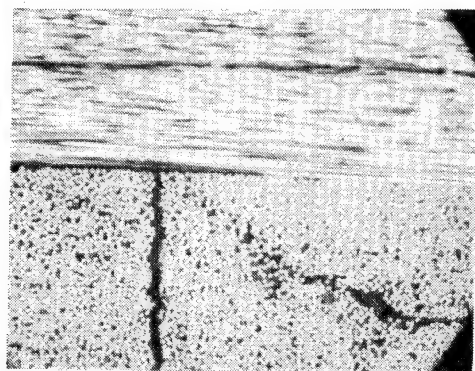
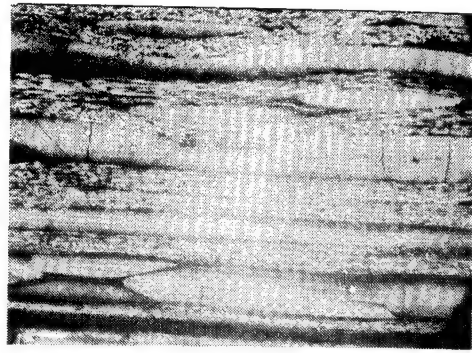
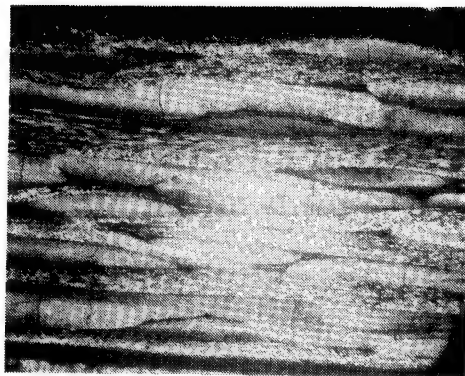


Figure 5. - 8 ply specimen after 258 hours of exposure at 473°F.

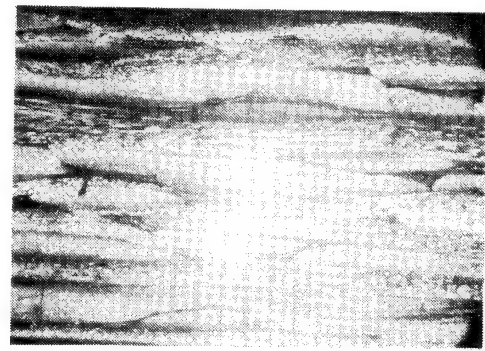
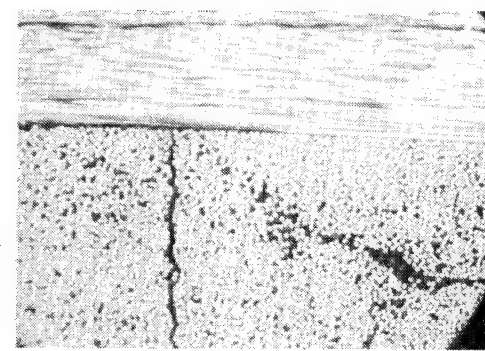


Figure 6. - 8 ply specimen after 391 hours of exposure at 473°F.

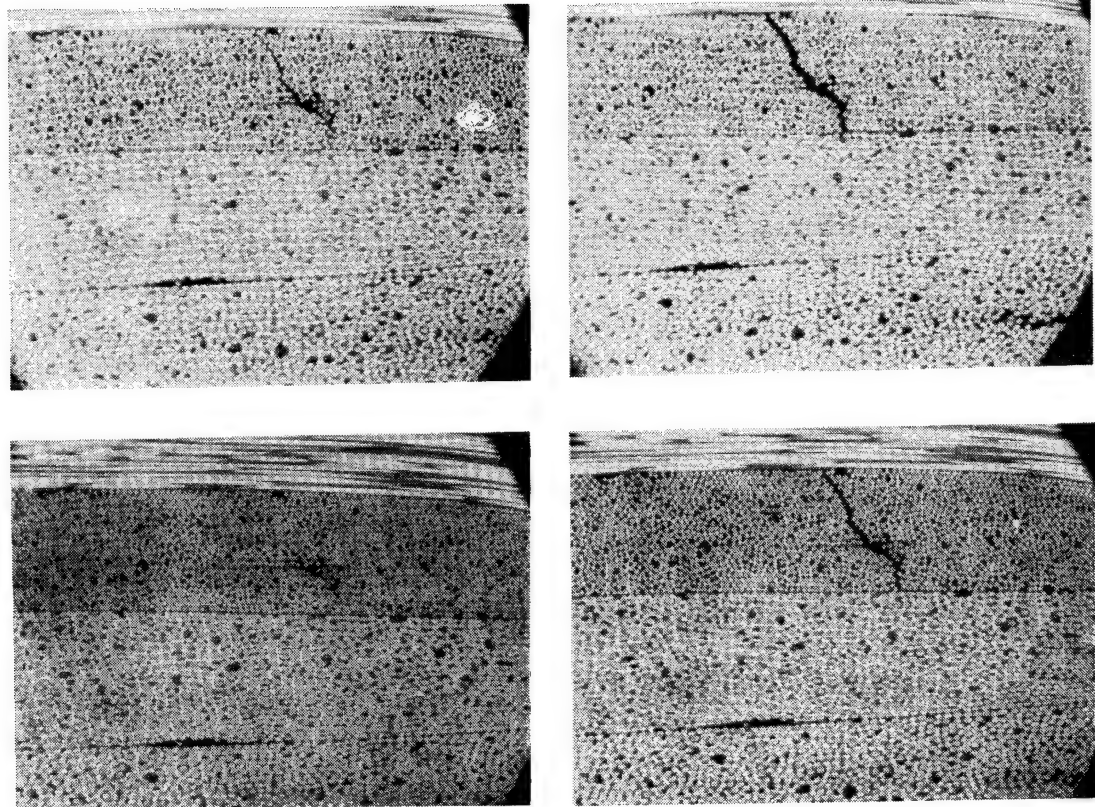


Figure 7. - Crack formation in 4-ply composite.

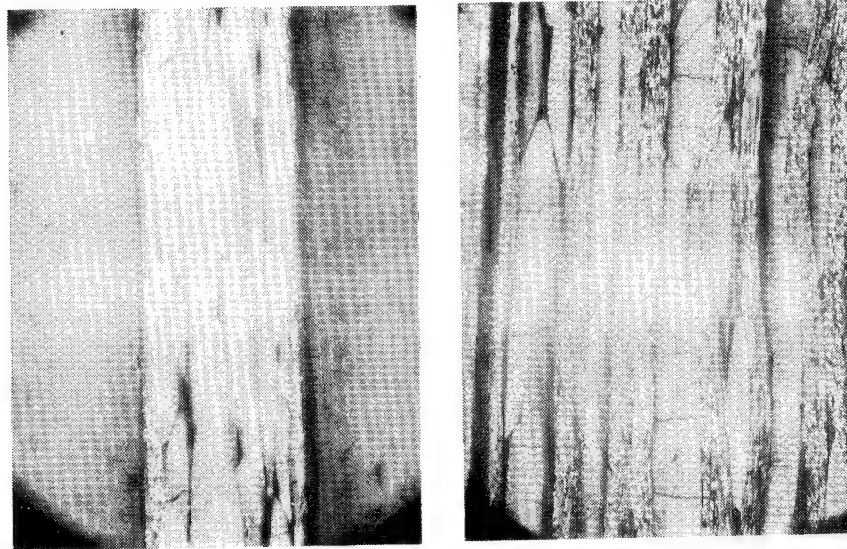


Figure 8. - 4 and 8-ply specimens following exposure at 473°F.

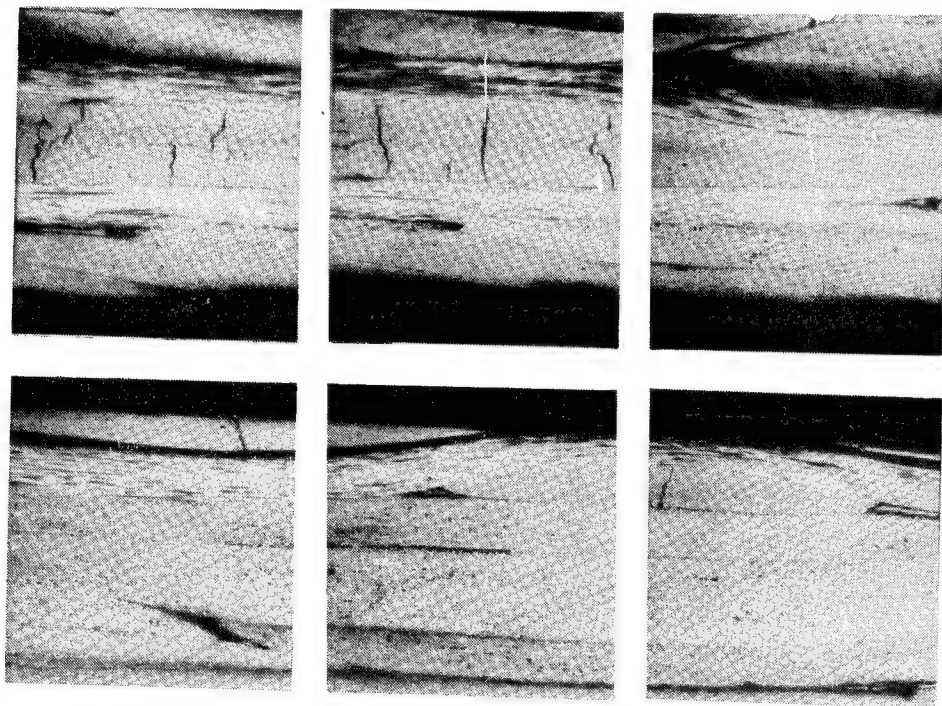


Figure 9. - 4 ply composite following exposure at 473°F.
(Top: Along +45° axis. Bottom: Along 90° axis.)

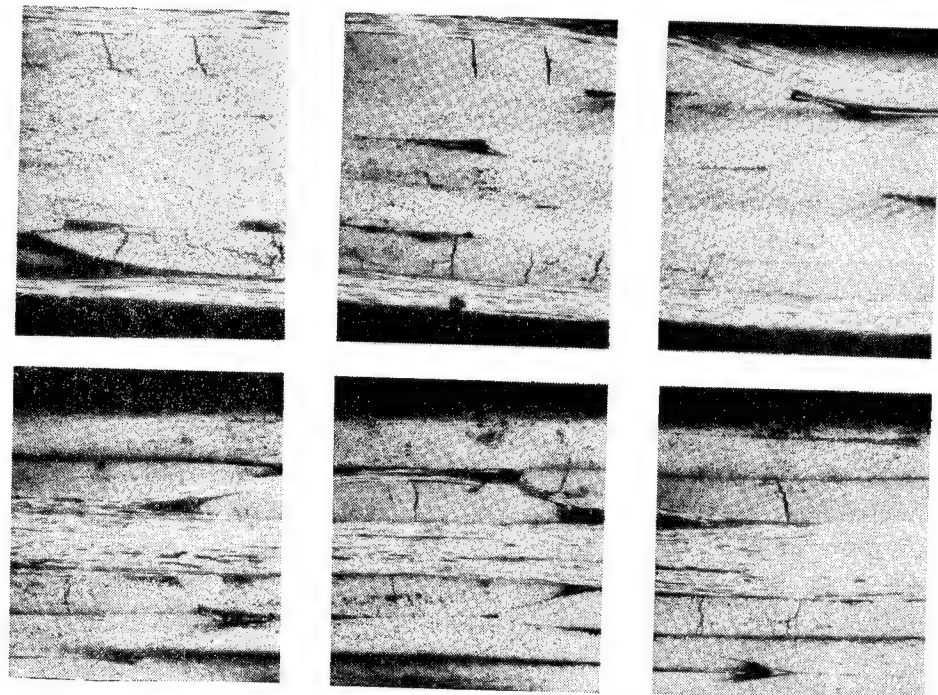


Figure 10. - 4 ply composite following exposure at 473°F.
(Top: Along 0° axis. Bottom: Along -45° axis.)

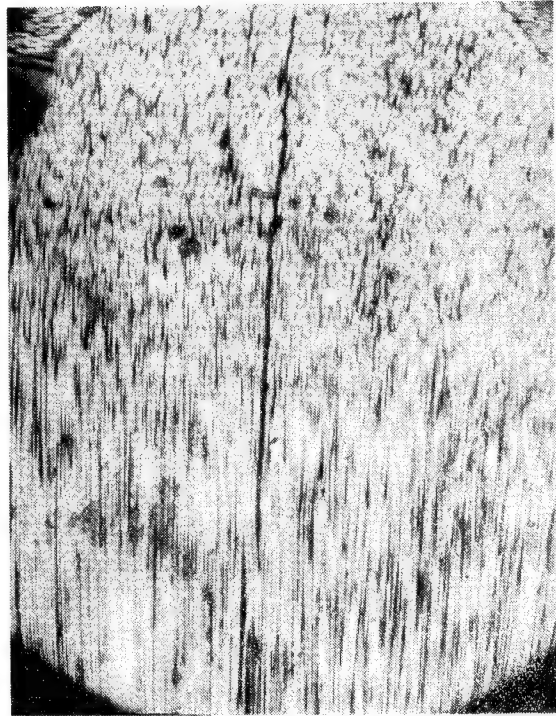
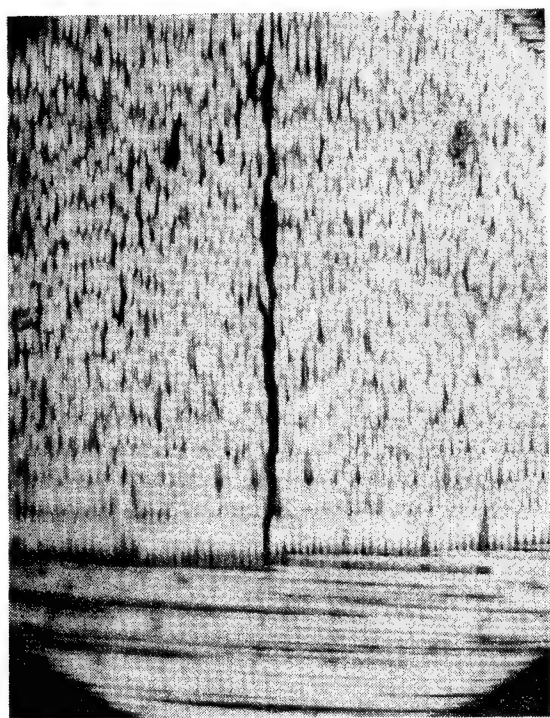
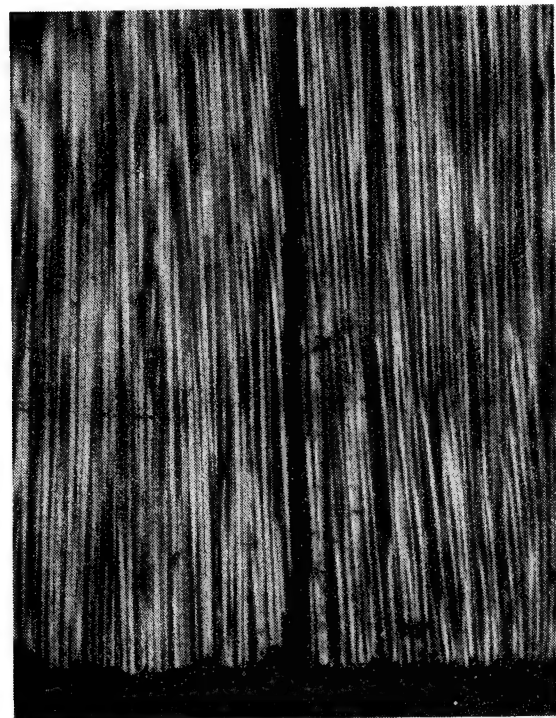


Figure 11. - Cracks along the outer surface following exposure at 473°F.

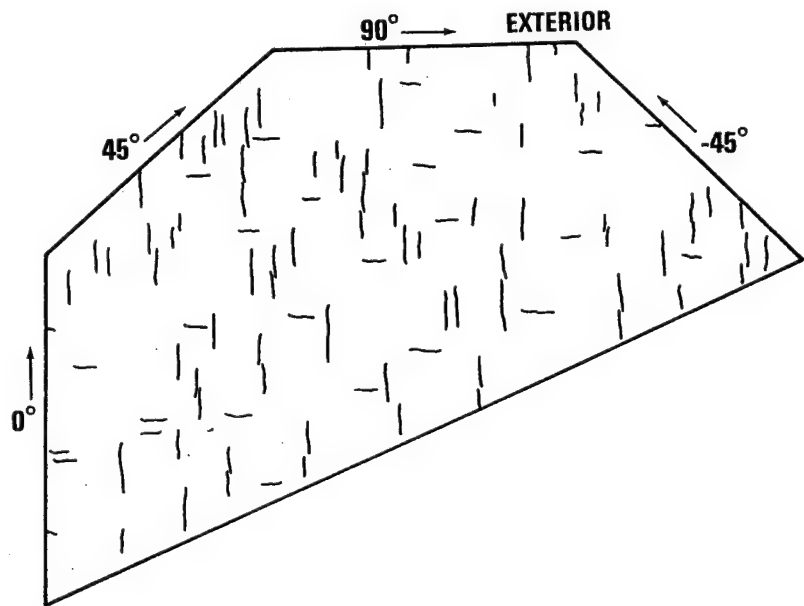


Figure 12. - 4 ply specimen after 400 hour exposure at 473°F.

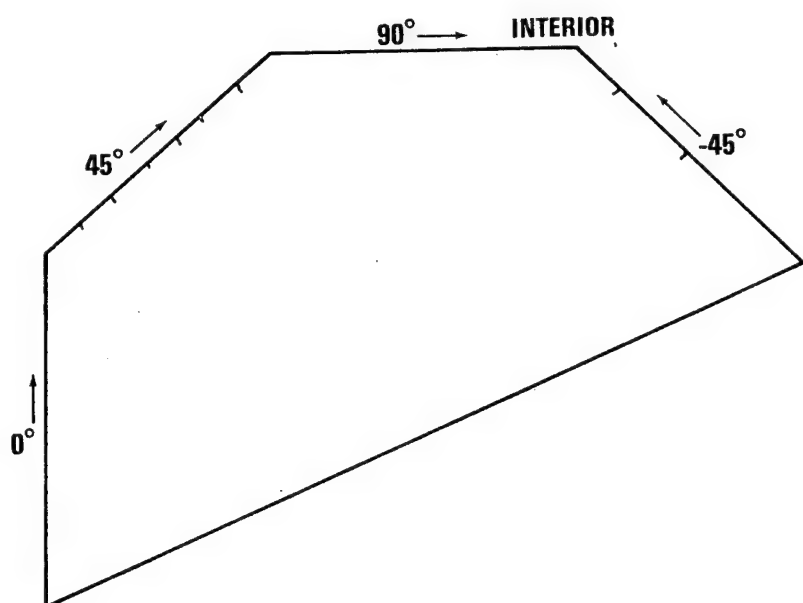


Figure 13. - 4 ply specimen after 400 hour exposure at 473°F.

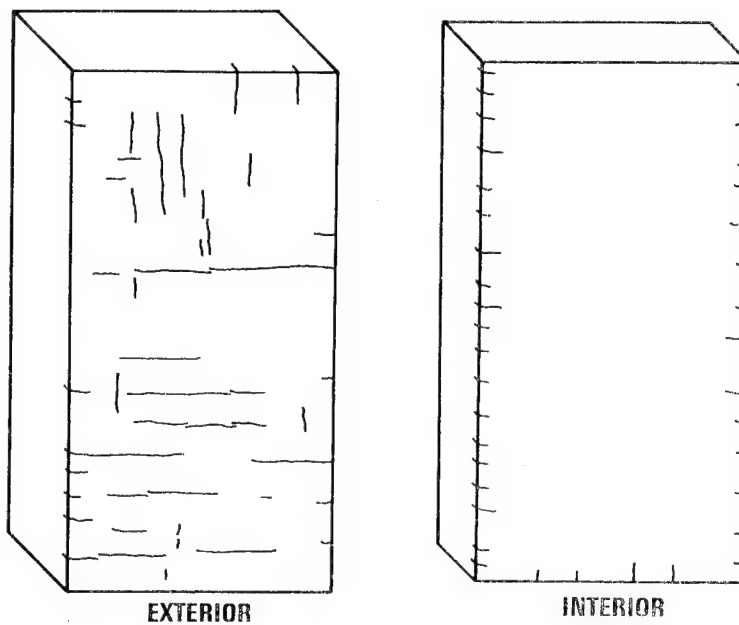


Figure 14. - 8 ply specimen after 400 hour exposure at 550°F.

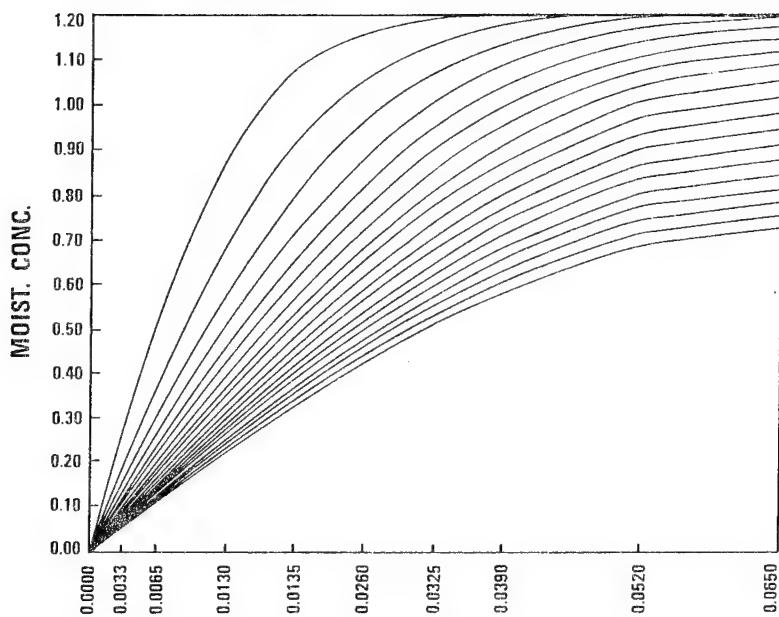


Figure 15. - Moisture concentration profile of a 4 ply specimen during thermal cycling.

EFFECTS OF REAL-TIME THERMAL AGING ON GRAPHITE/POLYIMIDE COMPOSITES*

*J.F. Haskins and J.R. Kerr
General Dynamics Convair Division*

As part of a program to evaluate high-temperature advanced composites for use on supersonic cruise transport aircraft, two graphite/polyimide composites have been aged at elevated temperatures for times up to 5.7 years. Work on the first, HT-S/710 graphite/polyimide, was started in 1974. Evaluation of the second polyimide, Celion 6000/LARC-160, began in 1980. Baseline properties are presented, including unnotched and notched tensile data as a function of temperature, compression, flexure, shear, and constant-amplitude fatigue data at $R = 0.1$ and $R = -1$.

Tensile specimens were aged in ovens where pressure and aging temperatures were controlled for various times up to and including 50,000 hours. Changes in tensile strength were determined and plotted as a function of aging time. The HT-S/710 composite aged at 450F and 550F is compared to the Celion 6000/LARC-160 composite aged at 350F and 450F. After tensile testing, many of the thermal aging specimens were examined using a scanning electron microscope. Results of these studies are presented, and changes in properties and degradation mechanisms during high-temperature aging are discussed and illustrated using metallographic techniques.

INTRODUCTION

Advanced composites will play a key role in the technology emerging for the design and fabrication of future supersonic vehicles.

Research and development during recent years has led to advances in fabrication techniques and characterization of short-time properties and has

provided limited supersonic flight experience for these materials.

However, information on the effects of long-time exposure to service environments representative of supersonic cruise aircraft on composite materials has not generally been available. An extensive program to generate such information has been in progress at General Dynamics Convair Division under NASA Contract NAS1-12308 since 1973 (Ref. 1).

Figure 1 illustrates the overall NASA study from which the material for this paper was taken. Changes in mechanical properties that occur over very long periods of time are being determined for ambient and thermal aging conditions and for random cyclic loading with cyclic temperature variations. These latter tests, the flight simulation exposures, are intended to provide data on the effect of 10,000, 25,000 and 50,000 hours of simulated supersonic flight service on residual properties of the composites. The purpose of the thermal aging study (conducted at constant temperature without load) was to assist in understanding the results of the more complex flight simulation program. While flight simulation tests are still in progress, the original thermal aging specimens have completed the required 50,000 hours of exposure, and the residual strength data is now available. The second polyimide, introduced later in the program, has completed thermal aging tests out to 10,000 hours.

This paper presents the results of these aging tests for two graphite/polyimide systems. Earlier work on thermal aging of HT-S/710 (Ref. 2) is compared to more recent work on Celion 6000/LARC-160. All exposures were conducted at ambient pressure. Previous work had shown a direct correlation of thermal aging and oxygen pressure on residual strength of resin-matrix composites (Ref. 1). In this paper, ambient pressure was

* Sponsored by the National Aeronautics and Space Administration, Langley Research Center, Hampton, Virginia, under Contract NAS 1-12308, monitored by Mr. Bland A. Stein.

chosen to compare the two systems, since most of the data has been generated at ambient pressure.

In actual use, a supersonic cruise vehicle would be at a very high altitude during much of the time at which the structure has reached its maximum temperature. Thus, if reduced oxygen pressure were taken into account, the composite materials could likely be used at high temperatures for longer periods of time.

EXPERIMENTAL

The graphite/polyimide composite systems employed in this program were HT-S/710 and Celion 6000/LARC-160. Six- and twelve-ply $[0^\circ \pm 45^\circ]$ crossplied laminates of each system were fabricated by Convair Division from vendor-supplied prepreg material using conventional autoclave processing methods. Quality assurance testing was conducted on both the as-received prepreg and the fabricated laminates. These acceptance tests included fiber, resin, and volatile contents, resin flow, and process gel for the prepreg material and ultrasonic C-scan, fiber content, specific gravity, and metallographic examinations for the panels. Table 1 lists information for the two composites.

Test specimens were cut from the panels using a diamond impregnated saw. Details of the specimen configurations for the various types of tests are presented in Table 2. Polyimide-quartz doublers were bonded to all but the flexure and short beam shear specimens using HT-424, a modified epoxy-phenolic film adhesive with an aluminum filler. For the thermal aging specimens, the doublers were attached after exposure.

Conventional test methods were used for the tensile, compression, flexure, and shear tests. The notched tensile specimens contained a center hole 0.25 inch in diameter, giving a theoretical stress concentration (K_t) of 2.43. Compressive strength

Table 1. Material systems.

Material System	Celion 6000/LARC-160	HT-S/710
Vendor	Fiberite	Hercules
Orientation	$[0^\circ \pm 45^\circ]_s$ $[0^\circ \pm 45^\circ]_{s2}$	$[0^\circ \pm 45^\circ]_s$ $[0^\circ \pm 45^\circ]_{s2}$
Fiber Content	67%	70%
Specific Gravity	1.56	1.48

was determined using a Celanese-type test fixture with an 18-ply specimen prepared by bonding together three six-ply panels. A similar 18-ply specimen was also used for the short beam shear tests.

Constant-amplitude fatigue tests were conducted at a constant frequency of 30 Hz. For elevated temperature tests, clamshell and ring furnaces were used. Temperature was monitored by a thermocouple attached to the specimen at the center of the gage section. A total of nine specimens was used to obtain an S-N curve for any given set of conditions. Test conditions were:

- Cycles: 10^3 to 10^7
- R values: -1 and 0.1
- Temperature: 75 and 350 or 450F
- Specimen configuration: unnotched and notched

Thermal aging exposures were conducted in specially constructed aging furnaces similar to the sketch in Figure 2. The heater plates consist of insulated wire sandwiched between two thin aluminum plates. All furnace temperatures were equilibrium-controlled; i.e., a constant amount of power was supplied to the heaters. The various aging temperatures were generally maintained to ± 5 F with infrequent excursions to a maximum of ± 10 F.

Table 2. Details of test specimens

Specimen Type	Length (in.)	Width (in.)	Plyes	Doublers Required
Unnotched Tensile	9	0.5	6	Yes
Notched Tensile	9	1	6	Yes
Compressive	5.5	0.25	18	Yes
Unnotched Fatigue	9	0.5	6 and 12	Yes
Notched Fatigue	9	1.0	6 and 12	Yes
Flexure	3	0.5	12	No
Short Beam Shear	0.6	0.25	18	No
Thermal Aging	9	0.5	6	Yes

The aging temperatures were: Celion 6000/LARC-160, 350F and 450F; and HT-S/710, 450 and 550F.

The procedure followed for the exposures was to cut the specimen blanks to final size, heat at 250F for 24 hours to remove absorbed moisture, and load into the aging furnaces. The specimens were supported at their ends by narrow strips of stainless steel so that almost the entire surface was exposed to the air atmosphere within the furnaces. At the required time intervals, the ovens were shut down, opened, and the specimens removed and stored in a desiccator until double bonding and tensile testing. Residual strength testing was performed at 350F for the Celion 6000/LARC-160 and at 450F and 550F for the HT-S/710. The data points shown in the residual strength-versus-time plots are averages obtained from three tensile specimens per test condition.

After tensile testing, many of the thermal aging specimens were sectioned and mounted for study using a scanning electron microscope. These studies were intended to detect changes that occurred in the composites during exposure to assist in identifying degradation mechanisms.

A more detailed account of the fabrication, quality assurance, baseline testing, and thermal aging procedures can be found in Reference 1.

RESULTS AND DISCUSSION

To establish sufficient baseline data, a number of tensile tests were performed. In Figures 3 and 4, the tensile properties for the two polyimide composites are shown for both the unnotched and notched configurations. Tests were performed at a number of temperatures between -67 and 650F. Each data point represents the average of at least three tests. A regression line was fitted to the data, as shown in Figures 3 and 4. Each set of data points was super-

positioned to 350F; the resulting Weibull distribution fit is shown in Figures 5 and 6. Each polyimide is compared for both the unnotched and notched conditions. The Weibull and normal distribution parameters for each of the four curves are listed in Table 3.

The data was pooled in this manner to provide the maximum use of the tensile data in setting load levels for the flight simulation tests shown in Figure 1. The loads in Table 3 can be converted to stress by dividing by the laminate thickness (approximately 0.03 inch).

Other baseline properties are given in Table 4. The data given compares flexural strength, shear strength, and compressive strength and modulus of HT-S/710 and Celion 6000/LARC-160. As was the case for tensile strength, the Celion 6000/LARC-160 composite is considerably stronger.

Results of the fatigue testing portion of the program are presented in Figures 7 through 10. These S-N plots compare the effects of stress ratio, R, notch configuration, and temperature on the fatigue strength of the two graphite/polyimide systems.

The data shows the fatigue life for a stress ratio of R = -1 to be much lower than for R = 0.1. The effect of test temperature or the presence of a center notch (hole with $K_t = 2.43$) was slight compared to the stress ratio effect.

Table 4. Baseline mechanical property data.

	HT-S/710		Celon 6000/LARC-160	
	(0-deg \pm 45)	(0-deg)	(0-deg \pm 45)	(0-deg)
Flexural strength (ksi)				
75F	94	171	137	196
350F	79	127	124	145
Shear strength (ksi)				
75F	5.4	7.0	8.8	9.0
350F	—	—	7.5	8.8
Compressive strength (ksi)				
75F	55	—	85	—
Compressive modulus (msi)				
75F	6.7	—	7.5	—

16033232-7

Table 3. Comparison of Weibull and normal distribution parameters for tensile loads of two polyimide composites.

Material & Specimen Configuration	Weibull α	Weibull β (lb/in.)	Standard Deviation	Average (lb/in.)	Coef. of Variation	No. of Data Points
Celion 6000/LARC-160 Unnotched	28	3,245	147	3,180	0.046	35
Celion 6000/LARC-160 Notched	14	2,377	192	2,290	0.083	35
HT-S/710 Unnotched	13	2,396	237	2,301	0.103	26
HT-S/710 Notched	12	1,675	145	1,611	0.090	29

The lines on each of the four graphs are regression lines drawn by computer. Differences in slope or slight changes in position are not considered significant. As for the mechanical properties, in general, the Celion 6000/LARC-160 S-N curves are about 25% higher than those for HT-S/710.

Residual tensile strength of the HT-S/710 system is plotted as a function of aging time in Figure 11. Curves for aging at 450 and 550F in 14.7 psi air are included. The material aged at 450F showed very little change in tensile strength for times up to 25,000 hours. However, when the aging temperature was raised to 550F, significant strength decreases were observed after 5,000 hours of exposure. After 50,000 hours, almost no resin was left in the specimens, only graphite fibers. The specimens were badly warped and delaminated, and were no longer suitable for tensile testing. All tensile tests were performed at 350F after the indicated aging times. Each point consists of the average of three tensile coupons.

Residual tensile strength of the Celion 6000/LARC-160 system is plotted as a function of aging time in Figure 12 for ambient air pressure. As in the case of the HT-S/710, each point represents the average of three tensile tests. Aging temperatures were reduced for the second polyimide to 350 and 450F. There was not enough difference in the data for the two temperatures to draw separate curves. As shown in Figure 12, there is some loss in strength for aging times as short as 500 hours. After 10,000 hours of exposure at 450F, a comparison of the two graphite/polyimide systems shows that each has about the same residual tensile strength. Based on the shape of the aging curves, however, the HT-S/710 system would appear to be superior for time periods greater than 10,000 hours.

Scanning electron microscope photomicrographs in Figures 13 through 15 show results of metallographic examination of the graphite/polyimide aging specimens. For the HT-S/710 system (Figure 13), specimens aged at 450F exhibited no oxidation or matrix degradation effects for the first 25,000 hours. After 50,000 hours, relief polishing around the graphite fibers, increased porosity, and more fiber-matrix separation were observed. Raising the aging temperature to 550F greatly increased the degree of matrix degradation of the HT-710 system. Figure 13 shows that, in

one-atmosphere air, 10,000 hours at 550F has a slightly greater effect on the microstructure than 50,000 hours at 450F.

For the Celion 6000/LARC-160 system, metallographic effects were much more evident for the thermal aging specimens. At lower magnifications, the degree of microcracking and relief polishing was found to be related to both the temperature and length of time of aging. This can be seen in Figure 14. As pointed out earlier, however, the results of the tensile tests did not indicate a significant temperature effect for at least 10,000 hours of exposure. At higher magnification, evidence of oxidation, similar in nature to that first observed in the A-S/3501 graphite/epoxy system (Ref. 3) was found. Figure 15 shows the results of the higher-magnification examinations. When the polyimide resin matrix oxidized, it was more prone to crumble and resulted in an increased amount of relief polishing around the individual fibers. After 10,000 hours of aging at both temperatures, considerable oxidation has occurred in the outer plies but almost none in the center plies. This would be expected for an oxidation mechanism where attack begins at the outer surfaces and proceeds inward. Careful examination of Figure 15 also reveals an effect of temperature on oxidation where the degree of relief polishing around the graphite fibers is slightly greater at 450F than at 350F.

CONCLUSIONS

The mechanical properties of the Celion 6000/LARC-160 system were, in general, at least 25% stronger than the HT-S/710 system. The fiber-dominated properties of the two polyimides were nearly independent of temperature for the region examined. The matrix-dominated properties showed a slight decrease in strength as the temperature was increased.

The fatigue results clearly show that the strength at 10^7 cycles for a stress ratio of $R = -1$ is 50% of that for $R = 0.1$. Differences between room and elevated temperature S-N curves were not statistically significant. Also, notching had little effect on the fatigue results.

During thermal aging of HT-S/710 at 450F in an air atmosphere, there was little change in tensile strength for times out to 25,000 hours. At 550F, the strength was reduced significantly by 5,000 hours. Aging of Celion 6000/LARC-160 at both

350F and 450F resulted in a 20% loss in strength after 5,000 hours and a 30% loss after 10,000 hours. Tests on these specimens are being continued to 25,000 hours.

Metallographic studies have shown an increase in microcracking with aging time for the Celion 6000/LARC-160 system. These examinations have also revealed evidence of conventional oxidation damage to the matrix with the effect initiating at the surface and progressing inward with time. A similar effect had been observed earlier for A-S/3501 graphite/epoxy. For the HT-S/710 system, metallographic examinations showed very little during the early stages of exposure. For the longer times, increased porosity and fiber-matrix separation accompanied by numerous fine cracks at the fiber-matrix interface were revealed. However, visual effects starting at the edges and moving inward as seen in the Celion 6000/LARC-160 and A-S/3501 systems were not observed.

REFERENCES

1. Kerr, J.R. and Haskins, J.F., "Time-Temperature-Stress Capabilities of Composite Materials for Advanced Supersonic Technology Application," General Dynamics Convair Division, Report No. NASA CR-159267 (GDC-MAP-80-001), Prepared for NASA-Langley Research Center, April 1980.
2. Kerr, J.R. and Haskins, J.F., "Effects of 50,000 Hours of Thermal Aging on Graphite/Epoxy and Graphite/Polyimide Composites," AIAA/ASME/ASCE/AHS 23rd Structures, Structural Dynamics, and Materials Conference, New Orleans, Louisiana, May 1982.
3. Haskins, J.F., Kerr, J.R., and Stein, B.A., "Flight Simulation Testing of Advanced Composites for Supersonic Cruise Aircraft Applications," AIAA/ASME 18th Structures, Structural Dynamics, and Materials Conference, San Diego, California, March 1977.

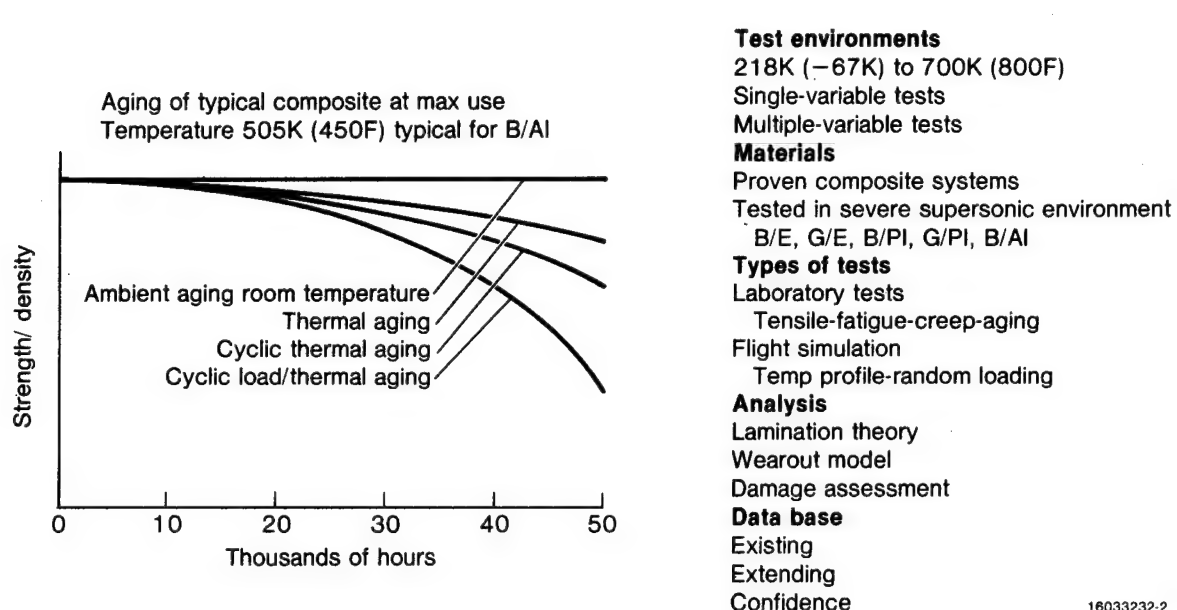


Figure 1. Characterization of composite material for up to 50,000 hours of supersonic cruise aircraft environment.

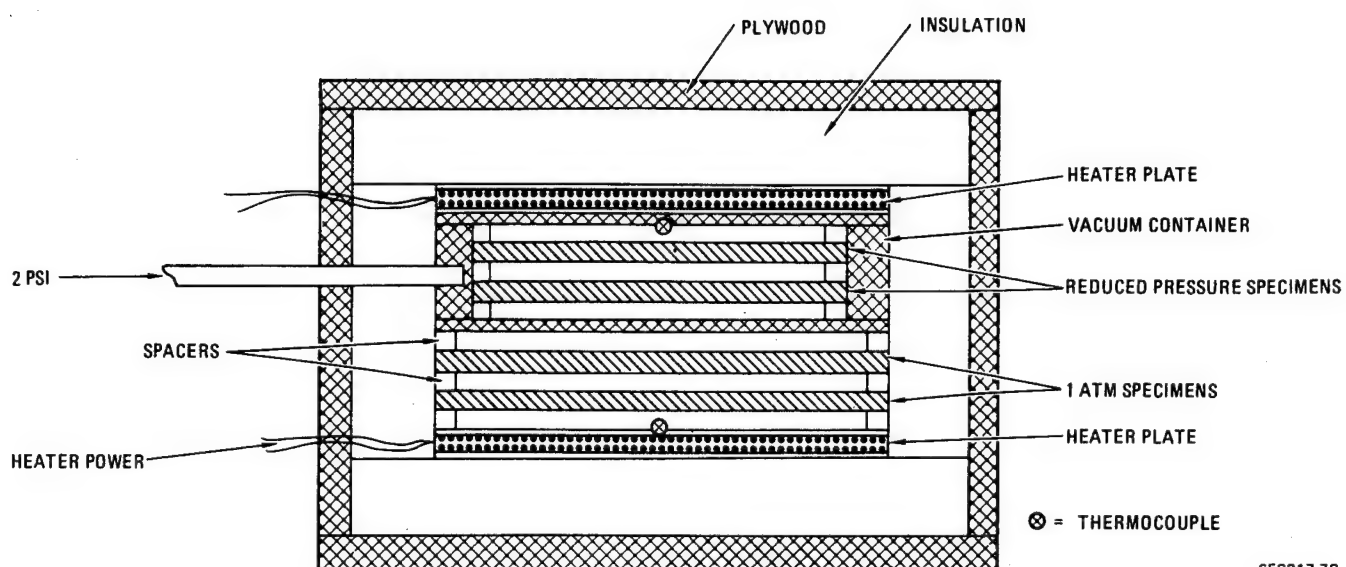


Figure 2. Thermal aging furnace configuration.

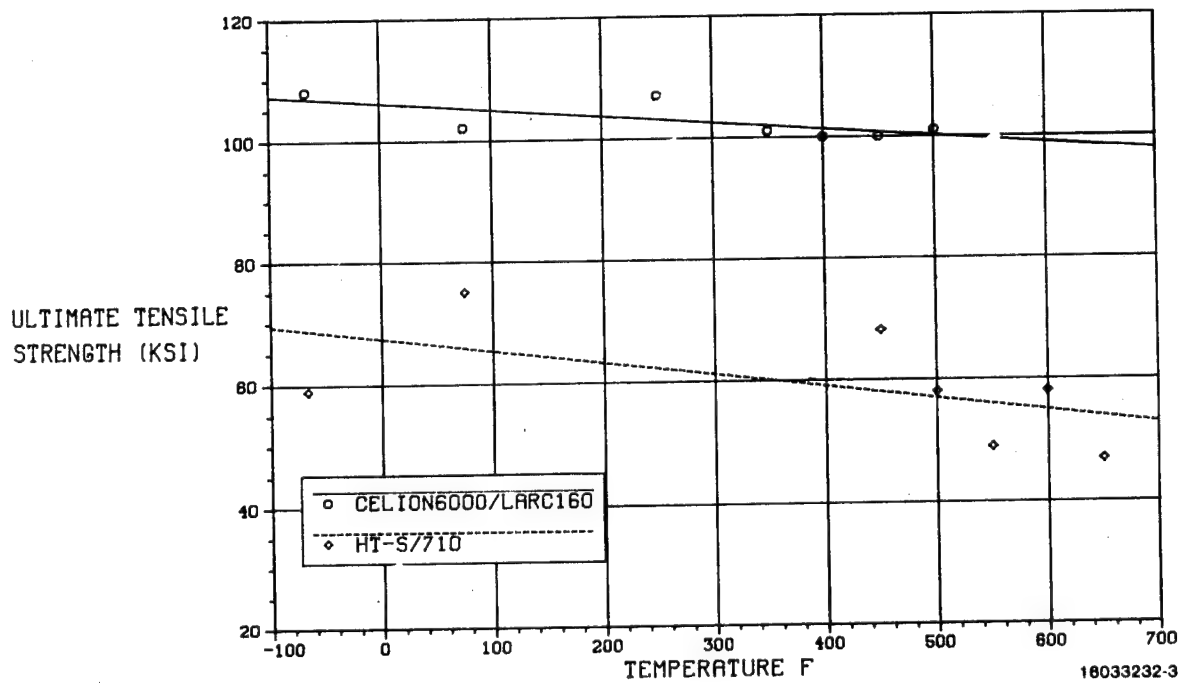


Figure 3. Baseline tensile results comparing unnotched Celion 6000/LARC-160 and HT-S/710 (0±45)_S polyimide composites.

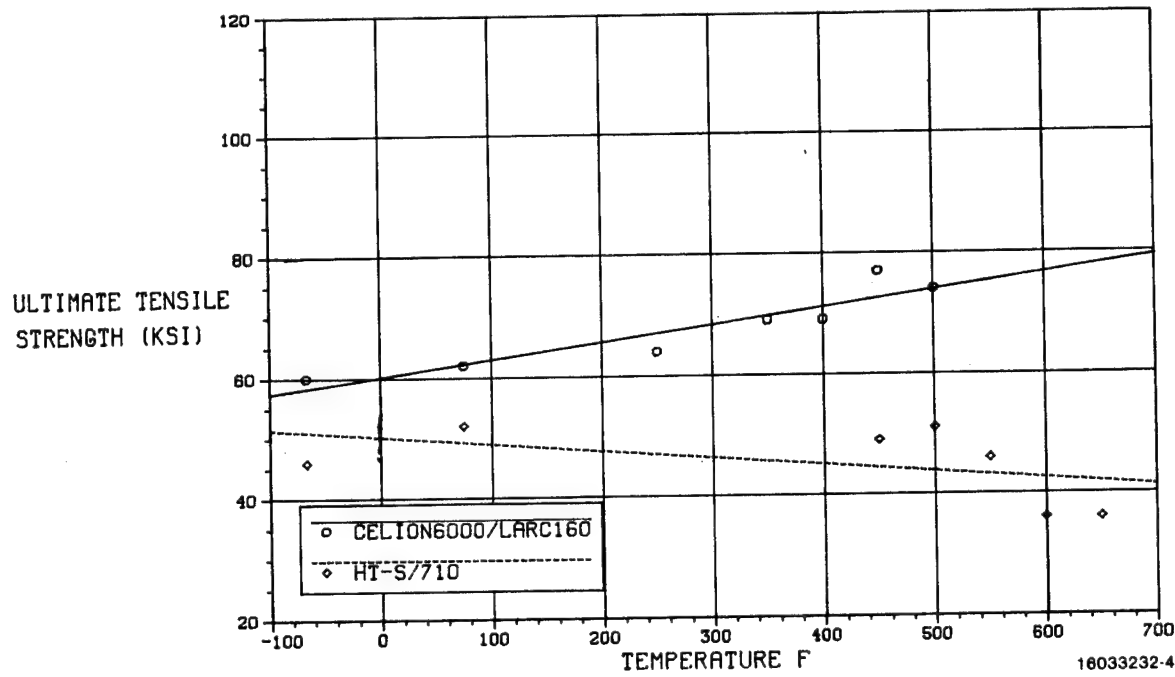


Figure 4. Baseline tensile results comparing notched Celion 6000/LARC-160 and HT-S/710 (0±45)_S polyimide composites.

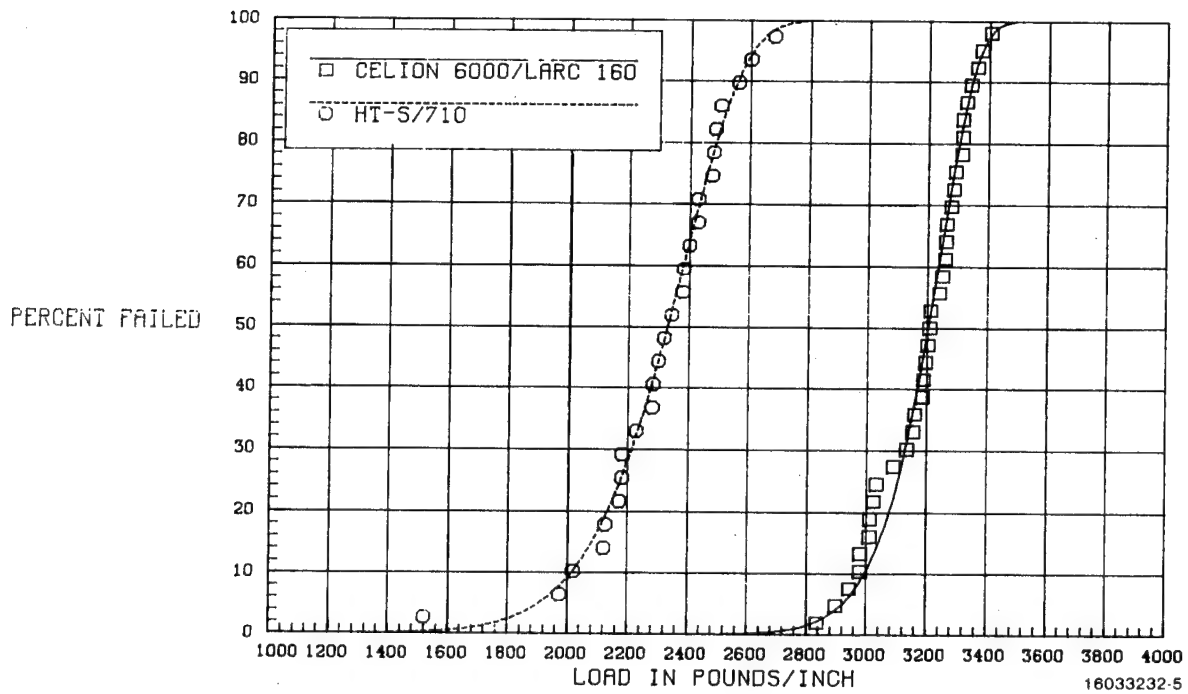


Figure 5. Comparison of unnotched tensile data for HT-S/710 and Celion 6000/LARC-160 (0 ± 45)_S (test points superpositioned to 350F for pooling).

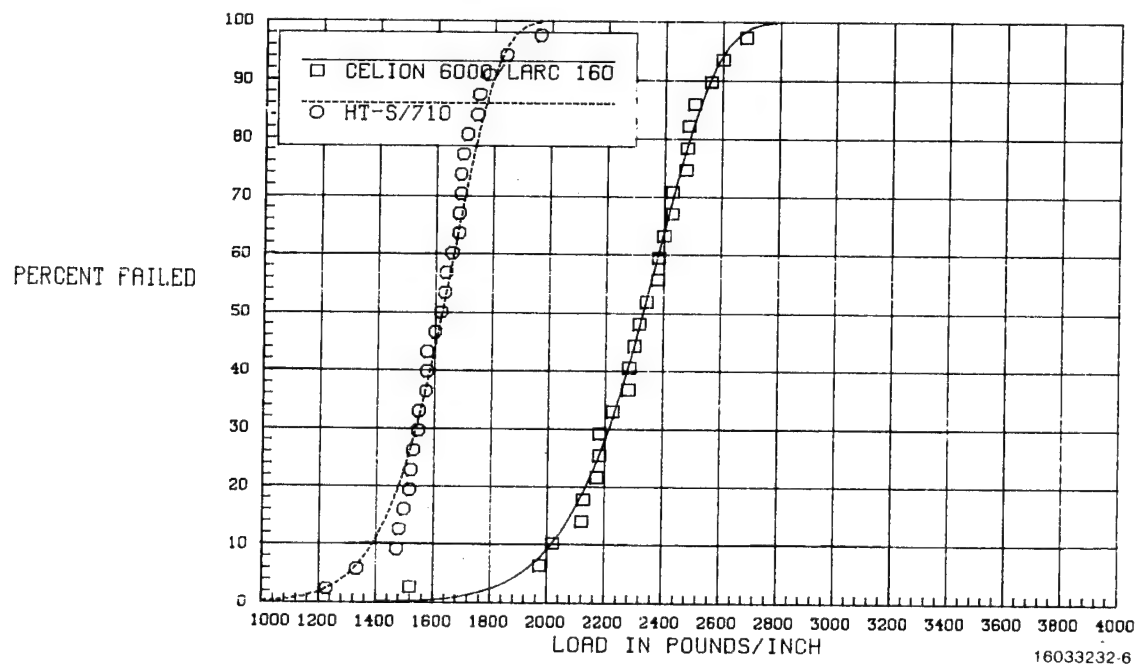


Figure 6. Comparison of notched tensile data for HT-S/710 and Celion 6000/LARC-160 (0 ± 45)_S (test points all superpositioned to 350F for pooling).

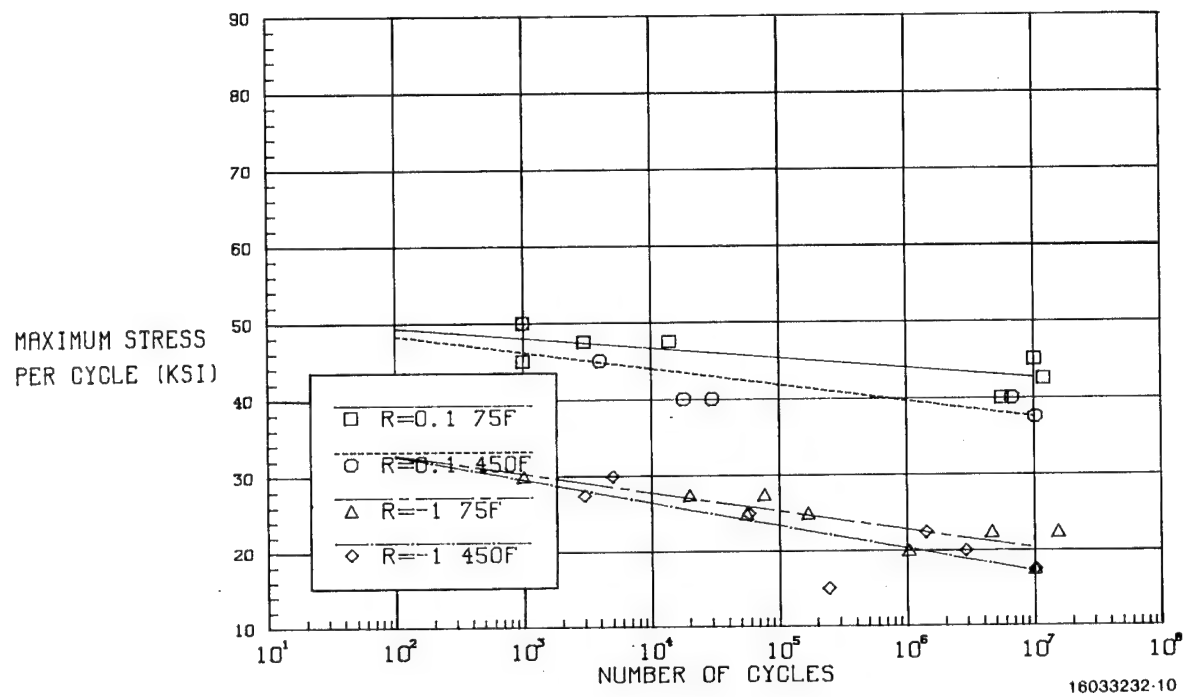


Figure 7. Axial fatigue data for HT-S/710 (0±45)_S G/PI, unnotched, $R=0.1$, $R=-1$.

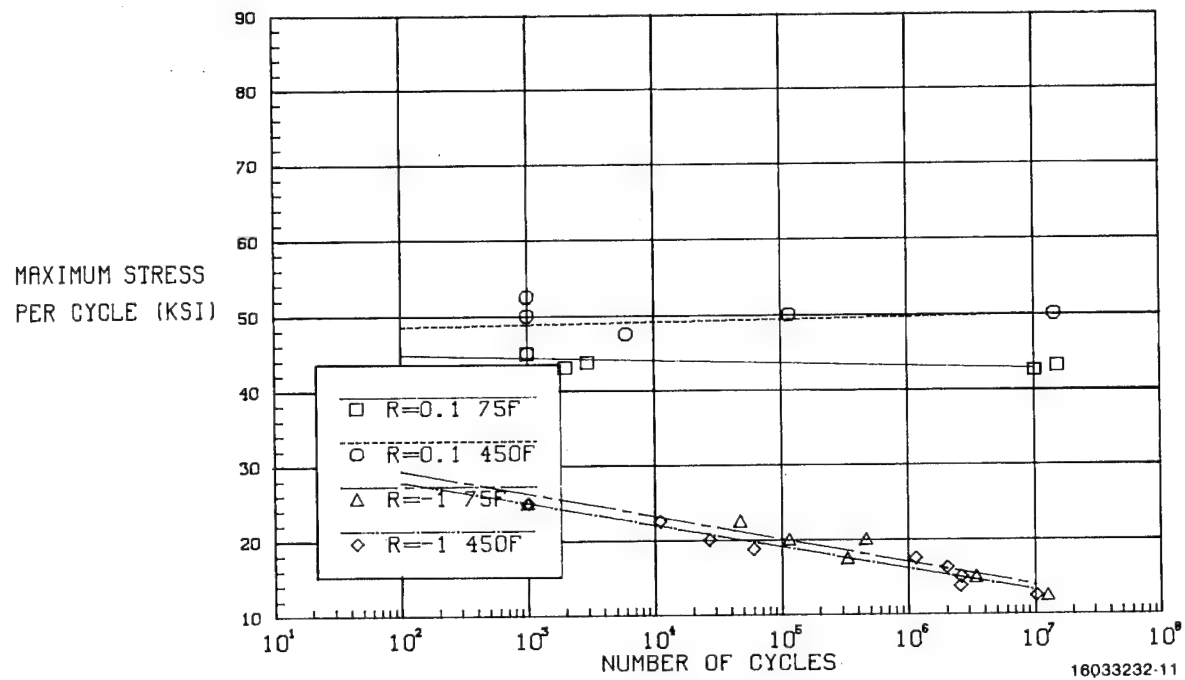


Figure 8. Axial fatigue data for HT-S/710 (0±45)_S G/PI, notched, $R=0.1$, $R=-1$.

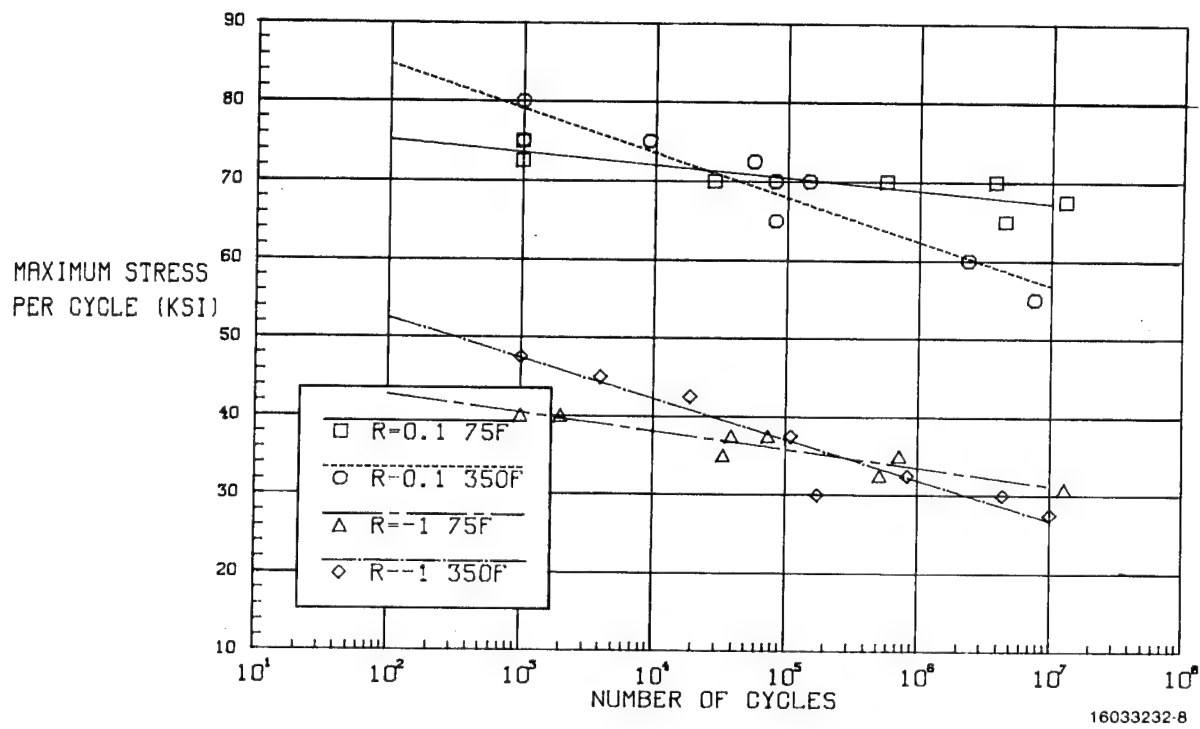


Figure 9. Axial fatigue data for Celion 6000/LARC-160 (0±45)_S G/PI, unnotched, R=0.1, R=-1.

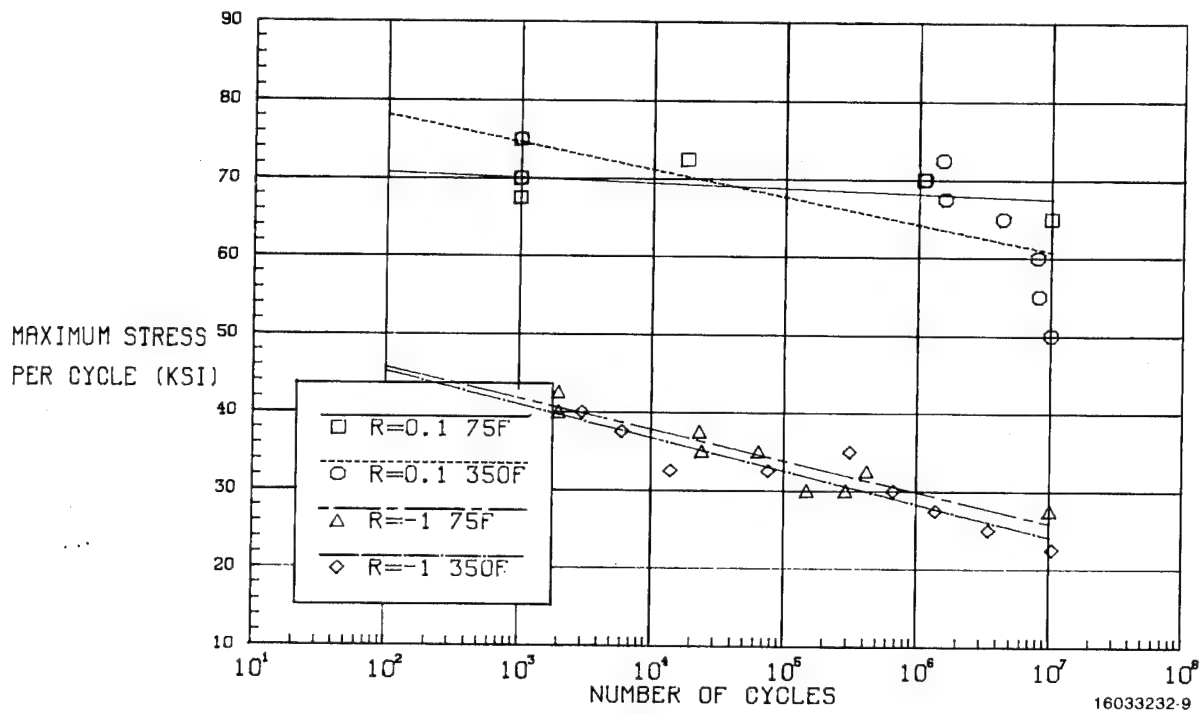


Figure 10. Axial fatigue data for Celion 6000/LARC-160 (0±45)_S G/PI, notched, R=0.1, R=-1.

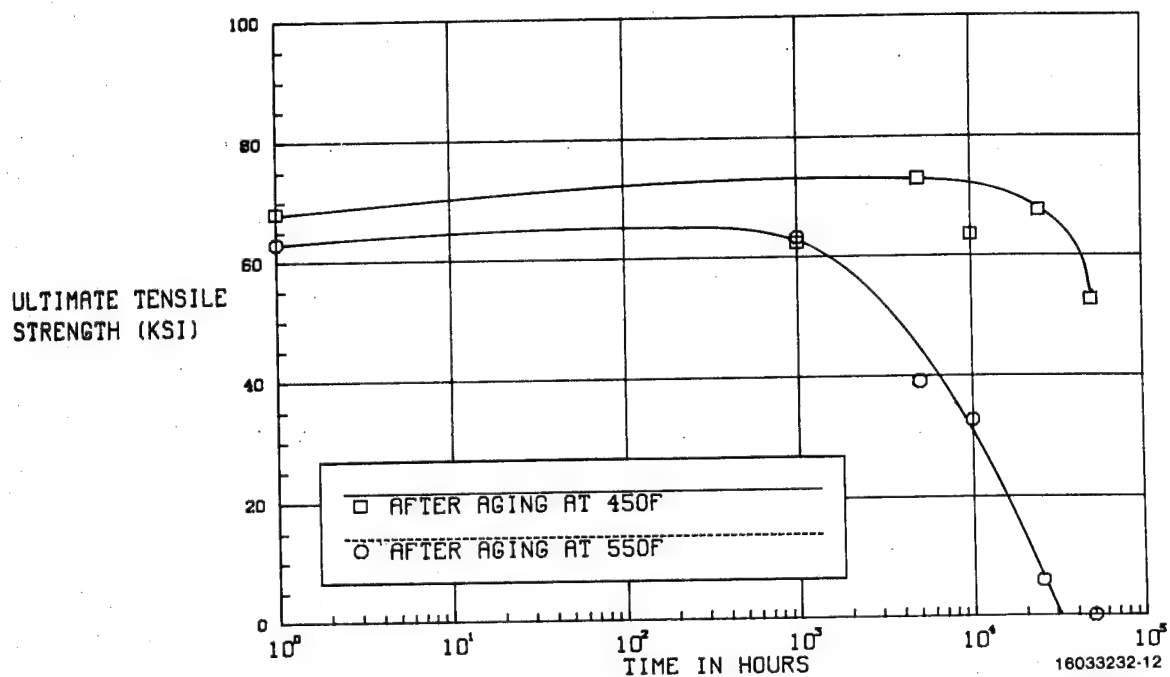


Figure 11. Tensile strength at aging temperature of HT-S/710 (0±45)s G/PI after thermal aging in 14.7 psi air at indicated temperatures.

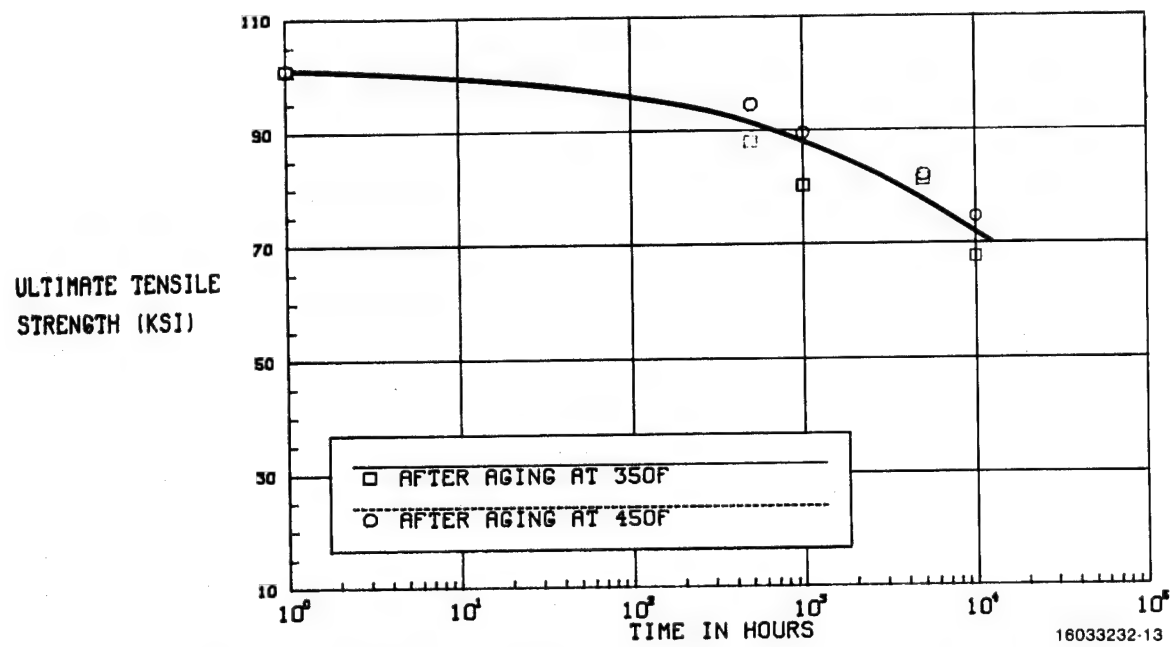
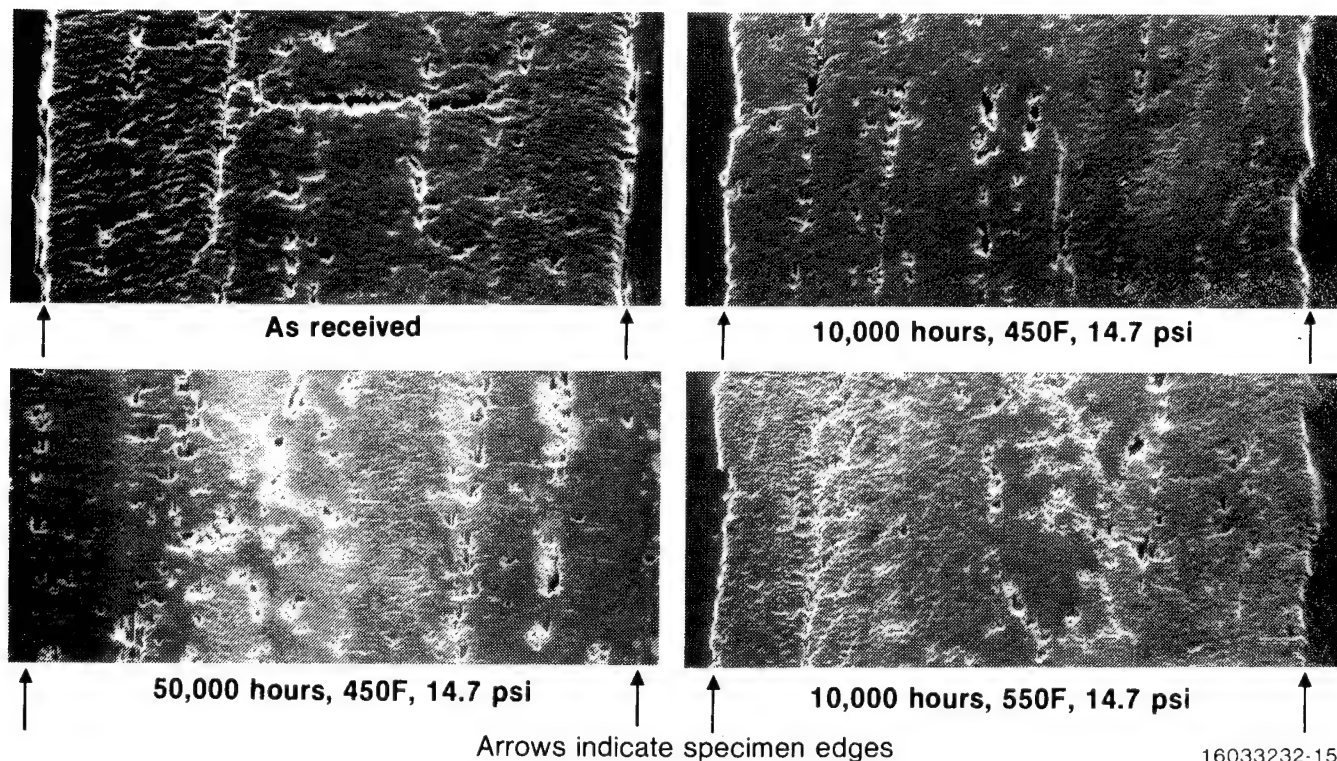


Figure 12. Tensile strength of Celion 6000/LARC-160 (0±45)s G/PI at 350F after thermal aging in 14.7 psi air at the indicated temperatures.



16033232-15

Figure 13. HT-S/710 graphite/polyimide after thermal aging at indicated conditions (100 \times).

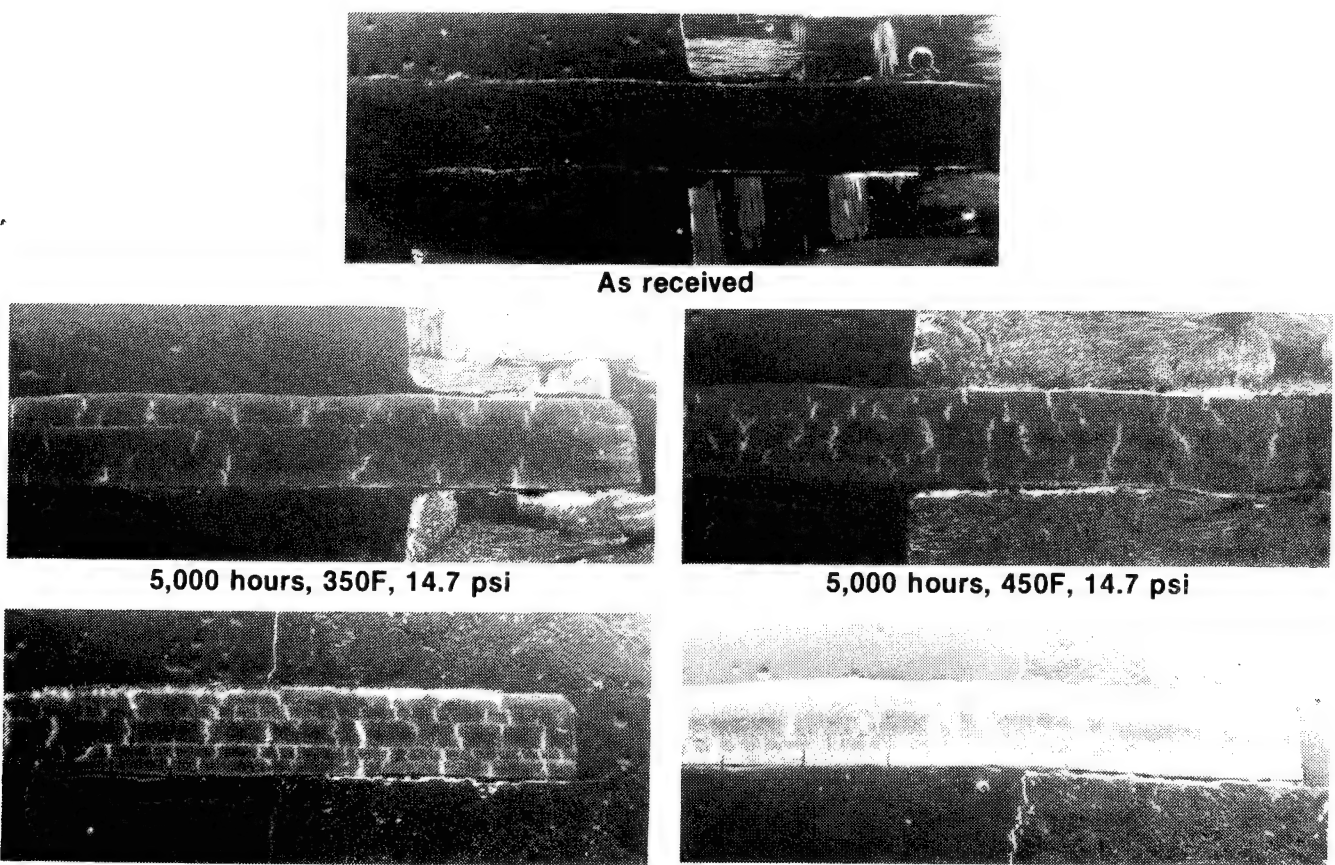
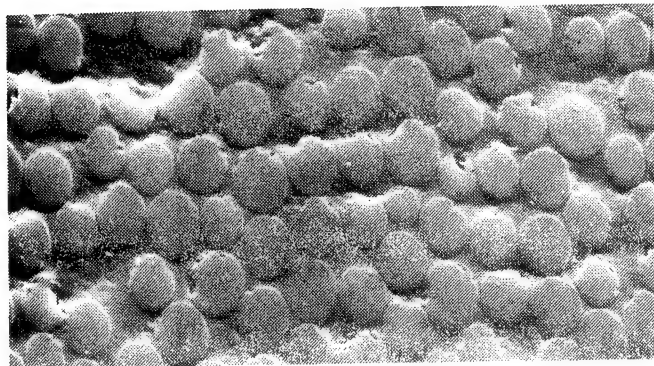
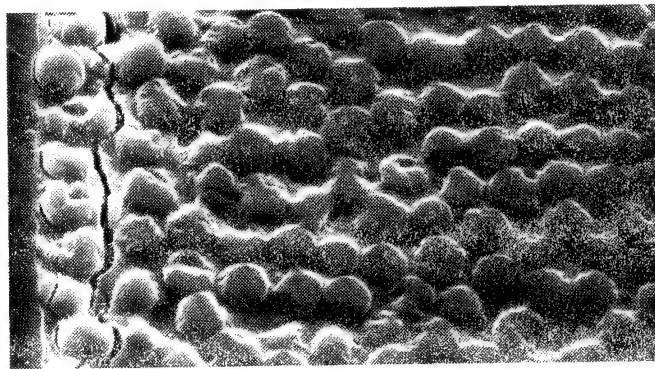


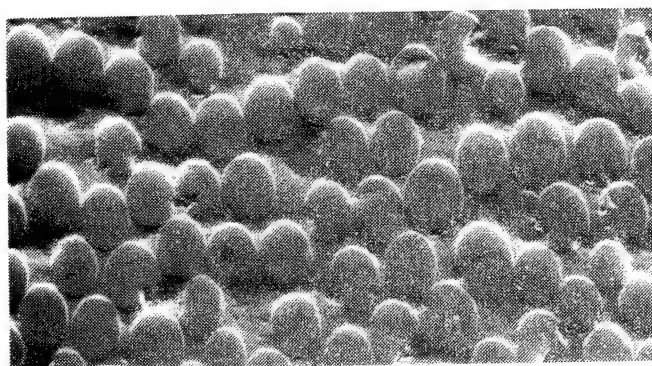
Figure 14. Celion 6000/LARC-160 graphite/polyimide after thermal aging at indicated conditions (13 \times).



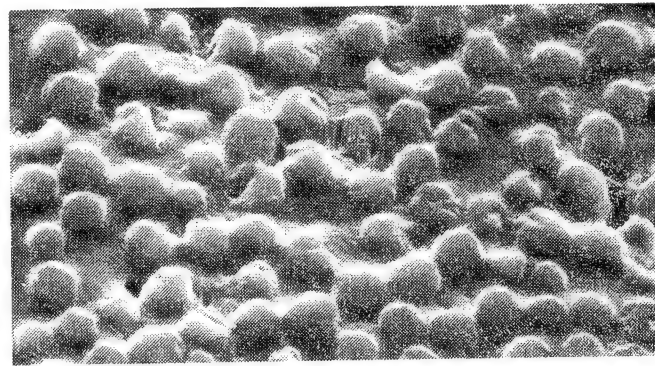
10,000 hours, 350F, 14.7 psi
Inner ply



10,000 hours, 350F, 14.7 psi
Outside ply



10,000 hours, 450F, 14.7 psi
Inner ply



10,000 hours, 450F, 14.7 psi
Outside ply

16033232-16

Figure 15. Celion 6000/LARC-160 graphite/polyimide after thermal aging at indicated conditions (1000 \times).

ENVIRONMENTAL STABILITY GRAPHITE/PMR-15 COMPOSITES

Clyde H. Sheppard and Doug McLaren
Boeing Aerospace Company
Boeing Commercial Airplane Company
Divisions of The Boeing Company

During the past few years The Boeing Company has been screening graphite composites for use in "hot areas" of engine nacelle structure. Structural and thermal analyses have shown that there is the potential for a 25 to 30 percent weight savings by using a graphite polyimide (Gr/PI) composite material in this type of structure.

Work conducted on the NASA CASTS program (Composites for Advanced Space Transportation Systems) amply demonstrated the capability of Graphite/PMR-15 for short term service (125 hours) at temperatures up to 589K (600°F). In addition, the CASTS program demonstrated that large structures could be fabricated using Gr/PMR-15. In commercial applications, however, the requirement exists for long term service capability (tens of thousands of hours) at temperatures ranging upwards from 449K (350°F). The results of Graphite/PMR-15 materials characterization efforts conducted at Boeing are presented in this paper, with emphasis on materials properties after isothermal aging at temperatures of 449K (350°F) and above.

BACKGROUND

The Boeing Aerospace Company (BAC) was selected by NASA Langley Research Center to demonstrate, over the 1977-1980 time period, the manufacturing of large structures using Graphite/PMR-15 polyimide broadgoods (ref. 1). Subsequently, BAC conducted four other NASA-sponsored programs, designed to refine the Quality Control of the PMR-15 graphite materials (ref. 2), the structural design capability using PMR-15 (refs. 3 and 4) and the characterization of PMR-15 polyimide prepgs (ref. 5). Based on the results of these first four programs, the Boeing Commercial Airplane Company (BCAC) instituted a long range development effort to adapt these materials to engine nacelle structures. The primary difference between the requirements posed by the NASA CASTS program and the requirements of commercial engine nacelle structure is the commercial requirement for very long times at moderate conditions (i.e., upwards of 30,000 hours at 449K (350°F) to 484K (450°F) with intermediate times (i.e., 5000 hours) at 545K (550°F)). To determine the suitability of PMR-15 materials under these conditions, the BCAC Propulsion Development Group initiated a series of programs which has extended from 1980. Interim data reported at the Hi Temple meeting at Las Cruz, New Mexico, in May 1982 was promising enough to reorient the isothermal aging program to include an evaluation of polyimide coatings and available sizings for the graphite fibers. This paper presents the interim results of that study.

Graphite/PMR-15 Composite Fabrication

Following the completion of the NASA Quality Control program (ref. 2) BAC adopted the PMR-15 Material Specification to the Boeing system and designated it as BMS 8-275. Additionally, the processes developed on the same program were also adopted, and designated as XBAC 5577. The Material Specification at Boeing includes:

- o Fiber properties
- o Graphite/PMR-15 prepreg properties
- o Graphite/PMR-15 composite properties
- o Chemical, physical and composite testing for properties

The processing document at Boeing includes:

- o Materials control
- o Layup procedure for:
 - flat laminates
 - hat sections
 - I beams
 - honeycomb panels
 - chopped graphite moldings
- o Quality Control accept and reject criteria

All materials used were subjected to the requirements of the Boeing material specification prior to release for composite panel manufacture. Those composite panels were in turn subjected to the requirements of the processing document (i.e., Nondestructive Inspection) and determined to be flaw free before use in the initial program. Results obtained in 1980-81 (Figures 1 and 2) indicated that the Graphite/PMR-15 performed extremely well and met the initial criteria i.e., 5000 hours at 545K (550°F). The material was also performing reasonably well at the lower 449K (350°F) temperature at 10,000 hours. Based on the results of that study, another test matrix was started (Figure 3). The purpose of this matrix was three fold:

- 1) To compare the aging characteristics of graphite fabric vs. graphite tape
- 2) To compare two commercially available fiber sizings (i.e., epoxy vs. polyimide)
- 3) To compare the effects of coating the Gr/PMR-15 composite on isothermal aging characteristics

The Gr/PMR-15 materials used in the above test matrix were obtained using reinforcements supplied by Celanese and one batch of PMR-15 resin manufactured by U.S. Polymeric. The materials met the requirements of the Boeing materials document, and the composite panels used in the aging studies were processed and met the Quality Control requirements of the Boeing processing documents. The tested specimens were machined from composite laminates which had been isothermally aged in panel form. The resulting test data are reported in Figures 4 thru 6.

Summary of Aging Studies

Preliminary analysis of the data obtained during the course of this program could be summarized as follows:

- o PMR-15 composites are suitable for long term use at the intermediate temperature range of 484K (450°F) thru 545K (550°) and short term use at 589K (600°F).
- o Preliminary indications are that the degradation modes of PMR-15 composites can probably be suppressed.

REFERENCES

1. Sheppard, C. H.; Hoggatt, J. T.; and Symonds, W. A.: Manufacturing Processes for Fabricating Graphite/PMR-15 Polyimide Structural Elements. NAS1-15009, 1979.
2. Sheppard, C. H.; Hoggatt, J. T.; and Symonds, W. A.: Quality Control Developments for Graphite/PMR-15 Polyimide Composites Materials. NASA CR-159182, 1979.
3. Skoumal, D. E.; and Arnquist, J. L.: Design, Fabrication and Test of Graphite/Polyimide Composite Joints and Attachments for Advanced Aerospace Vehicles. NASA CR-159111, 1980.
4. Cushman, J. B.; and McCleskey, S. F.: Design Allowables Test Program, Celion 3000/PMR-15 and Celion 6000/PMR-15, Graphite/Polyimide Composites. NAS1-15644, 1982.
5. Lindenmeyer, P. H.; and Sheppard, C. H.: Characterization of PMR-Polyimide Resin and Prepreg. NAS3-22523, 1983.

FIGURE 1

Celion 3000 Fabric/PMR-15

Interlaminar Shear Behavior of Conditioned (0.90)₁₀ Laminate

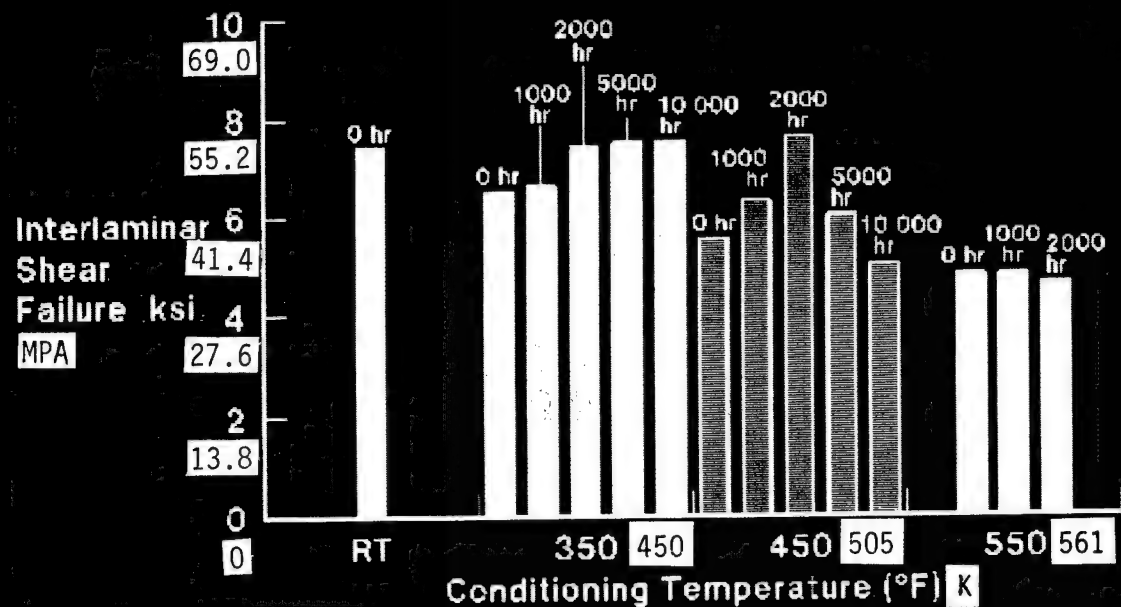


FIGURE 2

Celion 6000 Tape/PMR-15

Tensile Strength of Conditioned (0, ±45, 90)₈ Laminate

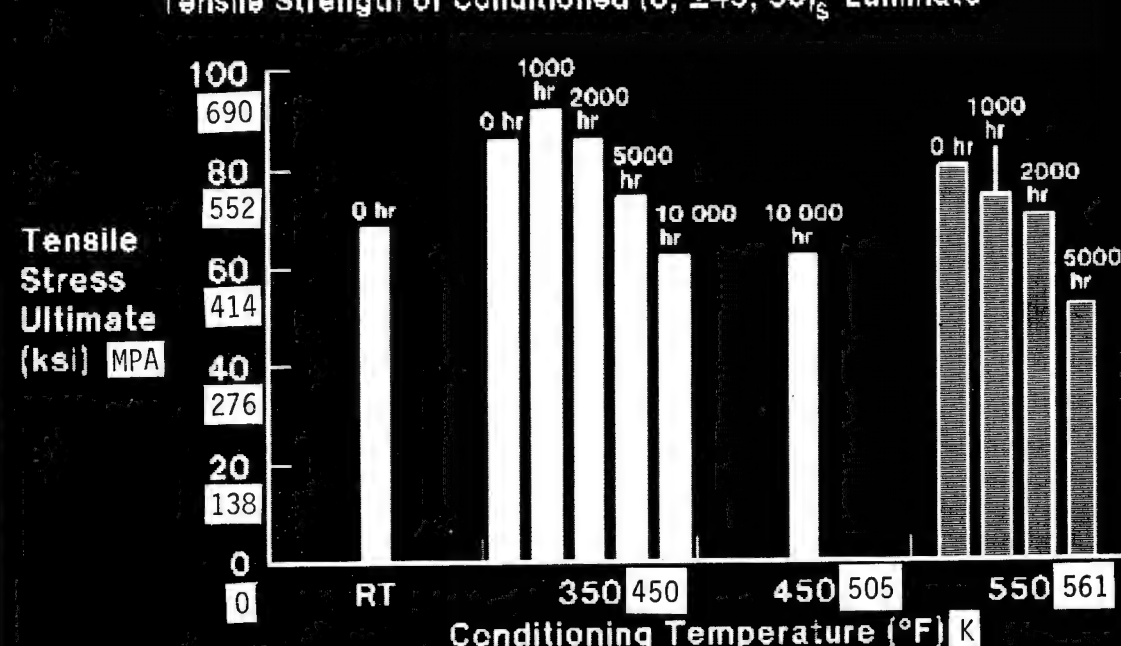


FIGURE 3
Test Matrix

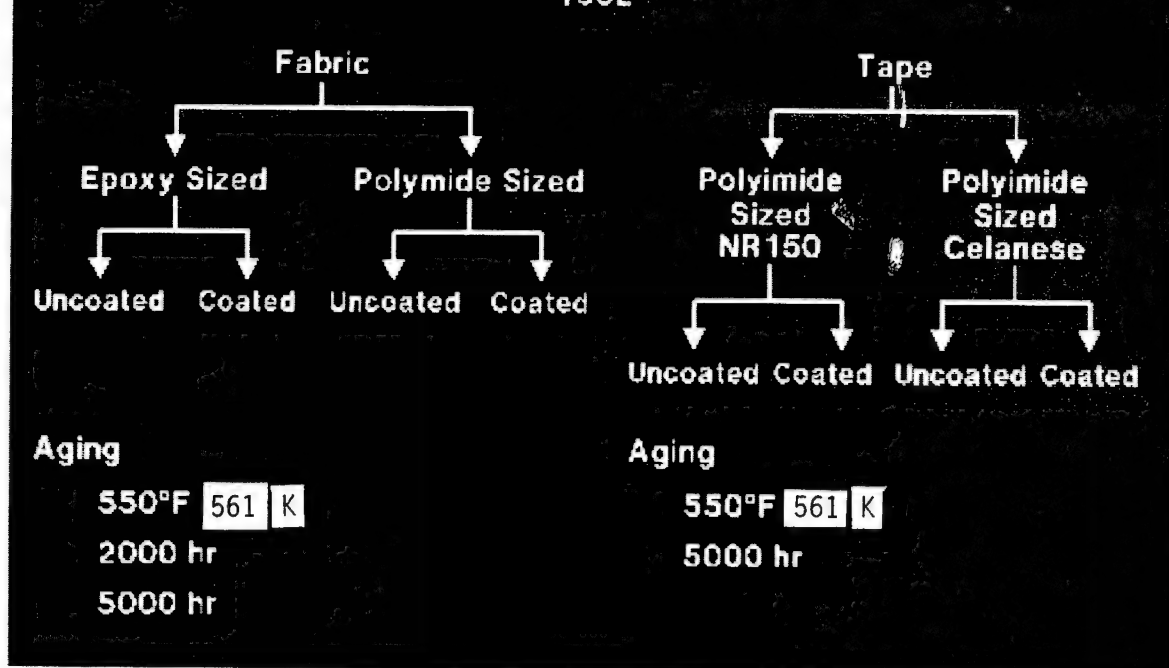
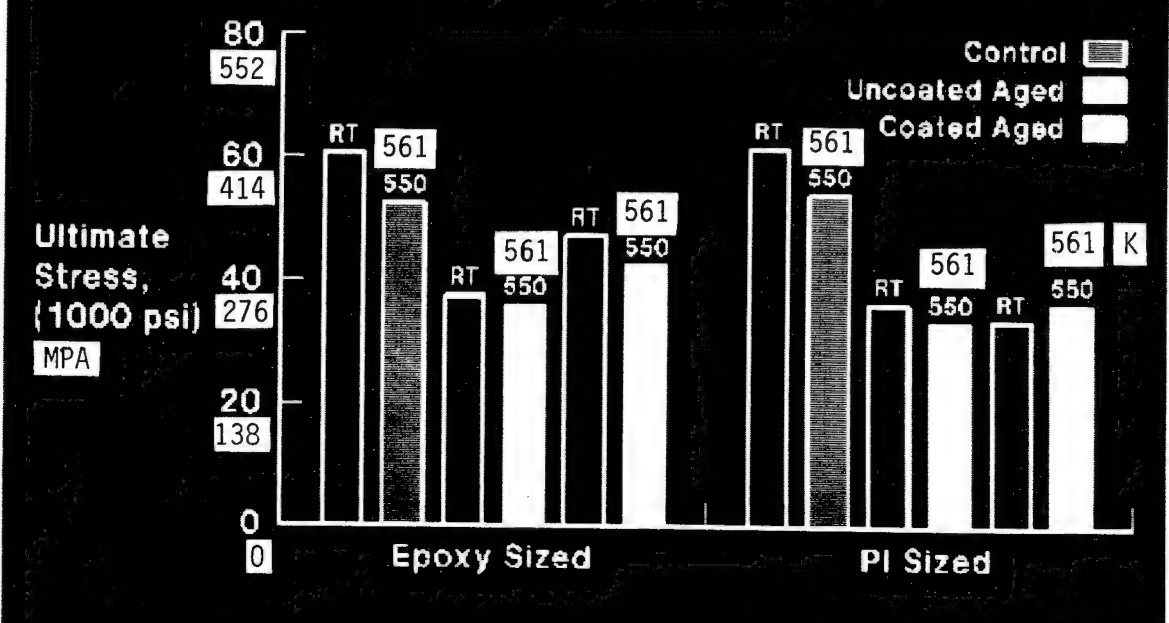
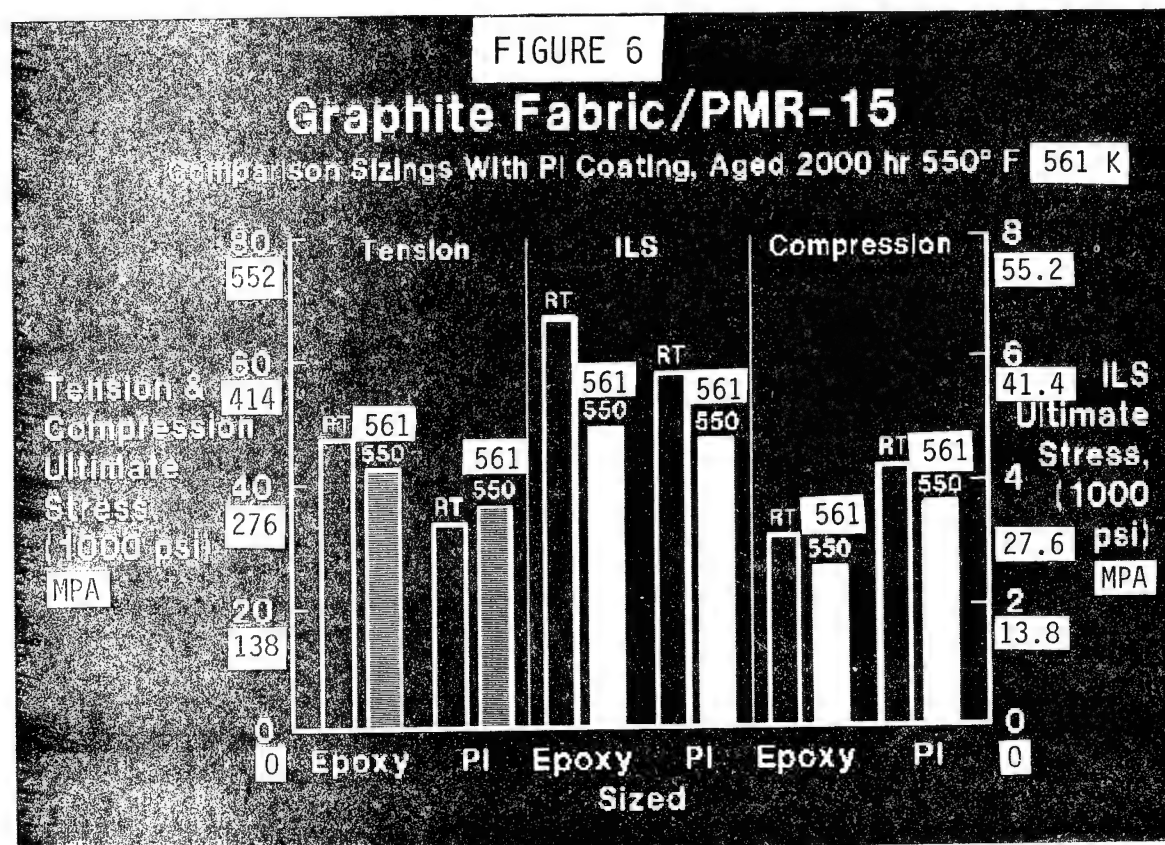
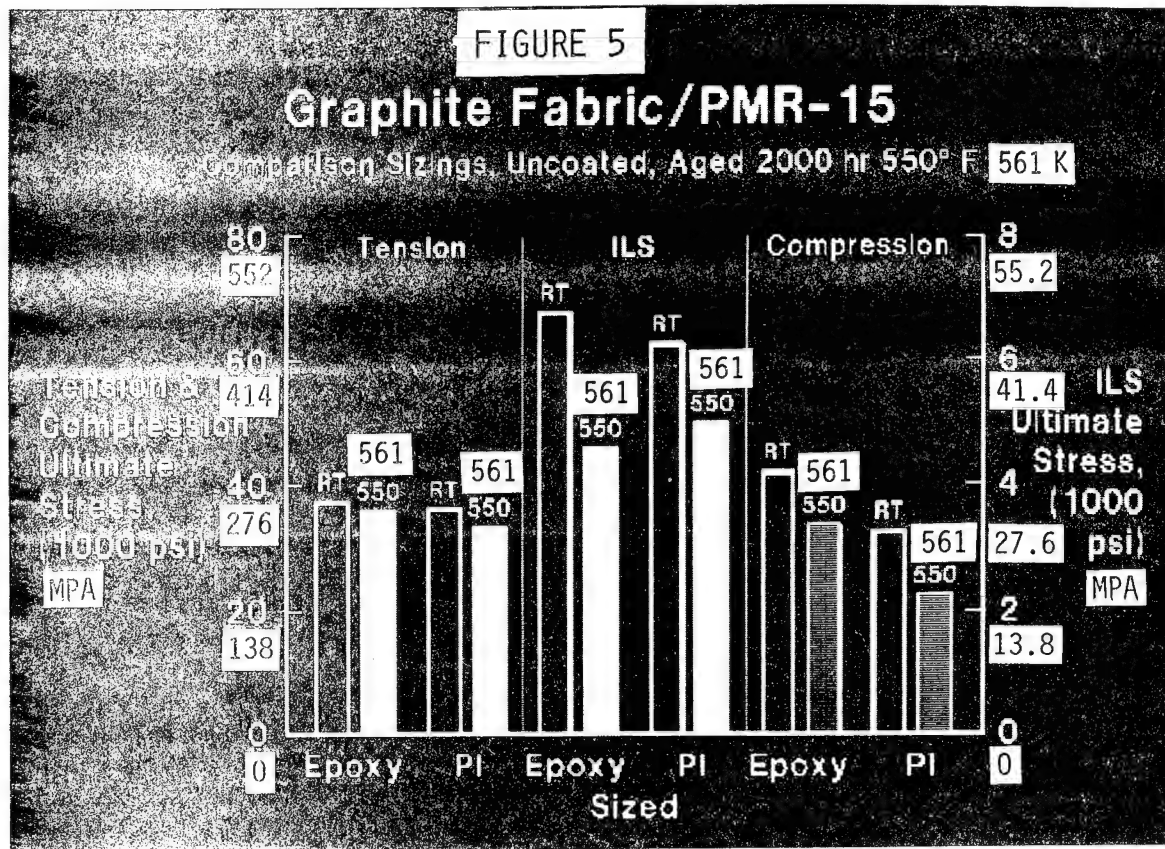


FIGURE 4





DEVELOPMENT OF DESIGN DATA FOR PROPULSION PMR-15 COMPOSITES

J. Postlewaite and D. McLaren
Boeing Commercial Airplane Company

The continuing development of PMR-15 composite materials and their associated design properties is pacing the implementation of this technology on commercial aircraft.

The guidelines that the FAA has issued regarding the certification of advanced composite structures are very significant with respect to future PMR-15 research and development activities.

FAA GUIDELINES

The FAA has issued an advisory circular dated 1-5-83 concerning guidelines for composite aircraft structures. Of particular significance to PMR-15 technology development is the reliance on combined environmental exposure and component testing, coupled with the stipulation that reliance on previous experience be limited to where common structures and materials have been used for a similar function.

Critical environmental exposures for commercial propulsion structures include 50 000 cycle service life, exposure to skydrol, moisture and other fluids, and nacelle fire conditions.

The structures currently being considered for PMR-15 are shown in figure 1.

DESIGN DATA DEVELOPMENT

Boeing is in the process of investigating PMR-15 composite characteristics of greatest significance to propulsion structures including:

- o Damage tolerance
- o Thermo-mechanical durability
- o Fire exposure performance

Figure 2 describes the results of a "through penetration" impact test on a B-3000/PMR-15 panel. Figure 3 demonstrates the "Post Impact Compression" strain capability of C-3000/PMR-15 under several conditions of temperature and fluid exposure.

Also under evaluation is the structural load carrying capability of Gr/PMR-15 panels damaged by fire. This information will allow the optimization of fire zone containment structures. The test fixture being used for the coincident application of fire and facesheet compression loads on a long beam bending sandwich specimen is shown in figure 4. Thermo-mechanical and thermo-oxidative durability and the effect of coatings and sizings has been addressed by C. Sheppard in a separate paper.

Given the guidelines recommended by the FAA, little of the large amount of information that is being, or has been generated regarding PMR-15 composites is of significance towards the certification of PMR-15 propulsion structures. The principal reasons for this are:

- (1) Variability of PMR-15 composites
- (2) Incomplete understanding of effect of resin chemistry and cure cycle on Thermo-mechanical stability of composites.
- (3) No capability to predict change in composite properties with service conditions.
- (4) Lack of service experience with representation structure and materials.

CONCLUSION

PMR-15 composites continue to show promise for application to commercial aircraft structure. However, at present PMR-15 structures are being built with considerable variety in specifications and procedure, the affect of which is not fully understood with respect to long term durability. Thus, this interpretation of the FAA guidelines implies that great expenses will be incurred by the industry in certifying these structures.

Critical needs for the efficient and effective implementation of PMR-15 composites to commercial aircraft include:

- (1) Establishment of an industry standard regarding:
 - (a) The control imposed by the materials and processing specifications on fibers, sizing, resin, and quality control.
 - (b) The methods used to generate long term durability and damage tolerance data for high temperature composites.
 - (c) The methods used to generate high temperature mechanical properties of high temperature composites.
- (2) Compilation of an industry wide database for the principle PMR-15 resins and cure cycles in use.
- (3) Development of capability to predict PMR-15 composite mechanical property responses to long term exposure to cyclic thermal environment, particularly with regard to damage and durability.
- (4) Gain in flight service experience with representative structures.

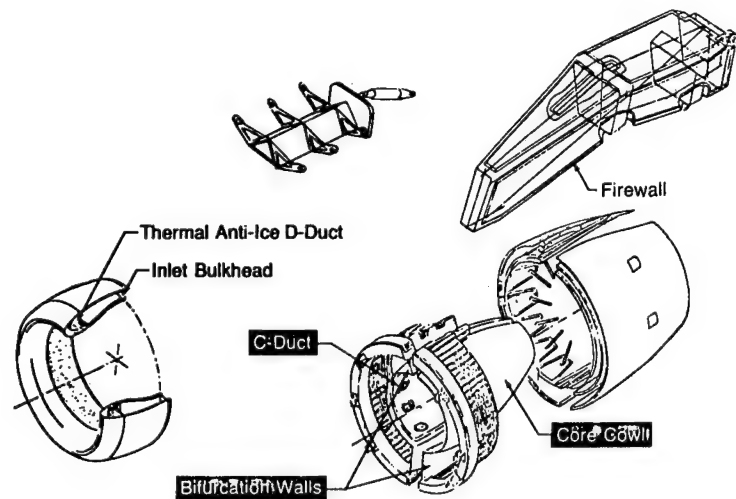


Figure 1. - PMR-15 applications.

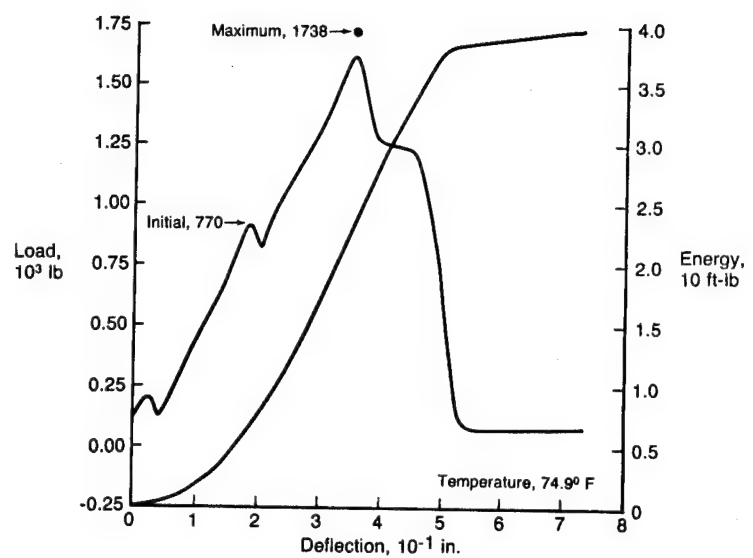


Figure 2. - Through penetration impact test.

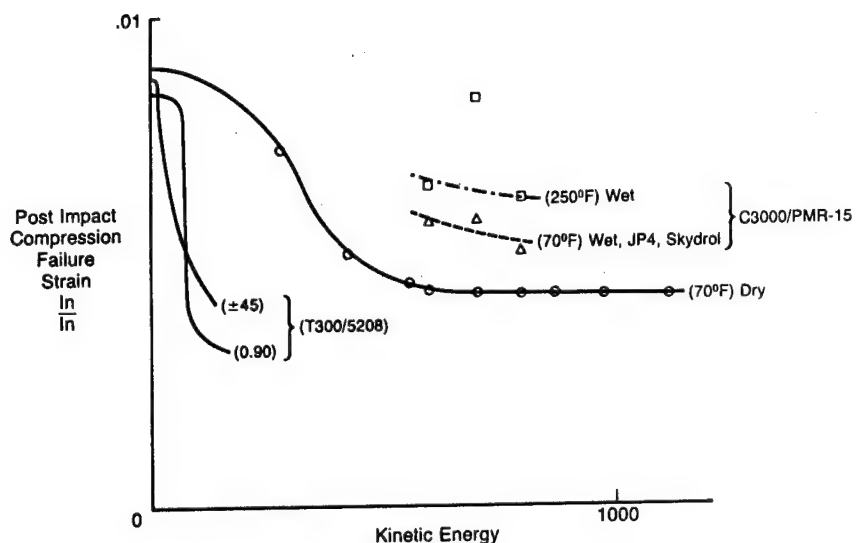


Figure 3. - Damage tolerance.

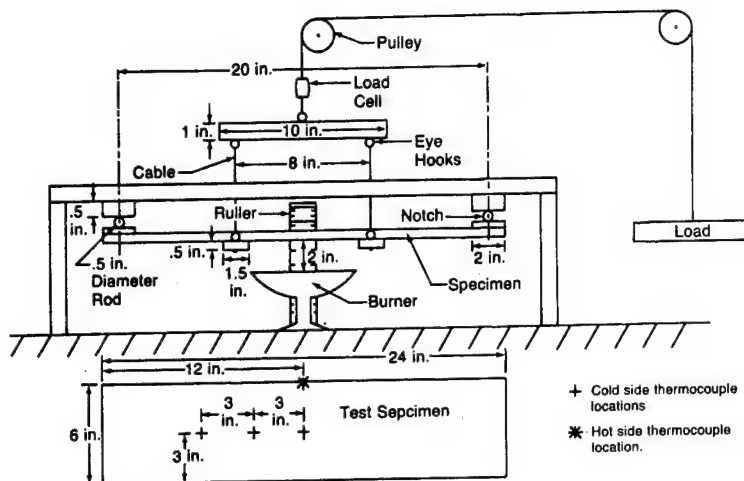


Figure 4. - Subcomponent hot side compression test rig.
(900°F-2600°F.)

POLYIMIDE COMPOSITES - APPLICATION HISTORIES

Leonard M. Poveromo
Grumman Aerospace Corporation

Advanced composite hardware exposed to thermal environments above 127°C (260°F) must be fabricated from materials having resin matrices whose thermal/moisture resistance is superior to that of conventional epoxy-matrix systems. A family of polyimide resins has evolved in the last 10 years that exhibits the thermal-oxidative stability required for high-temperature technology applications. The weight and structural benefits for organic-matrix composites can now be extended by designers and materials engineers to include structures exposed to 316°F (600°F). Polyimide composite materials are now commercially available that can replace metallic or epoxy composite structures in a wide range of aerospace applications.

Epoxy-matrix advanced composite materials were originally formulated to provide structurally efficient aerospace components for prolonged service at 177°C (350°F). However, due to thermal/humidity degradation their service temperature limitation is now generally recognized as 121° (250°F). The evolution of a family of Bismaleimide (BMI) polyimide resins with epoxy-like processing and excellent thermal resistance in the last few years is allowing the aerospace designer to design composite structure with 121°C - 232°C (250°F - 450°F) thermal envelopes. Graphite/BMI is commercially available from several sources, and is being used in aircraft production for the first time by Grumman on the DC-8 Nacelle Anti-Ice Plenum. Specific details of the Grumman programs and an industry overview are included in this paper.

INTRODUCTION

Polyimide advanced composite materials have reached a level of industrial maturity that make them viable construction materials offering the potential for weight reduction and improved structural performance. Polyimide composite materials are now commercially available that can replace metallic or epoxy composites for a wide range of aerospace structures. Table 1 describes the resin systems available versus structural service temperature requirements.

Epoxy-matrix advanced composite materials, as a result of long-term exposure to the environment, will absorb moisture in excess of 1% by weight. This combination of

TABLE 1. ORGANIC-MATRIX APPLICATION VS AIRCRAFT SERVICE TEMPERATURE

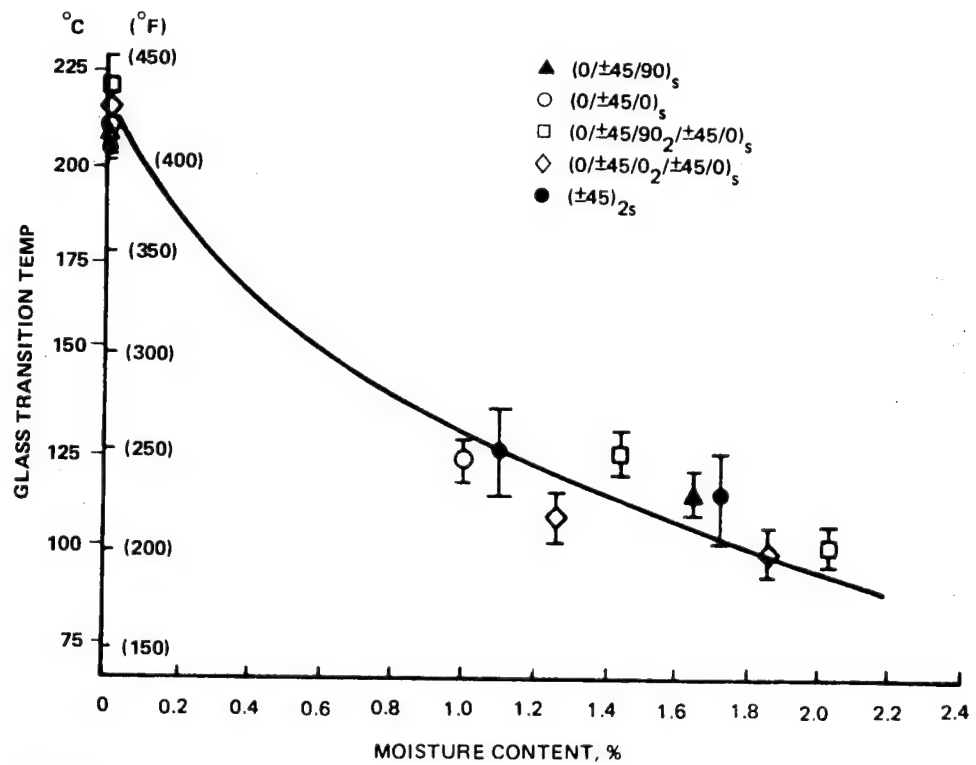
23° TO 127°C (73° TO 260°F)	127° TO 232°C (260 TO 450°F)	232° TO 316°C (450 TO 600°F)	> 316°C (600°F)
EPOXY <ul style="list-style-type: none"> • 3501 • 5208 • 976 	BMI <ul style="list-style-type: none"> • F-178 • V378A • 4001 	ADDITION POLYIMIDE <ul style="list-style-type: none"> • LARC-160 • PMR-15 • PMR-11 	CONDENSATION POLYIMIDE <ul style="list-style-type: none"> • NR-150B2 • THERMID 600
<ul style="list-style-type: none"> • ESTABLISHED DESIGN DATA • WIDESPREAD AEROSPACE EXPERIENCE • EASILY PROCESSED • DURABILITY CUT-OFF 127°C (260°F) 	<ul style="list-style-type: none"> • PROCESSIBILITY SIMILAR TO EPOXIES • PRELIMINARY STRUCTURAL DATA AVAILABLE • HOT-WET STATIC AND FATIGUE PROPERTIES TBD • DESIGN EXPERIENCE LIMITED 	<ul style="list-style-type: none"> • PROCESSING PARAMETERS INCLUDE 316°C (600°F) / 1.379 MPa (200 PSI) • BLEEDER/BREATHER SYSTEMS REQUIRE OPTIMIZATION • EXCELLENT THERMAL OXIDATIVE STABILITY • DURABILITY TBD • STRUCTURAL DATA MUST BE GENERATED 	<ul style="list-style-type: none"> • PROCESSING PARAMETERS INCLUDE 371°C (700°F) / 1.379 MPa (200 PSI) • BLEEDER/BREATHER SYSTEMS REQUIRE OPTIMIZATION • PRELIMINARY STRUCTURAL DATA AVAILABLE • EXCELLENT THERMAL OXIDATIVE STABILITY • DURABILITY TBD • DESIGN EXPERIENCE LIMITED • RESIN COSTLY

0385-014D

absorbed moisture with corresponding reduction in glass-transition-temperature (T_g) (fig. 1) and service temperatures in excess of 121°C (250°F) greatly reduces the compressive strength of conventional epoxy-matrix composites and minimizes their potential for weight savings (fig. 2). The BMI polyimide resins can be implemented on structurally efficient, composite designs with 121°C - 232°C (250°F - 450°F) thermal envelopes. All state-of-the-art BMI resins have processing or structural limitations; the optimal system is still to be developed. However, existing BMI composites can and are being utilized in applications tailored for their individual properties.

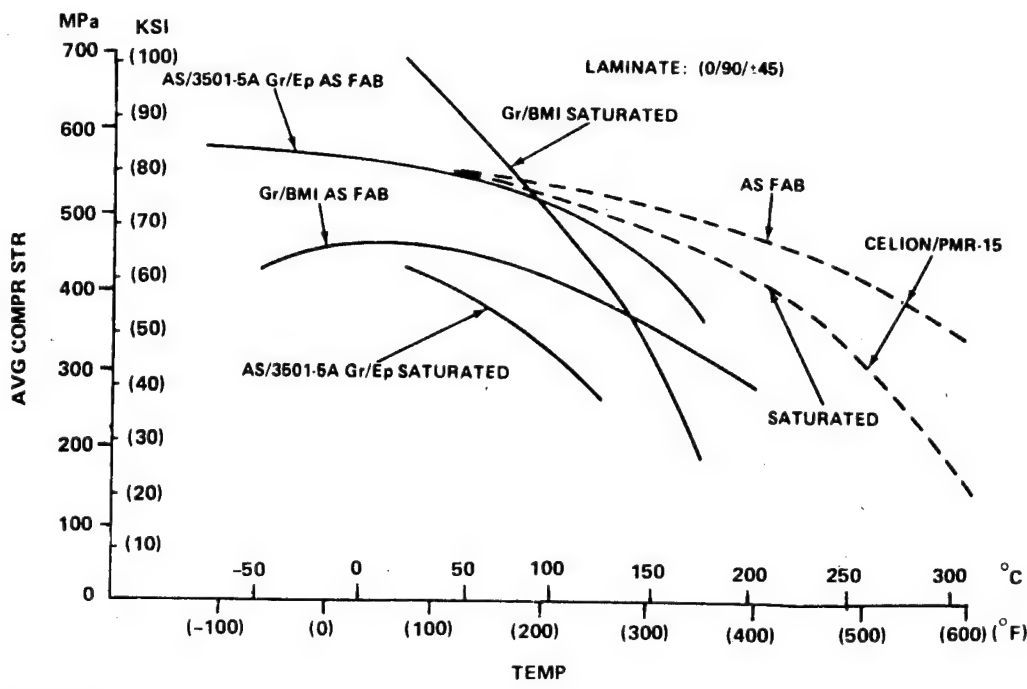
Grumman has successfully applied polyimide composite materials to advanced aerospace structures since the early 1970s. The pertinent funded development efforts and on-going production programs are listed in figure 3. The early requirements were for resins with long-term thermal stability 260°C (500°F) on high-speed aircraft with advanced electrical systems. Of the limited high-temperature resin systems available at that time, Grumman selected a condensation polyimide based on Monsanto's Skybond 709 resin. This material is derived from the reaction of a diacidester mixture and an aromatic amine. A manufacturing methodology was developed to fabricate heat-resistant fiberglass/polyimide and quartz/polyimide radomes for the EA-6B and A-6E Navy aircraft. The largest of the latter is the 4.5 x 0.5 x 0.6 m (15 x 1.5 x 2.0 ft) EA-6B T.J. Pod radome; more than 200 of these structures have been produced to date.

Springboarding off this technology during the mid-70s, the EF-111A Weapon Bay Radome (the largest all-polyimide-reinforced aerospace structure) was successfully designed, fabricated, and tested. This 4.9 x 0.6 x 0.6 m (16 x 2 x 2 ft) A-sandwich structure consists of fiberglass/polyimide facesheets bonded to polyimide honeycomb with polyimide film adhesive. This radome is presently in production as an integral part of the Air Force's EF-111A Tactical Jamming System.



0385-001D

Figure 1. Effect of moisture content on the glass transition temperature of AS/3501-5 Gr/Ep as measured by TMA



0385-002D

Figure 2. Comparison of compression strength of AS-1/3501-5A Gr/Ep, AS-4/4001 Gr/BMI and Celion/PMR-15 Gr/Pi laminates (as fabricated and saturated at 95% RH)

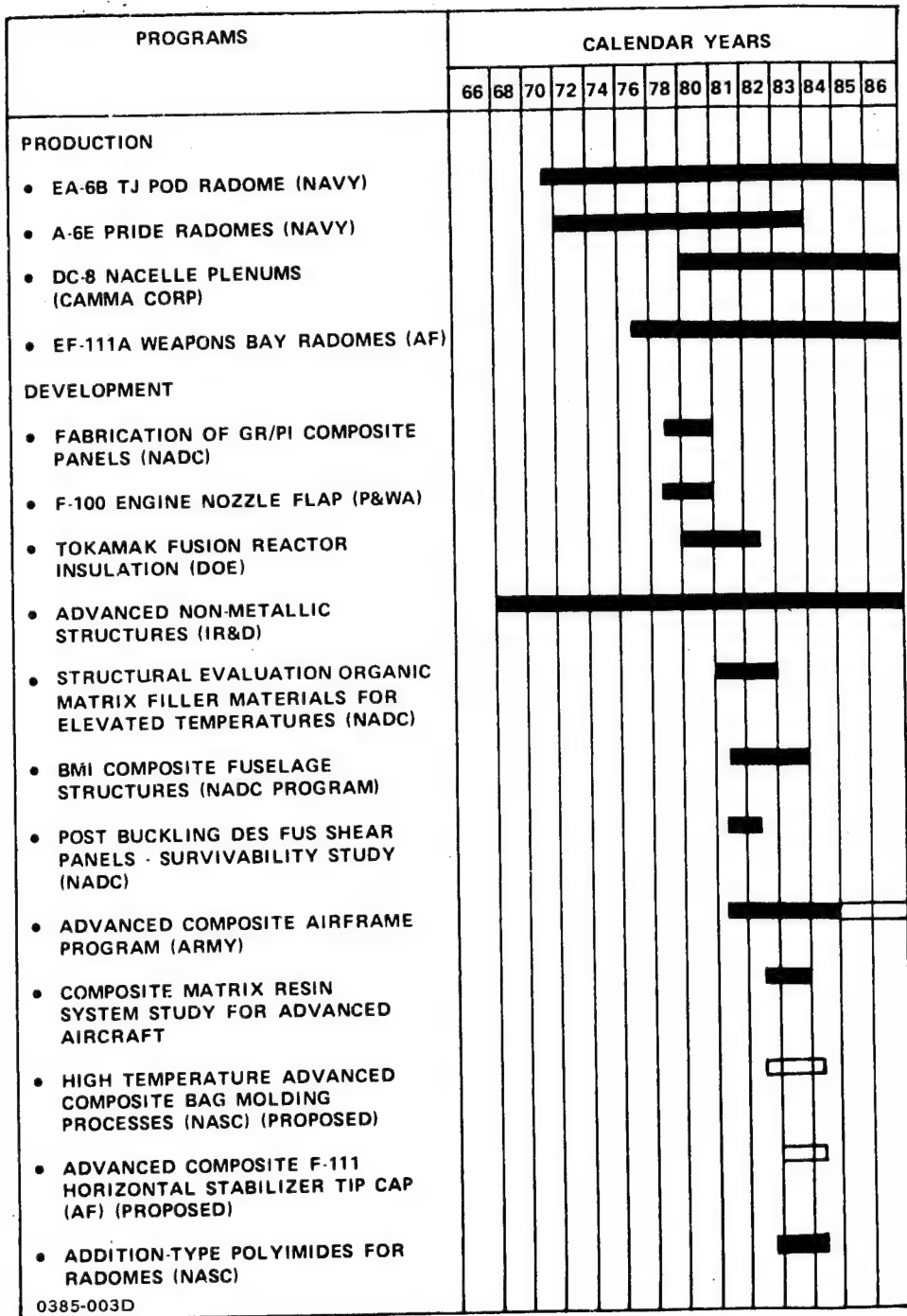
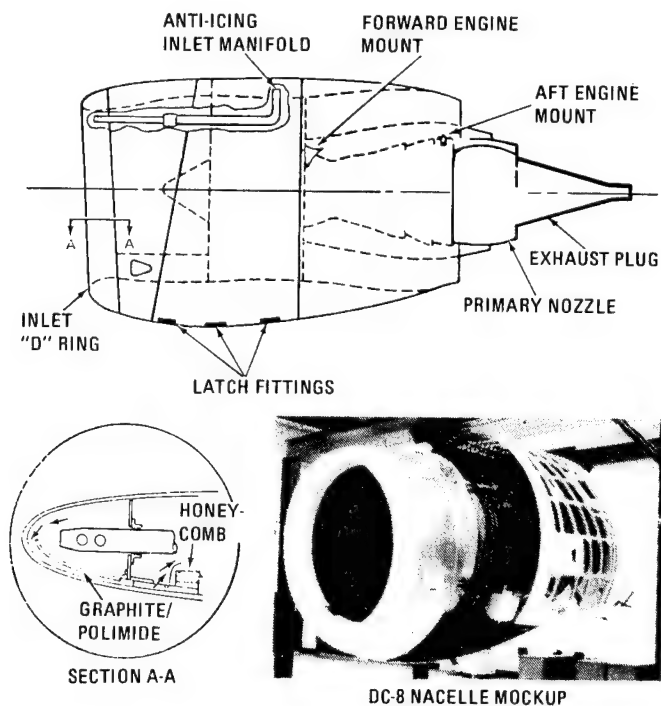


Figure 3. Grumman polyimide composite programs

DC-8/CFM 56 NACELLE ANTI-ICER PLENUM

Grumman designed and is fabricating the nacelles for Cammacorp's DC-8 re-engining program. The severe thermal/acoustic environment of the nacelle de-icer plenum (fig. 4) presented a design problem. A study of the maintenance records



0385-004D

Figure 4. Grumman-fabricated graphite/polyimide anti-ice plenum for DC-8 engine nacelle mockup

of the baseline titanium anti-ice skins in service showed high failure rates typified by multiple fatigue cracks with a tendency towards fragmentation. Since the cause was determined to be acoustic/thermal fatigue, a graphite/polyimide design with excellent fatigue resistance was developed. The processing requirements and 232°C (450°F) maximum service temperature of the part drove the matrix selection toward the bismalimide (BMI) addition-curing polyimides. Grumman has extensive experience in processing BMI polyimides since their introduction in the mid-70s. Initially, the resin was developed for substitution in fiberglass/polyimide radomes fabricated with condensation polyimides that had exhibited extensive processing problems. The two commercially available matrix systems were Hexcel's F-178 and USP's V-378A. The early Grumman BMI work involved development of woven graphite cloth/F-178 resin for advanced composite aircraft structures subjected to thermal environments between 127°C and 232°C (260°F and 450°F). In addition, Grumman has been working with the V-378A resin since its introduction and has established in-house materials and processing requirements for this system. The advantages of these BMI systems are that they are fully imidized and supplied without solvent. These resins do not emit volatile byproducts during the addition/free-radical curing mechanism. Void-free laminates are produced using standard 177°C (350°F) epoxy-prepreg bagging and curing procedures and production facilities.

Since the principal plenum design condition was thermal/acoustic fatigue, a test sequence involving noise levels up to 158 dB and 232°C (450°F) was developed (fig. 5) and a series of candidate laminates (table 2) were tested. The combina-

TABLE 2. ADVANCED COMPOSITE ACOUSTIC FATIGUE TEST PANELS

PANEL DESCRIPTION	NUMBER OF PLIES	THEORETICAL THICKNESS, MM (IN.)	LAYUP SEQUENCE
HYBRID 7781 GL/F-178 PI T-300 GR/F-178 PI	16	3.2 (0.124)	+45 _{GR} /-45 _{GR} /0 _{GR} /+45 _{GL} /90 _{GR} /-45 _{GL} /0 _{GL} /90 _{GL} /0 _{GR} /-45 _{GL} /90 _{GR} /+45 _{GL} /0 _{GR} /-45 _{GR} /+45 _{GR}
WOVEN GR/PI 24X23 8HS GR CLOTH F-178 & V-378A PI	9	3.0 (0.117)	+45 _{GR} /0 _{GR} /90 _{GR} /-45 _{GR} /0 _{GR} /-45 _{GR} /90 _{GR} /0 _{GR} /+45 _{GR}
HYBRID 7781 GL/V-378A PI T-300 GR/V-378A PI	20	4.2 (0.164)	+45 _{GR} /-45 _{GR} /0 _{GR} /+45 _{GL} /90 _{GR} /-45 _{GL} /0 _{GL} /90 _{GL} /0 _{GR} /-45 _{GL} /-45 _{GL} /0 _{GL} /90 _{GL} /0 _{GL} /-45 _{GL} /90 _{GR} /+45 _{GL} /0 _{GR} /-45 _{GR} /+45 _{GR}
LEGEND:			
GR - UNIDIRECTIONAL GRAPHITE/POLYIMIDE GL - WOVEN FIBERGLASS/POLYIMIDE			

0385-015D

tions included woven graphite/F-178, woven graphite/V-378A, woven fiberglass/unidirectional graphite/F-178 hybrid, and woven fiberglass/unidirectional graphite/V-378A hybrid. All the laminates successfully withstood the thermal/acoustic fatigue test. The woven graphite/BMI laminate was selected for use in the nacelle anti-ice plenum (fig. 6) because of ease of layup and thickness considerations. Subsequent fatigue and static tests (table 3) were conducted to verify the structural integrity of the graphite/BMI plenum configuration for FAA certification. The composite design resulted in a 30% weight savings and significant manufacturing/tooling cost savings over the alternative titanium plenum. A considerable amount of data was accumulated with respect to basic material properties and analytical procedures that helped to minimize batch-to-batch variations of incoming graphite/BMI prepreg.

BMI POLYIMIDE DEVELOPMENT PROGRAMS

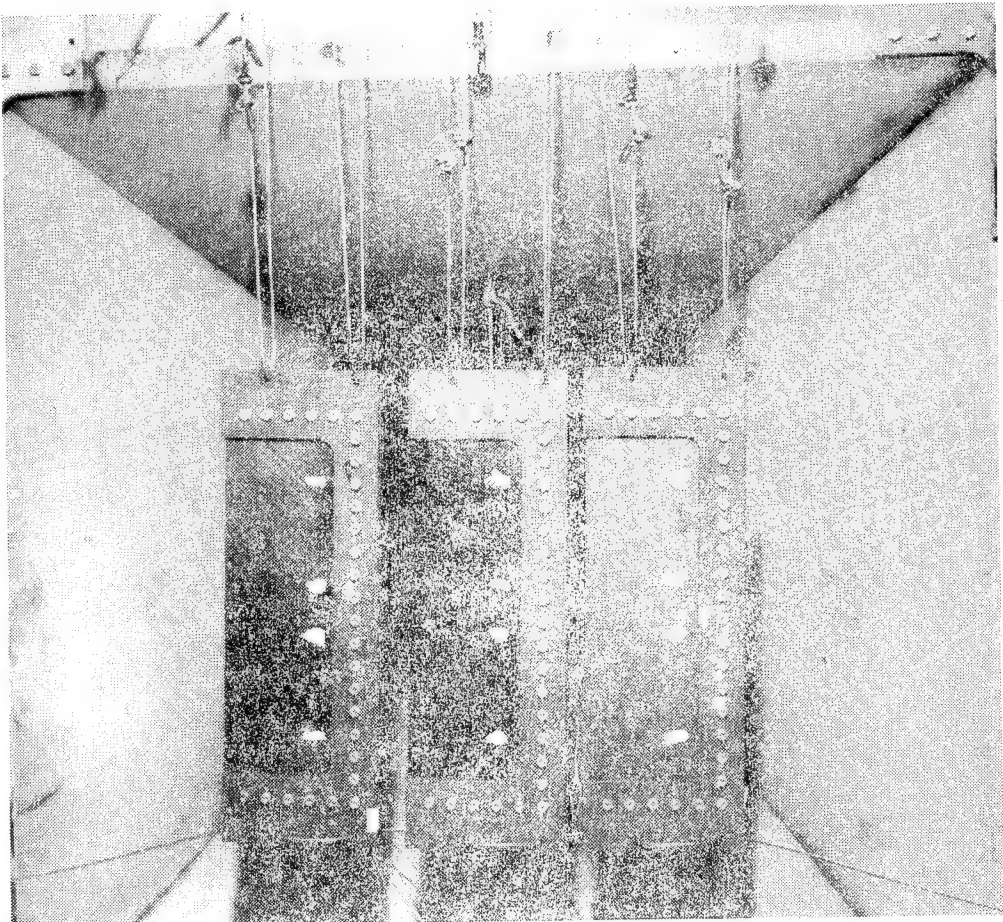
Prior to and during the above pioneering production program, Grumman was actively involved in development programs geared to generating BMI polyimide composite properties and structures. These programs are listed in figure 3. The specific details of the selected efforts are briefly described in the following subsections.

Fabrication of Graphite/Polyimide Panels (Naval Air Development Center-NADC)

The overall objective of this early program was the fabrication of over 300 T-300/F-178 graphite/BMI panels for environmental exposure to provide data for an NADC composite data base. Specific objectives included:

TEST PHASE	ELAPSED TIME, HR	TEST NOISE LEVEL IN ONE-THIRD OCTAVE BAND, dB	TEST TEMP., °C (°F)
1	10.0	152	23(73)
2	19.5	152	232(450)
3	42.5	155	232(450)
4	3.0	158	232(450)
	<u>75.0</u> (TOTAL)		

A. SEQUENCE



B. SETUP

0385-005D

Figure 5. Test procedure

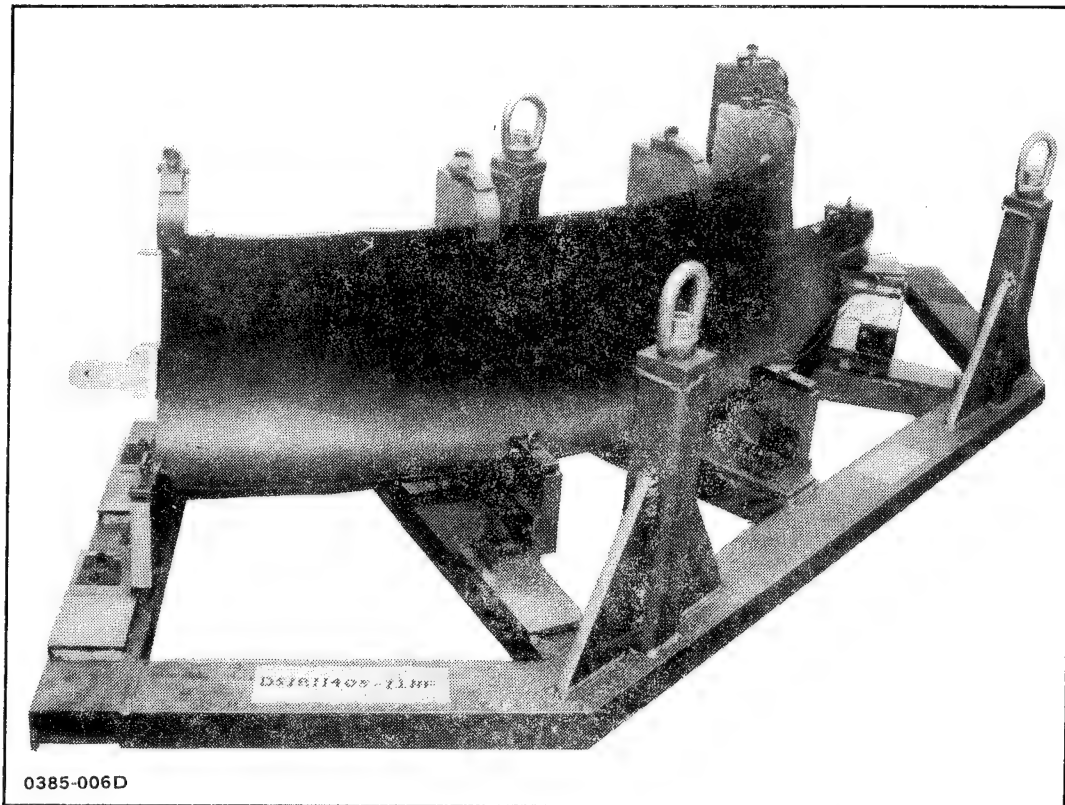


Figure 6. Section of graphite/polyimide DC-8 nacelle anti-ice plenum in postcuring fixture

- Material characterization of the as-received prepreg by chemical analysis
- Determination of the mechanical properties of autoclave-cured panels
- Determination of the environmental durability of autoclave-cured panels.

**Structural Evaluation of Organic Matrix Filamentary Materials
for Use at Elevated Temperatures (NADC)**

The purpose of this project was to demonstrate the suitability of graphite/BMI polyimide for high-temperature structural applications through the static and fatigue testing of quasi-isotropic coupons and hat-stiffened shear panels at room temperature—"dry" and at 177°C (350°F) "wet" conditions. The test matrix is shown in table 4. Testing involved the following:

- Static testing of unnotched and notched tension and compression coupons
- Static testing of horizontal shear specimens
- Constant-amplitude ($R=0$, $R=-1$) fatigue testing of unnotched and notched tension and compression coupons
- Spectrum fatigue testing of notched coupons

TABLE 3. SUMMARY OF STATIC TEST RESULTS ⁽¹⁾ OF GM3014-11 WOVEN
GRAPHITE/POLYIMIDE (F-178)

TEST	LAYUP ⁽²⁾ ORIENTATION	TEST TEMP, °C(°F)	ULTIMATE STRENGTH MPa(KSI)	MODULUS GPa(MSI)
TENSION	MULTI	23(73)WET 232(450)	356(51.9) 340(49.3)	48.0(6.98) 42.7(6.21)
	0/90	23(73)WET 232(450)	466(67.8) 500(72.6)	62.1(9.07) 57.5(8.38)
TENSION (OPEN-HOLE)	MULTI	23(73)WET 232(450)	327(47.5) 336(48.8)	— —
	0/90	23(73)WET 232(450)	422(61.2) 381(55.3)	— —
COMPRESSION (IITRI)	MULTI	23(73)WET 232(450)	429(62.1) 284(41.2)	— —
	0/90	23(73) 232(450)	562(81.8) 375(54.2)	— —
FLEXURE	MULTI	23(73)WET	430(62.4)	48.5(7.07)
RAIL SHEAR	MULTI	23(73)WET 232(450)	142(20.6) 110(16.0)	— —
	0/90	23(73)WET 232(450)	76(11.1) 55(8.0)	— —
BEARING AT 4% DEFLECTION	MULTI	23(73)WET 232(450)	436(63.2) 334(48.4)	— —
CTE	MULTI	—	1.5X10 ⁻⁶ ⁽³⁾	—
NOTES:				
(1) AVERAGE OF FIVE SPECIMENS				
(2) PLY ORIENTATION:				
MULTI: (0, +45, 0 -45, 0) _s TESTED IN 90°				
BI: (0/90) ₉ TESTED IN 90°				
(3) MICRO-UNITS				

0385-016D

TABLE 4. TEST MATRIX FOR ORGANIC-MATRIX FILAMENTARY MATERIALS
PROGRAM (NADC)

TEST CONFIGURATION	STATIC		FATIGUE					
			CONSTANT AMPLITUDE				SPECTRUM	
	R = 0.05		R = -1		RT DRY	350°F WET		
	RT DRY	350°F WET	RT DRY	350°F WET		RT DRY	350°F WET	
TENSION UNNOTCHED CENTER NOTCHED POST LOW VELOCITY IMPACT DAMAGE	10 ¹ 10	10 ¹ 10	6 6	6 6			2	2
COMPRESSION UNNOTCHED CENTER NOTCHED POST LOW VELOCITY IMPACT DAMAGE	10 ² 10	10 10			6 6	6 6	2	2
HORIZONTAL SHEAR	10	10						
SHEAR PANEL	1 ³	1			1 ³	1	1 ³	1

1 UNNOTCHED STATIC TENSION TESTS EMPLOYED CONVENTIONAL EXTENSOMETRY
 2 THREE OF THE TEN R.T. UNNOTCHED STATIC COMPRESSION SPECIMENS WERE INSTRUMENTED
 WITH 2 AXIAL GAGES
 3 R.T. SHEAR PANELS EACH USED TWO BACKED-UP, 2-ELEMENT ROSETTES PLUS 6 AXIAL GAGES

0385-017D

- Static and constant-amplitude fatigue testing of impacted coupons
- Static, constant-amplitude, and spectrum fatigue testing of hat-stiffened shear panels representative of a V/STOL aft-fuselage panel.

In addition, the temperature-dependent absorption characteristics of Gr/BMI were quantified in an early phase of the effort to permit accurate prediction of the expected in-service moisture contents and to enable adequate definition of the requisite conditioning and testing procedures for reliable simulation of these in-service conditions. The rate at which this material system absorbed moisture as a function of temperature (diffusivity) and the equilibrium moisture content as a function of relative humidity were established. The moisture desorption and re-absorption characteristics were also determined. Test panel configurations are shown in table 5. These parameters, together with environmental and aircraft mission scenarios, were inputted to a Grumman-developed semi-empirical computer model based on a Fickian diffusion process to estimate the total amount of moisture absorbed by Gr/BMI structures during the service life of future aircraft. (See figs. 7 through 10.) The effects of a range of impact energy levels on graphite/BMI were also determined visually and ultrasonically in order to determine the level that causes barely visible impact damage for subsequent tests as a "worst case" condition of subvisual damage. Grumman investigated the F-178 resin matrix in this program while Northrop evaluated the V-378A resin matrix in a parallel effort.

TABLE 5. CONFIGURATIONS OF T-300/F-178 GRAPHITE/POLYIMIDE MOISTURE CONDITIONING TEST PANELS

PANEL NO.	LAYUP SEQUENCE	THICKNESS, IN.	FIBER VOLUME, %	VOID CONTENT, %
X1	+45/-45/+45/-45/-45/+45/-45/+45 (MULTIDIRECTIONAL)	0.071	59.42	0.67
H2	[0]16 (UNIDIRECTIONAL)	0.080	61.54	0.56
T8	+45/0/+45/0/-45/0/90/90/0/-45/0/+45/0/+45 (MULTIDIRECTIONAL)	0.087	60.16	1.20
SPECIFIC GRAVITY:				
RESIN -- 1.2964 FIBER -- 1.7600				

0385-018D

Bismaleimide Composite Fuselage Structures
for High-Temperature Applications (NADC)

The objective of this on-going Bismaleimide Composite Fuselage Structures (BCFS) Program is to design and develop an advanced composite fuselage structure which can satisfy the load and environmental requirements of a Fighter/Attack (F/A) V/STOL aircraft. In so doing, this program will develop design criteria and data, and demonstrate manufacturing techniques for generic high-temperature composite fuselage structure designed to operate in the 177°C to 204°C (350°F to 400°F) temperature range. The component selected is a 3.7 x 1.2 m (12 x 4 ft) section of V/STOL aft fuselage. The specific design is a hat-stiffened post-buckled skin with J-section longerons and frames (fig. 11). The potential advantages of this structure are:

- Weight savings of 28% over an equivalent metallic baseline
- Damage-tolerance for both low- and high-energy impact
- Structural integrity, reliability, and maintainability
- Affordable production costs (10% less than metallic baseline).

Grumman used its polyimide design/manufacturing experience to aid in the developing the BMI resin matrix (Hercules 4001) used in this program.

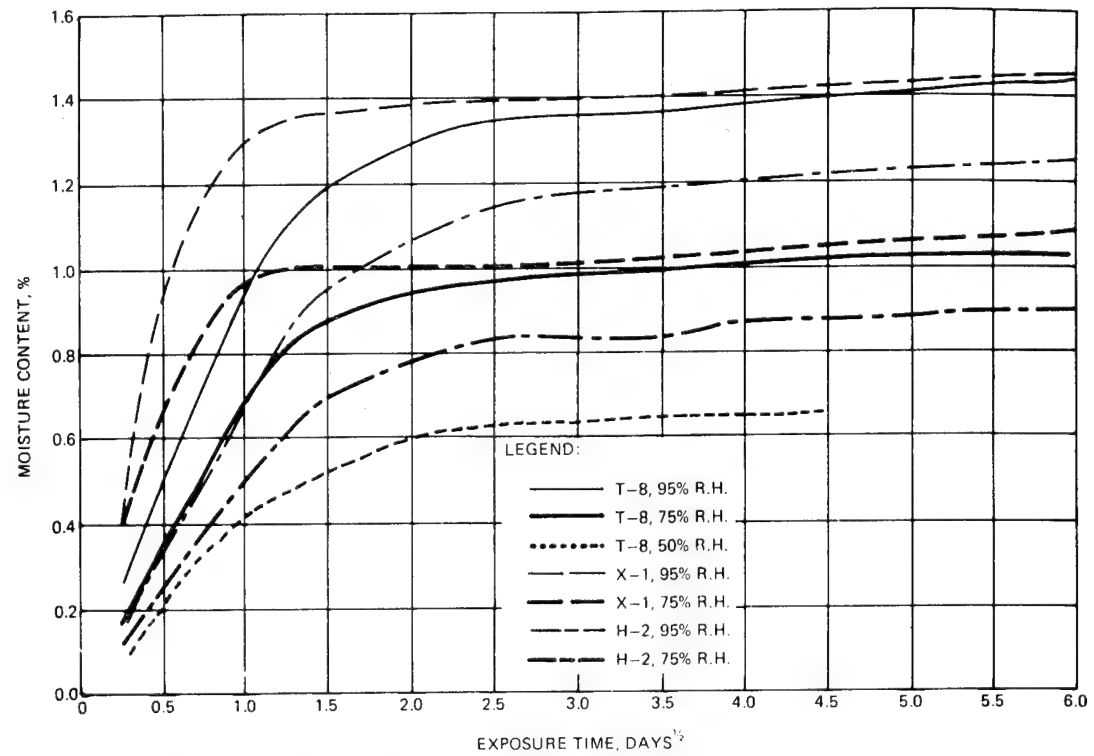


Figure 7. Effect of relative humidity on moisture content of 16-ply, T-300/F-178 graphite/polyimide panels at 77°C (170°F)

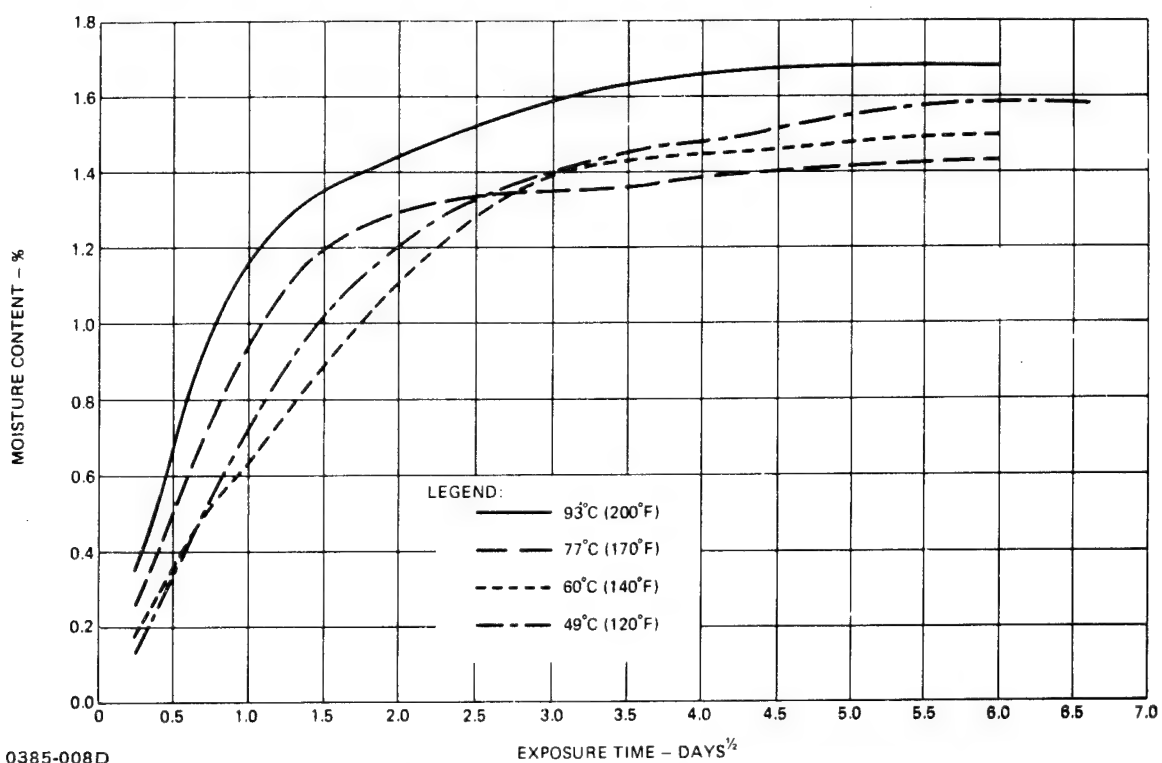
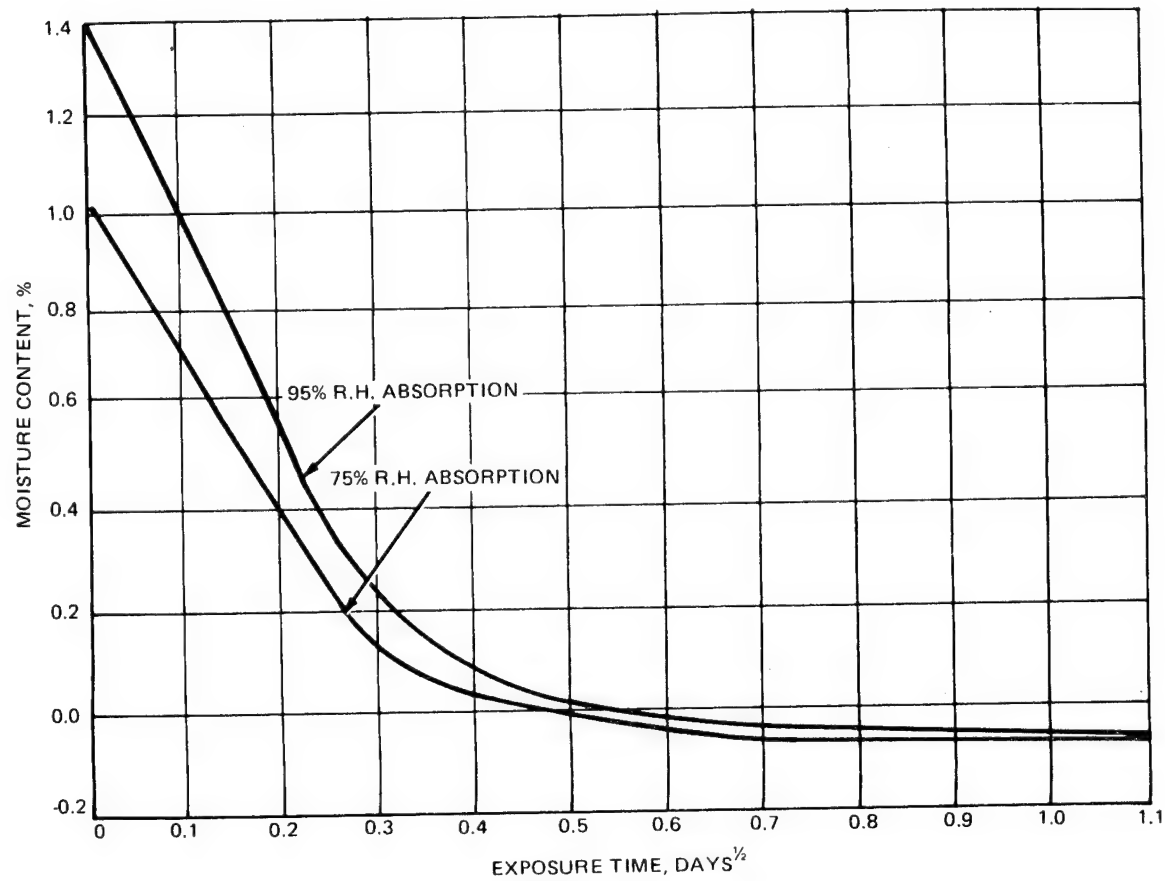
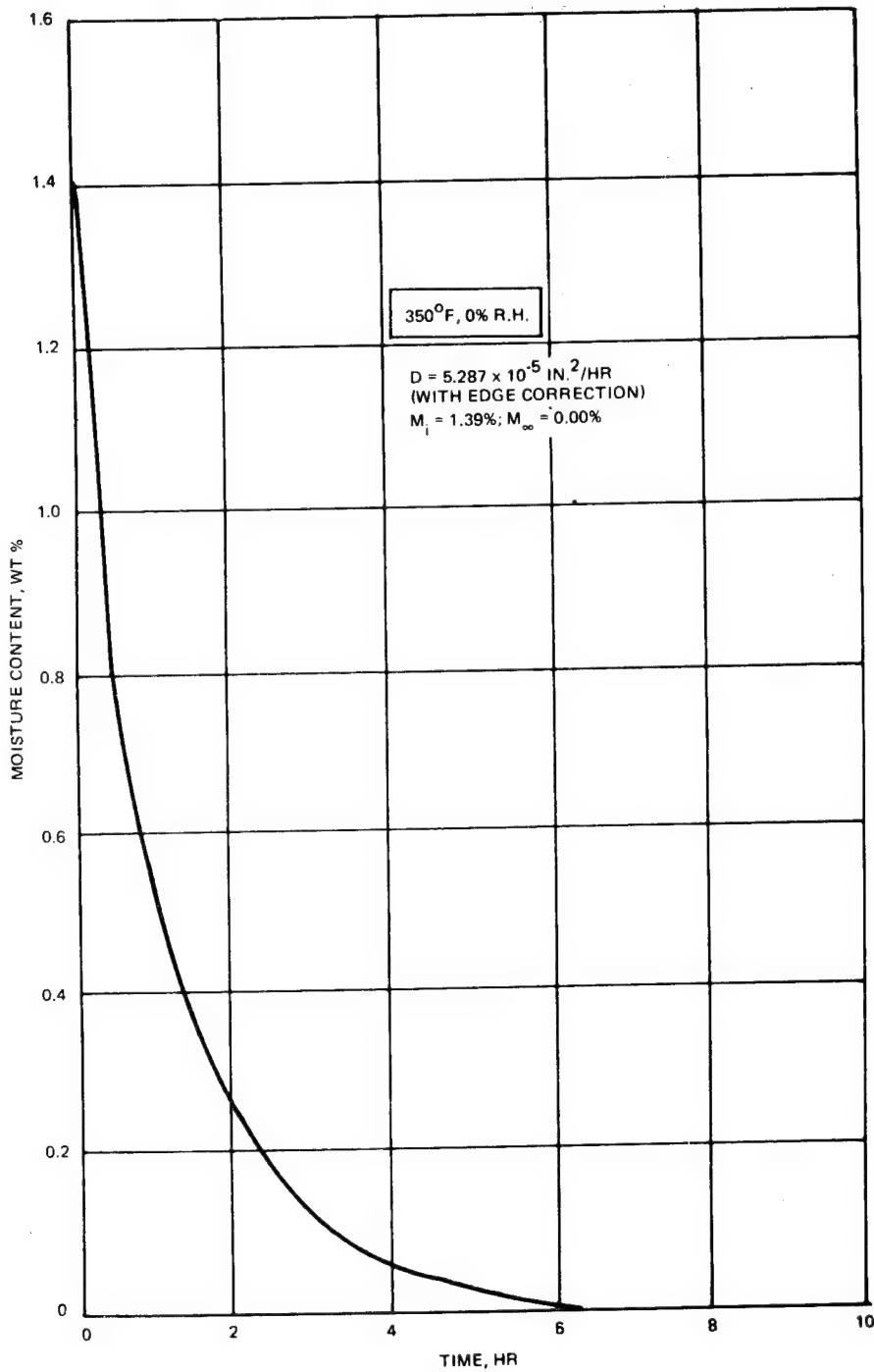


Figure 8. Effect of temperature on moisture diffusivity in 16-ply, T-300/F-178 graphite/polyimide panel No. T8 at 95% relative humidity



0385-009D

Figure 9. Moisture desorption at 177°C (350°F) from T-300/F-178 graphite/polyimide specimens



0385-010D

Figure 10. Projected moisture content time history for 16-ply graphite/polyimide specimens ($M_i = 1.39\%$, $M_\infty = 0.00\%$)

GRAPHITE BISMALEIMIDE (GR/BMI) COMPOSITE FUSELAGE PROGRAM

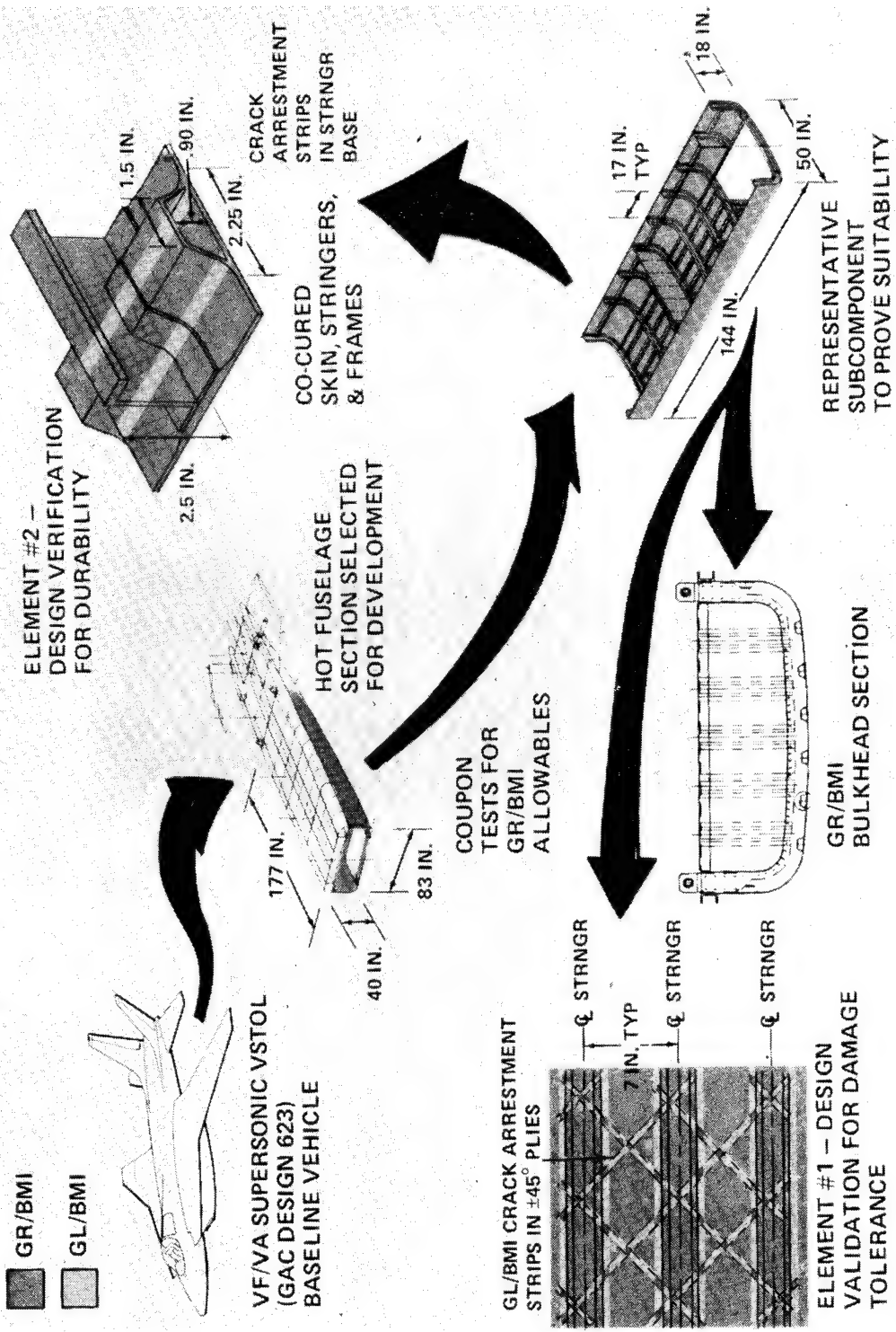
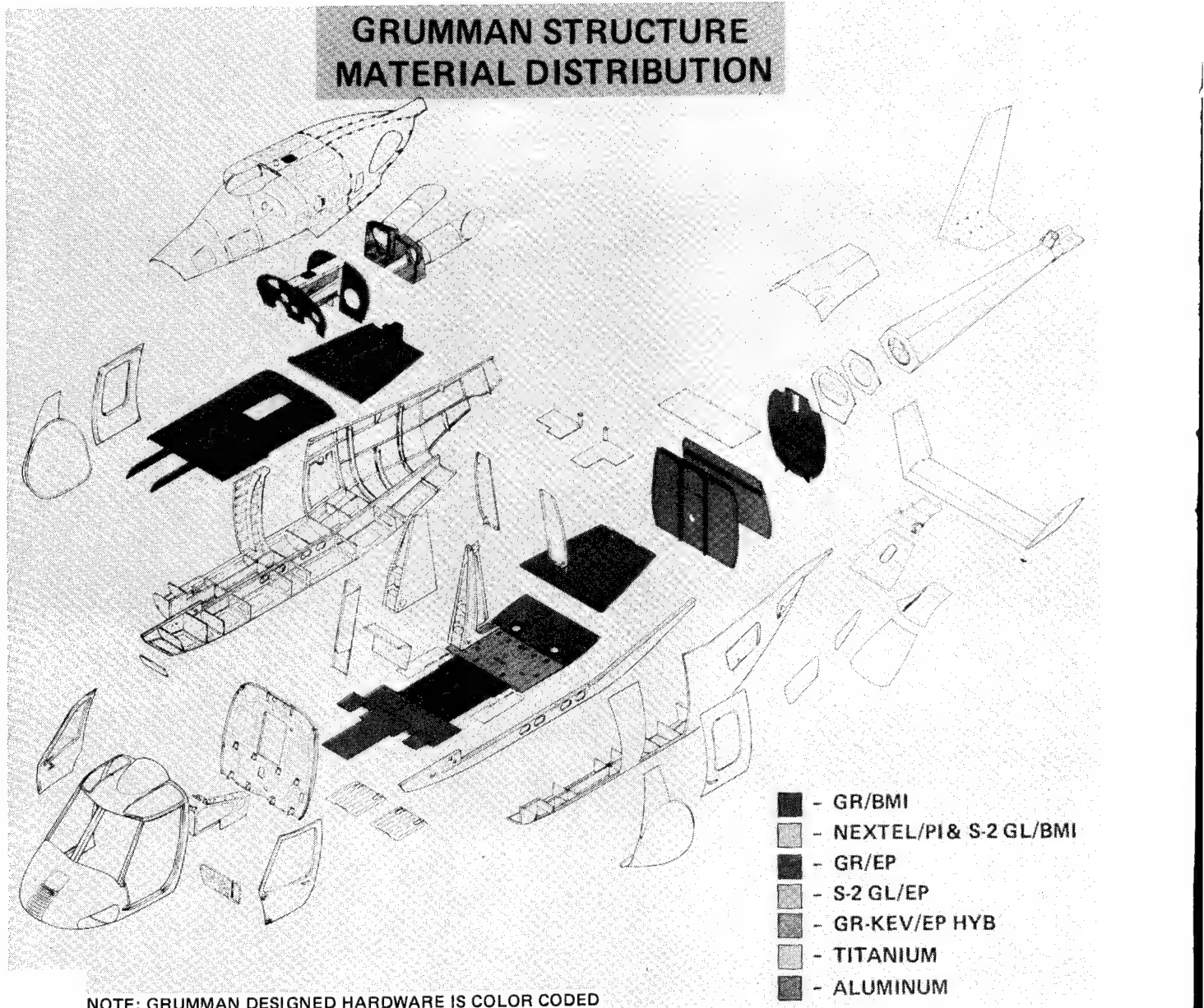


Fig. 11 Program Schematic for NADC - Funded BMI Composite Fuselage Program

0385-011D

Advanced Composite Airframe Program - ACAP (Army)

The objective of this program is to demonstrate how advanced composites, when applied in a helicopter airframe design, can provide weight/cost payoffs for future Army helicopters. Due to the operating service temperature [127°C (260°F)] and the fire-containment requirements of the Bell/Grumman ACAP design, a high-temperature resin system is required. Specifically, the aft roof is composed of two major components - the engine deck and the center beam assemblies. Both of these assemblies are fabricated using graphite/BMI. The engine deck is designed to contain a 1093°C (2000°F) fire for 15 minutes without backside penetration. The construction materials are HRP honeycomb core faced with fiberglass-graphite/BMI laminates. Outside of the fire containment area, the deck design consists of an integrally stiffened graphite/BMI skin with longitudinal hat stiffeners and transverse J-frames. The material distribution for this Grumman-designed structure is shown in fig. 12.



Composite Matrix Resin System Study for
Advanced Aircraft (NADC)

The objective of this new and innovative program is to select the optimal composite matrix system for service to 121°C (250°F) and in the 177°C to 232°C (350°F to 450°F) temperature range. The candidate graphite/resin system will be assessed for structural efficiency and environmental durability plus compatibility with cost-effective, reliable, and reproducible manufacturing processes. As a corollary to this effect, an evaluation of the compatibility of these resins with the new high-strain fibers will be investigated.

Industry-wide development efforts with BMI composites are growing, with every large aerospace company either actively evaluating these materials and/or planning their introduction into production. A partial listing of the programs that the author is aware of is shown in table 6.

TABLE 6. OTHER INDUSTRY BMI APPLICATIONS

COMPANY	APPLICATION	MATERIAL
GENERAL DYNAMICS/ FORT WORTH	F-16XL WING COVERS	GRAPHITE/V-378A
LTV	S-3 NACELLE DOOR	GRAPHITE/V-378A
MCDONNELL DOUGLAS/ ST. LOUIS	AV-8B HARRIER STRAKES, VENTRAL ANTENNA COVER & INBOARD TRAILING EDGE	FIBERGLASS/V-378A GRAPHITE/V-378A
ROCKWELL/BRUNSWICK (SUBCONTRACT)	B-1 RADOMES	FIBERGLASS OR QUARTZ/F-178
SNECMA	• ENGINE SHROUD • CFM 56 AIR OIL SEAL	• FIBERGLASS/ KERIMID 601 • KINEL 5504
ROLLS ROYCE	RB-211 TERMINAL BLOCK & STIFFENER RB-162 STATOR VANE & ROTOR BLADE	KINEL 5504

0385-019D

TOKAMAK FUSION REACTION - DIELECTRIC INSULATION

A unique polyimide program of interest at Grumman is the Tokamak Fusion Test Reactor (TFTR) which utilizes high-temperature polyimides. The overall TFTR is the largest project in the long-range program by the U.S. Energy Research and Development Administration (ERDA) to achieve a demonstration fusion power reactor by the late 1990's. The TFTR will be the first magnetic fusion system in the U.S. capable of producing fusion energy in significant quantities; it is being designed and developed at Princeton University's Plasma Physics Laboratory (PPPL). The prime industrial contractor working for PPPL is Ebasco, Inc., and their major subcontractor is Grumman Aerospace. In fabricating the TFTR torus, a doughnut-shaped container (high-temperature dielectric insulation) is used for magnetic confinement of plasma. This insulation prevents the flow of structure eddy currents that would distort the desired magnetic field of the Tokamak. The severe thermal [274°C (525°F)] and

electrical (0.75 kV) environment dictated a high-performance polyimide/fiberglass insulation material. Based on previous Grumman experience and the availability of industry data, the Polymeric Monomeric Reactant (PMR-15) polyimide resin system was selected as the matrix construction material. This resin system, originally formulated by NASA-Lewis Research Center, is prepared by combining two ester-acids and a diamine in methanol solvent. The 7781/PMR-15 fiberglass prepreg was available from several industry sources; Ferro's CPI-2237 material was selected.

Grumman generated material procurement and process specifications for the fiberglass/PMR-15 system. Extensive structural and electrical testing was conducted to characterize the material's performance in the unique Tokamak environment. Chemical evaluation of the prepreg consisted of establishing processing parameters and baseline control characteristics. Tests were run to determine the structural performance of the material: room-temperature compression creep; 1000-hour at 295°C (520°F) compression creep and coefficient of static friction; compression test under electric load (table 7); and electrical properties-dielectric strength, insulation resistance, dielectric constant, and dissipation factor (table 8). Following successful completion of the above testing, the required Tokamak dielectric insulation including 50 0.9 x 0.9 m (3 x 3 ft.) panels were fabricated and installed (fig. 13). Ring insulations for the Tokamak torus vacuum vessel outboard support pins were also successfully produced.

TABLE 7. ELECTRIFIED COMPRESSION PROPERTIES OF 7781 FIBER-GLASS/PMR-15

TEST TEMP, °C (°F)	APPLIED STRESS, MPa (KSI)	DC VOLTAGE, kV	MAX LEAKAGE CURRENT, μ A
127(260)	270(40)	0.75	NIL
127(260)	345(50)	0.75	NIL
271(520)	207(30)	0.75	0.72
271(520)	276(40)	0.75	0.78

0385-020D

TABLE 8. ELECTRICAL PROPERTIES OF 7781
FIBERGLASS/PMR-15

PROPERTY	AVERAGE VALUE
DIELECTRIC STRENGTH, V/MIL	1,023
INSULATION RESISTANCE, 10^{14} OHMS	>5.31
DIELECTRIC CONSTANT	5.17
DISSIPATION FACTOR	0.00010
TESTS PERFORMED AT ETL TESTING LABORATORIES, CORTLAND, N.Y.	

0385-021D

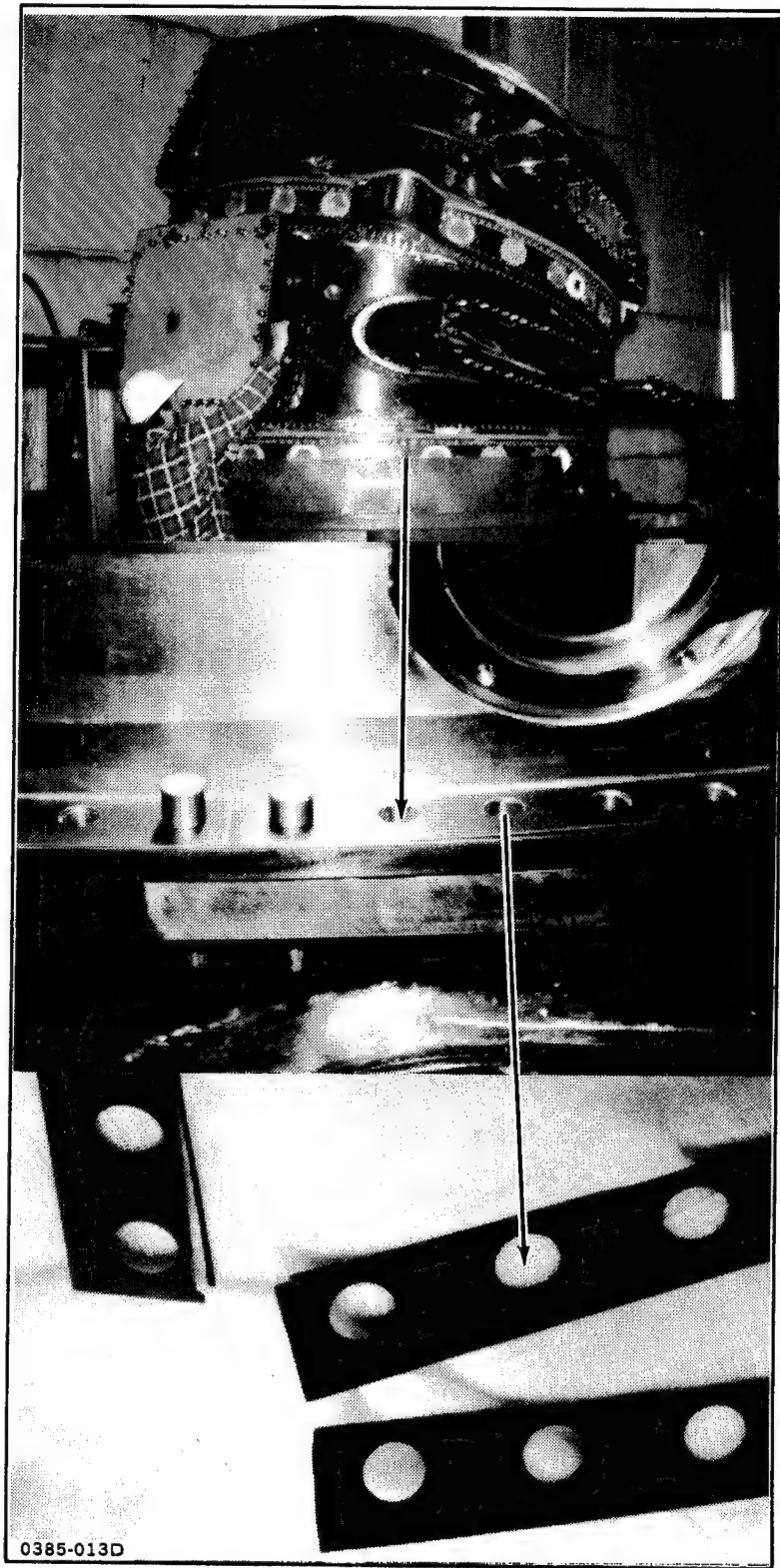


Figure 13. Location of 7781 fiberglass/PMR-15 dielectric insulation in Tokamak vacuum vessel

ACKNOWLEDGEMENTS

The author wishes to acknowledge the contributions of the following personnel and companies who helped make the programs described herein possible: R. Holden, J. Mahon, P. Palter, P. Pittari, J. Roman, M. Martin, S. DeMay, J. Lundgren, and C. Parente of Grumman; W. Redden and A. Brooks of Ebasco Services; Princeton Plasma Physics Laboratory; Cammacorp, and R. Trabacco, L. Buckley and T. Hess of NADC.

REFERENCES

1. L. Poveromo, "Polyimide Composites - Grumman Application Case Histories", 27th National SAMPE Symposium/Exhibition, May 1982.
2. L. Poveromo, "Polyimide Composites - Aerospace Case Histories", SPE First Technical Conference on Polyimides, November, 1982.

V-378A, A MODIFIED BISMALEIMIDE FOR ADVANCED COMPOSITES

S. W. Street
HITCO Materials Division

Addition polyimides cure with no evolution of gaseous by-products at relatively low temperatures and may be cured at low pressures to yield composites with excellent hot-wet strength retention. These properties have made them excellent candidates as matrix resins for advanced composites. However, commercially available bismaleimides are solids and difficult to handle in preimpregnated form.

V-378A is an addition polyimide composed of a mixture of bismaleimides and other reactive ingredients formulated to provide good prepreg properties and handling, facile cure and excellent composite mechanical properties. Several curing mechanisms are utilized to provide the characteristics exhibited by V-378A. Part of the mechanism is free radical and takes place at ambient temperature and above. Other mechanisms are principally Diels-Alder in nature. V-378A prepgs are tacky at ambient temperature but do not have long tacky outlife similar to some epoxies. V-378A yields composites which exhibit hot-wet strength retention which is superior to that provided by epoxy resin systems.

Epoxy resins, the dominant matrix system for high modulus graphite (HMG) do provide very good composite properties and have been extensively used in the manufacture of sporting goods and aircraft parts including ailerons, rudders, flaps, vertical and horizontal stabilizers, and complete wing sections for commercial and military aircraft. Epoxy resin prepgs are commonly supplied at relatively high resin contents requiring "bleeding" to achieve the desired resin content.

Use of this technique (bleeding) results in non-uniformity of resin content in the composite since more resin is removed next to the bleeder. This non-uniformity of resin content induces stresses and often results in warped parts. Use of a "net" resin concept tends to overcome these problems. V-378A exhibits excellent fiber wet out during the initial prepregging step and can thus be provided as a net resin prepg.

The 175°C curing epoxy resin systems exhibit long gel times at 175°C and very low "watery" viscosities which tend to make it difficult to achieve low void composites. Typically, 175°C curing epoxies require a "hold" at 150 - 175°C to build molecular weight (and viscosity) prior to full application of pressure. V-378A, in contrast, gels fairly rapidly at 125°C and exhibits moderate to low viscosity during heat up making it much easier to achieve very low void content composite structures. Pressure application is done at ambient temperature without the necessity of a hold.

LAY-UP AND CURE

V-378A exhibits light to medium tack at a prepreg net resin content of 30% which is significantly lower than epoxies typically supplied at 42%. The net resin concept is particularly useful for preparation of composites having both thick and thin sections. Due to the low temperature gel and relatively low exotherm, no difficulty has been encountered in curing virtually void-free laminates up to four inches in thickness.

Standard nylon vacuum bags and sealant tapes (same as used for 175°C epoxy) may be used versus expensive polyimide film bag and silicone sealant tape required for high temperature curing polyimides.

To cure the V-378A prepreg lay-up, 85 psi autoclave pressure and vacuum are applied at the beginning of the cycle, and the part heated to 60 - 90°C at a rate of 2 - 5°C/minute. The vacuum is released, the bag vented to the atmosphere, pressure increased to 100 psi and heat up continued to 175°C. The part is cured four hours at 175°C, cooled to ambient temperature, removed and post cured, unrestrained, from room temperature to 246°C for four hours. The four hour post cure at 246°C is required to develop good mechanical properties. Table 1 illustrates a study of $\pm 45^\circ$ tensile ultimate and strain using more extensive post cures and indicates the four hour post cure at 246°C to be satisfactory.

Use of a one to two hour hold at 60 - 90°C for very thick parts allows more time before gelation in order for air, trapped between plies during lay-up, to be released.

Figure 1 shows the effect on viscosity of heating the resin to 67°, 70° and 90°C with holds of 5 hours, 3-1/2 hours and 2-1/2 hours respectively. A heating rate of 1°C/minute was used.

Figure 2 illustrates the effect of heating rate with lower minimum viscosities obtained at faster heating rates.

EFFECTS OF MOISTURE ON PREPREG

The 175°C curing epoxy matrix resins have exhibited much variability in processing due to moisture pickup of the uncured prepreg. This affinity for moisture results in variations in gel time, foaming during cure and porosity in the cured composite.

In contrast, V-378A prepreg exposed to 100% RH and 52°C for one hour, then laid up and cured, exhibited no deleterious effects. Figures 3 and 4 exhibit the effect of a sixteen hour exposure at 90% RH, 24°C on uncured films of V-378A. No porosity or foaming was noted during the RDS viscosity determination.

MECHANICAL AND PHYSICAL PROPERTIES

Figure 5 exhibits a T_g of V-378A (via Rheometric Dynamic Spectroscopy) in excess of 370°C . Translation of properties on high modulus graphite are excellent. Table 2 lists mechanical properties of V-378A/T-300-6K tape composites. Retention of dry flexure at 310°C is approximately 40% of the ambient temperature value. Wet flexure retention (98% RH, 71°C , 30 days) at ambient and 175°C of 23 ksi/22,500 μ in./in. and 15.7 ksi/29,000 μ in./in., respectively are also impressive. It is of interest to note the increase in composite strain at 175°C rather than a decrease usually noted in 175°C epoxies. No significant degradation in ambient or 175°C ultimate or strain values of the $\pm 45^{\circ}$ tensile are exhibited after wet conditioning. Epoxies exhibit a significant drop in 175°C wet properties.

All wet elevated temperature testing was conducted using a five minute "soak" time, for the specimen to get to temperature in the preheated test chamber, in order to minimize drying of the specimen. V-378A composites lose moisture (and regain) at a more rapid rate than 175°C epoxies.

Transverse or 90° tensile ultimate and strain values of V-378A at ambient of 9.2 ksi/7,700 μ in./in. and 6.1 ksi/6,400 μ in./in. at 175°C are also higher than most 175°C epoxy systems.

EFFECTS OF PREPREG AGING AT 75°F

Table 3 exhibits flexure and shear tested at ambient and 177°C from prepreg which was laid up fresh and aged at 0, 7, 14 and 21 days intervals ambient temperature prior to cure. Ambient temperature tack retention, however, is much shorter than for typical 177°C curing epoxies. A vacuum bag debulk step is suggested at 2 - 3 hour intervals for large parts. Fresh prepreg should be laid up promptly and excess prepreg stored at -18°C . Storage stability of the prepreg is in excess of six months at -18°C .

GENERAL MECHANICAL PROPERTIES

Extensive mechanical properties on V-378A/T-300-6K unitape composites were determined by the University of Dayton Research Institute and reported under AF contract F 33615-78-C5172. This data includes 0° , $\pm 45^{\circ}$ and 90° tensile, 0° and 90° compressive, 0° and 90° flexure and shear at -55°C , 22°C , 177°C and 232°C as well as static and creep testing.

Two major aircraft companies have found V-378A to exhibit open hole tensile values 50 - 70% higher than 175°C curing epoxies.

Table 4 contains properties of V-378A/T-300-6K, 5 HS woven graphite fabric composites with flexure and shear tests up to 232°C . This is a relatively new style using the heavier weight 6000 filament yarn and may replace the 3000 filament yarn 8HS fabric in many applications due to the lower cost of the yarn.

Properties of V-378A/7781 E-glass fabric are listed in Table 5 and also exhibit excellent strength retention at temperatures up to 371°C.

Table 6 lists properties of V-378A/6781 S-glass and illustrates the higher strengths attainable with S-glass.

Some properties of HI-TEX graphite fiber, HITCO's recent entry in the high strength, high modulus field on V-378A are listed in Table 7.

ELEVATED TEMPERATURE STABILITY OF CURED COMPOSITES

Flexure and shear of .080" thick V-378A/T-300 tape composites after aging six months at 177°C and nine months at 232°C in circulating air ovens are listed in Table 8. Composite weight loss after six months at 177°C is less than 0.6%. Flexure at ambient and 177°C appear to have increased slightly. Six months aging at 232°C exhibited a weight loss of 2.3% and good retention of flexure. Nine month aging produced composite weight loss of 3.5%. Retention of shear and flexure was quite high both at ambient and 232°C. Degradation appeared to be greatest on the surface.

Two new sets of panels were prepared and one set coated with 1 mil of Skybond 703, a condensation type polyimide, as a protective coating. The control panel exhibited a weight loss of 4% while the Skybond 703 coated panel lost 2.3% weight after aging one year at 232°C. Test of flexure and shear indicated about 15% better retention of 232°C flexure and slightly better shear on the coated panel after the one year at 232°C.

SMOKE DENSITY

Figure 6 illustrates the very low smoke density exhibited by V-378A composites. After a 20 minute burn, the smoke density (NBS Smoke Chamber) is about 1.5.

APPLICATIONS

V-378A is being evaluated in a number of applications for commercial and military aircraft as well as industrial applications. One of the most impressive of these is for manufacture of the complete wing skins and ribs for the new F-16XL cranked arrow fighter plane. The first prototype of this new concept aircraft flew on July 3, 1982 and is under intensive evaluation by General Dynamics.

Figure 7 is a view of a V-378A/T-300-6K composite wing skin during lay-up. Figure 8 shows several skins in various stages of lay-up. Figure 9 is a completed skin removed from the tool and after post cure. This part had less than 0.030" warp after post cure. Extensive C-scans indicated essentially no voids. Figure 10 illustrates the completed wing structure with internal ribs mechanically fastened to the upper and lower wing skins. The root thickness of each skin is approximately 0.4" tapering to approximately 0.60" at the tip. The completed wing attached to the fuselage is shown in Figure 11. Figure 12 exhibits both wings attached to the fuselage and finally the finished cranked arrow, delta wing F-16XL is shown in Figure 13.

Proposed specifications for the F-16XL versus the current F-16A manufactured by General Dynamics, Ft. Worth, are listed in Table 9. Initial results from flight tests indicate performance is close to analytical predictions.

Figure 14 shows a wing flap from another prototype aircraft with integrally cocured V-378A/T-300 ribs bonded to a wing skin.

V-378A/T-300-6K is also being used to produce a firewall for an advanced concept helicopter and in numerous other applications.

SUMMARY

V-378A, a modified bismaleimide resin has been developed for composite applications requiring greater hot-wet strength retention than currently available with 175°C curing epoxy resins.

The new resin also exhibits good prepreg parameters, facile, epoxy-like, curing characteristics and appears useful for applications at temperatures of 232°C for extended periods of time and in areas where low smoke density is required.

Assistance from the U. S. Polymeric analytical, physical testing laboratories and from Lee McKague and Clarence Hart of General Dynamics for their help in providing photographs and technical assistance is gratefully acknowledged.

TABLE 1
EFFECT OF POST CURE ON $\pm 45^\circ$
TENSILE V378A/T-300 6K UNITAPE COMPOSITES

I. PRE-REG PROPERTIES		30.0 (NET) LIGHT - MEDIUM 18°C OR BELOW		30.0 (NET) LIGHT - MEDIUM 18°C OR BELOW		30.0 (NET) LIGHT - MEDIUM 18°C OR BELOW		30.0 (NET) LIGHT - MEDIUM 18°C OR BELOW	
RESIN CONTENT, % WT									
TACK									
RECOMMENDED STORAGE TEMPERATURE									
II. LAYUP AND CURE									
EIGHT PLIES V378A, $\pm 45^\circ$ (LOT 2W4872) WERE LAID UP ON A FREKOTE 33 RELEASED CAUL PLATE. ONE PLY TX1040 ADDED ON TOP OF LAYUP PLUS RELEASED TOP CAUL PLATE. COROPRENE SIDE DAMS APPLIED WITH 3 MIL TEDLAR ("L" SLITS AT EACH CORNER) TAPED TO TOP OF COROPRENE DAMS. TWO PLIES 1581 BREATHER OVER ENTIRE LAYUP TO VENT HOLES									
APPLY VACUUM PLUS 85 PSI AND HEAT FROM ROOM TEMPERATURE TO 82°C AT 3 \pm 2°C MIN. HOLD 30 AT 82°C, THEN VENT BAG TO ATMOSPHERE AND INCREASE PRESSURE TO 100 PSI. HEAT FROM 232°C TO 177°C. HOLD FOUR HOURS AT 232°C. COOL, REMOVE AND POST CURE AS NOTED BELOW:									
POST CURE	4 HR AT 246°C	8 HR AT 246°C	12 HR AT 246°C	24 HR AT 246°C	4 HR AT 246°C	90° TENSILE ULT. KSI, R.T.			
$\pm 45^\circ$ TENSILE ULT. KSI AT R.T.	21.49 23.71 23.77	22.97 22.46 23.04	23.41 22.31 21.74	21.16 20.15 19.62	19.60 19.31 19.62	19.60 20.15 19.62	19.60 20.15 19.62	19.60 20.15 19.62	19.60 20.15 19.62
AVERAGE	23.0	22.6	22.9	21.7	19.8	19.8	19.8	19.8	19.8
$\pm 45^\circ$ TENSILE STRAIN, μ IN./IN. AT R.T.	16740 16600 16700	17400 16960 17660	16820 16800 15000	15300 11400 15600	17000 16440 13500	$\pm 45^\circ$ TENSILE ULT. KSI, 177°C 45° TENSILE MODULUS, KSI, R.T.	$\pm 45^\circ$ TENSILE ULT. KSI, 177°C 45° TENSILE MODULUS, KSI, R.T.	$\pm 45^\circ$ TENSILE ULT. KSI, 177°C 45° TENSILE MODULUS, KSI, R.T.	$\pm 45^\circ$ TENSILE ULT. KSI, 177°C 45° TENSILE MODULUS, KSI, R.T.
AVERAGE	16680	17340	16170	14100	15650	0° TENSILE MODULUS, KSI, R.T. 0° TENSILE STRAIN, μ IN./IN. R.T.	0° TENSILE MODULUS, KSI, R.T. 0° TENSILE STRAIN, μ IN./IN. R.T.	0° TENSILE MODULUS, KSI, R.T. 0° TENSILE STRAIN, μ IN./IN. R.T.	0° TENSILE MODULUS, KSI, R.T. 0° TENSILE STRAIN, μ IN./IN. R.T.
$\pm 45^\circ$ TENSILE ULT. KSI AT 350°F	18.64 16.55	15.10 17.23 16.55	17.38 15.81 17.53	16.85 14.12 17.79	16.80 — 16.48	16.80 — 16.48	16.80 — 16.48	16.80 — 16.48	16.80 — 16.48
AVERAGE	17.5	16.1	16.4	16.8	16.6	16.6	16.6	16.6	16.6
τ 45° TENSILE STRAIN, μ IN./IN.	24600+ 28600+ 29400+	28000+ 27340+ 24000+	25600+ 21400+ 25000+	24400+ 25800+ 26600+	25000+ 21400+ 26400+	25400+ 25400+ 24100+	25400+ 25400+ 24100+	25400+ 25400+ 24100+	25400+ 25400+ 24100+
AVERAGE	27500+	26400+	25300+	24100+	24100+	25400+ 25400+ 24100+	25400+ 25400+ 24100+	25400+ 25400+ 24100+	25400+ 25400+ 24100+
LAMINATE DENSITY, GR/CC	1.56								
FIBER VOLUME, %	64.6								
VOIDS, %	0.1								
LAMINATE RESIN SOLIDS, % WT	27.2								

*5 MIN SOAK AT TEST TEMPERATURE
**% WEIGHT GAIN OF MOISTURE LISTED IN PARENTHESES

TABLE 2
TYPICAL MECHANICAL AND PHYSICAL PROPERTIES OF
CURED V-378A/T-300-6K, HM/G/PI TAPE COMPOSITES

TEST	"AS IS"	4 WK 71°C 98% RH	8 WK 71°C 98% RH
0° FLEXURE, ULT. KSI, R.T.	265.0	263.0 (1.73)*	254.0 (1.78)**
0° FLEXURE, ULT. KSI, 177°C	197.5	157.0	135.0
0° FLEXURE, ULT. KSI, 232°C	179.0	—	—
0° FLEXURE, ULT. KSI, 288°C	122.0	—	—
0° FLEXURE, ULT. KSI, 316°C	107.0	—	—
0° FLEXURE MODULUS, KSI, R.T.	19.8	20.7	18.4
0° FLEXURE MODULUS, KSI, 177°C*	19.7	20.7	18.3
0° FLEXURE MODULUS, KSI, 232°C	19.2	—	—
0° FLEXURE MODULUS, KSI, 288°C	18.4	—	—
0° FLEXURE MODULUS, KSI, 316°C	17.6	—	—
0° HORIZONTAL SHEAR, KSI, R.T.	18.3	16.1 (1.85)**	13.7 (1.91)**
0° HORIZONTAL SHEAR, KSI, 177°C	10.9	8.0	7.4
0° HORIZONTAL SHEAR, KSI, 232°C	9.2	—	—
0° HORIZONTAL SHEAR, KSI, 288°C	6.4	—	—
0° HORIZONTAL SHEAR, KSI, 316°C	5.8	—	—
90° TENSILE, ULT. KSI, R.T.	9.0	4.3 (1.74)**	4.6 (1.87)**
90° TENSILE, ULT. KSI, 177°C	5.9	1.40	1.58
90° TENSILE, ULT. KSI, 232°C	1.40	1.60	1.40
90° TENSILE, ULT. KSI, 288°C	1.40	1.60	1.40
90° TENSILE, ULT. KSI, 316°C	1.40	1.60	1.40
90° TENSILE MODULUS, KSI, R.T.	1.00	0.70	0.85
90° TENSILE MODULUS, KSI, 177°C	6.570	2.400	3.100
90° TENSILE STRAIN, μ IN./IN., R.T.	5.900	2.200	1.800
90° TENSILE STRAIN, μ IN./IN., 177°C	23.0	22.6 (1.60)**	22.3 (1.59)**
$\pm 45^\circ$ TENSILE ULT. KSI, R.T.	15.7	15.8	15.5
$\pm 45^\circ$ TENSILE MODULUS, KSI, R.T.	2.43	3.00	2.50
$\pm 45^\circ$ TENSILE MODULUS, KSI, 177°C	1.63	1.35	1.34
$\pm 45^\circ$ TENSILE MODULUS, KSI, 232°C	22.500	22.600	22.300
$\pm 45^\circ$ TENSILE MODULUS, KSI, 288°C	29.280	30.000	29.000
$\pm 45^\circ$ TENSILE MODULUS, KSI, 316°C	228.9	—	—
0° TENSILE MODULUS, KSI, R.T.	21.8	—	—
0° TENSILE STRAIN, μ IN./IN. R.T.	10,470	—	—

TABLE 3
EFFECT OF
PREPREG AGEING AT 23°C PRIOR TO CURE

TABLE 4
V-378A/S/T-300 . 6K, 5 HS
POLYIMIDE/BIDIRECTIONAL FABRIC,
LOT NO. D07220

I. PREPEG PROPERTIES		II. LAYUP AND CURE (NET RESIN, NO BLEEDER)		III. MECHANICAL PROPERTIES	
WET RESIN CONTENT, % WT	32.0	VOLATILES, % WT, 10' AT 135°C	7.0	TEST	RESULTS
FLOW, % — 15 PSI, 135°C, 15'	8.0	EIGHT PLIES V-378A/T-300 . 3K, 8HS FABRIC ON FREKOTE 33 RELEASED CAUL PLATE, ONE PLY TX1040			
0 FRESH	289.1/18.9	266.9/17.6	302.8/19.1	285.1/18.5	153/8.0
7-DAYS	280.2/19.0	268.2/19.3	287.8/18.9	260.8/19.2	135/7.7
14 DAYS	290.3/18.9	256.2/17.1	273.8/17.3	304.7/20.3	98/7.3
21 DAYS	263.0/18.3	273.4/16.7	295.5/18.6	270.0/18.8	
	—	262.9/18.4	274.1/18.4	285.2/19.0	
AVERAGE	280.7/18.8	265.5/17.8	286.8/18.5	281.2/19.2	
FLEX/MODULUS AT 177°C, KSI/MSI	228.4/17.1	218.6/17.8	208.3/19.4	198.4/18.3	
	243.4/19.6	218.1/17.3	209.8/18.4	204.8/17.5	
	225.0/17.7	224.2/18.1	206.2/18.3	205.0/17.3	
	231.0/18.6	222.2/19.4	205.6/18.6	202.4/17.6	
	—	216.3/18.5	216.1/17.2	194.8/18.2	
AVERAGE	232.0/18.3	220.9/18.2	209.2/18.4	201.1/17.8	
SBS AT R.T., KSI	17.1	18.2	17.5	17.1	
	17.8	18.4	18.0	17.0	
	18.5	18.4	17.8	—	
	16.9	18.2	18.1	15.8	
	17.9	17.2	18.1	15.9	
AVERAGE	17.7	18.1	17.9	16.5	
SBS AT 177°C, KSI	11.5	11.2	10.6	10.0	
	11.5	11.1	10.4	10.3	
	11.5	10.7	10.7	10.6	
	11.9	10.4	10.8	10.3	
	11.9	11.4	10.3	10.3	
AVERAGE	11.7	11.0	10.6	10.3	
DENSITY GR/CC	1.59	1.57	1.57	1.58	
RESIN SOLIDS, %	28.1	31.1	30.5	28.0	
FIBER VOLUME, %	65.1	61.5	62.0	64.4	
VOIDS, %	0.40	0.10	0.50	0.90	
VOID CONTENT, %					

TABLE 5
PRELIMINARY DATA
V-378A/7581 CS272, POLYIMIDE/BIDIRECTIONAL E-GLASS FABRIC

I. PREPREG PROPERTIES	
RESIN CONTENT, % WT	30%
II. LAYUP AND CURE (NET RESIN, NO BLEEDER)	
	TWELVE PLIES V-378A/6781 LOT NO. D07207 ON FREKOTE 33 RELEASED CAUL PLATE, ONE PLY TX1040 ON TOP LAYUP PLUS RELEASED TOP CAUL PLATE AND TEDLAR TOP RELEASE FILM WITH "L" SLITS AT CORNERS TAPE TO COROPRENE SIDE DAMS, TWO PLIES 7581 BREATHER OVER ENTIRE LAYUP PLUS VENT HOLES. APPLY NYLON VACUUM BAG WITH SEALANT
	APPLY VACUUM PLUS 85 PSI, HEAT FROM R.T. TO 177°C AT 3 ± 2°C/MIN, HOLD 30' AT 82°C THEN VENT BAG TO ATM AT 82°C AND INCREASE PRESSURE TO 100 PSI, THEN CONTINUE HEAT TO 177°C, CURE FOUR HOURS AT 177°C AND COOL TO 60°C OR BELOW BEFORE REMOVING. POSTCURE FOUR HOURS AT 246°C
III. MECHANICAL PROPERTIES	

RESULTS		RESULTS	
AS-IS	*WET	AS-IS	*WET
100/3.8	117/4.6	WARP ONLY - 4 EACH	WARP ONLY - 4 EACH
89/4.0	102/4.6	FLEX/MODULUS AT R.T. KSI/MSI	FLEX/MODULUS AT R.T. KSI/MSI
84/4.0	89/4.3	FLEX/MODULUS AT 177°C. KSI/MSI	FLEX/MODULUS AT 177°C. KSI/MSI
75/3.9	67/4.1	FLEX/MODULUS AT 232°C. KSI/MSI	FLEX/MODULUS AT 232°C. KSI/MSI
48/3.5	43/3.6	FLEX/MODULUS AT 316°C. KSI/MSI	FLEX/MODULUS AT 316°C. KSI/MSI
		FLEX/MODULUS AT 371°C. KSI/MSI	FLEX/MODULUS AT 371°C. KSI/MSI
		COMPRESSIVE/MODULUS AT R.T. KSI/MSI (ASTM D695 - DOGBONES)	COMPRESSIVE/MODULUS AT R.T. KSI/MSI (ASTM D695 - DOGBONES)
		COMPRESSIVE/MODULUS AT 177°C. KSI/MSI	COMPRESSIVE/MODULUS AT 177°C. KSI/MSI
		COMPRESSIVE/MODULUS AT 232°C. KSI/MSI	COMPRESSIVE/MODULUS AT 232°C. KSI/MSI
		TENSILE/MODULUS AT R.T. KSI/MSI	TENSILE/MODULUS AT R.T. KSI/MSI
		TENSILE/MODULUS AT 177°C. KSI/MSI	TENSILE/MODULUS AT 177°C. KSI/MSI
		TENSILE/MODULUS AT 232°C. KSI/MSI	TENSILE/MODULUS AT 232°C. KSI/MSI
		LAMINATE RESIN SOLIDS, % WT	LAMINATE RESIN SOLIDS, % WT
		LAMINATE DENSITY, GR/CC	LAMINATE DENSITY, GR/CC
		LAMINATE FIBER VOLUME, %	LAMINATE FIBER VOLUME, %
		LAMINATE Voids, %	LAMINATE Voids, %

*WET = 30 DAYS AT 71°C, 95-100% RH

*WET = 30 DAYS AT 71°C, 95-100% RH

TABLE 7
PRELIMINARY DATA
HIGH TEMPERATURE PROPERTIES, V-378A/HI-TEX-12K,
POLYIMIDE/HIGH MODULUS GRAPHITE UNIDIRECTIONAL COMPOSITE

TEST	RESULTS		0°
	0°	177°C	
0° FLEXURE/MODULUS, KSI/MSI, R.T.	324/18.5	1.60	1.62
0° FLEXURE/MODULUS, KSI/MSI, 177°C	243/18.2	—	1.57
0° SHORT BEAM SHEAR, KSI, R.T.	15.3	27.3	28.5
0° SHORT BEAM SHEAR, KSI, 177°F	10.8	—	—
LAMINATE DENSITY, GR/CC	1.60	—	—
LAMINATE RESIN SOLIDS, % WT	28.7	0.2	2.6
LAMINATE FIBER VOLUME, %	64.6	—	—
LAMINATE VOIDS, %	0.2	0.57	3.4

NOTE: 5 MIN SOAK AT TEST TEMPERATURE

TABLE 8
TYPICAL PROPERTIES OF
V-378A/T-300 UC309 LOT 2W4941, 5 MIL UNITAPE
COMPOSITES AGED AT SIX MONTHS AT 177°C AND 232°C

TEST	RESULTS		0°
	0°	177°C	
0° FLEXURE/MODULUS, KSI/MSI, R.T.	298/18.2	320/20.0	275/19.0
0° FLEXURE/MODULUS, KSI/MSI, 177°C	245/17.4	271/21.1	—
0° FLEXURE/MODULUS, KSI/MSI, 232°C	233/17.4	—	180/19.3
0° FLEXURE/MODULUS, KSI/MSI, 232°C	—	—	205/21.4
SHORT BEAM SHEAR, KSI, R.T.	15.8	—	—
SHORT BEAM SHEAR, KSI, 177°C	10.1	—	—
SHORT BEAM SHEAR, KSI, 232°C	7.7	—	—
SHORT BEAM SHEAR, KSI, 232°C	—	—	8.6

I. PREPREG PROPERTIES

WET RESIN CONTENT, % WT	30%
NONREACTIVE VOLATILES, % WT	0
TACK	LIGHT - MEDIUM
RECOMMENDED STORAGE TEMPERATURE	-18°C OR BELOW

II. LAYUP AND CURE (NET RESIN, NO BLEEDER)

FIFTEEN PLIES V-378A/HI-TEX12K (LOT 3W2320) 0° UNITAPE WERE LAID UP ON A FREKOTE 33 RELEASED CAUL PLATE, ONE PLI TX1040 ADDED ON TOP OF LAYUP PLUS RELEASED, TOP CAUL PLATE, COROPRENE SIDE DAMS APPLIED WITH 3 MIL TEDLAR WITH "L" SLITS AT EACH CORNER TAPED TO TOP OF COROPRENE DAMS. TWO PLIES 1581 BREATHER OVER ENTIRE LAYUP TO VENT HOLES

APPLY VACUUM PLUS 85 PSI AND HEAT FROM ROOM TEMPERATURE TO 82°C AT $3+2^\circ\text{C}/\text{MIN}$, HOLD 30°C AT 82°C , THEN VENT BAG TO ATMOSPHERE AND INCREASE AUTOCLAVE PRESSURE TO 100 PSI AND CONTINUE HEATING FROM 82°C TO 177°C . CURE FOUR HOURS AT 177°C , REMOVE, AND POSTCURE UNRESTRAINED FOUR HOURS AT 246°C

III. MECHANICAL AND PHYSICAL PROPERTIES, V-378A/T300-6K COMPOSITE

TEST	RESULTS		0°
	0°	177°C	
0° FLEXURE/MODULUS, KSI/MSI, R.T.	1.60	1.62	1.62
0° FLEXURE/MODULUS, KSI/MSI, 177°C	—	—	1.57
0° SHORT BEAM SHEAR, KSI, R.T.	27.3	28.5	26.6
0° SHORT BEAM SHEAR, KSI, 177°F	—	—	—
LAMINATE DENSITY, GR/CC	66.1	63.8	64.9
LAMINATE RESIN SOLIDS, % WT	0.2	0.2	2.6
LAMINATE FIBER VOLUME, %	—	—	—
LAMINATE VOIDS, %	0.57	2.3	3.4

TABLE 9
F-16XL SPECIFICATIONS

	F-16XL SCAMP	F-16A
WINGSPAN	32.4 FT	32.8 FT*
WING ROOT CHORD	499 IN.	195 IN.
WING AREA	646.4 SQ FT	300 SQ FT
OVERALL LENGTH	52.4 FT	47.6 FT
EMPTY WEIGHT	17,402 LB	15,137 LB
MAXIMUM TAKEOFF GROSS WEIGHT	37,500 LB	35,400 LB
FUEL CAPACITY	12,750 LB	6,972 LB
TAKEOFF ROLL (AIR-AIR COMBAT)	1,640 FT	2,425 FT
TAKEOFF ROLL (AIR-GROUND SUPPORT)	1,980 FT	3,030 FT
LANDING DISTANCE (AIR-AIR COMBAT)	1,990 FT†	2,480 FT
LANDING DISTANCE (AIR-GROUND SUPPORT)	2,230 FT**	2,830 FT
MAXIMUM SPEED	MACH 2.5	MACH 2.0
MAXIMUM CRUISE SPEED	MACH 2.2	MACH 0.93

*WITH WINGTIP MISSILES. WITHOUT MISSILES, SPAN IS 31 FT

†USING BRAKES ONLY. USING DRAG PARACHUTE, LANDING DISTANCE ESTIMATED
AT 1,180 FT

**USING BRAKES ONLY. USING DRAG PARACHUTE, LANDING DISTANCE ESTIMATED
AT 1,360 FT

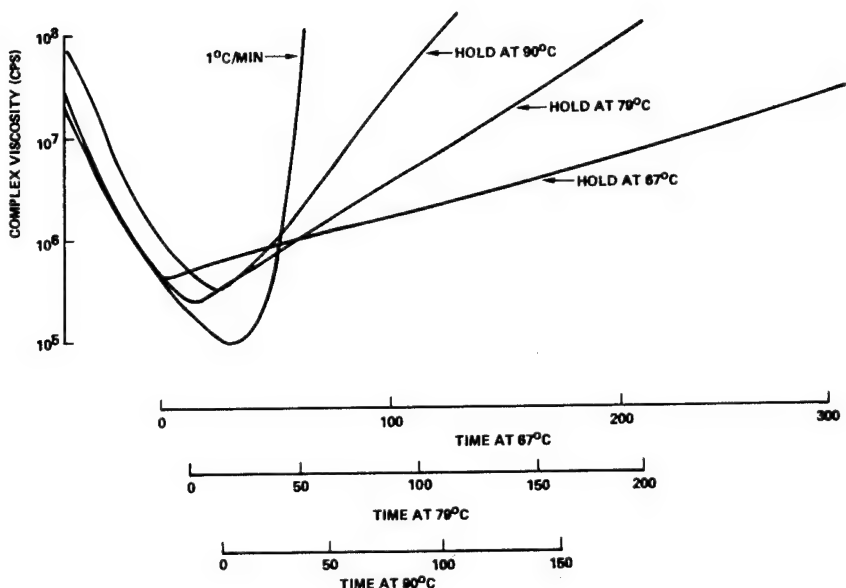


Figure 1. - USP V-378A (Lot WR6080) isothermal cure curves.

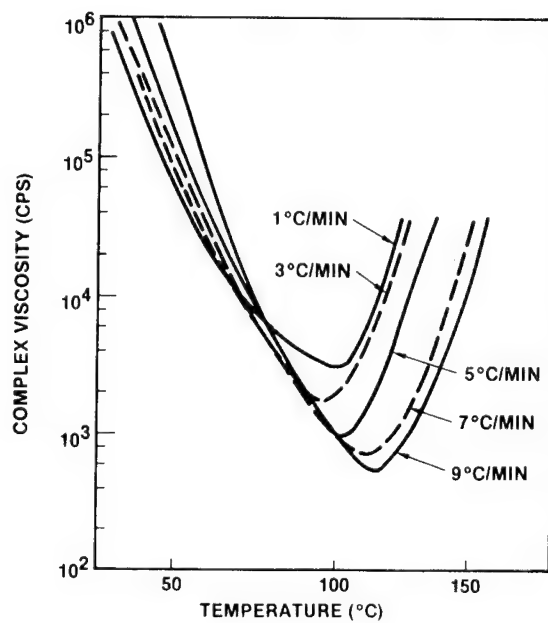


Figure 2. - USP V-378A, effect of heating rate.

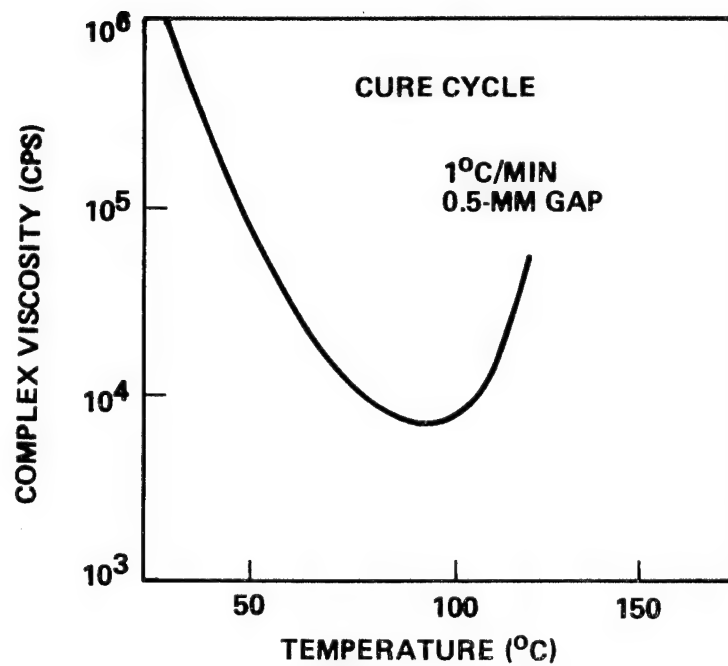


Figure 3. - USP V-378A exposed to 50 percent RH
at 24 °C (for 18 hr).

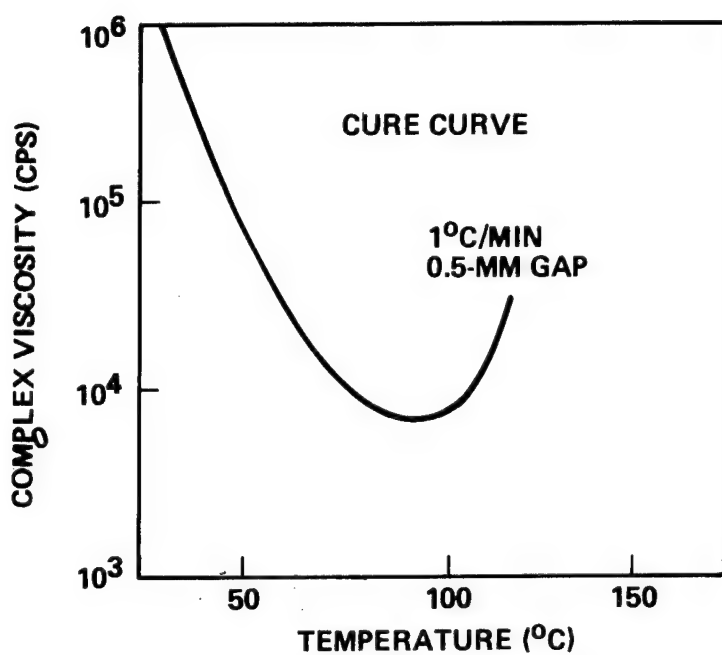


Figure 4. - USP V-378A exposed to 90 percent RH at 24 °C (for 16 hr).

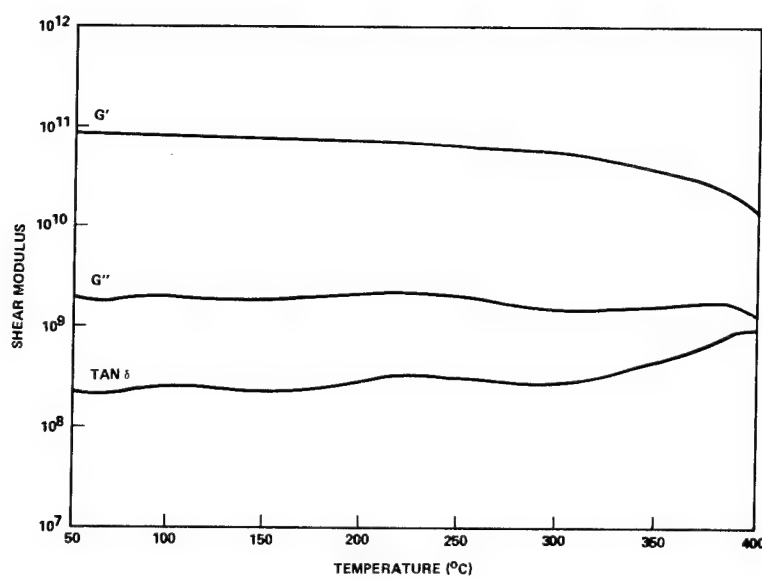


Figure 5. - Tg shear modulus by rheometric dynamic spectroscopy.

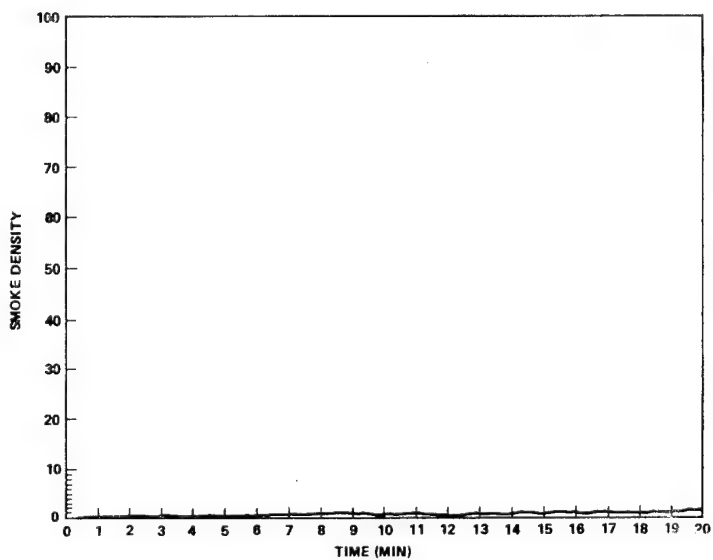


Figure 6. - V-378A/Celion, polyimide/graphite smoke density (NBS chamber).

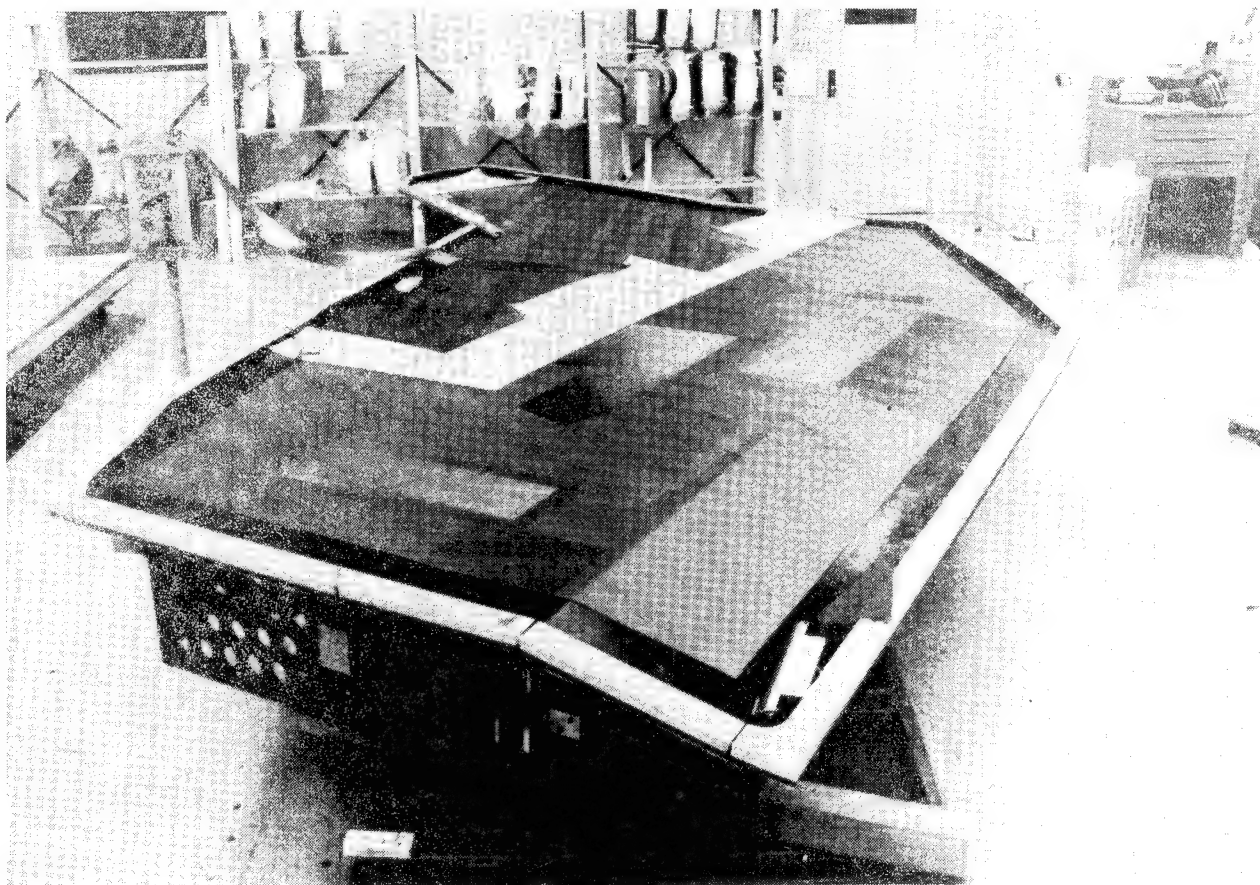


Figure 7. - V-378A/T-300-6K composite wing skin during lay-up.

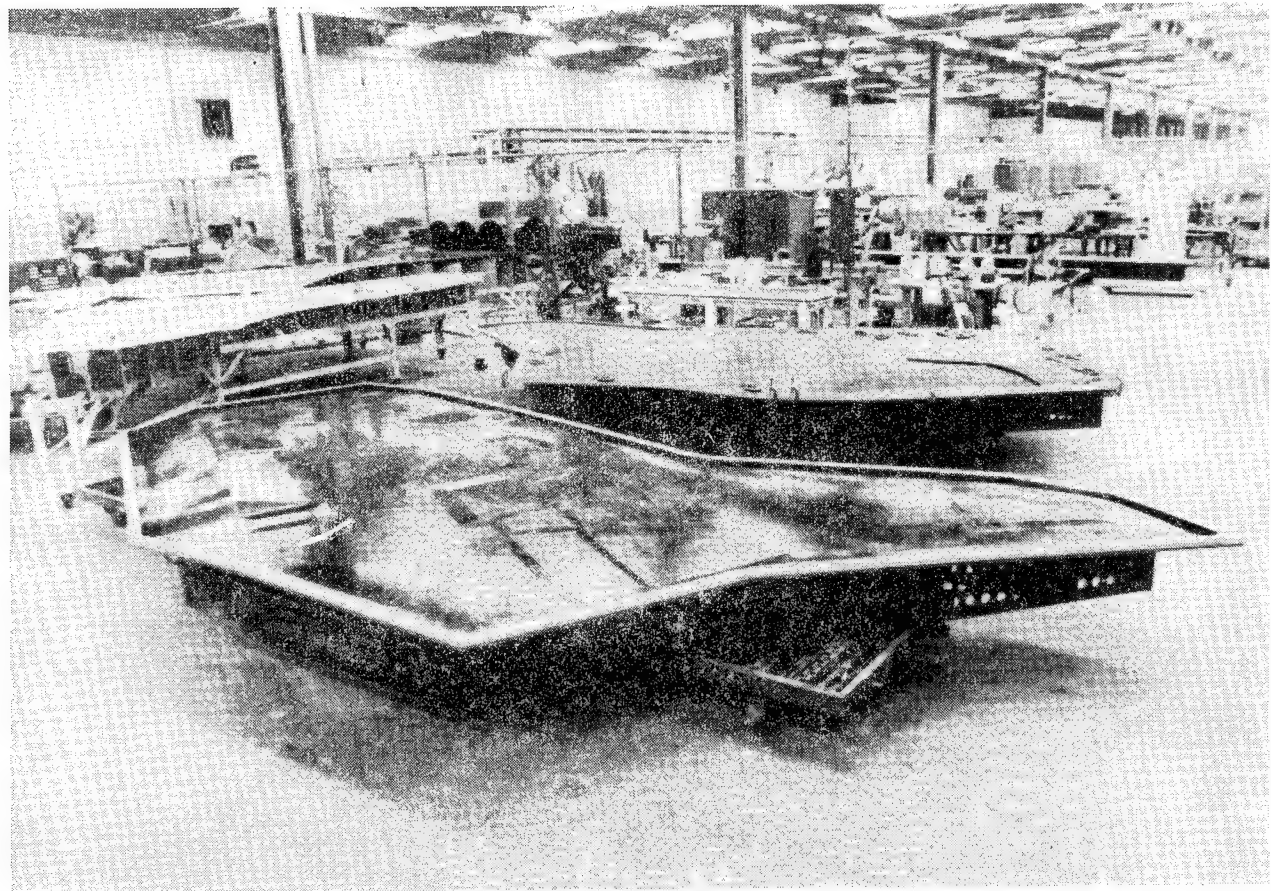


Figure 8. - Wing skins in various stages of lay-up.

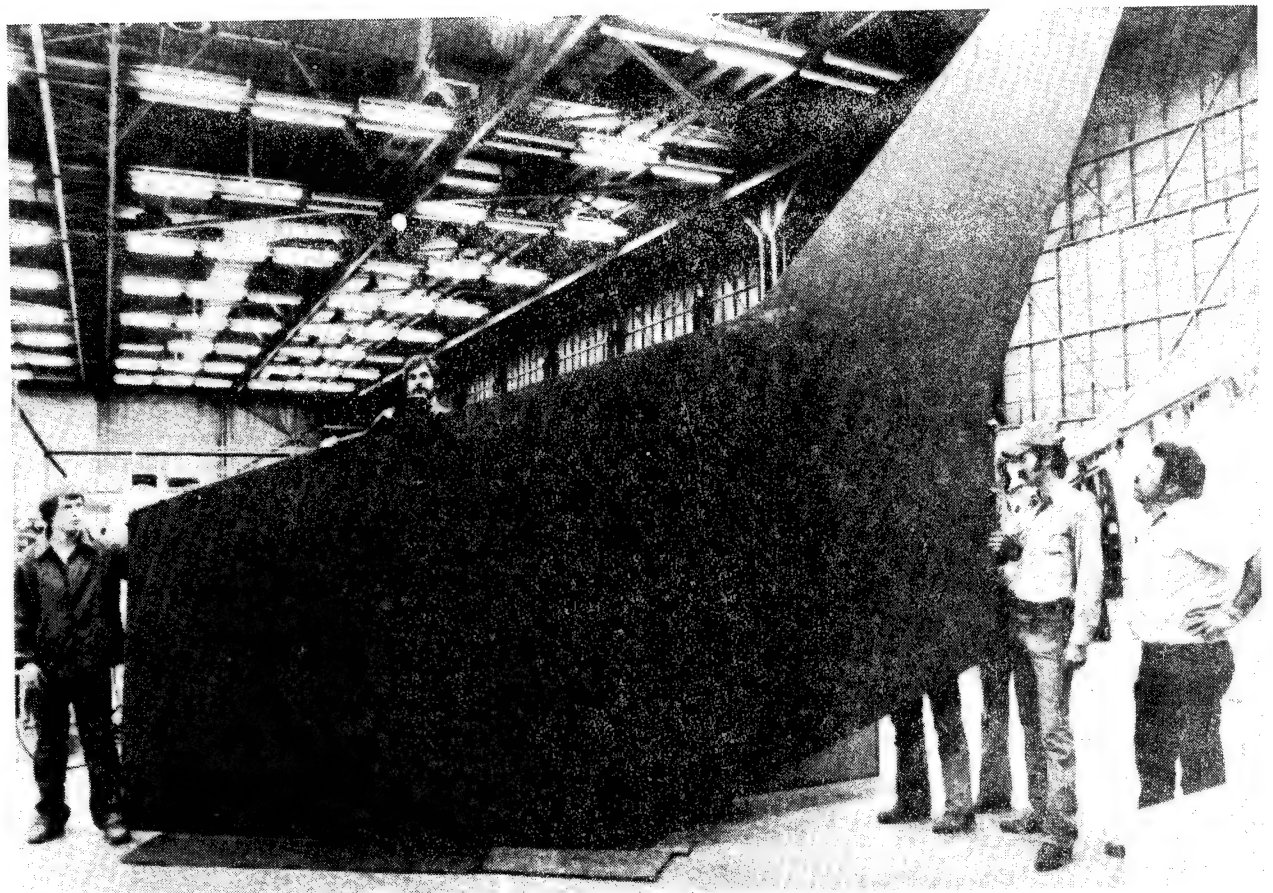


Figure 9. - Completed skin removed from tool after post cure.

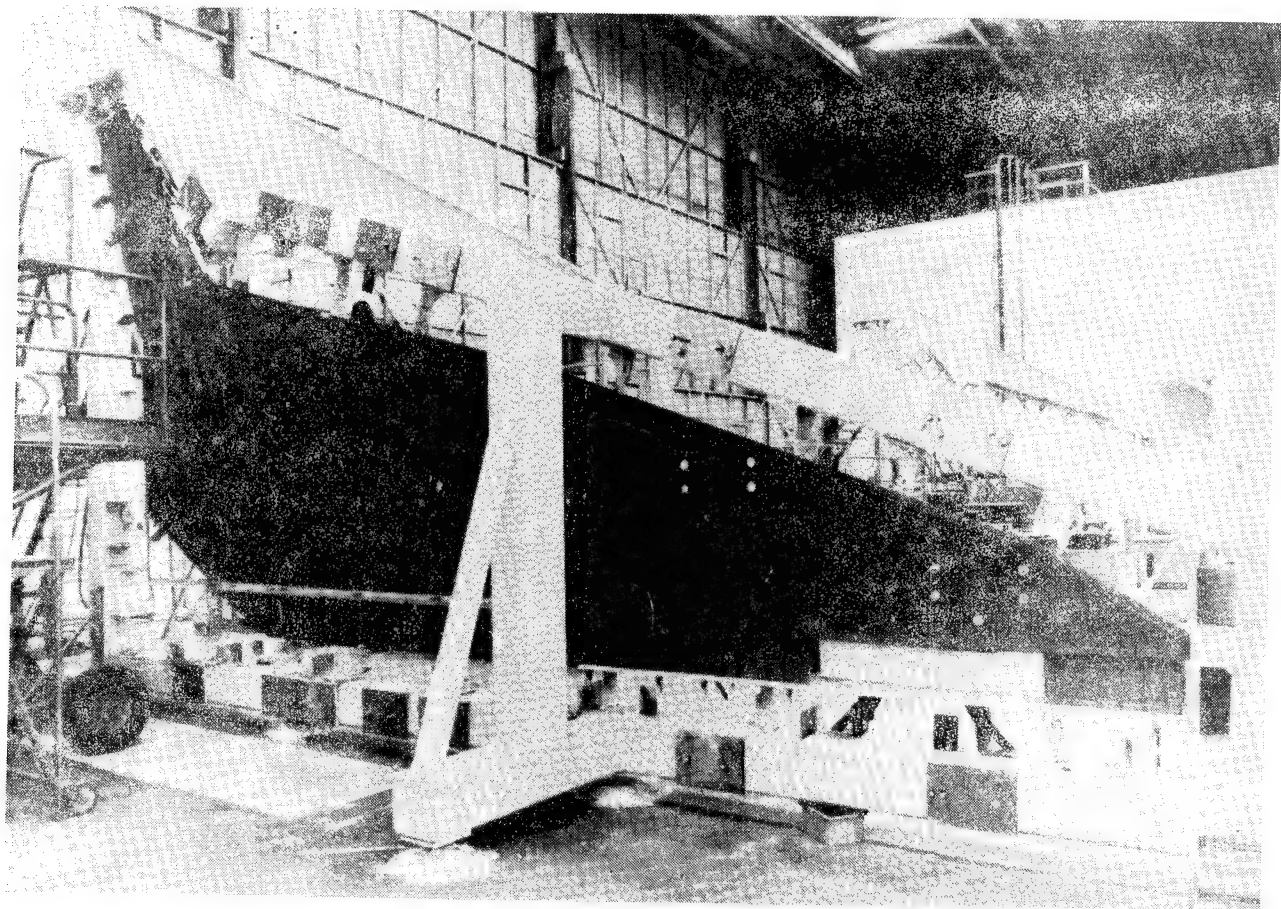


Figure 10. - Completed wing structure with internal ribs mechanically fastened to the upper and lower wing skins.

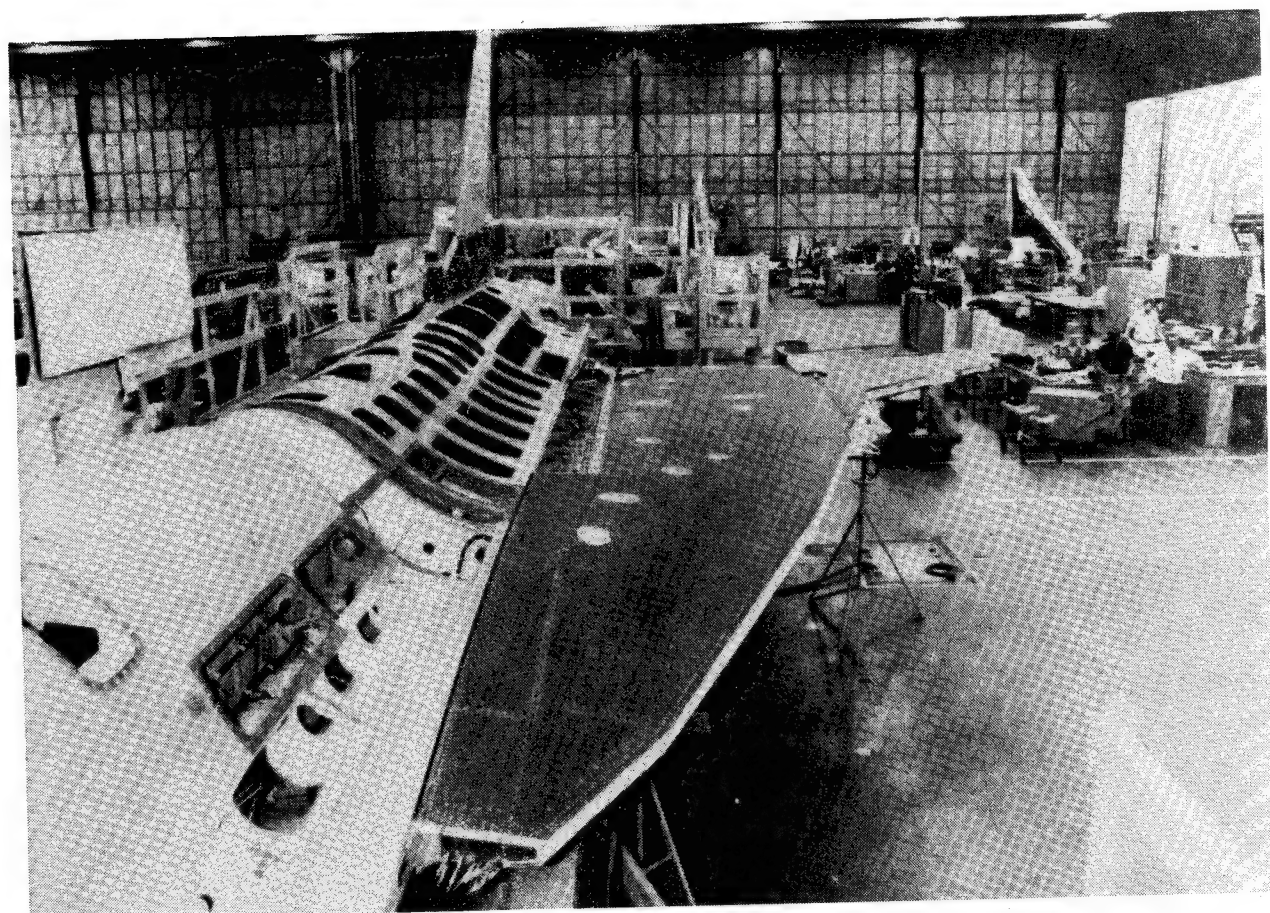


Figure 11. - Completed wing attached to fuselage.

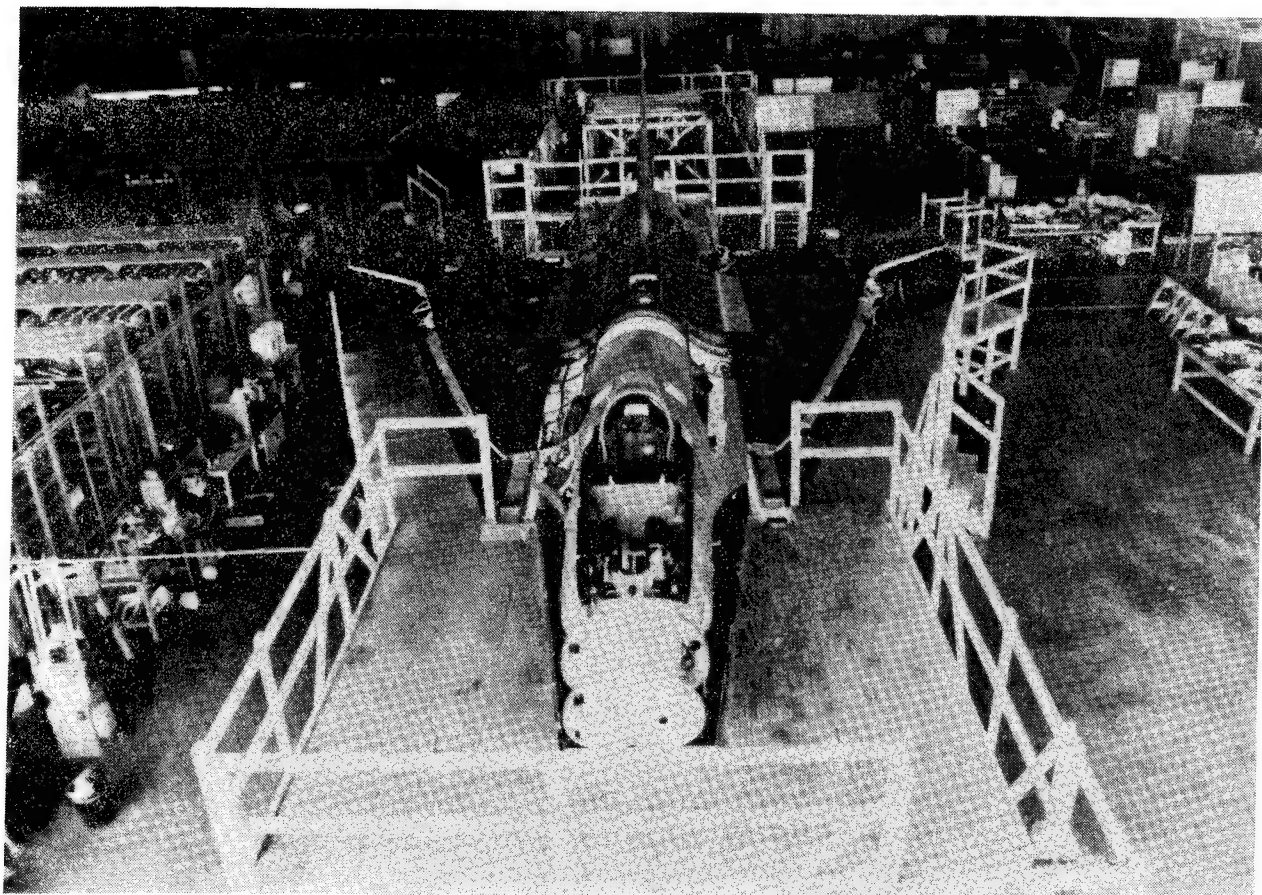


Figure 12. - Fuselage with both wings attached.

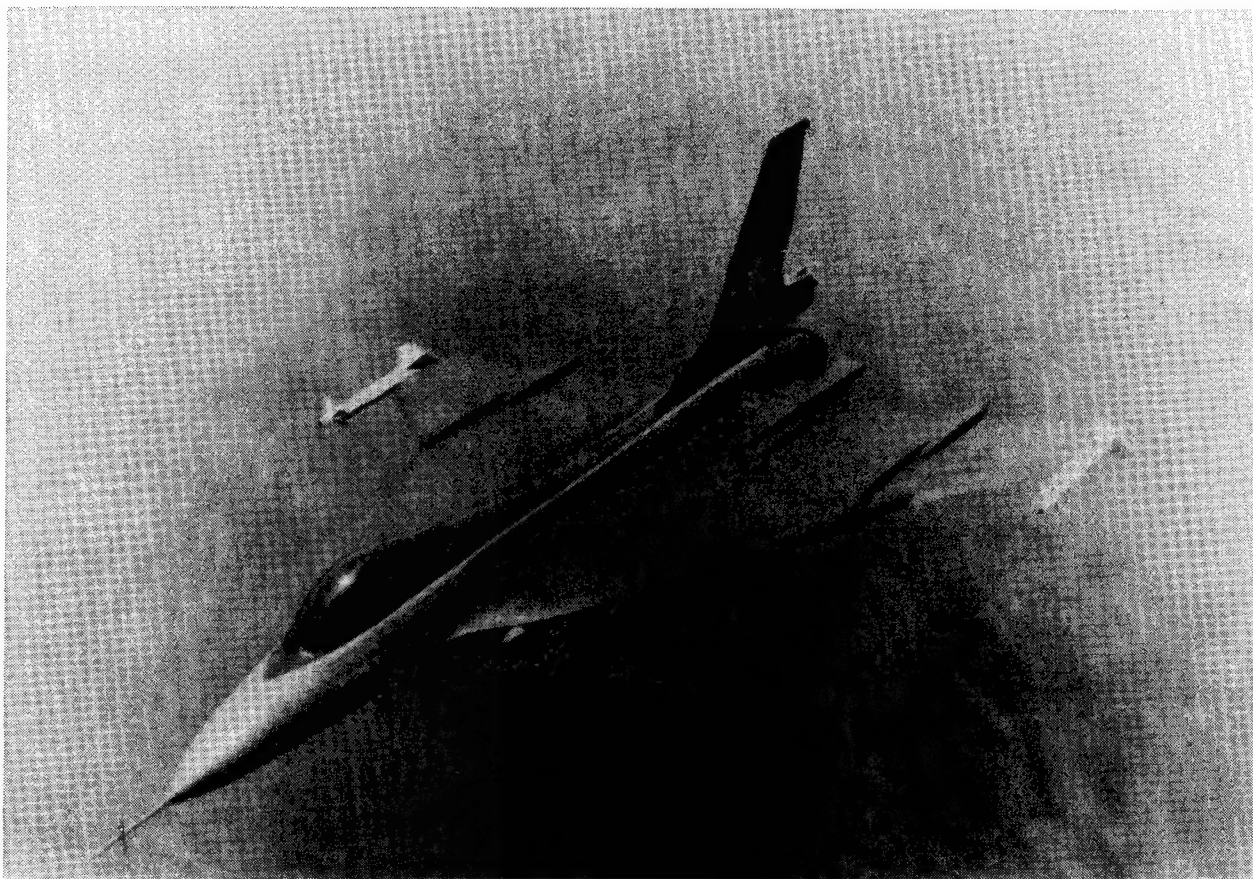


Figure 13. - Finished cranked arrow, delta wing F-16XL fighter plane.

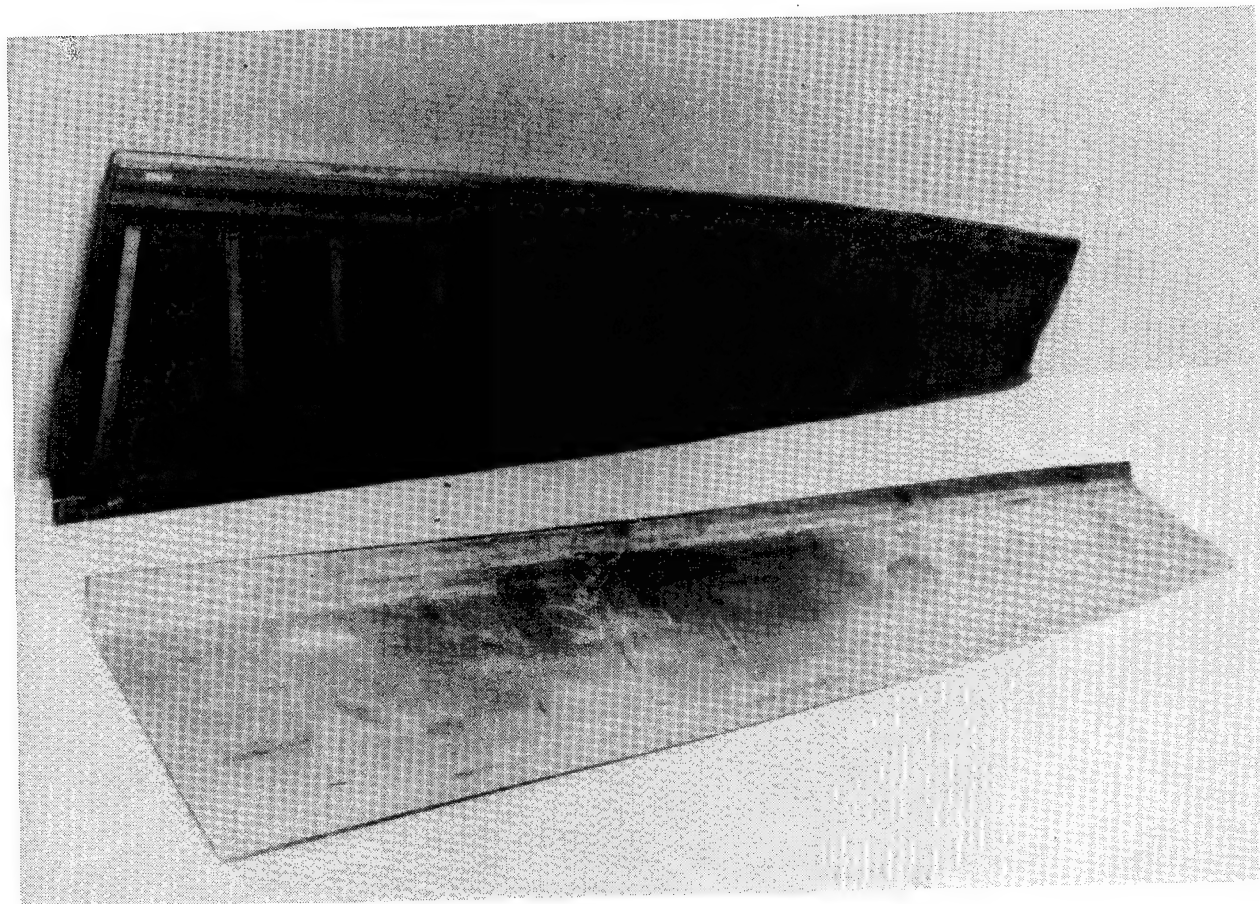


Figure 14. - Wing flap from another prototype aircraft with integrally cocured V-378A/T-300 ribs bonded to a wing skin.

TRANSFER MOLDING OF PMR-15 POLYIMIDE RESIN

J. P. Reardon, D. W. Moyer, and B. E. Nowak
Tribon Bearing Company

Transfer molding is an economically viable method of producing small shapes of PMR-15 polyimide. It is shown that with regard to flexural, compressive, and tribological properties transfer-molded PMR-15 polyimide is essentially equivalent to PMR-15 polyimide produced by the more common method of compression molding. Minor variations in anisotropy are predictable effects of molding design and secondary finishing operations.

INTRODUCTION

An intensifying interest in the aerospace community in PMR-15 polyimide resin is spawning programs to better characterize its physical properties, thereby leading to a variety of new applications. Because PMR-15 resin was designed for easy processing into structural composites, little has been done to utilize it for producing small components by common plastics molding techniques. Two years ago, however, we decided that the growing demands for a reasonably priced 600°F polymer warranted the effort to develop an economically feasible process for producing small parts from PMR-15 resin.

Among the standard molding techniques available for producing small parts, the first to suggest itself for mere simplicity is matched-die compression molding. Generally, however, cycle times greater than an hour are required to allow for heating and cooling the mold and for removing the molded piece from the mold cavity.

Hot isostatic pressing is suitable for making large billets, but the subsequent machining operations make this a rather expensive way of producing small parts. Similarly, extrusion yields rod stock which must then be machined into the finished shapes.

Injection molding has been developed to a high degree of sophistication and is probably capable of producing molded-to-size polyimide parts with minimum cycle times. But injection molding PMR-15 resin would be quite risky because of this resin's tendency to rapidly undergo extreme changes in viscosity during processing. An injection mold barrel frozen up with prematurely crosslinked PMR-15 polyimide would mean costly downtime.

A molding method with many of the good features of injection molding but less risk is transfer molding. Although it is less well-known than injection molding, transfer molding was the forerunner of injection molding, and it is still widely used for molding mundane thermosets such as phenolics. Because the mold itself is maintained at a single temperature and is capable of containing multiple cavities, transfer molding can produce a substantial number of parts with rather short cycle

times, and thus it can be a sound way of making small PMR-15 polyimide parts at a reasonable cost.

We have devoted enough effort to adapting transfer molding to the production of PMR-15 polyimide parts to have satisfied ourselves that the technique is economically sound as a manufacturing method. The subject of this paper is the results of our efforts thus far to demonstrate that the physical properties of transfer molded PMR-15 polyimide are equivalent to those of PMR-15 polyimide formed by the more usual compression molding.

PROCESS

The key to successful transfer or injection molding of a resin is the molding compound. Seldom are polymers molded neat. Fillers are selected to provide the particular blend of properties sought for in the final molded product. Once the formulation is decided upon, the processor proceeds as follows:

1. Blend the fillers into the resin solution.
2. Evaporate the solvent.
3. Imidize the resin.
4. Pulverize the imidized molding compound.
5. Press the powder into a preform pill.
6. Heat the pill immediately before inserting it into the transfer pot of the press.

The proper imidization of PMR-15 resin has been described in various technical papers (ref. 1-4). The imidized molding compound is reduced to a powder both as means of insuring homogeneity and of making it handleable. The powder, in turn, is compacted into a pill in a cold die in order to expel excess entrapped air. The size of the pill is determined by the size of the transfer pot and the volume of resin required to fill the mold cavities. The purpose of preheating the preform pills is to reduce the cycle time in the press.

The operation of the transfer press itself is easily described by referring to figure 1. The entire mold is maintained at the temperature required for curing the polymer. In the case of PMR-15 resin, the cure is effected by thermal crosslinking of the norbornenyl endcaps. At the start of the cycle, the mold is clamped shut. A hot preform pill of molding compound is dropped into the transfer pot of the mold and the hydraulic transfer ram is activated. The pressure of the ram and the heat of the mold rapidly liquify the molding compound. Molten material surges outward through narrow channels and into cavities in the mold base. A large enough preform pill is used to insure that a small amount of material remains in the hub (cull) directly under the ram, thereby keeping the curing resin under pressure. When enough time has passed to sufficiently cure the resin, the bottom platen drops down, lowering the lower half of the mold onto stationary ejector sleeves that force the molded pieces out of their cavities. The operator manually removes the pieces,

retracts the ram, and the cycle is ready to start over. The molded pieces themselves are later postcured in the free state to guarantee that the cure is complete and to enhance their oxidation resistance.

If the molding compound should setup prematurely, the worst that happens is that the cavities fill only partially and a thick cull remains. The hardened resinous mass can be ejected easily, the only loss being a small quantity of material and a few minutes of operating time.

RESULTS

Test Specimens

Figure 2 illustrates the three basic mold shapes from which specimens were taken for determination of physical properties. Rectangular plates as thick as 1.1 inch were formed by compression molding. Transfer-molded shapes included two cylinders, one being 1.50 in. OD x 0.37 in. ID x 1.16 in. and the other 1.03 in. OD x 0.53 in. ID x 2.41 in., and a standard test bar 4.0 x 0.50 x 0.25 inches. The point of resin injection ("gate") for the transfer-molded pieces is indicated in the sketch. Specimens were taken in two orientations 90° to each other as a check for anisotropy resulting from flow patterns into the mold cavity.

The flexural and compressive tests reported in this paper were run in accordance with ASTM D-790 and D-695, respectively. Wear tests were carried out in the conforming block configuration on a LFW-1 machine; a description of the test is given below.

Materials

Table I gives the composition of the material selected for this study. Material "N" is simply neat PMR-15 polyimide. The carbonaceous fillers found in materials "A," "B," and "C" represent typical formulations for self-lubricated, dry-running bearings and seals. The fillers consist of a high-quality natural graphite powder, a milled carbon fiber, and a calcined, finely divided amorphous carbon. The graphite provides lubricity, the carbon fiber reduces thermal expansion, and the amorphous carbon powder imparts hardness and wear resistance.

Flexural Properties

Table II presents a comparison of the four grades of PMR-15 polyimide in terms of the ultimate flexural strengths of specimens machined from compression-molded plates.

In table III, material "A" was chosen to illustrate the worst-case situation for the effect of the method of molding on the flexural strength. In the present context, "worst case" connotes the highest content of milled carbon fiber (33% by weight) and hence the most exaggerated anisotropy. The specimen orientations shown here favor preferred fiber orientation along the length of the specimens. The results are very much what one would normally anticipate. Because the transfer-molded test bar was end-gated, fiber orientation is dominant parallel to the length

of the bar, thereby providing maximum reinforcement. Resin flow downward into the cylindrical cavity is turbulent, giving the least reinforcement. In the compression-molded plate most fibers assume a horizontal posture but have no preferred orientation within the plane; this accounts for the intermediate flexural strength of compression-molded specimens.

Another factor that partially accounts for the variations in strength is the degree of machining required to prepare the test specimens. Thus, the transfer-molded test bars were tested as-molded, the compression-molded specimens were machined only along their edges, but specimens from the cylinders had to be machined on all faces. Because machining operations run the risk of inducing localized stresses and microscopic flaws in the test specimens, it is not surprising that the flexural strength of these specimens decreases with the amount of machining to which they have been subjected.

To complete the profile of these materials, figure 3 shows the drop off in flexural properties (in this instance, for material "A") with elevated temperatures up to 600°F. The curves shown are for transfer-molded test bars. Data for compression-molded specimens generate nearly identical curves.

Compressive Properties

A comparison of the ultimate compressive strength of our four PMR-15 grades is made in table IV. There is an indication of slight anisotropy in the compression-molded specimens. For material "N" this anisotropy is attributable to poor thermal conductivity of the neat resin promoting curing from the outside inward, thereby causing stratification within the molded plate. (Poor thermal conductivity also makes the neat resin very difficult to transfer mold.) Although material "A" exhibits good thermal conductivity, the preferred horizontal orientation of fibers within the molded plate provides greater reinforcement to perpendicularly applied compressive loads (i.e., in vertical specimens) because the stresses so generated are principally shear stresses.

Table V is a more detailed look at the relationship between compressive strength and method of molding for material "A." Once again, material "A" represents the "worst case" situation because of its high fiber content. Average compressive strengths of the two orientations of transfer-molded specimens fall within the one standard deviation range of each other. Values for the two orientations of the compression-molded specimens, however, barely overlap at three standard deviations, which confirms their anisotropy.

Tribological Properties

Tribon makes extensive use of Falex model #1 ring and conforming block test machines in screening materials for friction and wear properties. These machines are still commonly referred to as LFW-1 machines, after their original designation. LFW-1 tests do not predict precisely the wear that will occur in a given application, but they do rank materials. An experienced tribologist can utilize LFW-1 data effectively in selecting candidate materials for new applications.

The material to be tested is machined into a block with a radius that conforms to the test ring (figure 4). In all the tests reported in this paper the specimens

were run against the standard S-10 ring (SAE 4620 steel; Rc 60-62 hardness; 10-12 microinch rms finish), although the test ring may be made from any suitable material. The test ring is mounted on an electric motor-driven spindle and can be run at speeds variable from 4.5 to 1,000 ft./min. Load is applied to the test specimen by dead weights through a 30-to-1 lever system. Friction is measured by a force gage mounted tangentially to the contact area.

The terms and symbols used in wear testing are summarized as follow:

$$P = \text{unit load} = \text{load/area} = F/A \text{ (lb./in.}^2\text{)}$$

$$d = \text{diameter of test ring (in.)}$$

$$w = \text{width of test specimen (in.)}$$

$$n = \text{number of revolutions per minute}$$

$$V = \text{rubbing velocity} = \pi \cdot d \cdot n / 12 \text{ (ft./min.)}$$

$$D = \text{test material wear depth (in.)}$$

$$Q = \text{test material wear volume (in.}^3\text{)}$$

$$T = \text{test length (hr.)}$$

$$W = \text{wear rate} = D/T \text{ (in./hr.)}$$

$$K = \text{wear factor} = \frac{in.^3}{lb \cdot (ft/min) \cdot hr}$$

The usual unit of measurement for the operating conditions of self-lubricated bearings is pressure-velocity (PV), i.e., the product of unit load times the rubbing velocity. Unit load is calculated by dividing the applied load by the area. The expression of area most common in LFW-1 testing is the actual area of the arc in contact with the test ring (0.16 in.² in the present case). This expression differs sharply from the conventional expression used in journal bearing tests, which is for the projected area, namely, the shaft diameter multiplied by the bearing length, even though in actuality only an arc about the size of the LFW-1 test block supports the load. Ordinarily PV values derived from LFW-1 tests are considerably greater than those derived from journal bearing tests on the same material. We have found that if the PV values for LFW-1 tests are calculated as test ring diameter (d) times the test block width (w), LFW-1 wear rates approximate those obtained with journal bearing tests. Therefore, PV values reported below have been calculated on the basis of the conventional projected area.

The wear depth (D) of the test material is the difference in the height of the test block before and after tests. Wear rate (W), then, is calculated by dividing D by the test length (T). An alternate method of comparing wear rates of different materials under different operating conditions is by the wear factor K. This value, which is used extensively throughout the self-lubricated bearing industry, is normally a constant over the mild wear regime of a particular material. It is defined as the volumetric wear of the test material divided by the applied load, the rubbing velocity, and the test length. The ranges of K (all as 10-10 in English units) are:

1 to 50	Good self-lubricated materials such as carbon-graphites and graphite-filled polyimides, PTFE, nylons and acetals.
51 to 500	Unfilled polyimides, nylons and acetals.
501 to 5000	Unfilled PTFE and phenolics.
> 5000	Bronze and babbitt.

Table VI gives the test parameters and wear rates of compression-molded material "A" tested under ambient conditions. It can be seen that the wear factor K is relatively constant over the regime of mild wear, and that the mild wear regime has been exceeded at 1,000 fpm and 131,000 PV. When the same data are put into graphic form (figure 5), K appears as the slope of the W vs. PV curve. The solid curve in figure 5 represents the average value of K, with the two dashed lines indicating the ± 3 standard deviations that would be used by design engineers. All plotted data easily fall within these limits. Although K is usually considered a constant, our tests show an apparent slight increase in K with increasing rubbing velocity.

A similar presentation of wear data for transfer-molded material "A" is given in table VII and figure 6. The average K of 15.9 for the transfer-molded material is within one standard deviation of the average K of 19.8 for the compression-molded material. The two dashed lines in figure 6 are the same ± 3 standard deviation limits for compression-molded material as appeared in the previous figure. Once again, the wear rate for the transfer-molded material falls well within these limits. In light of the wide scatter of data ordinarily encountered in wear testing, these data for material "A" exhibit quite reasonable agreement.

The wear data obtained with material "B" (table VIII) corroborate the results just shown for material "A," namely, that the wear characteristics of PMR-15 based materials is not changed significantly by the method of molding. Similarly, neither specimen orientation nor test temperatures up to 600°F had any significant effect on the wear rates.

Table IX is a composite of some data already presented plus new data for material "C" and additional high-temperature data. It further illustrates the consistently low wear rate of PMR-15 based materials, whether they be compression-molded or transfer-molded.

CONCLUSIONS

Starting from the premise that transfer molding is an economically viable process for producing small parts from PMR-15 polyimide, we set out to determine whether transfer molding yields results comparable to the more common compression molding. According to the criteria examined in this paper, namely, the flexural, compressive, and tribological properties of the molded pieces, it can be concluded that the two molding techniques give essentially equivalent results, certainly within the ranges of variation that would normally be employed by design engineers. The minor discrepancies that were encountered are differences familiar to plastics molders and fall into two general categories, viz.,

- 1) Orientation effects attributable to resin flow patterns within a particular shape of mold cavity, and
- 2) The degree of secondary finishing required after molding.

Because these minor differences are predictable, they can be anticipated and accounted for in engineering designs.

There are, of course, other important physical and chemical properties of PMR-15 polyimide that need to be confirmed before the case is closed on transfer-versus compression-molded PMR-15 polyimide. Our work is continuing along this line, with emphasis on the thermal properties and thermo-oxidative stability of the molded PMR-15 polyimide. Even though the focus of this report has been on small shapes and bearing-grade composites, there is no intent to imply that the efficacy of transfer molding is limited to this combination. In fact, our current development work is on the transfer molding of larger, structural-grade compositions, the results of which will be reported as they become available.

REFERENCES

1. Cavano, P. J.: Resin/Graphite Fiber Composites, NASA CR-134727, 1974.
2. Lauver, R. W.: Kinetics of Imidization and Crosslinking in PMR-Polyimide Resin, NASA TM-78844, 1977.
3. Serafini, T. T., Delvigs, P., and Aiston, W. B.: PMR Polyimides - Review and Update, NASA TM-82821/AVRADCOM TR 82-C-3, 1982.
4. Serafini, T. T.: PMR Polyimide Composites for Aerospace Applications, NASA TM-83047, 1982.

TABLE I

COMPOSITION OF MATERIALS TESTED

Material	Composition, % by wt.			
	PMR-15	Graphite Powder	Milled Carbon Fiber	Calcined Carbon
N	100	0	0	0
A	56	11	33	0
B	60	10	15	15
C	63	37	0	0

TABLE II
COMPRESSION-MOLDED PMR-15 POLYIMIDE-BASED MATERIALS
(Specimens Machined from Flat Plates)

Material	No. of Sets Tested*	Flexural Strength psi at 73°F	% Standard Deviation	
			Within Sets	Among Sets
N	10	18,200	8.1	14.6
A	9	13,600	6.7	3.8
B	1	11,700	2.5	-
C	7	14,500	4.8	8.6

* 5 specimens per set

TABLE III
EFFECT OF MOLDING MODE ON FLEXURAL STRENGTH OF MATERIAL "A"

Molding	Stock	Specimen Orientation	Flexural Strength psi at 73°F	% Standard Deviation	
				Within Sets	Among Sets
Compression	Plate	⊥ (horizontal)	13,600	6.7	3.8
Transfer	Bar	⊥ (lengthwise)	17,800	4.8	4.2
Transfer	Cylinder	(vertical)	12,700	8.6	2.6

TABLE IV
COMPRESSIVE STRENGTH OF PMR-15 POLYIMIDE-BASED MATERIALS

Material	Compressive Strength, psi at 73°F			
	Compression-molded Plate		Transfer-molded Cylinder	
	Horizontal	Vertical	Horizontal	Vertical
N	24,300	27,100	-	-
A	26,200	29,900	27,700	26,800
B	30,600	-	30,600	30,300
C	27,300	-	-	-

TABLE V

COMPRESSIVE STRENGTH OF MATERIAL "A" ACCORDING TO METHOD OF MOLDING

Molding	Stock	Orientation	Compression, psi, at 73°F		No. of Tests
			Strength	% Std. Dev.	
Compression	Plate	⊥ (horiz.)	26,200	2.5	20
		(vertical)	29,900	1.9	5
Transfer	Bar	⊥ (width)	28,500	2.2	15
		(length)	27,800	2.3	21
Transfer	Cylinder	⊥ (horiz.)	27,700	2.8	8
		(vertical)	26,800	3.6	13

TABLE VI

WEAR RATE OF COMPRESSION MOLDED MATERIAL "A" AT VARIOUS PV LEVELS

Rubbing Velocity ft/min	PV 1b in ² x ft min	Wear Rate in/hr	Wear Factor	Number Of Tests
			in ³ 1b · ft/min · hr	
26	9,100	3.7 x 10 ⁻⁵	18.9 x 10 ⁻¹⁰	1
	18,200	6.9	17.8	1
	36,300	11.9	15.3	1
	45,400	14.5	14.9	1
71	24,800	13.7	25.8	7
	49,600	21.3	20.0	7
	74,400	27.8	17.5	8
	99,100	32.2	15.2	7
	123,900	46.2	17.4	4
1000	43,600	25.5	26.2	2
	87,200	54.9	29.4	2
	131,000	197.3	70.5*	1
	174,000	427.4	114.6	2

* These values not included in average

$$\text{AVERAGE WEAR FACTOR} = 19.8 \times 10^{-10}$$

$$\text{STANDARD DEVIATION} = 5.0 \times 10^{-10}$$

NOTE: Calculations have been made to give values corresponding to typical journal bearing tests results (see text, p. 5 above). Multiply PV by 2.15 to obtain values in usual LFW-1 format.

TABLE VII
WEAR RATE OF TRANSFER MOLDED
MATERIAL "A" AT VARIOUS PV LEVELS

Rubbing Velocity ft/min	PV lb/in ² x ft/min	Wear Rate in/hr	Wear Factor in ³ lb · ft/min · hr	Number Of Tests
71	24,800	14.4 x 10 ⁻⁵	27.2 x 10 ⁻¹⁰	4
	49,600	13.9	13.1	2
	74,400	18.4	11.6	2
	123,900	30.7	11.6	2

AVERAGE WEAR FACTOR = 15.9

NOTE: Calculations per method for journal bearing tests.
PV x 2.15 gives usual LFW-1 format.

TABLE VIII
WEAR FACTOR FOR MATERIAL "B"
FOR VARIOUS MOLDING METHODS

Molding Method	Orientation To Molding Direction	PV	K x 10 ⁻¹⁰	
			Amb.	600°F
Compression	Perpendicular	24,800	17.2	19.0
		49,600	11.6	N/T
Transfer	Perpendicular	24,800	21.8	N/T
		49,600	12.5	N/T
Transfer	Parallel	24,800	17.8	17.0
		49,600	10.6	N/T

N/T - Not Tested

NOTE: Calculations per method for journal bearing tests.
PV x 2.15 gives usual LFW-1 format.

TABLE IX
EFFECT OF COMPOSITION ON WEAR FACTOR

Material	Molding Method	PV	K x 10 ⁻¹⁰		
			Amb.	500°F	600°F
A	Transfer	24,800	27.2	33.0	34.3
		49,600	13.1	N/T	N/T
		74,400	11.6	9.0	N/T
		123,900	11.6	21.1	N/T
B	Compression	24,800	17.2	N/T	19.0
		49,600	11.6	N/T	N/T
	Transfer	24,800	17.8	N/T	17.0
		49,600	10.6	N/T	N/T
C	Compression	24,800	16.8	N/T	13.6
		49,600	9.6	N/T	N/T

N/T - Not Tested

NOTE: Calculations per method for journal bearing tests.

PV x 2.15 gives usual LFW-1 format.

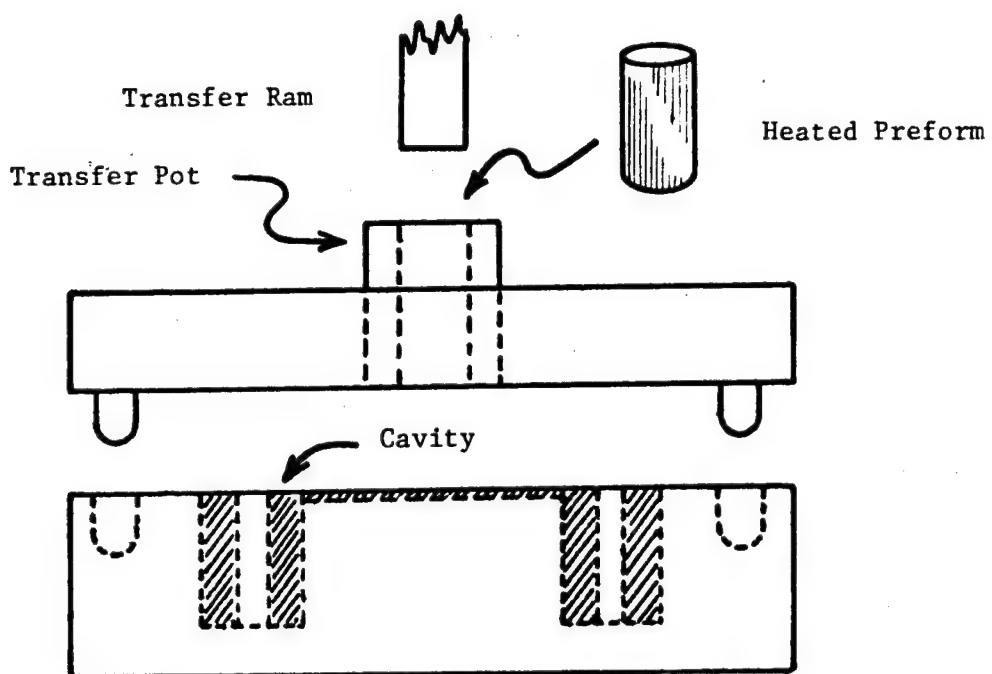


Figure 1. Simplified schematic of a typical transfer mold.

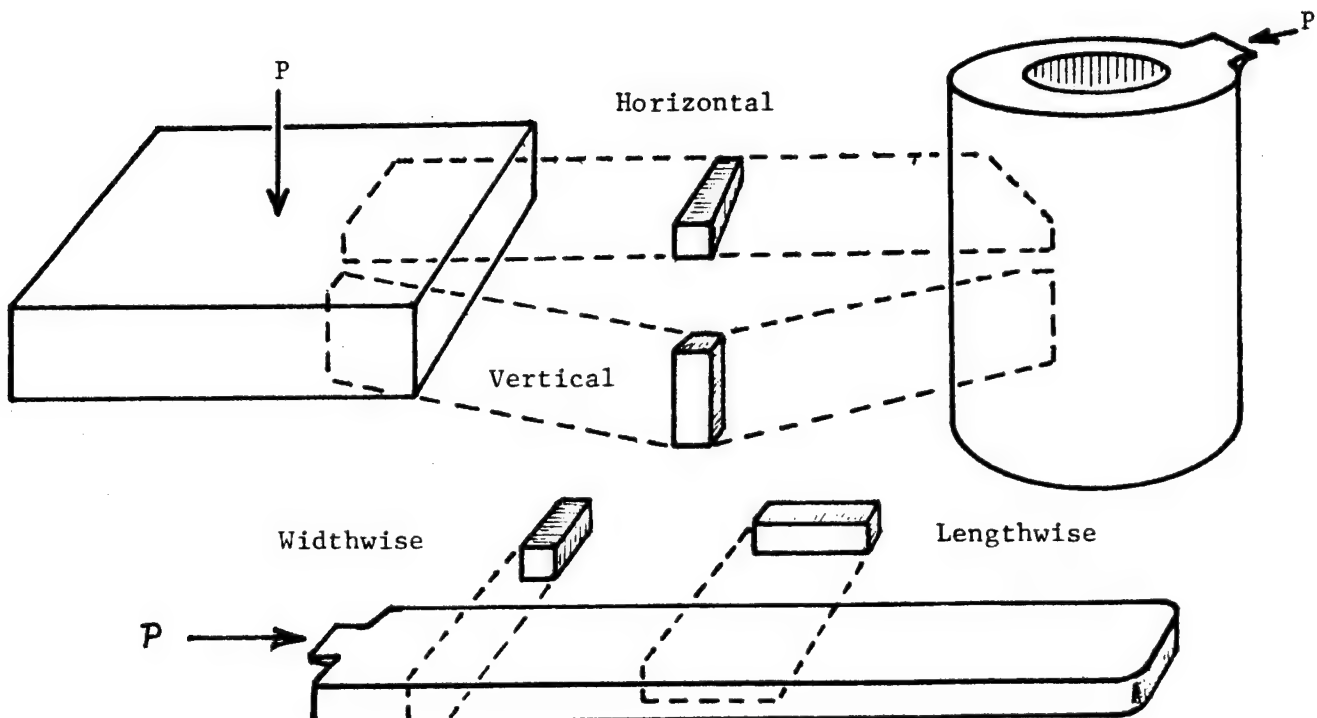


Figure 2. The three basic kinds of molded pieces from which test specimens were taken. "P" indicates the direction of applied pressure (compression molding) or the point of resin injection (transfer molding).

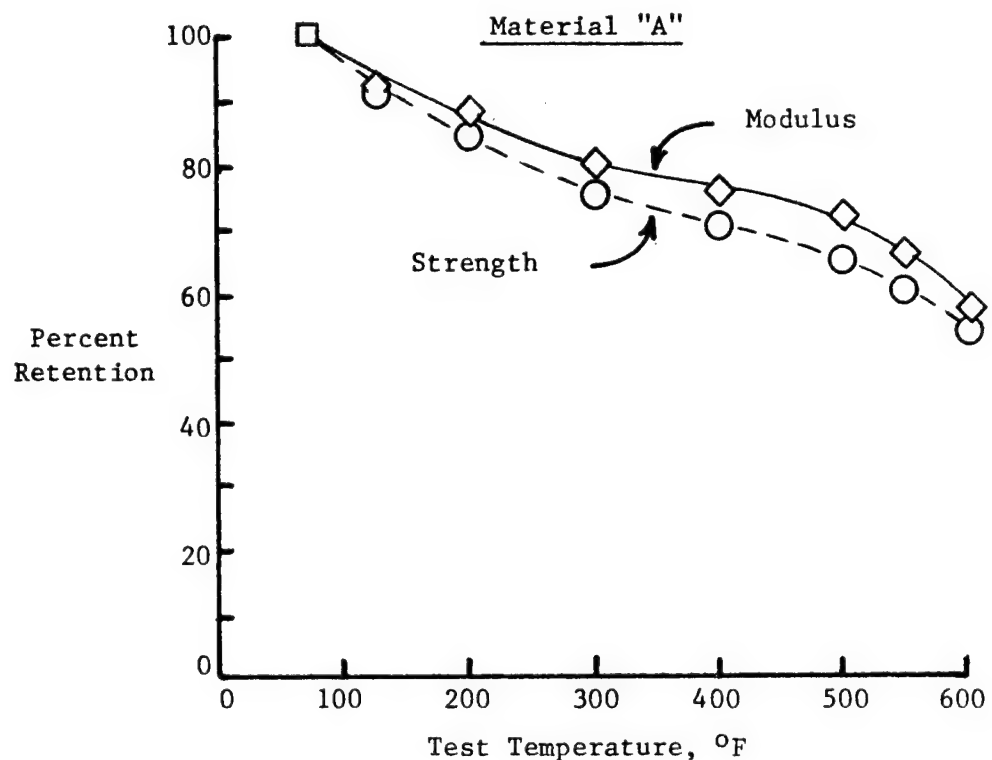


Figure 3. Effect of test temperature on the flexural properties of transfer-molded test bars of material "A".

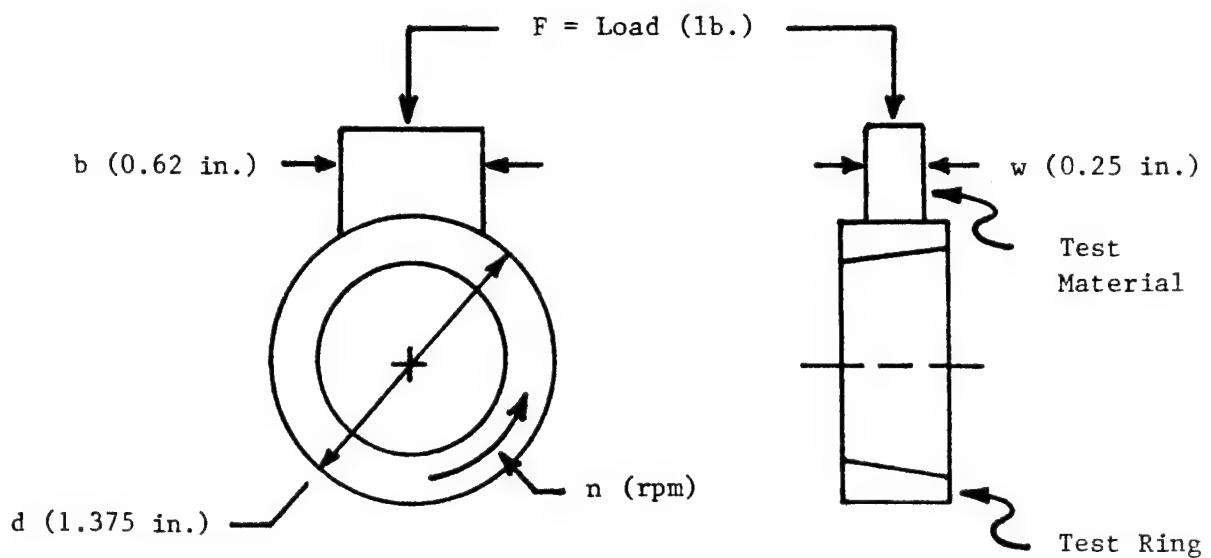


Figure 4. Ring and conforming block in the LFW-1 wear test.

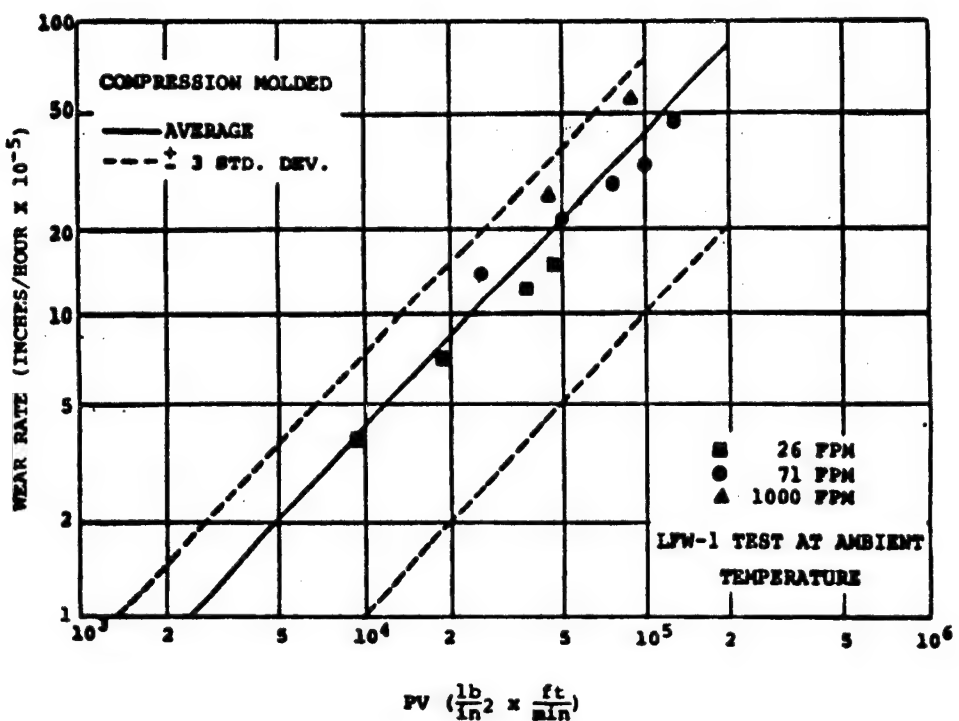


Figure 5. Wear of compression-molded material "A".

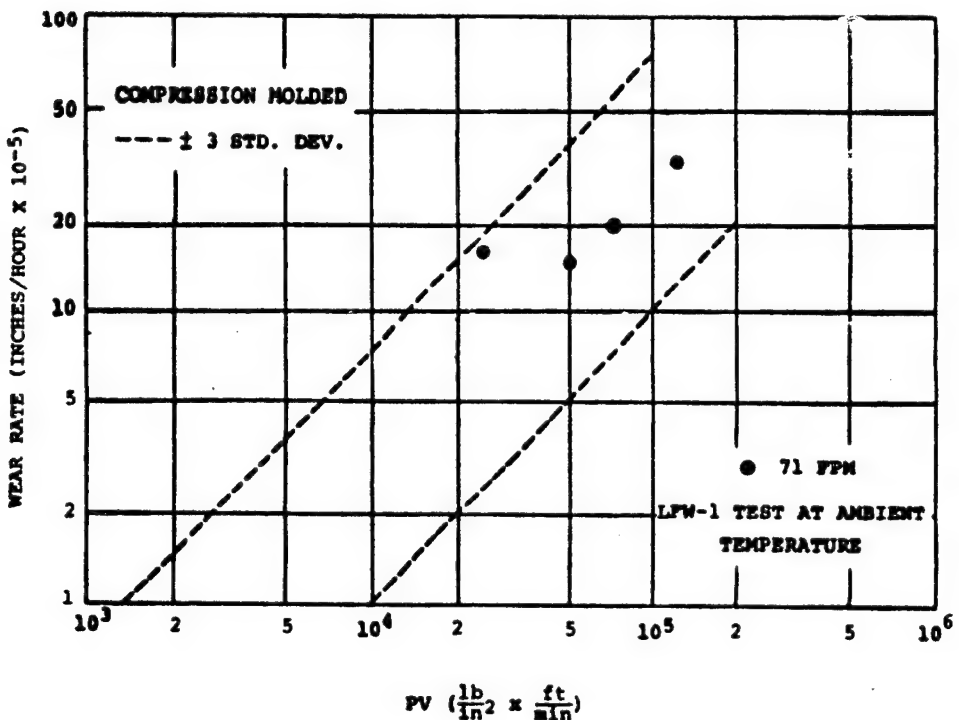


Figure 6. Wear of transfer-molded material "A".

APPLICATION OF GR/PMR-15 TO COMMERCIAL AIRCRAFT

PROPELLION INSTALLATION STRUCTURES

J. Postlewaite, K. Porter, and D. McLaren
Boeing Commercial Airplane Company

Following from early experience with polyimides on the SST program and Shuttle aft flap studies The Boeing Company is now working on collaborative programs with its principal nacelle suppliers to pursue the development of Gr/PMR-15 nacelle components.

Two programs are currently in effect. The first program is directed specifically towards the flight test and service evaluation at the earliest possible date of a 747 nacelle core cowl structure. The second program seeks to firmly establish the producibility and cost of a 757 thrust reverser "C" duct in a production environment.

The near term objectives of these programs include (a) the comparison of estimated cost and weight of Gr/PMR-15 versus metal structure, (b) the engine test of representative composite structure, (c) the preliminary design and analysis of the "C" duct structure, and (d) the preparation of cost data and time schedules for the development and producibility program.

In addition to powerplant structure, the propulsion ducting system has shown to be a strong candidate for Gr/PMR-15 application. Currently, the Boeing 747 Organization is evaluating the use of PMR-15 matrix composites to replace nearly 800 lb of titanium ducting per airplane.

BACKGROUND

For some years The Boeing Company has recognized the significance of polyimide high temperative resins for use in commercial aircraft. Early stimulus for applications research was given by the SST program in the late 1960's. Problems with the condensation type resins available at that time prevented full adoption of the composite structure concepts.

The Boeing Commercial Airplane Company, building on the background gained from participation in the NASA composites for Advanced Space Transportation Systems (CASTS), by the Boeing Aerospace Company has extended PMR-15 technology to commercial airplane propulsion structures (fig. 1). In 1980, a program was initiated to identify Gr/PMR-15 characteristic behaviors, including degradation trends and failure modes due to long term exposure to temperatures up to 550 °F. The result of that program coupled with favorable weight trade data compiled for use of composites on the powerplant installation of the next Boeing aircraft encouraged the search for methods to acquire data on which to base product design. It was decided to seek out cooperative programs with principal nacelle suppliers to further the development of Gr/PMR-15 technology for commercial structures (figs. 2 and 3).

COOPERATIVE PROGRAM

The major program currently in work is the design, analysis, fabrication, and test of the Thrust Reverser Fixed Structure "C" duct of the 757 aircraft powerplant installation (fig. 4). This structure has similarities in function to the NASA QCSEE PMR-15 inner cowl, but is quite dissimilar in size and operational requirements (fig. 5).

The functional requirements of this structure include thermal management of the engine core compartment, acoustic attenuation of fan duct airflow noise, carriage of normal operational and emergency loads without excessive deflection at all operational conditions, prevention of fire propagation from the core compartment into the fan duct; and accommodation of incidental damage and thermal transients throughout the 50 000 cycle required lifetime without compromising the functional capability of the structure.

This cooperative program focuses the resources of each partner into three tasks: Design and Analysis, Testing, and Specifications and Manufacturing. Each of these tasks addresses major parts of the overall program.

The generalized schedule indicates the ambitious nature of this program, with the following major milestones.

Producibility Assessment	- 2nd Quarter 1983
Design Complete	- 1st Quarter 1984
Fabrication Complete	- 2nd Quarter 1984
Structural Testing	- 1st Quarter 1985

MAJOR CONCERNS

This program has proceeded well into the design and analysis, testing, and producibility phases and has exposed some major concern areas.

Included among these are:

(1) Long term thermal exposure durability requirements of the "C" duct. These appear to necessitate use of weavable Pi sized fiber. However, the variable quality of currently available product is producing a downward bias in design data currently being generated.

(2) Current methods of obtaining high temperature design data provide results which are subject to excessive variability, and are obtained at high cost.

(3) Tooling techniques for building such a large, complex structure are presently unproven.

Efforts to alleviate these concerns are now underway among the participants in this program, with encouraging results being obtained.

TITANIUM DUCTING ALTERNATIVES

The 747 Engine Start and Thermal Anti-Icing Duct system has been identified as a very promising application for high temperature composites (fig. 6).

The current system, composed of titanium duct work, ranges from 2 to 7 in in diameter, and weighs upwards of 800 lb. Individual ductwork sections range from simple, 8 ft long pieces, to highly complex branched sections with varying diameters (figs. 7 and 8). All sections require end couplings and many sections have one or more bossed takeoffs (fig. 9).

The general design and objectives requirements of the composite system are as listed below.

- 50 psi maximum pressure
- 450° maximum temperature
- 50 ft/s maximum air flow
- 50 000 hr service life
- accommodate normal handling and service damage
- be repairable.

Due to the very long service life requirement in the 350 to 450 °F temperature range, PMR-15 matrix composites are considered to be prime candidates for this application. However, the considerations of material properties and manufacturing cost will provide a strong influence on the final choice of material.

At present, this project is in the early stages of feasibility assessment. One approach being considered is developing the manufacturing base concurrently with the investigation of the long term characteristics of the candidate materials operating in the duct system environment. Another important aspect of this application is that having demonstrated proper function, weight savings, and cost effective manufacture, composite ducting would be implemented immediately on new 747 aircraft, and on selected 747's on a refit basis. Similar applications exist on the 757 and 767 aircraft models as well.

CONCLUSION

In conclusion, Boeing Commercial Airplane Company is making considerable forward strides in the application of PMR-15 technology to commercial aircraft. This progress is a direct result of highly productive cooperative development programs with principal suppliers. With the current state of the commercial aircraft industry, the enthusiasm and commitment that these cooperative program members have shown must be applauded. Even as the program meets the challenges of developing a new material for propulsion systems, additional applications such as the 747 ducting have come forward, raising the possibility for further cooperative composite development programs.

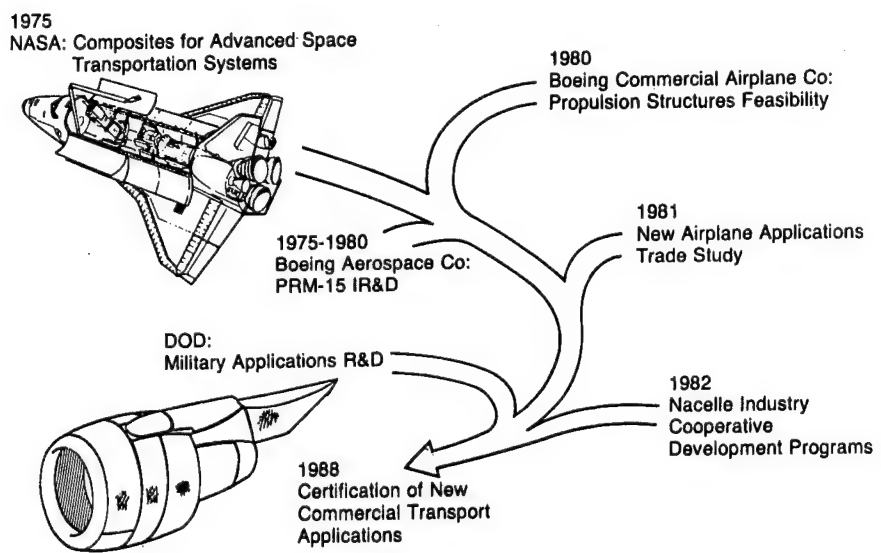


Figure 1. - Development of PMR-15 for commercial applications.

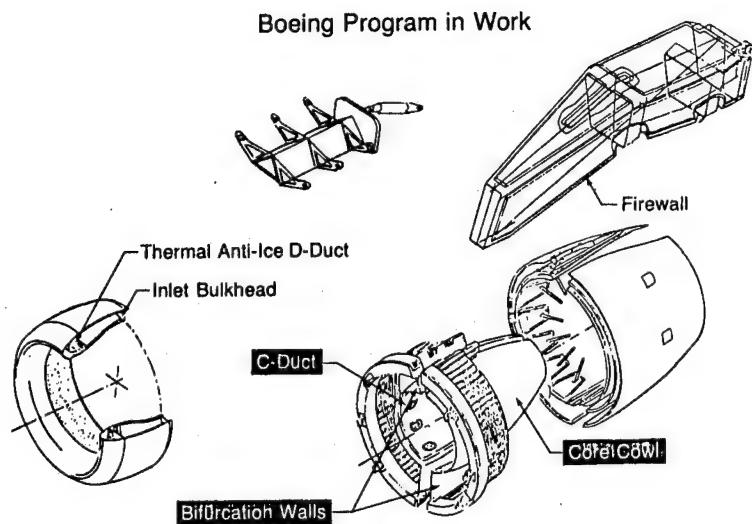


Figure 2. - PMR-15 candidate components.

<u>ITEM</u>	<u>WEIGHT (lb)</u>
Inlet bulkhead	60
Thrust reverser fixed structure	250
Core cowling	50
Ducting	50
Firewalls	30
PMR-15 composites weight	440 lb/nacelle or 880 lb/airplane
Weight savings	220 lb/airplane

Figure 3. - Weight estimate - propulsion installation
PMR-15 composite usage.

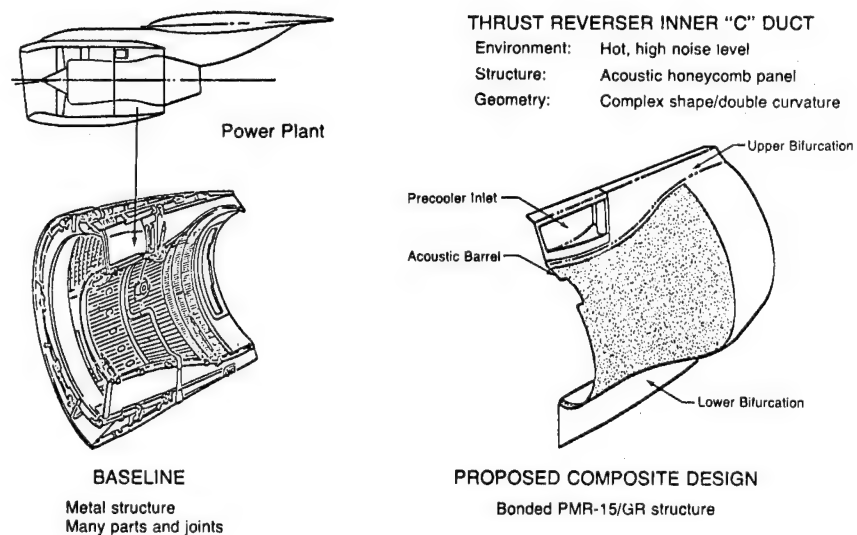


Figure 4. - Schematic of Thrust Reverser Fixed Structure "C" duct of 757 aircraft.

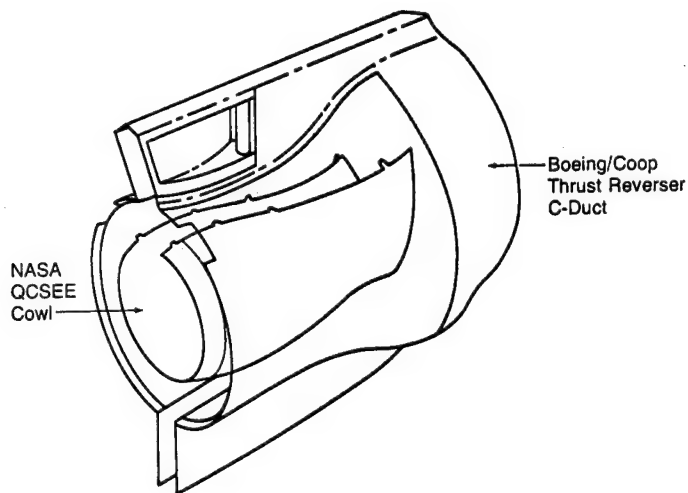


Figure 5. - Size comparison versus QCSEE inner duct.

747 Transport With Graphite/PMR-15 Ducting

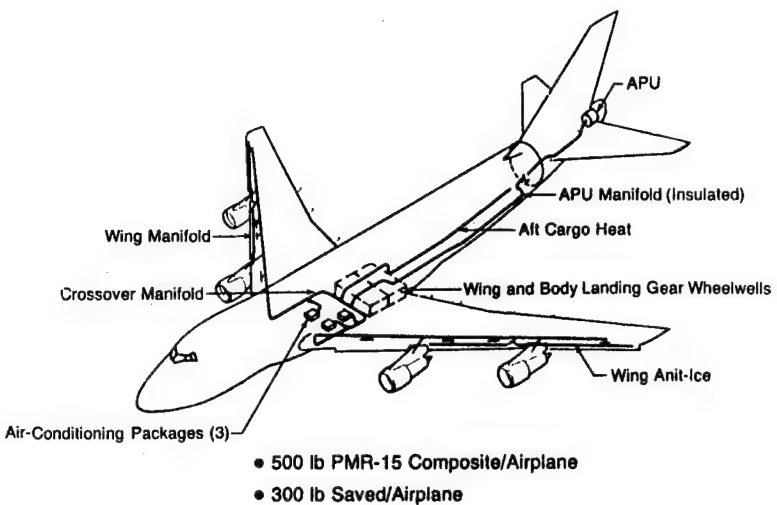


Figure 6. - Potential near term applications of PMR-15.

Straight Duct Section

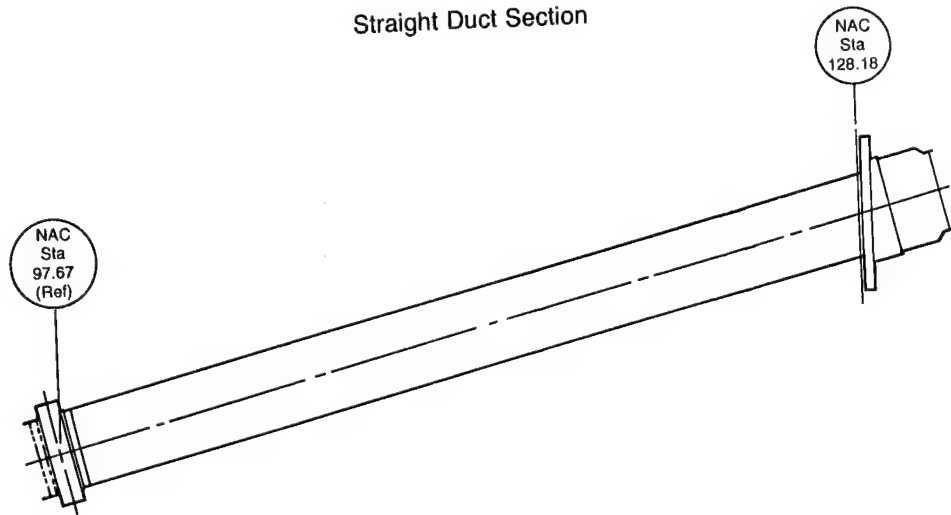


Figure 7. - 747 pneumatic duct.

Branched Duct Section

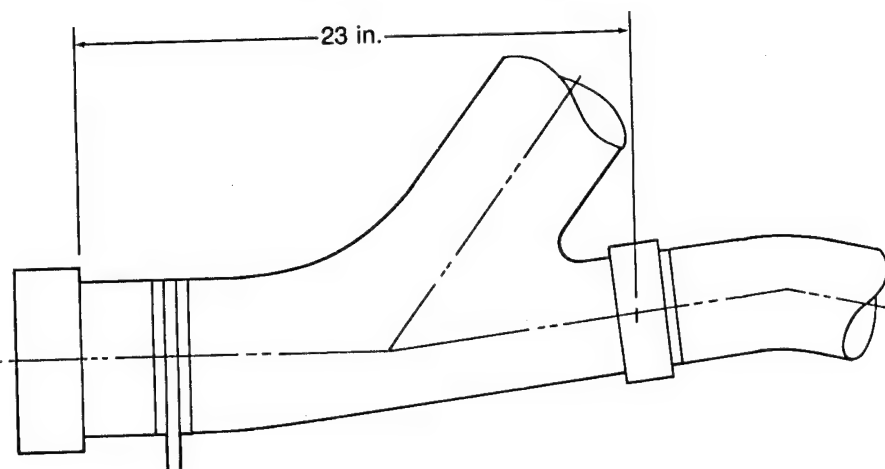


Figure 8. - 747 pneumatic duct.

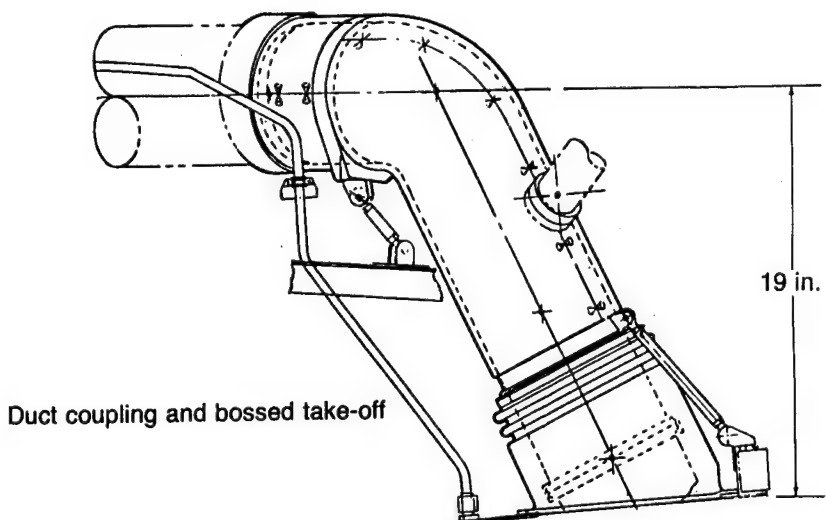


Figure 9. - 747 pneumatic duct.

FABRICATION PROCESS OF A HIGH TEMPERATURE POLYMER MATRIX ENGINE DUCT

R. D. Pratt and A. J. Wilson
General Electric Company
Aircraft Engine Business Group

The purpose of this paper is to discuss the process that was used in the molding of an advanced composite outer by-pass duct planned for the F404 engine. This duct was developed as a potential replacement for the existing titanium duct in order to reduce both the weight and cost of the duct. The work was performed under Contract NAS3-21854 and was funded by both NASA and the Navy.

The composite duct is now completing its development phase and is going into the manufacturing technology portion of the program under Navy ManTech sponsorship. The duct is fabricated using graphite cloth impregnated with the PMR15 matrix system developed by NASA/Lewis.

The General Electric Company has applied advanced polymeric composite materials in a variety of development jet engine components for the past decade. Among these components are fan blades, stator vanes, fan frames, fan ducting, cowlings, and shrouds. The matrix resins for composite parts with a service temperature up to 149°C (300°F), are mostly epoxies. For service temperatures of 149°C (300°F) to 316°C (600°F) several polyimide type systems have been explored. PMR15 polyimide resin, developed by NASA/Lewis Research Center, emerged as the matrix system selected by General Electric for the F404 composite outer duct. PMR15 offers several advantages over other polyimide systems that were tried in earlier projects. They are:

- 1) Uniform, high quality material, at competitive costs is available from several prepreg sources
- 2) Consistent low void processability in a variety of configurations has been demonstrated
- 3) The system has excellent physical and mechanical properties even after exposure to severe engine mission cycle environments
- 4) Adequate thermal stability.

The concept for making the duct was to vacuum bag-autoclave mold a cylindrical laminate shell of Graphite/PMR15 (Gr/PMR) on the outside of a steel mandrel mold. The mandrel mold allows for ease of laying-up the Gr/PMR prepreg and provides an as-molded surface on the airflow side of the finished part. The laminate would incorporate various changes in thickness and material orientation as required for strength, stiffness and configuration.

Sometime after molding, the duct shells would be cut into upper and lower half cylinders, titanium end flanges riveted into place, axial composite side doublers added, and all other fittings added to complete the duct. The composite portion of the duct would weigh approximately 13.6 kg (30 pounds) at assembly. The slightly tapered cylindrical duct is approximately 76 cm (30 inches) in diameter X 102 cm (40 inches) in length. From a design standpoint, the composite duct is required to be fully interchangeable with the titanium duct it replaces. (see Figure 1).

Producibility was perhaps the prime consideration in the selection of graphite fabric impregnated with PMR15 as the prepreg form of the Gr/PMR material for fabricating the F404 composite duct. Fabric could be cut into large easily handled laminae patterns and readily laid-up on the mold tool. (see Figure 2).

T-300 graphite fiber, produced by Union Carbide, woven into a 24 x 23-8 harness satin fabric was selected as the reinforcement for the duct. This selection was made in part because of the processing experience and a data base GE gained in designing and fabricating the Gr/PMR core cowling of the Quiet Clean Short-Haul Experimental Engines (QCSEE) GE built for NASA/Lewis. T-300 and PMR15 as a composite was shown to have adequate thermal stability as well as the strength and modulus of elasticity required for weight efficient duct design.

Allowance for thermal growth of the mold steel and the shrinkage of the Gr/PMR laminate material was provided for in fabricating an oversize (diameter) mold tool. Annular Gr/PMR test pieces were molded and then measured precisely to establish the final sizing of the mold. The mold tool was made with an axial spindle supported at each end with frames mounted to an all steel cart. This allowed for a convenient working height, rotating the mold during the lay-up, and mobility to and from the autoclave. (see Figure 3).

An assembly fixture was designed and built for positioning the end flanges to the composite duct shell. This fixture allows for match drilling the holes for rivets used in assembling the titanium end flanges to the duct body. A drill fixture for the axial split line doublers was also made.

The Gr/PMR materials was received in rolls as uncured prepreg with a colored polyethylene separator film on one side. The PMR15 contains a certain amount of free methanol, as received, which gives the material tack and drape in the prepreg form. In preparing the prepreg laminae for the duct, a second ply of polyethylene separator film of another color was applied to the exposed side of the material as it was unrolled for cutting. The Gr/PMR, now having polyethylene on both sides, could be cut into laminae patterns and handled without losing its tack and drape from evaporation of the methanol. The different color polyethylene film sides provided an easy means for retaining identity of the symmetrical laminae patterns with off-axis orientations. Laminae kits were then prepared for the duct lay-up, according to the engineering design.

Teflon mold release was applied to the mold tool prior to applying the first ply of laminae. It was necessary to add additional methanol to the mold side of this first ply after the polyethylene separator film was removed, so that the material would have sufficient tack to adhere to the mold surface during the preforming operation.

The Gr/PMR material, as received, can be debulked to about 406 to 432 microns (16 to 17 mils) prior to molding. Debulking is necessary to eliminate the potential for wrinkling the material during auto-clave molding.

After the final ply was layed-up a spiral wrap of heat shrinkable Dacron fabric tape, known as Ceconite, was then applied and shrunk tightly into place. The Ceconite fabric was used over the preform to permit venting of the volatiles produced when the preform was imidized. The preform was imidized in an air circulating oven according to the following schedule:

- o Room temperature to 77°C at 1/2°C/min
- o Hold 77°C for 60 minutes
- o Raise to 135°C at 1/2°C/min
- o Remove immediately from the oven to room temperature.

This schedule does not complete the imidization of the PMR15 system.

After imidization to 135°C, the preform was stripped of the Ceconite and release fabric and then recovered with porous release fabric and two plies of knit-fiberglass cloth breather. Four-inch wide strips of heavy tooling glass cloth were added parallel to the axis of the tool and overlapped two inches with each adjacent piece. The assembly was held tightly to the preform with a spiral wrap of glass cloth tape. A steel sash chain was wrapped into the glass cloth at each end of the preform to act as a 'header' for the venting of the vacuum bag to be applied. Kapton H film from DuPont was used as the vacuum bag. The bag was sealed with a high temperature sealant and checked for leaks by pulling a vacuum. The assembly was double bagged for insurance against loss in the autoclave with another ply of Kapton H. It was separated from the inner bag with a ply of style 1581 glass cloth breather and then checked for leaks with vacuum.

The entire assembly was moved into the autoclave and rechecked for leaks in the vacuum bags using the vacuum system in the autoclave. The assembly was autoclave molded according to the following schedule:

- o apply 13 kPa of vacuum
- o raise temperature to 204°C at 3.5°C/min
- o hold 204°C for 15 minutes, then apply full vacuum
- o raise temperature to 238°C at 2/3°C/min then apply 1277 kPa autoclave pressure and continue 1277 kPa and full vacuum throughout
- o raise temperature to 252°C in 30 minutes
- o hold 252°C for 30 minutes
- o raise temperature to 307°C at 1°C/min
- o hold 307°C/1277 kPa and full vacuum for 180 minutes

- o release the vacuum and pressure slowly (to prevent buckling) before lowering temperature
- o cycle complete - post cure later

The duct shells were easily removed from the mandrel tool after debagging. After a thorough visual inspection the duct shells were inspected by ultrasonic thru transmission with a 'C' scan readout. The 'C' scan indicates apparent defects as varying shades of grey on electro sensitive record paper. The grey scale is proportional to the attenuation of the ultrasonic signal and can be adjusted so as to show the extent of the laminates void content in the range level chosen. The design called for a maximum allowable void content of three (3) percent. The 'C' scan grey scale was adjusted to show a near black readout for this level of voids. The duct shells used were proven to contain less than three percent voids and no delaminations. A more thorough ultrasonic survey was also made by measuring the actual attenuation of the ultrasonic signal at grid locations marked on the ducts. Precise void content values were calculated and recorded for these locations. (see Figure 4).

The extensive hardware to be attached to the ducts at engine assembly required adding embossments to the duct shell in order to have spatial location identical to that on the titanium ducting to be replaced. These embossments along with areas requiring added stiffness or strength and the axial split line doublers, all made of Gr/PMR15, were then laid up on the duct shells. They were molded and bonded into position in several vacuum bag-autoclave cycles. These secondary laminations were not oven imidized separate from the autoclave as were the duct shells as it was necessary to hold the position of the various laminae for embossments, stiffeners and doublers with a vacuum bag. The operations used to add these secondary laminations were:

- o Mark the position of the buildup areas on the duct shell from precise mylar overlays
- o Prepare the surface for bonding using a chlorothene solvent wipe before and after a light grit blast
- o Prepare the prepreg kits for the buildups
- o Apply one ply of Style 120 glass cloth/PMR15 to the area (50% resin PBW). This material serves as an adhesive
- o Apply the buildup plies to the duct shell and dampen them with methanol, if required, to 'tack' them into position
- o Apply Teflon release fabric over the laminae
- o Apply glass fabric bleader and breather
- o Double envelope bag with Kapton film.

The secondary laminations were autoclave molded as follows:

- o Apply 13.6 kPa of vacuum

- o Raise temperature to 71°C at 0.83°C/min
- o Hold 71°C for 60 minutes
- o Raise temperature to 116°C at 0.42°C/min
- o Apply full vacuum
- o Raise temperature to 249°C @ 1.2°C/min
- o Apply 1277 kPa autoclave pressure
- o Hold 249°C for 30 minutes
- o Raise Temperature to 307°C at 1.2°C/min
- o Hold 307°C with full vacuum and 1277 kPa pressure for 180 minutes.

With all the secondary laminations completed, the duct was ready for machining and assembly to the end flanges. The sequence of events were:

- o Trim the duct and the axial doublers to dimension
- o Match drill the axial doublers with the duct shell for the bolting
- o Cut the duct shell into upper and lower halves
- o Using the assembly fixture, match drill and rivet the titanium end flanges to the duct shell
- o Complete all other machining of the embossments and mounting areas for the hardware assembly
- o Final ultrasonic inspection
- o Seal coat with Skybond 703 polyimide resin
- o Assemble and bond inserts
- o Post cure
- o Install studs
- o Part marking
- o Final inspection

The composite duct subjected to static load testing, exceeded requirements. The composite duct installed on a factory engine is still in test and performing well. The manufacturing technology portion of the program is now underway to ready the composite duct for production.

GE F404 Composite Duct Program

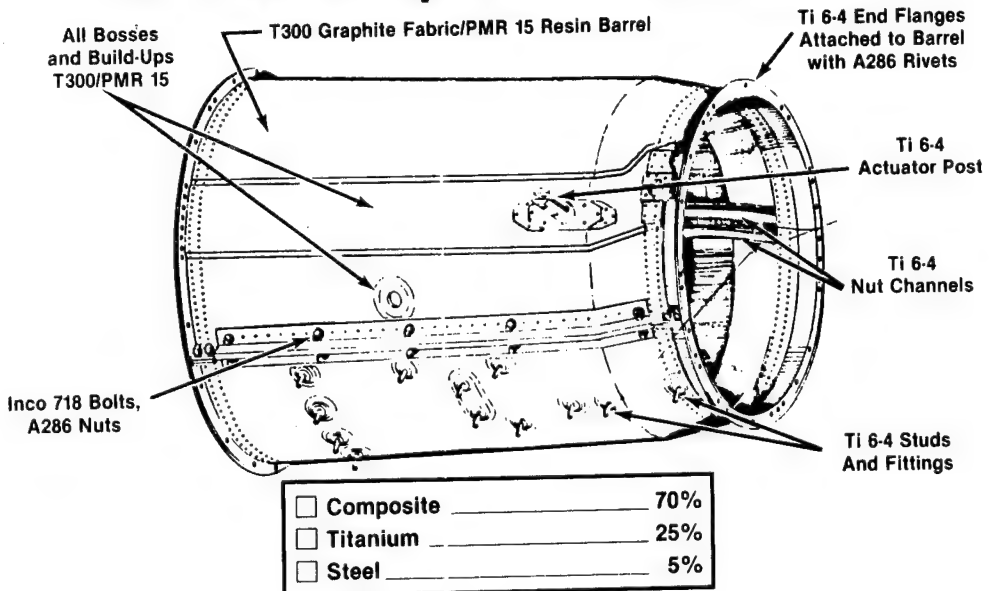


Figure 1

F404 Composite Duct Ply Arrangement

Ply	ΔA	Warp To Axis Δ
1	36°	0°
2	51°	-45°
3	24°	0°
4	39°	+45°
5	54°	-45°
6	42°	+45°
7	30°	-45°
8	45°	+45°
9	60°	0°
10	33°	-45°
11	48°	0°

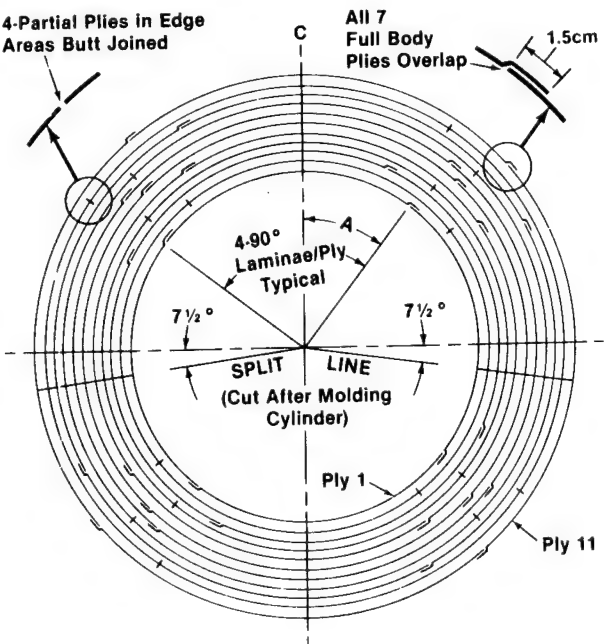


Figure 2

F404 Composite Duct Mold

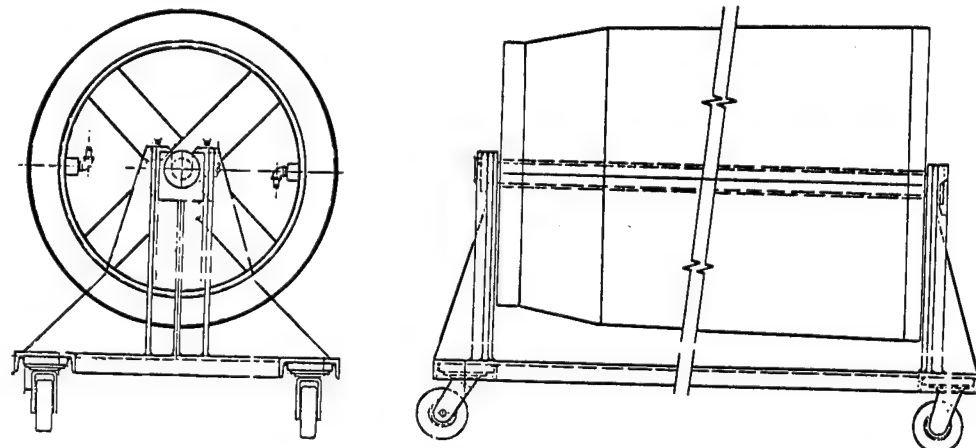


Figure 3

F404 Duct S/N 80003

Void Content Determined from the Attenuation of the Thru Transmission Ultrasonics

Degrees are CCW from Aft end

Dist. from Aft End	Top C 0°	60°	100° Ply Build Up	120°	153°	Bot C 180°	240°	260° Ply Build Up	300°
5cm	1.5%	1.5%	1.5%	1.5%		1.5%	1.5%	1.5%	1.5%
25cm	1.5%	1.5%	1.5%	2.5%		2.0%	1.5%	1.5%	1.5%
46cm	1.5%	1.5%	1.5%	3.0%		2.5%	1.5%	1.5%	1.5%
66cm	1.5%	1.5%	1.5%	2.0%	3.5%	3.5%	2.0%	1.5%	1.5%
86cm	1.5%	1.5%	1.5%	2.0%	5.0%	4.0%	2.0%	1.5%	1.5%
104cm	1.5%	1.5%	1.5%	1.5%		1.5%	1.5%	1.5%	1.5%

Figure 4

CURRENT AND FUTURE ENGINE APPLICATIONS OF Gr/PI COMPOSITES

P. J. Cavano and T. E. Schmid
Pratt & Whitney Aircraft
Government Products Division

The application of organic matrix composites to gas turbine engine components has been the subject of numerous Government and company funded programs since the 1960's.

The possibility of significant weight reductions, performance improvements and lower component costs have made the organic matrix composites extremely attractive to aircraft engine designers. But very little of this potential has been incorporated into production engines over the years even though a significant number of components have been designed, fabricated and tested. Some of the reasons behind the slow rate of incorporation include the following:

- A. Criticality - Since the engines are responsible for providing the power to achieve and maintain flight, the engine components must be designed and fabricated with materials that are extremely reliable. Composite materials have suffered from lack of cost effective, reliable non-destructive inspection methods for determining the integrity of small, complex shaped parts. To compensate for the inspection uncertainties, larger safety margins are often employed which result in reduced benefits.
- B. Temperatures - Gas turbine engine components generally operate at higher temperatures than the airframe components.

The thermal environment of a typical military gas turbine engine (Figure 1) is such that only parts near the front of the engine and on the outside of the engine operate at sufficiently low temperatures to be considered for organic matrix composites.

The development of the polyimide matrix materials, such as PMR-15, has significantly expanded the potential number component applications because of the 550 to 600°F capability of this material.

- C. Small component size - Most of the low temperature engine components are small in size and have extremely tight dimensional tolerances. As a result the fabrication methods must often employ compression molding which can have high tooling costs.

This is especially important during the development phase of an engine when designs may change rapidly. The small component sizes also make it very difficult to achieve the desired ply patterns in the thin sections and at attachment locations. This leads to design compromise in weight and cost.

- D. Small production volumes - The world market for gas turbine engines is not very large and as a result the economies of large scale production are rarely achieved. The turbine engine industry capital investment in metal working equipment represents a momentum that is difficult to overcome. Retooling for composite materials fabrication represents a major long-term investment that has been difficult to rationalize.
- E. Interfacing with metal components - Composite materials operate most efficiently in simple uniaxial or biaxial stress fields. At attachment locations the high stress concentrations are not easily accommodated which complicates the composite design and increases the cost. The other attachment problem that must often be overcome is the mismatch in coefficients of thermal expansion between composite materials and metals. The special metal part designs to accommodate the composite material properties often results in high costs and hence a reduction in the benefits which could result from the use of composite materials.

DISCUSSION

The weight advantage that can be obtained with the graphite/polyimide (Gr/PI) composites is a direct result of the high specific strength (strength/density) (Figure 2) and high specific modulus. While it would appear that weight reductions of 50% or more are obtainable over titanium alloy components, in practice because of the larger safety margins used and more complex and heavier attachment areas, the composite component weight savings is typically only 10 to 25%. These savings can be quite significant if the components are large as is the case with the high bypass ratio turbofan engines (Figure 3). Since these engines are best suited to low mach number operation on transport and bomber type aircraft, the inlet temperature are low enough (< 2500°F) for epoxy matrix composites to be used for the fan outer ducts. The inner ducts and cowlings operate at higher temperature because they are closer to the turbomachinery. These are a prime candidate for polyimide matrix materials such as PMR-15.

In the low bypass ratio augmented turbofan engines (Figure 4) that are best suited to fighter aircraft very few of the components operate at temperatures low enough for epoxy matrix composites. The number of components which are suited to the application of polyimide composites is quite significant, however. Using a maximum sustained operating temperature capability of 600°F with short term excursions to 650°F for the PMR-15 polyimide matrix material, the applications shown in Figure 4 have been defined.

Under a Navy sponsored program, both TRW and CHI fabricated (during the 1975-1977 time period) external engine components for evaluation on the F100 engine. The resin matrices used included NR-150B2, PMR-15 and Rhodia's K601 bismaleimide system. Figure 5 shows some of the components evaluated.

The cover plates, of both PMR-15 and NR-150B2 with chopped glass fiber, experienced compression creep at elevated temperature under the design bolt load. The unlined oil transfer tube, Kerimid 601 with chopped HT-5 fiber, was structurally adequate, but experienced seepage of hydraulic oil under 400 psig pressure. The oil tank brackets of chopped glass (with selective continuous reinforcement) with both NR-150B2 and PMR-15 matrices passed the required structural tests. Cost and weight reduction potential was demonstrated for these small components. Another small box bracket, not shown, was successfully engine tested for over 600 hours.

In 1976 work was initiated under company funded programs on the F100 exhaust nozzle external flap. The early prototype flaps were fabricated by a number of suppliers, including Composites Horizons, General Dynamics, Grumman and Hamilton Standard Division (HSD) of United Technologies. The HSD flaps were fabricated using the HMS/NR-160B2 system and are shown in Figure 6. A full set (15 pieces) has been flight tested on an F-15 aircraft at Edwards AFB. The high time part has collected over 700 total operating hours and 430 flight hours. This work led to a subsequent AF program (F33615-78-C-5099) in which a total of 52 parts were fabricated by Hamilton Standard from C-6000/NR-150B2. A schematic of the flap design is shown in Figure 7. These flaps have also accumulated a significant number of flight hours. Fifteen have 108 hours at EAFC and another set has collected 18 hours in a F-15 at NASA Hugh C. Dryden Flight Test Center (Figure 8). No significant difficulties have been encountered with any of these flaps and the two sets from the AF program will continue to be flight tested.

This latter design demonstrated a 22% weight reduction. Switching from the now-unavailable duPont NR-150B2 polyimide to the PMR-15 resin system and incorporating automated cutting and stacking under AF contract F33615-78-C-5218 has resulted in the composite flap being a cost effective alternative to the bill-of-material metal flap.

In 1979 P&WA performed static structural tests on three F100 Gr/PI augmentor ducts (Figure 9). These were fabricated by Rohr Industries (AS/703), Composite Horizons (C-6000/PMR-15), and General Dynamics (C-6000/NR-150B2). All the flanges were titanium, only the barrel was of composite. Weight savings, despite the fact that no design iterations were permitted, were 10 and 15% for the RI and CHI ducts. The Rohr duct passed all static structural tests and plans have been made to conduct sea level tests of the duct on a P&WA engine this year.

The CHI duct passed all of the static tests except for that portion involving an internal pressurization of the duct. In an attempt to extend maximum thermal performance, an elevated temperature posture was employed which induced matrix microcracking. The microcracking lead to gas leakage through the wall which made this duct unsuitable for subsequent engine testing.

It is clear that the usage of organic matrix composites in gas turbine engines is rapidly gaining acceptance. As a result of the current activities, the usage will increase rapidly in the later portion of the 1980's and early 1990's. This is shown schematically in Figure 10. As confidence is gained, through the successful application of composites, continued growth will occur which will have a beneficial effect on future engine weight, cost and performance.

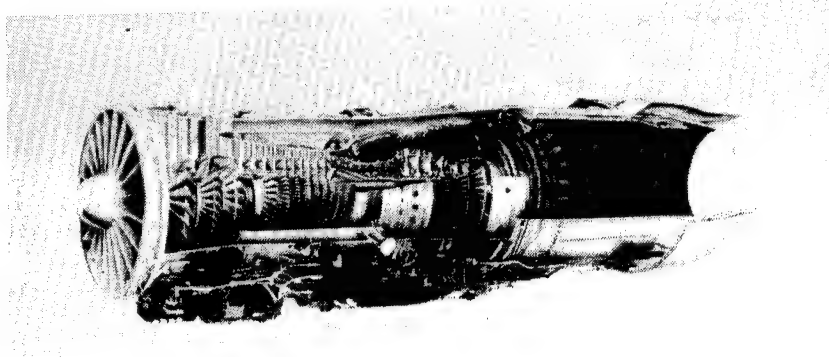


Figure 1. - F100 turbofan engine.

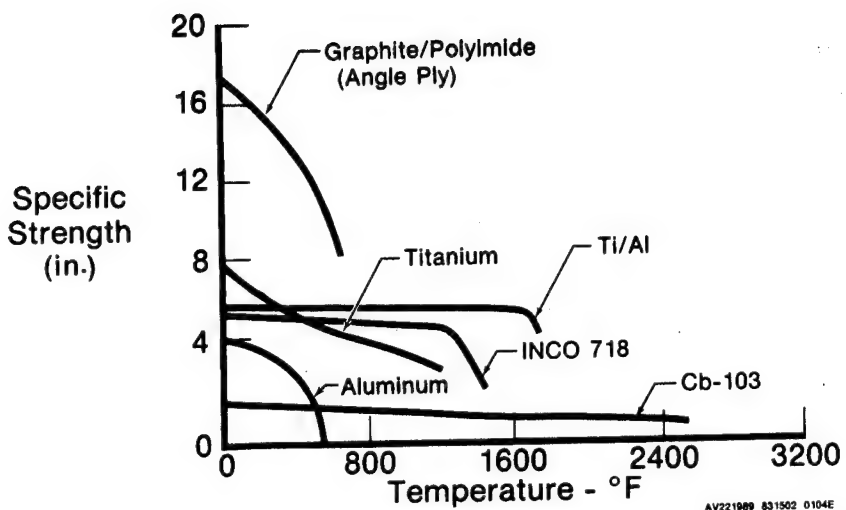


Figure 2. - Specific strength versus temperature.

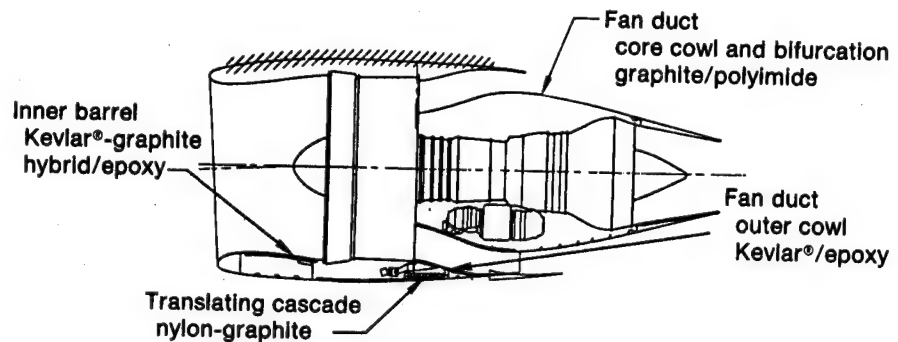


Figure 3. - Organic matrix composite applications in large turbofan engines.

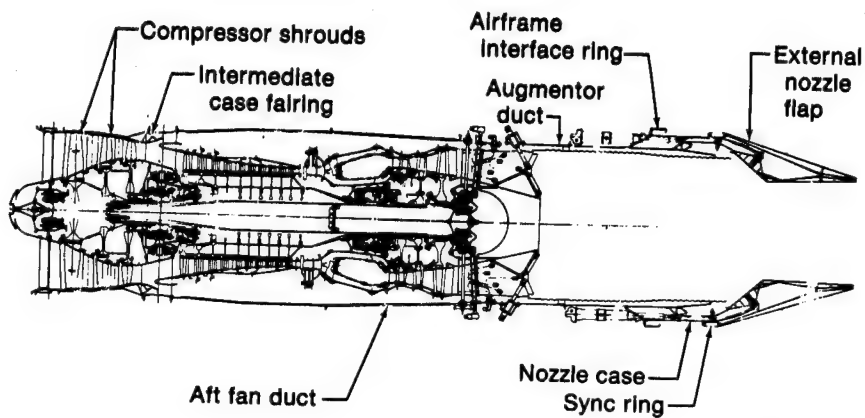


Figure 4. - Organic matrix composite applications in augmented turbofan engines.

AV227078 830902 2473B

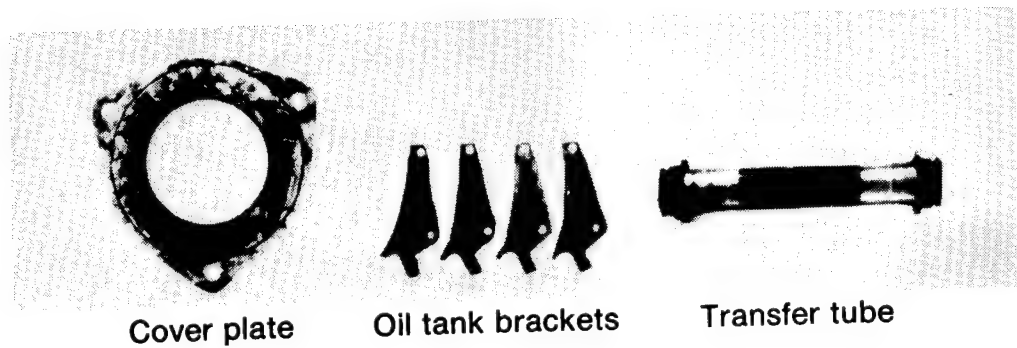


Figure 5. - External engine composite components.



Figure 6. - Prototype composite external nozzle flap.

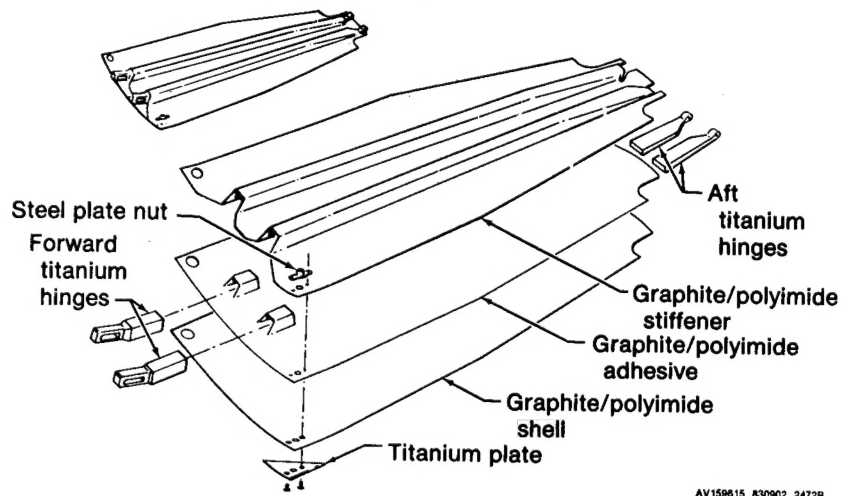


Figure 7. - Schematic of F100 composite nozzle flaps.

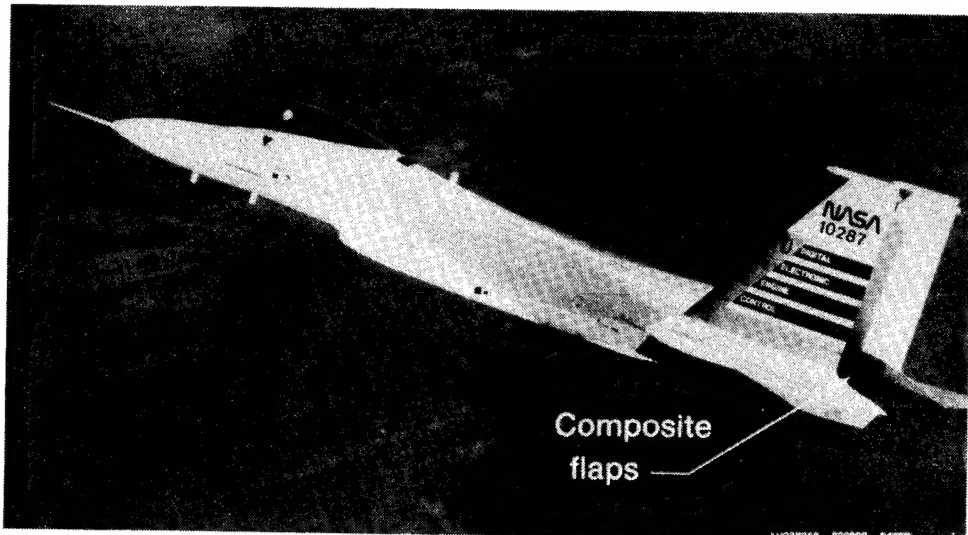
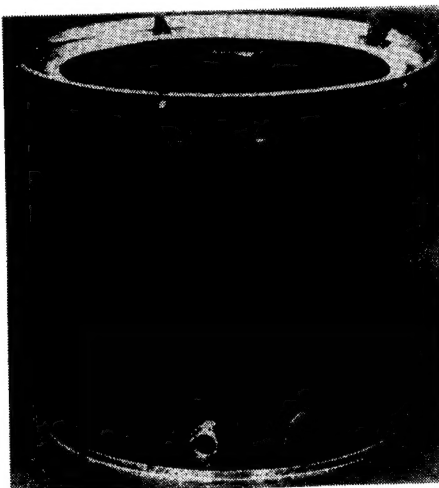


Figure 8. - Graphite/polyimide composite. External flaps on NASA F-15.



AV225401 830902

Figure 9. - Gr/PI composite augmentor duct.

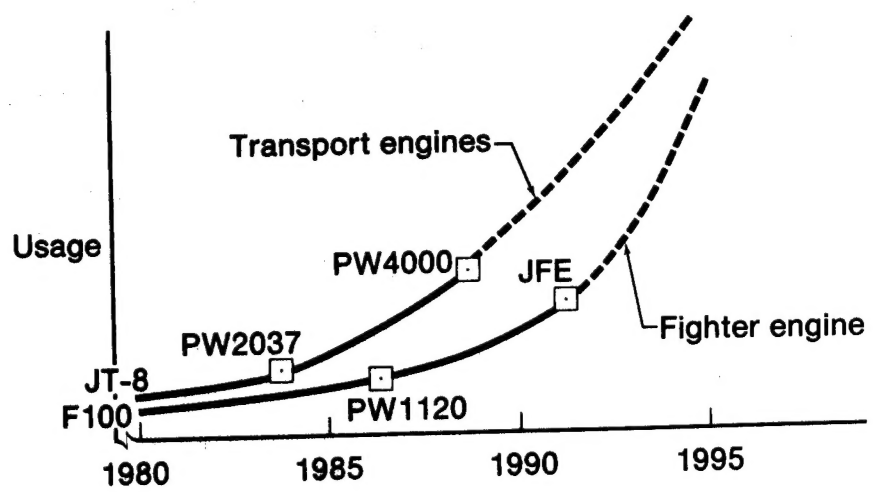


Figure 10. - Composite usage in engines is increasing.

1. Report No. NASA CP-2385	2. Government Accession No.	3. Recipient's Catalog No.	
4. Title and Subtitle High Temperature Polymer Matrix Composites		5. Report Date September 1985	
7. Author(s)		6. Performing Organization Code	
9. Performing Organization Name and Address National Aeronautics and Space Administration Lewis Research Center Cleveland, Ohio 44135		8. Performing Organization Report No. E-2425	
12. Sponsoring Agency Name and Address National Aeronautics and Space Administration Washington, D.C. 20546		10. Work Unit No. 11. Contract or Grant No.	
15. Supplementary Notes		13. Type of Report and Period Covered Conference Publication	
16. Abstract This is the proceedings of the High Temperature Polymer Matrix Composites Conference held at the NASA Lewis Research Center on March 16-18, 1983. The purpose of the conference was to provide scientists and engineers working in the field of high temperature polymer matrix composites an opportunity to review, exchange, and assess the latest developments in this rapidly expanding area of materials technology. Technical papers were presented in the following areas: 1. Matrix development 2. Adhesive development 3. Characterization 4. Environmental effects 5. Applications		14. Sponsoring Agency Code	
17. Key Words (Suggested by Author(s)) High-temperature resins; Polyimides; Composites; Adhesives; Environmental effects; Composite applications		18. Distribution Statement Unclassified - unlimited STAR Category 24	
19. Security Classif. (of this report) Unclassified	20. Security Classif. (of this page) Unclassified	21. No. of pages 423	22. Price* A18

National Aeronautics and
Space Administration

Washington, D.C.
20546

Official Business

Penalty for Private Use, \$300

SPECIAL FOURTH CLASS MAIL
BOOK

Postage and Fees Paid
National Aeronautics and
Space Administration
NASA-451



S 113.0 850813 S009420SR
DEPT OF THE ARMY
ARMY ARMAMENT RES & DEV COMMAND
PLASTICS TECH EVALUATION CTR
ATTN: MS MARY OLSEN, BLDG 351-N
DRSAC-SCH-02ARDC-AMCOM
DOVER NJ 07801



POSTMASTER: If Undeliverable (Section 158
Postal Manual) Do Not Return
